Copyright ©

Diversity and specificity of the teleost immune system

A transcriptome study on two fish species

Dissertation

zur Erlangung des Doktorgrades

- Dr. rer. nat. -

der Mathematisch-Naturwissenschaftlichen Fakultät
der Christian-Albrechts-Universität zu Kiel

vorgelegt von

David Haase

Kiel 2013

Diversity and specificity of the teleost immune system

A transcriptome study on two fish species

Dissertation

zur Erlangung des Doktorgrades

- Dr. rer. nat. -

der Mathematisch-Naturwissenschaftlichen Fakultät
der Christian-Albrechts-Universität zu Kiel

vorgelegt von

David Haase

Erster Gutachter: Prof. Dr. Thorsten B. H. Reusch

Zweiter Gutachter: Dr. Martin Kalbe

Tag der mündlichen Prüfung: 26.08.2013

Zum Druck genehmigt: 26.08.2013

gez. Prof. Dr. Wolfgang J. Duschl, Dekan

Content

Zusammenfassung

Alle Lebewesen sehen sich einer konstanten Bedrohung durch Krankheitserreger ausgesetzt. Schutz vor Infektionen wird dabei durch das Immunsystem gewährt. Bei Wirbeltieren unterscheidet man üblicherweise zwischen der sofort aktiven, unspezifischen angeborenen Immunantwort und der verzögert aktivierten, hochspezifischen adaptiven Immunantwort, welche lebenslange Resistenz gegen Krankheitserreger erzeugen kann. Bis vor wenigen Jahren fußte unser Verständnis von Prozessen des Immunsystems auf der Annahme, dass sie bei allen Kiefermäulern (Gnathostomata) gleich seien und dass eine spezifische Immunantwort nur in diesem Taxon zu finden sei. Mittlerweile konnte allerdings bereits gezeigt werden, dass auch Wirbellose (Invertebrata) zu einer spezifischen Immunantwort in der Lage sind. Fische gehören zu den ursprünglichsten Wirbeltieren, die sowohl ein angeborenes, wie auch adaptives Immunsystem besitzen. Da sie wechselwarme (poikilotherme) Organismen sind, wird ihr Immunsystem von der Umgebungstemperatur beeinflusst, was sich hauptsächlich auf das adaptive Immunsystem auswirkt. Damit verstärkt sich die Bedeutung des angeborenen Immunsystems in Fischen und unterstreicht die besondere Stellung, die diese Organismen in der Evolution des Immunsystems einnehmen.

In dieser Arbeit habe ich das Transkriptom, konkreter die vorhandene mRNA, von zwei Teleostei (Echte Knochenfische) mit Hilfe von Hochdurchsatz-Sequenziertechniken untersucht. Ziel war es, mehr Informationen über die Diversität des Immunsystems bei Wirbeltieren zu gewinnen. In meinem ersten Projekt habe ich das bis dato unbekannte Immungen-Repertoire der Grasnadel (*Syngnathus typhle*) untersucht. Mitglieder der Gattung Syngnathus zeichnen sich dadurch aus, dass die männlichen Tiere nach der Paarung die befruchteten Eier in einer Bauchtasche bebrüten. Studien konnten in diesem Zusammenhang bereits zeigen, dass dadurch das Immunsystem der Nachkommen beeinflusst wird. In meiner Untersuchung habe ich herausgefunden, dass die Grasnadel neben dem Dorsch die zweite Spezies darstellt, die einen Genverlust des MHC (Haupthistokompatibilität) Klasse II Komplexes aufweist, einem sehr wichtigen Bestandteil der Immunerkennung. Da sich die Zusammensetzung der fehlenden Gene zwischen Grasnadel und Dorsch unterscheidet, können wir davon ausgehen dass der Verlust von MHC II unabhängig stattgefunden hat. Diese Beobachtung unterstreicht den Einfluss evolutionärer Prozesse auf Komponenten des Immunsystems in Wirbeltieren.

Neben der Grasnadel habe ich mich noch mit Studien zur Genexpression von Dreistacheligen Stichlingen (*Gasterosteus aculeatus*), einem bedeutenden Modellorganismus der Ökologie und Evolutionsbiologie, beschäftigt. Die Immunantwort von Echten Knochenfischen auf Viren-Infektionen wurde bereits in diversen Studien untersucht.

Im Gegensatz dazu sind Informationen über Reaktionen auf parasitäre Würmer sehr spärlich. Daher habe ich die Genexpression von Stichlingen untersucht, die mit unterschiedlichen genetischen Linien einer parasitären Wurmart infiziert worden waren. Zunächst lag mein Augenmerk auf einer möglichen spezifischen Reaktion des angeborenen Immunsystems. Frühere Studien konnten bereits zeigen, dass der genetische Hintergrund innerhalb einer Parasitenart einen Effekt auf den Fisch haben kann, die dabei relevanten Immungene konnten jedoch bisher nicht gezeigt werden. In dieser Studie ist es mir gelungen sowohl Gene zu identifizieren, die eine allgemeine Reaktion auf die Wurmspezies darstellen, als auch eine Parasiten-Genotyp-spezifische Genexpression des angeborenen Immunsystems zu zeigen. Weiterhin habe ich den Effekt von wiederholten Infektionen verschiedener Parasiten-Linien auf die erworbene Immunität untersucht. Da angeborenes und adaptives Immunsystem unter gegenseitiger Einflussnahme stehen, hat mich besonders der Effekt Parasiten-Genotyp-spezifischer Immunisierung auf die Genexpressionsmuster interessiert. Die Resultate zeigen dabei einen großen Effekt kreuz-reaktiver Immunisierung und eine Reduzierung der Expression immunrelevanter Gene, unabhängig vom genetischen Hintergrund des Parasiten. Die in immunisierten Fischen aktiven Gene waren dabei größtenteils unterschiedlich zu denen, die in nicht-immunisierten Fischen zu finden waren. Dies zeigt, dass die adaptive Immunantwort einen Einfluss auf die Aktivierung von Genen des angeborenen Immunsystems ausübt und damit die Spezifität der Genexpression verändert. Aus meinen Resultaten kann ich schließen, dass die Immunantwort in Wirbeltieren sowohl von der untersuchten Spezies, als auch von möglichen vorherigen Infektionen abhängen kann. Daher ist es meines Erachtens nach wichtig, das Paradigma einer generellen Immunantwort in Gnathostomata hinter sich zu lassen und tiefer in die vergleichende Immunologie einzutauchen.

Summary

All living organisms are constantly surrounded by detrimental pathogens. Protection against those pathogens is realized by the immune system. In vertebrates, the immune system is classically divided into fast responding, unspecific innate immunity and slow-going, highly specific adaptive immunity, including immune memory. Until recently, our understanding of immune responses in vertebrates relied on the assumption that jawed vertebrates share common immune mechanisms and that adaptive immunity is a unique feature of this taxon. However, more recent studies have shown that invertebrates also possess specific immune responses and immune memory. Among extant vertebrates, fish are the most basal class of organisms which possess all elements of vertebrate immunity. As poikilothermic organisms, their adaptive immune response, in contrast to innate immunity, is strongly influenced by the surrounding temperature. This elevates the importance of innate immune mechanisms in fish and highlights their unique role in the evolution of the vertebrate immune system.

In this work I used high-throughput sequencing of mRNA (RNA-seq) to investigate the transcriptome of two teleost fish species and to shed light on the diversity of vertebrate immunity. In my first project I examined the transcriptome of an emerging model species, the broad-nosed pipefish (*Syngnathus typhle*). The genus *Syngnathus* exhibits male pregnancy and recent studies have shown that male pipefish contribute to the immunization of their offspring. Here I found that, next to atlantic cod, pipefish is the second vertebrate species lacking genes of the MHC class II complex, a central part of adaptive immune memory. Due to a different set of absent genes compared to cod, the loss of MHC II has likely been independent, emphasizing the importance of evolutionary processes to shape immune system components in vertebrates.

Next to pipefish I worked on gene expression patterns of three-spined sticklebacks (*Gasterosteus aculeatus*), an important model organism in ecology and evolutionary biology, infected with distinct lineages of parasitic worms. The immune response of teleost fish to viruses has already been addressed in several studies while our understanding of immune responses against parasitic worms is much less advanced. I studied the specificity of innate immune reactions in the transcriptome of three-spined sticklebacks. Earlier studies have shown an effect of parasite genotypes on the fish host, the corresponding immune genes however, have not been identified yet. I found genes to be differentially expressed as a response to the parasite per se as well as treatment specific gene expression, indicating parasite genotype specific responses of the innate immune system in sticklebacks. I further examined the effect of immune memory on the gene expression patterns induced by consecutive infections of different parasite lineages. Since innate and adaptive immunity can

influence each other I was interested in the effect of genotype specific immunization on the gene expression responses. The results show a large effect of cross-reactive immunization, reducing the amount of differentially expressed genes regardless of the genotypic background of the parasite. The genes responsible for an immune response in non-immunized fish were largely different to consecutively infected fish. This suggests that the adaptive immune system in three-spined sticklebacks modulates the extent to which innate immunity is activated and the specificity of the corresponding gene expression. Taken together, I conclude that vertebrate immune responses can depend on the species of interest and are influenced by previous infections, changing the gene expression of the host. Thus, it is important to go beyond the paradigm of a general vertebrate immune system and delve deeper into comparative immunology.

Introduction

The importance of immunity

All living species are constantly exposed to and attacked by parasites (Windsor 1997, 1998, Janeway et al. 2008). Parasite infections are usually detrimental to the fitness of an exploited host organism and thus host bodies need protection from invading pathogenic agents. This protection is realized by a variety of effector cells and molecules which compose the immune system (Janeway et al. 2008). Immunology as a science dates back to the late 18th century when Edward Jenners demonstrated in 1796 that an inoculation with cowpox confers resistance to the fatal smallpox, the invention of vaccination (Janeway et al. 2008). Since then scientists were not only able to identify the causing agents of different parasite induced diseases but also described many different immune responses resulting from those pathogenic challenges (Janeway et al. 2008). The high selective pressure, maintained by a huge variety of pathogenic agents, led to the emergence of a large repertoire of immune relevant molecules which can be generated by organisms across all phyla (Janeway et al. 2008). Even bacteria are known to possess an immune response to protect them from viral DNA and induce resistance against phages (Horvath and Barrangou 2010). In my thesis I will focus on the immune system of teleost fish. Fish are the most basal class of organisms which possess all elements of a vertebrate immune response and thus have a unique role in the evolution of the vertebrate immune system (Whyte 2007).

The vertebrate immune system

According to our current understanding the vertebrate immune response can be divided into four main steps. First, an invading pathogen is detected via receptor molecules, the "immunological recognition", with the crucial step of discriminating self from non-self. The infection then has to be contained and eliminated, which is done by various "immune effector functions". This response needs to be self-regulated due to its tissue damaging potential which leads to "immune regulation" as third main task. The last feature may involve "immunological memory" which will confer long lasting resistance to specific pathogens in some but not all immune pathways (Janeway et al. 2008). This last mechanism was long thought to be an unique attribute of the vertebrate adaptive immune system (Janeway et al. 2008), but recent experimental evidence also highlights immune priming, memory and specificity in invertebrate responses (Kurtz and Franz 2003, Little et al. 2003, Robalino et al. 2005, Schmid-Hempel 2005, Sadd and Schmid-Hempel 2006, Schulenburg et al. 2007, Roth et al. 2009). However, at present the cellular mechanisms are not fully understood.

Vertebrate immunity can be distinguished in two major parts, innate and adaptive immunity. The first line of defense against invading pathogens and parasites is the, evolutionary older, innate immune response (Janeway et al. 2008). Recognition of pathogens is constrained by a limited set of invariant pattern recognition receptors (PRRs) which respond to conserved pathogen-associated molecular patterns (PAMPs) (Janeway et al. 2008). These PAMPs are the key structure which allows distinguishing between self and non-self, thus preventing an immune reaction against self peptides (Janeway et al. 2008). Upon an infection macrophages try to engulf an invading pathogen and simultaneously start secreting signaling proteins which induce an inflammatory response. Another option of inducing an innate immune response with a subsequent inflammation is the complement system, a group of plasma proteins which can be activated upon pathogen recognition, coat foreign organisms and induce destruction, e.g. by recruited macrophages (Janeway et al. 2008). This inflammation mediates the recruitment of additional components of the innate immune response, including neutrophils and dendritic cells (Janeway et al. 2008). Neutrophils also bear PRRs and are heavily attracted to sites of ongoing inflammation processes. Dendritic cells take up pathogenic material, either by ingestion or via cell surface receptors, and present it to inactive T lymphocytes which activates the adaptive immune system (Janeway et al. 2008).

The adaptive immune system has evolved under strong selection mediated by rapidly adapting parasites/pathogens. Microparasites, in particular viruses and bacteria, have huge population sizes and short generation times which allows them to evade the immune recognition (Janeway et al. 2008). Within the innate immune pathways, PAMPs are only being recognized if they are largely conserved and not subjected to rapid evolutionary changes (Janeway et al. 2008). In contrast, the adaptive immune response has evolved to counteract invading pathogens with a higher degree of specificity via somatic hypermutation (Janeway et al. 2008). Lymphocytes, B cells and T cells, are the key element of phenotypic variability in an adaptive immune response. B cell receptors (BCR) on the cell surface bind an antigen, the result of processed pathogenic material, and induce proliferation of B cells into plasma cells which secrete antibodies, known as immunoglobulins, specific to the targeted antigen (Janeway et al. 2008). This specificity is mostly achieved by somatic hypermutation, a process which starts upon activation of a B cell by T cells with antigenic material (Janeway et al. 2008). During this process point mutations are introduced at very high rates, producing mutant B cell receptors on the cell surface. This is followed by a selection process allowing only B cells with highest antigen affinity to develop into antibody-secreting cells, a process called affinity maturation (Janeway et al. 2008).

T cell receptors (TCR) also proliferate upon antigen detection, but are distinct from the immunoglobulins. Activated effector T lymphocytes can be distinguished into cytotoxic T cells, helper T cells and regulatory T cells (Janeway et al. 2008). The first group can kill cells infected with intracellular pathogens, helper T cells enhance activation of antigen stimulated B cells and the last group is involved in the regulation of lymphocytes and other immune responses (Janeway et al. 2008).

The most intriguing difference between B cell receptor and T cell receptor is their way of binding foreign antigens. The T cell receptor cannot bind antigens directly, instead short peptides derived from antigens are bound to glycoproteins from the major histocompatibility complex (MHC) and presented upon cell surfaces (Janeway et al. 2008). These MHC molecules are highly polymorphic and can be distinguished into two molecule groups, MHC class I and MHC class II. CD8 T cells recognize MHC class I molecules bound to antigen peptides from the cytosol and CD4 T cells, which can also activate naive B cells, respond to MHC class II molecules generated in intracellular vesicles (Janeway et al. 2008). The diversity of the major histocompatibility complex is so important for the immune response against invading pathogens that it influences mate choice in many species, including mice, humans, salmon and sticklebacks (Wedekind et al. 1995, Penn and Potts 1998, Reusch et al. 2001b, Jobling et al. 2004, Consuegra and Garcia de Leaniz 2008).

Characteristics of the fish immune system

Fish are the crucial transition point between species which depend only on innate immunity, e.g. invertebrates, and those that rely heavily on adaptive immunity, e.g. mammals (Workenhe et al. 2010). They are the most basal class of vertebrates which possesses both components, innate and adaptive immunity (Whyte 2007). Adaptive immunity in this case is defined as the classical mechanism of immunoglobulin based specific immune responses and T cell mediated immune memory (Janeway et al. 2008). This is not including jawless vertebrates (agnathans) which possess a form of somatic cell rearrangement which is different from the V(D)J system in jawed vertebrates (Alder et al. 2005, Janeway et al. 2008). Teleost fish do not possess red bone marrow or lymph nodes, where the central immune cells, i.e. granulocytes, macrophages, dendritic cells and lymphocytes, of higher vertebrates (mammals) are produced (Workenhe et al. 2010). Instead the head kidney is morphologically and functionally resembling the red bone marrow, producing myeloid (granulocytes, macrophages, dendritic cells) and lymphoid (lymphocytes, natural killer cells) progenitor cells (Workenhe et al. 2010). Next to thymus and spleen, the head kidney is one of the major immune organs in fish, a major site of antibody production and together with the thymus the primary T cell and B cell organ (Press and Evensen 1999, Whyte 2007, Workenhe et al.

2010, Rauta et al. 2012). Studies on immune responses against viruses have shown that bony fish and mammals exhibit a high similarity in the major mechanisms of their respective immune response (Workenhe et al. 2010). There is however one important difference, since most teleost fish are poikilothermic organisms, i.e. their body temperature varies depending on the environment (Fry 1967, Workenhe et al. 2010). It appears that at least certain stages of the adaptive immune response seem to be more sensitive to low temperatures than the innate immune response (Workenhe et al. 2010). In contrast to mammals, external temperature changes can delay the activation of adaptive immunity in fish for several weeks (Magnadóttir 2006). Therefore, studies on the innate immune response of fishes are crucial for our understanding on the concerted effort of innate and adaptive immune responses in teleost fishes (Workenhe et al. 2010). Here, studies on host-parasite interactions can provide fruitful insight into mechanisms that induce an immune response against invading pathogens.

A classical fish model, the three-spined stickleback (*Gasterosteus aculeatus*)

Three-spined sticklebacks (*Gasterosteus aculeatus*) belong to the Gasterosteids and are small plated fish distributed over the whole Northern Hemisphere (Bell and Foster 1994). Originating from the marine habitat they colonized lakes and rivers after the last glaciation period with populations being marine, freshwater resident or anadromous, i.e. living in marine environments and migrating to fresh or brackish water for reproduction (Bell and Foster 1994). They have become famous for their elaborate mating behavior (Tinbergen 1952, Bell and Foster 1994). Due to their wide distribution in many ecologically distinct subpopulations (Reusch et al. 2001a, Berner et al. 2009, Eizaguirre et al. 2011), sticklebacks have become a major model organism in ecological and evolutionary research (Bell and Foster 1994, Gibson 2005). Their small size and ability to cope with laboratory environments make sticklebacks to a perfect model system for experimental studies in fish (Bell and Foster 1994). Numerous ecological and evolutionary research questions have been addressed with studies on sticklebacks, including mating behavior (Eizaguirre et al. 2009), plate and spine morphology (le Rouzic et al. 2011, Leinonen et al. 2011), population genetics (Bolnick et al. 2009) and host-parasite interactions (Kalbe et al. 2002). Several studies have shown the importance of MHC class II mediated immunity in three-spined sticklebacks (Wegner et al. 2003b, Kalbe et al. 2009, Lenz et al. 2009a, Matthews et al. 2010, McCairns et al. 2011, Eizaguirre et al. 2012a), making the species a classical model for studies on vertebrate immune reactions in fish. Sticklebacks have been shown to display an effect of parasite genotypes on host genotypes, indicating specific innate immune responses (Rauch et al. 2006). Studies on host-parasite interactions have revealed genes important for immune responses against macroparasites, with differences between parasite adapted and non-adapted stickleback

populations (Lenz et al. 2013). However, the genetic basis for host-parasite genotype x genotype interactions remains to be discovered.

An emerging model species, the broad-nosed pipefish (*Syngnathus typhle*)

Broad-nosed pipefish (*Syngnathus typhle*) belong to the teleost group of Syngnathids, including pipefish, seahorses and sea dragons, which share a specific feature: the eggs produced by females are bred and nourished by the males in a ventral brood pouch (Roth et al. 2011). *S. typhle* is an emerging model species in the context of evolutionary ecology with an emphasis on the immune responses under parasite pressure (Landis et al. 2012, Roth et al. 2012a, Roth et al. 2012b). It has been shown that pipefish adapt to local bacteria (Roth et al. 2012a) but also that macroparasites can locally adapt to pipefish populations (Landis et al. 2012). Studies have revealed that males, which breed the fertilized eggs, have an increased immune response compared to females (Roth et al. 2011) and are contributing to the immunization of offspring (Roth et al. 2012b). To understand how an immunological contribution of breeding males influences offspring survival, knowledge about the activity of immunological memory and thus the adaptive immune system is a valuable contribution to our understanding of the vertebrate immune system. But so far, the immune gene repertoire of pipefish has not even been characterized yet.

Macroparasites as models in evolutionary ecology research

Parasites are disease causing organisms, which exploit their host organisms for nutrients. Ectoparasites live on the host surface while endoparasites enter their host organisms. Unicellular eukaryotes (protozoa) as well as viruses and bacteria are sometimes termed microparasites, whereas macroparasites can usually be seen by the naked eye and are mostly parasitic insects or parasitic flatworms (platyhelminths). The generation time of macroparasites is usually much longer compared to microparasites (Viney and Cable 2011). This results in sophisticated life history strategies for survival inside the host and led to the evolution of mechanisms to actively manipulate the host immune response (Viney and Cable 2011). Parasitic platyhelminths can be distinguished in three main groups, Monogenea, Digenea and Cestoda, with the Monogenea having direct life cycles, i.e. infective stages are directly released, and the Digenea having indirect/complex life cycles with intermediate hosts (Viney and Cable 2011). The majority of trematodes maintains three host stages, including free living stages and asexual reproduction in one intermediate host (Rauch et al. 2005). Different explanations have been suggested for this phenomenon, including increased growth and/or fecundity (Parker et al. 2003, Benesh et al. 2013), higher transmission rates

(Morand et al. 1995), higher mating success (Brown et al. 2001) and increased intermixture of clonal genotypes (Rauch et al. 2005).

Studies on viruses have shed light on the corresponding immune response in teleost fish hosts (reviewed in Magnadóttir 2006, Whyte 2007, Workenhe et al. 2010) but the knowledge about responses against parasitic worms is much less advanced (Rauch et al. 2006, Janeway et al. 2008, Lenz et al. 2013). In my thesis I am aiming for this gap by studying the transcriptome response of three-spined stickleback (*G. aculeatus*) to infections with controlled laboratory lines of the parasitic trematode *Diplostomum pseudospathaceum*.

Except from studies on natural parasite populations there are few studies that have used controlled lab bred lines of macroparasites, especially trematodes and other parasitic worms, to control breeding design and thus genetic background of the parasites. One example is the tapeworm *Schistocephalus solidus*, which has been used to study parasite-induced immune-modulation (Scharsack et al. 2004) and host specificity (Henrich et al. 2013) and can be successfully maintained with in vitro cultures (Smyth 1946, Jakobsen et al. 2012).

An ideal candidate to test the consequences of host-parasite interactions are parasites from the genus *Diplostomum*. This eye flukes maintain a complex life cycle with two intermediate and one final host. In the final host, a piscivorous bird, the parasite reproduces sexually, laying eggs which leave the host via the feces (Chappell et al. 1994). Free swimming larvae, called miracidia, hatch from the eggs and infect fresh water snails (Chappell et al. 1994). In the snail the parasite transforms to a sporocyst which can produce hundreds of thousands of clonal cercariae, the infective stage which actively attacks a fish host, e.g. three-spined sticklebacks. The parasite enters the blood vessel of the host from where it migrates to the eye lens, which is free of any immune response, thus protecting the parasite (Chappell et al. 1994). The diplostomula impair the host's visual capacities, increasing the chance for predation by the final bird host (Chappell et al. 1994). Although the life cycle of *Diplostomum* is not easy to handle or maintain in the lab, the parasite provides several advantages for experimental studies on host-parasite interactions. First, the fish-infecting stage is replicated clonally in the host snail, which is detectable by published microsatellite primers (Reusch et al. 2004) and thus allows to control the genetic background of the parasite without losing the ability to conduct replicated studies (Rauch et al. 2006). Second, the migration to the fish's eye lens needs less than 24 hours (Chappell et al. 1994). Since the adaptive immune response in poikilotherm organisms like fish is considerably slowed, single infection-treatments need to be cleared by an innate immune response (Rauch et al. 2006). Third, the parasite load in the fish's eye lens can be counted non-invasively, leaving the potential for further experiments with the same fish including infection rate measurements (Wegner et al. 2007).

Transcriptome profiling via RNA-seq

My thesis attempts to characterize the innate and adaptive immune responses towards macroparasite infection via a characterization of the transcript abundance of all genes, also termed transcription profiling. To date, the most effective and insightful approach to sequence replicated expressed sequence tag libraries to a high depth of coverage is facilitated by next-generation sequencing technologies. The transcriptome can be defined as the total amount of transcripts expressed in the cell or tissue of an organism (Wang et al. 2009). This includes messenger RNA (mRNA) and all types of non-coding RNA (ncRNA) like tRNA and rRNA. Some ncRNAs, small interfering RNAs (siRNA), were even shown to induce post-transcriptional gene silencing, thus influencing the translation of mRNA to proteins (Hamilton and Baulcombe 1999). The presence of a transcript and its expression quantity can depend on the tissue type, developmental stage and/or physical condition (Wang et al. 2009). Considering these characteristics, including mRNA stability and translation efficiency, the abundance analysis of transcripts cannot be equated with the abundance of proteins but is still an essential tool to understand functional elements of the genome and how those vary under different conditions (Wang et al. 2009).

The research on transcriptome-wide gene expression has led to the development of various technologies, the most popular being microarray-based hybridization and sequence-based approaches (Wang et al. 2009). Hybridization via microarrays is usually realized by linking synthesized oligonucleotides on glass-like structures which then bind to fluorescent labelled cDNA fragments of interest (Maskos and Southern 1992, Wang et al. 2009). These approaches allow high-throughput estimation of gene expression combined with a relatively low cost per sample (Wang et al. 2009). They have been used to estimate expression of several thousand genes in fish, for example in medaka (Yao et al. 2012) or three-spined stickleback (Leder et al. 2009, Leder et al. 2010, Leveelahti et al. 2011, Sanogo et al. 2011). These approaches however are limited to existing knowledge, since the sequences needed for hybridization have to be synthesized beforehand (Wang et al. 2009). Thus they don't allow an estimation of the transcriptome without prior information.

Sequence-based approaches, which estimate the abundance of mRNA by direct sequencing of cDNA, have started with Sanger sequencing, leading to long but rather expensive nucleotide sequences (Shendure and Ji 2008, Wang et al. 2009). These have further developed into high-throughput sequencing technologies, also termed next-generation sequencing (NGS), different new sequencing methods capable of producing a large amount of short reads (Shendure and Ji 2008). Currently the three most widely distributed NGS-platforms for RNA sequencing are Illumina, 454 and SOLiD (Wang et al. 2009, Auer and

Doerge 2010). The general construction of sequencing libraries is similar for all technologies (Wang et al. 2009) with the general sequencing approach being quite diverse, ranging from color-coded nucleotide estimation (SOLiD) over pyrosequencing (454) to fluorescent labels in combination with Illumina bridge-PCR (Shendure and Ji 2008). Each technology has its advantages and disadvantages but all are very suitable for the estimation of gene expression even in non-model organisms without prior genetic information (Shendure and Ji 2008, Wang et al. 2009).

At first, the Sanger-based method of creating short tags to estimate expression of genes was transferred to NGS data, which allowed to estimate digital gene expression but was unable to distinguish between several isoforms of the same gene (Wang et al. 2009). Tag-based approaches have for example been used in three-spined sticklebacks to estimate immunological adaptation to macroparasites in connection with different habitats (Lenz et al. 2013). Later with increasing sequence (read) length the method was further developed to estimate the abundance of transcripts instead of sequence-associated tags, resulting in RNA sequencing (RNA-seq) approaches which allow mapping and quantification of the whole transcriptome (Wang et al. 2009) including the detection of unannotated transcripts and the estimation of splice variants (Trapnell et al. 2010). The increasing popularity of next-generation sequencing, including research on model and non-model organisms, facilitated the development of diverse software solutions for alignment (mapping) of large amounts of reads to a reference genome/transcriptome and for the de novo assembly of non-model organisms (Martin and Wang 2011). This included NGS technology specific solutions for de novo assembly and read mapping (Li and Durbin 2009, Mundry et al. 2012, Vijay et al. 2013) and the development of new statistical approaches (Auer and Doerge 2010, Soneson and Delorenzi 2013, Vijay et al. 2013). Since then, RNA-seq has been a widely used tool to investigate the transcriptome of several model and non-model fish (Greenwood et al. 2012, Gross et al. 2013, Palstra et al. 2013, Petzold et al. 2013, Yang et al. 2013) including studies on the fish immune system (Morera et al. 2011, Ordas et al. 2011, Zhang et al. 2011, Li et al. 2012, Sarropoulou et al. 2012, Sun et al. 2012).

In this work I used high-throughput sequencing of mRNA (RNA-seq) to explore the transcriptome of three-spined sticklebacks and broad-nosed pipefish. For the pipefish transcriptome I utilized a combination of 454 and Illumina reads. This approach combines the relatively long read length of 454 data and the high accuracy of the shorter Illumina reads to approximate the reconstruction of the whole pipefish transcriptome. In three-spined sticklebacks I used individual libraries of Illumina-sequenced reads aligned to a reference genome. The high amount of sequences produced by the Ilumina technology allows direct quantification of transcript abundance including an estimation of present splice variants.

Thesis outline

The results of my dissertation are structured in three chapters. All have the form of a manuscript, including: introduction, material & methods, results and discussion. The first chapter has already been published, the latter two are prepared for submission.

Chapter 1

In the first chapter I explored the immune repertoire of broad-nosed pipefish (*Syngnathus typhle*). For this purpose the transcriptome of wild caught individuals from the Baltic Sea and the Mediterranean Sea infected with pathogenic bacteria of the genus *Vibrio* was examined. Sequences were obtained via 454 and Illumina sequencing, assembled de novo and compared to a set of key immune genes that have been identified in other fish species.

Chapter 2

In the second chapter I investigated the specificity of the innate immune response in three-spined sticklebacks (*Gasterosteus aculeatus*). Therefore, clonal lineages of the parasite *Diplostomum pseudospathaceum* were isolated and used to infect naive, lab bred sticklebacks with either one of two clonal lineages or a clone mixture. Illumina-based transcriptome sequencing was performed on two immunologically relevant host organs (head kidney and gills) to estimate which genes are commonly expressed among all treatments, compared to specific expression as response to each genetically distinct parasite line.

Chapter 3

The third Chapter is tightly linked to the second chapter, since the same clonal parasite lines (*D. pseudospathaceum*) were used for infection experiments and subsequent transcriptome sequencing of RNA from three-spined sticklebacks (*G. aculeatus*) was performed. Here the focus was on the specificity of the memory effect of the immune response, to this end the sticklebacks were exposed weekly over the course of 5 weeks with either one of our two clones or a mix of clonal parasite lineages. This pre-exposure was followed by a final infection, either similar or different to the pre-exposure. This design allows to estimate how preexposure influences parasite load and gene expression in subsequent infections of the fish host.

Chapter 1

Absence of major histocompatibility complex class II mediated immunity in pipefish, *Syngnathus typhle*: evidence from deep transcriptome sequencing

David Haase[1,*], Olivia Roth[1,*], Martin Kalbe[2], Gisela Schmiedeskamp[2], Jörn P. Scharsack[3], Philip Rosenstiel[4] and Thorsten B. H. Reusch[1]

[1]Evolutionary Ecology of Marine Fishes, GEOMAR Helmholtz-Centre for Ocean Research Kiel, 24105 Kiel, Germany
[2]Max-Planck Institute for Evolutionary Biology, 24306 Plön, Germany
[3]Institute for Evolution and Biodiversity, University of Münster, 48149 Münster, Germany
[4]Institute for Clinical Molecular Biology, University of Kiel, 24105 Kiel, Germany

Biol. Lett. 2013 9, 20130044, published 27 February 2013

*equal contribution

Abstract

The major histocompatibility complex (MHC)-mediated adaptive immune system is the hallmark of gnathostome immune defense. Recent work suggests that cod-like fishes (Gadidae) lack important components of the MHC class II mediated immunity. Here, we report a putative independent loss of functionality of this pathway in another species, the pipefish *Syngnathus typhle* that belongs to a distantly related fish family (Syngnathidae). In a deep transcriptome sequencing approach comprising several independent normalized and non-normalized expressed sequence tag (EST) libraries with approximately 750 million reads, sequenced with two next generation platforms (454 and Illumina), we were unable to identify MHC class IIa/b genes as well as genes encoding associated receptors. Along with the recent findings in cod, our results suggest that immune systems of the Euteleosts may be more variable than previously assumed.

Introduction

Given the ubiquitous abundance of parasites and pathogens (Windsor 1998), immune systems are of crucial importance for any species. Parasite pressure has resulted in the evolution of highly specific immune defense (Schmid-Hempel and Ebert 2003) that

discriminates self from potentially dangerous non-self. Innate immune defense components recognize conserved pathogen-associated molecular patterns (Medzhitov and Janeway Jr 1997), but their repertoire diversity is limited. Hence, an important evolutionary innovation unique to gnathostomes (jawed vertebrates) is the adaptive immune system along with somatic diversification of receptors of the immunoglobulin family (Cooper and Alder 2006, Flajnik and Kasahara 2010). Foreign peptides (epitopes) are recognized upon presentation to specialized lymphocytes that requires the binding of epitopes to specialized receptor molecules, encoded by major histocompatibility complex (MHC) class I and II genes. Whereas MHC class I genes are expressed on all cells and present epitopes from within the cells, class II genes are only expressed on specialized antigen-presenting cells (APC) such as dendritic cells and macrophages. When APCs present motifs of extracellular danger signals from pathogens to specialized T cells (CD4+ type) the MHC II mediated immunity is activated.

Given the core function of the MHC class II mediated pathway in gnathostome immunity, it came as a surprise that members of the cod family lack MHC class IIa and b genes, as well as several important genes of this immune pathway (Star et al. 2011). Here, we report the absence of an MHC class II mediated immune pathway in a member of another, phylogenetically distant fish, the pipefish *Syngnathus typhle* (Syngnathidae) based on deep transcriptome sequencing, and compare the repertoire loss to the cod-like fishes.

Material and methods

Study species

As a sex-role reversed fish, the pipefish *S. typhle*, is a widely studied model species in evolutionary biology (Paczolt and Jones 2010, Roth et al. 2011). Females lay eggs into the male brood pouch, where they are fertilized and nourished (Kvarnemo et al. 2011). Pipefish are exposed to bacterial and metazoan pathogens in their coastal habitat (Landis et al. 2012, Roth et al. 2012a). Here, we analyzed pipefish from the Baltic Sea (Kiel Fjord) and from the Adriatic Sea (Lagoon of Venice). At both sites, fish are continually exposed to commensal and pathogenic Vibrio strains (Roth et al. 2012a). We thus assume that, if present, the MHC class II pathway would be activated. Individuals from Kiel Fjord were fed with live Vibrio isolated from their environment in order to stimulate their immune response. Individuals were killed with an overdose of MS222. RNA extracts were prepared immediately from freshly dissected organs.

Molecular methods

Our evidence of absence of the MHC class II pathway is based on three independent methodological approaches: (i) primer - directed approaches using conserved portions of the MHC class IIb-gene, (ii) preparation and sequencing of a normalized cDNA library and (iii) ultra-high-throughput sequencing of three non-normalized cDNA libraries using an Illumina HiSeq 2000 platform.

Using standard PCR-directed cloning and sequencing, we focused on the MHC class IIb-gene via primer-directed approaches with cDNA and gDNA as a template. Numerous published and self-developed primer pairs were tested in regions that are conserved across six acanthopterygian taxa according to alignments (see supplementary material, tables S.1.1 and S.1.2). PCR products were characterized using standard TA-cloning approaches and Sanger sequencing.

We performed deep-cDNA sequencing on a Roche 454 Titanium (normalized EST library, pool of individuals from Adriatic Sea/Baltic Sea) and on a Illumina Hi-Seq 2000 platform (non-normalized cDNA, supplementary material, tables S.1.3 and S.1.4, fish only from Baltic Sea challenged with Vibrio). RNA quality was checked on an Experion RNA analyser (Qiagen). A normalized cDNA library was prepared (pool of five pipefish individuals; pool of gill, liver, head kidney) by GATC (Konstanz, Germany), and sequenced with Roche 454 FLX Titanium chemistry (526491 reads after quality clipping). On an Illumina HiSeq 2000 platform, we characterized the transcriptome to ultra-high coverage analyzing three independent libraries of above organs separately, each derived from Vibrio-infected pipefish. In total approximately 750 million paired-end reads were produced (see the electronic supplementary material, table S.1.3; Genbank accession no. SRP018381).

Bioinformatic pipelines and analyses

The raw 454 reads were adaptor and quality-trimmed with SEQCLEAN (Chen et al. 2007), and reads less than 50 bp were discarded, resulting in 468126 reads (length 100 – 951 bp, mean 278 bp). Illumina data were cleaned using SEQPREP and overlapping read-pairs were merged. PRINSEQ (Schmieder and Edwards 2011) was used to maximize read quality by discarding all reads with an undetermined base content of greater than 10 percent. Random subsamples of merged reads obtained by Illumina-sequencing (length 50 – 186 bp) were the basis of two hybrid assemblies. They contained all 454 reads and either 10 million subsampled reads of Vibrio-infected pipefish gills, or 5 million reads of each of the three tissues head kidney, gills and liver. The assemblies conducted in MIRA3 (Chevreux et al.

2004) produced 96333 contigs for the 454-gill hybrid data, and 170726 contigs for all three organ types. To estimate assembly quality, we mapped reads against the contigs resulting from both de novo hybrid assemblies of 454 data and Illumina reads (see supplementary material, table S.1.4) using the software BOWTIE (Langmead et al. 2009). For annotation of gene models, the resulting contigs from both de-novo assemblies were blasted (BLASTx) against the non-redundant protein database from NCBI, using an e-value cut-off of 0.00001. In the three-tissue assembly these were 106154 of a total of 170726 contigs (62.18%).

As a second search strategy, we retrieved a number of cDNA sequences of the most important MHC II pathway genes from GenBank (see supplementary material, S.1.1) which were queried against all raw reads (approx. 750 million) obtained here. We used tBLASTx with very high cut-off values (e-value 100). For every target gene, we collected the 5000 best hits, which were then annotated using tBLASTx (e-value 0.00001) against NCBI non-redundant protein database.

To validate our approach (assembly + tBLASTx), we spiked the pipefish read data with short (101 bp) MHC II fragments derived from three-spined sticklebacks (*Gasterosteus aculeatus*) and seahorse (*Hippocampus abdominalis*), and found successful recovery (details in supplementary material S.1.2).

Table 1.1 Immune gene repertoire of broad-nosed pipefish, *Syngnathus typhle*. The immune gene repertoire is compared with cod (Star et al. 2011). The last column indicates how the transcript was identified, either via contig annotation, or via reciprocal best tBLASTx using teleost queries to the *S. typhle* database (see S.1.1 and S.1.2 §2 for details). The results of the tBLASTx search are presented in the tables S.1.5 and S.1.6.

gene abbreviation	pathway	pipefish, this study	cod	identification
MHC I	MHC I	yes	yes	contig annot
B2-microglobulin	MHC I	yes	yes	contig annot
TAP1	MHC I	yes	yes	contig annot
TAP2	MHC I	yes	yes	contig annot
Tapasin	MHC I	yes	yes	contig annot
PSME1	MHC I	yes	yes	contig annot
PSME2	MHC I	yes	yes	contig annot
PSME3	MHC I	yes	yes	contig annot
PSMB1	MHC I	yes	yes	contig annot
PSMB2	MHC I	yes	yes	contig annot
PSMB3	MHC I	yes	yes	contig annot
PSMB4	MHC I	yes	yes	contig annot
PSMB5	MHC I	yes	yes	contig annot
PSMB6	MHC I	yes	yes	contig annot
PSMB7	MHC I	yes	yes	contig annot
PSMB8	MHC I	yes	yes	tBLASTx
PSMB9	MHC I	yes	yes	tBLASTx
PSMB10	MHC I	yes	yes	tBLASTx
GranzymeB	MHC I	yes	yes	contig annot
Perforin	MHC I	yes	yes	contig annot
FasL	MHC I	yes	yes	contig annot
Fas	MHC I	yes	yes	contig annot
Erap1	MHC I	yes	yes	contig annot
Erap2	MHC I	yes	yes	contig annot
Irap	MHC I	yes	yes	contig annot
UNC93B	MHC I	yes	yes	contig annot
RFXANK	MHC II	yes	yes	contig annot
RFXAP	MHC II	yes	yes	contig annot
RFX5	MHC II	yes	yes	contig annot
RFX7	MHC II	yes	yes	contig annot
CIITA	MHC II	no	yes	n.a.
MHC II alpha	MHC II	no	no	n.a.
MHC II beta	MHC II	no	no	n.a.
Invariant chain	MHC II	not functional	no	contig annot
CD3e	T-cell receptors	yes	yes	contig annot
CD8a	T-cell receptors	yes	yes	contig annot
CD8b	T-cell receptors	no	yes	n.a.
CD4	T-cell receptors	no	truncated	n.a.
CD3 zeta	T-cell receptors	yes	yes	contig annot
CD3 g/d	T-cell receptors	yes	yes	contig annot
TCR beta	T-cell receptors	yes	yes	contig annot
TCR alpha	T-cell receptors	yes	yes	contig annot
TCR gamma	T-cell receptors	no	yes	n.a.
AIRE	T-cell receptors	yes	yes	tBLASTx

gene abbreviation	pathway	pipefish, this study	cod	identification
AICDA	T-cell receptors	yes	yes	contig annot
RAG1	T-cell receptors	yes	yes	contig annot
RAG2	T-cell receptors	yes	yes	tBLASTx
IL1B	Interleukins and interferons	yes	yes	contig annot
IL6ST	Interleukins and interferons	yes	yes	contig annot
IL8	Interleukins and interferons	yes	yes	contig annot
IL10	Interleukins and interferons	yes	yes	contig annot
IL12B	Interleukins and interferons	yes	yes	tBLASTx
IL15	Interleukins and interferons	yes	yes	contig annot
IL17D	Interleukins and interferons	yes	yes	contig annot
IL17A F1	Interleukins and interferons	yes	yes	tBLASTx
IL22	Interleukins and interferons	yes	yes	contig annot
IL2RG	Interleukins and interferons	yes	yes	contig annot
IL2RB	Interleukins and interferons	yes	yes	contig annot
IL4RA	Interleukins and interferons	yes	yes	contig annot
IL8RB-Like	Interleukins and interferons	yes	yes	contig annot
IL12RB2	Interleukins and interferons	yes	yes	contig annot
IL17RA	Interleukins and interferons	yes	yes	contig annot
IL17RD	Interleukins and interferons	yes	yes	contig annot
FOXP3	Interleukins and interferons	yes	yes	tBLASTx
TNFa	Interleukins and interferons	yes	yes	contig annot
TGFB	Interleukins and interferons	yes	yes	contig annot
IFNG	Interleukins and interferons	yes	yes	contig annot
IPS1	Interleukins and interferons	yes	yes	contig annot
IKKG	Interleukins and interferons	yes	yes	contig annot
MYD88	Interleukins and interferons	yes	yes	contig annot
C1qT4	Complement cascade	yes	yes	tBLASTx
C1qT5	Complement cascade	yes	yes	contig annot
C3	Complement cascade	yes	yes	contig annot
C4	Complement cascade	yes	yes	tBLASTx
C5	Complement cascade	yes	yes	contig annot
C6	Complement cascade	yes	yes	contig annot
C7	Complement cascade	yes	yes	contig annot
C8	Complement cascade	yes	yes	contig annot
C9	Complement cascade	yes	yes	contig annot
IgM	B cells and APC's	yes	yes	contig annot
Igb	B cells and APC's	yes	yes	contig annot
IgD	B cells and APC's	yes	yes	contig annot
PTPRC	B cells and APC's	yes	yes	contig annot
CD79A	B cells and APC's	yes	yes	contig annot
CD79B	B cells and APC's	yes	yes	contig annot
CD226	B cells and APC's	yes	yes	tBLASTx
CD40L	B cells and APC's	yes	yes	contig annot
CD40	B cells and APC's	yes	yes	contig annot
BLNK	B cells and APC's	yes	yes	contig annot
IGBP1	B cells and APC's	yes	yes	contig annot
CXCR2	Chemokines and receptors	yes	yes	contig annot
CXCR3	Chemokines and receptors	yes	yes	contig annot
CXCR4	Chemokines and receptors	yes	yes	contig annot
CCR5	Chemokines and receptors	yes	yes	contig annot
CCR6	Chemokines and receptors	yes	yes	contig annot
CCR7	Chemokines and receptors	yes	yes	contig annot
CCR9	Chemokines and receptors	yes	yes	contig annot

Results and discussion

The initial purpose of our study was to characterize a putative standard MHC-based immune system of a teleost species with sex-role reversal, the broad-nosed pipefish *S. typhle*. With primer-directed cloning and sequencing approaches, no gene fragment could be identified that even distantly resembled MHC class IIb. We subsequently performed deep transcriptome sequencing of pathogen-challenged pipefish individuals, where we failed to detect genes crucial for the MHC class II mediated adaptive immune pathways (table 1.1). Most notable is the absence of genes encoding the MHC class IIa and b chain, as well as the CD4+ receptor. By contrast, all genes important for the MHC class I pathway were present, in particular MHC I, b-2 microglobulin, TAP1 and 2 and the complete complement cascade (table 1.1). Further, several chemokine genes and associated receptors, interferones and interleukins were identified (table 1.1).

While the absence of genes directly encoding MHC class II molecules was similar to the situation in cod (Star et al. 2011), the receptor encoding gene (CD8b), which is involved in MHC I recognition via the T-cell receptor (TCR) was absent in pipefish but not cod (table 1.1). Note that CD8b is not mandatory for a MHC I mediated immune response, as CD8a molecules may function as a homodimer (Gao et al. 1997). The antigen recognizing TCRg was also absent. Because the majority of TCRs consist of a/b-heterodimers, functionality of the TCR is still likely (Janeway et al. 2008).

As opposed to cod, where the CD4+ receptor was truncated and non-functional, this gene could not be identified among pipefish transcripts. For the invariant-chain gene, our annotation returned two contigs that aligned almost perfectly to each other, suggesting the same transcript. When translated into the appropriate amino acid sequence, the putative gene model revealed a stop codon approximately 20 amino acid distant from the 3'-end of the gene in other teleosts (see supplementary material, table S.1.7), suggesting a truncated and non-functional invariant-chain gene. However, the invariant chain also binds to MHC class I molecules (Basha et al. 2012).

Thus, even if the identified transcript was functional, this would not provide conclusive evidence for the presence of MHC class II molecules in pipefish.

In our study, we have only captured transcribed genes and not analyzed the genome. It is, therefore, possible that too few APCs carrying MHC class II molecules were present in our RNA preparations. This is unlikely, because all individuals were immune challenged with Vibrio bacteria, the examined tissues harbor specialized cells involved in the MHC class II pathway, and express MHC class II genes (Wegner et al. 2006). Second, we identified

receptors that are uniquely expressed on specialized immune cells such as RAG1 and RAG2 demonstrating that these cell types were present (Oettinger et al. 1990).

It was reported earlier that seahorses and pipefish lack spleen and gut associated lymphatic tissue (Matsunaga and Rahman 1998) and thus possess no morphologically detectable organ where T cells can reside and proliferate (Rauta et al. 2012). Syngnathidae are thus supposed to suffer immune deficiency owing to secondary reduction of the adaptive immune system (Matsunaga and Rahman 1998). Nevertheless, among the Syngnathidae, seahorses (*Hippocampus abdominalis*) are reported to possess a single functional MHC class IIb-gene locus (Bahr and Wilson 2012) which is, however, divergent in terms of nucleotide sequences from all other Acanthopterygii, in particular in the second exon that codes for the peptide binding region (see supplementary material, table S.1.2). Because the *Syngnathus* genus diverged from the general Syngnathidae lineage 34 Mya (Wilson and Orr 2011), we postulate that the major immune system modification occurred during the cladogenesis of the genus *Syngnathus*.

All cod-like fishes examined thus far seem to lack the MHC class II pathway (Star et al. 2011), a trait previously thought to be a key innovation for vertebrate success. The families Syngnathidae and Gadidae are only distantly related and reciprocally monophyletic (Kawahara et al. 2008, Near et al. 2012), and fish orders that are phylogenetically younger than Syngnathidae possess MHC class II-genes (e.g. many Percomorpha—perch-like fishes). Hence, the absence of the MHC class II pathway in *Syngnathus* can only be explained as a secondary loss independent of (i.e. parallel to) that of cod-like fishes. In the Gadidae, it was speculated that habitats with few pathogens may have facilitated a loss of the MHC class II pathway. Given the ubiquity of macroparasites (Landis et al. 2012) and microparasites (Roth et al. 2012a) infecting *Syngnathus* species in shallow coastal waters, this explanation is unlikely to apply. This suggests that different selection pressures may result in a functional loss of MHC II mediated adaptive immunity. Moreover, the evolutionary flexibility in the organization of the vertebrate adaptive immune system seems to be higher than previously suggested (Star and Jentoft 2012).

Animal experiments were conducted under permission V312- 72241.121-19.

This project was financially supported through Volkswagen foundation (to O.R.), and the German Science Foundation (DFG, within SPP1399) to T.B.H.R. We thank Louis Du Pasquier for helpful comments and Katrin Beining for laboratory support.

Chapter 2

Redundancy of the innate immune system results in genotype specific host transcriptome responses to clonal trematode parasite lines in three-spined sticklebacks, *Gasterosteus aculeatus*

David Haase[1], Jennifer K. Rieger[1], Anika Witten[2], Monika Stoll[2], Erich Bornberg-Bauer[3], Martin Kalbe[4] and Thorsten B. H. Reusch[1]

[1]Evolutionary Ecology of Marine Fishes, GEOMAR Helmholtz-Centre for Ocean Research Kiel, 24105 Kiel, Germany
[2]Leibniz Institute of Arteriosclerosis Research, 48149 Münster, Germany
[3]Institute for Evolution and Biodiversity, University of Münster, 48149 Münster, Germany
[4]Max-Planck Institute for Evolutionary Biology, 24306 Plön, Germany

Summary

There is increasing evidence that the distinction between a specific adaptive and an unspecific innate immune response is an oversimplification. The large array of identified receptor types in innate immunity may result in a wide range of possible responses activated by multiple signaling pathways already upon the first encounter of a parasite. Here we used 486 million Illumina RNA-seq reads to show the transcriptomic responses of lab-bred three-spined sticklebacks (*Gasterosteus aculeatus*), singly infected with different clonal lineages of the trematode *Diplostomum pseudospathaceum*. Our data show 691 genes in head kidney and 1246 in gill tissue to be differentially expressed due to the parasite treatment with a clear distinction between shared and clone specific responses. Next to genes commonly expressed as a general response to *D. pseudospathaceum* infections (SOCS3, JUNB, THBS1, IRF4, IL4RA) we were able to detect the activation of distinct host response pathways depending on the parasite genotype, involving leukocyte-based or complement-based (C3, C4, C5) responses. Our data suggest that parasite genotype influences host receptor mechanisms, which can lead to alternative combinations of response pathways that might be activated upon first recognition of the parasite. The identified genes will provide insight into how the redundancy of the innate immune system can specifically counteract genetically different parasite lineages, further increasing our understanding about specific innate host immune responses.

Introduction

Vertebrate immunity consists of innate and adaptive components. Without delay, pathogens and parasites that enter a host organism are attacked by the innate immune response. It is mediated by macrophages and granulocytes, which detect conserved molecular patterns in pathogens, and enhanced through the activation of chemokines and cytokines (Janeway et al. 2008). Subsequently, after the processing of pathogenic epitopes, antigen-presenting cells trigger the proliferation of T-cells and B-cells, inducing a specific antibody-mediated adaptive immune response (Janeway et al. 2008). Since the receptors involved in innate immunity detect evolutionarily conserved molecular patterns (PAMP = pathogen associated molecular patterns), it is considered to be rather unspecific with respect to the pathogen species, let alone the genotype of a particular pathogen or parasite (Medzhitov and Janeway Jr 1997). However, growing evidence suggests that the distinction between the innate immune response being unspecific and the adaptive response being specific is an oversimplification (Flajnik and Du Pasquier 2004). For example, the large array of already identified receptor types may result in a wide range of possible innate immune responses activated by multiple signaling pathways (Kumar et al. 2011). Second, the innate immune response influences the subsequent activation of the adaptive immune system, for example through activation of T lymphocytes by antigen-presenting cells (Janeway et al. 2008). Taken together, we can expect a combination of innate immune responses and an antibody-mediated adaptive immunity, resulting in a very specific response to foreign pathogens (Nish and Medzhitov 2011). Both elements of the immune system co-occur for the first time in teleost fishes, making them a cornerstone for further understanding the evolution of basic features in vertebrate immune responses (Whyte 2007). Poikilothermic teleosts are well-suited organisms for studying the relative roles of innate vs. adaptive immunity because their adaptive immune system needs up to several weeks (Magnadóttir 2006) to be fully functional against a parasite or pathogen.

At the phenotypic level, it has been shown that upon first exposure the infection success of a parasite depends on the genotype x genotype interactions of host and parasite (Rauch et al. 2006, Lazzaro and Little 2009, Seppälä et al. 2009, De Roode and Altizer 2010), although the genetic basis is currently unknown. In line with these findings, host immune reactions were found to be parasite-clone specific (Koehler and Poulin 2012). This suggests a genetic basis for variation of the innate immune response (Rauch et al. 2006). If the variation exists during pathogen recognition, signaling and/or response is what we want to further explore with this study.

Our study species is the three-spined stickleback (*Gasterosteus aculeatus*), a recently emerging model fish species with outstanding genomic and transcriptomic resources (Gibson 2005, Jones et al. 2012, Feulner et al. 2013). Local adaptation of stickleback populations in northern Germany seems to be, at least partly, driven by different compositions of parasite species (Kalbe et al. 2002) and thus habitat specific immune gene responses (Lenz et al. 2012). Studies on the adaptive immune response of sticklebacks have shown a correlation between macroparasite fauna and diversity of antigen presenting MHC class II alleles in nature (Wegner et al. 2003b). This link between MHC II diversity and resistance to multiple parasite infections has also been proven in experimental studies (Wegner et al. 2003a).

In our experiment we used the digenean trematode *Diplostomum pseudospathaceum* to elicit a specific innate immune response in its fish host. This parasite has a complex life cycle, using freshwater snails and fish as intermediate hosts, before reproducing sexually in piscivorous birds (Chappell et al. 1994). Due to a clonal reproduction stage in the snail host, trematodes are ideal candidates to investigate genotype-specific performance of parasites (Koehler and Poulin 2012). The parasite invades the fish's eye lens to evade the adaptive immune system. Since the time between initial penetration and invasion of the eye lens is less than 24 h (Chappell et al. 1994), innate immunity serves as key response to *D. pseudospathaceum* (Kalbe and Kurtz 2006). In larger doses, the parasite reduces the visual capacities of its fish host, impending feeding efficiency and predator avoidance (Crowden and Broom 1980, Owen et al. 1993).

Here we used next generation mRNA sequencing (RNA-seq) to describe the transcriptional response of naive lab-bred three-spined sticklebacks (*G. aculeatus*) as hosts to mono-clonal and multi-clonal infections with the eye fluke *D. pseudospathaceum*. Transcriptome-wide RNA-seq is a powerful tool to assess expression patterns independent of a candidate gene approach by addressing the whole transcriptome, including the detection of low-expressed genes and alternative splice variants (Marioni et al. 2008). Gene expression differences can be affected by natural selection (Whitehead and Crawford 2006), leading to habitat specific immune responses (Lenz et al. 2013). This makes RNA-seq an appropriate method to investigate specific host gene expression patterns shaped by host-parasite antagonistic coevolution (Lenz et al. 2013).

We examined the mRNA expression patterns in head kidneys, the principal immune organ in fishes (Press and Evensen 1999, Rauta et al. 2012). Our second target organ was the gills, one of the preferred spots for cercarial penetration (Whyte et al. 1990).

We first investigated how a general transcriptomic response against *D. pseudospathaceum* in three-spined sticklebacks is realized by assessing all genes differentially expressed as a function of parasite treatment. Here we expect a set of genes to be differentially expressed in

all fishes treated with *D. pseudospathaceum.* In a second step we compared the genes uniquely expressed due to a specific monoclonal treatment, investigating the specificity of a transcriptomic response against a certain parasite genotype and how this influences gene expression patterns.

We also examined the expression of a set of prior defined immune relevant genes in *G. aculeatus*. Our objective was to identify a distinct subset of immune genes putatively responsible as key elements against infections with the parasitic trematode *D. pseudospathaceum* that possess polymorphism at the level of gene expression.

Material & Methods

Establishment of clonal parasite lineages & experimental infection

Clonal lines of *D. pseudospathaceum* were established by collecting parasite eggs from gull feces at the shore of the "Großer Plöner See" (Great Plön Lake) in Plön, Germany (54.159632°N, 10.425442°E). Hatched miracidia were used to infect lab bred freshwater snails of the species *Lymnaea stagnalis,* the first intermediate host of *D. pseudospathaceum*. Snails were exposed to single miracidia under controlled conditions in 12-well-plates, ensuring mono-miracidial infections. Eight weeks post infection, snails were isolated and exposed to light for 3h to check for cercaria production. From each of 4 snail pools, infected with miracidia from eggs originating from 4 different gull feces samples, the snail with the highest visible amount of cercaria production was chosen. Genotypes of cercariae emerging from snails were verified using the polymorphisms of 4 microsatellite loci (Diplo08, Diplo09, Diplo23 and Diplo29; Reusch et al. 2004). To increase the amount of available cercariae and avoid snail effects we decided to multiply and propagate specific clonal parasite lineages by establishing each lineage in several host snails. Therefore, groups of lab bred marine sticklebacks (*Gasterosteus aculeatus*) were exposed to cercariae from individual mono-miracidial infected snails to serve as parasite reservoirs. Those fish were sacrificed and fed together with the infective parasite stages to uninfected European Herring Gulls (*Larus argentatus*). We collected gull feces of all infected gulls over several weeks and used single hatched inbred miracidia to infect in total 692 lab bred *L. stagnalis*, thus increasing the amount of snails available for a specific clonal parasite lineage. For a larger experiment we thus created several inbred monoclonal parasite lines and outcrossed lines of several genotype combinations (Rieger et al. 2013). Only a subset of those lines was used in this study.

Lab bred three-spined stickleback (*G. aculeatus*) of 4 fish families, originating from the lake "Großer Plöner See", were bred and raised under standardized conditions (Kalbe and Kurtz 2006). After 7 months we randomly selected 12 fish per family and placed them in 1l aquaria. Three individuals per family were either exposed to 100 cercariae of clone I, clone XII, a clone mix (several clonal lineages, containing inbred and outcrossed parasite genotypes; Rieger et al. 2013) or not infected for use as control. All surviving infected snails were assessed for their respective parasite genotype prior to the infection experiment using microsatellites (Rieger et al. 2013). Only cercariae from snails where parasite genotype was unambiguous were used for the infection procedure.

Fish were killed 4h after infection by an incision into the brain, followed by immediate decapitation and separation of gills. Body cavities were opened for instantaneous exposure of inner organs to preserving buffer (RNAlater, Qiagen), in order to avoid RNA degradation. Likewise, fish bodies and separated gills were immediately stored in RNAlater. Since parasite larvae reach the fish eye lens and thus escape the immune system within only a few hours we decided to sample tissues that are likely to show a response to an ongoing infection.

On the other hand, since infection success cannot be reliably determined 4h post infection, an additional 3 fish from the same 4 fish families were exposed to the same parasite treatment under the exact same conditions as mentioned above. After 4 weeks, fish were dissected and eye lenses were checked for metacercariae of *D. pseudospathaceum*.

RNA extraction, library preparation & sequencing of cDNA libraries

After the experiment, whole fish were stored at -20°C in 5 ml tubes filled with RNAlater. Before extraction, gills and head kidney of 48 fish each were extracted via dissection and placed in lysis buffer and β-mercaptoethanol. Extraction was performed using the Macherey-Nagel NucleoSpin 96 RNA kit following the standard protocol. Quantity of RNA was checked using the Qubit Fluorometer (life technologies), and quality using an Experion Automated Electrophoresis system (Bio-Rad). Where RNA concentration was not sufficient, samples were replaced. Resulting total RNA was stored at -80°C. Samples were prepared for sequencing using the Illumina TruSeq RNA Sample Preparation Kit, following the standard protocol. Quality control and quantification of libraries was done using the LapChip® GX (Caliper) and the HT DNA High Sensitivity Kit. For sequencing, indexed libraries were diluted to 2 nmol/l and pooled. To control quality of the sequencing run, a 1% PhiX control library (PhiX Control Kit v3, Illumina) was added to each lane. cDNA libraries were sequenced on the Illumina HiScan SQ platform for 2*101 cycles (paired-end), yielding a read length of 101 bp on both ends of the target sequence. We sequenced 32 indexed samples (as part of a 96

sample setup) distributed over one flowcell. Raw image data were transformed and de-multiplexed using CASAVA 1.8 software.

DNA extraction & microsatellite PCR

Single cercariae emerging from infected snails were placed in 2 ml Eppendorf tubes. For extraction, 10 µl 5% Chelex suspension and 1 µl proteinase K (14 mg/ml dissolved in Tris-HCl, pH 7.5) were added, followed by shaking at 55°C for 15 minutes and 100°C for 30 minutes. Afterwards samples were immediately placed on ice. For PCR, 3 µl of extracted samples (centrifuged for 1 minute at 4000 rpm) were used. Conditions for PCR were initial denaturation 94°C, 3 minutes followed by 30 cycles of denaturation 94°C, annealing 56°C, elongation 72°C, 30 seconds each and final 72°C elongation for 5 minutes.

Data Analysis

Parasite infection statistics and data visualization

To estimate differences in parasite infection success, a two-way analysis of variance (ANOVA) was performed. Tukey's test was used as posthoc test, including Bonferroni correction to account for multiple testing. Data were square-root transformed to meet assumptions of normality and homogeneity of variances.

Visualization and modification of data sets, as well as statistical analysis of parasite infection data, was done with R (version 2.14.1) (R Core Development Team, 2012) including the software package CUMMERBUND, version 0.1.3 (Goff 2011) and custom made PYTHON scripts, version 3.1.2.

Read alignment and quantification of gene expression

Sequence reads were aligned to the *G. aculeatus* reference genome, version 67, available from ensembl (www.ensembl.org) using TOPHAT (Trapnell et al. 2009) with standard parameters. For statistical analysis we used normalized gene expression values as fragments per kilobase of exon model per million mapped reads (FPKM) modified for paired-end data after RPKM (Mortazavi et al. 2008). The software CUFFLINKS (version 1.3.0) was used for calculation of differential expression with parasite infections as treatments and fish families as replicates within a treatment. CUFFLINKS produces parsimonious sets of transcripts from alignment input leading to an estimation of relative abundances for those transcripts (Trapnell et al. 2010), thus taking biases of library preparation into account. In connection with the reference annotation based transcript (RABT) assembly method

(Roberts et al. 2011) we intended to obtain optimized alignment of reads to their respective gene down to the splice variant level. CUFFLINKS was used with the -N option, providing upper quartile normalization (see CUFFLINKS Manual) which improves the robustness of differential expression calls for less abundant transcripts. The software calculates log2 transformed fold change between two treatments for each gene of a stickleback reference transcriptome for each possible combination of treatments. P-values indicate significance of estimated fold changes with a correction for multiple testing (false discovery rate, FDR < 0.05; Benjamini and Hochberg 1995).

GO annotation and GO term enrichment analysis

The Gene Ontology (GO) project allows a standardized representation of genes and gene product attributes across species (www.geneontology.org). With GO terms we can test for enrichment of specific gene groups expressed under a given treatment against a reference set. This approach allows us to estimate differences between functional characteristics of two distinct gene sets.

Since the annotation of the stickleback reference transcriptome (version 67, www.ensembl.org) is incomplete, BLAST2GO was used for annotation of all reference-transcripts (Conesa et al. 2005). A Blastx search with an e-value threshold of 1e-05 was executed. In addition we performed a GO mapping for all sets of differentially expressed genes, using standard parameters.

GO term enrichment was done using the enrichment analysis function of BLAST2GO. The analysis conducts a Fisher's exact test, testing for the increased presence or absence of functional categories in a given subset of genes, compared to a different set. We tested for differences between both mono-clonal treatments as well as for all genes differentially expressed compared to control versus all known stickleback genes. FDR correction was applied after testing (FDR < 0.05).

Identifying immunity related genes

To estimate differential expression of genes known to be involved in an immune response we extracted human genes tagged with the GO-term "immune system process" (GO:0002376) from the ensembl database (www.ensembl.org) and compared to the stickleback transcriptome. Only genes that could be unambiguously identified in the genome of *G. aculeatus* were kept for further analyses. This set of putative immune relevant genes was completed with a set of selected core immune genes (Star et al. 2011, Haase et al. 2013), resulting in a list containing 1067 putatively immune relevant genes (Supplementary table S. 2.4).

Results

Parasite load (infection success)

Parasite load of infected sticklebacks ranged from 0-4 metacercariae in the eye lenses for *D. pseudospathaceum*-clone I, 0-6 for clone XII and 1-17 for the clone mix treatment (Fig. 2.1). Infection intensity varied significantly among parasite treatments (ANOVA, F = 9.595, P = 0.000867). Fish family as main factor and fish family x treatment interactions had no significant effect on parasite infection success (Table 2.1). A post-hoc test (Tukey's test) showed that differences in parasite infection success were driven by the difference among clone mix vs. single clone treatments (p = 0.0056 against clone I, p = 0.0034 against clone XII) while there were no significant differences between both single *D. pseudospathaceum* clones (Table 2.2).

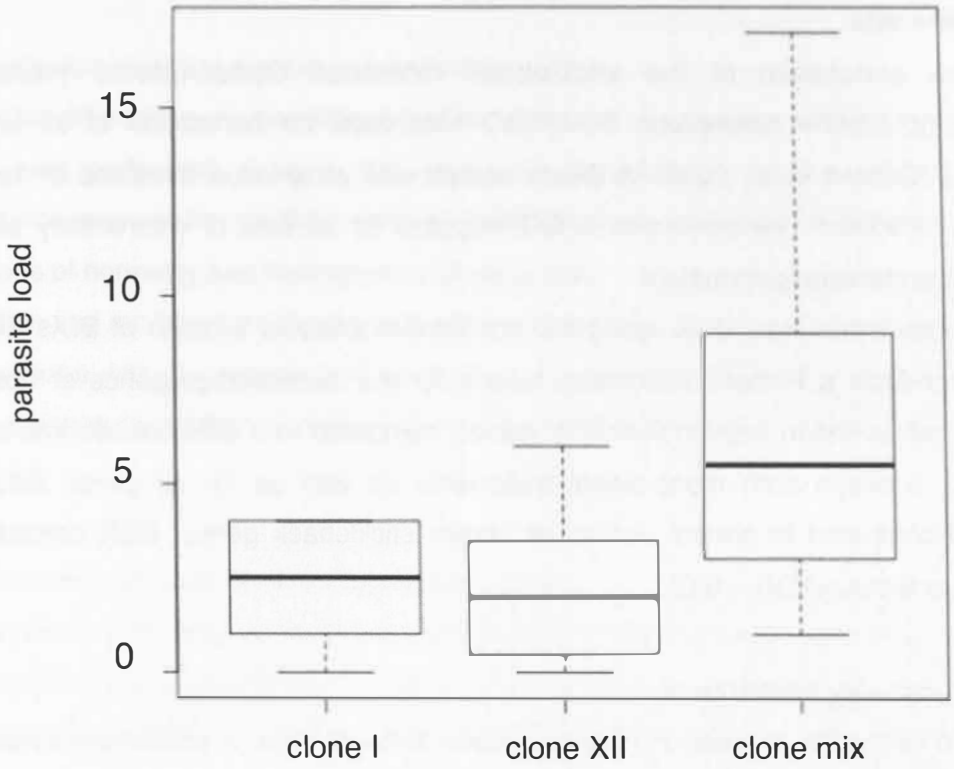

Fig. 2.1 Parasite load of three-spined sticklebacks, infected with *Diplostomum pseudospathaceum* cercariae. Distribution of total cercaria in stickleback eye lenses per infection treatment.

Table 2.1 Analysis of Variance (ANOVA) for testing differences in infection success of *D. pseudospathaceum* clones in three-spined sticklebacks (*G. aculeatus*) including treatment and fish family (sibship) interactions. Significance codes: *** 0.001 ** 0.01 * 0.05

	df	sum sq	mean sq	F-value	p-value
treatment	2	10.768	5.384	9.595	0.000867 ***
family	3	2.660	0.887	1.580	0.220169
treatment:family	6	7.428	0.8671	2.206	0.077697
residuals	24	13.467	0.561		

Table 2.2 Tukey multiple comparisons of means; 95% family-wise confidence level. The difference in the observed means is displayed by *diff*, *lwr* and *upr* are showing the lower and upper end point of the interval and *p adj* is giving the p-value after bonferroni adjustment for multiple comparisons.

	diff	lwr	upr	p adj
clone XII - clone I	-0.250000	-3.483550	2.983550	0.9803658
clone mix - clone I	4.416667	1.183117	7.650217	0.0055979 **
clone mix - clone XII	4.666667	1.433117	7.900217	0.0033804 **

Read mapping & differential gene expression

RNA sequencing on the Illumina platform led to 29 individual libraries with 486 million valid paired-end reads of 101 nucleotides length, after removal of two samples from gills (clone I, control) and one sample from head kidneys (control). Of those TOPHAT aligned 265 million reads with an average distribution of ~9 million reads per sample (supplementary table S. 2.1). Since CUFFLINKS calculates fold-changes for each gene of any possible combination of two treatments for all 4 treatments, 0.63 million comparisons were made of which 0.36 million were valid. Of those 37945 (10.5%) were significantly differentially expressed. To reliably account only for differences due to our infection treatments, only genes that were significantly different from the tissue specific controls were considered. This further data reduction (filtering) resulted in 1415 and 1060 differentially expressed gene comparisons in gills and head kidneys, respectively. When taking only unique transcripts that were differentially expressed into account, we found 1246 in gill and 691 in head kidney tissue (supplementary table S.2.2 and S.2.3). A subsequent multidimensional scaling plot (MDS, Robinson et al. 2010a) showed a clear distinction between all parasite treatments and a higher divergence among head kidney samples compared to gill tissue derived RNA (supplementary figure S. 2.1). Only a subset thereof was linked to known immune functions (figure 2.2). Distribution of differentially expressed genes can be further divided into genes only active due to a specific parasite clone treatment, genes shared between combinations of two treatments and genes differentially expressed due to the parasite infection in general (supplementary figure S.2.2).

GO term enrichment

We performed a GO term enrichment analysis for the general response against *D. pseudospathaceum*, including only up- or down-regulated genes in either of the two organs. We identified significant enrichment of GO terms under category "Biological Process" in gills as well as head kidneys. Genes belonging to the category "generation of precursor metabolites and energy" (GO:0006091) were down-regulated genes in gills, whereas in head kidneys 7 GO terms were enriched for down-regulated genes (supplementary table S.2.5). Important enriched down-regulated genes in head kidney tissue belonged to metabolic processes (GO:0008152) or to category "response to stimulus" (GO:0050896).

Up-regulated genes show a more complex pattern, revealing a higher number of enriched GO terms (supplementary table S.2.5). In gills, we can find GO terms corresponding to the development of cells and the organization of cellular components as well as genes playing a role in a response to stimulus or in signaling. Up-regulated genes in head kidney tissue revealed enrichment of GO terms related to cell production and cell organization. Abundant interleukins (IL22RA, IL4R, IL6) and interferons (IRF4) indicated the production of immune

relevant cells. This also applies to chemokines (c-c chemokine receptor type 9, c-c chemokine 19 precursor) which play a central role in inflammatory responses (Janeway et al. 2008). We found no GO terms significantly enriched as a function of the infection treatment.

Specific gene expression as a response to parasite genotype

To estimate genes expressed specifically due to a given treatment we assessed the specificity of the gene expression response in sticklebacks due to a mono-clonal infection treatment as well as the differences of a mono-clonal infection and a multi-clonal infection. In order to do so we investigated the expression of genes compared to a set of putative immune genes and observed differential expression in 139 out of 1067 genes. Broken down into tissue specific expression, this led to the detection of 55 immune genes in head kidney and 95 in gills (supplementary table S.2.6 and S.2.7; figure 2.2), which responded to the parasite infection. Interesting patterns emerged from the joint analysis of differential expression of immune relevant genes among both tissues. The majority of differentially expressed immune genes were down-regulated in head kidneys (31 out of 55) and up-regulated in gills (85 out of 95). Second, 20 out of 139 immune genes were related to the complement system, including several isoforms of complement component 3 (C3). The complement system is composed of several proteins and can be activated through three pathways: the classical pathway, involving antibodies, the antibody-independent alternative pathway, and the lectin pathway, all of which lead to the generation of factor C3 (Whyte 2007). The distribution of differentially expressed immune related genes allowed us to identify genes concertedly expressed between all treatments as a factor of *D. pseudospathaceum* infections in general. In head kidney samples, 6 genes were jointly up-regulated (THBS1, two isoforms of SOCS3, JUNB, IRF4, IL4RA). In gills only 3 shared up-regulated genes could be detected (THBS1, SOCS3, C4A).

Further, we were able to detect infection treatment dependent differences in expression of several genes (supplementary table S.2.6 and S.2.7). In up-regulated genes of head kidney samples, we find 2 only responding to infection by *D. pseudospathaceum*-clone I (HYAL2, PRF1), 3 to clone XII (RGCC, CYP27B1, CCR9) and 6 to the clone mix treatment (ITGA5, SIX1, ATP1B3, MEF2C, MLF1, MYLPF). Uniquely down-regulated were 3 genes in the clone I treatment (KYNU, C3, C7), 2 in clone XII (COL1A1, ZC3HAV1) and 1 in clone mix (VTN).

Up-regulated immune related genes in gills could only be found in clone XII (ITGB1, C6, SLC3A2) and clone mix samples (70 genes, see supplementary table S.2.7). Treatment with clone I resulted in 4 down-regulated genes (GATA2, CASP3, F11R, EPHA2), whereas treatment with the clone mix caused down-regulation of 6 genes (PFDN1, EXOSC5, ATG12, ELMOD2, PRDX3, MHC II beta).

A

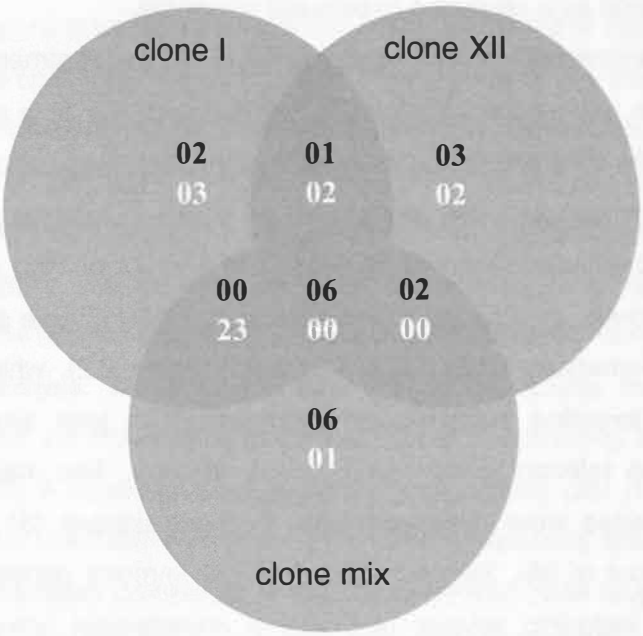

B

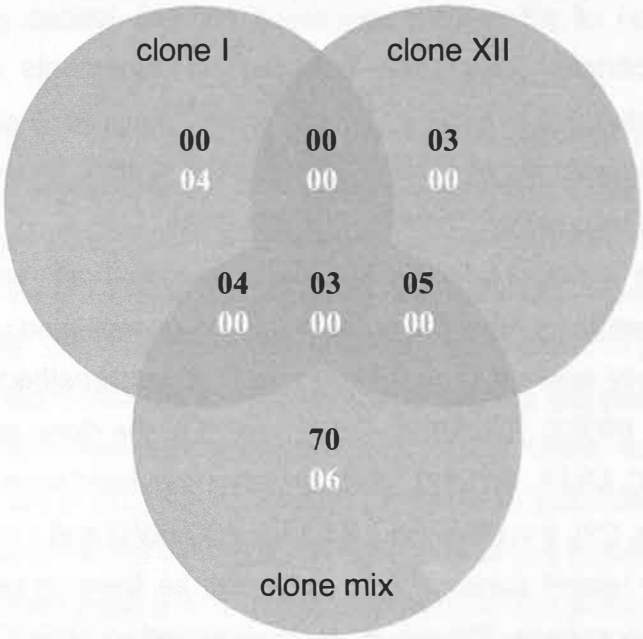

Fig. 2.2 Venn-Diagram for clone-wise distribution of differentially expressed immune genes in three-spined sticklebacks (*G. aculeatus*). Displayed are up-regulated (black) and down-regulated (white) genes in (A) head kidney and (B) gill tissue. Genes shared between treatments and regulated in both

Discussion

With this study we wanted to show differences in host gene expression patterns due to infections with genetically distinct parasite lineages. We provide transcriptomic evidence for innate immune responses in replicated three-spined sticklebacks that are specific to parasite genotypes infecting the fish host. Parasite clones collected under natural conditions are usually connected to a specific host snail individual. Thus, a clone-specific effect in an experimental setup cannot be distinguished from a snail-based effect (Koehler et al. 2012). Since we replicated clonal parasite lineages in a bird host and infected several snails with resulting miracidia, we can rule out this uncertainty.

Hence, we were able to discriminate between genes commonly expressed as a response to *D. pseudospathaceum* infections and those which are uniquely activated as a response against specific clonal lineages of the parasite. The innate immune system is characterized by a coordinated temporal sequence of activation of different parts, which can be activated upon epitope encounter while being down-regulated upon clearance of infection (Janeway et al. 2008). Depending on the receptor types activated during an infection a clone specific combination of innate immune responses might be induced (Kumar et al. 2011).

As a first step towards understanding the interaction of host x parasite genotype interactions, our experiment has not been designed to detect genetic effects on the host side. However, it is likely that host genotype specific changes in immune gene expression would have been detected with a larger setup (Rauch et al. 2006), given that immunity data of another study show that fish family influences immune responses at least partly (Jennifer Rieger, personal communication). Nevertheless, in one of the first deep RNA-seq approaches dealing with different genotypes of a macroparasite, we identified a number of responsive host immune genes that differed among clonal infection treatments.

At the phenotypic level, several studies have found lineage-specific differences in infectivity among trematode clonal lineages which suggest a role of the genetic background of the parasite in infection success (Rauch et al. 2006, Rauch et al. 2008, Koehler and Poulin 2012). In some of these studies, the genetic background of the host was also included into the design to estimate the influence of genotype specific host defenses on parasite infection success (Rauch et al. 2006).

Our data on the transcriptomic reaction of the host to *D. pseudospathaceum* infections are in line with those findings and represent a major step towards understanding the genetic basis of the reported differences. Although we did not observe a significantly different parasite load in sticklebacks between both mono-clonal infection treatments due to high variances, a diverse genetic background resulted in higher infection success compared to both mono-

clonal experimental infections (fig. 2.1). The expression of treatment specific genes seemed at odds with a realized infection rate that was not significantly different among parasite genotypes (table 2.2 and fig. 2.2). It is possible that our estimation of differential gene expression was more precise than the measurement of the infection success.

This was in line with our finding of significant differences in infection success of the multi-clonal infection treatment. It has been shown that the infection success of *D. pseudospathaceum* can be higher in mixed infections than in single genotypes, which is primarily due to the genetic diversity of exposure (Karvonen et al. 2012). In addition, a lake environment might harbor a dense population of infected snails, making simultaneous infections with several parasite genotypes more likely than single genotype infections (Rauch et al. 2005, Karvonen et al. 2012).

It has been hypothesized that multiple infections decrease the effectiveness of resource allocation in defense mechanisms (Jokela et al. 2000). If the enhanced diversity of combined *D. pseudospathaceum* lineages increases the pressure on the host, this can reduce the effectiveness of an immune response (Jokela et al. 2000). In this case theory predicts a shift from optimal resource allocation to damage toleration, which could explain the higher infection rates in the clone mix treatment (Jokela et al. 2000).

The down-regulation of genes in head kidneys termed as "response to stimulus" (GO:50896) indicates that the infection triggers a signal which induces the release of immune relevant cells from the head kidney to the site of infection. In gills we could observe that gene groups were involved in signaling (supplementary table S.2.5) and acting as a "response to stimulus" (GO:50896). Considered together, we interpreted this pattern as an activity of gene products released from the immune-relevant organ, head kidney (Press and Evensen 1999, Rauta et al. 2012), to the site of infection, gills (Whyte et al. 1990). Given this assumption, we expected genes which were down-regulated in head kidney samples to be migrating to the site of infection and thus not down-regulated because of deactivation.

The potential to detect significant enrichment of GO terms depends on the quality of an actual GO annotation. A low number of entries in the test sets, compared with an unknown GO-term quality might explain why we don't observe significant over- or underrepresentation between uniquely expressed gene sets. However, the vertebrate immune system is known to exhibit redundancy and alternative routes in a response against pathogens are likely (Nish and Medzhitov 2011). Thus, both gene sets might exert similar functions.

The general immune response against a parasitic worm seems to involve a wide variety of mechanisms. Upon recognition of the parasite the response starts with macrophages and the

activation of the complement system, which are generally present in the surrounding tissue (Janeway et al. 2008) and start attacking upon identification of the parasite. Macrophages are migratory phagocytic cells, capable of pathogen-recognition, cytokine production and antigen-presentation (Janeway et al. 2008). They are influenced by interleukins, which are cytokines produced by lymphocytes, white blood cells involved in the adaptive immune response (Janeway et al. 2008). The complement system is a set of different plasma proteins, involved in pathogen opsonization and induction of inflammatory processes (Janeway et al. 2008). Both macrophages and the complement system have been shown to significantly effect diplostomula survival in rainbow trout (*Oncorhynchus mykiss*; Whyte et al. 1990).

The activated macrophages are additionally expressing and attracting pro-inflammatory gene products like integrins, interferons and interleukins (Janeway et al. 2008). Those further attract macrophages, as well as eosinophil granulocytes, leukocytes which are typically considered the major response against macroparasites like digenean trematodes (Janeway et al. 2008).

For the general immune response against *D. pseudospathaceum* infections many genes were involved in macrophage activation, for example the interleukin-associated gene products THBS1, IRF4 and IL4RA. We can observe cytokine signaling (SOCS3, JUNB), where cytokines are small proteins that influence the behavior of other cells. In addition we find activation of the complement system (C4A). The complement system with its several effector proteins can be activated through three pathways all of which lead to the generation of factor C3 (Whyte 2007). The activation of C3 in turn, is involved in enhanced phagocytosis, recruitment of immune cells, stimulation of B-cell proliferation, activation of inflammatory responses and the membrane attack complex (Whyte 2007).

Among genes differentially expressed due to a specific clonal infection treatment we need to distinguish between head kidney and gill tissue. In head kidneys, we can observe up-regulation of genes involved in cytolytic processes (PRF1) as well as cytokine activation (HYAL2) due to the clone I treatment, but this can also be found in the clone XII treatment (RGCC, CYP27B1) (www.uniprot.org). Contrary to the clone I response we also find CCR9 to be up-regulated in the clone XII treated samples. CCR9 is a chemokine receptor interacting with its ligand TECK, which has been shown to attract dendritic cells and macrophages (Zaballos et al. 1999). Among down-regulated genes we can observe reduced interferon activity (KYNU in clone I, ZC3HAV1 in clone XII) suggesting a migration of macrophage-mediated immunity (Janeway et al. 2008). On the other hand, we observe down-regulation of complement genes in the clone I treatment (C3, C7) and a decreased amount of leukocyte

activity in the clone XII response (COL1A1) (www.uniprot.org). Since we expect immune-relevant cells to migrate from the head kidney to the gills as a response to the parasite treatment, these observations suggest an increased complement-based response due to the clone I treatment compared to an increased leukocyte activity due to the clone XII treatment. This is supported by the genes differentially expressed in the gill tissue, where we observe an increase in leukocyte related genes (ITGB1, SLC3A2) due to the clone XII treatment and a decrease in the clone I treatment (F11R, EPHA2) (www.uniprot.org). However, we do see complement activity due to clone XII (C6) as well as leukocyte activation as a response to clone I (GATA2, CASP3) (www.uniprot.org), which is mediated as decreased expression of negative leukocyte regulation.

Different isoforms of C3 have been detected in other fish species and it seems that antibody reactivities and binding affinities are affected by the type of isoform expressed (Whyte 2007). Interestingly, changes in expression of C3 isoforms due to *D. pseudospathaceum* infections seem to be limited to the treatments involving clone I and/or clone mix (supplementary table S.2.6 and S.2.7). The activation of C4A in gills of all infected fish indicates an activated classical pathway of the complement system, which should also involve C3 (www.uniprot.org). The up-regulation of C6 in gills of fish infected with clone XII however suggests an increased amount of activity for the membrane attack complex (www.uniprot.org). One possible interpretation would be that the complement system as central part in the response to *D. pseudospathaceum* infections is activated via different pathways depending on genotypic background of the parasite strain involved. It has already been proposed that the innate immune response shows a large amount of redundancy at the level of pathogen detection (Nish and Medzhitov 2011).

This redundancy of the innate immune system is also apparent in the clone specific up-regulation of the chemokine receptor CCR9 in gills as response to clone I and clone mix infections compared to an up-regulation in head kidneys as a response to clone XII (supplementary table S.2.6). The observed expression pattern may indicate a time shift in the host response to an infection against a specific parasite genotype mediated by a different combination of response pathways (Kumar et al. 2011). Since we cannot fully control the time point or location of an infection but have sequenced replicated fish RNA, the observed differences in expression of CCR9 can be attributed to specific parasite treatments. *D. pseudospathaceum* actively penetrates the skin and migrates to the eye lens of the fish host, it thus needs to produce enzymes capable of disrupting host tissue and protecting itself from the host immune system (Mikeš and Horák 2001). Unfortunately, we cannot distinguish between a delayed activation of specific genes due to an evasion strategy of the parasite

towards host immune responses or a delayed infection, e.g. through variable effectiveness of lytic enzymes.

Studies on host responses against pathogenic viruses have shown that the main mechanisms of both innate and adaptive immunity in bony fish are similar to those in mammals (Workenhe et al. 2010). Lenz and colleagues (2013) have shown that population-specific gene expression responses in *G. aculeatus* to parasite exposure, including *D. pseudospathaceum* exist, in line with local adaptation patterns of lake vs. river sticklebacks to their respective parasite assemblages (Lenz et al. 2013). The gene products involved in immune responses against macroparasites such as the genus *Diplostomum* seem to involve macrophages and the complement system but are still not well defined (Whyte et al. 1990, Janeway et al. 2008, Lenz et al. 2013). To the best of our knowledge, there are no data on the host gene expression levels as a function of within-species genetic affiliation and diversity in experimental infection by any macroparasite species.

The observed differences between both single clone treatments can be explained by the redundant possibilities for an innate immune response (Kumar et al. 2011, Nish and Medzhitov 2011). The interactions of host defense pathways can be described as cooperation, complementation and compensation (Nish and Medzhitov 2011). In cooperation, several individual pathways induce an optimal activation of the same effector mechanism, while complementation describes the activation of distinct effector mechanisms that have an additive effect in their combined response (Nish and Medzhitov 2011). Compensation becomes important when host defense pathways are inactivated, for example by parasite induced host immune-modulation or immune system evasion, and receptors can compensate for each other or different effector mechanisms exert functions that have a similar effect (Nish and Medzhitov 2011).

Thus, the genetic background of a specific parasite influences the combination of triggered host receptor mechanisms, resulting in alternative combinations of response pathways (Kumar et al. 2011). One could expect that genetically different *D. pseudospathaceum* lineages are recognized by a different set of receptor molecules, leading to the observed differences in gene expression. This might even involve a regulatory strategy concerning fitness costs, in terms of tissue damaging potential of the immune response, which dictates the order of activated response pathways (Nish and Medzhitov 2011).

Since we sequenced individual samples and used them as replicates in the statistical analysis, taking into account only genes that were differentially expressed compared to control, our findings can only be explained by the genetic background of parasite genotypes used in the infection treatments. This clearly indicates a specific transcriptomic response in the fish host due to a genetically defined parasite infection.

The genes determined to respond to an infection challenging the innate immune response will support new studies focusing on selected immune relevant genes, further increasing our knowledge about vertebrate immune systems.

Acknowledgements

We want to thank Gisela Schmiedeskamp, Gerhard Augustin and Daniel Martens for support with animal care and sample collection. The study was financially supported by the Deutsche Forschungsgemeinschaft (DFG, Priority Programme on Host-parasite Coevolution – SPP 1399), GEOMAR Helmholtz Centre for Ocean Research Kiel and the Max Planck Institute for Evolutionary Biology. Animal experiments were conducted under permission by the 'Ministry of Energy, Agriculture, the Environment and Rural Areas' of the state of Schleswig-Holstein, Germany (reference number: V 313-72241.123-34).

Chapter 3

Transcriptome analysis reveals complex interplay of adaptive and innate immunity in consecutively infected three-spined sticklebacks, *Gasterosteus aculeatus*

Jennifer K. Rieger[1,*], David Haase[1,*], Anika Witten[2], Monika Stoll[2], Erich Bornberg-Bauer[3], Martin Kalbe[4] and Thorsten B. H. Reusch[1]

[1]Evolutionary Ecology of Marine Fishes, GEOMAR Helmholtz-Centre for Ocean Research Kiel, 24105 Kiel, Germany
[2]Leibniz Institute of Arteriosclerosis Research, 48149 Münster, Germany
[3]Institute for Evolution and Biodiversity, University of Münster, 48149 Münster, Germany
[4]Max-Planck Institute for Evolutionary Biology, 24306 Plön, Germany

*equal contribution

Summary

While innate immune responses in vertebrates are the first line of defense against invading pathogens, the specific adaptive immune response can confer immunological memory and thus increased resistance to certain pathogens. The importance of components of the adaptive immune system in parasite resistance and mate choice have been shown in numerous studies. Additionally it has been shown that gene expression patterns may be specific to particular parasite genotypes, even if these can only be attacked by the innate immune system. However, how the vertebrate immune system reacts to repeated exposure of specific parasite genotypes is poorly understood. In this study, we used transcription profiling via next generation sequencing to investigate the effects of consecutive infections with distinct clonal lineages of the eye fluke *Diplostomum pseudospathaceum* on gene expression patterns in three-spined sticklebacks (*Gasterosteus aculeatus*). Specifically, we were interested in identifying a general adaptive immune response to *D. pseudospathaceum* on the one hand and specific adaptive responses to certain parasite lineages on the other. By subjecting fish to homologous exposures, as well as heterologous final and heterologous pre-exposures, we were able to investigate the relative contributions of immunization and final exposure on gene expression patterns. Finally, we examined differences between innate and adaptive immune mechanisms. We found a significant reduction of infection rates upon repeated exposure to *D. pseudospathaceum*. In general, the expression patterns of consecutively infected fish showed only very few differentially expressed immune genes regardless of whether they were exposed to homologous or heterologous parasite lineages.

Instead, the genetic identity of the first encounter with the parasite appeared to have a larger effect on immune gene expression. Very few genes were jointly up- or down-regulated in both single and multiple exposures. Additionally, the complement system appeared to play an important role for both naive and pre-exposed fish, which is an indication for the close connection of innate and adaptive immune responses.

Introduction

The vertebrate immune system is capable of precise and specific detection of parasites, with the ultimate goal to clear or at least prevent the proliferation of infections. While specificity to certain pathogen epitopes has classically been attributed to adaptive immunity, recent years have seen growing evidence of parasite genotype-specific innate responses on the host side. Both parts of the immune system are intertwined and many researchers are inclined to move away from the artificial dichotomy between the innate and adaptive system and towards an integrative understanding of immunity (Tort et al. 2003, Gardy et al. 2009, Criscitiello and de Figueiredo 2013). While the innate immune response has long been known to activate cell proliferation for an adaptive response (Janeway et al. 2008), adaptive regulation of the innate system is also being increasingly recognised (Shanker 2010).

Classical V(D)J-based adaptive immunity first evolved in poikilothermic jawed fish (Gnathostomata), and has long been regarded similar to that found in mammals (Sunyer 2013). Polymorphism at the major histocompatibility complex (MHC) loci plays a central role in the specific recognition of pathogens. One theory, the optimal diversity hypothesis (Nowak et al. 1992, Wegner et al. 2003a) posits that MHC diversity is under selection by two opposing forces. Selection for receptor diversity via gene duplication and allelic repertoire expansion allows the immune system to recognize more divergent foreign antigen molecules. On the other hand, models have predicted that too many different MHC alleles increase the risk of binding self peptides and autoimmune symptoms (Nowak et al. 1992, Woelfing et al. 2009), and there is empirical evidence from various taxa to supporting this assumptions (Wegner et al. 2003a, Wegner et al. 2003b, Westerdahl et al. 2005, de Bellocq et al. 2008, Kalbe et al. 2009, Lenz et al. 2009b). In three-spined sticklebacks (*Gasterosteus aculeatus*), this directly involves female mate choice for an optimal set of alleles (Reusch et al. 2001b), leading to enhanced fitness (Eizaguirre et al. 2009). Over longer time scales (~100s of generations) this possibly led to habitat specific immune responses (Lenz et al. 2013) and thus local adaptation of stickleback populations (Kalbe et al. 2002) with habitat-specific immunocompetence (Kalbe and Kurtz 2006).

Similar polymorphisms also play a role in innate immunity. For example, different studies have found that variation in toll-like receptor loci translates to variation in pathogen resistance (Schroder and Schumann 2005, Villasenor-Cardoso and Ortega 2011). Thus, genetic vanability in both innate and adaptive immune systems interact to determine the interactions of host and parasite populations. Studies have shown that there is reciprocal interaction between innate and adaptive immune components (Kurtz et al. 2006, Wegner et al. 2007, Shanker 2010) and that there are genotype x genotype interactions influencing parasite infection and innate immune responses in fish (Rauch et al. 2006, chapter 2). The extent to which the genetic diversity within single parasite species influences immune memory and the subsequent activation of adaptive and innate immune responses is still poorly understood.

Here, we use an RNA sequencing approach to investigate underlying gene expression patterns of an adaptive immune response in three-spined sticklebacks, a model fish species with increasing genomic and transcriptomic resources (Gibson 2005, Jones et al. 2012, chapter 2). The adaptive immune response was triggered by consecutive mono-clonal and multi-clonal infections with the eye fluke *Diplostomum pseudospathaceum* that involved homologous and heterologous challenges with respect to parasite genotype, as well as genetically less diverse (single genotype) and more diverse (multi-clonal = multiple genotype) challenges. This study is part of a larger experiment, where we examined RNA expression patterns of innate immune responses due to genotypically diverse parasite infections (chapter 2). In this paper, we will refer to our findings from the preceding publication and draw upon the data for direct comparison between innate and adaptive immune responses to *D. pseudospathaceum* clones. Our model parasite has a complex life cycle involving freshwater snails and fish as intermediate hosts, before undergoing sexual reproduction in the intestine of piscivorous birds (Chappell et al. 1994). The snail host harbours a clonal reproduction stage, making trematodes ideal candidates to investigate genotype-specific performance of parasites (Koehler and Poulin 2012). In the fish host, the parasite migrates to the eye lens where it causes cataracts and blindness, thus hampering feeding efficiency and predator avoidance (Crowden and Broom 1980, Owen et al. 1993). Since the parasite quickly invades the fish's eye lens, where it is protected from the immune system, it is of paramount importance for the host to be able to mount a fast and effective response.

The direct sequencing of whole transcriptomes (RNA-seq) is a powerful tool to assess expression patterns with the advantage of being independent of candidate genes (Wang et al. 2009). This includes the detection of low-expressed genes and the expression of alternative splice isoforms (Marioni et al. 2008, Trapnell et al. 2010). We examined the mRNA expression patterns in head kidneys, one of the major immune organs in fishes (Press

and Evensen 1999, Rauta et al. 2012) and gills, one of the preferred spots for cercarial penetration (Whyte et al. 1990).

Next-generation sequencing approaches have already revealed that adaptation of sticklebacks to different environments can lead to habitat-specific immune responses (Lenz et al. 2013). Since we used fish whose parents originated from a population naturally exposed to *D. pseudospathaceum*, we therefore expect similar adaptations in our experimental animals. To further investigate the genetic mechanisms underlying specific adaptive responses to distinct parasite lineages, we repeatedly subjected naïve, laboratory-bred fish to monoclonal or multiclonal mixes of *D. pseudospathaceum* cercariae. We were interested in investigating the expression patterns induced by repeated infection with distinct parasite lineages as well as finding out whether the genetic identity of the priming infections affects the outcome of the final infection. By switching the final infection treatment to a different lineage in part of the experimental fish, we were able to compare transcription patterns induced by homologous and heterologous infections.

In our previous experiment on naive fish (chapter 2), we identified general patterns of gene expression to infection with *D. pseudospathaceum* as well as specific responses to individual parasite clones. In line with these results, we hypothesize to find expression patterns in adaptive immunity that are shared between all consecutive treatments, as well as specific adaptive responses to different *D. pseudospathaceum* genotypes. In addition, we expect to identify genes differentially expressed as a result of a certain pre-exposure, as well as genes being influenced by the final treatment. Finally, by examining differences and similarities of gene expression patterns induced by consecutive infection treatments and those found in single infections, we will investigate the interplay between a mounting adaptive immune memory and innate immune processes.

We will tackle these hypotheses by comparison of different sets of single and consecutive infection treatments. The hypothesized effects on differential gene expression (up- or down-regulation) can be summarized as follows:

H1. General adaptive immune response to *D. pseudospathaceum*, i.e. expression patterns that are shared between all consecutive treatments;

H2. Parasite lineage-specific adaptive response to *D. pseudospathaceum*, i.e. expression patterns that are unique to specific homologous consecutive infections, and may be reflected in the phenotype as differing infection rates;

H3A. Effects of alternative final exposures, i.e. between groups pre-exposed to the same clones and

H3B. Effects of alternative pre-exposures, i.e. between groups with the same final exposure;
H4. Differences between innate and adaptive immune responses, i.e. comparison of singly exposed naïve fish with consecutively exposed fish.

Overall, this study aimed to reveal how specific different parasite genotypes, here of a digenean trematode, influence immune memory in fish and how this is reflected in the interaction of innate and adaptive immune responses.

Material & Methods

Initiation of clonal parasite lineages & experimental infection

Snails of the species *Lymnaea stagnalis* were exposed to single *Diplostomum pseudospathaceum* miracidia under controlled conditions. The polymorphisms of 4 microsatellite loci (Diplo08, Diplo09, Diplo23 and Diplo29) were used to verify genotypes of cercariae emerging from snails (Reusch et al. 2004). Lab bred marine sticklebacks (*Gasterosteus aculeatus*) were used as parasite reservoir, sacrificed and fed to uninfected European Herring Gulls (*Larus argentatus*). As part of a larger experiment, gull faeces of all infected gulls were collected over several weeks and lab bred *L. stagnalis* were infected with single hatched parasite larvae, called miracidia (Rieger et al. 2013). Thus we increased the amount of snails containing a specific clonal parasite lineage (see chapter 2 for a full description). Of those established lines the same subset was used as in chapter 2.

The same 4 fish families (sibships) of lab-bred three-spined stickleback as described in chapter 2 were used for the infection treatment. Fish were selected for infection trials 6 months after hatching. We randomly selected 36 fish per sibship and placed them in three 16l aquaria in groups of 12 fish. Over the course of 5 weeks we exposed the fish to either clone I, clone XII or a mix of clonal lineages, containing inbred and outcrossed parasite genotypes (Rieger et al. 2013). To do so, we pooled cercariae, the fish infecting parasite stage, collected from all available snails infected with the same parasite clone and estimated cercariae density per ml. We then added a volume of cercariae suspension to the fish tanks equivalent to the desired amount of 240 cercariae per tank, i.e. 20 per fish. This procedure will be termed pre-exposure throughout this study. Two weeks after the fifth pre-exposure, 6 fish per family pre-exposed to the clone mix and 12 fish per family pre-exposed to single clones (6*4+12*4*2 = 120) were placed into 1l aquaria. 3 fish per sibship per pre-exposure were either exposed to controlled doses of 100 cercariae of clone I, clone XII, clone mix or not infected for use as control (table 3.1); this procedure will be termed final exposure. To

ensure that parasite genotype was unambiguous, the respective parasite genotypes in all surviving infected snails were determined by microsatellite PCR prior to the infection experiment.

Penetrating *D. pseudospathaceum* larvae (termed metacercariae) can take up to 24h to reach the fish's eye lens (Chappell et al. 1994). In order to be able to reliably assess infection rates in fish used for RNA extraction, the controlled-dose infection was repeated after 2 days. Fish were sacrificed 4h after the final treatment (infection or control) by immediate decapitation, separation of gills and lateral incisions for faster penetration with preserving buffer (RNAlater, Qiagen). The fish heads were kept in 0.64% physiological NaCl solution for later assessment of infection rates. Fish were immediately stored in RNA later and frozen after 24h.

Table 3.1 Overview of pre-exposure - final exposure combinations. Including homologous (HO) and heterologous (HE) infections.

final exposure / **pre-exposure**	**I**	**XII**	**Mix**	**Control**
I	HO	-	HE	X
XII	-	HO	HE	X
Mix	-	-	HO	X
Control	X	X	X	X

RNA extraction, Library preparation & Sequencing of cDNA libraries

Gills and head kidneys were excised from 48 fish stored in preserving buffer and placed in lysis buffer and β-mercaptoethanol. RNA extraction was performed using the Macherey-Nagel NucleoSpin 96 RNA kit following the standard protocol. Quantity and quality measurements of RNA as well as library preparation and final sequencing were conducted as described in chapter 2 together with the samples analyzed in that study. We sequenced a 96 sample setup on one flow cell with 12 samples per lane distributed over 8 lanes respectively for 2*101 base pairs (paired-end).

DNA extraction & microsatellite PCR

We collected single cercariae from infected snails and placed them in 2ml Eppendorf tubes. Extraction of DNA was performed with 10μl 5% Chelex suspension and 1μl proteinase K (14mg/ml dissolved in Tris-HCl, pH 7.5), shaken at 55°C for 15 minutes and 100°C for 30 minutes. 3 μl of extracted samples were used for PCR. Conditions were initial denaturation for 3 minutes at 94°C followed by 30 cycles of denaturation 94°C, annealing 56°C, elongation 72°C, 30 seconds each and final 72°C elongation for 5 minutes (chapter 2).

Parasite infection statistics

All statistical analyses of parasite infection data were carried out using R (version 2.14.1; R Core Development Team, 2012). A full negative binomial generalized linear model was fitted to the infection rate data, including *pre-exposure*, *treatment*, *fish sibship* and interactions thereof as explanatory variables (Venables et al. 2002). We reduced the model by removing insignificant terms and compared it to the null model using the *anova* function. Individual levels of the treatments were compared with Tukey contrasts using the glht function (package multcomp). Since we were only interested in comparing the levels of the treatments and pre-exposures rather than the interactions, and since the treatments and pre-exposures were not fully factorial, contrasts were calculated from a reduced model excluding interaction terms.

The software package cummeRbund, version 0.1.3 (Goff and Trapnell 2011), edgeR (Robinson et al. 2010b) and custom made Python scripts, version 3.1.2, were used for data modification and visualization.

Read alignment and quantification of gene expression

Estimation of differential expression was performed as described in chapter 2. Version 67 of the *G. aculeatus* reference genome (www.ensembl.org) was used to align sequence reads using tophat (Trapnell et al. 2009) with standard parameters. Values for aligned reads were normalized as fragments per kilobase of exon model per million mapped reads (FPKM) modified for paired-end data after RPKM (Mortazavi et al. 2008). Differential expression was calculated with Cufflinks (version 1.3.0), including with parasite infections as treatments and fish families as replicates within a treatment (Trapnell et al. 2010). Calculations were made together with samples from chapter 2 to allow for direct compatibility of significantly expressed genes. Estimated fold changes were corrected for multiple testing (false discovery rate, FDR < 0.05, Benjamini and Hochberg 1995).

GO annotation & GO term enrichment

For estimation of GO term enrichment we used a self-made GO-annotation of the stickleback reference transcriptome (version 67, www.ensembl.org) as described in chapter 2. Blast2GO (Conesa et al. 2005) was used to calculate GO term enrichment. A Fisher's exact test was conducted, testing for the increased presence or absence of functional categories in a given subset of genes, compared to a different set.

In order to investigate the categories listed in the introduction, a total of 143 separate pairwise comparisons between treatment groups were carried out. These included both comparisons between pooled up- and down-regulated genes and between up-regulated and down-regulated genes considered separately. GO terms that were significantly over- or underrepresented in different treatment groups were determined by direct pairwise comparison of each combination of these groups according to the pre-formulated hypotheses, with always one arbitrary group serving as the respective reference. Groups consisted of genes that were either unique to a specific treatment groups or all genes differentially expressed within a given treatment group. For a general representation of GO terms, groups were also tested using the entire transcriptome as a reference. Only GO terms that are classed as 'biological process' include information on immune processes and were thus considered further. FDR correction was applied after testing (FDR < 0.05).

Putative immune genes

We estimated differential expression of putative immune-relevant genes by extracting human genes tagged with the GO-term "immune system process" (GO:0002376) from the ensembl database (www.ensembl.org) and compared them to the stickleback transcriptome (chapter 2). Only genes that could be unambiguously identified in *G. aculeatus* were kept for further analyses and completed with a set of selected immune genes identified in cod and pipefish (Star et al. 2011, Haase et al. 2013). This led to 1067 putatively immune relevant genes (supplementary table S.2.4). Since in our previous experiment on innate immunity (chapter 2) we found the complement system to play a key role in sticklebacks' immune defense against *D. pseudospathaceum*, the corresponding expression patterns have been regarded in more detail.

Results

Parasite infection rates

A total of 118 fish were infected, of which only a subset (one per sibship*pre-exposure*final exposure combination, equalling 48 fish) was subjected to mRNA-sequencing. Since not enough fish from sibship 10x15 that were pre-exposed to clone XII were available, 2 replicates had to be omitted. Thus, treatment groups XII- M and XII-control had to be reduced by 1 fish each (final no = two per sibship*pre-exposure*final exposure combination).

Infection rates ranged from 0-17 metacercariae per fish. The highest infection rates were caused by the clone mix (mean 3.3±3.8 metacercariae per fish). Treatment with clone I and XII resulted in mean infection rates of 1.25±1.42 and 1.8±1.4 metacercariae per fish, respectively. Pre-exposure to either clone considerably lowered infection rates in all treatment groups when compared to controls. On average, naive fish exhibited infection rates of 4.1±3.9 metacercariae per fish, whereas fish pre-exposed to clone I, XII or a mix of clones had 1.0±1.3, 1.0±1.3 and 0.8±1.6 metacercariae per fish, respectively (figure 3.1 & 3.2).

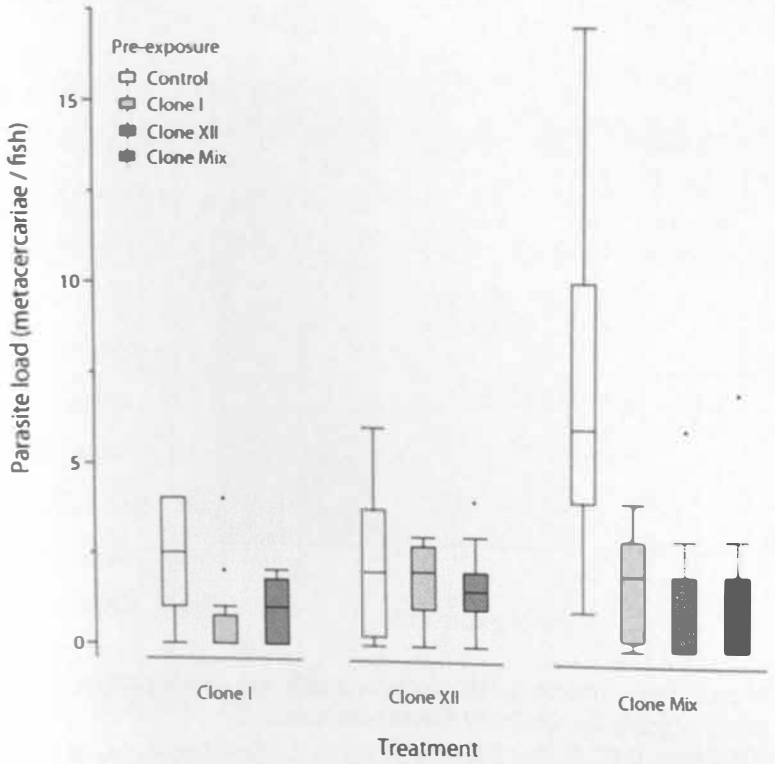

Figure 3.1 Boxplot showing infection rates within different final exposure and pre-exposure groups. The upper and lower boundaries of the boxes represent the upper and lower quartile, while bars above and below the boxes indicate the 10th and 90th percentiles. The line within the box marks the median.

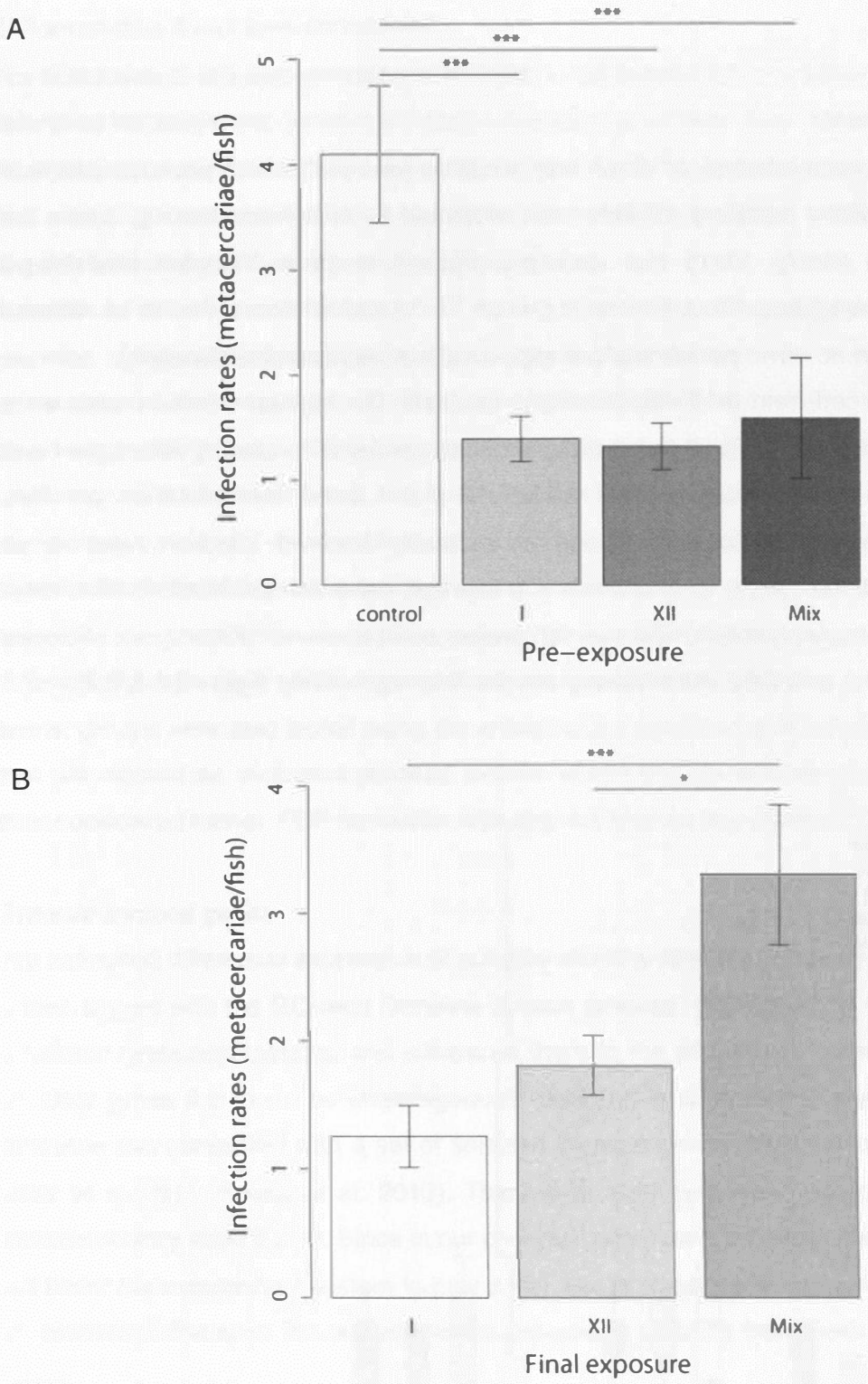

Figure 3.2 Barplot showing infection rates (mean ± SD) within A) different pre-exposure and B) different final exposure groups. Stars indicate the results of Tukey contrasts.
Significance codes: <0.001 '***', 0.001 '**', 0.01 '*'

The best fitting model included *final exposure*, *pre-exposure*, *fish sibship* as well as interactions between *final exposure* and *pre-exposure* and between *final exposure* and *sibship* (table 3.2A). Removing any of these terms from the model resulted in a worse model fit, as indicated by a higher AIC value (Akaike information criterion; see table 3.2B).

Table 3.2 Comparison of generalized linear models fit to infection rates of *Diplostomum pseudospathaceum* in the three-spined stickleback, *Gasterosteus aculeatus*. final=final exposure; pre=pre-exposure; sib=fish sibship; The Akaike information criterion (Akaike 1981) is defined as: _2 maximized log-likelihood + 2 number of parameters. Significance codes: <0.001 '***' 0.001 '**' 0.01 '*' 0.05 '.' 0.1 ' ' 1

	Model fit	Comparison to null model	
Effect (Model formula)	**Residual Deviance**	**AIC**	**P-value**
(A) pre + final + sib + pre:final + final:sib + pre:sib	127.40	455.62	$5.990e^{-09}$ ***
(B) pre + final + sib + pre:final + final:sib	132	446.24	$2.604e^{-10}$ ***
(C) pre + final + sib + pre:final	137.24	451.05	$1.683e^{-09}$ ***
(D) pre + final + sib + final:sib	134.97	451.07	$1.842e^{-09}$ ***

An analysis of deviance revealed a strong effect of both pre-exposure and final exposure (P<0.001, table 3.3), as well as an interaction effect of both final exposure and pre-exposure and final exposure and sibship (P=0.011 and 0.007, respectively). The latter may point to genotype x genotype interactions between host and parasite that have been observed earlier (Rauch et al. 2006). While the interaction term between pre-exposure and final exposure may suggest clone-specific priming effect, the post-hoc test suggests a rather stronger effect of pre-exposure, with all priming treatments being significantly different from controls but no differences between the different pre-exposures (table 3.4, table 3.5). The difference between final exposures is driven by infection rates caused by the clone mix, which is significantly higher than both those of clone I and clone XII. We fitted an additional generalized linear model to the data dividing experimental fish into homologous, heterologous and naive groups only. Infection rates significantly differed between these groups (analysis of deviance, p=9.208e-09). However, while all pre-exposed fish had significantly lower infection rates than naive fish, there was no significant difference between homologous and heterologous groups (Tukey contrasts, naive-homologous: z=-5.072, p<1e-05; naive-heterologous: z=-4.844, p<1e-05; homologous-heterologous: z=0.711, p=0.756).

Table 3.3 Results of deviance analysis, indicating the respective contributions of final exposure, pre-exposure, fish sibship and second-degree interactions to infection intensities of *Diplostomum pseudospathaceum* in three-spined stickleback, *Gasterosteus aculeatus*. Significance codes: <0.001 '***' 0.001 '**' 0.01 '*' 0.05 '.' 0.1 ' ' 1

Effect	Df	Deviance	Resid. Df	Resid. Dev	P-value	
pre-exposure	3	61.527	118	200.94	**2.773e-13**	***
final exposure	2	33.536	116	167.41	**5.220e-08**	***
sibship	3	4.697	113	162.71	0.195	
pre x final	4	13.059	109	149.65	**0.011**	*
final x sibship	6	17.600	103	132.05	**0.007**	**

Table 3.4 Tukey contrasts comparing the infection rates of single clones of *Diplostomum pseudospathaceum* (I, XII), as well as a mix of clones (M) in three-spined sticklebacks, *Gasterosteus aculeatus*, averaged over pre-exposure and sibship. Tukey contrasts were calculated from a reduced generalized linear model including final exposure, pre-exposure and fish sibship without interaction terms. Signif. codes: <0.001 '***' 0.001 '**' 0.01 '*' 0.05 '.' (Adjusted p values reported -- single-step method)

Comparison	Estimate	Std. Error	z value	P-value	
XII vs. I	0.4530	0.2334	1.941	0.1263	
M vs. I	1.0118	0.2162	4.681	**<1e-04**	***
M vs. XII	0.5588	0.1958	2.853	**0.0119**	*

Table 3.5 Tukey contrasts comparing infection success *of Diplostomum pseudospathaceum* in three-spined sticklebacks, *Gasterosteus aculeatus*, that were pre-exposed to different clones of *D. pseudospathaceum* (I, XII) a mix of clones (M), or sham-exposed as a control. Infection rates were averaged over final exposure and sibship. Tukey contrasts were calculated from a reduced model including final exposure, pre-exposure and fish sibship without interaction terms. Signif. codes: <0.001 '***' 0.001 '**' 0.01 '*' 0.05 '.' (Adjusted p values reported -- single-step method)

Comparison	Estimate	Std. Error	z value	P-value	
I vs. control	-1.0032	0.2055	-4.882	< 1e-04	***
XII vs. control	-1.0246	0.2090	-4.902	< 1e-04	***
Mix vs. control	-1.3374	0.3130	-4.273	0.000103	***
XII vs. I	-0.0214	0.2407	-0.089	0.999737	
Mix vs. I	-0.3342	0.3354	-0.996	0.743881	
Mix vs. XII	-0.3128	0.3385	-0.924	0.785206	

Read mapping & differential gene expression

Illumina sequencing produced a total of 990 million valid paired-end reads of 101 nucleotides length. 7 samples from gills were of low quality and had to be removed from further analyses. This led to samples with 4 replicates for the treatments I-I, I-C and XII-C in gills but only 3 replicates per treatment for I-M, XII-XII, M-M and 2 replicates for M-C and XII-M in gills. All samples of head kidney tissue were valid, resulting in a total of 57 individual libraries. Of those TOPHAT aligned 530 million reads with an average distribution of ~9 million reads per sample (supplementary table S.3.1).

We checked for differential expression of genes in all homologous consecutive treatments (H1, H2) and all heterologous consecutive treatments (H3a, H3b). Significant differences were filtered with reference to the respective control treatments, i.e. I-I and I-M compared to I-C, XII-XII and XII-M to XII-C and M-M to M-C. This will account for gene expression differences induced by the final exposure including the effect of the consecutive pre-exposure. We incorporated this filtering step to remove gene expression differences induced by the pre-exposure, which will allow us to identify only genes that were differentially expressed during the last step of the parasite treatments. We found 1946 differentially expressed gene comparisons, consisting of 1187 genes. 690 unique transcripts were differentially expressed in gill and 585 in head kidney tissue (supplementary table S.3.2 and S.3.3).

Identified genes were visualized in a multidimensional scaling plot (MDS, Robinson et al. 2010b). The plots display similarity of the treatments by means of proximity, i.e. increasing divergence between gene expression patterns with increasing distance. In gill tissue, we observed little differentiation between treatments on both axes without clear groupings; in particular the homologous treatments were not clearly separated from one another. In head kidney samples we observed a clear distinction between the homologous consecutive treatments and a tight clustering of heterologous samples. The heterologous treatments, on the other hand, were quite distinct from each other and from their respective homologous counterparts. Interestingly, in the first dimension we saw a clear grouping after final infection (I, XII or M) whereas the second dimension displays the pre-exposure with no clear distinction between monoclonal infections (I and XII) and a clear difference to the multi-clonal pre-exposure (figure 3.3).

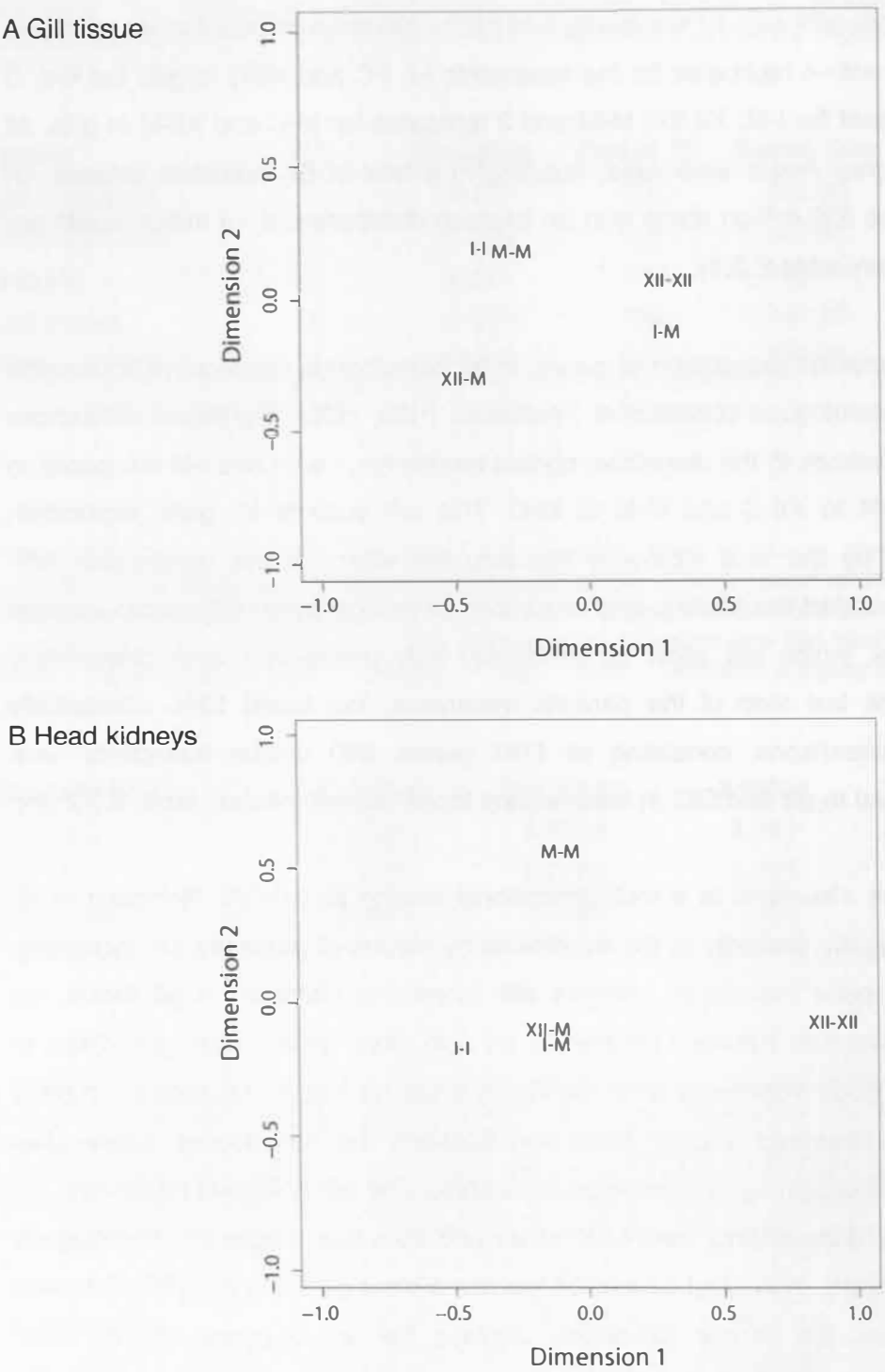

Figure 3.3 Multidimensional scaling (MDS) plot based on all genes differentially expressed in A) stickleback gill tissue or B) head kidneys in response to combinations of pre-exposure and treatment with different clones of *Diplostomum pseudospathaceum*. Consecutive treatments are labelled in the format *pre-exposure – final exposure*. Plots were made using the function plotMDS.DGEList of the R package edgeR. Distances are calculated as coefficients of variation of expression between samples for all genes given as input.

Gene ontology (GO) term enrichment

GO term enrichment revealed that most genes discriminating different treatment groups belonged to functional categories involving cellular movement, organization and signaling (see supplementary table S.3.4). Out of the 143 comparisons that were carried out, only 11 yielded significant differences in functional class 'biological process' and were thus considered further. The majority of significant differences were found in head kidneys. Most terms appeared in all of the 5 comparison categories (H1: general adaptive response, H2: specific adaptive response, H3a: effects of alternative final and H3b: alternative pre-exposures, H4: comparison of innate and adaptive immune mechanisms). It may be noted that, in groups treated with clone I, most GO terms were overrepresented when compared to groups treated with different clones. In addition, GO terms were always underrepresented in single-exposure groups when compared to multiple-exposure groups.

Specific gene expression

We compared all differentially expressed genes to the a priori list of putative immune genes. Out of 1067 putative immune-relevant genes, we were able identify 87 to be differentially expressed between the pre-exposure – final exposure combinations in our experiment. 49 putative immune genes were found in gill samples whereas 45 were distributed over head kidney samples. Among those we could identify up- and down-regulated genes with respect to a given treatment (supplementary table S.3.5 and S.3.6). An overview of the numbers of unique and shared genes in the different comparison categories can be found in figures 3.4.1 and 3.4.2. In the following section, we describe the treatment-specific gene expression for both organs and each hypothesis.

Gills

H1: General adaptive response

Among the shared genes, one (LGALS8 (2 of 2)) was different between I-I (up-regulated) and XII-XII (down-regulated) whereas one gene displayed common up-regulation in the XII-XII and M-M treatment (THBS1 (2 of 2)). No genes were jointly expressed between all three treatments.

H2: Specific adaptive response

The comparison of homologous consecutively exposed sticklebacks (I-I, XII-XII, M-M) showed 11 genes uniquely up-regulated in the I-I treatment (CASP3 (4 of 4), ELMOD2, GRAP2, PGLYRP2 (1 of 2), SLC3A2 (2 of 2), SOCS3 (1 of 2), ENSGACG00000001729, VIPR1 (2 of 2), CRISP3, RAG1, RAG2), one in the XII-XII (PVRL1 (2 of 2)) and two in the M-

M treatment (C3 (4 of 8), C7 (1 of 2)). Uniquely down-regulated were only 11 genes in the XII-XII treatment (GEM, ENSGACG00000012797, ENSGACG00000012799, ENSGACG00000012781, IRF4 (2 of 2), ATG12, TAL1, ENSGACG00000019078, ENSGACG00000012783, SOCS1 (2 of 2), ENSGACG00000000336).

H3a: Differences between alternating final exposures

The gene expression response of sticklebacks to an alternating final exposure was estimated by a comparison of I-I vs I-M and XII-XII vs XII-M. In I-I we found 10 genes uniquely up-regulated (LGALS8 (2 of 2), ELMOD2, GRAP2, PGLYRP2 (1 of 2), SLC3A2 (2 of 2), ENSGACG00000001729, VIPR1 (2 of 2), CRISP3, RAG1, RAG2) while in I-M 20 genes were uniquely up-regulated (ITGB1 (1 of 2), WAS, KLC1, KIFAP3 (2 of 2), CASP8, HYAL2 (1 of 2), ADSS, PIK3R1 (1 of 2), ENSGACG00000016298, DAB2, C4A, NCF1, ENSGACG00000012769, C6, NFKBIA (1 of 2), CCR9 (1 of 2), RSAD2, USP18, C7 (1 of 2), ENSGACG00000012792). No genes were uniquely down-regulated in either of both treatments, while two genes (CASP3 (4 of 4), SOCS3 (1 of 2)) were jointly up-regulated in I-I and I-M. In XII-XII two genes were uniquely up-regulated (THBS1 (2 of 2), PVRL1 (2 of 2)). Among down-regulated genes, 10 were unique in XII-XII (GEM, ENSGACG00000012781, IRF4 (2 of 2), ATG12, TAL1, ENSGACG00000019078, ENSGACG00000012783, SOCS1 (2 of 2), LGALS8 (2 of 2), ENSGACG00000000336) and four in XII-M (CXCL12 (2 of 2), C4A, IREB2, AP2S1). Both treatments showed joint down-regulation of two genes (ENSGACG00000012797, ENSGACG00000012799).

H3b: Differences between alternating pre- exposures

When comparing alternative pre-exposure (I-M, XII-M, M-M) we found 20 genes uniquely up-regulated in I-M (ITGB1 (1 of 2), WAS, KLC1, KIFAP3 (2 of 2), CASP8, HYAL2 (1 of 2), ADSS, PIK3R1 (1 of 2), ENSGACG00000016298, DAB2, NCF1, ENSGACG00000012769, CASP3 (4 of 4), C6, NFKBIA (1 of 2), CCR9 (1 of 2), RSAD2, USP18, SOCS3 (1 of 2), ENSGACG00000012792) and two in M-M (C3 (4 of 8), THBS1 (2 of 2)). Five genes were uniquely down-regulated in XII-M (ENSGACG00000012797, ENSGACG00000012799, CXCL12 (2 of 2), IREB2, AP2S1). Among shared genes, one (C4A) showed up-regulation in I-M while it was down-regulated in XII-M. One gene displayed common up-regulation between I-M and M-M (C7 (1 of 2)).

H4: Differences between innate and adaptive immune responses

The comparison of consecutive (I-I, XII-XII, M-M) vs single exposure (I, XII, M) showed 10 genes uniquely up-regulated in I-I (LGALS8 (2 of 2), ELMOD2, GRAP2, PGLYRP2 (1 of 2),

SLC3A2 (2 of 2), ENSGACG00000001729, VIPR1 (2 of 2), CRISP3, RAG1, RAG2) and six in I (COL1A1 (2 of 2), C4A, PIK3R1 (1 of 2), NFKBIA (1 of 2), CCR9 (1 of 2), THBS1 (2 of 2)). Uniquely down-regulated were only three genes in I (GATA2 (1 of 2), F11R, EPHA2 (1 of 2)). Shared expression of genes showed one jointly up-regulated in I and I-I (SOCS3 (1 of 2)) as well as one gene (CASP3 (4 of 4)) with up-regulation in I-I and down-regulation in I.
Between XII-XII and XII, one gene was uniquely up-regulated in XII-XII (PVRL1 (2 of 2)) and 10 genes in XII (ITGB1 (1 of 2), C4A, DAB2, C6, SLC3A2 (2 of 2), JUNB (2 of 2), SOCS3 (2 of 2), ITGA5 (1 of 2), ADAM8 (1 of 2), SOCS3 (1 of 2)). Among down-regulated genes only XII-XII showed 12 to be differentially expressed (GEM, ENSGACG00000012797, ENSGACG00000012799, ENSGACG00000012781, IRF4 (2 of 2), ATG12, TAL1, ENSGACG00000019078, ENSGACG00000012783, SOCS1 (2 of 2), LGALS8 (2 of 2), ENSGACG00000000336). One gene was jointly up-regulated of XII-XII and XII (THBS1 (2 of 2)). Among mixed clone exposure, two genes were uniquely up-regulated in M-M (C3 (4 of 8), C7 (1 of 2)) and 81 genes in M (see supplementary table S.2.7 for M and S.3.6 for M-M). Among down-regulated genes, six were present in M (PFDN1, EXOSC5, ATG12, ELMOD2, ENSGACG00000000336, PRDX3). One gene was jointly up-regulated in M-M and M (THBS1 (2 of 2)).

Head kidney

H1: General adaptive response

Among shared genes, one was commonly down-regulated in XII-XII and M-M (MYLPF (2 of 2)) whereas one was down-regulated in XII-XII and up-regulated in I-I (MASP1 (2 of 2)). Furthermore 19 genes were down-regulated in XII-XII and up-regulated in M-M, 10 of them complement related genes (APOB (1 of 5), APOB (5 of 5), C3 (1 of 8), C3 (2 of 8), C3 (3 of 8), C3 (4 of 8), C3 (5 of 8), C8A, C8G, C9, CFB, CFP, ENPP2 (2 of 2), ENSGACG00000003030, ENSGACG00000014811, ENSGACG00000014852, PGLYRP2 (2 of 2), SERPING1, SUSD2).

H2: Specific adaptive response

When looking at homologous consecutively exposed sticklebacks (I-I, XII-XII, M-M) we found four genes uniquely up-regulated in I-I (ELMOD2, VTN (2 of 2), APOB (2 of 5), PRG4), five in XII-XII (STXBP2, AP2S1, KIF23 (2 of 2), RPA1 (1 of 2), CDK1) and four genes in M-M (ADAMTS13, C8B, CHIA, PVRL1 (2 of 2)). Among uniquely down-regulated genes, we found four in XII-XII (PLG, KYNU, IRF6, C4A) and one in M-M (ADSSL1).

H3a: Differences between alternating final exposures

The alternating final exposure (I-I vs I-M and XII-XII vs XII-M) showed no immune-related genes in I-M, thus only in I-I were 5 genes uniquely up-regulated (ELMOD2, PRG4, VTN (2 of 2), APOB (2 of 5), MASP1 (2 of 2)). Between XII-XII and XII-M, five genes were uniquely up-regulated in XII-XII (STXBP2, AP2S1, KIF23 (2 of 2), RPA1 (1 of 2), CDK1) and one gene in XII-M (ITGA6 (1 of 2)). Among down-regulated genes, 15 were found in XII-XII (PLG, ENSGACG00000014811, C3 (4 of 8), APOB (5 of 5), C3 (3 of 8), C9, APOB (1 of 5), C3 (1 of 8), C3 (5 of 8), C3 (2 of 8), MASP1 (2 of 2), KYNU, SERPING1, ENPP2 (2 of 2), C4A) and seven in XII-M (MYLPF (1 of 2), ADSSL1, PGLYRP2 (1 of 2), ATP1B3, C7 (1 of 2), APOB (2 of 5), GAS6). Jointly down-regulated in XII-XII and XII-M were 10 genes (C8A, C8G, CFB, CFP, ENSGACG00000003030, ENSGACG00000014852, IRF6, MYLPF (2 of 2), PGLYRP2 (2 of 2), SUSD2).

H3b: Differences between alternating pre- exposures

The comparison of genes differentially expressed due to an alternating preexposure (I-M, XII-M, M-M) showed 15 genes uniquely up-regulated in M-M (ADAMTS13, ENPP2 (2 of 2), SERPING1, C9, C3 (5 of 8), APOB (1 of 5), C3 (1 of 8), C3 (3 of 8), C3 (4 of 8), C8B, C3 (2 of 8), CHIA, APOB (5 of 5), PVRL1 (2 of 2), ENSGACG00000014811) and one in XII-M (ITGA6 (1 of 2)). Among down-regulated genes only XII-M showed seven to be differentially expressed (MYLPF (1 of 2), IRF6, PGLYRP2 (1 of 2), ATP1B3, C7 (1 of 2), APOB (2 of 5), GAS6). Shared genes were two jointly down-regulated in XII-M and M-M (ADSSL1, MYLPF (2 of 2)) and eight down-regulated in XII-M while up-regulated in M-M (C8A, C8G, CFB, CFP, ENSGACG00000003030, ENSGACG00000014852, PGLYRP2 (2 of 2), SUSD2).

H4: Differences between innate and adaptive immune responses

The comparison of consecutive (I-I, XII-XII, M-M) vs single exposure (I, XII, M) showed four genes uniquely up-regulated in I-I (ELMOD2, APOB (2 of 5), PRG4, MASP1 (2 of 2)) and nine in I (HYAL2 (1 of 2), IRF4 (2 of 2), JUNB (1 of 2), ENSGACG00000016298, PRF1 (2 of 5), THBS1 (2 of 2), SOCS3 (2 of 2), JUNB (2 of 2), SOCS3 (1 of 2))). Unique down-regulation of 31 genes was observed in I (APOB (5 of 5), PGLYRP2 (2 of 2), APOB (1 of 5), C8G, C3 (1 of 8), C8B, C3 (4 of 8), C3 (5 of 8), C3 (3 of 8), PLG, CFP, C8A, SUSD2, C9, ENSGACG00000003030, G6PD (2 of 2), ENSGACG00000014811, C3 (2 of 8), ENSGACG00000014852, PVRL1 (2 of 2), CFB, SERPING1, C6, ENPP2 (2 of 2), KYNU, C7 (1 of 2), ADSSL1, C3 (8 of 8), MYLPF (2 of 2), C3 (7 of 8), ADAMTS13). One gene was up-regulated in I-I while down-regulated in I (VTN (2 of 2)).

When looking at XII-XII and XII, we found five genes uniquely up-regulated in XII-XII (STXBP2, AP2S1, KIF23 (2 of 2), RPA1 (1 of 2), CDK1) and 13 in XII (ADAMTS13, IRF4 (2 of 2), RGCC, ENSGACG00000016298, CYP27B1, THBS1 (2 of 2), JUNB (1 of 2), CCR9 (1 of 2), CRIP2 (2 of 2), PIP5K1C (2 of 2), JUNB (2 of 2), SOCS3 (2 of 2), SOCS3 (1 of 2)). Down-regulated were genes 22 in XII-XII (C8G, PLG, PGLYRP2 (2 of 2), ENSGACG00000014811, C8A, C3 (4 of 8), APOB (5 of 5), C3 (3 of 8), C9, APOB (1 of 5), C3 (1 of 8), C3 (5 of 8), C3 (2 of 8), SUSD2, CFP, MASP1 (2 of 2), CFB, KYNU, SERPING1, ENPP2 (2 of 2), IRF6, C4A) and three genes in XII (PVRL1 (2 of 2), COL1A1 (2 of 2), ZC3HAV1). Among shared genes, one was jointly down-regulated in XII-XII and XII (MYLPF (2 of 2)), while two were down-regulated in XII-XII and up-regulated in XII (ENSGACG00000003030, ENSGACG00000014852).

The mixed clone exposure revealed three genes uniquely up-regulated in M-M (ADAMTS13, CHIA, PVRL1 (2 of 2)) and 14 in M (IRF4 (2 of 2), ITGA5 (1 of 2), THBS1 (2 of 2), ENSGACG00000016298, SOCS3 (2 of 2), SIX1, JUNB (2 of 2), PIP5K1C (2 of 2), ATP1B3, CRIP2 (2 of 2), MEF2C (2 of 2), SOCS3 (1 of 2), MLF1, MYLPF (1 of 2)). Uniquely down-regulated was one gene in M-M (MYLPF (2 of 2)) and six genes in M (VTN (1 of 2), PLG, G6PD (2 of 2), VTN (2 of 2), C6, C3 (8 of 8)). Among shared genes, one (ADSSL1) was down-regulated in M-M and up-regulated in M, whereas 20 genes were up-regulated in M-M while down-regulated in M (APOB (1 of 5), APOB (5 of 5), C3 (1 of 8), C3 (2 of 8), C3 (3 of 8), C3 (4 of 8), C3 (5 of 8), C8A, C8B, C8G, C9, CFB, CFP, ENPP2 (2 of 2), ENSGACG00000003030, ENSGACG00000014811, ENSGACG00000014852, PGLYRP2 (2 of 2), SERPING1, SUSD2).

Among differentially expressed genes, the clearest pattern could be found in the regulation of genes involved in the complement and coagulation cascades. Genes of the complement system (C3, C4, C5, C6, C7, C8, C9, CFP, CFB, PLG, MASP1, SERPING1) were found to be active in all treatments. When clustered for similarity of expression, head kidney samples of consecutively exposed fish showed a clear distinction between I-I and XII-XII, whereas samples with M as final exposure (I-M, XII-M, M-M) cluster in between, with a I-M and XII-M being more similar to each other than to M-M (figure 3.5).

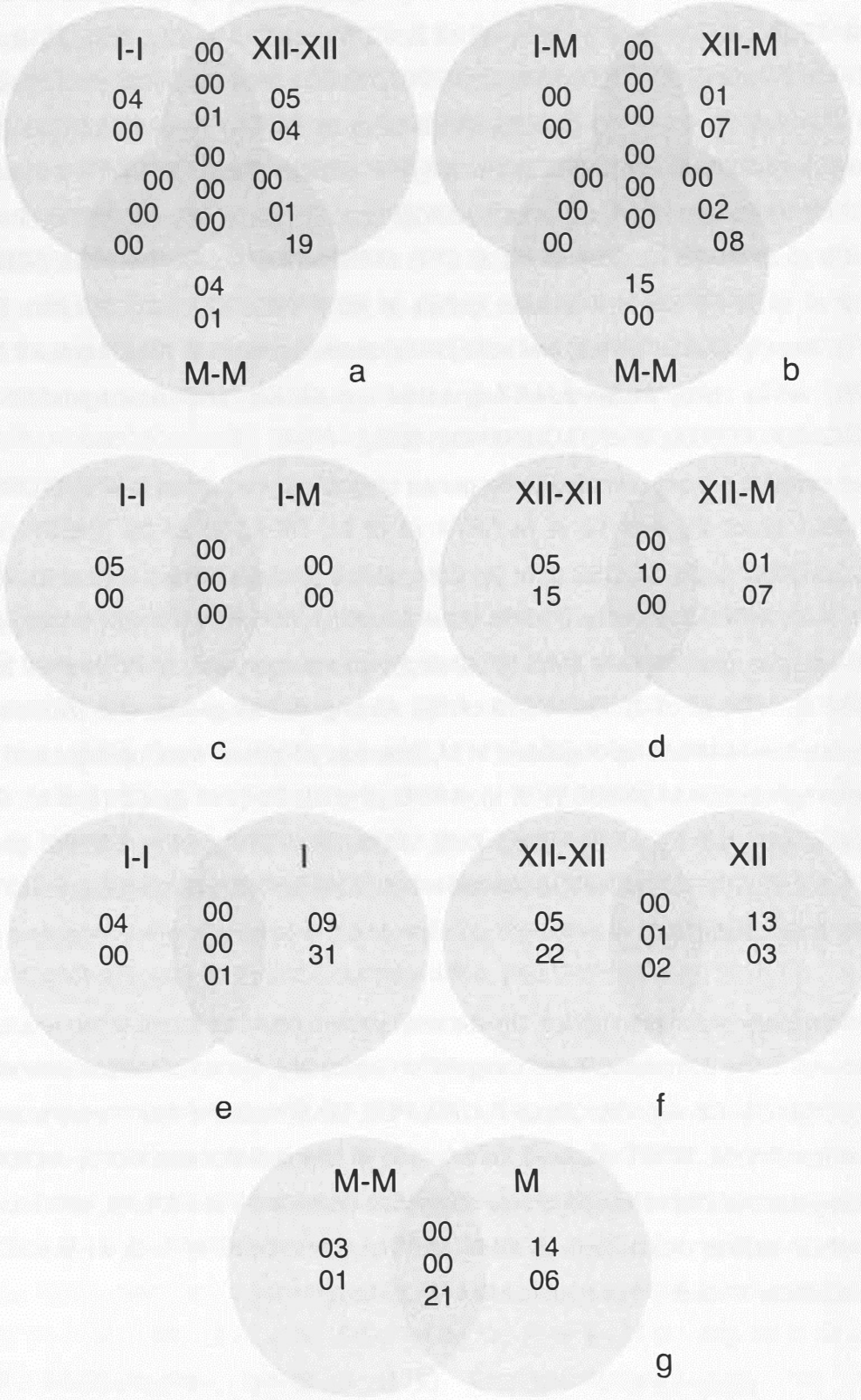

Figure 3.4.1 Differentially expressed immune genes in head kidney samples. Shown are up- and down-regulated genes (numbers from top down, first and second) as well as genes with different direction of regulation (third number if present) and whether they are shared or uniquely expressed between treatments. a) consecutive homologous infections; b) alternative pre-exposure; c & d) alternative final exposure; e - g) multiple vs single exposure. See also supplementary table S.3.5.

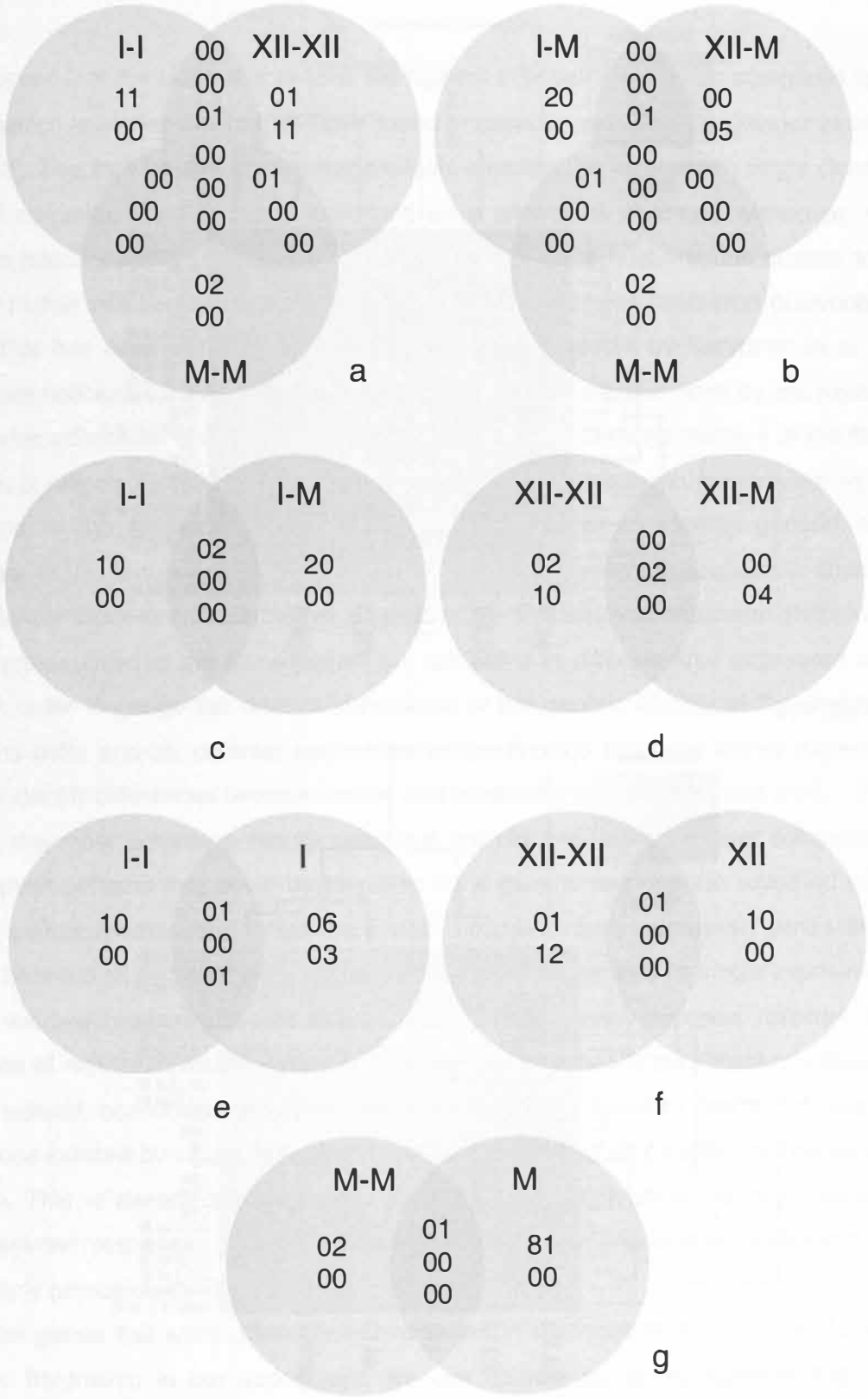

Figure 3.4.2 Differentially expressed immune genes in gill samples. Shown are up- and down-regulated genes (numbers from top down, first and second) as well as genes with different direction of regulation (third number if present) and whether they are shared or uniquely expressed between treatments. a) consecutive homologous infections; b) alternative pre-exposure; c & d) alternative final exposure; e - g) multiple vs single exposure. See also supplementary table S.3.6.

A Gill tissue

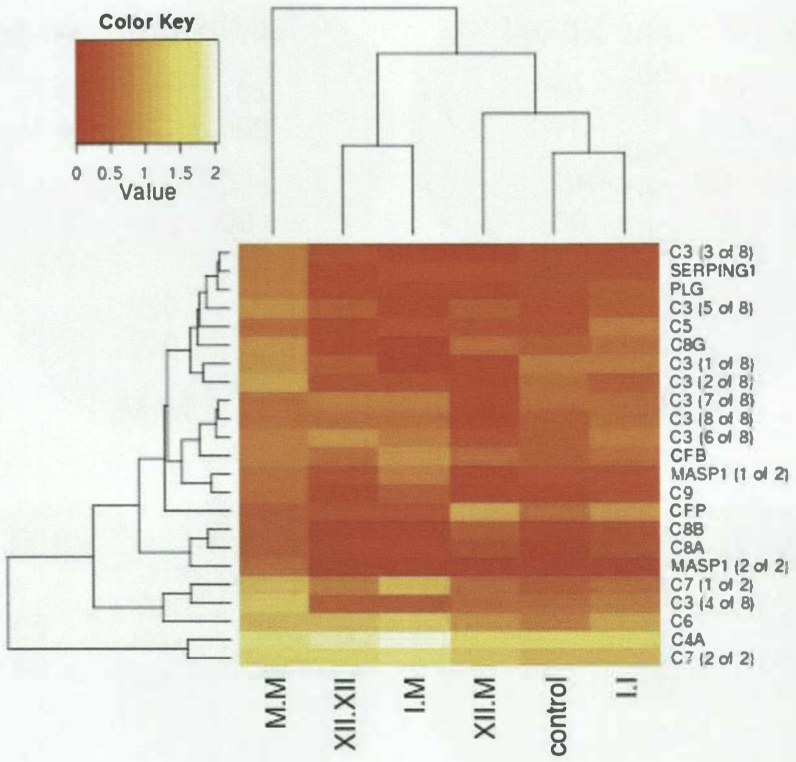

B Head kidneys

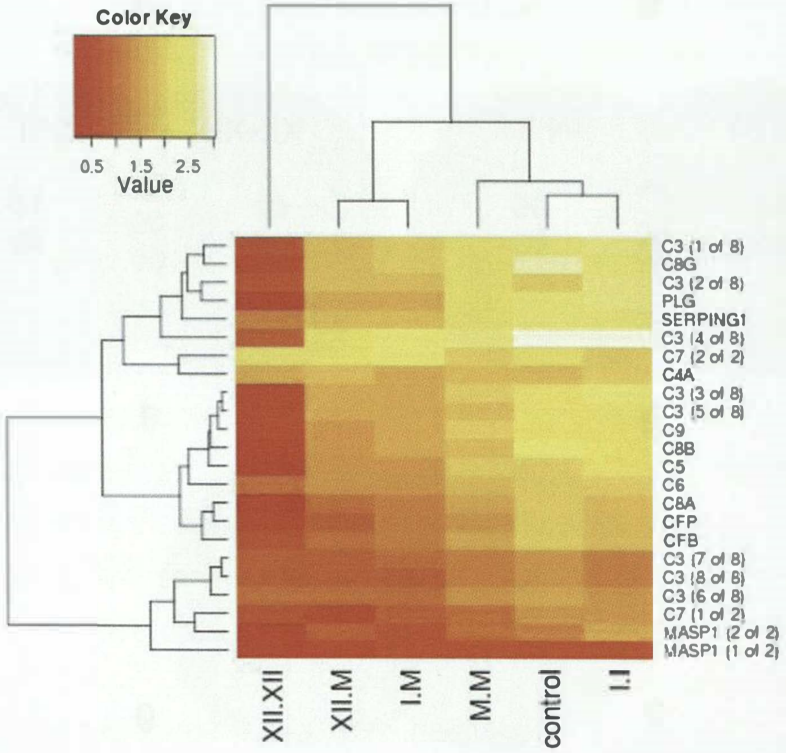

Figure 3.5 Heatmap of gene expression values of genes in the complement pathway in A) gill tissue and B) head kidneys of consecutively infected sticklebacks. Treatments are coded pre-exposure.final_exposure, showing homologous (I.I, XII.XII, M.M) and heterologous (I.M, XII.M) treatments as well as uninfected controls. Hierarchical clustering was performed on log10+1 transformed FPKM values with the function heatmap.2 of the R-package gplots.

Discussion

We observed that the clone mix caused the highest infection rates when compared to single clones, which is similar to what we have found in previous experiments (Rieger et al. 2013, chapter 2). This may be due to inbreeding effects lowering the virulence in single clonal lines, whereas cercariae used in mixed infections were allowed to outcross. Moreover, multiple genotype infections may pose an additional challenge for the host immune system and thus result in higher infection rates, a process generally referred to as facilitation (Karvonen et al. 2012). This has been demonstrated for *D. pseudospathaceum* by Karvonen et al (2012). Even more noticeable, however, was the reduction in final infection rates by pre-exposure to *D. pseudospathaceum* which points to a gradual built up of immune memory in the fish host. How this is reflected in the gene expression patterns, in particular in immune genes, will be elucidated in the following section where we will attempt to identify general adaptive responses to *D. pseudospathaceum* in the transcription patterns measured in sticklebacks (H1); identify clone-specific adaptive responses to *D. pseudospathaceum* (H2); compare groups pre-exposed to the same clones but subjected to different final exposures and vice versa in order to gauge the relative importance of the genetic identity of the first and final infections (H3a and b); contrast our results to the findings from our earlier experiment in order to identify differences between innate and adaptive immune responses (H4).

One of the most surprising results was that we did not find clear and consistent gene transcription patterns that could be identified as a general response to repeated infections with *D. pseudospathaceum.* While there were no differentially expressed genes that were shared between all samples in gill tissue as a function of repeated vs single exposure (figure 3.4.2), the few genes that were shared among head kidney samples followed different directions of regulation, thus they are not indicating a functionally consistent response (figure 3.4.1). Instead, consecutive infection lead to a transcription pattern that is not only distinct from those induced by single infections, but also differs between parasite genotypes entering the fish. This is already apparent from the MDS plot, which shows a clear distinction of transcriptomic responses between different homologous consecutive infections, and is particularly pronounced in the head kidney (figure 3.3).

From the genes that were differentially expressed in response to the different consecutive parasite treatments in our experiment, we can deduce some mechanisms that may be involved in specific immunity against individual clones of *D. pseudospathaceum*. The differing up-regulation of immune genes in head kidneys of homologous-consecutively infected fish indicates a variety of mechanisms in the response to the different parasite genotypes. In treatment I-I we see genes involved in phagocytosis (ELMOD2) and cell migration (VTN and

APOB), whereas XII-XII treated fish show activity of genes involved in endocytosis (STXBP2, AP2S1) and antigen presentation (KIF23). In fish subjected to M-M, interleukin related (ADAMTS13, CHIA) and complement activation genes (C8B) are up-regulated (www.uniprot.org). In contrast, we found no or only few differentially expressed genes in heterologous consecutive infections.

When considering the gills as representatives of the periphery of the fishes' bodies, where contact and interaction between parasite and immune system actually takes place, it appears that only fish pre-exposed to clone I exhibit pronounced expression of immune-related genes. Here we find indications of T- and B-cell activation in treatment I-I (up-regulation of CASP3, IL8, RAG1, RAG2) on the one hand, down-regulation of interferon gamma (PGLYRP2) and cytokine signalling (SOCS3) on the other, both of which are involved in macrophage activation (www.uniprot.org). We previously found macrophage activity to be among the first reactions to *D. pseudospathaceum* (chapter 2). Gene expression patterns in I-I suggest a shift from macrophage activity to a specific adaptive immune response. In I-M treatments we additionally see more complement genes (C4, C6, C7) as well as interleukin (IL4RA), chemokine (CCR9) and immunoglobulin (IgM) activity when compared to I-I (www.uniprot.org). Fish subjected to the M-M and XII-XII treatments show little or no differential expression of immune genes in gill tissue (supplementary table S.3.5 and S.3.6).

Comparison of alternative pre-exposures showed hardly any immune genes that were commonly regulated between fish subjected to the same final treatment. So again, we find a strong effect of parasite genotype upon gene expression patterns. Alternative final exposures on the other hand indicated slightly more similarities between different treatment groups pre-exposed to the same parasite genotype. While treatment I-M showed no differentially expressed immune genes and thus no overlap with treatment I-I, treatment groups XII-XII and XII-M shared more differentially expressed genes than XII-M and I-M (figure 3.4.1 and 3.4.2). In combination with the generally low amount of differentially expressed genes, this indicates that the nature of the final infection influences the composition of the immune response only little, regardless of its genotypic diversity (single clone or clone mix). Instead, the immune response appears to be influenced more strongly by the first encounter with the parasite. This is also reflected by the infection rates, which show a significant decrease of infection success in pre-exposed sticklebacks, regardless of the parasite's genotype or whether the infection was homologous or heterologous.

When comparing our results to the immune response of naïve fish receiving only a single infection (chapter 2), it is clear that consecutive exposure to *Dipostomum* cercariae leads to a more effective immune response, visible as lowered infection rates. Since single and

consecutive infections with the same parasite genotype do not share many differentially expressed genes, the observed pattern is unlikely to be caused solely by a reactivation of proteins already present during an innate response in naive fish (figure 3.4.1 and 3.4.2). Instead, it is possible that consecutive infections induce a number of signaling cascades that in turn activate components of the adaptive immune response. When looking more closely at the response of putative immune genes, however, it is difficult to discern expression patterns that would be unambiguously classified as belonging to the adaptive immune system. This may be due to the nature of RNA sequencing: since our data set encompasses all mRNA present in head kidneys and gills at the time of sampling, we have not only quantified transcripts of cellular immune activity but also any cell migration and proliferation that goes along with it. This is also reflected in the GO term analysis, where enriched terms showed mainly cell movement and organization activity as a response to different parasite treatments (supplementary table S.3.4). These terms were present in all 5 comparison categories (H1: general adaptive response, H2: specific adaptive response, H3a: alternative final exposure, H3b: alternative pre-exposure, H4: innate vs. adaptive), which may indicate replication and migration of immune-relevant cells but cannot be directly identified as immunity related processes.

The clearest pattern within the combined dataset can be found in the complement system, which is best known for eliminating pathogens directly by forming pores in their cell surfaces (Peitsch and Tschopp 1991), but is also involved in opsonization, attracting phagocytes and modulating the adaptive immune response (Winkelstein 1973, Frank and Fries 1991, Carroll 1998). The presence of a large array of complement isoforms when compared to mammals indicates a particularly important role of the complement system in fish, possibly because of the delay in mounting an adaptive immune response in poikilothermic animals (Whyte 2007). In our previous experiment, we already found considerable differences in complement gene expression between fish subjected to the individual clone treatments (chapter 2).

In consecutively exposed fish, a clear clustering could only be observed in head kidney samples, while gill samples showed a generally weaker expression of genes and no distinct treatment clusters (figure 3.5). In fish pre-exposed to clone XII (XII-M, XII-XII), we find a down-regulation of complement genes in head kidneys without a simultaneous up-regulation in gills (supplementary tables S.3.5 and S.3.6). This may be an indication of immune-modulatory activities by the parasite, or of migration of effector cells to peripheral areas of the body other than the gills. Interestingly, a similar set of genes found down-regulated in XII-XII samples was up-regulated in head kidneys in the M-M treatment (supplementary table S. 3.5). Gills of both I-I and XII-XII treated fish showed no differential expression of complement-related genes, whereas C3 and C7 were up-regulated in M-M (supplementary table S.3.6).

This highlights the importance of the complement system in both effecting innate immunity as well as mediating adaptive responses. The differences between the expression patterns in the different clonal treatments demonstrate the potential of the stickleback immune system to react specifically to certain parasite genotypes on both innate and adaptive levels. There are indications that the pre-exposure plays a larger role than the final infection itself, as we can see from heterologous consecutive infections (H3). Accordingly, in the XII-M treatment, complement genes are also down-regulated in head kidney (C7, C8, CFP, CFB) as well as gill tissue (C4) (www.uniprot.org). In I-M treated fish, we find no up- or down-regulation of complement genes in HK and up-regulation of C6 and C7 in gills. Thus, expression profiles of treatments with alternating final exposure (I-M, XII-M) are more similar to those found in homologous-infected fish pre-exposed to the same genotypes (I-I, XII-XII) than to each other. This is in line with our findings concerning parasite infection rates, where pre-exposure had the strongest effect and only weak interactions between pre-exposure and treatment could be observed.

Different strategies to attack and clear pathogenic infections have been shown to exist in different fish species. For example, Atlantic cod have recently been shown to have lost the entire MHC class II gene pathway (Star et al. 2011) without compromising their ability to withstand parasite attacks. In pipefish, MHC II also appears to be functionally absent (Haase et al. 2013). In stickleback populations, it has been shown that MHC diversity coincides with the amount and diversity of parasites the fish are likely to encounter during their lifetime (Eizaguirre et al. 2012b). Experiments have confirmed that fish with intermediate, optimised numbers of alleles have the highest parasite resistance (Wegner et al. 2003a, Kurtz et al. 2004), and maximal lifetime reproductive success (Kalbe et al. 2009), when compared to individuals with very high or very low numbers of alleles. MHC based adaptive immunity has also been demonstrated to be subjected to female mate choice (Reusch et al. 2001b), leading to enhanced fitness (Eizaguirre et al. 2009).

It is likely that any adaptation to specific habitats and their characteristic parasite/pathogen assemblage also acts on components of the immune system other than the MHC pathway. For instance, previous studies have shown stickleback ecotypes from lake and river habitats to have differing immunocompetences, probably owing to the larger diversity of parasites present in lakes (Kalbe and Kurtz 2006, Lenz et al. 2013). The evolution of specific responses to certain parasite genotypes, however, is likely to depend on the ecology and population genetics of the respective parasite species. *D. pseudospathaceum,* for example, is a generalist parasite with regard to its fish vector, infecting many freshwater species (Chappell et al. 1994). In addition, it has highly mobile final hosts that are able to disperse the worms over long distances and thus cause admixing. Therefore, populations of *D.*

pseudospathaceum are genetically highly diverse while exhibiting little genetic structuring over large geographical ranges (Louhi et al. 2010). In a study by Rauch et al (2005) very few instances of stickleback infected with more than one of any given *D. pseudospathaceum* clone were found (Rauch et al. 2005). As fish accumulate metacercariae in their eye lenses during the summer season, we would expect sticklebacks to mount an adaptive immune response that is effective against different clones in order to reduce the risk of cataracts and blindness. Nevertheless, genotype x genotype interactions between *D. pseudospathaceum* and uninfected three-spined sticklebacks have been demonstrated (Rauch et al. 2006). Due to considerable redundancy within both innate and adaptive immune systems (Nish and Medzhitov 2011), it is possible that different pathways all lead to similar responses. In addition, many specific immune receptors are able to cross-react with different antigens. A recent study has demonstrated that humans can harbour specific immune memory against foreign antigens which they have not been exposed to (Su et al. 2013). Even though natural populations of *D. pseudospathaceum* are genetically highly polymorphic, our results suggest similar antigenic patterns that may be recognised by the immune system.

While we found genotype-specific immune gene expression in response to different parasite clones in naive fish (chapter 2), pre-exposed fish did not exhibit specific adaptive immune mechanisms that coincided with the genotype of the final infection. This may be an indication of the necessity to mount an effective adaptive immune response covering as much genetic parasite diversity as possible. Nevertheless, our results indicate that the genetic prerequisites for specific immune responses are available as the necessary components for local adaptation. This is in line with the findings of Wegner et al (2007), who found that resistance to *D. pseudospathaceum* in sticklebacks increased within only one generation of artificial selection (Wegner et al. 2007). The importance of complement-based immunity in an immune response against *D. pseudospathaceum* as well as the observed differences between singly and consecutively infected fish may be interpreted as a representation of the close interconnection between the innate and adaptive immune systems (Gardy et al. 2009, Shanker 2010, Criscitiello and de Figueiredo 2013). By showing the complex parasite genotype dependencies of host gene expression, our results contribute significantly to the current understanding of the diversity of immune mechanisms in vertebrates. While mRNA abundance cannot be taken as a proxy for protein activity (Feder and Walser 2005), RNA sequencing provides us with a holistic view of the molecular mechanisms triggered upon exposure to a parasite.

Acknowledgements

We would like to thank Gisela Schmiedeskamp, Gerhard Augustin and Daniel Martens who were very helpful with animal care and sample collection. The study was financially supported by the Deutsche Forschungsgemeinschaft (DFG, Priority Programme on Host-parasite Coevolution – SPP 1399), GEOMAR Helmholtz Centre for Ocean Research Kiel and the Max Planck Institute for Evolutionary Biology. Animal experiments were conducted with permission of the 'Ministry of Energy, Agriculture, the Environment and Rural Areas' of the state of Schleswig-Holstein, Germany (reference number: V 313-72241.123-34).

Discussion

Beyond the vertebrate paradigm

In this thesis I have explored transcriptome-wide expression patterns of broad-nosed pipefish (*Syngnathus typhle*) and three-spined sticklebacks (*Gasterosteus aculeatus*) to investigate the specificity and diversity of teleost immune responses. I have shown that broad-nosed pipefish (*S. typhle*) do not show expression of MHC class II associated immune genes (chapter 1). This extraordinary feature has to date been shown only in one other species, the atlantic cod (*Gadus morhua*), although MHC mediated immune memory has long been thought to be a key element in specific immune memory of jawed vertebrates (Janeway et al. 2008, Star et al. 2011). The assumption that only long-lived vertebrates are able to mount a specific immune response with subsequent immune memory has been found to be an oversimplification. Recent experimental work was able to point out immune priming, memory and specificity in invertebrate immune responses (Kurtz and Franz 2003, Little et al. 2003, Robalino et al. 2005, Schmid-Hempel 2005, Sadd and Schmid-Hempel 2006, Schulenburg et al. 2007, Roth et al. 2009). The cellular mechanisms of those immune systems are to date not fully understood.

I have also shown that innate immune responses can depend on the genotypic background of an invading pathogen (chapter 2). On the phenotypic level this has been known before (Rauch et al. 2006) but in the experiment presented here I was able to identify gene expression changes attributable to genetically very distinct trematode infections. Apparently, the innate immune system possesses a variety of receptor mechanisms with the ability to detect pathogenic invaders by several receptor types (Gardy et al. 2009, Nish and Medzhitov 2011). The resulting responses thus show a large amount of diversity within defense mechanisms. They can be limited to certain tissue types and depending on a hierarchy determined by fitness costs of a specific response (Nish and Medzhitov 2011). This knowledge however is mostly based on pathogenic bacteria and viruses, with little knowledge of the mechanisms of innate immunity as a response to macroparasites, such as trematodic worms (Nish and Medzhitov 2011). Due to the tissue damaging potential, innate immunity needs to be efficiently controlled to prevent damage to the host while exerting sufficient pressure on the invading pathogen (Goldszmid and Trinchieri 2012). This control seems to be partly mediated by the activated adaptive immune response (Shanker 2010). It has been shown for example, that T-cells can suppress an innate immune response by down-regulating associated genes (Kim et al. 2007, Shanker 2010). This process even requires MHC molecules but is independent of antigen specificity (Kim et al. 2007, Shanker 2010). Interactions among innate and adaptive immunity in vertebrates have been known for

some time. For example, parts of the innate immune response activate and mediate adaptive T cell and B cell based immune responses (Janeway et al. 2008).

To examine the effect of an activated adaptive immune system on gene expression patterns of fish, sticklebacks were consecutively infected over several weeks, including alternating final infections to estimate specificity and variability of the resulting immune gene responses (chapter 3). Interestingly, next to parasite genotype specific responses and a strong effect of previous infections on the gene expression patterns, also differences in genes related to innate immunity were found. Apparently, next to suppression, adaptive immunity can also activate parts of an innate immune response, compensate absent innate responses and can induce combined effects of innate and adaptive immunity resulting in fine-tuning of a maximized host defense (Shanker 2010). Additionally, characteristics of immunological memory have been shown in components of the innate immune system with NK cells bearing virus-specific receptors and macrophages undergoing differentiation and adaptation to repeated exposure (Foster and Medzhitov 2009, Sun et al. 2009, Shanker 2010). The idea that features of adaptive immunity are present in the evolutionary older innate immune system (Shanker 2010) is supported by the accumulating evidence for specific immune responses and immune memory in invertebrates which do not possess a classical V(D)J-based adaptive immunity (Kurtz 2004).

The complexity of an immune system response is not limited in the interaction of adaptive and innate components. Furthermore, expression of immune relevant genes is controlled via post-transcriptional regulation by microRNAs and post-translational modifications (Gardy et al. 2009). The reaction to repeated pathogen exposure in macrophages for example involves modification of gene packaging histones (Foster and Medzhitov 2009, Shanker 2010). Protein-protein interactions can vary depending on nucleotide variation in the protein binding sites of the host population and innate responses can also depend on the species examined (Gardy et al. 2009). It has already been shown that mouse models, which are commonly used in clinical studies, differ at several points of the adaptive and innate immune system when compared to humans (Mestas and Hughes 2004, Gardy et al. 2009). Although the mechanisms of innate and adaptive immune systems in fishes have been regarded as being similar to mammals (Workenhe et al. 2010, Sunyer 2013), their repertoire and combination of immune relevant mechanisms is more different than previously thought. Teleost fish seem to lack antibody isotope switching (Sunyer 2013) while their innate immune repertoire is more diverse than in mammals (Magnadóttir 2006, Sunyer 2013). Although antibody diversity in fish is lower than in mammals (Du Pasquier 1982, Magnadóttir 2006), with only three immunoglobulin (Ig) classes, IgM, IgD and IgT (Fillatreau et al. 2013), the complexity of immunoglobulin loci of some fish is at least as large as in mammalian species (Fillatreau et

al. 2013). Natural antibodies, as part of an innate immune response, and phagocytic B-cells also seem to play a large role in fish, but similarities to the situation in mammals have still to be examined (Magnadóttir 2006, Whyte 2007). In cod, which lack a MHC class II mediated adaptive immune response (Star et al. 2011), natural antibodies have been shown to mimic a specific antibody response (Magnadóttir 2006). Another feature of teleost fish is the adaptation of the complement system to cold environments where it can remain active at very low (0-4°C) temperatures (Whyte 2007). It is additionally more diversified with several isoforms of C3, one of the central complement component proteins (Whyte 2007), a pattern which plays a role in innate immune reactions of sticklebacks to parasite infections (chapter 2).

Technology under development: issues in obtaining and analyzing RNA-seq data

In my thesis I studied the transcriptomes of two fish species and their gene expression responses to pathogenic challenges. The most popular approaches to study global patterns of RNA abundance are microarray-based hybridization and sequence-based approaches (Wang et al. 2009). Microarray approaches however rely on synthesized sequences and thus are limited to existing knowledge (Wang et al. 2009). RNA-seq is a powerful tool to estimate transcript levels without the need for candidate genes. Both approaches rely on the expectation that a specific stress response induces measurable changes in the transcription of genes. Since mRNA abundances do not equal protein levels, due to several subsequent RNA modification steps, gene expression changes should not be mistaken as indicators for fitness differences (Feder and Walser 2005). Instead I used the transcriptome approach to estimate the presence of transcribed genes (chapter 1) and to identify genes linked to a specific stress response (Feder and Walser 2005, chapter 2, chapter 3).

In next-generation sequencing, the production of millions of reads is a multistep procedure containing some pitfalls which have to be additionally accounted for when preparing and analyzing RNA-seq data. The preparation of sequencing libraries for instance can introduce a bias, depending on the fragmentation method used (Wang et al. 2009). Most challenges however, come after the sequencing step. All NGS platforms have distinct error profiles that should be accounted for when analyzing the respective sequence data (Miller et al. 2010, Nakamura et al. 2011), although the effects of sequencing errors seem to have low effect on the estimation of differential gene expression (Vijay et al. 2013).

After assessing the quality of my data sets, I either aligned the sequenced reads to a reference genome (chapter 2, chapter 3) or assembled them de novo (chapter 1). To this end many software tools for alignment of reads, like BOWTIE, SOAP and ELAND, or de novo assembly of transcriptomes/genomes, e.g. ABYSS, VELVET or MIRA, have been developed

(see www.seqanswers.com for an extended list). The amount of contigs, i.e. contiguous sequences built from short reads, in de novo assemblies depends on the assembly software, coverage and parameters used (Mundry et al. 2012, www.seqanswers.com). In case of the MIRA-assembled pipefish transcriptome different transcript isoforms and intronic sequences led to an unusually high amount of contigs. Further filtering steps were not appropriate to gain support for the absence of specific transcripts (chapter 1).

The aligned stickleback reads were further subjected to statistical software packages for quantification and comparison of transcript abundances. To estimate differential expression of transcripts between samples, reads need to be either mapped to a reference genome/ transcriptome or to de novo assembled gene models, quantified and subsequently analyzed by appropriate statistical approaches (Vijay et al. 2013). Statistical analyses of microarray studies have been developed over several years, including guidelines for research design and the development of study-specific statistical models for a better explanation of the observed data (Brazma et al. 2001, Cui and Churchill 2003, Gibson 2003, Zang et al. 2007, Nam and Kim 2008). Since RNA-seq is a relatively new method, compared to microarrays, the statistical framework is less developed, with a higher degree of uncertainty which mathematical model describes the data best (Auer and Doerge 2010, Katz et al. 2010, Trapnell et al. 2010, Kvam et al. 2012, www.seqanswers.com). I decided to analyze the stickleback transcriptome data with respect to potentially differential expression of splice variants (chapter 2, chapter 3). For this purpose I chose a software package which combined fast read alignment to a reference genome with the estimation of splice variants and a subsequent statistical test including corrections for multiple testing (Trapnell et al. 2010).

After alignment and quantification of reads I performed an assessment of functional gene categories and their distribution over the dataset. GO term analysis, the characterization of genes into gene groups defined by their "Biological Process", "Molecular Function" or "Cellular Component", is widely used (www.geneontology.org). However, the definition of a certain gene belonging to a specific functional group depends on an annotation process not always directly backed by experimental evidence (www.blast2go.com, Conesa et al. 2005). Functional categorizations can be different between annotations, depending on the parameters used (chapter 2, Conesa et al. 2005). This can lead to incomplete GO annotations or the attribution of genes to very basic functions, e.g. "Biological Process", which have no further discriminatory value. Still the approach is valid to characterize the composition of a set of genes or to examine differences between given datasets, if the limitations of a given GO annotation are known. To extract immune function related genes by their GO term annotation if important immune relevant genes, e.g. the complement system, are not termed as immune related would be misleading (chapter 2). Nonetheless, it is still

possible to estimate differences between gene groups and then have a detailed look at the genes driving an observed difference.

During the fish transcriptome analyses I experienced a more general obstacle in the analysis of NGS data, limitations in computing resources. The output of sequencing machines in terms of base-pairs is increasing since the invention of next-generation sequencing (Mardis 2011), combined with an exponential decrease of the costs per sequenced base (Stein 2010). While large re-sequencing projects such as the "1000 Genomes Project" massively increase the available amount of sequence data via parallel genome sequencing of human genomes (http://www.1000genomes.org/), the cost of storage space is predicted to overtake the costs of data acquisition during the coming "tsunami of genome data" (Stein 2010). Next to hard disk space, bioinformatic analyses can require large amounts of RAM (random-access memory), in de novo assemblies currently exceeding the hundredfold of memory available in desktop computers, or CPUs (central processing unit), e.g. in BLAST annotations. I experienced both limitations during the analysis of the *S. typhle* data, which forced me to subsample datasets for the de novo transcriptome assembly (chapter 1). These analyses require the maintenance of local computing clusters, which need additional resources and need to be upgraded regularly to keep pace with increasing amounts of data (Stein 2010). Bioinformaticians already work on enhancement and development of algorithms to reduce computer resources needed. This includes digital normalization of sequence data, including a reduction of sequence errors (Brown et al. 2012) and enhanced read mapping by including graphical processing power (GPU) to increase performance (http://cibiv.github.com/NextGenMap/). Another solution might be cloud computing, where a distinct amount of computer resources can be virtually rented, allowing calculations without maintaining expensive cluster systems (Stein 2010). However, to date this approach is limited by network bandwidth, not fully developed for NGS data analyses and at the moment marginally more expensive then maintaining an own computer cluster (Stein 2010).

The diversity of immune gene expression in fish

With the onset of next-generation sequencing technologies, studies on repertoire and evolution of fish immune systems have greatly expanded (Morera et al. 2011, Ordas et al. 2011, Star et al. 2011, Zhang et al. 2011, Li et al. 2012, Sarropoulou et al. 2012, Sun et al. 2012, Lenz et al. 2013, Sunyer 2013). With my thesis I contributed to this growing knowledge, being able to show that more than one fish species lack certain features of the adaptive immune response (chapter 1, Star et al. 2011). I have shown that innate immunity shows specific transcriptomic responses depending on the genotypic background of a certain parasite species and that gene expression patterns of consecutively infected sticklebacks are

influenced by previous infections (chapter 2, chapter 3). Especially innate immunity of teleost fish has been of special interest in the last years (Magnadóttir 2006, Whyte 2007, Workenhe et al. 2010). As teleost fish are poikilothermic, adaptive immunity is relatively slow and hence, innate immunity is supposed to play a much more important role in the defense against invading pathogens (Whyte 2007). As with humans and mice, the importance of the innate immune response has been shown to be depending on the fish species of interest and can be different compared with others (Whyte 2007). These findings underline the importance of variation in immune responses in general. Unraveling this variation is our main objective as evolutionary biologists since variation is not only the product but also the source of adaptation and diversification in living organisms. From an evolutionary perspective I can clearly say that the observed gene expression differences are likely the result of selective processes. Depending on the fish species this led to selection against central components of V(D)J-mediated immune memory in pipefish (chapter 1), as well as to a vast amount of possibilities for a specific innate immune response (chapter 2) and parasite genotype dependent cross-reactive immunization mechanics in sticklebacks (chapter 3). Taken together I want to underline that the idea of one archetypical pathway for all vertebrate species is an oversimplification by classical molecular immunology and thus a paradigm which should be changed.

Perspectives

In my thesis I have shown that immune related gene expression of three-spined sticklebacks depends on the genotypic background of a parasite strain (chapter 2, chapter 3). As a next step I want to investigate the genetic contribution of the host to gene expression patterns of an innate immune response. More precisely, I want to disentangle how much of the variability can either be attributed to a random composition of several alternative immune responses or is predetermined by the genetic background of the host in response to the interaction with a certain parasite genotype, which would then be expressed as heritability. To this end a selection experiment was performed with the clonal *Diplostomum pseudospathaceum* lineages from chapter 2 and chapter 3 to infect three-spined sticklebacks (*G. aculeatus*) and then those individuals were selected for breeding, which were infected the lowest. Studies on sticklebacks infected with *Diplostomum* have already shown that one generation of selection for resistance can decrease the susceptibility of stickleback offspring against the respective parasite (Wegner et al. 2007). Sticklebacks with a defined genetic background were already selected for resistance against different genotypic lineages of *D. pseudospathaceum*. I will analyze the transcriptome of those fish by means of Illumina-based RNA-seq to estimate gene expression patterns of fish bred resistant against and then infected with the same or different lineages of *Diplostomum*. To embed those transcriptome data into an integrated approach, infection success of the parasite and diverse body condition parameters including immune cell production have already been taken. Combined with a thorough statistical analysis this study will boost our understanding on the heritability of gene expression patterns under a selective environment in combination with an in depth knowledge of the phenotypic responses.

I have shown that the transcriptome of broad-nosed pipefish (*S. typhle*) lacks the expression of MHC class II related genes (chapter 1). Together with the absence of MHC class II in cod (*Gadus morhua*), this provides strong evidence that even within the jawed vertebrates different frameworks of adaptive immunity can exist. Different hypotheses are discussed as possible explanations for this unexpected phenomenon (Star and Jentoft 2012). However, evidence in favor for one hypothesis is still scarce (Star and Jentoft 2012). It has been shown that big-belly seahorse (*Hippocampus abdominalis*), a close relative to the Syngnathidae, possess an MHC class II mediated adaptive immune response (Bahr and Wilson 2011), although allelic diversity is surprisingly low (Bahr and Wilson 2012). This, among other factors, makes it very likely that both species lost their MHC class II genes independently,

raising the question of the underlying evolutionary processes which shaped the immune repertoire of both species (chapter 1). These findings challenge our view that differences in the evolution of adaptive immunity in jawed vertebrates are only limited to different preferences in the generation of immunoglobulin diversity (Janeway et al. 2008). Since I could only show that pipefish don't express MHC class II related genes, the amount of traces possibly left in the genome are not known. There are clearly differences in the absence of genes compared to cod, thus further genomic information might highlight species specific compensation for the loss of MHC II in *S. typhle* (chapter 1). Additionally, the sequencing of a pipefish genome would facilitate new studies on different research fields, including ecology, evolution and immunity. We have seen already, that the components of a fish immune system and the importance of adaptive and innate responses depends on the fish species (Whyte 2007) and our understanding on fish immunity comes from a limited subset of the 40,000 known fish species (Fillatreau et al. 2013). Therefore, the immune repertoire of pipefish will be further investigated by a genome sequencing project.

These two projects will help us to unravel the composition of immune relevant genes in broad-nosed pipefish and the heritability of gene expression patterns in three-spined sticklebacks. Taken together this will further increase our knowledge about the evolution of vertebrate immunity and the diversity of immune responses in fish.

Eidesstattliche Erklärung

Hiermit erkläre ich, dass ich die vorliegende Dissertation mit dem Titel:

Diversity and specificity of the teleost immune system

A transcriptome study on two fish species

selbstständig, mit der Unterstützung meiner Betreuer, verfasst habe. Ich habe keine anderen als die angegebenen Hilfsmittel und Quellen verwendet und die Arbeit unter Einhaltung der Regeln guter wissenschaftlicher Praxis der Deutschen Forschungsgemeinschaft erstellt.

Diese Arbeit wurde an keiner anderen Stelle im Rahmen eines Prüfungsverfahrens vorgelegt und ist mein bisher erstes und einziges Promotionsverfahren.

Kapitel 1 dieser Arbeit wurden in der wissenschaftlichen Fachzeitschrift „Biology Letters" veröffentlicht. Die Koautoren aller drei Kapitel finden sich zu Beginn des jeweiligen Kapitels in der Autorenliste. Der Anteil der Autoren an den Manuskripten wird im Abschnitt „Author contributions" erläutert.

Kiel, im Mai 2013 David Haase

Author Contributions

Chapter 1

Haase D*, Roth O*, Kalbe M, Schmiedeskamp G, Scharsack JP, Rosenstiel P, Reusch TBH (2013) Absence of major histocompatibility complex class II mediated immunity in pipefish, *Syngnathus typhle*: evidence from deep transcriptome sequencing. Biol. Lett. 2013 Feb 27;9(2) *equal contribution

TBHR and OR conceived the project. OR performed PCR directed cloning and analyzed the data. PR contributed with sequencing facilities. **DH analyzed high-throughput sequencing data. TBHR wrote the manuscript together with DH and OR.** All authors contributed to the manuscript.

Chapter 2

Haase D, Rieger JK, Witten A, Stoll M, Bornberg-Bauer E, Kalbe M, Reusch TBH: Redundancy of the innate immune system results in genotype specific host transcriptome responses to clonal trematode parasite lines in three-spined sticklebacks, *Gasterosteus aculeatus* (prepared for submission)

TBHR conceived the project. TBHR, EBB and MS applied for funding. **DH and JKR designed and conducted the experiment under the supervision of TBHR and MK.** MK also took part in the experiment. MS and AW contributed with sequencing facilities, EBB with bioinformatic input. **DH analyzed the data and wrote the manuscript under supervision of TBHR.** All authors contributed to the manuscript.

Chapter 3

Rieger JK*, **Haase D***, Witten A, Stoll M, Bornberg-Bauer E, Kalbe M, Reusch TBH: Transcriptome analysis reveals complex interplay of adaptive and innate immunity in consecutively infected three-spined sticklebacks, *Gasterosteus aculeatus* (prepared for submission) *equal contribution

TBHR conceived the project. TBHR, EBB and MS applied for funding. **DH and JKR designed and conducted the experiment under the supervision of TBHR and MK.** MK also took part in the experiment. MS and AW contributed with sequencing facilities, EBB with bioinformatic input. **DH and JKR analyzed the data and wrote the manuscript under supervision of TBHR.** All authors contributed to the manuscript.

Danksagung

Zuerst möchte ich Prof. Dr. Thorsten Reusch für die Gelegenheit zu Promotion, sowie seine Betreuung und Unterstützung bei der Fertigstellung der Arbeit danken.

Dr. Martin Kalbe gebührt großer Dank für seinen unermüdlichen Einsatz im Aufbau und der Durchführung der Experimente. Unvergessen bleibt seine neuentdeckte Freude an Heatmaps und die große Begeisterung bei der Möwenaufzucht.

Ich möchte mich auch bei Jennifer Rieger für die gute Zusammenarbeit bedanken. Ohne ihre Unterstützung wäre dieses Projekt sehr viel schwieriger zu bewältigen gewesen.

Der B45-WG danke ich für den besten Büroalltag, den man sich vorstellen kann. Danke auch an Christophe und Livia für die fachliche Unterstützung. Vielen Dank auch an Sören, Kai, Philipp, Susie, Simone, Regina, Tina und Katrin für die Hilfe bei Fischen, Würmern und anderen Nöten sowie an die EV für die kollegiale Atmosphäre und das tolle Arbeitsklima.

Großer Dank geht auch an Gerhard Augustin und Daniel Martens vom MPI Plön für die viele Hilfe bei der Versorgung der Fische, sowie an Gisela Schmiedeskamp für ihre Unterstützung bei der Möwenaufzucht.

Danke an Mini und Chaperone für Starthilfe und Rückhalt.

Vielen Dank an meine Familie, inklusive Kira. Ebenfalls vielen Dank an Natascha für ihre Unterstützung und die Geduld an stressigen Schreibtagen.

Zu guter Letzt möchte ich noch der “wilden 13” und den “glorreichen 7” für ihren unermüdlichen Einsatz in der Parasitenvermehrung danken. Sollte Ihnen, lieber Leser, einmal eine Möwe auf dem Kopf sitzen, einfach Katzenfutter hinzugeben.

List of publications

I have coauthored the following publication during the time of my dissertation but not included it in my thesis:

Rieger JK, Haase D, Reusch TB, and Kalbe M (2013) Genetic compatibilities, outcrossing rates and fitness consequences across life stages of the trematode *Diplostomum pseudospathaceum*. International journal for parasitology 43:485-491.

References

Akaike H (1981) Citation Classic - a New Look at the Statistical-Model Identification. Cc/Eng Tech Appl Sci:22-22.

Alder MN, Rogozin IB, Iyer LM, Glazko GV, Cooper MD, and Pancer Z (2005) Diversity and function of adaptive immune receptors in a jawless vertebrate. Science 310:1970-1973.

Auer PL and Doerge RW (2010) Statistical design and analysis of RNA sequencing data. Genetics 185:405-416.

Bahr A and Wilson AB (2011) The impact of sex-role reversal on the diversity of the major histocompatibility complex: insights from the seahorse (*Hippocampus abdominalis*). BMC evolutionary biology 11:121.

Bahr A and Wilson AB (2012) The evolution of MHC diversity: evidence of intralocus gene conversion and recombination in a single-locus system. Gene 497:52-57.

Basha G, Omilusik K, Chavez-Steenbock A, Reinicke AT, Lack N, Choi KB, and Jefferies WA (2012) A CD74-dependent MHC class I endolysosomal cross-presentation pathway. Nat Immunol 13:237-245.

Bell MA and Foster SA (1994) The evolutionary biology of the threespine stickleback. Oxford University Press, Oxford ; New York.

Benesh DP, Chubb JC, and Parker GA (2013) Complex Life Cycles: Why Refrain from Growth before Reproduction in the Adult Niche? Am Nat 181:39-51.

Benjamini Y and Hochberg Y (1995) Controlling the false discovery rate - A practical and powerful approach to multiple testing. Journal of the Royal Statistical Society Series B-Methodological 57:289-300.

Berner D, Grandchamp AC, and Hendry AP (2009) Variable Progress toward Ecological Speciation in Parapatry: Stickleback across Eight Lake-Stream Transitions. Evolution 63:1740-1753.

Bolnick DI, Snowberg LK, Patenia C, Stutz WE, Ingram T, and Lau OL (2009) Phenotype-dependent native habitat preference facilitates divergence between parapatric lake and stream stickleback. Evolution 63:2004-2016.

Brazma A, Hingamp P, Quackenbush J, Sherlock G, Spellman P, Stoeckert C, Aach J, Ansorge W, Ball CA, Causton HC, Gaasterland T, Glenisson P, Holstege FCP, Kim IF, Markowitz V, Matese JC, Parkinson H, Robinson A, Sarkans U, Schulze-Kremer S, Stewart J, Taylor R, Vilo J, and Vingron M (2001) Minimum information about a microarray experiment (MIAME) - toward standards for microarray data. Nature Genetics 29:365-371.

Brown CT, Howe A, Zhang Q, Pyrkosz AB, and Brom TH (2012) A reference-free algorithm for computational normalization of shotgun sequencing data. arXiv preprint arXiv: 1203.4802.

Brown SP, Renaud F, Guegan JF, and Thomas F (2001) Evolution of trophic transmission in parasites: the need to reach a mating place? Journal of Evolutionary Biology 14:815-820.

Carroll MC (1998) The role of complement and complement receptors in induction and regulation of immunity. Annual review of immunology 16:545-568.

Chappell LH, Hardie LJ, and Secombes CJ (1994) Diplostomiasis: the disease and host-parasite interactions. Pp. 59-86 *in* A. W. Pike, and J. W. Lewis, eds. Parasitic diseases of fish. Samara Publishing Limited, Dyfed, UK.

Chen YA, Lin CC, Wang CD, Wu HB, and Hwang PI (2007) An optimized procedure greatly improves EST vector contamination removal. BMC genomics 8:416.

Chevreux B, Pfisterer T, Drescher B, Driesel AJ, Müller WEG, Wetter T, and Suhai S (2004) Using the miraEST Assembler for Reliable and Automated mRNA Transcript Assembly and SNP Detection in Sequenced ESTs. Genome Research 14:1147-1159.

Conesa A, Gotz S, Garcia-Gomez JM, Terol J, Talon M, and Robles M (2005) Blast2GO: a universal tool for annotation, visualization and analysis in functional genomics research. Bioinformatics 21:3674-3676.

Consuegra S and Garcia de Leaniz C (2008) MHC-mediated mate choice increases parasite resistance in salmon. Proceedings. Biological sciences / The Royal Society 275:1397-1403.

Cooper MD and Alder MN (2006) The evolution of adaptive immune systems. Cell 124:815-822.

Criscitiello MF and de Figueiredo P (2013) Fifty Shades of Immune Defense. Plos Pathog 9.

Crowden AE and Broom DM (1980) Effects of the eyefluke, *Diplostomum spathaceum*, on the behaviour of dace (*Leuciscus leuciscus*). Animal Behaviour 28:287-294.

Cui XQ and Churchill GA (2003) Statistical tests for differential expression in cDNA microarray experiments. Genome biology 4.

de Bellocq JG, Charbonnel N, and Morand S (2008) Coevolutionary relationship between helminth diversity and MHC class II polymorphism in rodents. Journal of Evolutionary Biology 21:1144-1150.

De Roode JC and Altizer S (2010) Host-parasite genetic interactions and virulence-transmission relationships in natural populations of monarch butterflies. Evolution 64:502-514.

Du Pasquier L (1982) Antibody diversity in lower vertebrates--why is it so restricted? Nature 296:311-313.

Eizaguirre C, Lenz TL, Kalbe M, and Milinski M (2012a) Divergent selection on locally adapted major histocompatibility complex immune genes experimentally proven in the field. Ecology letters 15:723-731.

Eizaguirre C, Lenz TL, Kalbe M, and Milinski M (2012b) Rapid and adaptive evolution of MHC genes under parasite selection in experimental vertebrate populations. Nature communications 3:621.

Eizaguirre C, Lenz TL, Sommerfeld RD, Harrod C, Kalbe M, and Milinski M (2011) Parasite diversity, patterns of MHC II variation and olfactory based mate choice in diverging three-spined stickleback ecotypes. Evol Ecol 25:605-622.

Eizaguirre C, Yeates SE, Lenz TL, Kalbe M, and Milinski M (2009) MHC-based mate choice combines good genes and maintenance of MHC polymorphism. Mol Ecol 18:3316-3329.

Feder ME and Walser JC (2005) The biological limitations of transcriptomics in elucidating stress and stress responses. J Evol Biol 18:901-910.

Feulner PGD, Chain FJJ, Panchal M, Eizaguirre C, Kalbe M, Lenz TL, Mundry M, Samonte IE, Stoll M, Milinski M, Reusch TBH, and Bornberg-Bauer E (2013) Genome-wide patterns of standing genetic variation in a marine population of three-spined sticklebacks. Molecular Ecology 22:635-649.

Fillatreau S, Six A, Magadan S, Castro R, Sunyer JO, and Boudinot P (2013) The astonishing diversity of Ig classes and B cell repertoires in teleost fish. Frontiers in immunology 4:28.

Flajnik MF and Du Pasquier L (2004) Evolution of innate and adaptive immunity: can we draw a line? Trends in immunology 25:640-644.

Flajnik MF and Kasahara M (2010) Origin and evolution of the adaptive immune system: genetic events and selective pressures. Nature reviews. Genetics 11:47-59.

Foster SL and Medzhitov R (2009) Gene-specific control of the TLR-induced inflammatory response. Clin Immunol 130:7-15.

Frank MM and Fries LF (1991) The role of complement in inflammation and phagocytosis. Immunology today 12:322-326.

Fry FEJ (1967) Responses of vertebrate poikilotherms to temperature. Pp. 375-409 *in* A. H. Rose, ed. Thermobiology. A.C. Press.

Gao GF, Tormo J, Gerth UC, Wyer JR, McMichael AJ, Stuart DI, Bell JI, Jones EY, and Jakobsen BK (1997) Crystal structure of the complex between human CD8 alpha alpha and HLA-A2. Nature 387:630-634.

Gardy JL, Lynn DJ, Brinkman FS, and Hancock RE (2009) Enabling a systems biology approach to immunology: focus on innate immunity. Trends Immunol 30:249-262.

Gibson G (2003) Microarray analysis - Genome-scale hypothesis scanning. Plos Biol 1:28-29.

Gibson G (2005) The Synthesis and Evolution of a Supermodel. Science 307:1890-1891.

Goff L and Trapnell C (2011) cummeRbund: The finishing touch on your Tuxedo workflow. Analysis, exploration, manipulation, and visualization of Cufflinks HTS data.

Goff LT, Cole (2011) cummeRbund: The finishing touch on your Tuxedo workflow. Analysis, exploration, manipulation, and visualization of Cufflinks HTS data.

Goldszmid RS and Trinchieri G (2012) The price of immunity. Nat Immunol 13:932-938.

Greenwood AK, Cech JN, and Peichel CL (2012) Molecular and developmental contributions to divergent pigment patterns in marine and freshwater sticklebacks. Evolution & development 14:351-362.

Gross JB, Furterer A, Carlson BM, and Stahl BA (2013) An Integrated Transcriptome-Wide Analysis of Cave and Surface Dwelling Astyanax mexicanus. PloS one 8:e55659.

Haase D, Roth O, Kalbe M, Schmiedeskamp G, Scharsack JP, Rosenstiel P, and Reusch TBH (2013) Absence of major histocompatibility complex class II mediated immunity in pipefish, *Syngnathus typhle*: evidence from deep transcriptome sequencing. Biology Letters 9.

Hamilton AJ and Baulcombe DC (1999) A species of small antisense RNA in posttranscriptional gene silencing in plants. Science 286:950-952.

Henrich T, Benesh D, and Kalbe M (2013) Hybridization between two cestode species and its consequences for intermediate host range. Parasites & Vectors 6:33.

Horvath P and Barrangou R (2010) CRISPR/Cas, the immune system of bacteria and archaea. Science 327:167-170.

Jakobsen PJ, Scharsack JP, Hammerschmidt K, Deines P, Kalbe M, and Milinski M (2012) In vitro transition of *Schistocephalus solidus* (Cestoda) from coracidium to procercoid and from procercoid to plerocercoid. Experimental parasitology 130:267-273.

Janeway C, Murphy K, Travers P, Walport M, and Janeway C (2008) Janeway's immunobiology. Garland Science.

Jobling MA, Hurles M, and Tyler-Smith C (2004) Human evolutionary genetics : origins, peoples & disease. Garland Science, New York.

Jokela J, Schmid-Hempel P, and Rigby MC (2000) Dr. Pangloss restrained by the Red Queen – steps towards a unified defence theory. Oikos 89:267-274.

Jones FC, Grabherr MG, Chan YF, Russell P, Mauceli E, Johnson J, Swofford R, Pirun M, Zody MC, White S, Birney E, Searle S, Schmutz J, Grimwood J, Dickson MC, Myers RM, Miller CT, Summers BR, Knecht AK, Brady SD, Zhang H, Pollen AA, Howes T, Amemiya C, Baldwin J, Bloom T, Jaffe DB, Nicol R, Wilkinson J, Lander ES, Di Palma F, Lindblad-Toh K, and Kingsley DM (2012) The genomic basis of adaptive evolution in threespine sticklebacks. Nature 484:55-61.

Kalbe M, Eizaguirre C, Dankert I, Reusch TBH, Sommerfeld RD, Wegner KM, and Milinski M (2009) Lifetime reproductive success is maximized with optimal major histocompatibility complex diversity. Proceedings of the Royal Society B: Biological Sciences 276:925-934.

Kalbe M and Kurtz J (2006) Local differences in immunocompetence reflect resistance of sticklebacks against the eye fluke Diplostomum pseudospathaceum. Parasitology 132:105-116.

Kalbe M, Wegner KM, and Reusch TBH (2002) Dispersion patterns of parasites in 0+ year three-spined sticklebacks: a cross population comparison. Journal of Fish Biology 60:1529-1542.

Karvonen A, Rellstab C, Louhi K-R, and Jokela J (2012) Synchronous attack is advantageous: mixed genotype infections lead to higher infection success in trematode parasites. Proceedings of the Royal Society B: Biological Sciences 279:171-176.

Katz Y, Wang ET, Airoldi EM, and Burge CB (2010) Analysis and design of RNA sequencing experiments for identifying isoform regulation. Nature methods 7:1009-1015.

Kawahara R, Miya M, Mabuchi K, Lavoue S, Inoue JG, Satoh TP, Kawaguchi A, and Nishida M (2008) Interrelationships of the 11 gasterosteiform families (sticklebacks, pipefishes, and their relatives): A new perspective based on whole mitogenome sequences from 75 higher teleosts. Mol Phylogenet Evol 46:224-236.

Kim KD, Zhao J, Auh S, Yang X, Du P, Tang H, and Fu YX (2007) Adaptive immune cells temper initial innate responses. Nature medicine 13:1248-1252.

Koehler AV and Poulin R (2012) Clone-specific immune reactions in a trematode-crustacean system. Parasitology 139:128-136.

Koehler AV, Springer YP, Randhawa HS, Leung TLF, Keeney DB, and Poulin R (2012) Genetic and phenotypic influences on clone-level success and host specialization in a generalist parasite. Journal of Evolutionary Biology 25:66-79.

Kumar H, Kawai T, and Akira S (2011) Pathogen Recognition by the Innate Immune System. International Reviews of Immunology 30:16-34.

Kurtz J (2004) Memory in the innate and adaptive immune systems. Microbes and Infection 6:1410-1417.

Kurtz J and Franz K (2003) Innate defence: evidence for memory in invertebrate immunity. Nature 425:37-38.

Kurtz J, Kalbe M, Aeschlimann PB, Häberli MA, Wegner KM, Reusch TBH, and Milinski M (2004) Major histocompatibility complex diversity influences parasite resistance and innate immunity in sticklebacks. Proceedings of the Royal Society of London. Series B: Biological Sciences 271:197-204.

Kurtz J, Wegner KM, Kalbe M, Reusch TB, Schaschl H, Hasselquist D, and Milinski M (2006) MHC genes and oxidative stress in sticklebacks: an immuno-ecological approach. Proceedings. Biological sciences / The Royal Society 273:1407-1414.

Kvam VM, Liu P, and Si Y (2012) A comparison of statistical methods for detecting differentially expressed genes from RNA-seq data. American journal of botany 99:248-256.

Kvarnemo C, Mobley KB, Partridge C, Jones AG, and Ahnesjo I (2011) Evidence of paternal nutrient provisioning to embryos in broad-nosed pipefish *Syngnathus typhle*. J Fish Biol 78:1725-1737.

Landis SH, Kalbe M, Reusch TB, and Roth O (2012) Consistent pattern of local adaptation during an experimental heat wave in a pipefish-trematode host-parasite system. PloS one 7:e30658.

Langmead B, Trapnell C, Pop M, and Salzberg S (2009) Ultrafast and memory-efficient alignment of short DNA sequences to the human genome. Genome biology 10.

Lazzaro BP and Little TJ (2009) Immunity in a variable world. Philosophical Transactions of the Royal Society B: Biological Sciences 364:15-26.

le Rouzic A, Ostbye K, Klepaker TO, Hansen TF, Bernatchez L, Schluter D, and Vollestad LA (2011) Strong and consistent natural selection associated with armour reduction in sticklebacks. Mol Ecol 20:2483-2493.

Leder EH, Cano JM, Leinonen T, O'Hara RB, Nikinmaa M, Primmer CR, and Merila J (2010) Female-Biased Expression on the X Chromosome as a Key Step in Sex Chromosome Evolution in Threespine Sticklebacks. Mol Biol Evol 27:1495-1503.

Leder EH, Merila J, and Primmer CR (2009) A flexible whole-genome microarray for transcriptomics in three-spine stickleback (*Gasterosteus aculeatus*). BMC genomics 10:426.

Leinonen T, Herczeg G, Cano JM, and Merila J (2011) Predation-imposed selection on threespine stickleback (*Gasterosteus aculeatus*) morphology: a test of the refuge use hypothesis. Evolution 65:2916-2926.

Lenz TL, Eizaguirre C, Rotter B, Kalbe M, and Milinski M (2012) Exploring local immunological adaptation of two stickleback ecotypes by experimental infection and transcriptome-wide digital gene expression analysis. Molecular Ecology:n/a-n/a.

Lenz TL, Eizaguirre C, Rotter B, Kalbe M, and Milinski M (2013) Exploring local immunological adaptation of two stickleback ecotypes by experimental infection and transcriptome-wide digital gene expression analysis. Mol Ecol 22:774-786.

Lenz TL, Eizaguirre C, Scharsack JP, Kalbe M, and Milinski M (2009a) Disentangling the role of MHC-dependent 'good genes' and 'compatible genes' in mate-choice decisions of three-spined sticklebacks *Gasterosteus aculeatus* under semi-natural conditions. J Fish Biol 75:2122-2142.

Lenz TL, Wells K, Pfeiffer M, and Sommer S (2009b) Diverse MHC IIB allele repertoire increases parasite resistance and body condition in the Long-tailed giant rat (*Leopoldamys sabanus*). BMC evolutionary biology 9:269.

Leveelahti L, Leskinen P, Leder EH, Waser W, and Nikinmaa M (2011) Responses of threespine stickleback (*Gasterosteus aculeatus*, L) transcriptome to hypoxia. Comp Biochem Phys D 6:370-381.

Li C, Zhang Y, Wang R, Lu J, Nandi S, Mohanty S, Terhune J, Liu Z, and Peatman E (2012) RNA-seq analysis of mucosal immune responses reveals signatures of intestinal barrier disruption and pathogen entry following *Edwardsiella ictaluri* infection in channel catfish, *Ictalurus punctatus*. Fish Shellfish Immunol 32:816-827.

Li H and Durbin R (2009) Fast and accurate short read alignment with Burrows-Wheeler transform. Bioinformatics 25:1754-1760.

Little TJ, O'Connor B, Colegrave N, Watt K, and Read AF (2003) Maternal transfer of strain-specific immunity in an invertebrate. Current biology : CB 13:489-492.

Louhi K-R, Karvonen A, Rellstab C, and Jokela J (2010) Is the population genetic structure of complex life cycle parasites determined by the geographic range of the most motile host? Infection, Genetics and Evolution 10:1271-1277.

Magnadóttir B (2006) Innate immunity of fish (overview). Fish & Shellfish Immunology 20:137-151.

Mardis ER (2011) A decade's perspective on DNA sequencing technology. Nature 470:198-203.

Marioni JC, Mason CE, Mane SM, Stephens M, and Gilad Y (2008) RNA-seq: An assessment of technical reproducibility and comparison with gene expression arrays. Genome Research 18:1509-1517.

Martin JA and Wang Z (2011) Next-generation transcriptome assembly. Nature reviews. Genetics 12:671-682.

Maskos U and Southern EM (1992) Oligonucleotide hybridizations on glass supports: a novel linker for oligonucleotide synthesis and hybridization properties of oligonucleotides synthesised in situ. Nucleic acids research 20:1679-1684.

Matsunaga T and Rahman A (1998) What brought the adaptive immune system to vertebrates? - The jaw hypothesis and the seahorse. Immunol Rev 166:177-186.

Matthews B, Harmon LJ, M'Gonigle L, Marchinko KB, and Schaschl H (2010) Sympatric and allopatric divergence of MHC genes in threespine stickleback. PloS one 5:e10948.

McCairns RJS, Bourget S, and Bernatchez L (2011) Putative causes and consequences of MHC variation within and between locally adapted stickleback demes. Molecular Ecology 20:486-502.

Medzhitov R and Janeway Jr CA (1997) Innate Immunity: The Virtues of a Nonclonal System of Recognition. Cell 91:295-298.

Mestas J and Hughes CCW (2004) Of Mice and Not Men: Differences between Mouse and Human Immunology. The Journal of Immunology 172:2731-2738.

Mikeš L and Horák P (2001) A protein with lectin activity in penetration glands of *Diplostomum pseudospathaceum* cercariae. International journal for parasitology 31:245-252.

Miller JR, Koren S, and Sutton G (2010) Assembly algorithms for next-generation sequencing data. Genomics 95:315-327.

Morand S, Robert F, and Connors VA (1995) Complexity in Parasite Life-Cycles - Population Biology of Cestodes in Fish. J Anim Ecol 64:256-264.

Morera D, Roher N, Ribas L, Balasch JC, Donate C, Callol A, Boltana S, Roberts S, Goetz G, Goetz FW, and MacKenzie SA (2011) RNA-Seq reveals an integrated immune response in nucleated erythrocytes. PloS one 6:e26998.

Mortazavi A, Williams BA, McCue K, Schaeffer L, and Wold B (2008) Mapping and quantifying mammalian transcriptomes by RNA-Seq. Nat Meth 5:621-628.

Mundry M, Bornberg-Bauer E, Sammeth M, and Feulner PG (2012) Evaluating characteristics of de novo assembly software on 454 transcriptome data: a simulation approach. PloS one 7:e31410.

Nakamura K, Oshima T, Morimoto T, Ikeda S, Yoshikawa H, Shiwa Y, Ishikawa S, Linak MC, Hirai A, Takahashi H, Altaf-Ul-Amin M, Ogasawara N, and Kanaya S (2011) Sequence-specific error profile of Illumina sequencers. Nucleic acids research.

Nam D and Kim SY (2008) Gene-set approach for expression pattern analysis. Brief Bioinform 9:189-197.

Near TJ, Eytan RI, Dornburg A, Kuhn KL, Moore JA, Davis MP, Wainwright PC, Friedman M, and Smith WL (2012) Resolution of ray-finned fish phylogeny and timing of diversification. Proceedings of the National Academy of Sciences of the United States of America 109:13698-13703.

Nish S and Medzhitov R (2011) Host Defense Pathways: Role of Redundancy and Compensation in Infectious Disease Phenotypes. Immunity 34:629-636.

Nowak MA, Tarczyhornoch K, and Austyn JM (1992) The optimal number of major histocompatibility complex molecules in an individual. Proc Natl Acad Sci USA 89:10896-10899.

Oettinger MA, Schatz DG, Gorka C, and Baltimore D (1990) Rag-1 and Rag-2, Adjacent Genes That Synergistically Activate V(D)J Recombination. Science 248:1517-1523.

Ordas A, Hegedus Z, Henkel CV, Stockhammer OW, Butler D, Jansen HJ, Racz P, Mink M, Spaink HP, and Meijer AH (2011) Deep sequencing of the innate immune transcriptomic response of zebrafish embryos to *Salmonella* infection. Fish Shellfish Immunol 31:716-724.

Owen SF, Barber I, and Hart PJB (1993) Low level infection by eye fluke, Diplostomum spp., affects the vision of three-spined sticklebacks, *Gasterosteus aculeatus*. Journal of Fish Biology 42:803-806.

Paczolt KA and Jones AG (2010) Post-copulatory sexual selection and sexual conflict in the evolution of male pregnancy. Nature 464:401-404.

Palstra AP, Beltran S, Burgerhout E, Brittijn SA, Magnoni LJ, Henkel CV, Jansen HJ, van den Thillart GE, Spaink HP, and Planas JV (2013) Deep RNA sequencing of the skeletal muscle transcriptome in swimming fish. PloS one 8:e53171.

Parker GA, Chubb JC, Ball MA, and Roberts GN (2003) Evolution of complex life cycles in helminth parasites. Nature 425:480-484.

Peitsch MC and Tschopp J (1991) Assembly of macromolecular pores by immune defense systems. Current opinion in cell biology 3:710-716.

Penn D and Potts W (1998) MHC-disassortative mating preferences reversed by cross-fostering. Proceedings. Biological sciences / The Royal Society 265:1299-1306.

Petzold A, Reichwald K, Groth M, Taudien S, Hartmann N, Priebe S, Shagin D, Englert C, and Platzer M (2013) The transcript catalogue of the short-lived fish Nothobranchius furzeri provides insights into age-dependent changes of mRNA levels. BMC genomics 14:185.

Press CM and Evensen Ø (1999) The morphology of the immune system in teleost fishes. Fish & Shellfish Immunology 9:309-318.

Rauch G, Kalbe M, and B.H. Reusch T (2008) Partitioning average competition and extreme-genotype effects in genetically diverse infections. Oikos 117:399-405.

Rauch G, Kalbe M, and Reusch TBH (2005) How a complex life cycle can improve a parasite's sex life. Journal of Evolutionary Biology 18:1069-1075.

Rauch G, Kalbe M, and Reusch TBH (2006) One day is enough: rapid and specific host–parasite interactions in a stickleback-trematode system. Biology Letters 2:382-384.

Rauta PR, Nayak B, and Das S (2012) Immune system and immune responses in fish and their role in comparative immunity study: A model for higher organisms. Immunology letters 148:23-33.

Reusch TB, Wegner KM, and Kalbe M (2001a) Rapid genetic divergence in postglacial populations of threespine stickleback (*Gasterosteus aculeatus*): the role of habitat type, drainage and geographical proximity. Mol Ecol 10:2435-2445.

Reusch TBH, Haberli MA, Aeschlimann PB, and Milinski M (2001b) Female sticklebacks count alleles in a strategy of sexual selection explaining MHC polymorphism. Nature 414:300-302.

Reusch TBH, Rauch G, and Kalbe M (2004) Polymorphic microsatellite loci for the trematode *Diplostomum pseudospathaceum*. Molecular Ecology Notes 4:577-579.

Rieger JK, Haase D, Reusch TB, and Kalbe M (2013) Genetic compatibilities, outcrossing rates and fitness consequences across life stages of the trematode *Diplostomum pseudospathaceum*. International journal for parasitology 43:485-491.

Robalino J, Bartlett T, Shepard E, Prior S, Jaramillo G, Scura E, Chapman RW, Gross PS, Browdy CL, and Warr GW (2005) Double-stranded RNA induces sequence-specific antiviral silencing in addition to nonspecific immunity in a marine shrimp: convergence of RNA interference and innate immunity in the invertebrate antiviral response? Journal of virology 79:13561-13571.

Roberts A, Pimentel H, Trapnell C, and Pachter L (2011) Identification of novel transcripts in annotated genomes using RNA-Seq. Bioinformatics 27:2325-2329.

Robinson MD, McCarthy DJ, and Smyth GK (2010a) edgeR: a Bioconductor package for differential expression analysis of digital gene expression data. Bioinformatics 26:139-140.

Robinson MD, McCarthy DJ, and Smyth GK (2010b) edgeR: a Bioconductor package for differential expression analysis of digital gene expression data. Bioinformatics 26:139-140.

Roth O, Keller I, Landis SH, Salzburger W, and Reusch TB (2012a) Hosts are ahead in a marine host-parasite coevolutionary arms race: innate immune system adaptation in pipefish *Syngnathus typhle* against Vibrio phylotypes. Evolution 66:2528-2539.

Roth O, Klein V, Beemelmanns A, Scharsack JP, and Reusch TB (2012b) Male pregnancy and biparental immune priming. Am Nat 180:802-814.

Roth O, Sadd BM, Schmid-Hempel P, and Kurtz J (2009) Strain-specific priming of resistance in the red flour beetle, *Tribolium castaneum*. P Roy Soc B-Biol Sci 276:145-151.

Roth O, Scharsack JP, Keller I, and Reusch TB (2011) Bateman's principle and immunity in a sex-role reversed pipefish. J Evol Biol 24:1410-1420.

Sadd BM and Schmid-Hempel P (2006) Insect immunity shows specificity in protection upon secondary pathogen exposure. Current Biology 16:1206-1210.

Sanogo YO, Hankison S, Band M, Obregon A, and Bell AM (2011) Brain Transcriptomic Response of Threespine Sticklebacks to Cues of a Predator. Brain Behav Evolut 77:270-285.

Sarropoulou E, Galindo-Villegas J, Garcia-Alcazar A, Kasapidis P, and Mulero V (2012) Characterization of European sea bass transcripts by RNA SEQ after oral vaccine against V. anguillarum. Mar Biotechnol (NY) 14:634-642.

Scharsack JP, Kalbe M, Derner R, Kurtz J, and Milinski M (2004) Modulation of granulocyte responses in three-spined sticklebacks Gasterosteus aculeatus infected with the tapeworm *Schistocephalus solidus*. Diseases of aquatic organisms 59:141-150.

Schmid-Hempel P (2005) Natural insect host-parasite systems show immune priming and specificity: puzzles to be solved. Bioessays 27:1026-1034.

Schmid-Hempel P and Ebert D (2003) On the evolutionary ecology of specific immune defence. Trends in ecology & evolution 18:27-32.

Schmieder R and Edwards R (2011) Quality control and preprocessing of metagenomic datasets. Bioinformatics 27:863-864.

Schroder NW and Schumann RR (2005) Single nucleotide polymorphisms of Toll-like receptors and susceptibility to infectious disease. The Lancet infectious diseases 5:156-164.

Schulenburg H, Boehnisch C, and Michiels NK (2007) How do invertebrates generate a highly specific innate immune response? Mol Immunol 44:3338-3344.

Seppälä O, Karvonen A, Tellervo Valtonen E, and Jokela J (2009) Interactions among co-infecting parasite species: a mechanism maintaining genetic variation in parasites? Proceedings of the Royal Society B: Biological Sciences 276:691-697.

Shanker A (2010) Adaptive control of innate immunity. Immunology letters 131:107-112.

Shendure J and Ji H (2008) Next-generation DNA sequencing. Nature biotechnology 26:1135-1145.

Smyth JD (1946) Studies on tapeworm physiology, the cultivation of *Schistocephalus solidus* in vitro. The Journal of experimental biology 23:47-70.

Soneson C and Delorenzi M (2013) A comparison of methods for differential expression analysis of RNA-seq data. BMC bioinformatics 14:91.

Star B and Jentoft S (2012) Why does the immune system of Atlantic cod lack MHC II? Bioessays 34:648-651.

Star B, Nederbragt AJ, Jentoft S, Grimholt U, Malmstrom M, Gregers TF, Rounge TB, Paulsen J, Solbakken MH, Sharma A, Wetten OF, Lanzen A, Winer R, Knight J, Vogel J-H, Aken B, Andersen O, Lagesen K, Tooming-Klunderud A, Edvardsen RB, Tina KG, Espelund M, Nepal C, Previti C, Karlsen BO, Moum T, Skage M, Berg PR, Gjoen

T, Kuhl H, Thorsen J, Malde K, Reinhardt R, Du L, Johansen SD, Searle S, Lien S, Nilsen F, Jonassen I, Omholt SW, Stenseth NC, and Jakobsen KS (2011) The genome sequence of Atlantic cod reveals a unique immune system. Nature 477:207-210.

Stein LD (2010) The case for cloud computing in genome informatics. Genome biology 11:207.

Su LF, Kidd BA, Han A, Kotzin JJ, and Davis MM (2013) Virus-Specific CD4(+) Memory-Phenotype T Cells Are Abundant in Unexposed Adults. Immunity 38:373-383.

Sun F, Peatman E, Li C, Liu S, Jiang Y, Zhou Z, and Liu Z (2012) Transcriptomic signatures of attachment, NF-kappaB suppression and IFN stimulation in the catfish gill following columnaris bacterial infection. Developmental and comparative immunology 38:169-180.

Sun JC, Beilke JN, and Lanier LL (2009) Adaptive immune features of natural killer cells. Nature 457:557-561.

Sunyer JO (2013) Fishing for mammalian paradigms in the teleost immune system. Nat Immunol 14:320-326.

Tinbergen N (1952) The Curious Behavior of the Stickleback. Scientific American 187:22-26.

Tort L, Balasch JC, and Mackenzie S (2003) Fish immune system. A crossroads between innate and adaptive responses. Immunología 22:277-286.

Trapnell C, Pachter L, and Salzberg SL (2009) TopHat: discovering splice junctions with RNA-Seq. Bioinformatics 25:1105-1111.

Trapnell C, Williams BA, Pertea G, Mortazavi A, Kwan G, van Baren MJ, Salzberg SL, Wold BJ, and Pachter L (2010) Transcript assembly and quantification by RNA-Seq reveals unannotated transcripts and isoform switching during cell differentiation. Nat Biotech 28:511-515.

Venables WN, Ripley BD, and Venables WN (2002) Modern applied statistics with S. Springer, New York.

Vijay N, Poelstra JW, Kunstner A, and Wolf JB (2013) Challenges and strategies in transcriptome assembly and differential gene expression quantification. A comprehensive in silico assessment of RNA-seq experiments. Mol Ecol 22:620-634.

Villasenor-Cardoso MI and Ortega E (2011) Polymorphisms of innate immunity receptors in infection by parasites. Parasite immunology 33:643-653.

Viney M and Cable J (2011) Macroparasite life histories. Current biology : CB 21:R767-774.

Wang Z, Gerstein M, and Snyder M (2009) RNA-Seq: a revolutionary tool for transcriptomics. Nature reviews. Genetics 10:57-63.

Wedekind C, Seebeck T, Bettens F, and Paepke AJ (1995) MHC-dependent mate preferences in humans. Proceedings. Biological sciences / The Royal Society 260:245-249.

Wegner KM, Kalbe M, Kurtz J, Reusch TBH, and Milinski M (2003a) Parasite Selection for Immunogenetic Optimality. Science 301:1343.

Wegner KM, Kalbe M, Rauch G, Kurtz J, Schaschl H, and Reusch TB (2006) Genetic variation in MHC class II expression and interactions with MHC sequence polymorphism in three-spined sticklebacks. Mol Ecol 15:1153-1164.

Wegner KM, Kalbe M, and Reusch TBH (2007) Innate versus adaptive immunity in sticklebacks: evidence for trade-offs from a selection experiment. Evol Ecol 21:473-483.

Wegner KM, Reusch TBH, and Kalbe M (2003b) Multiple parasites are driving major histocompatibility complex polymorphism in the wild. Journal of Evolutionary Biology 16:224-232.

Westerdahl H, Waldenstrom J, Hansson B, Hasselquist D, von Schantz T, and Bensch S (2005) Associations between malaria and MHC genes in a migratory songbird. P Roy Soc B-Biol Sci 272:1511-1518.

Whitehead A and Crawford DL (2006) Variation within and among species in gene expression: raw material for evolution. Molecular Ecology 15:1197-1211.

Whyte SK (2007) The innate immune response of finfish – A review of current knowledge. Fish & Shellfish Immunology 23:1127-1151.

Whyte SK, Chappell LH, and Secombes CJ (1990) Protection of rainbow trout, Oncorhynchus mykiss (Richardson), against *Diplostomum spathaceum* (Digenea): the role of specific antibody and activated macrophages. Journal of Fish Diseases 13:281-291.

Wilson AB and Orr JW (2011) The evolutionary origins of Syngnathidae: pipefishes and seahorses. J Fish Biol 78:1603-1623.

Windsor DA (1997) Equal rights for parasites. Perspectives in biology and medicine 40:222-229.

Windsor DA (1998) Most of the species on Earth are parasites. International journal for parasitology 28:1939-1941.

Winkelstein JA (1973) Opsonins: their function, identity, and clinical significance. The Journal of pediatrics 82:747-753.

Woelfing B, Traulsen A, Milinski M, and Boehm T (2009) Does intra-individual major histocompatibility complex diversity keep a golden mean? Philosophical transactions of the Royal Society of London. Series B, Biological sciences 364:117-128.

Workenhe ST, Rise ML, Kibenge MJT, and Kibenge FSB (2010) The fight between the teleost fish immune response and aquatic viruses. Mol Immunol 47:2525-2536.

Yang CH, Wang C, Chen X, Chen SD, Zhang YN, Zhi F, Wang JJ, Li LM, Zhou XJ, Li NY, Pan H, Zhang JF, Zen K, Zhang CY, and Zhang CN (2013) Identification of seven serum microRNAs from a genome-wide serum microRNA expression profile as potential noninvasive biomarkers for malignant astrocytomas. Int J Cancer 132:116-127.

Yao ZL, Wang H, Chen L, Zhou K, Ying CQ, and Lai QF (2012) Transcriptomic profiles of Japanese medaka (*Oryzias latipes*) in response to alkalinity stress. Genetics and molecular research : GMR 11:2200-2246.

Zaballos Á, Gutiérrez J, Varona R, Ardavín C, and Márquez G (1999) Cutting Edge: Identification of the Orphan Chemokine Receptor GPR-9-6 as CCR9, the Receptor for the Chemokine TECK. The Journal of Immunology 162:5671-5675.

Zang SZ, Guo RF, Zhang L, and Lu YY (2007) Integration of statistical inference methods and a novel control measure to improve sensitivity and specificity of data analysis in expression profiling studies. J Biomed Inform 40:552-560.

Zhang Y, Stupka E, Henkel CV, Jansen HJ, Spaink HP, and Verbeek FJ (2011) Identification of common carp innate immune genes with whole-genome sequencing and RNA-Seq data. Journal of integrative bioinformatics 8:169.

Appendix

Appendix Chapter 1

The following Appendix is identical to the supplementary material from the publication:
Haase D, Roth O, Kalbe M, Schmiedeskamp G, Scharsack JP, Rosenstiel P, Reusch TBH (2013) Absence of major histocompatibility complex class II mediated immunity in pipefish, *Syngnathus typhle*: evidence from deep transcriptome sequencing. Biol. Lett. 2013 Feb 27;9(2)

Content

Supplementary material S.1.1 Nucleotide sequences and accession numbers of nucleotide sequences retrieved from GENBANK used to query all 750 mio. Illumina reads via a reciprocal tBLASTx-approach.

Supplementary material S.1.2 Detailed description of validation of bioinformatical search strategies to identify MHC class IIβ genes

Supplementary Table S.1.1 Overview on PCR-primers used in the targeted cloning

Supplementary Table S.1.2 Nucleotide alignment of MHC class IIβ coding sequences of 6 Actinopterygii species along with the seahorse (*Hippocampus abdominalis*, Syngnathidae).

Supplementary Table S.1.3 *Syngnathus typhle*: expressed sequence tag (EST) library types, tissue, sequence reads statistics

Supplementary Table S.1.4 *Syngnathus typhle*: mapping statistics of reads

Supplementary Table S.1.5 Bit scores and read statistics for 7 immune genes identified via reciprocal tblastx search in 750 mio *S. typhle* ESTs.

Supplementary Table S.1.6 Read and annotation statistics of 4 immune genes with contigs that were identified in the reciprocal tBLASTx search

Supplementary Table S.1.7 Amino acid alignment of putative invariant chain genes from 10 teleost species including *Syngnathus typhle*

Supplementary material S.1.1 Nucleotide sequences and accession numbers of nucleotide sequences retrieved from GENBANK or ENSEMBL used to query all 750 mio. Illumina reads via a reciprocal tblastx-approach.

```
>gi|226443287 Salmo salar T-cell surface glycoprotein CD4 (cd4), mRNA
AGATTTCAGATAAAATGTTCAATATGAAGACTTTCTCCTGGTTTGTGTTCGCCCTGTGTATTCTCCATGT
GGTGGGTGAGGTGATCTACAAGACAAAGGGGCACTCTGTCAATATTGATTGCGGATTCAAGACGTCTAAC
AAGGATGTAGAGTGGAGACATAAAGCTGTGGGTGGAAGTGAATCTGTGCTGATCATGGACATTAAAGGGA
AGAGTGGCAAGCAGCGGAAAGGAAAGGCTCCCATGGTTGAAAGGGCGAAAGTGAGAGGGGACGGGCTGGA
AATCTCTGCTCTAAATGATGGTGATGCCGGACTTTACATCTGTATGGTGGACAGGAAAGAGATGGATCAC
AGACTCGACTTTGTCACAGTCAATGTCCACCCCTCCAATGTCCTCATCGAAGGCACCAATGCTATCCTCG
AGTGCCAGGTGACAGGAGTGGATCCCTTGCCCAGTGTGGAGTGGCGTAGTCCAGGTGGAACGGTGGAAGG
GGCCCCTGGACGACCTGGCTCTTGGAAAGTCTCTTTCAACTCTGTGGCCCTGTCAGACACAGGAGACTGG
ACATGTCAGATTACTCAGGATGAGAAGACACACAAAGAGACTCAGACCATCAACGTGAGAAGTTTGTCGC
CGGACAAGGGCCAAGATGATGGGCAGGGGCACAGTGGACCTAACTCTAATGTAAACACAGTGACACCTTG
CAATCACTGTACCACAGGCAGCCAGCAGCCCGTTGAGTGGGTGTCCATTCTGGGCTTAAGCCTGTGGGTG
TGGGTGGCAGTGGGAGCAGGATGCCTGGTGGTGGTCTTACTCCTGGTGACCATTGTTCTCCTGCACCTCA
GGAACAAAAGAATGAAGAGAAGAGACCGGAAGATGAAGAACATCAGAGTGCCCCTGAAGTCCAACGACTA
CTGCCAGTGTAACCGCACACTAGAGGGTCCACCACGGAGGACGCAGTGAGAGAAGCCTTCGGCTGTACCA
CGGAAACAGCGCTGATGGAGCGGAGTATTATGGGCTGGAACATGATTGCTTGACGACACGGGGCGGATGG
AAGAATGATAGAGAGAGAGAGAAAAGTAGTCTTATACAGTTAGAGCGATTACAAGGGAGAGAGAGAGAAA
GAGAGGGGGGAGATCATGTAAATGGGCTTATGTCTGTTTCAAAAATATGAATGATGAAATTATATAAACT
GAAAATCACACATTGAAAATAATCACATATTCTTACCTATATGTTATTGAATGTCATCTGACGTCTTCCT
CGCATTGTCAGAGCATCCTCTACTGCATTGCATCTTTGTGCTTAGATCATTTTCAATGATTATTCATTTT
CACACAAAGACGGATACTTATACTGTACGGTTTTAGAATGATTCTTGCTGTGATATCATTTAGTGTGGCA
TATTTACAAATGCTTGTTATGTTATGAATTAATATACCTGTTAAATTAAAGTGTTTTCTTGTTGAAGGGA
ATATAGATCA

>gi|319921951|gb|GU550706.1| Siniperca chuatsi T cell surface glycoprotein
CD4 mRNA, complete cds
GGACTCAACAACAGTTACGTGTGACTGAGATGAAGAACTTAATTAAATCCATCCTCATTCTCATCCCTGT
GCTCATGTCAACAACAGGGACAGAAGAGGTGGTATATGCTCAGGTGGGAGATACGGTTACGCTAAAGCCT
CCAAGGAGGGATAATTTAAAGGATCATTATTTGTACTGGTCATTTGGTCATGAGGACCTTCAACTTGCCT
GGCGGAATCCCCATGGCGGACAGGGGTTCGACAAAAGCCCATGGAACCATTCTTTGTCCATGTCTGACGA
CTCACTGGTCATCCACCACATCAAACAAGAACACTTTGGGACTTTTATCTGTAAACTGACTATGAATCGT
AATTCATTCGTAATCACATATAAACTACTCAAACTCAACGTGATTATGAACCCACCATTTCCTCTGTTGC
CTTTGGAATCTCTGTCTCTGGTCTGCAACGCAGAGTCTCCTCAGAGTCTCATGAAGCCAGAGATATACTG
GCTGACTCCCCAGGGAGAGAAAATAAAAATTAACGAAGGAAGACTCACCATGAGAGCCACAAGCCAACAC
AGTGGCGAGTGGACCTGTGTTGTGACAAATGGTGAAAAAGAATACAAGGCCACAGAATCTGTTATAGTTG
TGGACCTCTCCCCAGCTCCTTTACGTCCTCAGTATACGTCTAAATCCTCGCCTCTCACTGTCCCCTCTCC
TCAGAGTCTCATGAAGCCAGAGATATACTGGCTGACTCCCCAGGGAGAGAAAATAAAAATTAACGAAGGA
AGACTCACCATGAGAGCCACAAGCCAACACAGTGGCGAGTGGACCTGTGTTGTGACAAATGGTGAAAAAG
GATACAAGGCCACAAAATCTGTTATAGTTGTGGACCTCTCCCCAGCTCCTTTACGTCCTCAGTATACGTC
TAAATCCTCGCCTCTCACTGTCCCCTGTTCCATTGCCCCTCACATCTCCTGGGACAAAATCATAGCCAAG
GGCATCCAGGGAGCTCACTGGGACTTCTTCCCTATATCAGGTCTCAGTTCTGCTGTTCCACAGAAGCTCT
TCTCCCTGTGTCTGGGGGATGAACTGACCTGGAAGACAGAAAAAAACACAGGACTGAAACCCGTGAAAGA
CCTTAAAAAAGGAAATTTGACTTTGATCGGAAAACTACGGAGTGAAGAAGACGCAGGGGACTATGTGTGC
GCCCTGAATTTCACAAATGGTGTAGTTCTGAAGAGGACTGTACATGTAAATGTGCTGCAAATCATCTCCT
CCCCAGGAACAGACTTCATTTCTGGCCAGCAGGTCAACCTGACTTGCAGCATTGGCCATCCGCTGCCCTC
TGACCTGCAAGTGAAATGGATCCCACCTAAAGCATTGTCCCTTCCGTCTCTGAGACCTGACCATCACCAT
CTCACCATCCCGGAAGTGGGGACAGGAGATAGCGGACCATGGAGGTGTGAGCTGTGGCAGAACAGCACAC
TGCTGACGTCAGCTACGATAGTGCTGAAGATTGAATCCAAGCTGAGTGTGTGGATGCTGGTGATCATATG
TAGTGTCATAGTCATCGCAATCCTCCTCCTCGTACTCATTTTCATCCTCTACCGACGCAAACAACGGAAG
ATGAGACACCTCAGGCATCGACTCTGCCAATGCAAAAACCCAAAGCCCAAAGGATTCTACAGAACATAAT
ATCTCCCACAAAGACATTTTCAAGAGGACATCGCAACCAATTGAATTTCTGTCCAGATAAGATGGATTTT
TCTGTCATATTTACTAAACTGTGAACCTCTGTTAGGTGTGTGATGCGGGCCTGAAAGTTCAGTCATTGTT
GAAATGTCAGAAAATGTATTTTACAGTTGTACATATCAGCCAGTTTGGATAGTTTTTATATTTGTAATGT
AACATGTAATTGATTTCTTCGGGACTTTTATATTTCACAGAATTTCTCATTGAAACTATGCTATGTTCCA
```

CCTAATTATCATTTTAACATTATTGTTTGCGATTATTACTGTTAATAATTGTTTATGTTATACTCTTTCA
TTCACATTGTTTTCAGATTTGTCTTTTTGTCATGTTATGTAATTTTTACGACGCTCTATGATACTGCTTG
TTACTTTTATAAATATTTACCAATATATAATTTAGAAAGTGAGCAAATGTTGATACTAAATATACAAATT
AGGATACTTAAACCAAATAGATCAAATTTTTGTCAGAAAATTGTTTATTTGTTGAAACAAACAAACTGTA
AAAACAGTTGCCAGTGAAGTTTTTGAATAAAGTATCAATATCTTTCACAAAAAAAAAAAAAAAAAAAAAA
AAA

>gi|118344617|ref|NM_001078623.1| Takifugu rubripes T-cell surface glycoprotein CD4 (cd4), mRNA
AGAGCTGAGGTCTTCGCTGTACAGACAACATCACATGTGTCTTCCATCAGAATCAGAATCACCGCGCCAC
ATGCACGCTCGCATCCGCGGAGGAGACCGTGTGAGCGCGTGAAATCCAGCCAGCGTTGGTGCACGCCGCC
AGGCCGGGAGGAAGAAGGCTGCGTGCGGTAGCCGCACGTTACAGGAGCTGAGACGCCAAGCCTCAGAGGG
AACAGAAGCAGGCCAACCGCCGGAGAGGGAGGCGCTTTAAAGGCGAGGCTGCGATAAATACGCCACCTTT
CATCCTGGCCCCAGAACCGGGCCCCGGCGCACACGTATGACCTTCGTCAGCAGACACATTCCGGACATGG
AACCGCTTCCCTCTGGCCTCCTGCTGCTCACTGCGCTCCTGTCAGCATCACGAGCCGAAGAGCTCATATA
TGCCCAGGTGGGACAGACGGTCACTCTGAAACCTCCAGAAAATTATAAGACACCGACCTACTACTTGTCC
TGGCATTTCGGAGAACTTGAGCTGGCCTGGACTAATCACATGAGTGGAAACAAAGTCATAAAACATGAAA
ACTGGGACACGGCATTGTCGGACAACTCTCTGGTTGTGAAAGAAATCCGTCAAAATCAATTTGGGATTTA
CAAATGTAATGTGAATGAGAAGATATGGACCTACAAAGTTCTCCGTCTCAAGGTGTCGGCAGAGCCGCCG
TCTCTGGTGCTTTCTGGACGAACCGTGACTCTGGTCTGCGATGCAGAACCTCCCAACAGTCTGCAGAAGC
CGGGGATACACTGGCTGAACCCACAGGGAGAGAAAATTACCCAGGCGACTCACAGCGTGCAAGTCAGCAG
CCGCCACAGCGGTCGGTGGACCTGCGTCGTCACCCTGGATAGAAAAGAAGCCACGGCCCAGATCTCCGTC
ACGGTGGTCGACCTCTACTCGCCCCCCATGGCGTATACATCCACATCCTCCCCCCTGGCCGTCCCCTGCT
CCGTCCCCAAAGTTTCCTGGGAGCAAATCAAATCCCTGGGCCTCCGAGAGGGACACTGGCAGTTCTTCCC
CAGATCGAAGTCAAACCTGGTTTCTGCTGACGCGCAGAGGCTCTTCACCCTCTCCCTGGAGGAGCCGGTC
TCCTGGAAGGCCAACCAAACCAGAGGCCTGACCCCGGTTTCAGATTTCAAAACCCCTAATCTCTCCTTGG
GCAGAACGCTGGGGAGAGCCAACGACCGCGGTGACTACGTGTGCACCCTGAAGTTTGAAAGCGGCCCACC
GCTCAGCACGACCGTTCGGGTGAACGTGTTGGAAATTGCCGCGTCGCCGGGAACAGTCTTGATTTCGGGC
CAGCAGCTCAACCTGACCTGCGGCCTCGGCGTCCCCCTGACCTCTGACCTGCATCTGAAATGGATCTCAC
CCGAGAGGGCGACAATACGATCCGGCCAGCTCACCATCCCGGCGGTGGGGGCGGGGAATTCCGGGAAGTG
GAGGTGTGAGCTGTGGCGGAACGATACCCGGCTGACGTCAGCCGTGATAACGCTGAAGATTGAGCCCAAG
CTGAGCGTGTGGATGCTGGTGATCATATGCAGCGTCGCAGTCATCGTCCTCCTCCTCCTCCTCCTCGGTT
TCATCCTCTGCCGGCGCAGACGAGCACGGGTGAGACACGTCAGACATCAACTGTGCCAGTGCAAAAACCC
CAAACCTAAAGGCTTCTACAGGACGTGACGCCTCCCGCTGAGTCGACCCCACGAGCTTCAAACTCCTGCC
GGCTGCACTGAGATGAGGCTGCGGGGAAAGTTTAGAGCGCAGAACAAAGTATATTAAACTTGTTTTATTC
GTATCGACCACGTTCTTCCTGTTAGATGTGGACAGGAATAATCCCAATCTGCATCATGTACATTGTAAAT
ATTGCGCAACATTGTTTATTATGTTCTTTAATTCACCGTCATATATGTGATGATGCTCTTGTATGTTATT
GAGCAAATGCTCACAGGCAAATGATAATGGGCATTTAACAATAGCTGATACATAGCATTAAAAATTAGCC
CGACAAAATTAGACGTTTGTTTTTTAAATCAGAATAATTAGAATCAATCTCTCAAAAGAAAAACTAATTC
TTCTGTCTGGTAAAGGGGGGGTTCTAAATAGTAACCAATTATTAGTTTCTAAAAACAAAGGTATGATGTG
AAGATGATCATATTTATTTATTACCACCAGATGTCTGCTGTGCCTCTCCAGCAGTGTCAACACTGCTGTT
TGTCCATTTATTATTTAATTCTTGGCATTTATTCCCCCAGCCATCGTCAGCAGCTCCACTTCCAGAGGCT
GGGTTATTCTAACCGAGCTAATTAAACCAGAGGAGAGCAGGAGTGTCTGTTTATCTCTGCCTGTAGTTCC
TGAGCTTCGATTTGTAGTTGTGATTGAAGTTAAATCTTGCTGGTTGGTCCTTCGGGCTTGTTTTTTAGGC
TCTATTTTTTAACTTCAATTTTCCGGGGTGTCATGTTTATGTTTAACATGGTCCCACATCATCACAATTA
GAAAAATAGCTCTTTCCTAAGACAGCATATAGGTTCTGTGACTAAATGGTGCTAAATGTTCTCCTTACAA
ACCATATAAAACGGTAATTAAATTGATTTATTAAAGGAAATGTGTCGTAAAAAAAAAAAAAAAAAAAAAA
AAAA

>gi|145870286|gb|ES376374.1|ES376374 Tra_Liver_1-3_B01 Guppy pDNR_LIB Tranquille Liver Poecilia reticulata cDNA clone Tra_Liver_1-3_B01 5' similar to low molecular mass polypeptide subunit PSMB8 [Takifugu rubripes], mRNA sequence
GACAAGGAAATCATTGATCAGCTTCGCCAAACGCTTTCTGGTTTCTAGAGCGTTTGTAGGAATTATATCA
GACAGCTATCATATTAAATAAGGTCTGATATTTACGACACAATGGCACTTTTTGAAGTGAGCGGTTTTAA
GCCTTATTCTGAAGTCCGTGCGCAGATTCTTCCGTTCGGTCAGACTCGGCTTGTGGACCGACCGAACCAC
TACACCTTCAACACCAAAACCCAGGAGTTTGCTGTCCCTCTGGGTGAGGACCCCTCCGGGTTTCTAAAGT
CCTGTAACCATGACGGAGGAGTTTGCATTGACCTGAACCATGGTACCACCACTTTGGCTTTCAAGTTCAG
GCATGGAGTCATCGTGGCCGTGGACTCCAGAGCTTCAGCTGGGAACTACCTGGCATCAAAAGATGCCAAC
AAGGTGATAGAAATCAACTCGTACCTACTGGGGACCATGTCAGGTAGCGCAGCCGACTGCCAGCACTGGG
AGCGGCTACTGGCCAAAGAATGCAGGCTGTACAGGTTGAGAAACGGTCACAGGATTTCTGTGGCTGCTGC
ATCAAAGCTGCTGTCAAACATGATGTTGGGCTACAGAGGCATGGGCCTCTCCATGGGAAGCATGATCTGT
GGATGGG

>gi|253945025|gb|GR705396.1|GR705396 cNOnTE2024_D17.ab1_c Tilapia adult testis library Oreochromis niloticus cDNA 5' similar to Proteasome subunit beta type-8 in Bos taurus (Q3T112), mRNA sequence
GGGGAGTCTTCACGATTGAGCTCATTTATGCAAATGGTTGCATCTCGGTATTATTTTGTTTAGAATGTTT
GTATCGTTTTTAAAAGAAAAGAAAATTTAATATTTTAAACGAGCCATTAAAAACCCTTTCACTTTCTATT
TCTTTGTCACGTACAAGGAAATCACCCTTGGCGTCAATCGCATTCGTCCTTTTTAGAAAACTCGAAACCT
ACTAGATATATATACATTTAAAATATAATTTATCTGCTTTAACAGGTTATGGCACTTCTTCAAGTGAGCG
ACTTTCAGTGTGTTTCTGAAGTCCGCGGACAGATTCTTCCAGTGAAACAGAGGTACCTCGTCGACCGAAC
CAACCACTACAATTTTGGGAGCAAAACTCAAGAATTTGCGGTTCCGCCTGGTGTAGAGCCTTCTGGGTTT
CTGAAGTCCTGCAACCGTGATGGAGGTGTGTGTATTGAAATGAACCACGGGACCACCACTCTGGCCTTCA
AGTTCAGGCATGGAGTCATCGTGGCTGTGGACTCCAGAGCTTCAGCTGGCCGTTACTTAGCATCCAACGA
TGTGAACAAGGTGATAGAGATCAACCCATACCTGCTGGGCACCATG

>gi|224230652|gb|GH692384.1|GH692384 CBZB36091.g1 CBZB: Normalized channel catfish cDNA library from head kidney, gill, intestine, spleen, skin and liver (mixed tissue 1, AUK_M) Ictalurus punctatus cDNA 3' similar to zebrafish RefSeq, NP_571467.2, proteasome (prosome, macropain) subunit, beta type, 8 [Danio rerio], mRNA sequence
CAGTGTTTAGTCTGAAAACCATCTTTATTTTCATTACTGAATACAGATACAGGGTTTGTGTGCGTATCAA
AGCTCATGTGCACTCAAAACATTCCTTTCCTGTACTTATGGATTAGATCTGATACGTCCTCCTTGCACAC
CTTAATCCAACCGTCCTCCTTCATGTGATAGAGGTTCACGACTCCACCAGAGTAGGCGTCTCTGTGTGTG
GCGTGAGCAATGCCACGGCGGCCGAGCTCATATGCCTCTTCCACTGTCATATCCTCACGGTAGCCACTGT
CAATCACCCCGTATGCATAGCTGTTACCACAGCCCGTGGAAAACATTTGCCCTGAGAGGCGTGTTCCATT
ATGATCTACATAATAAAGACCAGGACCCTTCTTGTCCCAGCCACAGATCATGCTACCCATAGACAGGCCC
ATGCCTCTATAACCAAGCATCATGTTAGACAGCAGCTTGGAAGCTGCAGACACTGAGATCCTCTGCTTGT
TACGGAGCTGGTAAAGCCTGCACTCCTTAGCCAGAAGTCTCTCCCAATACTGACAATCTGCAGCACTACC
AGACATGGTGCCCAACATGTAAGGGTTGATCTCAATCACCTTATTCGCCTCCTTTGAATCGATATAGCGT
CCAGCCGAGGCTCTGGAGTCGACGGCTACATGACGCCA

>ENSGACG00000001293|PSMB8 (1 of 10)
ATGGCTCTTTTCCAAGTATCTGGTTTGAAGTCTTATGCTGAACTCCGTGAGCAGATTCTTCCAGCCAGAC
AGACGCATCTCTTCGACCGAACCAACCACTACAACTTCGGGACCAAAACGCAGGAATTTGCTGTCCCTCT
GGGTGTAGACCCTTCAGGGTTTCTAGGAACCTGCAGCCGTGATGGTGGTGTGAGTATAGACCTGAACCAC
GGGACGACCACCCTGGCCTTCAAGTTCAGACATGGAGTCATTGTGGCTGTGGACTCCAGAGCCTCAGCAG
GCCGTTACTTGGCGTCCAACGACGTCAACAAGGTGATAGAGATCAACCCCTACCTGCTGGGCACCATGTC
GGGCAGCGCTGCAGACTGCCAGTACTGGGAGAGACTCCTGGCCAAAGAATGCAGGCTGTACAGGCTGAGG
AGCAACCACAGGATCTCTGTGGCTGCTGCCTCCAAGCTGCTGTGCAACATGATGCTGGGCTACAGAGGCA
TGGGCCTCTCTATGGGAAGCATGATCTGTGGATGGGACAAAGAGGGTCCCGGTCTGTACTACGTGGACGA
CCGAGGGACGCGTCTGTCCGGCCGCATGTTCTCCACCGGCTGTGGGAGCAGCTACGCCTACGGCGTGGTG
GACAGCGGCTACAGGGAGGACATGGCGGTGGAGGAGGCGTACGAGCTGGGCCGCCGGGGCATCGCTCACG
CCACACACAGGGACGCCTACTCTGGAGGGGCGGTCAACATGTACCACATGCAGCAGGACGGCTGGATAAA
GGTGTGTAAGGACGACGTATCCGAGTTGATCCACCGCTACAGGAAGGGAATGTTCTGAATGCTCAGCACT
CTGAACACGACTGATGATGCGTTTCTTCCCAAAAGATTCTTTGTCCACTTTTCTAATAGTGATTTTGGAA
ATGATCCCACTGACGTCTCACAGCAGAGAAATGCTGTAGAAACGTTTCTTTCCTTACACATGAACCTGAA
CTCTACAGAACCAAACTGTCTCTAAGCTGCTGAGCTCATTGTTTGCTGTTTGTTCTTAGTGATGTAATGC
AGGTTCTGTGTGTGTTGATCCTCACGTGCTTCTGTGTAGTAGTTTGTTCTTTGTTAACCAGACATGCTGT
TAAAATACTTTCACCAAAACAACACACAGTCCCAA

>gi|145871330|gb|ES377418.1|ES377418 Tra_Liver_7-4_F01 Guppy pDNR_LIB Tranquille Liver Poecilia reticulata cDNA clone Tra_Liver_7-4_F01 5' similar to PSMB9 [Oryzias latipes], mRNA sequence
GGGAAAAAATGGAGTCTGTCTGATGTTTTAATAATGGAATGGTGTGTAACTCCAATTGCTAGGCACTTTT
GAGCGTTACATATCGGTTTCTAAATCAAGTGAACCGCTGCAAACAAGGTCTACTCCTTCCGCGTCAGTGA
GTGTCAGCTTCTGGTAAGTTACACTAATTCCAGTTCGGCGTCGTCGTTAAAAAGAGTCTGCCATGTTGGG
AGAAACGGAGCCGCAGTGGTTGTCCGAAGAAGTGAAAACTGGAACAACCATCATTGCCATAGAGTTTAAT
GGAGGCGTCGTATTAGGGTCTGATTCCAGAGTGTCTGCTGGGGAGTCGGTGGTTAACAGGGTGATGAATA
AATTGTCTCCACTTCATGATAAGATTTACTGTGCCCTGTCAGGATCTGCAGCAGATGCTCAAACCATTGC
TGAGGCAGTCAACTACCAACTAGATGTCCACAGTATGGAAATAGGTGAGGACCCAAAGGTTCGATCAGCT
GCCACTTTGGTGAAGAACATTTCATACAAATACAAGGAGGAGCTGTCGGCTCATTTCATTGTTGCAGGAT
GGGACAGAAAAGATGGAGGACAGGTTTTTGCAACCATGAAAGGTTTCCTGACCAGACAGCCTTTCGCTGT
TGGCGGGTCAGGCAGCTCCTACGTTTATGGATTTGTTGATGCTGAGTATCGAAAAGGAATGAGCAGGGAG
GAGTGCCAGCAGTTTGTGGTTAACACCCTCGCTTTGGCCATGAACCGTGACGGCTCCAGCGGTGGTGTGG

CCTACTTGGTCACCATTGATGAACACAACACAGAGGAGAAAGTCATTTTGGGAAATGACCTGCCCACTTT
CTTTGATCAGTGATACAGCAATCACTGTATTGTTGGAATTCATTAAAATAATAAAAAAGAAAAAAAAAAA
AAAAAAAAAAAAAAAAAAA

>gi|327414615|gb|FF280943.1|FF280943 AQAH-SP-0340 Spleen of Oreochromis niloticus infected with Streptococcus agalactiae Oreochromis niloticus cDNA clone SP466 5' similar to Proteasome subunit beta type 9 precursor, mRNA sequence
CGCAGAGGCATGAGAAAGGAGGAGTGCCAGCAGTTTGTTGTCAACACTCTCTCTTTGGCAATGAACCGTG
ATGGCTCCAGCGGAGGCGTGGCCTACATCGTCACCATCGATAAACACGGCACAGAGGAGAAAGTCGTTCT
AGGAAATCAGTTACCCACCTTCTTTGATCAGTAACATGTTTGTTGTCCTCACAGCAGCTGTGGCAAACCT
GTCAACCAAGTCAGCTTGTAATATGTAAACACTGAACATCACTTTTTGCCAATAATTAAATAAAAGAAAA
ATAACTAAAAAAAAAAAAAAAAAA

>gi|294489128|gb|GW787388.1|GW787388 NBFGR-CbSpn1650 Normalized Clarias batrachus spleen cDNA library Clarias batrachus cDNA clone S1650 5' similar to ACO08445.1 Proteasome subunit beta type 9 precursor (Oncorhynchus mykiss), mRNA sequence
AGCTTTTGAAGTTTGGTCCTCACGGCTCCAGATTTCACGTTGTGTCTAGCTGGGGAGACAGTGGTGAATC
GAGTTATGAACAAACTCTTCTCAACTACATGACAAGATCTACTGTGCTTTGTCAGGGTCAGCCGCTGATG
CCCAGACTATTGCTGAGGTTGTCAACTACCAACTGGATGTACATAGTATTGAGCTGGATGAAGACCCCTT
GGTTCGCTCAGCTGCTACATTAGTGAAGAACATTTCCTACAAGTATAAAGAGGAACTATCAGCACATCTG
ATTGTTGCAGGTTGGGACAAGAGATATGGGGGACAAGTCTATGTGACTTTGGATGGCCTACTTTCGCAGC
AGCCGTTTGCTATTGGCGGCTCTGGTAGTTCATACATCTATGGGTTTGTTGACGCAGAATACCGGAAAGG
CATGACAAGAAAAGAATGCCAGAAGTTTGTTGTAGATGCACTGACACTTGCAATGAGCAGAGATGGTTCT
AGTGGAGGCGTAGCATACGTCGTTTACCATAGATGAAAATGGAGCAGAAACAAGTGCATTCTGGGAAATG
AGCTACCTACATTTTTTAATGAGTGAAAAAGGGGGCACAAGCAAAACTATTTTTTAAACATTGCATTTAT
TTCTTTTATTGGGGTTGTAATGTCAAGTAACCCCATAAACATTCACTTCATAGAAAAATTTTGCACCATT
TTTCACTTTTTAAATTCAATCCAGAGAAAATGCTGGTTAAATAAAGATTAT

>ENSGACG00000000129|PSMB9 (1 of 5)
ATGTTGCAGGAGACGGGGACGGAGTGGTTGTCTCAGGAGGTGAAGACCGGAACCACCATCATCGCCGTAG
AGTTTGACGGAGGGGTCGTGCTGGGGTCTGATTCCAGAGTGTCTGCAGGGGCGTCGGTGGTGAACAGGGT
GATGAACAAGCTGTCTCCCCTCCATGACAAGATCTACTGTGCTCTGTCCGGCTCTGCAGCCGACGCTCAG
ACCATCGCCGAGGTCGTCCACTACCAGCTCGATGTCCACAGTATCGAGATCGATGAGGACCCACAGGTTC
GCTCAGCGGCCACTCTGGTGAGGAACATCTCGTACAAGTACAAAGAGGAGCTGTCGGCCCATCTCATCGT
GGCCGGCTGGGACAGAAGAGACGGGGGACAGGTGTTTGCCACCCTGAGTGGTCTCCTGACGAGGCAGCCC
TTTGCCGTGGGCGGCTCTGGAAGCTCACATGTTTATGGGTTTGTTGATGCTGAGTTTCGCGGAGGCATGA
GCAAGGAGGAGTGCCAGCAGTTTGTTGTCAACACTCTGTCTTTGGCGATAAACCGCGATGGCTCCAGTGG
AGGCGTGGCCTATATTGTGTCCATTGATGAACACGGCACGGAGGAGAAAGTGGTTCTAGGAAATGACTTA
CCCACCTTCTTTGACCAGTGA

>gi|115425768|gb|CX348814.1|CX348814 pls_0003H06.z1.abd spleen expressed sequence tags library Larimichthys crocea cDNA 5' END, mRNA sequence PSMB10
AGTGTGCTGGAATTCGGCCATTACGGCCGGGGAGTCAGATGCAGTATGGCGCTATCAAATGTCCTCGAAC
CTCCTGTCTCTGGGTTTAATTTCGACCGAAGCGCAGCGAGGAATGCTGCATTAGAGGGTCTGTTTGAATG
GAGGACAGGCACCTAAACCTCTGAAAACAGGCACCACGATCGCAGGAGTGGTGTTCAAGGATGGGGTGGT
GCTCGGAGCAGACACGAGAGCTACCTCCAGTGAAGTGGTGGCCGACAAGATGTGTGCAAAGATCCATTAC
ATTGCTCCAAATATATACTGTTGTGGAGCAGGTACAGCAGCAGATACAGAGAAGACCACAGAGCTCCTCT
CCTCCAACCTCACCATCTTCTCTCTGAACAGCGGGAGGAACCCTCGTGTCGTCATGGCTGTCAACATACT
ACAGGACATGCTGTACAGGTATCACGGTCAAATTGGTGCTAATCTTATACTGGGAGGAGTAGATTGCACT
GGGAATCACCTGTACACAGTGGGGCCATATGGAAGTGTAAATCAGGTGCCTTACCTTGCAATGGGATCTG
GTGATCTGGCTGCTCTTGGGATCCTAGAGGACGGGTTCAAACCCGATCTAGAGTTGGAAAAGGCAAAGGA
GCTCGTGCGTAATGCCATCCA

>gi|224274161|gb|GH683973.1|GH683973 CBZB31134.g1 CBZB: Normalized channel catfish cDNA library from head kidney, gill, intestine, spleen, skin and liver (mixed tissue 1, AUK_M) Ictalurus punctatus cDNA 3' similar to zebrafish RefSeq, NP_571752.1, proteasome subunit, beta type, 10 [Danio rerio], mRNA sequence
CCAGGATATCATGCATTTATTACAAAATCATTATATCAATAACCATTAACAAAAGTTATTGATGATGGTA
ATAAATGGTGAATAAATGGTACTGAATAACAAACATCATGACTGATTGTGCTTTCTTAGCTCAGGCTGTT
TCCATAGTCTGAACTGTCTCGTGCAGTAGCTCCAGATCCAGACGAACCACATTCTCTGTCAAAACTGGGG

TGGTACCTGGCTTATACTTATACTTGTCCTTTCTTGTGTCTTTGTATTCAGACTCCTGATAAGGTCTGAT
GTAATCAACCCCTTGTCTGGTGATCACACACAGGTCTGTATTGTGACCTGAACCAAGATCACTCATGATG
CCCGAATGGATCGCATCACACACCAATGCCTTAGCCTCATCTAGCTCCATATTGGCTTTAAATCTGTCCT
CCAGGATACCCATAGCAGCTAAATTGCCAGATCCCATTGCAAGATATGGAAGCTTGTCCATGCTCCCATA
GGGCCCCACTGTGTAGAGATGATTCCCTGTGAAGTCGACCCCTCCTAGAATTAAATTTGCCCCAATCATA
CCTCGATATCTGAAGAGCATATCCTGTAGTATGTGAGCTGCCATGGTGACTCTGGGGTTCCTCTCGCTAT
TCAAGGAGAAAATGGCGAGGTTGGAAGAGAGCAATTCTGTAGTTTTAAATGTGTCTGCTGCTGTCCCTGC
TCCGCAA

>gi|200928525|gb|FC996846.1|FC996846 CBNG3047.b1 CBNG: Normalized channel catfish cDNA library from head kidney, gill, intestine, spleen, skin and liver (mixed issue 1, AUK) Ictalurus punctatus cDNA 5' similar to zebrafish RefSeq, NP_571752.1, proteasome subunit, beta type, 10 [Danio rerio], mRNA sequence
TACTGTCAAGACTGGCACAACCATCGCAGGAGTGGTGTTTAAGGATGGTGTGGTCCTGGGAGCTGACACA
AGGGCTACCTCCCGCGAAGTATAAGCTGACAAAATGTGTGAAAAAATTCACTACATTGCTCCAAACATAT
ATTGTTGCGGAGCAGGGACAGCAGCAGACACATTTAAAACTACAGAATTGCTCTCTTCCAACCTCAC

>ENSGACG00000018551|PSMB10
ATGGCCAACATTTTGAAGTCTTATGATTCGGTGACTGGAGGATTCTGTTTTGAGAACAGCCGCAGGAATG
CAGTATTGGAGTGCAGTCTGTCAGAGTCCGGCTACAAAGCTCCCAGTGCCAGAAAGACAGGGACCACTAT
TGCTGGGATTGTTTACAAGGATGGCGTGATCCTGGGAGCAGACACCAGGGCTACAGATGACATGGTGGTT
GCCGACAAGAACTGCATGAAGATTCACTACATCGCTCCAAAGATCTACTGCTGTGGTGCTGGCGTGGCTG
CAGACGCAGAGATCACCACTCAGATCATGGCATCCAACGTAGAGCTGCACATGCTCAACACTGGGCGGCC
CCCGCTCGTCGCCATGGTAACTCGACAGCTGAAACAGATGCTGTTCAGGTACCAGGGTCACGTTGGTTCT
TCTCTGATCGTCGGAGGAGTCGATGTGAATGGTGCTCACCTGTACAGTGTTTACCCACACGGCTCCTACG
ACAAACTGCCTTTTGTCACCATGGGTTCTGGAGCTGCAGCTGCTGTGTCTGTGTTTGAGGACAGATTCAA
ACCAAACATGGGGCTGGAAAAGGCAAAGCAGCTGGTACGAGACGCCATCACTGCAGGGATTTTGTGTGAC
CTGGGCTCAGGCAGCAACGTGGACTTGTGCGTTATCACTGAGGCCGGAGTGGAGTACCTGCGAGCCTACG
ACACGCCCGCGAAGAAGGGCAAAAGAGAGGGACAGTACAGGTATGAGCCCGGCACCACGGCCGTCCTGAC
TAAAACTGTGACCCCCTTCTCTCTGGATGTGGTCGACGAATCAGTTCAGTTCATGAACAGGGATTTCACA
TTT

>gi|25134315|gb|CA589737.1|CA589737 hab37g08.y1 Fugu UT6 adult gut Takifugu rubripes cDNA clone IMAGE:6350798 5' similar to TR:O78109 O78109 MHC CLASS II TRANSACTIVATOR CIITA FORM IV. [1] ;, mRNA sequence
AGAAAACGCAACAGGGAAGAGAACCAGCCAAAGAACACATTCTGCTGTGGGCCAATCCTTACCTGCAGAG
CTACCTGGCGGCGCTCCATTTGTGCCTGTCAAGGGTGGTTTCACATCGCACTTTCTTCAAGAGCCTCCCT
CTCCTGTCGGGCCCAAAGTCCTGCCGGCGCTGCCAACGGGAAGTGCTGGAGCTCACTCAGCGGTTCGCTT
TTGGAATTTTGATGGAAAAGCTAGAGACACTCGACGCTGAGGCCAGTCTCAGAGACGCGCTCGTCGCCAA
ACAGACTTTATTGACCAAACACCTTGAGGATCTCTCACACGGCGGCCTGAGTCCGGCTCAGCTTCTGCAG
GCTTGCCACTATGTTTATGAAGTGAGTTTGATACGTGGCAGTCCGAGCACGGATGGGAGTGACACAGAAT
TAAAGCGTCAGTCAAAGCTACCGGAGGTCCTGGCGTTTCGTGGCGTTCCCATCGACCCTTTGGATG

>gi|211910008|gb|GE616627.1|GE616627 cd8b Oreochromis niloticus adult liver Oreochromis niloticus cDNA clone cd8b, mRNA sequence
CATTATGCTGAGTGATATCTTTTTTTTTACAGCCTAATGATGGCCTCCTTCACTTGCATCAACAACTTTT
TGGACCTCATTTTGAGAATTTCAGTAAAAAGCTGGAAAATACAAATTCAACACTTGAAATTGATTCCAGA
TATTTTGTCTGCTTAATGTGTCACAGAGCAACAAGAAAATAGGCCTCACGTGGCCTTAAAACTACCTTCT
CAACTGACCAATTATTTTTAAGCCTCTGAAAATAGGGCACTGTAACTCCTAGACTGTTGATGCAATACTT
TTGATAAAGCTCTTCATATCCCCAGCATTTAGTGAGGGTTAAT

>ENSGACG00000008960 CD8 beta chain
CTTTCCATTCTTGCGAAACGTTGGGTTACAGTTGTAGGTTTTGTACCATATTACCAACTTCAGGACACGG
TGAAGATTCAGTATCCCGTGCTCCACAGTACGGAGGTCATTGAATGTGACTGCGGTAACGTCCTATGTGA
CAATGTGTACTGGTTCCGCAGCATCCACAACCACGAAAAACTAGAGTTCCTCGGCAGATTCAACAACGCT
GGCCGTGGATCTCCAGTGGACGAGGCCCACTTCAAATTAAGCAGGAAGAGCAATACGTGCTTTGCGCTAT
TCATCATCAACGTGACAGAGGAGGACACAGGGATTTATTCTTGTGTTCTGAAGGACAGGAAAAACACAGA
AACATGGAAGTCCGGGATTCTTCTTCGGCCGGGAGTGACCGCTCCAACGCTACCTCCTCACACGAAACCC
AAACCCCCAGTGGAGCCAGTGTGCGGCTGCCCTACGAAGGATCCTTCACAGGGCGACTGCGGCTCCCTGG
TGCTGTGGCCCTTGGTTGGACTGGTTGCGGCGTTGGCTCTGGCCCTCATCGGCACCCTGTACTACTTCAG
CCGGCTACCCAAAAAATGTCGGCACCACTTTGTGAATAAGAATCGTTCTGTTAAA

>gi|78229885|gb|DV569890.1|DV569890 Pf_IL_305C11_TriplEx-5LD Flounder IL Induced Liver library Platichthys flesus cDNA clone Pf_IL_305C11 5' similar to AB076073 (Paralichthys olivaceus) T cell receptor gamma chain V-J-C1 %ID = 57 E-value = 2.00E-52, mRNA sequence
CAGATGGTTAAAGTCTGAGTCTCTTTCACTGTGTGGTTCATCTTCGGCTCAGGAACCAAATTGTTCGTAA
CTGATCGGCCGGTGGTGACTCCGGTGGTGAGCGTGTACCCGGCAGCTTCCATAGCCGCCCTGGACGGGAA
GAGCTCCCTGCTGTGTGTGGCCTCCAACATGGTTCCTCCTCTGGTCCAGTTCTCCTGGACAAGACAGAGG
GAGGGTGGTCCTCTGGAGACGCTGTCCTCTGATGATGGAGAGCAGCTGGAGCTCAGAGGGGCAGGACGCA
CCGCCGCCATCATGGTGGTCGACCGGCACGTTTCCTACAAATACAACTACAGCTGCCACGTCAGGCATGA
GGGAGGCGCAGTGGAGGCCCCGGCAGAGCAAGAGGTTTCTGCTAATCCAGCACCGACGACTCAGGCACAG
ACGGCTCAAATACCGACGACTCCAGCACCGACGACTCCAGCACCGACGCCTCCAGCACAGACGCCTCTGG
CGGCCTGGGCCTGGTCTCATCGGCAGGTGAAGCTGCTGTGGCTGCTCTACACGCTGCTGATGGTGAAGAG
TCTGGTTCACTGCGGTGGACTCGCTCTGATCCACATCCTGAGGAACAGGGAGCGTCCAGCCGCTGCTCAC
CAGACCACGGAGTTTCCTGCAGCAGCTTCAACTTCTCACTGACTCCTGTTCACTTCACTCTGCTTCTCTT
TCACTGCAAACATTCATCTGAACTGTAACTTTGNCAAGTATCAAATAAAGATTTTATTCT

>gi|52852390|gb|CF752916.1|CF752916 om_C001.58 12hr LPS Zap Express Library Oncorhynchus mykiss cDNA 5' similar to T cell receptor gamma chain V-J-C1, mRNA sequence
GGTGAAGGCTCGAATTTGGCTCTGGCACGACACTTTATGTGACAGATGGCATTCAACGAAAACCCAAAGT
GACGCTGTACTCAGCGTCCAACTCTGAGTCGAATGAGAAGACCACCCTGCTATGTCTGGCTAGAGACATG
TTTCCAGACTTGGTCAAGATCTCATGGAAGATGGAGGATGCAAACGGCGGAAGAACGGAGGTGCCCAAAG
CAGAGGGGGAACAGCTGGAGCAGAGGGAGGAAGAACAGACGACCAGTATGATCATCATTGATAAAGACAA
TACGTACAGGAACAAATACATCTGTTCTGTGGAGCATGAATGGGGTGCTCAACATTTAGTCATCCCAAAA
GATACTCCAACCACCATGTCTGCACCAGCGTTCAGAAATGACACCCAGGAGTCACTGACTCTGCAGTTTA
CCGAAGATTCCTTCCAGTCAACGTGCAGTCTGAACCTGGCCTCTGTGGTTTACACAGTGATGATAGTGAA
AAGCATGGTGTATTGCTGTGGGCTCTCTCTCCTGCTGCACAACAGGATCCTGGGAAGAGGACCCAGCACC
TGAAGACCTCTATGAGGAAAATAATTTACGTGCTTTTTTACATTGATACAATGTTGTTGTTTTTTTTTGT
TTTTTTTTACATTGATACAGCTTGCATGACATTTTCCTTGCCTAACACAGCCTGCTCAAATTAACTAAGT
TGCTCAAAATAACCATATTATTTCAGATGAGGATGCCTTTGTGAACAAAATGTTGCAGCAACAATGGTTC
TGTAAATGATTGTAAAAATACATTTTTACAGTTCCGTGCTGTTTTCAATGATAAAGGTTACTTTAAACCC
CCAAAAAAAAAAAAAAAAA

>ENSGACG00000015763 T cell receptor gamma chain
CCCGTGGTGAGCGTGTACCCAGCAGCATCCAGCGCCCACCTGCAGGGGAGGAGCTCCCTGCTGTGTGTGG
CCTCCTCCATGTTTCCTCCTCTGGTCCGGTTCTCCTGGAGGAGACGTGAGGAGCACAGTTCTCTGCAGGA
GAAGGTCCCTGATGATGCAGAGCAGCTGGAGTTCACAGAGTCCGGACGCACCGCCTCCATCTTGCTGCTC
CATCAGCAGGAGACCAGCCGCTATCGATACCGCTGCTACGTCCACCACGAGGGGGGAAAGGTGGAGGCCC
CGAGCGAACAAGAGGACAGAGTTCCTCCATCAGCTCCTCCATCAGCTCCTCCGTCAGCTCCTCCATCAGC
TCCTCCGTCAGCTCCTCCGTCAGCTCCTCCGTCAGCTCCTCCGTCAGCTCCGGGCCCGTCTCCGTACCAG
GTGAAGCTGCTGTGCCGGCTGTACGTCGTGCTGATAGTGAAGAGCCTGGTGTTCTGCTGTGGAGTCTCTC
TGGTGATGGTCCTCAGGAACACGGCTCACATGTAGGACTTCTCTCCTCATCTCCTCCCATCAGTTTGTCC
CTCTGATCAGCAAACATCTGCTGATCTTCACATGTTGAACACCATCATCCTAAAGGCATGAACACATACA
TGTGTGTATTCTACCAATAGTTGCAGTAGATCCGTGTAAATCATTTCTCGTGTTAGTTGGAGTATTTCTA
CTTAAATATCTGATATAAAACAACATGATGCTGAATCATCAGCTGTCTGTTAAATATTCTTCTTTTCCTT
CAAATGAATGTTGATTCTCTGTTTGTTGAGTTGCTTTTATACGGAATATTGATGAAGTCTGTTGATGTTC
TTTGTGTTTGTTTCTTCATGTGTTGAACACGTTA

>ENSGACG00000008369 Autoimmune regulator
GAATCTCTGCGCGCAAAATCCGCAAATGGAGCCTGTCTCACGTTGGATTTAACGTCCACCAAGAACGAAT
GTTTCTGTGGAACCACACATGGACCCGATGGACTGGCTGGAGAACCACGAACTCTTGCGGTTTTTCCGCC
GTCATAAAACCGAAATGTCTTGCATGGAGAAGCCGCGCACGTTCCTCTGCCAGCTCAGGGATCACGACCT
GGTCCCTGAGGACCGATACAAGAAGGTGAGCTGCATGAGGAGTAAAGACAACATGAGGAAAGGTCTCTAT
GAAATTCTGGACTGGTTTGAGAGAGAGCGATCACAGAAGGTCAGAGAGTTCTGGAGCTGCGTGTTCAAGG
ACTCCATCCTGAACCAGTATCCCACGCTGCGACTGCTGCGCAACAGCCTCATGGACGGGACTCGTGGGAA
GAGTATTCGCACTGAGACGAGCTGGATGACCCCGGTGGAGTTCCTGGAGTTGGCACTTGGTCGGAAGGAT
GCCTCTTGGAAGAAAGACATTGAATGTGAAGGGAAGCCACTCTTTGTCCTCATAAAGGCCAAGACCCTGA
GGATCCACTCTCTGCTGTGTAATTGCAGCCTGTGCAAACCAGATGACGAAGACCAGGTGAGTTTGTTCAT
CAGACAGTGTCCTCATTCTGCACCGTCCTTCATTAAACAACACGATGGCCGTGTCATCAGTGACATTAAA
TAGTCCCACTTCTCTCACGATGAGATACGGCACAACAAGAAACCCTTTTCTGTCGGATGCATATAACATG
TAACTGTGTAATTGGCCGTGCCGTCATGTTTGTCTTGGCAGAGGAATCAGAAAAACGATGATGAGTGTTG
CATCTGTAGG

>gi|9913504|gb|BE630816.1|BE630816 uu49c07.x1 Soares_thymus_2NbMT Mus musculus cDNA clone IMAGE:3375276 3' similar to TR:Q9Z0E3 Q9Z0E3 AIRE PROTEIN. ;, mRNA sequence
TTACATAGAAGTGACTTTAATTCCAGGATATGGGGTGGCCTTGCATCTCTACAAAGATCAGGGCCATCTG
CAAGCTGAGTCCAGCAGGCCAGAACCTGCCAGCTCTTGGTCCTAATCAGCCCAGGCCTCTCAGAACAGAG
TGCCTCATCCGATGGGGCTGGGTGGGGAGGGAGCCAATGCTGTGCTGCCCACCCCTTCCTGGGCCACCTG
TCATCAGGAAGAGAAGGGTGGTGTCTCGGCCAGCGGGCGTGACATGCTCTGGATGGCCCACTGCAGGATG
CCGTCAAATGAGTGCTCATTGAGGAGGGACTCCAGGTCGTCCCTATGTAGAACAGGGTCGTGACTAGCAG
AGTCGTCCCCTACCTTGGCAAGCCCAGGTGCTGGACGGGGCCCAAAAGTGGGTACAGCTTCNCCCGGTGT
GCCCGCGGTGGAGTCGAGTCTGCAGAGCAGGATTTGCAGCGGAGATTGGGCCCCGGCCGGGCGGGGGCCT
CCGGAAAGTGCAGCGCCAGTG

>gi|5884455|gb|AI981427.1|AI981427 pat.pk0053.c5.f chicken activated T cell cDNA Gallus gallus cDNA clone pat.pk0053.c5.f 5' similar to AUTOIMMUNE REGULATOR (APECED PROTEIN) AIRE-1, mRNA sequence
AGCAGGAGGCCTGAGAAGGAGCCCAGGAGAAGTGGCAGGGCCACTAACCACGACAGCTGCGATAGCTGCA
AGGAAGGAGGGGACCTGCTGTGCTGCGATCACTGCCCCGCCGCTTTCCACCTCCAGTGCTGCAACCCTCC
GCTCAGCGAAGAAATGCTGCCTCCAAAGGGGAGTGGATGTGTCACCGCTGCACCGTGCGCCGAAAGAGCG
AGAACAGAAGAAANGACTGGGGCANGTTAATGGATTGGTGGGCAAAACTGGGAAAAGGACCACCTCCCAA
CCAGTGACGCAGACTGTTGGACAGGTCTAGCAGCAGCATCAGGGCTAATGCGCATGCCAGGATCTTGGAA
AGGGAGACAAGCCGGCTGGCACTCCCACATCAATGCCANCACGAGNCCCCANTCAGAGCANATGTNNCAT
GNGGAATNTTNCTGGATATGNCCCCCNTTGNAAAATGGCTGNGGCCCCCNGTGAACCACNTTTGAGCTTC
TATTGCTGCCGCCATGGAAAGGACCANNTATTCAGCTGCCNAATTATTCCNNCACACATACCTCAGGTCN
AGCAGGNGGNGAGAAAGGACCACNCNGAANNCTNAAGC

>ENSGACG00000011461|RAG2
ATGACCCTTCAACCATTAACTCCAGTGAACTGTGCAGGCCTTCTGCAGCCCGGCTTCTCTCTGCTGCAGC
TGGATGGGGAAGTTCTTCTGTTTGGCCAGAAGGGTTGGCCCAAGCGCTCATGTCCAACTGGCATGTTTAG
TGTTCGCTTTAAATGTGGAGAGATGAAGCTGAGGGCCATCTCCTTCTCCAACGACTCATGCTACCTCCCT
CCATTGCGCTGCCCGGCTGTTTGCCGCCTTGACCCGTACGACGGCCTCCCAGAGAGTTACCTCATCCACG
GCGGCCGCACCCCAAACAACGAGATCTCCTCCAGCCTCTACGTGCTGACCACAGACAGCCGCGGCTGCAA
TCGCAAGCTCACCCTGTGCTGCAAAGAGAAGGAACTCGTGGGAGAAGTGCCGGGGGCCAGGTACGGCCAC
ACAATGAGCGTGGTCCACAGCCACGGGAAGACGGCCTGTGTGTTGTTCGGCGGTCGATCTTACATGCCTG
CGGGGGAGCGGACCACGGAGAGCTGGAACAGCGTCGTCGACCGCCCGCCTCAGGTGTTCCTGTTTGACTT
GGAGTTCGGTTGCTGCTCCGCCCACGCTCTCCCCGCGCTCACAGACGGCCAGTCTTTCCATCTGGCCCTC
GCCAGAGAAGACTGCGTCTACCTCATCGGGGGTCACTCCGTGGCCTCTGACTCTCGGCCCCCTCGGCTCT
TCCGTCTACGCGTGGAGCTCCTGCAGGGCAGCCCCTTGCTTTCCTGTGAGACTCTTACGACGGGCATGTC
CATCTCCAGTGCCATAATTAACCGCACAGGTCGCGCTCACAATTACATCATATTGGGCGGGTATCAGTCG
GACTCTCAGAAGAGGATGGAGTGCAGCGCTGTGAGCGTCAATGAGAGCGGGATCCATTTTGAGCCACTGG
AATCACCCAGGTGGACTCCTGACATCACCCATAGCCGCACCTGGTTTGGCAGCAGCGTGGGGGAGGGGAG
CATCCTACTCGCTGTCCCCACTGAAGGAAGGCCATCCCAAGCCGATATGCATTACTTCTACAAGGTGAGC
TTCCCGACAGAAGAAGAGGCCAGGGAGGAAGAAGGAACCCAGGGCTGCAGCCAGGATTCAACCGAGTACG
ACGACTCCACTCCCCTGGAAGACTCCGAGGAGCTCTACTTCGGTCGCGAGCCGCACGAGCTGGAGGACAG
CGACGACGGACGAGTTGATAATTACAACGAGGAGGACGAGGAAGACGAATCGCAAGCGGGCTACTGGATC
AAATGCTGCCTGGGCTGTCAGGTGGACCCCAACATCTGGGAGCCCTACTACTCCACCGAGCTCCACCGGC
CGGCCATGATCTTCTGCTCCAGAGGGGAAGGGGGACACTGGGTCCATGCCCAGTGCATGGACCTGTCTGA
GACCCTGCTGCTCAGACTCTCACAGGGCAGCAAAAGGTACTTCTGCCTGGACCACGGAGGCCTGCCTCAC
CAGGAGATGACCCCGCCCCGACAGGTCCAGCCTCTGAAGCTCACACCCATGAAGGTTAAGGACAGGAAAA
CTCCTCCTACAATTAAGATGTCCCCTGCCAAAAAACTCTTTTTGAGAAGGCTTTTTGAATGA

>ENSGACG00000008005|IL2RB
CTGGTGAGCCGGAGGAGGTGCTCTGCAACTCCTCTCACACAGCGTTGTGAGGCTTCCTTTCTTTCTTCTG
TTTCTCGTGTCCCTGAAGGACTCTCCTGCGTGAATGACTTTGTGAACAACGTGAGCTGCACGTGGGACGG
CTCTGGACTGGACTGCTGGATCGTTGGTATGAAGATTACCTGGGCCAAACGGGCAACGATTATTCGAAGC
TGCAAACTGAAACAACACCGGAACTCTCCGTCAGGGTGCAGTTTTGTCTTTGAAAATGAAGAGTTCAACC
CTTTTATGAAGGAGATGCCCTACATACGAGTGGAGTGTAACGGGACGATGGTGGAGAACATCACAAACTA
TTCACCATTCAATCACGTCAAAATGCATCCTCCGAGCGTTCCCAATGTCAGCTGCACGCCCAACAGGACC
CTGATATCCTGGAGCCCAGGAGGTCCTCCGTCAGACTACTTCAAATCCTTCAACTTCCAGGTTCAGATCA
AACAGAAAAACAAGTCATGGAATGAGTCCAACACTTTGTTCACACAAGAACAAGAGCTGATCGTAGCCAG
TTGGAAAGTGAAGGGGCCCTGCCAGGTCCGGGTGAGAGTCAAACCCGTTTTTCTCCGGACAAGCAGCCAC
TGGAGCGACTGGAGTCCTACGACATCCTGGCTGGGTGCAACAGACACGGGGACAACAACACAGGATGAAG
GGTTGTGCGAGCAGATGTTGGCTTGTGTGTCTGTCTTTGTGTGCACGTGCGCCATGTCTTTTCTAATGGC
TCGCTTTTGTCATTCCAGGCTCCTCAAAGGGAGGCCAGTACCAAACCCTTCTAAATATTTCCACACTCTC

CACTCTGTACACGGAGGCAATGTGAAGGAATGGCTGAATCCTCCGTCGGCTGCTGAGTCGTTCTTCACAG
CCCAGCCGTGCGACAGCATCTCCCCAGTTGAGATATGCGAAGGCTGGGACGTGGTCGCCACCACCTCTCC
CTCCTCCAGCTCCAGCAGCGCCCTGCTTCACTCCAGGCACGACCCTCGGACCGCCGGCTCGGACACCAGC
GGCGTGGTTGACGATTCCTCCTCCTCTTCATCCTTCTTCTCCAACGTGGGCTACTTCATATCCAGCTCCT
CCGGCAGCTTGGCACCAACTGGCCTCGGCCCGGCTCACCCGGCCTGTCGGGACGATTTCCGCAACACCCT
CAACCTCCGCCTCTCCCTCCACCCGGCGCTCGACGGCTGTCCAACCTACGAGAGCTTGACGAGGGAGCCG
CACAGCCCCGACTCCGGCTTAGGCATCGCAAAGGAAGACGAAGACGGCGATGAAGACACGTGCCCCTGTG
CTCCACCCGCTCCTAACGCTCCCACTCTGACTACCATAGCGAATAAGAGCCAACAGGCGGAGGTATCTGT
GGCAGCTGCTCATGGCCACTATGCGGCCTGGCCCGTGCCCGGCGCCATGTGCCGGTCTTCCTCCATGCCC
GTGGAGCCCTGCAAGACGGGCTATCTGACACTCAAAGAGCTGCAGACGACATTCAGCAATAAATCTATCT
GA

>gi|50569243|gb|CO647749.1|CO647749 ILLUMIGEN_MCQ_40902 Katze_MMPB2 Macaca mulatta cDNA clone IBIUW:23374 5' similar to Bases 334 to 964 highly similar to human IL2RB (Hs.75596), mRNA sequence
TTGGGGAACTGTGTGTGTTGCAGGGGGGCGGTCACTCCCCAACTCCCTCTTTAATCACAGAGTCCCACGA
GTTTAGGCTCTGAAGCATCACTCCTCTCCAGCCCTGCAGCTGTTCACCAGTATCAGTCCTCGAGGCTCTC
CAGGGCTCCTTGCCCTGACCTCCTCCCTGGGTTTTCGGCCCCAGCCTCCTCCCCTCCCCTCCACCTCCAC
AGGGCAGCCTGAATGTGCTTTCCAAAACCCAAATATGGCCATGCTCCTCCTCGGTTCAAAACCTTGCACG
GGCCGCACTGCCCTCAGCCCCATTTCTCAGCCCCATTTCTCAGCCCCATTTCTCAGGCTATTCCCTGGGC
CTGCTGTGCTCTCCCCCTTATCCGGGTGACAAACTTCCCTGACCCCTCAAATGCCGGTTTTGCTTCCCCT
GGAGGGAAGCACTGCCTCCCTTAATCTGCCAGAAACTTCTAGCATCAGTGCTGGAGGGAGAAGCTGTCAG
CAACCCAGTGCGCCTGGAGAAAGAGGCCCTGTTACTCTTCCCTTGGGATCTCTGAGACCTCAGAGTGCTT
GGCTGCTGCATCCTTAATGCTGGGGCCCAAGTATGGGCACAGATGCCCCCACAAAGTGGACGCCTGCTGC
ATCTTCCCACAGTGGCTTCACAGACCCACAAGAGAAGCTGCTGGAGAGTAAACCCTGGAGTCTGAGGCCC
GGGCAGCAGTCCCCTCCTAGTAGTGGGCCCTGATGCTGCCAGGCCTGGGACCTCCCACTCTCCCTCCACC
GGAGAGTCTCCTCTGCAGCTCAGGGACTGGCACACTGGCCTTTCAGAAGGACGGCTTCACAGGGCAGGGC
CTCATCATCTTTTCCTGCCCCAGAACAGTGGCCAGGGCCCCATGTATACCCGGGGTGAATGAATTAATTA
CCGGGACCCCCCTCCTCCGGGGCCCCCTGCCCTGGAAATTCCCCCAAAAAAGCAA

>ENSGACG00000012777|FOXP3
GCCCTGTTTGTGAGTGGCTTCTGTCGCTGGCCGGGCTGTGACGTGATGTCTGAAGATTTCCCTAGTTTCT
TAAAGCATCTCCATTCTGAACACAGTCATGGGGAGAAAAGCATTGCGCAGTGGAAGGTCCAGCAAGATAT
TGTTCAGTGCATGGAAAGTCAGCTCATCCTGGAAAAACAGAAACTCATTGCGATGCAACTTCATCTGCAC
CTATCTGGACACAAACACACTGATATGACTCTTGAATGTACTTTTTGTCATTCTGTGCTGAAGGCAGCGT
CTGAGTGGCCGCACAGTCTTCCTCTGTTCCTGCCCCAGCCTCAGCATGGCTACAGCATGGCTGCTGGGGC
CGCACACATTCTCCCAGGTACCACACTTTTTATGGTTTTTATGGTAAATATTGAATGTTACAAATACAGC
AACATCAGGCCTCCGTACACCTACGCATACTTGATAAGATGGTCGATCCTGGAGTCTGTAGACAAGCAGC
GCACTCTGAATGAGATTTACAACTGGTTCACCACCATGTTCTTCTACTTCAGACACAACACTGCTACCTG
GAAGAATGCAGTGCGGCACAACCTCAGCCTGCACAAGTGTTTTGTGCGA

>ENSGACG00000017381|C1QTNF4 (1 of 2)
CAGACGCCATGCTGCTCCCGGCGGTCGCTCTGATTGGCCTGCTGTGCCTGGGCCACGCCCCCCGCGCGCT
GGGATTGGCCCGGCTGTCGGAGGACGCGGAGCTGCGCTCGGCCTTCTCGGTGGCGCGCACCAACAGCATG
GAGGGCGGGCCCAAGATGACCGTGACCTTCGACGCCGTCTACGTCAACATCGGCGGGGACTTCGACCCCA
AAGCCGGCCTGTTCCGCTGCCGCGTGGCGGGCGCGTACTACTTCTCCTTCACGGTGGGGAAGTTCCCCCA
CAAGGACCTGTCCGTCATGCTGATGAAGAACCGGAACGAGGTGCAGGCCATCGTGTACGAGGAGAACGCC
GGCGAGGAGCGGAAGGTGCAGAGCCAGAGCGTCATGCTGCAGCTGGAGTTCGGCGACACCGTGTGGCTCC
GTCTCCACGGCGACCCTCGCTACGCCCTCTACAGCAACACCGGCCACTACACCACCTTCAACGGCTACCT
GGTCTACCCGGACACCTACGCACCACCACCCGCGGCCCCAGCAGCAGGACGACCAGGCAGATCCGCCTTC
TCGGTGGGGCGCACCCAGAGCATCGTGGGGGTCAACCAGGCCGGCCTGCCGCAGCACCGCCCCGTCGGCT
TCGACGCCGCCTTCGTCAACATCGGCGGCGACTTCAACGTGACGGAGGGCCTGTTCACCTGCCGCGTGGC
CGGCGCCTACTACTTCTCCTTCAACGTGGGCAAGCTGCCGCAGAAGACGCTGTCCGTCAAGCTGATGAAG
AACCGCCTGGAGGTGCAGGCCATGATCTACGACGACAGCCAGGGCGAGAAGGCGCTGCAGAGCCAGAGCC
TGATGCTGGCGCTGAGGGCGGGCGACACCGTGTGGCTCTACTCGCACCAGAGGGACGGCTTCGGGGCGTA
CAGCAACCACGCCAAGTACATCACCTTCACGGGCTTCCTGGTCTACCCGGACTTCGCAGCGGCGGGACCC
TCCCCGACCCTTCGGTCCGCGTGGACC

>ENSGACG00000007933|C4A
GAAGCTGCACGATGGGGCGCTACGTCTTTTGCTTTTTGTTCCTGATCTCGACTGTGGAGTGTTCGGCGGG
GAGATTCTTCATATCAGCCCCCCATGTTTTTCACGTGGGTGTTAATGAGAAAGTGTTTGTCCAGATGGGA
AACTCTTATCTTAATAATCCTGTCACTCTCTACCTGGAGCACGAGGCTACCGGTACTCTTGTGTCTGAGA
AGAAAACCGATGGAACCACAACGGAAGGACAGATTAAAACAGTTGAGCTAATGATAGAAAGGAATCTAAT

CTCAACATTGTCTGAACGTTTTGGCCTCAGCTACCTTCTGCTGGTGGCAGAGAGCCCCTCCTTCGGTAGG
ATTAGGAAGGTAACAAGAGTTATGGTATCAAAACGAAGGGGCTACATCTTCATTCAGACTGATCAGCCAA
TCTATACCCCGGCACAGAATGTGCGATACAGGATATTCACTCTTGACCACACATTGAGGCCTCATGATGA
GGTGTTCCACATAAAAGTATATAATTCTGCTGGAAATAGAGTCATCAAAAGCCAAAAGATTGCAGATAGA
GGAATACTCCAAGGATCATTTCCGCTACCTGATGTATCAAAACAAAGATTGGGCACATGGAAGATTACAG
CACACTATGTTGATGATGCATATGCTGCTTCCCGAGAGTTCAAAGTCCAAAAATTTGTTTTACCAAGTTT
TGAGGTGAACATTGAAATGGAGCAGAGGTTTATTTTGTTGAAGACAGAACAGCTCAACTTCTCCATATCG
GCAAAGTATTCGCATGGCGAGCAAGCAAAAGGGGCTTACCACTGCCAATTTGGAGTGATAGAAAGAGATA
AAACCCACGGCCAAAAAACGAAGCCTGTGTTTATCAGGGGGTTGGAGCTAACTGGGAGGATCAACGGTGG
CGCCGAAGCAGCATCTGTTCAGATAGCAAACCTAAATGCTCACCTCGAAAAACAGCAGAACAAATCCTTC
TCTGAGCTACAGCGAAGTGGAGGACAACTATACTTGAGAGTATTTGTAACCAATATACAAAGTGGTGAAA
CGCAAGAGGCGGAAGTAAACCTTCCTATCATCTCCCATAAATACACCTTGGATCTCTCTCGAACTCGCTC
ATATTTCCTCCCCGGATACCCACTAGATGTGGTGCTGGTCGTGAGTCTCCCCGACGGGTCCCCAGCAGCT
GGTGTGGGAGTAAAGATTGATGTTCCCACCTCTACAGAGACATCTTGGGAAGGCAAAACCGACGGGGAGG
GGGCAGTGTTTCCTGTCTTTAATATTCCCTCTGGTGCTCAGATTACAGTTGACGTGTCGGCAGACGGCCA
GACGCAAACAAAAGTGCTTCGGCGCGCTTCATCTCCGACTAATAGCTACCTTTACCTGAGTTTTACCAAC
AGGATGTACTCTGTGGGCGAGTCAATGACAGTAACTTACAACACCATCAACAGCCCAAACGTTGGGTTTA
TATACTTCATGGTCTTAAGTCGCGGGATCCTAATAAAACATGGCTCTCTCCGATTGGGCACTTCAGTGAA
AGACCACCTGCAAATAACATCTGATATGGTGCCATCCTTCCGTCTGATTGGCTACTACTACAACGAGCGC
GGTGACATCATTGCAGACTCTGTGTGGGTAGATGTCAGCGATGAGTGTGAGATGAAAGTCAAGGTGGAGG
CACAAGGTCTGTTCGAACCGGGGAAAAAAGCTGCGATAGAATTTGATTTATATGGTCAGAGAGCCACAGT
GGCTTTATTGGCTGTGGATAAGGCAATCTACGCTCTGAATGCCGATAATAAACTCACAGGCAAACAGGTG
TTTTCCTCCATGCAGTCATATGACCTCGGGTGCTCGTACAGCGGAGGATCTGATCCTGCAGCTGTACTAA
CAAATGCTGGCCTGTCTTCTGTATCTCAGTCGCAGTCAATGTGGAAAAGATCTGACTGCGGTTCACAAAA
TGCACGACAAAAGCGCGCAGTGGACCTTCAACAAGAAATGATGACCATAAAATCAAATTTTTCCGATGAA
CAGATGCAAGAATGTTGTGTTCGCGGGTTTTCTCTCATCCCTATGAGACGAACATGTCAGGAAAGAGTGA
AGAGAGTCTCTATGGTGAAGAATAATCCTGCTTGTGCAGACACCTTTTTAAAATGCTGCCTTGAAGGACA
GCGACTGAGACAAAAAAAGATTCGAGACGACGCCGAGAAAGGACTTGGCAGGACTGCGGAAGTAGCAGAC
ATTGAGCAGTTCTTCTGGGACACTGGTGCTCAATACATTCGACGATATTTCCCCCCGAGCTTTGGATTCA
CAACATCTGATATAAATGGGAAAGGACGGATGTCTTTGACTCTGCCTGACTCAATCACCACATGGGAGAT
TCAGGTTGTCACTTTGTCTGCAGCCACTGGTTTCTGTGTAGTTAAGCCGTTGGAGGTCAGATCGTTCAAG
GCGGCATTTGTCTCCCTGCAACTTCCTTACTCAGTGAAGAGATATGAGCAAATATCCATTTCGCCTGTTA
TCTACAACTATGGCCAGGACCAACTGCAGGTGGCAGTTCATATGGAACAAACTGAAGGCCTTTGCTCCCC
CGGCTCAGCCACCGCCGTGGCTTTTGTTAACATTACTGTGGAGCCAGAGTCGTCACAGTTAGTGTCCTTC
TCCGCTGTTCCCATGGTAACCGGCTCAATACCCATCAAAATACGTCTCTATGACATGGAGAAAGAGTTTG
GAATTGATGCAATTGAAAAGACTTTGAGCGTGATGACAGAAGGACTGGAAAAGAGAATACAAGAAACCCA
AGTGTTTAAATTAGACGGGAAGAGCACAAAATCATTCCAAATTGACGGAATGTTACCAGATGAAACAGTC
CCAGACTCCACCTCCAACATTTTCATTTCAGCGGAAGCGGATGGATTCAGCAGTCCACTTGTGAGGAACC
TTCTTTCGCCTGAGAAGGTTTTCAGTCTGATCCAATTGCCTACAGGATGTTTACAACAGACAACGTTAAG
ACTCACCCCAACATTGTCAGCCGTGCGCTACCTCGACATGAGTGACCAGTGGGAAGACCTGCCTCCTGGT
ACCAGAGATGATGCCCTTGATAAAATCGAGACAGGCTTTATAAGGATATTTCCAAAGGAGAAACCCAATA
GTTCTTATGGATCATGGTTTTCAACGCCAGCTAGTAATTGGTTGACTGCACTCATACTGAAAGTGCTATC
GTTGATGGCGGAGCGTCAGTCAGTGGCTTTTGGAGAGAAGGGCCGAAAGACTACGATCGCACCTGATGAA
AAGATCAAAAACGTAGTCAATTACTTGCTCACAGCCCAGAACACTGATGGGTCATTCCGTGACCCAAATC
CAGTGCTACACAGAGGAGTTCTGAATGGACCAGACCAACACGCAGCCATGACGGCATTCATAAATCTTGC
CCTGAACCGGTCCCTTCAATTCCTGAACACTGACTTGAAAAGTAATGCGGAAGCAAGCATTACCAGATCA
ACAAACTATCTCCTGTTGCACCTGGAGGAGCTTCAGCATCCATTGGCTGTTGCCATCACAGTCTACTGCC
TCGCAGTCTGCCTTCCACAGGGAACAGATCATTCATCTGCCTGGACAAGACTCAAAACAATGGCTACTCA
AGATGACAATGGCTGTTATCTGTGGACAACAACCCAACGGAATCAAGTCCGTGCAGACGCCATCACAGTA
GAGACCACCGCCTATGCTCTGCTCGCAGCAGTGGAACTCGGACATACTAAGGAGGCAGACAAAATAGCCT
GCTGGTTAACCACCCAAGAAAACTATTTTGGAGGCTATAAATCATCACAGGATACAATCATGGTATTGGA
AGCCCTGGCAGAGTATGAGCTGAAGGGGCCCGTCCGCTCTGAAGTAAATCTAGTAGCTGAGTTCACAGTC
CAAGGAAGGAAAGACATCATACAACTTGTCTTGGATAATAAGAAAGAAAAAGTGGAAACAGACCTCAAGA
AGTTTTCTGGGAACAACATTAAGGTGCAAATGACAGGAAACGGCGATGCCAAGATTAAAATCGTTAAGGC
CTACCATGTGCTGGACCCTGTGGACAGTTGTGACTTACTGTCAATCAGTGTCACGGTGGAAGGGAAAGTC
AAGTACACCGACAAGATCATAGAAAACTATGAATACTACGATGACGATGATAACAAGGAGGAAAAGGAGG
GGCGCCGAAACAAGAGAGACCTTGATAGTAACTTCATTTCAGAAGATGCTGTCACCTACACAATCTGTGT
CAGTCATAGCCTGAAGAGGAATCTCACAGGGATGGGTATTGCTGACGTCACACTTCTGAGTGGATTTGAG
GTCGTTATCGAGGACTTGGACAAGCTACGAGAGACACCTGAGGAATACATTTCTCATTATGAGGTCTCCA
ATGGAAGAGTGCTGCTTTATTTCAATGAGCTCTTTGACTCAGAGGAATGTATTAGTTTTGATGCCATACA
GAGAGTACCAGTTGGTCTTCTACAGCCTGCTTCAGCTGTGTTCTATGATTATTATGAACCAAACAGAATG
TGCACTGTGTCCTACTCCGCCCCCCGAAGGAGCAACATGGTCTCCAGACTGTGCTCAGAGGATGTGTGCC
AATGTGCAGAAAGACCCTGTCATAAAATACAAAATACATTCAAATCACAAATTCGTCAGAAGGTCCCCAA

GAGTGTCCGTCTAGAACATGCTTGCTTCTTCCCTACAGTGGATTACGCATACTTGGTGGAAATCCTTAAC
GTTTCCATGAAGAGTAACTTTGACATGTACAAAACGCGTGTAAACGAGGTGCTCAGATCACATGGAGATA
CGGGAGTGGGTGAGGATTCTATTCGAGTGTTCGCTAAGCGGCGTCAGTGCAAAGGACAGTTGGACGTGGG
AAAACAGTATCTCATCATGGGCAAAGATGGCTCCACGACGGACTCCAGTGGGAAGATTCAGTATCTTTTG
GAGTCCAACACTTGGGTGGAAAGAAAGCCTTTGGAAGAAGAATGCAAAAAATCTGCACATAGAACCGCCT
GCTCACGGTTTAATGTGTTTAAAGATGAGTACAAGATATATGGCTGCAGACAGTGAAACGGACAAGTCCT
TTCATCCACGGGACGCACCCTCAGCATAAATGTTTGGTGCTCTTTTTTAACCTTTTATAATCATAAACGC
ATAGTATGAGAACATGCTTGAGATTATTGCTTGATAGACAGTAAGTGAACGACAACTTTAGTATAATTTG
AAAGTTTACTACACTTGGAATGAGACTATTGCCCATGAATTCATGTCCAATACAGCTACCAGTTTTTAAA
TAAATAAAAACCTTTACCTTTGAATGTATTATGTTTTAAAATAATGATTTCAAAATGTAACCTTCACTC

>gi|387145078|gb|JK823217.1|JK823217 CA1110_P14 Clinocottus analis liver, muscle, gill library Clinocottus analis cDNA clone 1110_P14 5' similar to Complement C4 (Fragments), mRNA sequence
ACTTAAATTTAGACGAGCATGTCACCTACACAGTCTGCGTCAGTAACAGCCTGAACAGCACTCTCACAGG
AATGTCTATCGCTGACATCACACTTCTGAGTGGATTTGAGGCTGTAACTCAGGACCTGGACGCGCTAAAG
AAGTCACCTGAGCAATACATTTCCCATTACGAGATCTCAAACGGAAGAGTGCTGATCTACTTTAATGAGC
TCTTTGAATCAAAGGAATGTATTAGTTTCGATGCTGTACAGAGAGTACCAATTGGTCTTCTACAGCCCGC
TCCAGCTGTATTCTATGATTATTGCGAACCAAACAGAAAGTGTACTGTGTTCTACTCCGCCCCCAAACGG
AGCAAAATGGTCTCCAAACTGTGTTCAGAGGATGTGTGCCAATGTGCAGAAAGACCATGTCATAAAATAA
AAAATACATTCCTGTCAGAACGTGGTCGGGGAATCACAAAGTATGCCCGTTCAAAACATGCTTGCTTCTT
CCCAACAGTAGATTACGCATACATGGTTGAAGTCCTCAATGTGTCCATGAAGAATAACTTTGAGCTGTAC
AACATTAATGTAGAGGAGGTACTCAGATCACATGGAGACATCGAAGTGAGTGAGAATTCGATTCGAGTGT
TTGTTAAGAGGCAGCAGTGTAAAGAACAGTTAGACGTAGGAAACCAGTACCTGCTCATGGGAAAAGATGG
CTCCACAACGGACTCAAATGGAATGATGCGGTATCTGTTGGAGTCAAACACCTGGGTTGAAGGAAAGCCT
TCTGCAGAAGAATGTAAAAAATCTGCATATAAAGTGGCCTGCAGAGAGTTTAACGTGTTTACAGATGAGT
ACAAGATAGACGGCTGCAGACAGTGAAACGGACACATTATTTTAATCAAACTTTTGCTTTAGTAGTTTCC
CATGGNNGCTTANNNCNCATGGATGTTTAGAGCTCTTTTTTTTAACC

>gi|338827443|gb|GW606365.1|GW606365 LFSSH-Li-Nor-Hyp-#230 P. annectens normoxia and hypoxia SSH library Protopterus annectens cDNA 5' similar to Complement C4, mRNA sequence
AAGACCATCATGGTGACAAAGGCTGGAAGAAGTATACAAGAAGATTTACAGTTTCCTCTAGGAACCAAAA
TTAATGTTGATGTTCGAGGAAAGGGAAAAGGAGCCATAAGTATTATGAGACTGTATAATGTCATAGACGT
TGACAACAGCACTTGCACAGACATAAAAATTGAAGTGACTTTGAGAGGAGAGGTGAAGTATGAACCAGCT
GAAGACTATGATTATGACTATGGTGACGCAATGGCTGATGAACCCTTCAGCAAAATCAGCTGGTTTGACC
GGCGGAACAGAAGGAGGAGAGAAGCAGCAGCTCCCGGCAGCAGTGATAAAGCCGTGATATATGACATCTG
CATATGGAGAGACCCAAAAGCAAAGGTGTCCGGTATGGCTATTGCTGACATTACCATGCTGAGTGGCTTT
GAGCCAAACAGTGCTGACCTTGATAAGTTGGTTTCACTTACCGAACAATATATCAGTCACTATGAGTTCA
AGGAAGGGAGACTACTACTTTACTTTGATGAGATTCCAAAAGAAAAAGATTGCATATCCTTTGAAGCAAA
GCAAATTCTACCAATTGGACTACTTCAGCCCACTAGCGCAAGTCTTTATGATTTTTATGAACCAGGTC

>gi|253919982|gb|GR677478.1|GR677478 cNOnOV1017_J07.ab1_c Tilapia adult ovary library Oreochromis niloticus cDNA 5' similar to Complement C4 in Rattus norvegicus (P08649), mRNA sequence
GGGGAACCCAAGGATGATTGTGACCATCTGTTAATCAGTGTCAGAGTGGAGGGGAAAGTGAAGTACACAC
TTCCGGTATTAGAAAACTATGAATACTATGACTACGACGATGAGAAACAAGACCAGGAAGACTTGGGACG
AACAGCCATTGAGGGGTCTGATGCTCACACCCGATACAGGAGAACTGTTGATAACAACTTAAGTACAAAA
GAGGCTGTTACTTACACTGTCTGTGTCAGGCAGAAGAGCAATCTTACAGGAATGGCCATTGCTGACATCA
CATTACTGAGTGGATTTAAGGCTGAAACTAAAACTTTGGAGAGGATCGAAAGTGTACTGTGTTCTATTCT
GCACCGCAAAGAAGCAAGATGGTCTCCAAATTGTGTTCAGAGGACGTGTGCCAATGCGCAGAAAGACCTT
GTCATAAACTACAAGATACATTCAATCGAAGAAGAAGAATTAGGAAGATTAACCGTGTCCAACATGCTTG
CTTCTTCCCTATCGTAGATTATGCATATATTGTTGAAGTCTCCAGCATTTCTGTGAAGAGTAACTTTGAG
CTGTACACTACTTCTGTAATTGACGTTCTCAGATCAAATAACGATGTGTCAGTGAGTGAG

>gi|118496533|gb|EE993227.2|EE993227 AUF_IfSpn_231_p21 Ictalurus furcatus spleen cDNA library Ictalurus furcatus cDNA 5' similar to CD226 antigen; adhesion glycoprotein; platelet and T cell activation antigen 1; DNAX accessory molecule-1; T lineage-specific activation antigen 1 antigen, mRNA sequence
CCACGCGTCCGGAGAGTCATCCGGATTCTCAGAACCCGAGTTATCGTGAAAGAGCTCATTTCTTCATTGA
GGAGATCGCTCAGGGAAACTTCTCTCTCTTCCTTACGAACGTGACCCGGGAAGACGCAGGAGTTTATAAG
TGTGCTGTTTACACAAACCATGACTCCTATGAAACTCTGATTGAAATAAAGGAGATTGAGCGTTTGATCG

TGTCTGGAGCCCATGTCATATCTGCGTATGCGGGTGAAGATATCACTCTGAATTGCTCTGTAGACTCACA
TATCCCAGCGGAAAATATAGAACAGGTCTCATGGAGGAAAACGGATGGAGAGATCTTAGTGCTGCTCTAT
GAACATGGTGAGGTCCACACAGACTCGTCCCATGAGAGATACATGGACAGAGTGGAATTGTTCAGCGCTG
AAGAAAGAAACAAAGGAAACTTCTCATTGAGACTGAAGGATGTCCGAACTGACGATAAAGGGCTGTATAC
ATGTTCAGCATTCTCTGGGGCATTCTCAGATCACACAACTGTGGAAGTACAGCAGCTGAATTAAGATGGA
GATAACCCAGAAGCCAGAAGCCAGAAGCACCCACCATGACATGCTGACAGGGAAGGAGATAAACCCGCCA
CATTCTCTCTCAGTTCTCGCTGTCTCTCATTCTTTCTCTTTCCATCTTCTTCACTGTGATGAACTACAAG
CACGTAGCACATTCCTTCAGAAATCTCTCTCTCACACACACATACAAGCTATGCACACACACACACACAC
ACACACACACTCACACACACACACACACACACACGTGGTGGAAGATACACATTTNCTGGTACGCAGTGGTTC
ATTCCTGGTATCCAAATGGTTTTTCTCTAAAAAATAAAGGTAAACCACTGCTTTTTCTCAAAAAAAAAAA
AAAAAAAAACGCGGGC

>ENSGACG00000002708|CD226
AAAGGACCACTGGTACTTCGTGGTACTCCTCTTTCTTCCCCTTCTTGAAGGCGCGGCCCACGTTGCCATT
GTCAATCTCCAAGAAGGGATGGTCCTCAACTGTGTGTGCCCCTGGAGCGGCAACCTCAGCATGGTGTCCT
GGACCAAAGTGCCGGAAAAGTATCCGGTAGCCGTTTTCCACCCAGAGTATGGAGTGACCTTCTCCCACCA
TTACCGGGAGAGGATAGAGTTCCTGAGGACCACGCCTATGGATGGAAGTATTTCCATGAGGAACGTAACT
CACCAGGATATAGGGGTCTACCACTGCTCTGTTCAGACCTTCCCTCGAGGTCCCTGGACAAAGGACGTCC
AGGTGGAAGACTTAGACGAGCCCCCAGACGAAGAGAGCGAAGGCTCTGAGGCGATGGAGCCGTACGCGGA
GCAGGTGGCGGAGTCCGGCAACAACGCGACCATCCGCTGCGACCACCAGCACAGCGGCACCGTTCACCAG
GTCATTTTGGAGATGATGCCCCACGGCCAACCCTGGGGCATCATCGGTGTGTGTAAAAAGGTGGACGGGC
GCCTGGTGAGCGAGGACTACGGCGACAGGGGGACGATCGGCTGTGCGGACAGCCTGGACGCCAGTCTGCA
CCTGACGGGCGTGGTGCGGGAAGATGGCGGCTTCTACCGCTGCAGCTTCAGCACGGACGCCGGGTTGCTG
ACCACCACTGTGCTGCTCACCGTGTCCCCCCCAGGTGGATTCAGCCTGACGGTGTACATGATGTACATCT
ACATCGGGGCCGGAGCATCTGGGCTTCTTCTACTCATCGCCATCATTGCAGTGGCAGTGAAGCACAGG

> il17a_f3-001 ENSDART00000061523
ATGCGGCTCTCACGGGTTTTCAGAGCTGTGCTGCTGCTGTTTCTGCTCATGCTTTTGTTA
GATGCTGCTCTCTCTGAGAATAGGACTAAAAGAAAAAGATGTTCTGGTGTGAAGAAGTGT
ACTAGTGCTGGATGTAAATCAAGATGTCAAAGAAAGACAGCTTGGGTCATTCTAAACTCA
GCTTGGGACAATATAATGAGTGACACTCCGTCTCCAGACAGATCTCTGTCGCCTTGGACA
TACACAACTTCTGTTGATGAGTCACGAATCCCATCAACAATCTCAGAGGCAAAATGTGAA
AAAAGAGGCTGTTTAACAAAAGACGGTGAGGAGGACCTGGGACTGGAGTCCCAACCCATT
TACTACCAGATCAACATCCTGAGACGAGTGAAGAAAAAAAATTCAACATTTTACGCTCTT
AAACTGGAGACGAAAAAAGTTAGTGTTGGCTGCACATGCGTTTTACCAATTGTTTTGCCT
CAGAACTAG

> Il17a-001 ENSMUST00000027061
ATGAGTCCAGGGAGAGCTTCATCTGTGTCTCTGATGCTGTTGCTGCTGCTGAGCCTGGCG
GCTACAGTGAAGGCAGCAGCGATCATCCCTCAAAGCTCAGCGTGTCCAAACACTGAGGCC
AAGGACTTCCTCCAGAATGTGAAGGTCAACCTCAAAGTCTTTAACTCCCTTGGCGCAAAA
GTGAGCTCCAGAAGGCCCTCAGACTACCTCAACCGTTCCACGTCACCCTGGACTCTCCAC
CGCAATGAAGACCCTGATAGATATCCCTCTGTGATCTGGGAAGCTCAGTGCCGCCACCAG
CGCTGTGTCAATGCGGAGGGAAAGCTGGACCACCACATGAATTCTGTTCTCATCCAGCAA
GAGATCCTGGTCCTGAAGAGGGAGCCTGAGAGCTGCCCCTTCACTTTCAGGGTCGAGAAG
ATGCTGGTGGGTGTGGGCTGCACCTGCGTGGCCTCGATTGTCCGCCAGGCAGCCTAA

> IL17A-001 ENST00000340057
ATGACTCCTGGGAAGACCTCATTGGTGTCACTGCTACTGCTGCTGAGCCTGGAGGCCATA
GTGAAGGCAGGAATCACAATCCCACGAAATCCAGGATGCCCAAATTCTGAGGACAAGAAC
TTCCCCCGGACTGTGATGGTCAACCTGAACATCCATAACCGGAATACCAATACCAATCCC
AAAAGGTCCTCAGATTACTACAACCGATCCACCTCACCTTGGAATCTCCACCGCAATGAG
GACCCTGAGAGATATCCCTCTGTGATCTGGGAGGCAAAGTGCCGCCACTTGGGCTGCATC
AACGCTGATGGGAACGTGGACTACCACATGAACTCTGTCCCCATCCAGCAAGAGATCCTG
GTCCTGCGCAGGGAGCCTCCACACTGCCCCAACTCCTTCCGGCTGGAGAAGATACTGGTG
TCCGTGGGCTGCACCTGTGTCACCCCGATTGTCCACCATGTGGCCTAA

>gi|363409072|gb|JN398460.1| Hippocampus abdominalis MHC class II antigen beta chain (Hiab-DAB) gene, Hiab-DAB*19 allele, exon 2 and partial cds
ATGGCTACCTGTGGCATGCGGACACTGGTTGTGTGTTCAACTCGAGTGACCTGAATGACATCGAGTACTT
CGAGATTTACAACTACAACAAACTGAAGCTTTTCCGCTTCAGCAGCACTTTGGATAAGTTCGTCGGCTAC
ACCGAGTTTGGCATCAAGCAGGCTACCGTCTTCAACAACAACAAAGACATCATCGCCGACGCCAGAGCCA
GGAAAGAATACATTTGTTTAAACAATATTAAGATTGACTACGAAAGTGCGCTCACCAAGTCAG

>gi|148277545|ref|NM_001098262.1| Danio rerio similar to MHC class II antigen beta chain (LOC100002901), mRNA
AAACAGAACCACTTTTTACCAGCACAACGGAACTAATTGTTCTTTATACAGCTTTAAGACGAGTCTTTTC
AACGACAGACATGGAAGTGTTCACTGTCCGAGCATCTCTGTTAACTCTTCTGCTGTATCCACACATCATC
ATAACATGGACAGATTACCATACAGTAAATATTCTGGCCTACACAAGGGTGATGGGAAACGGCTCCATAG
ATCAGACAGTGGTTGTTTTAGTAAACGACGCCATATTTGCACACTTTGACAAAGCGAACAACACATTTGC
CTTAAATCCCACTGCAAGTGCTGGCTTTTCAGTTCTGGAGAAACGTGAAAGCATTTTCTGCCTCGGAGAG
GTGAATAAGGGATTTCATCGACAAACCGAATACCTGGAGAAACTTAAAAAAGAAACAAAATCCTCAAAGA
CACTTTTTGTACGCCCTTCAGTCATTATGTATGCTGAGTTTCCTGAAGAAGAAGGAAAAGCAAATGTCCT
TTACTGCTATGCTACCGGGTTTTACCCTGGTGACATTGATATAAGATTTTTCCTAAATGGCCAAAAATCC
ACTGCAAAACTAGAGACATCTGACCTAATGTATGGGGAAGACTGGACCTTCAGAGTCTTCAAGTATATGA
AGATCACCCCACAGACTGGAGACGAGTACACATGTGAAGTCAGACACAGCAGCATGTCTGAACCCAAAAT
CACAGTGTGGAGGCCTGAGTTTTCATCATCAACATCACATCCATACTGGGCTTATACAACGGCTCTCGGG
GTCATGTCGGGCATCGGGACATCTACCCTGATTTTGAAAAGAAAACATTGCTCTCAACTTTAAAGGCTTA
ATACTGGGTCCTGTTTTGTTCTCCCTTTACTTCCGTTAGGAAAAATTTGTGAAAAGCATGGCATAAATTA
CCATCTATATGCTGATGACTCTCAAATCTACTTCCCTATAAAATCTACACTACAAAAATTCGGCTAATTT
AAAAGTAAACAAAAATGTCAATTACTTTTAAACAATATTTAACTTGTAGCAACCCAAAGAAATTGAGTTG
ATAACTCAATTTTTCCACGTTAATGGAGTTGTTTTGTATATTTCCACACACTGATGTTTTTGCTGTTTTT
TATACTGATAATATGGAACACTACATGTTTTTGTTTTGTAAAACAATAAAAACCTGTTTTATATAAAAAA
TATATATATTACTGAAAAACAAAAAAAAAAAAAAAAAAAAAAAAAAAAAAAAAAAAAAAAAAAAAAAAAA

>gi|374082910|gb|JN827383.1| Gasterosteus aculeatus clone GN709K12 MHC class II antigen beta chain (Gaac-DXB) gene, exon 2 and partial cds
GAGTTCATCGACTCTTATTACTACAACAAGTTAGAACTCACGAGGTTCAGCAGCTCAGTGGGGAAGTATG
TCGGCTTCACTGAGTACGGAGTGAGGAACGCTGAATACTGGAACAACGACGCTTCACTTCTGAGTGCTAT
GAGAGCTCAGAAGGAGGTTTACTGTCTGAACCACGTCCCGGTCTATTACAGCAATGCTCTGACTAAGTCC
GGTGAGTCAGAGCGACATTATTATTATCATCGTTATTATTATCACATTATGATAAATGTCATTACATTAT
TATCACATATTGATCAAATAACGTGAACTAAACGCTGACGTCAGACTGAAGTCTTTCTCCACCTTGTGGT
GAAGTTGTGCTACTACAGCTCCGACTAATATTACTACTTATTCATGTGCTCATCACTCATCACCTCATCG
GACCCGAGAATCACTTCTTCATCTTCTCATGAACATTTTATATCAAATCAATCCATTAAACGATCCAATC
AGGAATATTACAAAGTCATTTAGTAAAATGACTTAAATAAATAAAGTCTGCTGTATTTAACTTCAAATCT
GAGCTTCAACTTTGTAAAATAGTTTAAAATAGTTTATAATAGTTAATATAATCAAATCAAAGAGAAAATC
ACGCGGTAGTTTATTCTAAAGTAAAGATCATTTATTAGGAAATCCAACTAGAACCTGATACACATCTTCT
GTAATAAATGATTCACGTTGTTATACATATTTTATATAGTTTACTCGTGTGGTTTAATATGTAACACATT
TATAAATAATATAATGATGTTGTTTTACACCAAATCATATAATATAATTATATGATCAAATATTAAACAG
AAGAAACACTTTGAATTCAAGTATCAAGTATTTATGGACACTTTATGGATATTATTGAGTAGAACATTTT
ATCTGTGAGTACATGACTGGTACTTGTACTGCAGCTGGTACTACTGCTACTACCTTAAGTACTCCTAGTA
CTAATCCTCGTACCTGTAAGCTCATAGAACAAACCCTCACCATGTCATATATTGTCTCCAG

>gi|300791239|gb|HM596888.1| Salmo trutta MHC class II antigen beta chain (Satr-DAB) gene, Satr-DAB*n allele, partial cds
GATGGATATTTTTATCAGAGGGTGGCAGAGTGCCGATTCTCCTCAAAGGACCTGCAGGGTATAGAGTTGA
TAGACTCTTATGTTTTCAATCAGGCTGAACATATCAGATTCAACAGCACTGTGGGGAAGTATGTTGGATA
CACTGAGCATGGAGTGTACAATGCAGAAGCCTGGAACAGTGATGCTGCGTTCCTGGCTCAAGAGCGAGGG
GAGCTGGAGCGTGTCTGTAAGCATAACGCTGATCTCCACTACAGCGC

Supplementary material S.1.2 Detailed description of validation of bioinformatical search strategies to identify MHC class IIβ genes in *Syngnathus typhle*

To validate our bioinformatical approaches for identifying key immune genes in the transcriptome of *Syngnathus typhle* (assembly + tBLASTx) we spiked the real read data with short MHC II fragments derived from three-spined sticklebacks (*Gasterosteus aculeatus*) and seahorse (*Hippocampus abdominalis*) and found successful recovery.

1. To test de novo assembly and contig annotation, a MHC class IIβ gene from *Gasterosteus aculeatus* was randomly cut into 15 sequences of 101 bp length, resembling typical Illumina sequences. These sequences were added to a subsample of 10 million reads and then used in a de novo assembly. Subsequent annotation of resulting contigs successfully recovered an annotated MHC class IIβ contig consisting of stickleback sequences.

2. To test the tBLASTx sensitivity, a MHC class IIβ gene from *Hippocampus abdominalis* (JN398460) was randomly shortened to 15 sequences 101 bp long, resembling typical Illumina sequences. These sequences were added to 250 million single end rawreads. The modified raw reads were transformed into a blast database and used in a subsequent tBLASTx search, using MHC class II sequences from 3 fish species as query. Hippocampus sequences were excluded as query to account for a possible sequence divergence due to phylogenetic distances. The approach identified 13 of the 15 *Hippocampus* sequences (87%), all by amino acid sequence similarity to *Gasterosteus aculeatus*.

A clustalw based alignment between translated coding sequences of stickleback (gil 374082910|gb|JN827383.1) and seahorse (gil363409072|gb|JN398460.1) MHC class IIβ chains reveals 70 overlapping amino acids, of which 33 (47%) are a perfect match, 25 (36%) are non-perfect similarities and 12 (17%) are total substitutions. Since we include the *Hippocampus* MHC class IIβ sequence in our regular tBLASTx search and seahorses are more closely related to pipefish than to sticklebacks, we are confident that our approach would display detectable MHC class II sequences of pipefish. To account additionally for complexity based assembly problems, MHC class IIβ sequences of seahorses and sticklebacks were analysed via RepeatMasker, using *Danio rerio* (zebrafish) settings as reference (the only teleost, see www.repeatmasker.org). Of the longer stickleback sequence, 5.67% were marked as simple repeats, while the rest was free of any repeat structure. In the seahorse sequence no repeats could be detected. Thus, abundant repeats in our major target genes cannot be responsible for any failure to detect MHC.

Supplementary Table S.1.1 Overview on PCR-primers used in the targeted cloning approaches to identify MHC class IIβ-genes, either in combination, or in a 3'-RACE approach. The nucleotide alignment that served to design our own primers is given in Supplementary Table S2.

Primer	Nucleotide sequence 5'->3'	Reference
Sato GA11	AACTCCACTGAGCTGAAGGACATC	Sato et al. 1998
Sato GA11 mod1	AACTCCACGGAGCTGAAGGACAT	own alignment
Pipe_MHCf2	CGTCTACGACTTCTACCCCA	own alignment
Pipe_MHCf3	CGACTTCTACCCCAAACAGATC	own alignment
Pipe_MHCr1	TGGACCTGGTAGTACCAGTC	own alignment
Pipe_MHCr2	GAGTGGATCTGGTAGTACCAGTC	own alignment
Pipe_MHCr3	TAGACCAGGTGAGAGTGGA	own alignment
Pipe_MHCr4	CCAGGTGGGAGTGGA	own alignment
MHC_pipe_wob_r1_2	GAGTGGATCTGGTAGTACCAGTC	own alignment
MHC_pipe_wob_r3_4	TAGACCAGGTGAGAGTGGA	own alignment
MHC_pipe_fr3	GATCTGTTTGGGGTAGAAGTCG-	own alignment
Sato_Ga11_mod_rev	ATGTCCTTCAGCTCCGTGGAGTT-	own alignment
Sato_Ga11_wob_rev	ATGTCCTTCAGCTCAGTGGAGT	own alignment
GAIIEx1F	CAGCGTCTCCCTCCTCTTCA	Lenz et al. 2009
GAIIEx2startF	GTCTTTAACTCCACGGAGCTGAAGG	Lenz et al. 2009
GAIIExon2R_RSCA	ACTCACCGGACTTAGTCA	Lenz et al. 2009
MHCIIB-E3F2	GCCTTACGTCAGACTTCACTCG	Bahr & Wilson 2012
MHCIIb-E3R3	GGCGTGTAGACCAGGTGAGA	Bahr & Wilson 2012

Supplementary table S.1.2 Nucleotide alignment of MHC class IIβ coding sequences of 6 Actinopterygii species along with the seahorse (*Hippocampus abdominalis*, Syngnathidae). Given are the locations of all 18 PCR primers used for cloning approaches.

```
                                 ....|....| ....|....| ....|....| ....|....| ....|....| ....|....|
....|....| ....|....| ....|....| ....|....|
                                        10         20         30         40         50         60
70         80         90        100
BT027207.1|Gasterosteus a   ATGGCTCCAT CCTTCATCAG CGTCTCCCTC CTCTTCAT-- ---CGGCCTC CACGCAGCAG
ATGGATTCAT GGAGTTTAGG ACGTTTCGTT GTGTCTTTAA
gb|EF681865.1|Larimichthy   ATGGCTTCAT CCTTCATCAG CTTCTCCCTG CTCTTCATCA ---GCCTCTG CACAG--CAG
ATGGATTCAT GGAATCATTT TTGGGCCGTT GTGTTTTTAA
gb|DQ821113.1|Dicentrarch   ATGGCTTCAT CCTTTCTCAG CTTCTCCCTC CTCTTCATCA TCAGCCTCTA CACAG--CAG
ATGGATTCCG GAGTTATGAC ATAGATCGCT GTGTGTTTAA
gb|EU399186.1|  Epinephel   ATGGCTTCAT CCTTTCTCAG CTTCTCCCTC CTCTTCAT-- -CAGCCTCTA CACAG--CAG
ATGGGTTTAG GTGTTATAGT CTGTTCCGCT GTGACTTTAA
gb|EU909404.2| Archoplite   ---------- ---------- ---------- ---------- ---------- ----------
---------- ---------- ---------- ----------
gb|AY158838.1| Stizostedi   ATGGCTTCAT CCTTTCTCAG CGTCTCCCTG CTCTTCAT-- -CAGCCTCTA CACAG--CAG
ATGGATTCAT GGAATATAAT CTGGCCCGTT GTGTGTTCAA
AFI42568.1 [Hippocampus a   ATGGCTACGT TTGCTCGGGT CGCCTGCCTC CTTTTCCTCA CCTTCTACGT GACAGATGGC
TACCTGTTTC ATACGGACGT TGGTTGTGTG TTCAACTCGA
primerSato_GA11             ---------- ---------- ---------- ---------- ---------- ----------
---------- ---------- ---------- --------AA
primerSato_GA11_mod1        ---------- ---------- ---------- ---------- ---------- ----------
---------- ---------- ---------- --------AA
MHC_pipe_f2                 ---------- ---------- ---------- ---------- ---------- ----------
---------- ---------- ---------- ----------
MHC_Pipe_f3                 ---------- ---------- ---------- ---------- ---------- ----------
---------- ---------- ---------- ----------
MHC_pipe_r1                 ---------- ---------- ---------- ---------- ---------- ----------
---------- ---------- ---------- ----------
MHC_pipe_r2                 ---------- ---------- ---------- ---------- ---------- ----------
---------- ---------- ---------- ----------
MHC_pipe_r3                 ---------- ---------- ---------- ---------- ---------- ----------
---------- ---------- ---------- ----------
MHC_pipe_r4                 ---------- ---------- ---------- ---------- ---------- ----------
---------- ---------- ---------- ----------
MHC_pipe_wob_r1_2           ---------- ---------- ---------- ---------- ---------- ----------
---------- ---------- ---------- ----------
MHC_pipe_wob_r3_4           ---------- ---------- ---------- ---------- ---------- ----------
---------- ---------- ---------- ----------
MHC_pipe_fr3                ---------- ---------- ---------- ---------- ---------- ----------
---------- ---------- ---------- ----------
SatoGA11_mod_1              ---------- ---------- ---------- ---------- ---------- ----------
---------- ---------- ---------- --------AA
SatoGA11_wob_1              ---------- ---------- ---------- ---------- ---------- ----------
---------- ---------- ---------- --------AA
GAIIEx1F                    ---------- -------CAG CGTCTCCCTC CTCTTCAT-- ---------- ----------
---------- ---------- ---------- ----------
GAIIEx2startF               ---------- ---------- ---------- ---------- ---------- ----------
---------- ---------- ---------- --GTCTTTAA
GAIIExon2R_RSCA             ---------- ---------- ---------- ---------- ---------- ----------
---------- ---------- ---------- ----------
MHCIIB-E3F2                 ~~~~~~~~~~ ~~~~~~~~~~ ~~~~~~~~~~ ~~~~~~~~~~ ~~~~~~~~~~ ~~~~~~~~~~
~~~~~~~~~~ ~~~~~~~~~~ ~~~~~~~~~~ ~~~~~~~~~~
MHCIIb-E3R3                 ~~~~~~~~~~ ~~~~~~~~~~ ~~~~~~~~~~ ~~~~~~~~~~ ~~~~~~~~~~ ~~~~~~~~~~
~~~~~~~~~~ ~~~~~~~~~~ ~~~~~~~~~~ ~~~~~~~~~~


                                 ....|....| ....|....| ....|....| ....|....| ....|....| ....|....|
....|....| ....|....| ....|....| ....|....|
                                       110        120        130        140        150        160
170        180        190        200
BT027207.1|Gasterosteus a   CTCCACGGAG CTGAAGGACA TCGAGTACAT CGACTCGTAT TTCTTCAACA AGTTAGAACT
CACGAGGTTC AGCAGCTCAG TGGGGAAGTT TGTCGGCTTC
gb|EF681865.1|Larimichthy   CTCGACTGAT CTGAAGAACA TTGAGTTCAT CGCCTCTTGG TATTACAACA AGATGGAGTA
CACCAGGTTC AGCAGCAGTG TGGGGAAGTT TGTTGGATTC
gb|DQ821113.1|Dicentrarch   CTCCACTGAT CCGAAGAACA TCGAGTACAT CTACTCTCAA TATTACAACA AGTTGGAGTT
CACCAGGTTC AGCAGCAGTG TGGGAGAGTA TGTTGGTTAC
gb|EU399186.1|  Epinephel   CTCCACTGAT CTGAAGGACA TCGAGTACAT CTACTCTGAA TATTACAACA AGCTGGAGAT
CGCCAGGTTC AGCAGCAGTG TGGGGAAGTA TGTTGGATAC
```

```
gb|EU909404.2| Archoplite   ---------- ---------- ---------- ---------- ------AACA ATGACGAGTA
CATCAGGTTC AGCAGCAGTG TGGGGCAGCA TGTTGGATAC
gb|AY158838.1| Stizostedi   CTCCTCTGAT CTGAAGGACA TCGAGTTCAT CTACTCAATG TACTACAACA AGTTAGAGTT
CATCAGGTTC AGCAGCAGTT TGGGGAAGTA TGTTGGATAC
AFI42568.1 [Hippocampus a   GTGACCTGAA TGACATCGAG TACTTCCAGA TTTACAACTA CAACAAACTG AAGCTTTTCC
GCTTCAGCAG CACTTTGGAT AAGTACGTCG GCTACACAGA
primerSato_GA11             CTCCACTGAG CTGAAGGACA TC-------- ---------- ---------- ----------
---------- ---------- ---------- ----------
primerSato_GA11_mod1        CTCCACGGAG CTGAAGGACA T--------- ---------- ---------- ----------
---------- ---------- ---------- ----------
MHC_pipe_f2                 ---------- ---------- ---------- ---------- ---------- ----------
---------- ---------- ---------- ----------
MHC_Pipe_f3                 ---------- ---------- ---------- ---------- ---------- ----------
---------- ---------- ---------- ----------
MHC_pipe_r1                 ---------- ---------- ---------- ---------- ---------- ----------
---------- ---------- ---------- ----------
MHC_pipe_r2                 ---------- ---------- ---------- ---------- ---------- ----------
---------- ---------- ---------- ----------
MHC_pipe_r3                 ---------- ---------- ---------- ---------- ---------- ----------
---------- ---------- ---------- ----------
MHC_pipe_r4                 ---------- ---------- ---------- ---------- ---------- ----------
---------- ---------- ---------- ----------
MHC_pipe_wob_r1_2           ---------- ---------- ---------- ---------- ---------- ----------
---------- ---------- ---------- ----------
MHC_pipe_wob_r3_4           ---------- ---------- ---------- ---------- ---------- ----------
---------- ---------- ---------- ----------
MHC_pipe_fr3                ---------- ---------- ---------- ---------- ---------- ----------
---------- ---------- ---------- ----------
SatoGA11_mod_1              CTCCACGGAG CTGAAGGACA T--------- ---------- ---------- ----------
---------- ---------- ---------- ----------
SatoGA11_wob_1              CTCCACWGAW CTGAAGWACA T--------- ---------- ---------- ----------
---------- ---------- ---------- ----------
GAIIEx1F                    ---------- ---------- ---------- ---------- ---------- ----------
---------- ---------- ---------- ----------
GAIIEx2startF               CTCCACGGAG CTGAAGG--- ---------- ---------- ---------- ----------
---------- ---------- ---------- ----------
GAIIExon2R_RSCA             ---------- ---------- ---------- ---------- ---------- ----------
---------- ---------- ---------- ----------
MHCIIB-E3F2                 ~~~~~~~~~~ ~~~~~~~~~~ ~~~~~~~~~~ ~~~~~~~~~~ ~~~~~~~~~~ ~~~~~~~~~~
~~~~~~~~~~ ~~~~~~~~~~ ~~~~~~~~~~ ~~~~~~~~~~
MHCIIb-E3R3                 ~~~~~~~~~~ ~~~~~~~~~~ ~~~~~~~~~~ ~~~~~~~~~~ ~~~~~~~~~~ ~~~~~~~~~~
~~~~~~~~~~ ~~~~~~~~~~ ~~~~~~~~~~ ~~~~~~~~~~


                            ....|....| ....|....| ....|....| ....|....| ....|....| ....|....|
....|....| ....|....| ....|....| ....|....|
                                     210        220        230        240        250        260
270        280        290        300
BT027207.1|Gasterosteus a   ACTGAGTACG GAGTGAGGAA CGCTGAATAC TGGAACAACA ACCCTTCATA TCTGAGTGCT
ATGAAGGCTC AGAAGGAGGT TTACTGTCTG AACCACGTCC
gb|EF681865.1|Larimichthy   ACAGAGTACG GTGTGAAGAA CGCAGAGTAC TGGAACAATG ATGCTTCATT TCTGGCTCAG
ACGAGAGGCG AGAAGGAGAG ATACTGTCTG AACCACATTC
gb|DQ821113.1|Dicentrarch   ACTGAGTTCG GAGTGAAACA GGCTAAATAC TTTAACAGTA ATCCTTCAAT ACTGGCTCAG
AGGAGAGGTG AGAAGGAGAG GTACTGCCTG AACCACGTTA
gb|EU399186.1|  Epinephel   ACTGAGTTTG GTGTGAAGCA GGCTGAGAAC TGGAACAAAG ATTCTTCAGA ACTGGCTCGG
AGGAGTGCTG AGAAGGAGAG GTTCTGTCTG AACAACATTG
gb|EU909404.2| Archoplite   ACTGAGCATG GAGTGAAGAA CGCTGAGGCC TGGAACAAAG ATGCTGGAAA ACTGGCTGCG
ATGAGAGCTC AGAAGGAGAC GTACTGCCTA AACAACGTTG
gb|AY158838.1| Stizostedi   ACTGAGTTTG GAGTGAAGAA CGCAGAACGT CTCAACAATG ATCCTTCAGA ACTGGCTCGG
AGGAAAGCTG ATAAGGAGAG ATACTGCAAA CACAACATTG
AFI42568.1 [Hippocampus a   GTTTGGCATC AAGCAGGCTA CCGCCTTCAA CAACGACAAA G-ACATCATC GCCGACGCCA
GAGCCAGGAA AGAATACATT TGTTTAAACA ATATTAAGCT
primerSato_GA11             ---------- ---------- ---------- ---------- ---------- ----------
---------- ---------- ---------- ----------
primerSato_GA11_mod1        ---------- ---------- ---------- ---------- ---------- ----------
---------- ---------- ---------- ----------
MHC_pipe_f2                 ---------- ---------- ---------- ---------- ---------- ----------
---------- ---------- ---------- ----------
MHC_Pipe_f3                 ---------- ---------- ---------- ---------- ---------- ----------
---------- ---------- ---------- ----------
MHC_pipe_r1                 ---------- ---------- ---------- ---------- ---------- ----------
---------- ---------- ---------- ----------
MHC_pipe_r2                 ---------- ---------- ---------- ---------- ---------- ----------
---------- ---------- ---------- ----------
MHC_pipe_r3                 ---------- ---------- ---------- ---------- ---------- ----------
---------- ---------- ---------- ----------
```

```
MHC_pipe_r4                 ---------- ---------- ---------- ---------- ---------- ----------
---------- ---------- ---------- ----------
MHC_pipe_wob_r1_2           ---------- ---------- ---------- ---------- ---------- ----------
---------- ---------- ---------- ----------
MHC_pipe_wob_r3_4           ---------- ---------- ---------- ---------- ---------- ----------
---------- ---------- ---------- ----------
MHC_pipe_fr3                ---------- ---------- ---------- ---------- ---------- ----------
---------- ---------- ---------- ----------
SatoGA11_mod_1              ---------- ---------- ---------- ---------- ---------- ----------
---------- ---------- ---------- ----------
SatoGA11_wob_1              ---------- ---------- ---------- ---------- ---------- ----------
---------- ---------- ---------- ----------
GAIIEx1F                    ---------- ---------- ---------- ---------- ---------- ----------
---------- ---------- ---------- ----------
GAIIEx2startF               ---------- ---------- ---------- ---------- ---------- ----------
---------- ---------- ---------- ----------
GAIIExon2R_RSCA             ---------- ---------- ---------- ---------- ---------- ----------
---------- ---------- ---------- ----------
MHCIIB-E3F2                 ~~~~~~~~~~ ~~~~~~~~~~ ~~~~~~~~~~ ~~~~~~~~~~ ~~~~~~~~~~ ~~~~~~~~~~
~~~~~~~~~~ ~~~~~~~~~~ ~~~~~~~~~~ ~~~~~~~~~~
MHCIIb-E3R3                 ~~~~~~~~~~ ~~~~~~~~~~ ~~~~~~~~~~ ~~~~~~~~~~ ~~~~~~~~~~ ~~~~~~~~~~
~~~~~~~~~~ ~~~~~~~~~~ ~~~~~~~~~~ ~~~~~~~~~~


                            ....|....| ....|....| ....|....| ....|....| ....|....| ....|....|
....|....| ....|....| ....|....| ....|....|
                                     310        320        330        340        350        360
370        380        390        400
BT027207.1|Gasterosteus a   CGGTCTATTA CAGCAATGCT CTGACTAAGT CCGCTGAGCC CTACGTCAGG CTGCACTCTG
AGACGCCCCC TGGTGGTGGA CCTTTGTCCA TGTTGGTCTG
gb|EF681865.1|Larimichthy   AGGCCTGGTA CAGCCACACT CTGGATAAGT CAGCTAAGCC GTATGTCAGG CTGCACTCTG
TGACGCCCCC TGGTGGTCAC CATCCCTCCA TGCTGGTCTG
gb|DQ821113.1|Dicentrarch   ACGCTTACTA CCCGCATGCT CTGGATAAAT CAGTTAAGCC CTATGTCAGA CTGCGCTCGG
TGGCGCCCCC TGCTGGTAAA CATCCCTCCA TGTTGGTCCG
gb|EU399186.1|  Epinephel   AGGCTTTCTA CCCAAATATT CTGACTAAGC CAGCTGAGCC GTATGTCAGG CTGCACTCTG
TGACGCCCTC TGGAGGTAAA CATTCAGCCA TGTTGGTCTG
gb|EU909404.2| Archoplite   GGATCGACTA CCAGGCTGCT CTGACTAAGT CAGCTGAGCC CTACGTGTTC CTGAGCTCTG
TGACGCCCCC TGGTGGTAAA CATCCCTCCA TGTTGGTCTG
gb|AY158838.1| Stizostedi   ATATCCGGTA CCACGCTGCT CTGACTAAAT CAGCTGAGCC GTATGTCAGA CTGAGCTCTA
CGGCGTCCCC TGGTGGTAAA CATTCAGCCA TGTTGGTCTG
AFI42568.1 [Hippocampus a   TGACTACGAA AGTGCGCTCA CCAAGTCAGC CAAGCCTTAC GTCAGACTTC ACTCGGAGTC
TCCT~~~~CC GGAGGGCTCC CACTCCGCCA TGCTGGTGTG
primerSato_GA11             ---------- ---------- ---------- ---------- ---------- ----------
---------- ---------- ---------- ----------
primerSato_GA11_mod1        ---------- ---------- ---------- ---------- ---------- ----------
---------- ---------- ---------- ----------
MHC_pipe_f2                 ---------- ---------- ---------- ---------- ---------- ----------
---------- ---------- ---------- ----------
MHC_Pipe_f3                 ---------- ---------- ---------- ---------- ---------- ----------
---------- ---------- ---------- ----------
MHC_pipe_r1                 ---------- ---------- ---------- ---------- ---------- ----------
---------- ---------- ---------- ----------
MHC_pipe_r2                 ---------- ---------- ---------- ---------- ---------- ----------
---------- ---------- ---------- ----------
MHC_pipe_r3                 ---------- ---------- ---------- ---------- ---------- ----------
---------- ---------- ---------- ----------
MHC_pipe_r4                 ---------- ---------- ---------- ---------- ---------- ----------
---------- ---------- ---------- ----------
MHC_pipe_wob_r1_2           ---------- ---------- ---------- ---------- ---------- ----------
---------- ---------- ---------- ----------
MHC_pipe_wob_r3_4           ---------- ---------- ---------- ---------- ---------- ----------
---------- ---------- ---------- ----------
MHC_pipe_fr3                ---------- ---------- ---------- ---------- ---------- ----------
---------- ---------- ---------- ----------
SatoGA11_mod_1              ---------- ---------- ---------- ---------- ---------- ----------
---------- ---------- ---------- ..........
SatoGA11_wob_1              ---------- ---------- ---------- ---------- ---------- ----------
---------- -----..... .......... ..........
GAIIEx1F                    ---------- ---------- ---------- ---------- ---------- ----------
---------- ---------- ---------- ----------
GAIIEx2startF               ---------- ---------- ---------- ---------- ---------- ----------
---------- ---------- ---------- ----------
GAIIExon2R_RSCA             ---------- ---------- CTGACTAAGT
CCGGTGAGT- .......... .......... .......... .......... .......... ..........
MHCIIB-E3F2                 ~~~~~~~~~~ ~~~~~~~~~~ ~~~~~~~~~~ ~~~~~~~GCC TTACGTCAGA
CTTCACTCG. .......... .......... .......... ..........
```

```
MHCIIb-E3R3                 ~~~~~~~~~~ ~~~~~~~~~~ ~~~~~~~~~~ ~~~~~~~~~~ ~~~~~~~~~~ ~~~~~~~~~~
~~~~~~~~~~ ~~~~~~~~~~ ~~~~~~~~~~ ~~~~~~~~~~


                            ....|....| ....|....| ....|....| ....|....| ....|....| ....|....|
....|....| ....|....| ....|....| ....|....|
                                     410        420        430        440        450        460
470        480        490        500
BT027207.1|Gasterosteus a   CAGCGTCTAT GACTTCTACC CCAAGAAGAT CATAGTGAGG TGGACCAGAG ACGG~AGGCC
AGAGACCACC GGGGTCACTT CTACCGACGA GCTGGCAGAC
gb|EF681865.1|Larimichthy   CAGCGTCTTC GACTTCTACC CCCAACACAT CAAGGTGAGC TGGATCAGAG ACGGA~AGGA
AGTCACCTCT GATGTCACTT CCACTGATGA GCTGGCAGAC
gb|DQ821113.1|Dicentrarch   CAGCGTCTAC GACTTCTTCC CCAAACACAT CAGAGTGAGC TGGCTCAGAG ACGGA~AGGA
AGTCACCTCT GATGTCACTT CCACTGATGA GCTGGCAGAC
gb|EU399186.1|  Epinephel   CAGCGTCTTC AACTTCTACC CCAAAAAGAT CAAAGTCAGC TGGCTCAGAG ACGGA~AGGA
AGTCACCTCT GATGTCACTT CCACTGATGA GCTGGCAGAC
gb|EU909404.2| Archoplite   CAGCGTCTTC GACTTCTACC CCAAACAGAT CAGAGTGGGC TGGCTCAGAG ACGGA~AGGA
AGTCAGCTCT GATGTCACTT CCACTGATGA GCTGGCAGAC
gb|AY158838.1| Stizostedi   CAGCGTCTAC GACTTCTACC CCAAACAGAT CAGAGTGAGC TGGACCAGAG ACGGA~AGGA
AGTCACCTCT GATGTCACTT CCACTGATGA GCTGGCAGAC
AFI42568.1 [Hippocampus a   CATCGTCTAC GACTTCTACC CCAAGCAGAT CCGCGTCAAC TGGCTGAGGG ACGGCCAGGA
AGCCACGGGC GAGGTGACCT CCACCGACGA GATGCCCGAC
primerSato_GA11             ---------- ---------- ---------- ---------- ---------- ----------
---------- ---------- ---------- ----------
primerSato_GA11_mod1        ---------- ---------- ---------- ---------- ---------- ----------
---------- ---------- ---------- ----------
MHC_pipe_f2                 ---CGTCTAC GACTTCTACC
CCA....... .......... .......... .......... .......... .......... .......... ..........
MHC_Pipe_f3                 ---------C GACTTCTACC CCAAACAGAT
C......... .......... .......... .......... .......... .......... ..........
MHC_pipe_r1                 ---------- ---------- ---------- ---------- ---------- ----------
---------- ---------- ---------- ----------
MHC_pipe_r2                 ---------- ---------- ---------- ---------- ---------- ----------
---------- ---------- ---------- ----------
MHC_pipe_r3                 ---------- ---------- ---------- ---------- ---------- ----------
---------- ---------- ---------- ----------
MHC_pipe_r4                 ---------- ---------- ---------- ---------- ---------- ----------
---------- ---------- ---------- ----------
MHC_pipe_wob_r1_2           ---------- ---------- ---------- ---------- ---------- ----------
---------- ---------- ---------- ----------
MHC_pipe_wob_r3_4           ---------- ---------- ---------- ---------- ---------- ----------
---------- ---------- ---------- ----------
MHC_pipe_fr3                ---------C GACTTCTACC CCAAACAGAT C--------- ---------- ----------
---------- ---------- ---------- ----------
SatoGA11_mod_1              .......... .......... .......... .......... .......... ..........
.......... .......... .......... ..........
SatoGA11_wob_1              .......... .......... .......... .......... .......... ..........
.......... .......... .......... ..........
GAIIEx1F                    ---------- ---------- ---------- ---------- ---------- ----------
---------- ---------- ---------- ----------
GAIIEx2startF               ---------- ---------- ---------- ---------- ---------- ----------
---------- ---------- ---------- ----------
GAIIExon2R_RSCA             .......... .......... .......... .......... .......... ..........
.......... .......... .......... ..........
MHCIIB-
E3F2                   .......... .......... .......... .......... .......... ..........
.......... .......... .......... ..........
MHCIIb-E3R3                 ~~~~~~~~~~ ~~~~~~~~~~ ~~~~~~~~~~ ~~~~~~~~~~ ~~~~~~~~~~ ~~~~~~~~~~
~~~~~~~~~~ ~~~~~~~~~~ ~~~~~~~~~~ ~~~~~~~~~~


                            ....|....| ....|....| ....|....| ....|....| ....|....| ..
                                     510        520        530        540        550
BT027207.1|Gasterosteus a   GGGGATTGGT ACTACCAGAC CCACTCCCAC CTGGAGTACA CGCCC..... ..
gb|EF681865.1|Larimichthy   GCTGATTGGT ACTACCAGAT CCACTCTCAC CTGGAGTACA CGCCC..... ..
gb|DQ821113.1|Dicentrarch   GCTGATTGGT TCTACCAGAT CCACTCTCAC CTGGAGTACA CGCCC..... ..
gb|EU399186.1|  Epinephel   GGTGATTGGT ACTACCAGAT CCACTCTCAC CTGGAGTACA CGCCC..... ..
gb|EU909404.2| Archoplite   GGGGACTGGT ACTACCAGGT CCACTCTCAC CTGGAGTACA CGCCC..... ..
gb|AY158838.1| Stizostedi   GGTGATTGGT ACTACCAGAT CCACTCTCAC CTGGAGTACA CGCCC..... ..
AFI42568.1 [Hippocampus a   GGCGACTGGT ACTACCAGGT CCACTCTCAC CTGGTCTACA CGCCGCGACT GA
primerSato_GA11             ---------- ---------- ---------- -------... .......... ..
primerSato_GA11_mod1        ---------- ---------- ---------- -------... .......... ..
MHC_pipe_f2                 .......... .......... .......... .......... .......... ..
MHC_Pipe_f3                 .......... .......... .......... .......... .......... ..
MHC_pipe_r1                 --GACTGGTA CTACCAGGTC CA........ .......... .......... ..
MHC_pipe_r2                 ---GCTGGTA CTACCAGATC CACTC..... .......... .......... ..
MHC_pipe_r3                 ---------- --------TC CACTCTCACC TGGTCTA... .......... ..
```

```
MHC_pipe_r4                 ---------- --------TC CACTCCCACC TGG....... .......... ..
MHC_pipe_wob_r1_2           --GACTGGTA CTACCAGWTC CACTC----- -------... .......... ..
MHC_pipe_wob_r3_4           ---------- --------TC CACTCWCACC TGGTCTA... .......... ..
MHC_pipe_fr3                ---------- ---------- ---------- -------... .......... ..
SatoGA11_mod_1              .......... .......... .......... .......... .......... ..
SatoGA11_wob_1              .......... .......... .......... .......... .......... ..
GAIIEx1F                    ---------- ---------- ---------- -------... .......... ..
GAIIEx2startF               ---------- ---------- ---------- -------... .......... ..
GAIIExon2R_RSCA             .......... .......... .......... .......... .......... ..
MHCIIB-E3F2                 .......... .......... .......... .......... .......... ..
MHCIIb-E3R3                 ~~~~~~~~~~ ~~~~~~~~~~ ~~~TCTCACC TGGTCTACAC GCC....... ..
```

Supplementary Table S.1.3 *Syngnathus typhle*: EST library types, tissue, sequence reads statistics

Library type	tissue	#individuals	Raw reads (10^6)	Reads after clipping (10^6)	Merged only (10^6)	Mean length merged (bp)
454 normalized	Head kidney/ gill/liver	5 (3 Baltic, 2 Adriatic Sea)	0.90	0.57	84	278
Ilumina paired end	Head kidney	1 (Baltic)	257	213	84	149
Ilumina paired end	liver	1 (Baltic)	240	220	38	146
Ilumina paired end	gill	1 (Baltic)	246	123	93	149

Supplementary Table S.1.4 *Syngnathus typhle*: mapping statistics of all quality checked reads against mixed assembly (454 plus 5 mio reads each tissue)

Illumina library	Total reads (10^6)	Reads mappable (10^6)	Reads left (10^6)
Head kidney	220	177	42
liver	123	98	25
gill	213	167	45

Supplementary Table S.1.5 Bit scores and read statistics for 11 immune genes identified via reciprocal tBLASTx search in 750 mio *Syngnathus typhle* ESTs. Genes with several identified reads (PSMB8, RAG2, complement C4 and C1qT4, IL12A, IL17A) were successfully assembled into respective contigs based on the short reads identified via tblastx. The retrieved sequence reads representing genes PSMB9, PSMB10, AIRE, FOXP3 and CD226 were not sufficient in number to produce contigs. However, here annotation metrics for single sequences are similar or better than in the assembled genes and above commonly used thresholds (supplementary table S6). This suggests that the annotation of those reads is correct as well.

gene_name	bit_score	e-value	read retrieved
AIRE	62	3.00E-08	HWI-ST758:61:B0272ACXX:7:1304:1508:118853 1:N:0:
C1QT4	62	3.00E-08	HWI-ST758:61:B0272ACXX:5:1303:2064:126331 2:N:0:
C1QT4	64.3	6.00E-09	HWI-ST758:61:B0272ACXX:7:1204:19035:199665 2:N:0:
C1QT4	73.9	8.00E-12	HWI-ST758:61:B0272ACXX:5:1303:2064:126331 1:N:0:
C1QT4	60.5	9.00E-08	HWI-ST758:61:B0272ACXX:7:2106:9864:124661 1:N:0:
C1QT4	72.4	2.00E-11	HWI-ST758:61:B0272ACXX:5:1302:2389:105196 1:N:0:
C1QT4	57.8	6.00E-07	HWI-ST758:61:B0272ACXX:7:2302:16517:143923 1:N:0:
C1QT4	55.8	2.00E-06	HWI-ST758:61:B0272ACXX:5:2308:16930:62378 1:N:0:
C1QT4	64.3	6.00E-09	HWI-ST758:61:B0272ACXX:7:1204:19035:199665 1:N:0:
C1QT4	55.5	3.00E-06	HWI-ST758:61:B0272ACXX:5:2306:4682:89923 1:N:0:
C1QT4	68.2	4.00E-10	HWI-ST758:61:B0272ACXX:5:1207:12107:179321 1:N:0:
C1QT4	68.9	3.00E-10	HWI-ST758:61:B0272ACXX:5:1105:12955:119811 1:N:0:
C1QT4	62.8	2.00E-08	HWI-ST758:61:B0272ACXX:5:1108:9040:115759 1:N:0:
C1QT4	64.7	5.00E-09	HWI-ST758:61:B0272ACXX:7:2107:9602:22927 1:N:0:
C1QT4	64.3	6.00E-09	HWI-ST758:61:B0272ACXX:5:2301:13356:32512 1:N:0:
C1QT4	61.2	5.00E-08	HWI-ST758:61:B0272ACXX:7:2302:16517:143923 2:N:0:
C1QT4	63.5	1.00E-08	HWI-ST758:61:B0272ACXX:7:2105:15452:137119 1:N:0:
C1QT4	60.5	9.00E-08	HWI-ST758:61:B0272ACXX:7:2206:3891:60758 1:N:0:
C1QT4	68.2	4.00E-10	HWI-ST758:61:B0272ACXX:5:1101:7058:145154 1:N:0:
C1QT4	62.4	2.00E-08	HWI-ST758:61:B0272ACXX:5:1101:7058:145154 2:N:0:
C1QT4	73.9	8.00E-12	HWI-ST758:61:B0272ACXX:7:1101:7776:98987 2:N:0:
C1QT4	62.4	2.00E-08	HWI-ST758:61:B0272ACXX:7:1203:4549:143045 1:N:0:
C4	43.5	0.011	HWI-ST758:61:B0272ACXX:6:1208:5336:200109 1:N:0:

C4	37.4	0.81	HWI-ST758:61:B0272ACXX:6:1107:15871:189465 1:N:0:
C4	38.1	0.48	HWI-ST758:61:B0272ACXX:6:1304:11188:95458 1:N:0:
C4	45.8	0.002	HWI-ST758:61:B0272ACXX:5:2303:5338:9783 1:N:0:
C4	43.9	0.009	HWI-ST758:61:B0272ACXX:6:1205:18270:88600 1:N:0:
C4	42.4	0.025	HWI-ST758:61:B0272ACXX:6:1204:10963:162144 1:N:0:
C4	41.6	0.043	HWI-ST758:61:B0272ACXX:6:1202:16419:25413 1:N:0:
C4	41.6	0.043	HWI-ST758:61:B0272ACXX:6:1103:9493:96981 1:N:0:
C4	47.4	8.00E-04	HWI-ST758:61:B0272ACXX:6:1205:3425:145758 1:N:0:
C4	43.1	0.015	HWI-ST758:61:B0272ACXX:6:1305:4469:52712 1:N:0:
C4	39.7	0.16	HWI-ST758:61:B0272ACXX:6:1308:8340:120393 1:N:0:
C4	38.1	0.48	HWI-ST758:61:B0272ACXX:6:1108:13369:25399 1:Y:0:
C4	42.4	0.025	HWI-ST758:61:B0272ACXX:6:1101:14449:195331 1:N:0:
C4	45.1	0.004	HWI-ST758:61:B0272ACXX:6:1202:5574:165585 1:N:0:
C4	42.4	0.025	HWI-ST758:61:B0272ACXX:6:1303:17014:40973 1:N:0:
C4	42.4	0.025	HWI-ST758:61:B0272ACXX:6:1108:7308:33557 1:Y:0:
C4	47.4	8.00E-04	HWI-ST758:61:B0272ACXX:6:1301:9506:96445 1:N:0:
C4	38.5	0.37	HWI-ST758:61:B0272ACXX:6:1108:15170:32787 1:N:0:
C4	42.4	0.025	HWI-ST758:61:B0272ACXX:6:1307:3128:23958 1:N:0:
C4	43.1	0.015	HWI-ST758:61:B0272ACXX:6:1208:18541:63322 1:N:0:
C4	41.6	0.043	HWI-ST758:61:B0272ACXX:6:1101:20086:193057 1:N:0:
C4	43.5	0.011	HWI-ST758:61:B0272ACXX:6:1308:8297:78269 1:N:0:
C4	43.9	0.009	HWI-ST758:61:B0272ACXX:6:1107:14404:139980 1:N:0:
C4	42.7	0.019	HWI-ST758:61:B0272ACXX:6:1202:20789:56796 1:N:0:
C4	42.7	0.019	HWI-ST758:61:B0272ACXX:6:1205:17187:2520 1:N:0:
C4	47.4	8.00E-04	HWI-ST758:61:B0272ACXX:6:1305:15018:145829 1:N:0:
C4	41.6	0.043	HWI-ST758:61:B0272ACXX:6:1108:17995:195062 1:N:0:
C4	45.4	0.004	HWI-ST758:61:B0272ACXX:6:1207:15676:65975 1:N:0:
CD226	59.7	2.00E-07	HWI-ST758:61:B0272ACXX:5:1302:19959:117238 1:N:0:
CD226	71.6	4.00E-11	HWI-ST758:61:B0272ACXX:6:1107:12197:143109 1:N:0:
CD226	68.2	4.00E-10	HWI-ST758:61:B0272ACXX:5:2308:12201:95985 1:Y:0:
CD226	69.3	2.00E-10	HWI-ST758:61:B0272ACXX:5:1102:14786:42822 1:N:0:

CD226	63.5	1.00E-08	HWI-ST758:61:B0272ACXX:5:2308:12201:95985 2:Y:0:
CD226	63.9	8.00E-09	HWI-ST758:61:B0272ACXX:5:1107:18373:170532 1:N:0:
FOXP3	74.7	5.00E-12	HWI-ST758:61:B0272ACXX:6:1103:18464:146927 1:N:0:
FOXP3	63.2	1.00E-08	HWI-ST758:61:B0272ACXX:6:2201:1976:27936 2:Y:0:
PSMB10	67	1.00E-09	HWI-ST758:61:B0272ACXX:7:2305:4496:54842 1:N:0:
PSMB10	52.4	2.00E-05	HWI-ST758:61:B0272ACXX:7:2304:10049:73896 1:N:0:
PSMB8	54.3	6.00E-06	HWI-ST758:61:B0272ACXX:7:2102:8017:148789 1:N:0:
PSMB8	45.1	0.004	HWI-ST758:61:B0272ACXX:7:1301:12993:187278 1:N:0:
PSMB8	60.5	9.00E-08	HWI-ST758:61:B0272ACXX:5:1305:15838:28010 1:N:0:
PSMB8	49.7	2.00E-04	HWI-ST758:61:B0272ACXX:7:2206:5522:122302 1:N:0:
PSMB8	57	1.00E-06	HWI-ST758:61:B0272ACXX:7:1203:18495:95027 1:N:0:
PSMB8	44.7	0.005	HWI-ST758:61:B0272ACXX:5:2108:17397:140779 1:N:0:
PSMB8	56.2	2.00E-06	HWI-ST758:61:B0272ACXX:7:2202:15441:186712 1:N:0:
PSMB8	55.8	2.00E-06	HWI-ST758:61:B0272ACXX:5:1304:19264:13475 1:N:0:
PSMB8	59.7	2.00E-07	HWI-ST758:61:B0272ACXX:5:1203:5360:151559 1:N:0:
PSMB8	57.8	6.00E-07	HWI-ST758:61:B0272ACXX:7:2208:14055:27771 1:N:0:
PSMB8	42.4	0.025	HWI-ST758:61:B0272ACXX:7:1303:2436:182110 1:N:0:
PSMB8	54.3	6.00E-06	HWI-ST758:61:B0272ACXX:7:1103:16385:7695 1:N:0:
PSMB8	54.3	6.00E-06	HWI-ST758:61:B0272ACXX:5:2102:15231:187289 1:N:0:
PSMB8	58.5	3.00E-07	HWI-ST758:61:B0272ACXX:5:2208:14134:197344 1:N:0:
PSMB8	56.2	2.00E-06	HWI-ST758:61:B0272ACXX:7:1304:8742:187782 1:N:0:
PSMB8	42.7	0.019	HWI-ST758:61:B0272ACXX:6:1207:16182:65882 1:N:0:
PSMB8	55.8	2.00E-06	HWI-ST758:61:B0272ACXX:5:1102:6504:99697 1:N:0:
PSMB8	57.8	6.00E-07	HWI-ST758:61:B0272ACXX:6:1208:20666:168709 1:N:0:
PSMB8	56.6	1.00E-06	HWI-ST758:61:B0272ACXX:7:1102:9359:118970 1:N:0:
PSMB8	52.4	2.00E-05	HWI-ST758:61:B0272ACXX:5:2204:17690:90029 1:N:0:
PSMB8	45.5	0.003	HWI-ST758:61:B0272ACXX:7:2108:20239:140194 1:N:0:
PSMB8	49.7	2.00E-04	HWI-ST758:61:B0272ACXX:7:1108:10208:171825 1:N:0:
PSMB8	54.3	6.00E-06	HWI-ST758:61:B0272ACXX:7:2201:5387:20281 1:N:0:
PSMB8	53.5	1.00E-05	HWI-ST758:61:B0272ACXX:5:2208:8952:182418 1:N:0:
PSMB8	55.8	3.00E-06	HWI-ST758:61:B0272ACXX:7:1104:15433:125689 1:Y:0:

PSMB8	55.5	3.00E-06	HWI-ST758:61:B0272ACXX:5:2208:7212:190335 1:N:0:
PSMB8	58.5	3.00E-07	HWI-ST758:61:B0272ACXX:7:1202:4052:183177 1:N:0:
PSMB8	53.9	8.00E-06	HWI-ST758:61:B0272ACXX:5:2203:6719:23707 1:N:0:
PSMB8	52.8	2.00E-05	HWI-ST758:61:B0272ACXX:7:2208:9259:170110 1:N:0:
PSMB8	55.8	2.00E-06	HWI-ST758:61:B0272ACXX:7:2108:4215:36681 1:N:0:
PSMB8	54.7	5.00E-06	HWI-ST758:61:B0272ACXX:7:1105:10360:190457 1:N:0:
PSMB8	58.5	3.00E-07	HWI-ST758:61:B0272ACXX:5:2303:6784:184938 1:N:0:
PSMB8	56.6	1.00E-06	HWI-ST758:61:B0272ACXX:7:2304:4534:179269 2:N:0:
PSMB8	48.5	4.00E-04	HWI-ST758:61:B0272ACXX:7:1208:2854:31543 1:Y:0:
PSMB8	38.1	0.48	HWI-ST758:61:B0272ACXX:7:2307:12673:76874 1:N:0:
PSMB8	57	1.00E-06	HWI-ST758:61:B0272ACXX:7:1107:18994:121708 2:N:0:
PSMB9	69.7	1.00E-10	HWI-ST758:61:B0272ACXX:6:1107:19813:33744 2:N:0:
PSMB9	38.1	0.48	HWI-ST758:61:B0272ACXX:7:2105:8896:37271 1:N:0:
RAG2	66.6	1.00E-09	HWI-ST758:61:B0272ACXX:5:1203:7888:280301:N:0:
RAG2	61.6	4.00E-08	HWI-ST758:61:B0272ACXX:5:2306:8921:1873631:N:0:
RAG2	65.5	3.00E-09	HWI-ST758:61:B0272ACXX:5:2207:11226:1117871:N:0:
RAG2	68.9	3.00E-10	HWI-ST758:61:B0272ACXX:5:1104:7486:813092:N:0:
RAG2	56.6	1.00E-06	HWI-ST758:61:B0272ACXX:5:1303:20920:1529011:N:0:
RAG2	64.3	6.00E-09	HWI-ST758:61:B0272ACXX:5:1303:12044:838381:N:0:
RAG2	69.3	2.00E-10	HWI-ST758:61:B0272ACXX:5:1205:13304:1538021:N:0:
RAG2	63.2	1.00E-08	HWI-ST758:61:B0272ACXX:5:2203:2640:1288891:N:0:
RAG2	59.7	2.00E-07	HWI-ST758:61:B0272ACXX:5:2102:15722:1648461:N:0:
RAG2	50.8	7.00E-05	HWI-ST758:61:B0272ACXX:5:2208:18308:1332641:N:0:
RAG2	57	1.00E-06	HWI-ST758:61:B0272ACXX:5:2205:20343:169212:N:0:
RAG2	57.4	8.00E-07	HWI-ST758:61:B0272ACXX:5:2201:8406:1340201:N:0:
RAG2	67.4	7.00E-10	HWI-ST758:61:B0272ACXX:5:2207:12567:1167311:N:0:
RAG2	60.1	1.00E-07	HWI-ST758:61:B0272ACXX:5:2303:15121:44132:N:0:
RAG2	71.2	5.00E-11	HWI-ST758:61:B0272ACXX:5:2203:11708:841682:N:0:
RAG2	57	1.00E-06	HWI-ST758:61:B0272ACXX:5:2202:16912:1012982:N:0:
RAG2	68.6	3.00E-10	HWI-ST758:61:B0272ACXX:5:2201:13057:776461:N:0:
RAG2	55.1	4.00E-06	HWI-ST758:61:B0272ACXX:5:1205:4564:848922:N:0:

RAG2	43.5	0.011	HWI-ST758:61:B0272ACXX:5:1107:16468:683711:N:0:
RAG2	55.1	4.00E-06	HWI-ST758:61:B0272ACXX:5:1106:6404:1156192:N:0:
RAG2	63.9	8.00E-09	HWI-ST758:61:B0272ACXX:5:1205:4564:848921:N:0:
RAG2	57.8	6.00E-07	HWI-ST758:61:B0272ACXX:5:2101:11373:85912:N:0:
RAG2	67	1.00E-09	HWI-ST758:61:B0272ACXX:5:1304:4933:1582451:N:0:
RAG2	71.6	4.00E-11	HWI-ST758:61:B0272ACXX:5:2105:8559:778292:N:0:
RAG2	71.2	5.00E-11	HWI-ST758:61:B0272ACXX:5:2106:10244:281702:N:0:
RAG2	67	1.00E-09	HWI-ST758:61:B0272ACXX:5:1108:13951:1141761:N:0:
RAG2	58.2	4.00E-07	HWI-ST758:61:B0272ACXX:5:1302:19609:1637261:N:0:
RAG2	55.1	4.00E-06	HWI-ST758:61:B0272ACXX:5:1303:3166:767302:N:0:
RAG2	67	1.00E-09	HWI-ST758:61:B0272ACXX:5:2206:18528:155402:N:0:
RAG2	39.3	0.21	HWI-ST758:61:B0272ACXX:5:2108:18419:1019181:N:0:
RAG2	66.2	2.00E-09	HWI-ST758:61:B0272ACXX:5:1201:6019:80592:N:0:
RAG2	58.9	3.00E-07	HWI-ST758:61:B0272ACXX:5:1305:4088:1555121:N:0:
RAG2	53.9	8.00E-06	HWI-ST758:61:B0272ACXX:5:2302:20525:825621:N:0:
RAG2	71.2	5.00E-11	HWI-ST758:61:B0272ACXX:5:2206:21096:1748262:N:0:
RAG2	46.6	0.001	HWI-ST758:61:B0272ACXX:5:2206:19001:698591:N:0:
RAG2	53.5	1.00E-05	HWI-ST758:61:B0272ACXX:5:1206:16951:521741:N:0:
RAG2	64.7	5.00E-09	HWI-ST758:61:B0272ACXX:7:2207:3809:1143341:N:0:
RAG2	62.8	2.00E-08	HWI-ST758:61:B0272ACXX:5:1304:19224:1839201:N:0:
RAG2	55.8	2.00E-06	HWI-ST758:61:B0272ACXX:7:1308:8984:1996511:Y:0:
RAG2	68.9	3.00E-10	HWI-ST758:61:B0272ACXX:5:1206:6016:969591:N:0:
RAG2	62.8	2.00E-08	HWI-ST758:61:B0272ACXX:5:2108:6240:983361:N:0:
RAG2	63.2	1.00E-08	HWI-ST758:61:B0272ACXX:5:2206:12309:250031:N:0:
RAG2	60.8	7.00E-08	HWI-ST758:61:B0272ACXX:5:1108:19677:1941892:N:0:
RAG2	66.2	2.00E-09	HWI-ST758:61:B0272ACXX:7:1302:10176:1089701:N:0:
RAG2	62	3.00E-08	HWI-ST758:61:B0272ACXX:5:1107:14960:494941:N:0:
RAG2	48.5	4.00E-04	HWI-ST758:61:B0272ACXX:5:1108:14666:1600011:N:0:
RAG2	65.1	4.00E-09	HWI-ST758:61:B0272ACXX:5:1107:4097:1331482:N:0:
RAG2	60.5	9.00E-08	HWI-ST758:61:B0272ACXX:5:1206:15216:404402:N:0:
RAG2	70.5	9.00E-11	HWI-ST758:61:B0272ACXX:5:1208:9491:226111:N:0:

RAG2	55.1	4.00E-06	HWI-ST758:61:B0272ACXX:5:1303:3639:911252:Y:0:
RAG2	69.3	2.00E-10	HWI-ST758:61:B0272ACXX:5:2104:16038:440401:N:0:
RAG2	44.3	0.007	HWI-ST758:61:B0272ACXX:5:1207:4940:1932441:N:0:
RAG2	45.1	0.004	HWI-ST758:61:B0272ACXX:5:2106:8426:45571:N:0:
RAG2	57.4	8.00E-07	HWI-ST758:61:B0272ACXX:5:1207:8368:1502781:N:0:
RAG2	61.2	5.00E-08	HWI-ST758:61:B0272ACXX:5:2206:14239:365452:N:0:
RAG2	51.6	4.00E-05	HWI-ST758:61:B0272ACXX:5:1207:8598:1870001:N:0:
RAG2	66.2	2.00E-09	HWI-ST758:61:B0272ACXX:5:2208:2082:1204351:N:0:
RAG2	63.2	1.00E-08	HWI-ST758:61:B0272ACXX:7:2308:5092:176821:N:0:
RAG2	67.8	6.00E-10	HWI-ST758:61:B0272ACXX:7:1107:13505:886651:N:0:
RAG2	55.8	2.00E-06	HWI-ST758:61:B0272ACXX:5:2202:8809:938851:N:0:
RAG2	56.6	1.00E-06	HWI-ST758:61:B0272ACXX:5:1107:4097:1331481:N:0:
RAG2	61.2	5.00E-08	HWI-ST758:61:B0272ACXX:5:2204:4838:876652:N:0:
RAG2	57.4	8.00E-07	HWI-ST758:61:B0272ACXX:5:1106:3308:1766791:Y:0:
RAG2	56.6	1.00E-06	HWI-ST758:61:B0272ACXX:5:1208:17481:723041:N:0:
RAG2	65.1	4.00E-09	HWI-ST758:61:B0272ACXX:5:2102:12591:397022:N:0:
RAG2	65.1	4.00E-09	HWI-ST758:61:B0272ACXX:5:2205:12993:1397391:N:0:
RAG2	55.8	2.00E-06	HWI-ST758:61:B0272ACXX:5:2106:6735:312141:N:0:
RAG2	33.5	0.012	HWI-ST758:61:B0272ACXX:5:2103:4525:212261:N:0:
RAG2	57	1.00E-06	HWI-ST758:61:B0272ACXX:5:1303:13015:1206252:N:0:
RAG2	60.1	1.00E-07	HWI-ST758:61:B0272ACXX:5:2104:1651:819491:N:0:
RAG2	56.6	1.00E-06	HWI-ST758:61:B0272ACXX:5:1205:14568:90671:N:0:
RAG2	68.2	4.00E-10	HWI-ST758:61:B0272ACXX:5:2204:20896:493701:N:0:
RAG2	65.1	4.00E-09	HWI-ST758:61:B0272ACXX:5:1204:13133:1297942:N:0:
RAG2	50.4	9.00E-05	HWI-ST758:61:B0272ACXX:5:2108:12303:436891:N:0:
RAG2	56.6	1.00E-06	HWI-ST758:61:B0272ACXX:5:1106:17261:950291:N:0:
RAG2	66.6	1.00E-09	HWI-ST758:61:B0272ACXX:5:2105:21054:1092551:N:0:
RAG2	45.8	0.002	HWI-ST758:61:B0272ACXX:7:1303:11617:1921651:N:0:
RAG2	66.6	1.00E-09	HWI-ST758:61:B0272ACXX:5:2304:12243:1161782:N:0:
RAG2	65.5	3.00E-09	HWI-ST758:61:B0272ACXX:5:2202:16912:1012981:N:0:
RAG2	55.8	2.00E-06	HWI-ST758:61:B0272ACXX:5:1201:10420:1725471:N:0:

RAG2	55.1	4.00E-06	HWI-ST758:61:B0272ACXX:5:2104:5840:753171:N:0:
RAG2	70.1	1.00E-10	HWI-ST758:61:B0272ACXX:5:1308:13425:298731:N:0:
RAG2	55.5	3.00E-06	HWI-ST758:61:B0272ACXX:5:1103:7098:1851491:N:0:
RAG2	53.9	8.00E-06	HWI-ST758:61:B0272ACXX:5:2208:11210:856262:N:0:
RAG2	60.1	1.00E-07	HWI-ST758:61:B0272ACXX:5:1102:1546:667852:N:0:
RAG2	55.1	4.00E-06	HWI-ST758:61:B0272ACXX:5:2106:17337:549112:Y:0:
RAG2	67.4	7.00E-10	HWI-ST758:61:B0272ACXX:5:2203:3771:1947282:N:0:
RAG2	66.2	2.00E-09	HWI-ST758:61:B0272ACXX:5:2205:2664:222401:N:0:
RAG2	63.9	8.00E-09	HWI-ST758:61:B0272ACXX:5:2107:8046:59211:N:0:
RAG2	55.8	2.00E-06	HWI-ST758:61:B0272ACXX:5:2202:9496:1138061:N:0:
RAG2	68.2	4.00E-10	HWI-ST758:61:B0272ACXX:5:2308:9828:463552:N:0:
RAG2	53.9	8.00E-06	HWI-ST758:61:B0272ACXX:5:1102:2747:1043761:N:0:
RAG2	56.6	1.00E-06	HWI-ST758:61:B0272ACXX:5:2108:8706:1139452:Y:0:
RAG2	60.8	7.00E-08	HWI-ST758:61:B0272ACXX:5:2202:15493:1303211:N:0:
RAG2	64.7	5.00E-09	HWI-ST758:61:B0272ACXX:5:2305:2369:1024081:N:0:
RAG2	70.1	1.00E-10	HWI-ST758:61:B0272ACXX:5:1306:17892:725782:N:0:
RAG2	63.9	8.00E-09	HWI-ST758:61:B0272ACXX:5:2107:20771:1299832:N:0:
RAG2	57	1.00E-06	HWI-ST758:61:B0272ACXX:5:1302:10952:114911:N:0:
RAG2	55.8	2.00E-06	HWI-ST758:61:B0272ACXX:5:2208:13709:823271:N:0:
RAG2	60.8	7.00E-08	HWI-ST758:61:B0272ACXX:5:2102:19868:732531:N:0:
RAG2	70.1	1.00E-10	HWI-ST758:61:B0272ACXX:7:2107:7775:34572:N:0:
RAG2	67.8	6.00E-10	HWI-ST758:61:B0272ACXX:5:1101:3645:1399041:N:0:
RAG2	58.9	3.00E-07	HWI-ST758:61:B0272ACXX:5:1102:18614:380881:N:0:
RAG2	55.5	3.00E-06	HWI-ST758:61:B0272ACXX:5:1207:12052:1814052:N:0:
RAG2	64.3	6.00E-09	HWI-ST758:61:B0272ACXX:5:2101:1959:1925521:N:0:
RAG2	59.7	2.00E-07	HWI-ST758:61:B0272ACXX:5:2108:10403:261012:N:0:
RAG2	63.5	1.00E-08	HWI-ST758:61:B0272ACXX:5:2107:10413:55201:Y:0:
RAG2	63.9	8.00E-09	HWI-ST758:61:B0272ACXX:5:2203:4957:487101:N:0:
RAG2	61.6	4.00E-08	HWI-ST758:61:B0272ACXX:5:2301:15417:1387491:N:0:
RAG2	67	1.00E-09	HWI-ST758:61:B0272ACXX:5:1108:5808:1000561:N:0:
RAG2	62.8	2.00E-08	HWI-ST758:61:B0272ACXX:5:1105:5437:1630552:N:0:
RAG2	51.6	4.00E-05	HWI-ST758:61:B0272ACXX:5:1206:7889:89471:N:0:

RAG2	59.7	2.00E-07	HWI-ST758:61:B0272ACXX:5:1208:16939:1507821:Y:0:
RAG2	55.1	4.00E-06	HWI-ST758:61:B0272ACXX:5:1203:14958:168821:N:0:
RAG2	70.5	9.00E-11	HWI-ST758:61:B0272ACXX:5:2202:7941:182662:N:0:
RAG2	48.5	4.00E-04	HWI-ST758:61:B0272ACXX:5:1203:8378:1980591:N:0:
RAG2	65.5	3.00E-09	HWI-ST758:61:B0272ACXX:5:1105:5437:1630551:N:0:
RAG2	64.7	5.00E-09	HWI-ST758:61:B0272ACXX:5:2106:21192:1466282:N:0:
RAG2	53.9	8.00E-06	HWI-ST758:61:B0272ACXX:5:1207:19232:602731:N:0:
RAG2	66.2	2.00E-09	HWI-ST758:61:B0272ACXX:7:1101:7957:606191:N:0:
RAG2	56.6	1.00E-06	HWI-ST758:61:B0272ACXX:5:2103:1810:1760991:Y:0:
RAG2	81.3	5.00E-14	HWI-ST758:61:B0272ACXX:7:2104:16053:1367511:N:0:
RAG2	56.6	1.00E-06	HWI-ST758:61:B0272ACXX:5:2106:20468:827031:N:0:
RAG2	61.6	4.00E-08	HWI-ST758:61:B0272ACXX:5:2107:5705:1167591:N:0:
RAG2	65.9	2.00E-09	HWI-ST758:61:B0272ACXX:7:2102:18773:1135511:N:0:
RAG2	67.8	6.00E-10	HWI-ST758:61:B0272ACXX:5:2104:13568:1488201:N:0:
RAG2	60.5	9.00E-08	HWI-ST758:61:B0272ACXX:7:2203:8164:436241:N:0:
RAG2	70.1	1.00E-10	HWI-ST758:61:B0272ACXX:5:1202:15128:971901:N:0:
RAG2	67.4	7.00E-10	HWI-ST758:61:B0272ACXX:5:1201:10726:1925872:N:0:
RAG2	57	1.00E-06	HWI-ST758:61:B0272ACXX:5:1203:10908:1140601:N:0:
IL12B	56,6	1,00E-06	HWI-ST758:61:B0272ACXX:5:1307:11362:152989 1:N:0:
IL12B	54,3	6,00E-06	HWI-ST758:61:B0272ACXX:5:1308:10350:89504 1:N:0:
IL12B	57	1,00E-06	HWI-ST758:61:B0272ACXX:5:1305:15764:82865 2:N:0:
IL12B	57	1,00E-06	HWI-ST758:61:B0272ACXX:5:1104:13591:130392 2:N:0:
IL12B	59,3	2,00E-07	HWI-ST758:61:B0272ACXX:5:1101:2747:25400 2:N:0:
IL12B	54,3	6,00E-06	HWI-ST758:61:B0272ACXX:5:1104:19117:56844 2:N:0:
IL12B	59,3	2,00E-07	HWI-ST758:61:B0272ACXX:7:1101:13556:143617 1:N:0:
IL12B	54,3	6,00E-06	HWI-ST758:61:B0272ACXX:7:1105:1545:89558 2:N:0:
IL17A	54,29	6,44E-06	HWI-ST758:61:B0272ACXX:7:1301:2749:143329 2:N:0:
IL17A	62,77	1,81E-08	HWI-ST758:61:B0272ACXX:7:2106:18709:200715 2:N:0:
IL17A	55,83	2,21E-06	HWI-ST758:61:B0272ACXX:7:2206:14404:129038 2:N:0:
IL17A	55,06	3,77E-06	HWI-ST758:61:B0272ACXX:7:2305:18032:47034 2:N:0:
IL17A	86,65	1,19E-15	HWI-ST758:61:B0272ACXX:5:2108:11269:58964 1:N:0:
IL17A	60,46	9,03E-08	HWI-ST758:61:B0272ACXX:5:2301:15999:147251 1:N:0:

IL17A	85,11	3,46E-15	HWI-ST758:61:B0272ACXX:5:1106:9953:128048 1:N:0:
IL17A	69,32	1,96E-10	HWI-ST758:61:B0272ACXX:5:1307:18409:198874 1:N:0:
IL17A	71,63	3,92E-11	HWI-ST758:61:B0272ACXX:5:2207:15090:171603 1:N:0:
IL17A	64,69	4,82E-09	HWI-ST758:61:B0272ACXX:5:2208:4721:182741 1:N:0:
IL17A	55,06	3,77E-06	HWI-ST758:61:B0272ACXX:5:1206:2716:6001 1:N:0:
IL17A	59,69	1,56E-07	HWI-ST758:61:B0272ACXX:5:1105:16236:200307 1:N:0:
IL17A	56,22	1,74E-06	HWI-ST758:61:B0272ACXX:5:2304:18427:10652 1:N:0:
IL17A	60,07	1,17E-07	HWI-ST758:61:B0272ACXX:5:1208:13261:22642 1:N:0:
IL17A	62,77	1,81E-08	HWI-ST758:61:B0272ACXX:5:1105:16413:26952 1:N:0:
IL17A	62,77	1,81E-08	HWI-ST758:61:B0272ACXX:5:1302:11483:8784 1:N:0:
IL17A	62,77	1,81E-08	HWI-ST758:61:B0272ACXX:5:1101:13228:165881 1:N:0:
IL17A	68,55	3,40E-10	HWI-ST758:61:B0272ACXX:5:2203:2862:130019 1:N:0:
IL17A	59,69	1,57E-07	HWI-ST758:61:B0272ACXX:5:2106:16260:82621 1:N:0:

Supplementary Table S.1.6 read and annotation statistics of 6 immune genes that were identified in the reciprocal tBLASTx search where single retrieved reads could be re-assembled into contigs.

PSMB 8 36 reads of which 34 were assembled into a contig; bit score 92.4; evalue 2e-20

>PSMB8_tblastx_20130107_c01
gtctgtggctgggacaagagaggcccagggctgtactacgttgactcggaaggaagccga
gtttgcggcgacatattctcactgggctctgsctccatctacgcctacggtgtgatggac
agcggctttcggcaagatctgaccgtggaggaagcctgcg

RAG2 130 reads, which resulted in 2 non-overlapping contigs

RAG2 contig 01; 90 reads; bit score 230; e-value 5e-70

>RAG2_tblastx_20130107_c02
ccaagagctaacagacaattccactcctctcgargattcagatgagctmtattttggccg
tgagcctcaagagcttgatgatagtagtgagggtgaaggtratacctacaatgagaaaga
tgaggagsatgagtcgcaatatggctactggatsaaatgttgccgtggttgtcagctgga
tgtcaatrcwtgggagccgtattactccactgagctccaatggccagccatgatcttttg
ttccaaaagagaggccggacactgggtccatgcccagtgcatggggctgtctgaaacaat
gctcctcgaactgtcgcagggaaacaaaaaatacttctgccgagaacacgggggtcttcc
gaagcaggagatgaccccacctcaaaaggttataccactaacacataagcctttaaaagt
caagcaaaggaaatcgca

RAG2 contig 02; 36 reads; bit score 128; e-value 2e-33

>RAG2_tblastx_20130107_c03
ggatgactctgcaaccattaaagccagtcaactgcgaarrtcttctgcaacctggctgtt
ctsttctgcagcttgacggtgaagttctcctgtttggccagaaaggatggccaaagcgct
cctgtccaacaggagtatttggtgtgcgcttgaaacatggygagctgaggttgagagcca
tatctttctccaatgactcccagtaccttcctc

C1qT4: 21 reads of which 9 were assembled into 1 contig; bit score 159; evalue 1e-45

>syt_C1qT4_tblastx_20130107_c05
agcgagggtcgccatggaggcggagccagatgctgtcaccaaactccagctgcagcatga
cactctggctctgtaccttcctctcctctccagcattctcttcatacacaatggcttgca
cctcatttctattcttcatcagcatcacagacaagtctttatgagggaactttcccactg
taaaggagaagtagtaggccccagggatgcgacagcgaaacaagcc

C4 28 reads of which 26 were assembled into 1 contig; bit score 55.5; evalue 2e-07

>syt_C4_tblastx_20130107_c04
gcctccagagtcaagaccgtgtcctgcagtgagtagaatccctscccgtagtgctgatcc
wgggtcagccaggacacgatggggktggcgtacggaatccggccmttcagyagcgcsctg
agcarcccktaggctgtcgtctccaccgtcakgccactggc

IL17A/F1 19 reads of which 18 were assembled into a contig; bit score 94.0; e-value 1e-22

```
>IL17A/F1_tblastx_20130107_rep_c6
gcgcgtctgatgcgggtgggcgcccgacgacttgacgcggcgcagcagcagaacctgatg
caggatgggccgcgactccagcctcaggtcttccacgcygctcgagtccaggcagccgcg
caacacgcagcgggcctcagacacgggaggaaagagcgccgcgtcctgcgacacgttata
cgtccagggtgagatggagcggttgtgcagcg
```

IL12B 8 reads; bit score 76.6; e-value 1e-15

```
>IL12B_tblastx_20130107_c7
ctcttcttggtgaagtcctcttgaataaggacaacagtgtaattgagaagagatccattt
gagctgtggcagctgtagttgcctcctcccaaactctcctcgagctttaccaggtatgaa
ttacccctctgtgccttttc
```

Supplementary table S.1.7 Amino acid alignment of putative invariant chain genes from 10 teleost species and a truncated gene found in Syngnathus typhle (pos 279 of alignment, bottom).

```
                                    ....|....| ....|....| ....|....| ....|....|
....|....| ....|....| ....|....| ....|....|
                                            10        20        30        40
50        60        70        80
Q8JFN4| [Oncorhynchus mykiss]     ---------- --MEEQQQQR HDDALLERAG SQDVILPITT
NTRASNSRAF KVAGLTVLAC LLLAGQALTT YLVLNQRGQI
Q6EE25| [Siniperca chuatsi] MH   ---------- ---MADSAED APMARGSLAG SDEALILPAG
PTGGSNSRAL KVAGLTTLTC LLLASQVFTA YMVFGQKEQI
B6VAR1_EPIAK [Epinephelus akaa   ---------- ---MAEPAEG APLAAGSLAS SEEDLLPLTA
QRGGSNSRAL KIVGLTTLAC LLLASQVFTA VMVFDQKQQI
Q06KB6_[Dicentrarchus labrax]    ---------- ---MAHS-ED APLATGSLAG SEEALVLSGR
PTGGSNSRAL KIAGLTTLAC LLLASQVFTA YMVFGQKEQI
ACM09693.1| [Salmo salar] HLA    ---------- --MEEQQQQR HDDALLERAG SQDVILPITT
NTRASNSRAF KVAGLTVLAC LLLAGQALTA YLVFNQRGQI
ACO13218.1| [Esox lucius] H-2    ---------- --MEEQQQ-I HNEALLERTA SDEAILPSVR -
RRTSNSRAF KVAGFTLLAC LLLAGQGLTA YLVFNQRGQI
ACO10022.1| [Osmerus mordax] H   ---------- --MEDHQP-- QDDSLLR-AG SEEALVSPRA
PPGGSNNRAF KVAGLTVLAC LLLASQGLTA YLVISQRGQI
AAS77256.1| [Siniperca chuatsi   ---------- ---MADSAED APMARGSLAG SDEALILPAG
PTGGSNSRAL KVAGLTTLTC LLLASQVFTA YMVFGQKEQI
ABH09445.1| [Dicentrarchus lab   ---------- ---MAHS-ED APLATGSLAG SEEALVLSGR
PTGGSNSRAL KIAGLTTLAC LLLASQVFTA YMVFGQKEQI
47215554| [Tetraodon nigroviri   ---------- ---MADGQED APLARGSVAG SEEGLILRAR
PAGGSNSHAL KVAGLTTLVC LLLGSQVFTA YMVFGQRQQI
hybrid_3x5mio_20120605_c6693_S   LWVQCNRKKL AVKQSQMEKT GENTPMQRTG SAEPLVGGAR
YRGRPTGYAL KVASLTILAC LLVASQVFVA IMVFSQKQQI

                                    ....|....| ....|....| ....|....| ....|....|
....|....| ....|....| ....|....| ....|....|
                                            90       100       110       120
130       140       150       160
Q8JFN4| [Oncorhynchus mykiss]     YDMQKSNGNM RKQLRNRPPA VAPVKMQTPM LNMARLIDFT
DEDVKT---- PMTNLEATAV AIVSLEEQVK NLLQ-NPQLP
Q6EE25| [Siniperca chuatsi] MH   HTLQKNSERM SKQLTRSSQA VAPMKMHMPM NSLPLLMDFT
PNED---SKT PLTKLQDTA- -VVSVEKQLK DLMQ-DSQLP
B6VAR1_EPIAK [Epinephelus akaa   HSLQRNSDKL GRQLTRSSQA VAPVRMHMPM NSLPLLMDFD
ADANTKPKKT PLTKLQEA-- -VVSVEAQLK ELLQEDSQLP
Q06KB6_[Dicentrarchus labrax]    HTLQKNSERM TKQLTRSSQA VAPVRMHMPM SSLPMLMDFT DEDSK-
ATKT PLTKLQDT-- -VVSVEKQVK DLIQ-DSQLP
ACM09693.1| [Salmo salar] HLA    HDMQKSNDNM RKQLRNRPLA VAPVKMQMPM LNMARLIDFT
DEDSKT---- PMTNLEATAI AIVSLEDQVK DLLQ-NPQLP
ACO13218.1| [Escx lucius] H-2    NDMQKNNDNM RKQLRNRP-P VAPVQMHMPM LNMPRLIDFS
EEDSQTTKNS PMTKLENTAV AIQSLEKQVK DLLQ-NPELP
ACO10022.1| [Osmerus mordax] H   HNLQKNTDKM NKKITIRS-H VAPVQMHVPM NTMPLLKDFS
DEEPKE-AQT PMSKLQFT-- AIVSVEKQVK DLLQ-NVSLP
AAS77256.1| [Siniperca chuatsi   HTLQKNSERM SKQLTRSSQA VAPMKMHMPM NSLPLLMDFT
PNED---SKT PLTKLQDTA- -VVSVEKQLK DLMQ-DSQLP
ABH09445.1| [Dicentrarchus lab   HTLQKNSERM TKQLTRSSQA VAPVRMHMPM SSLPMLMDFT DEDSK-
ATKT PLTKLQDT-- -VVSVEKQVK DLIQ-DSQLP
47215554| [Tetraodon nigroviri   RELQGNNKRI SNQLTRSSQ- -APVRMQVPM RSLPMMRAFD
PDTDT--PIM PKAAVQET-- -VVSVETQVK DLLQ-NFTLP
hybrid_3x5mio_20120605_c6693_S   HTLQKDFDGL SRQLHAAQ-- VAPFKLRQPM NHFPQMQAFA
DLDSVA-TKA PVKQEEKK-M ESIGVDEMLG -LMEENFEMP

                                    ....|....| ....|....| ....|....| ....|....|
....|....| ....|....| ....|....| ....|....|
                                           170       180       190       200
210       220       230       240
```

```
Q8JFN4| [Oncorhynchus mykiss]    QFNETFLANL QSLKKQVEET EWEGFETWAR YWLLFQMAQE
KPPVLPTPQP ---------- ---------- ----------
Q6EE25| [Siniperca chuatsi] MH   QFNETFLANL QGLKQQMNES EWKSFESWMR YWLIFQMAQQ K-
PVPPTADP ASLIKTKCQM ESAPGVSKIG SYKPQCDEQG
B6VAR1_EPIAK [Epinephelus akaa   QFNETFLANL QGMKQHVNET DWKSFESWMR YWLIFQIAQR T-
PAPPTAEP TTAPLTKCQQ EAAPGPSKIG SYKPQCDEQG
Q06KB6_[Dicentrarchus labrax]    QFNETFMANL QSLKQHINES EWQSFESWMR YWLIFQMAQK T-
PVPPTADP ASLIKTKCQM EAAPGPSKIG SYKPQCDEQG
ACM09693.1| [Salmo salar] HLA    QFNETFLANL QSLKQQVEET EWEGFETWVR YWLLFQMAQE
KPPAPPTPQP ---------- ---------- ----------
ACO13218.1| [Esox lucius] H-2    QFNETFLANL QGLKKQMESN EWKDFETWTR NWLIFQMAQE
KTAVSATPKP STGLQTKCSE VKDSLKHMLG TYVPQCDEQG
ACO10022.1| [Osmerus mordax] H   EFNQSFLKNV QSLQTKMESE EWMSFETWMR HWLIFQMAQQ
SPPVPASALQ TKCR------ ---LQTRILG SYQPQCDAQG
AAS77256.1| [Siniperca chuatsi   QFNETFLANL QGLKQQMNES EWKSFESWMR YWLIFQMAQQ K-
PVPPTADP ASLIKTKCQM ESAPGVSKIG SYKPQCDEQG
ABH09445.1| [Dicentrarchus lab   QFNETFMANL QSLKQHINES EWQSFESWMR YWLIFQMAQK T-
PVPPTADP ASLIKTKCQM EAAPGPSKIG SYKPQCDEQG
47215554| [Tetraodon nigroviri   AFNSTFASNL LALKSQMDQT TWQKLESWMQ SWLIFQMAQE K-
PPTITATP AP-VMTKCQK EAASVKHLLG TRKPQCDELG
hybrid_3x5mio_20120605_c6693_S   KFNDTVLGNL KSLKKQLNQS NWKSFESWLR NWIIFHMSQQ
TPPTPTGSST KT----KCQI RAEVKSSQLD PFRPVCDLKG


                                 ....|....| ....|....| ....|....| ....|....|
....|....| ....|....| ....|....| ....|....|
                                         250        260        270        280
290        300        310        320
Q8JFN4| [Oncorhynchus mykiss]    ---------- ---------- ----VP---- ---------- -----
HQRRP SYPRMMQLKE YKNE------ ----------
Q6EE25| [Siniperca chuatsi] MH   RYKPMQCWHA TGFCWCVDET -GAVIEGTTM RGRPDCQRR- --
ALAPRRMA FAPSLMQKTI SIDDQ----- ----------
B6VAR1_EPIAK [Epinephelus akaa   RYKPMQCWHA TGFCWCVDEF -GNVVEGTRM RGRPDCQRA- --
SLYPRRVM LAPRLMQKTL SLDDDTN--- ----------
Q06KB6_[Dicentrarchus labrax]    RYKPMQCWHA TGYCWCVDET -GTAIEGTTM RGRPDCQR-- --
GSMPRRVM LAPRLMQKTL SFDDQ----- ----------
ACM09693.1| [Salmo salar] HLA    ---------- ---------- ----VP---- ---------- -----
HQRMA AYPRMMQLKE YKNE------ ----------
ACO13218.1| [Esox lucius] H-2    NYLPMQCWHA TGFCWCVDKT -GQTIPGTAV RGRASCN--- ---
QGFRRVA APPMMMQVKE FKEE------ ----------
ACO10022.1| [Osmerus mordax] H   HFMPMQCWHS TGYCWCVDSE -GTAIPGTEM RGKPTCGGVP
KPAPGLRRMV PMLKTMQLES DVQDK----- ----------
AAS77256.1| [Siniperca chuatsi   RYKPMQCWHA TGFCWCVDET -GAVIEGTTM RGRPDCQRR- --
ALAPRRMA FAPSLMQKTI SIDDQ----- ----------
ABH09445.1| [Dicentrarchus lab   RYKPMQCWHA TGYCWCVDET -GTAIEGTTM RGRPDCQR-- --
GSMPRRVM LAPRLMQKTL SFDDQ----- ----------
47215554| [Tetraodon nigroviri   QYTPIQCWPA VGMCWCVDSS -GTAVPGTAV RGHPNCPR-- ---
ASPRHMM LAPLREMAAV DVEVKLRKDA VSFRLSQVKL
hybrid_3x5mio_20120605_c6693_S   RYEAIQCWHV IGVCWCVDVD SGAAIEGTFT KGRPKCETG-
---------- ---------- ---------- ----------


                                 ..

Q8JFN4| [Oncorhynchus mykiss]    --
Q6EE25| [Siniperca chuatsi] MH   --
B6VAR1_EPIAK [Epinephelus akaa   --
Q06KB6_[Dicentrarchus labrax]    --
ACM09693.1| [Salmo salar] HLA    --
ACO13218.1| [Esox lucius] H-2    --
ACO10022.1| [Osmerus mordax] H   --
AAS77256.1| [Siniperca chuatsi   --
ABH09445.1| [Dicentrarchus lab   --
47215554| [Tetraodon nigroviri   NI
hybrid_3x5mio_20120605_c6693_S   --
```

Appendix Chapter 2

Supplementary figure S.2.1 Multidimensional scaling plot for *D. pseudospathaceum* infection treatments. FPKM values for all genes significantly differentially expressed, compared to control, in either gills (A) or head kidney (B) were used for calculations.

A

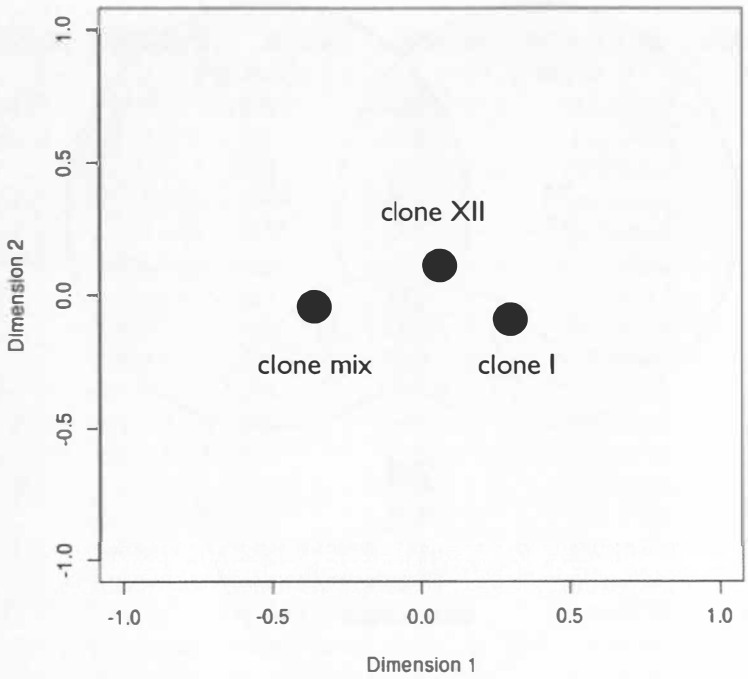

B

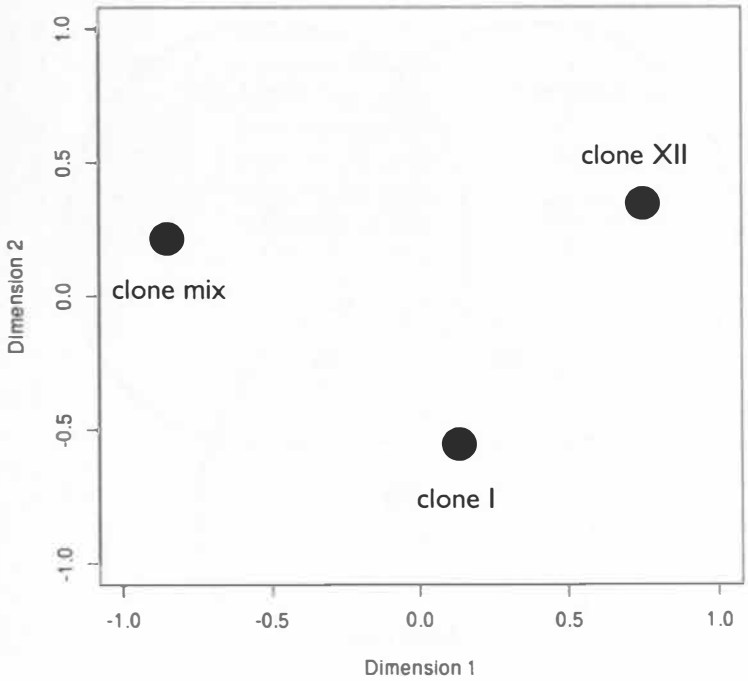

Supplementary figure S.2.2 Venn-Diagram for differentially expressed genes. Displayed are number of genes significantly differentially expressed due to either one, two or all infection treatments. Up-regulated genes are written in black, down-regulated genes in grey. Genes where expression was significantly different in more than one treatment and regulated in both directions are not shown. See also supplementary tables S.2.2 and S.2.3.

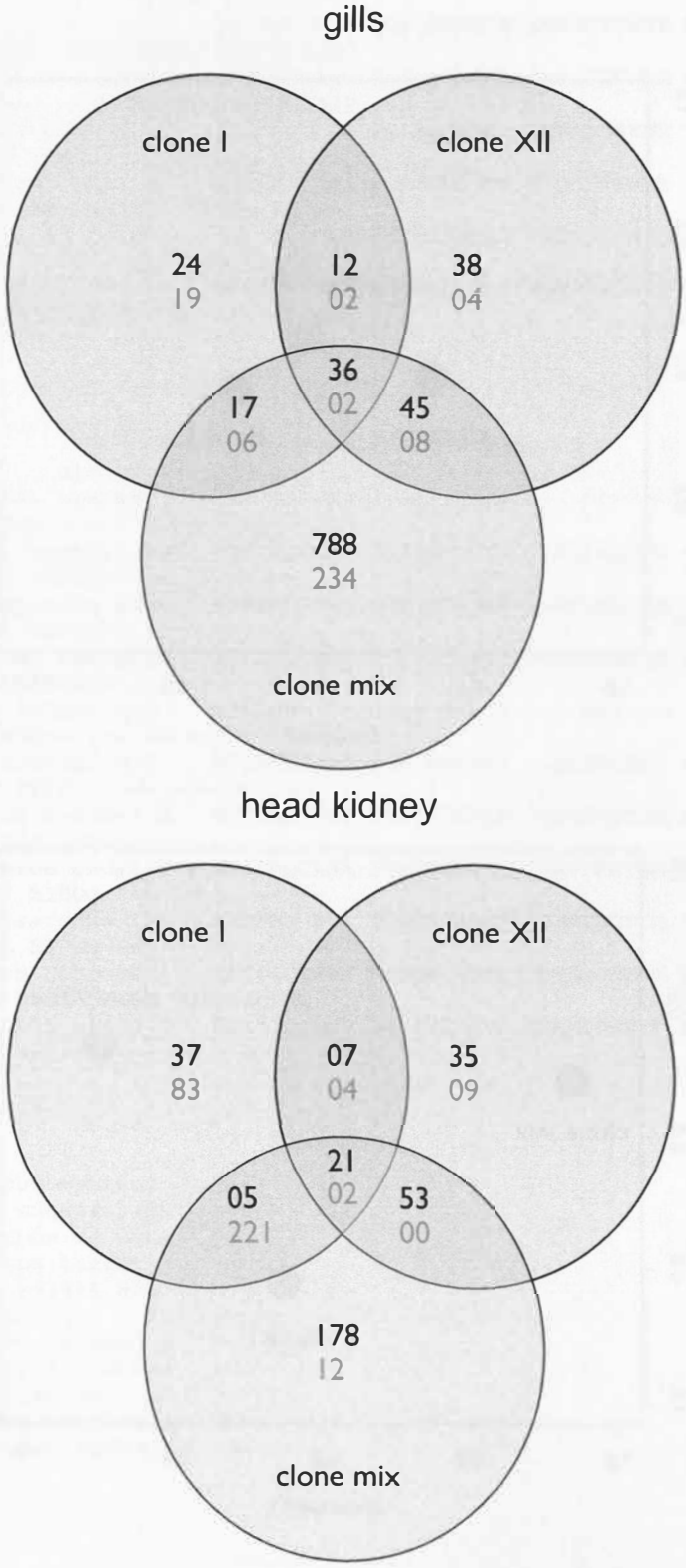

Supplementary table S.2.1 Number of reads per sample, including treatment, fish family, organ type, flowcell lane number, total reads and mapped reads. Two samples from gills and one sample from head kidney were of reduced quality and had to be removed from further analysis. This led to 4 samples in gills (clone XII, clone mix) and head kidney (clone I, clone XII, clone mix) as well as 3 samples in gills (clone I, control) and head kidney (control), resulting in 29 individual libraries.

sample	fish family	treatment	organ	lane no	total reads	aligned reads	% aligned
1	10-10x15	control	gills	L006	11193950	6374910	56,95
2	10-13x12	control	gills	L001	6542490	3710021	56,71
3	10-2x1	control	gills	L002	11781202	6625186	56,24
4	10-10x15	clone mix	gills	L007	9034308	4817625	53,33
5	10-11x16	clone mix	gills	L006	10700158	6461189	60,38
6	10-13x12	clone mix	gills	L004	24710382	11990896	48,53
7	10-2x1	clone mix	gills	L003	12123212	6914101	57,03
8	10-10x15	clone I	gills	L004	11070914	5252831	47,45
9	10-11x16	clone I	gills	L008	12455600	6233762	50,05
10	10-13x12	clone I	gills	L004	13034054	6891659	52,87
11	10-10x15	clone XII	gills	L008	14880032	6888039	46,29
12	10-11x16	clone XII	gills	L007	9508384	4819680	50,69
13	10-13x12	clone XII	gills	L006	9498616	5792914	60,99
14	10-2x1	clone XII	gills	L005	9015786	4803562	53,28
15	10-10x15	control	head kidney	L005	10356510	5845850	56,45
16	10-11x16	control	head kidney	L008	16185886	8286884	51,20
17	10-2x1	control	head kidney	L004	19945222	10646606	53,38
18	10-10x15	clone mix	head kidney	L001	31556086	17647114	55,92
19	10-11x16	clone mix	head kidney	L008	20305784	9906271	48,79
20	10-13x12	clone mix	head kidney	L005	14366550	7398995	51,50
21	10-2x1	clone mix	head kidney	L006	18581584	11015042	59,28
22	10-10x15	clone I	head kidney	L005	14538858	7900850	54,34
23	10-11x16	clone I	head kidney	L007	14744676	8186321	55,52
24	10-13x12	clone I	head kidney	L004	20077788	11469317	57,12
25	10-2x1	clone I	head kidney	L003	28496486	19646137	68,94
26	10-10x15	clone XII	head kidney	L008	23881298	12756204	53,42
27	10-11x16	clone XII	head kidney	L008	42804942	21061942	49,20
28	10-13x12	clone XII	head kidney	L003	22337552	12241427	54,80
29	10-2x1	clone XII	head kidney	L001	22988590	13737901	59,76

Supplementary table S.2.2 Cufflinks output, list of differentially expressed genes in head kidney tissue of three-spined sticklebacks. Differentially expressed is defined by comparison to uninfected controls. The term "gene" is the name for a specific gene as taken from the *G. aculeatus* reference genome, "sample_2" is the infection treatment group, log2(fold change) displays the transformed fold change in "sample_2" compared to control, p value and q value are given for each test (only significant differences shown).

gene	sample_2	log2(fold_change)	p_value	q_value
A1CF	clone I	-8,26234	6,08E-012	1,27E-009
ABCB11	clone I	-7,66416	1,63E-007	9,85E-006
ABCB4	clone I	-6,98155	2,19E-007	1,27E-005
ABCF2	clone I	1,75392	0,000936081	0,0145583
ACADL	clone I	-3,58254	0,000302908	0,00577917
ACMSD	clone I	-6,47473	9,33E-006	0,000312622
ADAMTS13	clone I	-1,96941	0	0
ADSSL1	clone I	-3,14657	0,000262256	0,00513046
AGT	clone I	-6,03987	2,12E-008	1,69E-006
AGXT (1 of 2)	clone I	-6,34674	6,64E-008	4,54E-006
AGXT (2 of 2)	clone I	-5,85821	2,24E-008	1,77E-006
AGXT2 (1 of 2)	clone I	-5,05852	8,35E-006	0,000284477
AGXT2L1	clone I	-3,88978	8,53E-005	0,00201361
AKR1D1 (1 of 2)	clone I	-2,94657	0,00159121	0,0223358
AKR1D1 (2 of 2)	clone I	-6,31304	3,02E-009	3,10E-007
ALDH1L1	clone I	-3,87058	6,48E-005	0,00160033
ALDH8A1	clone I	-6,32151	9,65E-007	4,54E-005
ALDH9A1 (1 of 2)	clone I	-2,12538	1,25E-005	0,000401432
ALDOA (1 of 2)	clone I	-3,66488	0	0
ALDOB	clone I	-4,55834	0,00293298	0,036396
ALLC	clone I	-4,82042	1,18E-006	5,37E-005
AMBP	clone I	-6,70697	3,67E-007	1,98E-005
AMDHD1	clone I	-3,28757	0,000437006	0,00782273
ANGPTL3 (1 of 2)	clone I	-4,02717	5,61E-005	0,00141944
ANGPTL4 (2 of 2)	clone I	-2,42623	0,00050154	0,00875473
APOA1	clone I	-6,49435	0,00231658	0,0301725
APOB (1 of 5)	clone I	-6,97217	2,25E-011	4,07E-009
APOB (5 of 5)	clone I	-7,29866	3,55E-015	1,43E-012
APOE (2 of 2)	clone I	-7,18521	8,66E-011	1,35E-008
APOH (2 of 2)	clone I	-5,77363	1,28E-006	5,77E-005
ARG1	clone I	-4,34149	1,80E-008	1,47E-006
ARHGEF38 (1 of 2)	clone I	-4,69825	0,00115952	0,0173272
ARL14 (2 of 2)	clone I	-1,80E+308	0,000483262	0,00849264
ARRDC2	clone I	1,25342	0,00124141	0,0183076
ASGR1	clone I	-6,56246	3,28E-008	2,47E-006
ATP2A1 (1 of 2)	clone I	-2,83553	0,000225118	0,00452056
ATP2A1 (2 of 2)	clone I	-3,71322	9,01E-005	0,00210823
ATP7B	clone I	-5,99769	0,00102015	0,0156127
BAIAP2L1 (1 of 2)	clone I	-4,01322	0,00284242	0,03549
BCO2 (3 of 3)	clone I	-4,31316	2,00E-005	0,000595804
BRIX1	clone I	0,938478	0,00308099	0,037834
C3 (1 of 8)	clone I	-6,88346	1,17E-007	7,41E-006
C3 (2 of 8)	clone I	-5,45179	8,49E-007	4,07E-005

gene	sample_2	log2(fold_change)	p_value	q_value
C3 (3 of 8)	clone I	-6,41276	3,83E-006	0,000146982
C3 (4 of 8)	clone I	-6,65395	0,000252949	0,0049805
C3 (5 of 8)	clone I	-6,51416	1,17E-006	5,37E-005
C3 (7 of 8)	clone I	-2,72404	0,00157496	0,0221546
C3 (8 of 8)	clone I	-3,05116	0	0
C6	clone I	-3,96029	0	0
C6orf58	clone I	-5,7995	4,61E-009	4,49E-007
C7 (1 of 2)	clone I	-3,47181	0,000115251	0,0025901
C8A	clone I	-6,25739	2,04E-008	1,63E-006
C8B	clone I	-6,86441	6,66E-016	3,01E-013
C8G	clone I	-6,95663	1,16E-009	1,34E-007
C9	clone I	-5,89096	1,15E-006	5,27E-005
CA6 (1 of 2)	clone I	3,38416	3,35E-006	0,000131179
CASQ1 (1 of 2)	clone I	-5,2741	0,000254702	0,00500872
CD2	clone I	-0,85864	0,00420864	0,0483043
CDO1	clone I	-2,93771	0,000690453	0,011363
CEBPB	clone I	2,13349	0,000583176	0,0098995
CELA1 (1 of 2)	clone I	-3,38608	0,00348941	0,0417143
CETP	clone I	-7,11618	3,70E-010	4,89E-008
CFB	clone I	-4,35573	9,21E-006	0,000309066
CFP	clone I	-6,34205	1,73E-008	1,42E-006
CIDEB	clone I	-6,30322	4,00E-007	2,13E-005
CKM (1 of 2)	clone I	-3,10984	0,000456821	0,00811188
CKM (2 of 2)	clone I	-3,348	0,000214047	0,00433574
CLDN2	clone I	-4,28803	0,000852125	0,0134805
CLDN3 (2 of 4)	clone I	2,66856	3,38E-005	0,000927284
CNDP1	clone I	-7,2812	0,00187385	0,0254777
CREB3L3	clone I	-4,19135	0,000135954	0,00297071
CROT (2 of 2)	clone I	-1,28362	1,25E-006	5,65E-005
CSRNP1 (1 of 2)	clone I	2,51791	0,00139468	0,0200985
CTBS	clone I	-0,301773	0,00121522	0,017992
CYP24A1	clone I	-5,54853	0	0
CYP2C9	clone I	-6,1389	0,000127764	0,00282169
CYP2J2 (1 of 6)	clone I	-5,94602	2,25E-011	4,07E-009
CYP2J2 (2 of 6)	clone I	-5,9798	9,89E-007	4,63E-005
CYP2J2 (3 of 6)	clone I	-5,91664	3,62E-010	4,79E-008
CYP2W1 (1 of 5)	clone I	-6,70341	1,05E-011	2,06E-009
CYP46A1	clone I	-1,59514	0,000147666	0,00318336
CYP7A1	clone I	-4,02521	0	0
CYP8B1	clone I	-5,38991	2,05E-006	8,64E-005
DDIT4 (1 of 2)	clone I	3,897	6,75E-009	6,25E-007
DENND4A (2 of 2)	clone I	4,08973	1,24E-010	1,86E-008
DGAT2	clone I	-3,12191	0,000455311	0,00808893
DIABLO (1 of 2)	clone I	-6,89981	1,27E-007	7,95E-006
DMGDH	clone I	-4,27203	1,06E-005	0,000347971
DNAJC22	clone I	-1,80E+308	0,000506774	0,00882908
DPYS	clone I	-4,99891	3,89E-005	0,00104265
DUSP1	clone I	1,94075	0,000484509	0,00851018
DUSP26 (2 of 2)	clone I	-6,65077	0,000703562	0,0115414
EGFR (2 of 2)	clone I	-2,9445	0,000583696	0,00990652
ELL (2 of 2)	clone I	2,65453	5,22E-005	0,00133663
ELTD1	clone I	0,992205	0,00328525	0,0397884
ENPP2 (2 of 2)	clone I	-3,92879	3,94E-005	0,00105437

gene	sample_2	log2(fold_change)	p_value	q_value
ENSGACG00000000007	clone I	-7,10752	1,98E-008	1,59E-006
ENSGACG00000000231	clone I	-4,28609	8,84E-005	0,00207364
ENSGACG00000000272	clone I	-3,81325	0,000297829	0,00569912
ENSGACG00000000614	clone I	0,893794	0,00392023	0,0457139
ENSGACG00000000665	clone I	-3,51876	0,000458751	0,00813988
ENSGACG00000001260	clone I	-6,43989	2,16E-006	9,02E-005
ENSGACG00000001261	clone I	-4,31609	4,04E-005	0,00107651
ENSGACG00000001432	clone I	-8,0299	4,12E-012	8,94E-010
ENSGACG00000001548	clone I	1,84892	0,0008311	0,0132074
ENSGACG00000001733	clone I	-7,0658	6,48E-012	1,34E-009
ENSGACG00000001736	clone I	-2,71167	0,00338299	0,0407239
ENSGACG00000001742	clone I	-2,87035	0	0
ENSGACG00000002588	clone I	-2,37304	0,00364568	0,0431855
ENSGACG00000002805	clone I	-1,80E+308	0,00120415	0,0178592
ENSGACG00000002832	clone I	-5,69265	0,000632226	0,0105763
ENSGACG00000003030	clone I	-5,77693	3,55E-005	0,000967877
ENSGACG00000003461	clone I	-6,36104	2,41E-006	9,90E-005
ENSGACG00000003467	clone I	-7,05614	0,000534784	0,00922841
ENSGACG00000003473	clone I	-6,33723	7,29E-007	3,57E-005
ENSGACG00000003808	clone I	-3,54307	0,000528889	0,00914422
ENSGACG00000004324	clone I	0,936529	3,75E-005	0,00101272
ENSGACG00000004413	clone I	-7,06247	4,44E-016	2,06E-013
ENSGACG00000004463	clone I	-4,34166	0,000950603	0,0147431
ENSGACG00000004822	clone I	-4,60546	0,000123834	0,00274885
ENSGACG00000005023	clone I	-5,27403	8,65E-005	0,00203782
ENSGACG00000005067	clone I	-3,09301	0,00221705	0,029132
ENSGACG00000005133	clone I	-1,01577	0,00126775	0,0186172
ENSGACG00000005228	clone I	-3,1393	0,00218601	0,0288072
ENSGACG00000005264	clone I	-6,58423	0,000716258	0,0117097
ENSGACG00000005482	clone I	-2,15647	0,0039549	0,0460253
ENSGACG00000005760	clone I	2,20893	2,16E-005	0,000636833
ENSGACG00000005883	clone I	-6,58054	4,48E-012	9,65E-010
ENSGACG00000006029	clone I	-6,55171	0,00152758	0,021618
ENSGACG00000006351	clone I	-4,32696	0,000116311	0,00260974
ENSGACG00000006545	clone I	-5,56062	4,17E-007	2,21E-005
ENSGACG00000006644	clone I	-7,4846	7,51E-010	9,13E-008
ENSGACG00000006790	clone I	-4,17966	1,71E-006	7,40E-005
ENSGACG00000006829	clone I	-5,56502	1,23E-007	7,73E-006
ENSGACG00000006833	clone I	-1,80E+308	0,000126401	0,00279651
ENSGACG00000007038	clone I	-7,45594	0,000196193	0,00403245
ENSGACG00000007329	clone I	-1,4746	6,95E-007	3,43E-005
ENSGACG00000007337	clone I	-3,08122	0,000482589	0,00848312
ENSGACG00000007411	clone I	-1,98952	5,30E-007	2,71E-005
ENSGACG00000007505	clone I	-6,23203	0,00154558	0,0218252
ENSGACG00000007507	clone I	-4,21283	2,99E-005	0,000836944
ENSGACG00000007640	clone I	-4,81786	1,90E-005	0,000571725
ENSGACG00000007642	clone I	-6,57212	1,64E-006	7,15E-005
ENSGACG00000007954	clone I	-6,85502	1,87E-009	2,04E-007
ENSGACG00000008053	clone I	2,95615	7,16E-005	0,00173896
ENSGACG00000008055	clone I	2,70934	0,000204268	0,0041701
ENSGACG00000008064	clone I	3,18569	0,00143956	0,0206125
ENSGACG00000008353	clone I	1,64659	0,00227412	0,0297279
ENSGACG00000009173	clone I	-6,7297	4,21E-007	2,23E-005

gene	sample_2	log2(fold_change)	p_value	q_value
ENSGACG00000009188	clone I	2,31671	0,00144135	0,0206325
ENSGACG00000009200	clone I	2,50991	8,86E-006	0,000299218
ENSGACG00000009583	clone I	-5,6853	1,41E-006	6,26E-005
ENSGACG00000009592	clone I	-6,1302	2,16E-011	3,93E-009
ENSGACG00000009633	clone I	-4,31968	3,77E-008	2,78E-006
ENSGACG00000009880	clone I	-6,41272	8,53E-007	4,09E-005
ENSGACG00000009883	clone I	-6,70551	9,91E-008	6,42E-006
ENSGACG00000009952	clone I	-5,55089	6,20E-008	4,28E-006
ENSGACG00000010000	clone I	-4,00092	2,08E-005	0,000615638
ENSGACG00000010018	clone I	-4,6013	9,43E-006	0,000315442
ENSGACG00000010050	clone I	2,44672	3,63E-007	1,96E-005
ENSGACG00000010145	clone I	-6,23799	2,48E-008	1,94E-006
ENSGACG00000010196	clone I	-6,79781	7,43E-008	5,01E-006
ENSGACG00000010247	clone I	-1,80E+308	0,00338142	0,040709
ENSGACG00000010476	clone I	4,33386	6,27E-009	5,86E-007
ENSGACG00000010478	clone I	-1,22907	5,48E-006	0,000199077
ENSGACG00000010933	clone I	-6,7886	7,76E-007	3,77E-005
ENSGACG00000011392	clone I	-7,01174	0	0
ENSGACG00000011617	clone I	-6,61204	0,000225791	0,00453209
ENSGACG00000011633	clone I	-2,4338	0,00273144	0,0343844
ENSGACG00000011676	clone I	1,82014	0,00203001	0,0271622
ENSGACG00000011846	clone I	-6,39995	1,44E-012	3,47E-010
ENSGACG00000011851	clone I	-6,55997	0	0
ENSGACG00000011882	clone I	-4,29853	0,00351179	0,0419258
ENSGACG00000012174	clone I	-3,01963	0,000368091	0,00679049
ENSGACG00000012189	clone I	-2,0248	0,00316587	0,0386472
ENSGACG00000012381	clone I	-5,7883	1,40E-008	1,18E-006
ENSGACG00000012390	clone I	-2,36126	4,05E-006	0,000154115
ENSGACG00000012414	clone I	-6,07395	7,40E-006	0,000256922
ENSGACG00000012464	clone I	4,27211	1,63E-007	9,85E-006
ENSGACG00000012473	clone I	-2,96294	0,00304768	0,0375179
ENSGACG00000013449	clone I	-3,7927	0,000543925	0,00935562
ENSGACG00000013769	clone I	-6,61335	0,000185053	0,00384112
ENSGACG00000013793	clone I	-5,87914	3,30E-007	1,81E-005
ENSGACG00000013996	clone I	-4,65379	0,000300255	0,00573683
ENSGACG00000014312	clone I	1,92572	0,00105527	0,0160488
ENSGACG00000014348	clone I	-5,24718	1,37E-006	6,11E-005
ENSGACG00000014547	clone I	-2,84255	0,000275864	0,00534929
ENSGACG00000014675	clone I	-2,25811	0,00101936	0,0156029
ENSGACG00000014699	clone I	-1,80E+308	0,000131837	0,00289605
ENSGACG00000014752	clone I	-3,99578	7,08E-006	0,000247575
ENSGACG00000014811	clone I	-5,51263	8,13E-006	0,000278366
ENSGACG00000014852	clone I	-4,45739	5,17E-005	0,0013255
ENSGACG00000014915	clone I	1,54522	3,58E-006	0,000138829
ENSGACG00000015411	clone I	-7,4861	6,66E-016	3,01E-013
ENSGACG00000015464	clone I	-5,98109	0	0
ENSGACG00000015472	clone I	-6,76234	1,54E-009	1,72E-007
ENSGACG00000015778	clone I	-3,83301	0,00126482	0,0185838
ENSGACG00000015857	clone I	-5,85485	1,08E-008	9,39E-007
ENSGACG00000015947	clone I	-6,76683	1,59E-007	9,63E-006
ENSGACG00000016093	clone I	-4,65403	1,06E-005	0,000347233
ENSGACG00000016104	clone I	-7,09803	2,61E-007	1,48E-005
ENSGACG00000016168	clone I	-3,7682	0,000207965	0,00423221

gene	sample_2	log2(fold_change)	p_value	q_value
ENSGACG00000016298	clone I	2,68674	1,75E-007	1,05E-005
ENSGACG00000016669	clone I	-5,09526	3,08E-013	8,60E-011
ENSGACG00000016687	clone I	-4,86618	3,64E-006	0,000140877
ENSGACG00000016696	clone I	-4,46761	1,11E-005	0,000360747
ENSGACG00000016946	clone I	3,74269	6,34E-005	0,00157196
ENSGACG00000017299	clone I	-3,22936	0,000295118	0,0056563
ENSGACG00000017655	clone I	-5,14812	0,00314064	0,0384026
ENSGACG00000017681	clone I	-5,83825	1,44E-009	1,62E-007
ENSGACG00000017758	clone I	5,49079	0,0022066	0,029023
ENSGACG00000018216	clone I	1,08904	1,39E-005	0,000437473
ENSGACG00000018662	clone I	5,08244	1,20E-006	5,49E-005
ENSGACG00000019066	clone I	-8,0083	2,02E-010	2,86E-008
ENSGACG00000019454	clone I	-4,9021	7,96E-007	3,85E-005
ENSGACG00000019517	clone I	-5,63956	1,22E-005	0,000392214
ENSGACG00000019604	clone I	-6,1084	0,000206805	0,00421261
ENSGACG00000019794	clone I	-0,975571	5,67E-008	3,95E-006
ENSGACG00000019954	clone I	-1,80E+308	0,000184771	0,00383646
ENSGACG00000019958	clone I	-4,65059	0,00024363	0,00482813
ENSGACG00000020003	clone I	1,51637	0,00371209	0,0438077
ENSGACG00000020047	clone I	-6,28332	1,89E-009	2,06E-007
ENSGACG00000020141	clone I	3,18032	0,000240639	0,00477727
ENSGACG00000020145	clone I	3,23431	0,00232098	0,0302184
ENSGACG00000020249	clone I	-5,39847	0,00274362	0,0345076
ENSGACG00000020469	clone I	5,55826	3,01E-006	0,000119773
ENSGACG00000020566	clone I	-6,44754	1,79E-007	1,07E-005
ENSGACG00000020613	clone I	-5,35313	0,0020998	0,0279061
ENSGACG00000020614	clone I	-3,66215	0,00239987	0,0310392
ENSGACG00000020653	clone I	-7,47581	2,22E-015	9,22E-013
ENSGACG00000020833	clone I	-1,80E+308	0,00120415	0,0178592
ENSGACG00000020873	clone I	-5,45036	0,00237727	0,0308005
ENSGACG00000020917	clone I	-5,5049	2,26E-011	4,10E-009
EPS8	clone I	-2,30336	0,000745276	0,0120925
F10	clone I	-6,60835	2,13E-008	1,69E-006
F2	clone I	-5,8185	2,46E-005	0,000709851
F3 (1 of 2)	clone I	3,10255	0,000143546	0,00310933
F5	clone I	-5,99715	5,07E-007	2,61E-005
F9 (1 of 2)	clone I	-5,29892	5,86E-005	0,0014714
F9 (2 of 2)	clone I	-5,0986	7,02E-007	3,46E-005
FABP1	clone I	-5,38724	2,38E-006	9,79E-005
FETUB (1 of 3)	clone I	-4,91123	6,29E-006	0,000223929
FETUB (2 of 3)	clone I	-5,86012	7,13E-006	0,000249092
FETUB (3 of 3)	clone I	-7,04398	5,88E-007	2,97E-005
FGA	clone I	-6,22383	5,93E-011	9,64E-009
FGB	clone I	-6,65833	3,13E-005	0,000869675
FGG	clone I	-6,16835	1,54E-005	0,000477944
FKBP5	clone I	3,27635	1,15E-007	7,28E-006
FOSL1	clone I	6,12055	1,24E-007	7,82E-006
FOXA3	clone I	-5,23203	2,89E-005	0,000813889
FRZB	clone I	-1,77075	0,000531798	0,00918551
G0S2	clone I	-5,91183	6,03E-007	3,03E-005
G6PC (1 of 2)	clone I	-4,32502	3,60E-006	0,000139466
G6PC (2 of 2)	clone I	-5,5826	6,79E-009	6,28E-007
G6PD (2 of 2)	clone I	-5,75639	0,0010316	0,0157559

gene	sample_2	log2(fold_change)	p_value	q_value
GADD45A (2 of 2)	clone I	2,20338	0,000304648	0,00580618
GAPDH (1 of 2)	clone I	-3,23816	5,24E-010	6,64E-008
GAPDH (2 of 2)	clone I	-6,33017	3,35E-009	3,39E-007
GLUL (1 of 2)	clone I	1,73336	0,000330657	0,0062155
GPX4 (2 of 4)	clone I	-4,63893	3,23E-006	0,000127237
GPX4 (3 of 4)	clone I	-4,68482	0,001237	0,0182546
GRAMD3 (2 of 2)	clone I	-1,80E+308	0,000678638	0,0112038
GSTZ1	clone I	-3,03798	0,00195257	0,026323
GZMM (2 of 5)	clone I	-1,00054	0,000693498	0,0114051
GZMM (3 of 5)	clone I	-1,18532	1,62E-006	7,08E-005
HAAO	clone I	-7,22313	9,77E-015	3,62E-012
HABP2 (1 of 2)	clone I	-8,10124	1,11E-015	4,85E-013
HABP2 (2 of 2)	clone I	-6,99357	6,58E-010	8,12E-008
HAL	clone I	-5,62892	5,81E-007	2,94E-005
HAO1	clone I	-5,51087	2,55E-010	3,52E-008
HGD	clone I	-6,0564	5,24E-006	0,000191702
HNF1A	clone I	-4,51967	0,000572722	0,00975457
HNF4A	clone I	-5,88247	2,07E-006	8,69E-005
HNMT (2 of 2)	clone I	-2,78906	0,00117596	0,0175251
HPD	clone I	-7,23769	1,98E-007	1,16E-005
HPN	clone I	-5,19908	0,000132058	0,00289982
HPX	clone I	-6,49736	4,00E-015	1,59E-012
HSD17B3	clone I	-4,90298	8,25E-007	3,97E-005
HYAL2 (1 of 2)	clone I	1,17095	0,00281202	0,0351816
IGFALS	clone I	-5,30884	2,22E-006	9,25E-005
IGFBP1 (2 of 2)	clone I	-5,31957	5,43E-006	0,000197849
IGFBP2 (2 of 2)	clone I	-4,3574	0,00369335	0,0436332
IL22RA1	clone I	1,80E+308	0,000758843	0,0122712
ILDR1 (1 of 2)	clone I	-5,08095	4,75E-006	0,00017641
IRF4 (2 of 2)	clone I	1,41405	0,00137279	0,0198463
ITIH2	clone I	-7,41664	5,28E-011	8,71E-009
ITIH4 (2 of 2)	clone I	-5,96859	3,83E-005	0,00102914
IYD	clone I	-3,55059	0,00126153	0,0185457
JUNB (1 of 2)	clone I	2,3601	0,000315549	0,00597811
JUNB (2 of 2)	clone I	3,92283	8,39E-007	4,03E-005
KL	clone I	-5,42654	2,58E-006	0,000105166
KMO	clone I	-3,75426	0,000639928	0,0106796
KNG1	clone I	-7,19528	1,37E-009	1,55E-007
KYNU	clone I	-3,68863	0,00144268	0,0206476
LCAT,PLA2G15	clone I	-1,7575	0,0011699	0,0174532
LECT2	clone I	-6,76975	8,65E-010	1,03E-007
LIPC	clone I	-5,81958	1,28E-010	1,91E-008
LPAR2 (2 of 2)	clone I	-0,858139	0,00306445	0,0376745
LRCH2	clone I	1,30146	0,000121702	0,00270948
LRG1	clone I	-5,4962	1,73E-007	1,04E-005
LYZ	clone I	-6,36612	9,20E-009	8,18E-007
MAT1A (2 of 2)	clone I	-8,99792	1,04E-005	0,000342925
MCFD2	clone I	-2,55399	0,00186398	0,0253707
METTL21C (2 of 2)	clone I	-4,61001	0,00101504	0,0155482
MINPP1 (1 of 2)	clone I	-3,96668	4,04E-005	0,00107799
MIOX	clone I	-6,84743	4,34E-007	2,29E-005
MLXIPL	clone I	-6,44768	4,23E-007	2,24E-005
MMD2 (2 of 2)	clone I	-4,66782	0,000384744	0,00704481

gene	sample_2	log2(fold_change)	p_value	q_value
MOGAT2	clone I	-6,00351	0,000310383	0,00589669
MOV10 (2 of 2)	clone I	1,64233	0,00185727	0,0252981
MPHOSPH10	clone I	0,745934	0,000788192	0,0126571
MPZL3	clone I	-4,84542	0,00428842	0,0490083
MST1P9	clone I	-6,83764	2,11E-007	1,23E-005
MYBPC2 (1 of 2)	clone I	-4,06022	2,64E-006	0,000107191
MYL1	clone I	-4,15649	1,76E-005	0,000534414
MYLPF (2 of 2)	clone I	-2,82307	0,00135674	0,0196593
NAALADL1	clone I	-2,52696	0,00425799	0,0487389
NCOA7 (2 of 2)	clone I	2,43613	0,000503136	0,00877779
NIPSNAP1	clone I	-4,45659	3,87E-005	0,00103927
NME4	clone I	-6,77302	7,06E-008	4,79E-006
NR0B2	clone I	-1,80E+308	0,00178359	0,0244808
NR1H4	clone I	-5,0432	1,92E-008	1,55E-006
OVGP1 (3 of 5)	clone I	-6,17641	2,05E-008	1,64E-006
PACSIN3	clone I	-2,90943	0,00230907	0,030093
PCSK6	clone I	-5,51117	0,000114506	0,00257593
PDIA4	clone I	1,00239	0,00338362	0,0407297
PFKFB3	clone I	2,3248	0,00241536	0,0311969
PFKM (2 of 2)	clone I	-4,48603	9,92E-006	0,000329235
PGAM2	clone I	-4,72246	1,13E-005	0,000367394
PGC	clone I	3,15127	0,000825514	0,0131358
PGLYRP2 (2 of 2)	clone I	-7,08313	0	0
PIM1	clone I	2,39227	0,000228829	0,00458258
PIPOX	clone I	-4,85111	0,000737502	0,0119907
PKLR	clone I	-2,07291	0,0014538	0,020775
PLA2G12B (1 of 2)	clone I	-3,53177	0,000886224	0,0139178
PLG	clone I	-6,41262	0	0
PPDPF (2 of 2)	clone I	-4,08053	1,75E-005	0,000532905
PPM1J	clone I	1,41616	0,00151534	0,0214775
PPP1R15B	clone I	1,67019	0,00309817	0,0379965
PRF1 (2 of 5)	clone I	2,79254	0,000972212	0,0150142
PRHOXNB	clone I	-6,48664	2,70E-006	0,000109325
PROC	clone I	-4,77604	1,97E-007	1,16E-005
PRODH2	clone I	-3,72383	0,00435356	0,0495752
PROM1 (1 of 2)	clone I	-3,7078	0,000649955	0,0108147
PROZ (2 of 2)	clone I	-5,96644	9,34E-010	1,11E-007
PVRL1 (2 of 2)	clone I	-4,41888	0,000704906	0,0115593
PYGM (2 of 2)	clone I	-4,48498	7,17E-006	0,000250079
QPCT	clone I	-3,91134	0,00018762	0,00388518
QPRT	clone I	-4,33523	0,000374656	0,00689165
RARG (1 of 2)	clone I	1,6569	0,00361315	0,0428832
RFK	clone I	1,05868	0,00205034	0,0273804
RGS5	clone I	0,761822	0,000332895	0,00624974
SCARF1	clone I	2,43577	0,00359746	0,0427396
SDC2	clone I	-2,26818	0,00343504	0,041209
SERPINA10 (1 of 2)	clone I	-6,75361	2,00E-015	8,36E-013
SERPINC1	clone I	-6,76305	4,78E-007	2,48E-005
SERPIND1	clone I	-6,89117	3,78E-009	3,78E-007
SERPINF2	clone I	-6,12086	2,34E-009	2,48E-007
SERPING1	clone I	-4,31792	0,000175318	0,00367152
SHBG	clone I	-5,24712	1,28E-006	5,77E-005
SLC13A3	clone I	-4,19113	7,39E-005	0,00178488

gene	sample_2	log2(fold_change)	p_value	q_value
SLC13A5 (2 of 2)	clone I	-6,13999	1,22E-008	1,05E-006
SLC1A5	clone I	2,50444	2,28E-005	0,000665632
SLC22A13	clone I	-5,19422	0,00109333	0,016519
SLC22A14	clone I	-3,48402	0,000883453	0,0138823
SLC22A16	clone I	-6,38717	0,0013388	0,0194484
SLC25A34	clone I	-3,30934	0,00260614	0,0331358
SLC27A2 (1 of 3)	clone I	-4,73123	1,42E-005	0,000447399
SLC27A2 (2 of 3)	clone I	-2,99604	0,000794409	0,0127377
SLC27A6	clone I	-3,54959	0,00021688	0,00438382
SLC2A2	clone I	-1,80E+308	0,00418103	0,0480541
SLC7A2	clone I	-3,35522	0,00321126	0,0390847
SMOX	clone I	4,79144	3,71E-014	1,24E-011
SOAT2	clone I	-2,97793	9,41E-005	0,00218518
SOCS3 (1 of 2)	clone I	5,02142	5,49E-011	9,00E-009
SOCS3 (2 of 2)	clone I	3,52158	2,31E-005	0,00067399
SUSD2	clone I	-5,9516	0,00287635	0,0358288
TAT	clone I	-5,62239	2,27E-008	1,79E-006
TDO2	clone I	-7,12716	2,49E-007	1,42E-005
TF	clone I	-6,59198	0,0010223	0,0156394
TFR2	clone I	-3,453	0,00131914	0,0192224
THBS1 (2 of 2)	clone I	2,96688	5,01E-006	0,000184648
TIMP2 (1 of 2)	clone I	1,70064	0,00389634	0,0454923
TLR3	clone I	-3,94611	9,93E-006	0,000329494
TM4SF4	clone I	-1,80E+308	8,85E-005	0,00207617
TM7SF2	clone I	-3,43438	0,000767822	0,0123918
TMEM79 (1 of 2)	clone I	-3,65948	0,00214352	0,0283688
TNNC2 (1 of 2)	clone I	-3,35039	0,000219396	0,00442627
TNNI2 (1 of 5)	clone I	-3,46452	0,00180689	0,0247394
TNNI2 (3 of 5)	clone I	-3,42707	0,000178817	0,00373263
TNNT3 (2 of 2)	clone I	-3,31293	0,00101584	0,0155582
TPM2	clone I	-0,698659	5,27E-005	0,00134639
TTC36	clone I	-4,17839	1,50E-005	0,00046637
TYMP	clone I	-4,915	1,64E-006	7,12E-005
UCP1	clone I	-4,89081	5,12E-008	3,62E-006
UGT2A3 (3 of 4)	clone I	-1,93469	0,00321186	0,0390901
UGT2A3 (4 of 4)	clone I	-3,99779	0,00187631	0,0255049
UPB1	clone I	-3,73042	3,37E-007	1,84E-005
UPP2	clone I	-5,37939	7,27E-006	0,000253128
UROC1	clone I	-5,03856	3,59E-007	1,94E-005
VTN (2 of 2)	clone I	-6,63193	0	0
ZFP36	clone I	1,5808	0,00349363	0,0417529
ZNFX1	clone I	1,4393	0,00211641	0,0280832
A1CF	clone mix	-9,45232	3,57E-009	3,58E-007
ABCB11	clone mix	-7,20081	1,08E-006	4,99E-005
ABCB4	clone mix	-5,10158	9,21E-006	0,000309099
ACAA2	clone mix	1,7751	9,61E-005	0,00222532
ACMSD	clone mix	-5,96738	8,37E-007	4,02E-005
ACSF2 (2 of 2)	clone mix	-3,3142	4,28E-005	0,00113007
ACSL4	clone mix	1,21208	0,00124195	0,0183141
ACTN2	clone mix	7,04617	9,38E-008	6,12E-006
ADPRH	clone mix	2,39927	0,00168406	0,0233792
ADPRHL1	clone mix	6,84139	1,39E-006	6,17E-005
ADSSL1	clone mix	4,31808	0,000163499	0,00346497

gene	sample_2	log2(fold_change)	p_value	q_value
AGT	clone mix	-7,72347	1,96E-008	1,58E-006
AGXT (1 of 2)	clone mix	-8,48385	2,78E-005	0,000786698
AGXT (2 of 2)	clone mix	-8,02024	3,67E-008	2,72E-006
AGXT2 (1 of 2)	clone mix	-4,88925	0,00024886	0,00491356
AHSG	clone mix	-9,47625	0	0
AKR1D1 (2 of 2)	clone mix	-7,87448	1,55E-008	1,29E-006
ALDH8A1	clone mix	-7,33055	4,87E-006	0,000180375
ALLC	clone mix	-5,00936	3,43E-006	0,000133802
ALPK3 (1 of 2)	clone mix	5,71732	8,82E-005	0,00207101
ALPK3 (2 of 2)	clone mix	6,36627	7,19E-006	0,000250879
AMBP	clone mix	-8,36261	5,34E-007	2,73E-005
AMDHD1	clone mix	-4,93734	0,000186495	0,0038655
ANGPTL3 (1 of 2)	clone mix	-5,8661	2,38E-005	0,000691078
ANGPTL5	clone mix	2,82959	0,000890158	0,0139683
ANGPTL7	clone mix	6,88492	0,000942395	0,0146378
ANK3 (1 of 2)	clone mix	2,93732	0,000919295	0,0143441
ANXA6	clone mix	4,22764	5,88E-005	0,00147707
APOA1	clone mix	-9,06207	2,51E-005	0,000722663
APOB (1 of 5)	clone mix	-8,46904	1,26E-009	1,44E-007
APOB (5 of 5)	clone mix	-9,07721	8,88E-016	3,93E-013
APOBEC2 (2 of 2)	clone mix	4,66589	1,21E-006	5,52E-005
APOE (2 of 2)	clone mix	-1,80E+308	0,000207215	0,00421955
APOH (2 of 2)	clone mix	-6,5211	2,25E-005	0,000659304
ARG1	clone mix	-3,79611	0,00069419	0,0114144
ARHGEF38 (1 of 2)	clone mix	-4,77493	0,000542882	0,00934037
ARL14 (2 of 2)	clone mix	-1,80E+308	0,000483262	0,00849264
ASB2 (1 of 2)	clone mix	5,63141	0,000235194	0,00468914
ASB5	clone mix	5,61327	0,00182838	0,0249823
ASGR1	clone mix	-8,05254	2,91E-009	3,01E-007
ATP1B3	clone mix	4,15556	0,000122693	0,00272753
ATP2A1 (1 of 2)	clone mix	5,55016	9,79E-007	4,59E-005
ATP2A2 (1 of 2)	clone mix	2,45458	0,00252052	0,032273
ATP7B	clone mix	-5,43213	5,28E-005	0,00134971
BMP10 (2 of 2)	clone mix	6,16807	0,000354888	0,0065878
BVES	clone mix	2,84616	0,000755338	0,0122242
C3 (1 of 8)	clone mix	-7,32688	1,64E-006	7,15E-005
C3 (2 of 8)	clone mix	-6,09692	4,24E-006	0,000160231
C3 (3 of 8)	clone mix	-7,56018	5,76E-007	2,92E-005
C3 (4 of 8)	clone mix	-7,97252	2,27E-005	0,000663285
C3 (5 of 8)	clone mix	-7,33536	7,55E-007	3,68E-005
C3 (8 of 8)	clone mix	-2,97549	2,22E-016	1,07E-013
C6	clone mix	-3,91856	0	0
C6orf58	clone mix	-7,17017	2,82E-008	2,17E-006
C8A	clone mix	-8,172	3,60E-007	1,95E-005
C8B	clone mix	-9,58731	5,96E-006	0,000213696
C8G	clone mix	-8,88119	1,19E-010	1,79E-008
C9	clone mix	-6,48627	1,47E-006	6,49E-005
CA6 (1 of 2)	clone mix	4,4725	4,47E-007	2,34E-005
CA6 (2 of 2)	clone mix	4,4454	0,000531458	0,00918072
CACNG1 (2 of 2)	clone mix	4,86771	0,00112121	0,0168613
CAP2	clone mix	4,37013	1,12E-006	5,15E-005
CASQ1 (1 of 2)	clone mix	2,62435	0,00028387	0,00547686
CAV3	clone mix	3,64534	1,17E-005	0,000377137

gene	sample_2	log2(fold_change)	p_value	q_value
CBX7 (2 of 2)	clone mix	1,6102	0,00200657	0,026912
CCRN4L (2 of 2)	clone mix	1,86769	0,00103641	0,0158156
CDH15	clone mix	4,23794	0,000667444	0,0110521
CETP	clone mix	-8,57613	2,71E-007	1,53E-005
CFB	clone mix	-5,21265	1,15E-005	0,000374249
CFP	clone mix	-7,5473	4,38E-007	2,31E-005
CHCHD3 (2 of 2)	clone mix	1,01126	0,00194734	0,0262684
CIDEB	clone mix	-7,08005	4,82E-008	3,44E-006
CKMT2 (1 of 2)	clone mix	6,38005	0	0
CLDN2	clone mix	-1,80E+308	0,00263022	0,0333755
CLIC5 (2 of 2)	clone mix	4,13361	0,00073087	0,0119035
CNDP1	clone mix	-7,21208	0,000148379	0,00319605
CORO6	clone mix	3,15266	0,000214551	0,00434446
COX6B1 (1 of 2)	clone mix	3,9819	0,000809981	0,012938
COX7A1	clone mix	2,89271	0,00167906	0,0233233
CPT1B	clone mix	4,03752	8,17E-005	0,001942
CREB3L3	clone mix	-4,86036	0,000995133	0,0153012
CRIP2 (2 of 2)	clone mix	4,18652	0,000814347	0,0129932
CROT (2 of 2)	clone mix	-1,21466	1,72E-005	0,000524368
CSRP3	clone mix	6,68479	0,000769387	0,0124122
CTDSPL (1 of 2)	clone mix	2,16458	0,000360289	0,00667151
CYP24A1	clone mix	-7,47787	4,30E-011	7,25E-009
CYP2C9	clone mix	-6,59934	0,000173139	0,00363377
CYP2J2 (1 of 6)	clone mix	-6,90308	1,13E-009	1,31E-007
CYP2J2 (2 of 6)	clone mix	-7,58652	0,000513823	0,00893042
CYP2J2 (3 of 6)	clone mix	-3,98974	0,000150853	0,00324077
CYP2W1 (1 of 5)	clone mix	-1,80E+308	0,000180018	0,0037538
CYP7A1	clone mix	-4,33877	9,23E-010	1,10E-007
CYP8B1	clone mix	-4,81158	0,000105939	0,00241293
DAG1 (1 of 2)	clone mix	2,29277	0,00435256	0,049567
DDIT4 (1 of 2)	clone mix	4,37605	3,67E-007	1,98E-005
DENND4A (2 of 2)	clone mix	4,71111	2,65E-008	2,05E-006
DES	clone mix	5,9404	9,54E-009	8,45E-007
DHRS7C (1 of 2)	clone mix	4,11315	0,000480846	0,00845817
DHRS7C (2 of 2)	clone mix	4,24917	2,75E-005	0,000781284
DIABLO (1 of 2)	clone mix	-8,63579	5,87E-008	4,08E-006
DMD	clone mix	3,33467	0,000235213	0,00468941
DNAJC22	clone mix	-1,80E+308	0,000506774	0,00882908
DPYS	clone mix	-1,80E+308	8,28E-006	0,00028259
DTNA	clone mix	4,88119	2,56E-005	0,000735057
DUSP26 (2 of 2)	clone mix	-4,84748	1,24E-005	0,000397841
EGF	clone mix	3,04227	0,00246946	0,0317477
ELL (2 of 2)	clone mix	3,00113	0,000263951	0,00515684
ELTD1	clone mix	1,60145	0,00246475	0,0317003
ENO3	clone mix	2,9872	0,00141613	0,0203434
ENPP2 (2 of 2)	clone mix	-3,66921	0,00101657	0,0155675
ENSGACG00000000007	clone mix	-8,11472	1,83E-009	2,00E-007
ENSGACG00000000272	clone mix	3,54269	3,55E-005	0,000966521
ENSGACG00000000300	clone mix	4,92423	5,55E-007	2,82E-005
ENSGACG00000000547	clone mix	4,74245	0,00202181	0,0270772
ENSGACG00000001073	clone mix	5,16748	0,0010648	0,0161686
ENSGACG00000001260	clone mix	-8,16523	1,06E-007	6,81E-006
ENSGACG00000001261	clone mix	-4,9603	7,43E-006	0,000257758

gene	sample_2	log2(fold_change)	p_value	q_value
ENSGACG00000001432	clone mix	-8,38559	2,16E-009	2,32E-007
ENSGACG00000001733	clone mix	-7,26937	9,46E-009	8,38E-007
ENSGACG00000001742	clone mix	-2,84172	0	0
ENSGACG00000002089	clone mix	5,01119	8,53E-007	4,09E-005
ENSGACG00000002738	clone mix	3,1554	0,00275341	0,0346035
ENSGACG00000002791	clone mix	1,80E+308	0,000800079	0,0128101
ENSGACG00000002805	clone mix	-1,80E+308	0,00120415	0,0178592
ENSGACG00000002832	clone mix	-5,58718	9,02E-005	0,00211034
ENSGACG00000002902	clone mix	7,61526	0,000600187	0,0101358
ENSGACG00000003003	clone mix	8,67502	0,000237202	0,00472103
ENSGACG00000003030	clone mix	-5,21788	0,00049831	0,00870816
ENSGACG00000003435	clone mix	-5,39212	0,00422824	0,0484796
ENSGACG00000003461	clone mix	-8,65825	4,69E-008	3,36E-006
ENSGACG00000003467	clone mix	-9,94776	2,22E-006	9,23E-005
ENSGACG00000003473	clone mix	-6,1975	6,61E-006	0,000233408
ENSGACG00000003501	clone mix	2,71534	0,00343187	0,0411803
ENSGACG00000003651	clone mix	3,67353	0,00113529	0,0170326
ENSGACG00000004200	clone mix	10,4072	2,85E-008	2,19E-006
ENSGACG00000004413	clone mix	-9,54121	9,05E-012	1,81E-009
ENSGACG00000004463	clone mix	-4,79157	0,00120635	0,0178864
ENSGACG00000004822	clone mix	-4,28271	0,000809453	0,0129317
ENSGACG00000004971	clone mix	4,617	4,61E-006	0,000172237
ENSGACG00000005023	clone mix	3,96559	0,0003643	0,00673245
ENSGACG00000005264	clone mix	-5,09263	4,94E-005	0,00127506
ENSGACG00000005365	clone mix	2,97659	0,000240806	0,00478006
ENSGACG00000005883	clone mix	-6,39573	1,67E-008	1,38E-006
ENSGACG00000005916	clone mix	-5,06856	0,00372467	0,0439226
ENSGACG00000005973	clone mix	2,65704	0,000610459	0,0102753
ENSGACG00000006029	clone mix	-9,14545	1,45E-005	0,000454108
ENSGACG00000006109	clone mix	4,1981	0,00104704	0,0159464
ENSGACG00000006351	clone mix	-3,66544	0,00138272	0,0199588
ENSGACG00000006530	clone mix	4,30505	8,60E-005	0,0020269
ENSGACG00000006644	clone mix	-7,50861	6,77E-010	8,32E-008
ENSGACG00000006790	clone mix	-4,44725	4,46E-005	0,00117029
ENSGACG00000006829	clone mix	-1,80E+308	0,00348204	0,0416455
ENSGACG00000006833	clone mix	-7,19262	1,09E-005	0,000357722
ENSGACG00000007038	clone mix	-8,0323	2,59E-005	0,000743096
ENSGACG00000007411	clone mix	-1,67337	9,99E-015	3,70E-012
ENSGACG00000007507	clone mix	-3,96162	0,000458463	0,00813578
ENSGACG00000007622	clone mix	3,18314	0,000789668	0,0126754
ENSGACG00000007640	clone mix	-5,83486	0,000106101	0,00241612
ENSGACG00000007661	clone mix	7,941	1,40E-005	0,000439815
ENSGACG00000007954	clone mix	-7,64659	1,12E-007	7,15E-006
ENSGACG00000008064	clone mix	3,41811	0,00204422	0,0273142
ENSGACG00000008706	clone mix	3,18777	0,000956924	0,0148199
ENSGACG00000009173	clone mix	-9,32742	1,57E-006	6,89E-005
ENSGACG00000009200	clone mix	2,15006	0,000803965	0,0128611
ENSGACG00000009409	clone mix	8,714	1,18E-010	1,77E-008
ENSGACG00000009583	clone mix	-4,34612	0,00107373	0,0162786
ENSGACG00000009592	clone mix	-5,19627	5,11E-013	1,36E-010
ENSGACG00000009633	clone mix	-4,62296	2,74E-005	0,000777028
ENSGACG00000009821	clone mix	4,14856	0,00128021	0,0187634
ENSGACG00000009825	clone mix	0,80967	0,0029731	0,0367932

gene	sample_2	log2(fold_change)	p_value	q_value
ENSGACG00000009880	clone mix	-9,2888	6,70E-007	3,32E-005
ENSGACG00000009883	clone mix	-9,40461	2,37E-005	0,000689702
ENSGACG00000009952	clone mix	-7,60972	0,00274343	0,0345057
ENSGACG00000010050	clone mix	2,44667	1,04E-005	0,000343556
ENSGACG00000010126	clone mix	7,15861	2,19E-005	0,000644025
ENSGACG00000010127	clone mix	3,4267	0,00198807	0,0267137
ENSGACG00000010145	clone mix	-5,98309	5,24E-007	2,69E-005
ENSGACG00000010184	clone mix	5,39047	4,63E-006	0,000172874
ENSGACG00000010196	clone mix	-8,07504	1,34E-006	5,99E-005
ENSGACG00000010476	clone mix	3,6596	1,46E-006	6,45E-005
ENSGACG00000010623	clone mix	8,28426	1,49E-006	6,56E-005
ENSGACG00000010757	clone mix	3,60422	0,00070724	0,0115896
ENSGACG00000010837	clone mix	3,30196	0,00311893	0,0381901
ENSGACG00000010933	clone mix	-7,76623	3,35E-007	1,83E-005
ENSGACG00000011294	clone mix	2,05134	0,00229546	0,0299512
ENSGACG00000011392	clone mix	-9,67169	3,24E-014	1,10E-011
ENSGACG00000011617	clone mix	-9,09182	1,69E-006	7,31E-005
ENSGACG00000011846	clone mix	-9,1225	1,61E-011	3,02E-009
ENSGACG00000011851	clone mix	-9,65967	9,97E-010	1,17E-007
ENSGACG00000011882	clone mix	-1,80E+308	0,00318018	0,0387864
ENSGACG00000012174	clone mix	5,41496	0,00235428	0,0305623
ENSGACG00000012381	clone mix	-8,60602	8,21E-006	0,00028048
ENSGACG00000012414	clone mix	-9,20094	3,91E-008	2,87E-006
ENSGACG00000012464	clone mix	2,8934	0,000917222	0,0143167
ENSGACG00000012473	clone mix	-4,25753	0,00373041	0,043977
ENSGACG00000012546	clone mix	4,36428	5,41E-007	2,76E-005
ENSGACG00000012590	clone mix	3,62915	0,000539175	0,00928892
ENSGACG00000012592	clone mix	3,17343	0,000859312	0,0135726
ENSGACG00000012654	clone mix	8,432	1,17E-005	0,000377388
ENSGACG00000012657	clone mix	7,79734	2,75E-007	1,54E-005
ENSGACG00000012663	clone mix	4,59504	5,12E-005	0,0013149
ENSGACG00000012954	clone mix	6,47443	2,11E-005	0,00062499
ENSGACG00000012962	clone mix	9,61108	3,13E-007	1,73E-005
ENSGACG00000013326	clone mix	2,23475	0,0029096	0,036166
ENSGACG00000013564	clone mix	1,80E+308	6,01E-005	0,00150263
ENSGACG00000013583	clone mix	2,93448	0,0015206	0,021538
ENSGACG00000013712	clone mix	1,4635	0,00363968	0,043131
ENSGACG00000013769	clone mix	-6,08426	0,00243402	0,0313869
ENSGACG00000013782	clone mix	8,88738	2,55E-008	1,98E-006
ENSGACG00000013793	clone mix	-6,19303	1,90E-006	8,11E-005
ENSGACG00000013996	clone mix	-4,5489	0,000458371	0,00813449
ENSGACG00000014348	clone mix	-5,64324	1,36E-005	0,000430949
ENSGACG00000014547	clone mix	-3,55635	0,0010022	0,01539
ENSGACG00000014699	clone mix	-5,99861	3,25E-006	0,000127809
ENSGACG00000014752	clone mix	4,26222	0,000336452	0,00630562
ENSGACG00000014811	clone mix	-8,47799	3,14E-008	2,37E-006
ENSGACG00000014852	clone mix	-4,8164	4,56E-005	0,00119375
ENSGACG00000014922	clone mix	4,24362	2,37E-005	0,000688445
ENSGACG00000014948	clone mix	8,17823	0,00306636	0,0376933
ENSGACG00000014960	clone mix	8,77795	8,05E-009	7,29E-007
ENSGACG00000015168	clone mix	4,84033	8,30E-006	0,000283264
ENSGACG00000015248	clone mix	4,14657	1,74E-005	0,000529666
ENSGACG00000015265	clone mix	4,51299	5,69E-005	0,00143615

gene	sample_2	log2(fold_change)	p_value	q_value
ENSGACG00000015407	clone mix	3,10252	0,0020882	0,0277831
ENSGACG00000015411	clone mix	-9,40632	2,53E-005	0,000728333
ENSGACG00000015464	clone mix	-7,79816	2,62E-009	2,74E-007
ENSGACG00000015472	clone mix	-8,22622	4,39E-008	3,17E-006
ENSGACG00000015778	clone mix	4,63744	8,36E-005	0,00198065
ENSGACG00000015857	clone mix	-8,36516	1,55E-009	1,73E-007
ENSGACG00000015947	clone mix	-7,9605	1,98E-007	1,17E-005
ENSGACG00000016031	clone mix	3,70453	0,000381856	0,0070004
ENSGACG00000016045	clone mix	5,50674	5,66E-006	0,000204499
ENSGACG00000016073	clone mix	3,14627	0,0020555	0,0274327
ENSGACG00000016093	clone mix	-5,64742	5,49E-005	0,00139269
ENSGACG00000016104	clone mix	-10,0841	5,78E-009	5,46E-007
ENSGACG00000016298	clone mix	2,55669	4,71E-005	0,00122545
ENSGACG00000016669	clone mix	-4,98091	9,28E-011	1,44E-008
ENSGACG00000016687	clone mix	-4,92367	4,74E-005	0,00123278
ENSGACG00000016696	clone mix	-6,64583	2,20E-005	0,000646483
ENSGACG00000017655	clone mix	-4,32298	0,00206708	0,0275538
ENSGACG00000017681	clone mix	-6,17273	3,25E-006	0,000128022
ENSGACG00000017683	clone mix	4,7162	7,79E-006	0,000268433
ENSGACG00000017758	clone mix	5,88708	0,00151364	0,0214597
ENSGACG00000018177	clone mix	-1,80E+308	0,000538967	0,00928614
ENSGACG00000018499	clone mix	4,18979	3,73E-005	0,00100711
ENSGACG00000018662	clone mix	4,50171	8,58E-005	0,00202406
ENSGACG00000018776	clone mix	-8,21294	1,13E-010	1,71E-008
ENSGACG00000018832	clone mix	4,38728	0,000241803	0,00479694
ENSGACG00000018908	clone mix	3,77047	7,13E-005	0,00173363
ENSGACG00000018934	clone mix	3,60144	0,000579002	0,00984081
ENSGACG00000019066	clone mix	-9,12381	9,66E-010	1,14E-007
ENSGACG00000019454	clone mix	-5,88264	1,20E-005	0,000385487
ENSGACG00000019517	clone mix	-1,80E+308	0,00305528	0,0375886
ENSGACG00000019604	clone mix	-1,80E+308	1,01E-007	6,52E-006
ENSGACG00000019624	clone mix	4,32767	0,00138722	0,0200102
ENSGACG00000019744	clone mix	7,66271	5,68E-008	3,96E-006
ENSGACG00000019784	clone mix	6,30711	4,12E-007	2,18E-005
ENSGACG00000019954	clone mix	-5,33707	1,24E-005	0,000396448
ENSGACG00000019958	clone mix	-3,80775	0,00397733	0,0462224
ENSGACG00000020047	clone mix	-7,57813	1,28E-008	1,09E-006
ENSGACG00000020469	clone mix	4,38933	0,000880791	0,0138487
ENSGACG00000020566	clone mix	-1,80E+308	5,70E-005	0,00143887
ENSGACG00000020614	clone mix	-4,16206	0,00219492	0,0288996
ENSGACG00000020615	clone mix	-3,85397	0,00177518	0,0243874
ENSGACG00000020653	clone mix	-8,53252	1,66E-010	2,41E-008
ENSGACG00000020833	clone mix	-1,80E+308	0,00120415	0,0178592
ENSGACG00000020917	clone mix	-7,70784	8,34E-009	7,52E-007
ESYT2 (2 of 2)	clone mix	4,01851	0,00101574	0,0155568
F10	clone mix	-7,67275	4,09E-008	2,98E-006
F2	clone mix	-7,10922	4,66E-006	0,000173562
F3 (1 of 2)	clone mix	3,31364	0,000319824	0,00604585
F5	clone mix	-6,60978	5,83E-006	0,000209847
F9 (1 of 2)	clone mix	-5,78317	0,00113102	0,016982
F9 (2 of 2)	clone mix	-5,86491	3,68E-008	2,72E-006
FABP1	clone mix	-7,52754	0,000137803	0,00300485
FABP2 (2 of 2)	clone mix	5,54522	1,41E-005	0,000442383

gene	sample_2	log2(fold_change)	p_value	q_value
FER1L6	clone mix	6,02657	0,00344332	0,0412879
FERMT2	clone mix	1,29243	0,00133136	0,0193611
FETUB (1 of 3)	clone mix	-5,58163	1,47E-005	0,00046061
FETUB (2 of 3)	clone mix	-5,17161	0,00023219	0,004639
FETUB (3 of 3)	clone mix	-8,28839	1,22E-007	7,71E-006
FGA	clone mix	-9,38095	1,04E-010	1,59E-008
FGB	clone mix	-8,85037	6,79E-008	4,63E-006
FGG	clone mix	-8,72605	2,01E-007	1,18E-005
FHL1 (1 of 2)	clone mix	3,24257	3,18E-009	3,24E-007
FHL2 (1 of 2)	clone mix	4,38662	9,49E-006	0,000317191
FHOD3 (1 of 2)	clone mix	3,98885	4,19E-005	0,00111007
FILIP1 (1 of 2)	clone mix	4,25565	4,04E-005	0,00107757
FKBP5	clone mix	4,23206	2,38E-007	1,37E-005
FLNC (1 of 2)	clone mix	3,24023	9,09E-005	0,00212351
FLNC (2 of 2)	clone mix	5,28118	5,25E-008	3,70E-006
FOSL1	clone mix	4,77764	0,000150351	0,00323166
FPGT-TNNI3K	clone mix	3,52345	0,00118923	0,0176817
FSD2	clone mix	2,55681	0,00356731	0,0424511
G0S2	clone mix	-4,65133	3,37E-005	0,000926008
G6PC (1 of 2)	clone mix	-6,11379	3,21E-007	1,77E-005
G6PC (2 of 2)	clone mix	-6,78698	3,49E-005	0,000954266
G6PD (2 of 2)	clone mix	-4,83302	0,000422036	0,00760138
GAPDH (1 of 2)	clone mix	4,68969	4,62E-008	3,31E-006
GMPR	clone mix	3,39691	0,000386271	0,00706693
GPM6B (2 of 2)	clone mix	1,48908	0,00139709	0,0201277
GPX4 (2 of 4)	clone mix	-4,92659	3,26E-005	0,000899041
GPX4 (3 of 4)	clone mix	-4,6933	0,0021903	0,0288513
GPX4 (4 of 4)	clone mix	-4,61245	0,00347004	0,0415363
GRAMD3 (2 of 2)	clone mix	-1,80E+308	0,000678638	0,0112038
GZMM (2 of 5)	clone mix	-1,88621	1,91E-008	1,55E-006
HAAO	clone mix	-9,01293	1,98E-012	4,63E-010
HABP2 (1 of 2)	clone mix	-9,47468	4,38E-008	3,16E-006
HABP2 (2 of 2)	clone mix	-9,71789	4,33E-014	1,43E-011
HAL	clone mix	-5,81666	2,32E-005	0,000677307
HAO1	clone mix	-1,80E+308	1,32E-006	5,93E-005
HGD	clone mix	-5,13121	0,000716314	0,0117104
HHATL (2 of 2)	clone mix	6,38591	2,90E-007	1,62E-005
HIVEP2 (2 of 2)	clone mix	5,08855	0,000298069	0,0057026
HNF1A	clone mix	-4,15424	0,00394509	0,0459396
HNF4A	clone mix	-7,10406	0,000244939	0,00484946
HPD	clone mix	-7,79804	4,83E-007	2,50E-005
HPN	clone mix	-4,2277	0,00120046	0,0178164
HPX	clone mix	-8,95519	9,22E-013	2,31E-010
HRC	clone mix	4,72011	1,35E-005	0,000426888
HSD17B3	clone mix	-3,89208	5,96E-007	3,00E-005
HSP90AA1 (2 of 2)	clone mix	5,41141	0,00021015	0,00426972
HSPB1	clone mix	3,78324	8,28E-008	5,50E-006
HSPB7	clone mix	5,4009	2,65E-006	0,000107539
IGFALS	clone mix	-6,09706	6,34E-006	0,00022534
IGFBP1 (2 of 2)	clone mix	-6,58674	1,71E-006	7,39E-005
IGFN1 (4 of 5)	clone mix	8,46113	8,21E-006	0,000280692
IGSF5 (2 of 2)	clone mix	-4,78368	0,000871581	0,0137298
ILDR1 (1 of 2)	clone mix	-3,47813	1,20E-005	0,000385761

gene	sample_2	log2(fold_change)	p_value	q_value
IPO13 (2 of 2)	clone mix	3,80229	0,00214249	0,0283576
IRF4 (2 of 2)	clone mix	1,78947	0,000811916	0,0129617
ITGA5 (1 of 2)	clone mix	2,31389	0,00213492	0,0282792
ITIH2	clone mix	-8,56165	7,14E-008	4,84E-006
ITIH4 (2 of 2)	clone mix	-5,80946	0,00015352	0,00328764
JPH1 (1 of 2)	clone mix	4,44618	5,61E-005	0,0014192
JPH2	clone mix	3,92328	1,08E-005	0,000354458
JUNB (2 of 2)	clone mix	3,41232	0,000229937	0,00460136
KBTBD10 (1 of 2)	clone mix	3,9268	0,000124546	0,00276196
KBTBD12	clone mix	4,52109	3,72E-005	0,00100584
KCNJ14	clone mix	5,2533	0,00362084	0,0429571
KL	clone mix	-5,27582	2,99E-005	0,000836716
KLF13	clone mix	3,31945	0,00164226	0,0229142
KLF9	clone mix	2,68032	0,000737203	0,0119868
KLHL30	clone mix	4,86814	7,33E-006	0,000254858
KLHL31	clone mix	5,55851	3,86E-008	2,84E-006
KLHL38 (2 of 2)	clone mix	5,93881	3,83E-006	0,000147046
KNG1	clone mix	-8,23173	8,27E-010	9,96E-008
LDB3	clone mix	4,31541	0,000156193	0,00333485
LECT2	clone mix	-9,45427	3,62E-009	3,63E-007
LIMCH1 (2 of 2)	clone mix	2,89254	0,00439358	0,0499249
LIPC	clone mix	-6,18618	1,07E-008	9,33E-007
LMOD3	clone mix	2,24621	0,00118012	0,0175748
LRG1	clone mix	-8,44941	7,86E-005	0,00188079
LRRC14B	clone mix	2,9663	0,00317895	0,0387757
LRRC2	clone mix	3,74612	0,000351851	0,00654066
LYZ	clone mix	-8,08362	3,11E-009	3,19E-007
MAT1A (2 of 2)	clone mix	-8,37152	7,87E-009	7,15E-007
MDH1 (2 of 2)	clone mix	2,95913	0,0023995	0,031035
MEF2C (2 of 2)	clone mix	4,59457	0,000129711	0,00285762
MICAL2 (2 of 2)	clone mix	2,28887	0,00419306	0,0481628
MINPP1 (1 of 2)	clone mix	-3,91478	0,000484058	0,00850407
MIOX	clone mix	-9,41505	3,18E-007	1,75E-005
MLF1	clone mix	4,79993	0,00427236	0,0488688
MLXIPL	clone mix	-2,91059	0,00197395	0,0265615
MMP9	clone mix	1,99427	5,33E-010	6,73E-008
MOGAT2	clone mix	-7,02163	0,000875855	0,0137844
MPZL3	clone mix	-3,90013	0,000748888	0,0121397
MSS51	clone mix	3,32715	0,00136932	0,0198057
MST1P9	clone mix	-8,37176	8,86E-007	4,22E-005
MYL1	clone mix	3,71807	0,00209093	0,0278127
MYL7	clone mix	7,67761	2,24E-007	1,30E-005
MYLK	clone mix	2,3793	0,00238843	0,030918
MYLK4 (1 of 2)	clone mix	6,40473	2,67E-005	0,000760614
MYLK4 (2 of 2)	clone mix	4,33414	1,96E-005	0,00058648
MYLPF (1 of 2)	clone mix	11,08	1,32E-005	0,000419886
MYO18A (2 of 2)	clone mix	5,3749	1,32E-005	0,000420355
MYOC	clone mix	5,15953	0,00071554	0,0117003
MYOM1 (2 of 2)	clone mix	4,39973	2,69E-008	2,07E-006
MYOZ1 (1 of 2)	clone mix	5,16977	1,98E-006	8,38E-005
MYOZ2 (1 of 2)	clone mix	5,87713	4,85E-007	2,51E-005
MYOZ2 (2 of 2)	clone mix	3,94155	0,000852697	0,0134876
MYOZ3	clone mix	3,87792	0,00368452	0,0435503

gene	sample_2	log2(fold_change)	p_value	q_value
MYPN	clone mix	3,99614	0,00262405	0,0333144
NAALADL1	clone mix	-3,52012	0,000124103	0,00275382
NBEA (2 of 2)	clone mix	1,74561	0,000199285	0,00408555
NDRG2	clone mix	2,24207	0,00319011	0,0388804
NDUFA4 (2 of 2)	clone mix	5,47042	0,000224137	0,00450499
NEB	clone mix	5,26732	8,88E-016	3,93E-013
NEBL	clone mix	3,55025	0,0020965	0,0278716
NEXN	clone mix	4,20174	6,03E-006	0,000215899
NIPSNAP1	clone mix	-4,37953	8,55E-005	0,00201707
NR0B2	clone mix	-5,25379	0,00241866	0,0312296
NR1H4	clone mix	-7,39419	1,52E-005	0,000473756
NRAP	clone mix	3,8403	0,00365405	0,0432675
OBSCN	clone mix	4,26785	2,77E-009	2,87E-007
OBSL1 (2 of 2)	clone mix	5,42834	7,21E-006	0,00025144
OVGP1 (3 of 5)	clone mix	-8,19648	8,96E-009	8,00E-007
PABPC4	clone mix	5,16538	1,99E-007	1,17E-005
PCSK6	clone mix	-5,21122	0,000123615	0,00274499
PDLIM1	clone mix	6,03339	1,51E-008	1,26E-006
PDLIM7	clone mix	2,23115	0,000412819	0,00746505
PFKFB3	clone mix	3,42098	4,48E-005	0,00117453
PFKFB4 (2 of 2)	clone mix	0,656039	0,000712586	0,0116608
PFKM (1 of 2)	clone mix	3,99804	0,000256282	0,00503408
PFKM (2 of 2)	clone mix	3,27751	0,00064485	0,0107454
PGAM2	clone mix	3,52473	0,000101531	0,00233007
PGLYRP2 (2 of 2)	clone mix	-9,26656	4,80E-006	0,000178235
PIP5K1C (2 of 2)	clone mix	3,61921	0,000692464	0,0113909
PLA2G12B (1 of 2)	clone mix	-4,59073	0,000347477	0,00647535
PLG	clone mix	-9,12264	2,33E-011	4,20E-009
PPM1J	clone mix	1,9346	0,00101316	0,0155252
PPM1K (2 of 2)	clone mix	3,94667	0,000393509	0,00717548
PPP1R27 (1 of 2)	clone mix	4,36266	2,91E-005	0,000817678
PRHOXNB	clone mix	-1,80E+308	8,85E-005	0,00207617
PRODH2	clone mix	-5,19772	0,00203898	0,0272568
PROZ (2 of 2)	clone mix	-8,18804	2,32E-005	0,000676432
PYGM (2 of 2)	clone mix	3,65248	0,000539476	0,00929305
QPCT	clone mix	-3,60227	0,00369209	0,0436205
QPRT	clone mix	-3,69464	0,0035321	0,042121
RAMP1 (2 of 2)	clone mix	4,45678	0,00229099	0,0299031
RBM24 (1 of 2)	clone mix	3,57947	0,00432338	0,0493158
RGR	clone mix	4,31277	0,00409694	0,0472994
RPL3L	clone mix	5,371	1,48E-005	0,000462417
RRAD	clone mix	3,81035	0,0012415	0,0183088
RYR1 (1 of 2)	clone mix	4,43723	1,88E-005	0,000567537
RYR1 (2 of 2)	clone mix	5,84703	6,73E-007	3,33E-005
SCN4A (2 of 2)	clone mix	3,10989	0,00175349	0,0241486
SERPINA10 (1 of 2)	clone mix	-6,69702	5,52E-013	1,45E-010
SERPINC1	clone mix	-8,55003	3,57E-008	2,65E-006
SERPIND1	clone mix	-8,75629	1,15E-008	9,93E-007
SERPINF2	clone mix	-7,83308	2,59E-008	2,01E-006
SERPING1	clone mix	-3,96492	0,0017837	0,0244818
SGCA	clone mix	4,67637	0,0026369	0,033442
SGCG	clone mix	1,94602	0,00379814	0,0445955
SHBG	clone mix	-7,27206	2,53E-007	1,44E-005

gene	sample_2	log2(fold_change)	p_value	q_value
SIX1	clone mix	3,41225	0,000122339	0,00272123
SLC13A3	clone mix	-5,52726	4,13E-005	0,00109701
SLC13A5 (2 of 2)	clone mix	-8,04321	2,99E-010	4,05E-008
SLC1A5	clone mix	2,8761	0,000146143	0,00315609
SLC22A13	clone mix	-1,80E+308	0,000223494	0,00449408
SLC22A16	clone mix	-2,8213	0,00434832	0,0495314
SLC25A43	clone mix	4,95184	1,33E-005	0,000421351
SLC26A11	clone mix	1,21159	0,000101424	0,00232801
SLC27A2 (1 of 3)	clone mix	-4,5458	0,000133652	0,00292919
SLC27A6	clone mix	-3,57811	0,000981181	0,015127
SLC2A2	clone mix	-1,80E+308	0,00418103	0,0480541
SLC34A2 (1 of 2)	clone mix	5,43395	4,17E-005	0,00110654
SLC41A3 (1 of 2)	clone mix	4,75892	0,00216692	0,0286111
SLC4A3	clone mix	4,90025	2,79E-005	0,000789973
SLC8A1 (2 of 2)	clone mix	7,94778	5,91E-005	0,00148222
SMOX	clone mix	5,1103	5,75E-008	4,00E-006
SMPX	clone mix	4,3406	1,19E-005	0,000382418
SNRNP70	clone mix	0,687726	0,000727284	0,0118546
SOAT2	clone mix	-6,06704	3,02E-006	0,000120103
SOCS3 (1 of 2)	clone mix	4,7558	9,08E-008	5,95E-006
SOCS3 (2 of 2)	clone mix	2,95157	0,00197091	0,026528
SORBS1	clone mix	2,23338	0,000668673	0,0110688
SORBS2	clone mix	4,46058	0,000325318	0,00613056
SPAG17	clone mix	4,65399	0,00213446	0,0282737
SPEG (1 of 2)	clone mix	3,0298	0,0020106	0,0269555
SPEG (2 of 2)	clone mix	2,72837	0,00121844	0,0180301
SPP2	clone mix	-6,30087	0,000202476	0,00413994
SPTBN1 (1 of 2)	clone mix	0,912046	0,00335708	0,0404783
SRL (1 of 2)	clone mix	4,59616	6,80E-006	0,000239138
SRL (2 of 2)	clone mix	3,17943	0,000336483	0,00630598
SUSD2	clone mix	-6,4255	0,000127073	0,00280852
SVIL (2 of 2)	clone mix	2,95952	0,000662983	0,0109918
SYNE2 (1 of 3)	clone mix	5,21479	2,08E-006	8,75E-005
SYNPO2L (1 of 2)	clone mix	4,28236	0,000148378	0,00319605
SYNPO2L (2 of 2)	clone mix	6,82575	1,59E-005	0,000490919
TAT	clone mix	-6,321	5,87E-006	0,00021096
TCAP	clone mix	4,34303	3,60E-005	0,00097753
TDO2	clone mix	-8,39853	3,12E-007	1,72E-005
TF	clone mix	-7,44169	0,000461348	0,00817794
THBS1 (2 of 2)	clone mix	2,41748	0,00310704	0,0380761
TJP1 (1 of 2)	clone mix	2,0736	0,0030529	0,0375677
TKT (2 of 2)	clone mix	4,89647	8,14E-005	0,00193685
TLR3	clone mix	-4,06587	4,65E-005	0,00121238
TM4SF4	clone mix	-1,80E+308	8,85E-005	0,00207617
TM4SF5	clone mix	-3,87002	0,00403026	0,046702
TM7SF2	clone mix	-4,31474	0,00129959	0,0189922
TMEM182	clone mix	4,92927	4,99E-011	8,28E-009
TMOD1	clone mix	3,64627	0,00225948	0,029573
TMOD4	clone mix	2,09525	4,77E-007	2,48E-005
TNNC1	clone mix	8,92128	9,06E-008	5,94E-006
TNNC2 (1 of 2)	clone mix	4,19605	0,000130627	0,00287404
TNNC2 (2 of 2)	clone mix	3,46013	0,000301462	0,00575604
TNNI2 (1 of 5)	clone mix	3,15294	0,00209209	0,0278249

gene	sample_2	log2(fold_change)	p_value	q_value
TNNI2 (3 of 5)	clone mix	2,98901	0,0041025	0,047349
TNNI2 (4 of 5)	clone mix	6,23861	0,000744837	0,0120866
TNNI2 (5 of 5)	clone mix	6,30029	2,80E-007	1,57E-005
TNNT2 (1 of 2)	clone mix	7,7103	3,13E-006	0,000123832
TNNT2 (2 of 2)	clone mix	2,69605	0,00315082	0,0385008
TNNT3 (2 of 2)	clone mix	3,2295	0,000167344	0,00353286
TPM2	clone mix	3,05966	0,000576159	0,0098013
TPM3	clone mix	5,07827	2,34E-005	0,000681963
TRAK1 (1 of 2)	clone mix	1,01685	0,00134123	0,0194768
TRDN	clone mix	4,39318	2,88E-006	0,000115199
TRIM63	clone mix	3,61258	0,00018636	0,00386321
TTN	clone mix	5,64727	6,33E-006	0,000225115
TXLNB (1 of 2)	clone mix	4,6162	3,25E-007	1,78E-005
TXLNB (2 of 2)	clone mix	5,16277	1,21E-006	5,52E-005
TYMP	clone mix	-3,9567	0,000999553	0,0153574
UCP1	clone mix	-7,74551	1,09E-007	6,97E-006
UPP2	clone mix	-6,33611	1,24E-005	0,000396673
UROC1	clone mix	-8,00731	8,50E-007	4,07E-005
USP13	clone mix	5,67653	4,49E-007	2,35E-005
USP2	clone mix	3,69078	0,000154815	0,00331004
USP28	clone mix	4,96192	1,36E-006	6,07E-005
VTN (1 of 2)	clone mix	-9,96102	2,06E-009	2,22E-007
VTN (2 of 2)	clone mix	-4,25722	8,86E-009	7,92E-007
XIRP2 (1 of 2)	clone mix	3,63989	7,51E-005	0,00181064
ZFP106 (1 of 2)	clone mix	3,63206	6,70E-005	0,00164672
ACADL	clone XII	1,90467	1,30E-009	1,49E-007
ACE	clone XII	1,22001	0,0025577	0,032646
ACSL4	clone XII	1,51213	0,00169672	0,0235202
ACTN2	clone XII	6,14374	0,000200904	0,00411318
ADAMTS13	clone XII	0,797039	3,60E-007	1,95E-005
ADPRHL1	clone XII	5,29602	0,000216518	0,00437762
ALPK3 (1 of 2)	clone XII	5,03258	0,00176154	0,0242358
ALPK3 (2 of 2)	clone XII	4,49	0,00195363	0,0263343
ANO1 (1 of 2)	clone XII	1,41167	0,00158354	0,0222503
ANXA6	clone XII	3,58389	0,00145263	0,0207619
AVPI1	clone XII	2,65988	0,00373378	0,0440063
BAG3	clone XII	3,88254	0,00277896	0,0348567
BLVRB	clone XII	-1,06469	0,00280186	0,0350824
BMP10 (2 of 2)	clone XII	5,7565	0,000991652	0,015258
CA6 (1 of 2)	clone XII	4,91299	1,17E-006	5,37E-005
CA6 (2 of 2)	clone XII	4,93474	0,000150373	0,00323204
CASQ1 (1 of 2)	clone XII	-5,09569	5,92E-005	0,00148545
CASQ2 (1 of 2)	clone XII	2,7988	0,00031225	0,00592639
CCR9 (1 of 2)	clone XII	3,61821	0,00142329	0,0204245
CCRN4L (1 of 2)	clone XII	4,21047	0,00179793	0,0246392
CKMT2 (1 of 2)	clone XII	2,55885	0,000207135	0,00421821
COL1A1 (2 of 2)	clone XII	-1,17237	7,04E-005	0,00171469
COX6B1 (1 of 2)	clone XII	3,99961	0,00249279	0,0319907
CPO (1 of 2)	clone XII	3,36757	0,00337791	0,0406752
CRIP2 (2 of 2)	clone XII	3,83058	0,00372596	0,0439342
CSRNP1 (1 of 2)	clone XII	3,29314	0,000344783	0,00643374
CSRP3	clone XII	6,64921	0,000953306	0,014776
CYP27B1	clone XII	2,77632	0,000286586	0,00552035

gene	sample_2	log2(fold_change)	p_value	q_value
DDIT4 (1 of 2)	clone XII	5,13059	3,45E-006	0,000134727
DENND4A (2 of 2)	clone XII	4,02434	1,17E-005	0,000377426
ELL (2 of 2)	clone XII	3,14847	0,000483939	0,00850258
ELTD1	clone XII	2,64973	8,27E-005	0,00196096
ENSGACG00000001073	clone XII	5,75389	0,000355838	0,00660242
ENSGACG00000001311	clone XII	-4,17047	0,0041242	0,0475451
ENSGACG00000001522	clone XII	-4,25436	0,00053952	0,00929369
ENSGACG00000003030	clone XII	5,79286	0,00150825	0,021398
ENSGACG00000005023	clone XII	-4,2235	0,000690882	0,0113689
ENSGACG00000005760	clone XII	2,27393	8,93E-005	0,00209134
ENSGACG00000006109	clone XII	4,58495	0,00389729	0,0455018
ENSGACG00000007447	clone XII	1,29747	0,00173823	0,0239772
ENSGACG00000007661	clone XII	7,83442	9,50E-005	0,00220425
ENSGACG00000008053	clone XII	3,26477	0,000614647	0,0103346
ENSGACG00000008055	clone XII	2,90306	0,0014699	0,0209609
ENSGACG00000008064	clone XII	4,14393	0,000476233	0,00839255
ENSGACG00000008242	clone XII	-3,19841	0,00156927	0,0220915
ENSGACG00000009559	clone XII	3,11869	0,00416257	0,0478894
ENSGACG00000009825	clone XII	1,63884	4,68E-007	2,44E-005
ENSGACG00000010050	clone XII	3,63451	4,18E-011	7,08E-009
ENSGACG00000010126	clone XII	6,79735	0,000132529	0,00290846
ENSGACG00000010476	clone XII	5,40943	2,64E-005	0,000754814
ENSGACG00000010623	clone XII	7,30947	0,000218405	0,00440972
ENSGACG00000011845	clone XII	4,5453	0,000459224	0,00814659
ENSGACG00000011846	clone XII	-3,66598	0,00154755	0,0218473
ENSGACG00000012228	clone XII	4,29271	2,65E-005	0,000756896
ENSGACG00000012245	clone XII	3,18824	0,00422023	0,0484099
ENSGACG00000012464	clone XII	3,54413	4,64E-005	0,00120915
ENSGACG00000012654	clone XII	7,71157	6,99E-005	0,00170479
ENSGACG00000012657	clone XII	6,79796	0,000186833	0,00387162
ENSGACG00000012663	clone XII	4,17545	0,00247655	0,0318205
ENSGACG00000013326	clone XII	2,27882	0,00423595	0,0485501
ENSGACG00000013782	clone XII	5,83863	0,000288207	0,00554683
ENSGACG00000014752	clone XII	-3,47107	0,00123559	0,0182374
ENSGACG00000014852	clone XII	5,28503	0,00333253	0,0402405
ENSGACG00000014960	clone XII	7,82835	1,87E-005	0,000565075
ENSGACG00000015110	clone XII	3,481	0,000352268	0,00654712
ENSGACG00000015175	clone XII	2,63764	0,00373337	0,0440022
ENSGACG00000016298	clone XII	2,67699	1,52E-005	0,000473464
ENSGACG00000016813	clone XII	2,17407	6,35E-006	0,000225556
ENSGACG00000018662	clone XII	5,35673	4,25E-006	0,000160752
ENSGACG00000019744	clone XII	7,05129	0,00017644	0,0036912
ENSGACG00000020727	clone XII	4,31392	6,65E-006	0,000234774
ENTPD4	clone XII	1,07019	0,000659864	0,0109496
FAM102B (2 of 2)	clone XII	3,32537	0,00331975	0,0401188
FERMT2	clone XII	1,32919	0,00331657	0,0400882
FHL1 (1 of 2)	clone XII	2,4312	0,00437216	0,0497423
FHL2 (1 of 2)	clone XII	4,21511	0,00235361	0,0305561
FKBP5	clone XII	5,3293	3,14E-005	0,000872874
FLNC (2 of 2)	clone XII	4,67479	0,000596803	0,0100888
FOSL1	clone XII	6,5125	9,47E-007	4,47E-005
GADD45B (1 of 2)	clone XII	2,20549	0,00386086	0,0451694
GZMM (3 of 5)	clone XII	-2,84743	0	0

gene	sample_2	log2(fold_change)	p_value	q_value
HGF (1 of 2)	clone XII	3,89189	0,00333421	0,0402571
HSP90AA1 (2 of 2)	clone XII	5,57397	0,00113414	0,0170196
HSPB1	clone XII	3,4532	0,000223452	0,00449394
HSPB7	clone XII	5,37516	0,000531145	0,00917649
IGFBP1 (1 of 2)	clone XII	5,87281	0,00046516	0,00823314
IRF4 (2 of 2)	clone XII	2,25575	0,000622756	0,0104458
JPH2	clone XII	3,32459	0,00134064	0,0194701
JUNB (1 of 2)	clone XII	2,83099	0,00422861	0,0484831
JUNB (2 of 2)	clone XII	4,51802	1,85E-005	0,000558641
KLF13	clone XII	3,26084	0,00269023	0,0339758
KLF9	clone XII	3,73408	0,000394239	0,00718671
LDB3	clone XII	3,8337	0,00161777	0,0226343
LMOD2 (1 of 2)	clone XII	5,25465	0,00299241	0,0369881
LRCH2	clone XII	1,05445	0,00428167	0,0489486
LRRC10	clone XII	4,99886	0,00169482	0,0234988
LRRFIP1 (1 of 2)	clone XII	1,11668	2,50E-006	0,000102155
MYBPC2 (1 of 2)	clone XII	-3,53404	0,00014781	0,00318601
MYL1	clone XII	-4,26532	0,000338662	0,00633876
MYL7	clone XII	7,1239	0,000123576	0,00274436
MYLK4 (1 of 2)	clone XII	5,95708	0,000782943	0,0125899
MYLK4 (2 of 2)	clone XII	3,76457	0,000976123	0,015064
MYLPF (2 of 2)	clone XII	-3,0921	0,0030704	0,0377321
MYOM1 (1 of 2)	clone XII	4,21035	1,14E-008	9,83E-007
MYOZ2 (1 of 2)	clone XII	5,02413	9,01E-005	0,00210714
NR0B2	clone XII	-3,10311	0,00254404	0,0325081
OBSCN	clone XII	3,1224	0,000261055	0,00511107
PAFAH1B3	clone XII	-0,571056	2,69E-010	3,68E-008
PFKFB3	clone XII	3,07407	0,000609832	0,0102663
PFKM (1 of 2)	clone XII	-4,38725	0,00280291	0,0350929
PIP5K1C (2 of 2)	clone XII	3,94477	0,000274262	0,00532287
PLEKHG5	clone XII	2,028	4,29E-006	0,000162043
PRAM1	clone XII	-2,57198	0,00125151	0,0184265
PROM2	clone XII	3,10851	0,00253599	0,0324275
PVRL1 (2 of 2)	clone XII	-4,35336	0,00377867	0,0444195
RGCC	clone XII	2,47955	0,00392402	0,0457509
RRAD	clone XII	3,7178	0,00109305	0,0165155
SCARF1	clone XII	3,54394	0,000702598	0,0115278
SEMA3A (2 of 2)	clone XII	3,84738	0,000124828	0,0027673
SIK1	clone XII	3,52691	0,000226519	0,00454395
SLC13A2 (1 of 2)	clone XII	4,39743	7,41E-006	0,000257352
SLC1A5	clone XII	3,51114	7,14E-005	0,00173578
SLC25A43	clone XII	2,00662	1,08E-009	1,26E-007
SLC2A9	clone XII	0,575455	0,00261144	0,0331865
SLC41A3 (1 of 2)	clone XII	5,34339	0,00109175	0,0165003
SLC8A1 (2 of 2)	clone XII	7,03531	0,00217029	0,0286471
SMOX	clone XII	5,81048	2,61E-006	0,00010597
SMTNL2	clone XII	3,57082	0,00185121	0,0252328
SNRNP70	clone XII	0,705332	2,72E-006	0,000109908
SOCS3 (1 of 2)	clone XII	6,20923	1,96E-007	1,15E-005
SOCS3 (2 of 2)	clone XII	4,52403	7,45E-005	0,00179809
SORBS2	clone XII	4,05282	0,00120357	0,0178536
SYNPO2L (2 of 2)	clone XII	6,2532	0,000135171	0,00295699
TCAP	clone XII	4,51621	7,74E-005	0,00185575

gene	sample_2	log2(fold_change)	p_value	q_value
THBS1 (2 of 2)	clone XII	2,7921	0,00139455	0,0200972
TJP1 (1 of 2)	clone XII	2,10649	0,00335018	0,0404128
TNNC1	clone XII	8,53184	2,09E-006	8,77E-005
TNNC2 (1 of 2)	clone XII	-3,43356	0,00206096	0,0274915
TNNI2 (1 of 5)	clone XII	-4,43371	0,000839432	0,0133171
TNNI2 (3 of 5)	clone XII	-4,21155	0,00032296	0,00609449
TNNT2 (1 of 2)	clone XII	7,51055	5,15E-005	0,00132201
TPM2	clone XII	-1,23705	4,44E-016	2,06E-013
UROS	clone XII	-1,20225	0,00202598	0,0271208
ZC3HAV1	clone XII	-0,707299	0,00264566	0,0335286

Supplementary table S.2.3 Cufflinks output, list of differentially expressed genes in gill tissue of three-spined sticklebacks. Differentially expressed is defined by comparison to uninfected controls. The term "gene" is the name for a specific gene as taken from the *G. aculeatus* reference genome, "sample_2" is the infection treatment group, log2(fold change) displays the transformed fold change in "sample_2" compared to control, p value and q value are given for each test (only significant differences shown).

gene	sample_2	log2(fold_change)	p_value	q_value
ACE	clone I	1,1921	6,35E-006	0,00022556
ADPRHL1	clone I	3,4272	0,0039553	0,0460285
AOC2	clone I	1,56223	0,0019519	0,0263151
ARRDC2	clone I	2,45006	1,32E-007	8,25E-006
ASL	clone I	-0,635794	0,0029484	0,0365495
BTBD10 (1 of 2)	clone I	-0,3405	0,0013549	0,0196386
C4A	clone I	0,753185	0,0013315	0,0193631
CANT1 (1 of 2)	clone I	-0,659822	0,0032816	0,0397541
CASP3 (4 of 4)	clone I	-0,73709	0,0001404	0,00305316
CCR9 (1 of 2)	clone I	1,47913	0,0003232	0,00609843
CDCP1 (1 of 3),CDCP1 (3 of 3)	clone I	-0,897406	0,0035536	0,0423252
CEBPB	clone I	1,90909	1,93E-005	0,00057973
CEBPD	clone I	1,52203	0,0014414	0,0206331
CKMT1A	clone I	0,96786	0,0010129	0,0155223
COL11A1 (2 of 2)	clone I	1,83854	0,0012542	0,0184586
COL1A1 (2 of 2)	clone I	0,701278	0,001486	0,0211432
CYP1B1	clone I	1,29966	0,0037904	0,0445283
DDIT4 (1 of 2)	clone I	3,48533	2,11E-011	3,84E-009
DIO3	clone I	2,30949	0,0024666	0,0317198
DYNLL1	clone I	-0,742202	1,82E-005	0,00055031
EHF	clone I	-0,774701	0,0001261	0,00279071
EIF4G2 (1 of 2)	clone I	0,396751	0,0036589	0,0433112
ENSGACG00000000208	clone I	2,99665	0,0006386	0,0106607
ENSGACG00000000614	clone I	2,07415	8,88E-016	3,93E-013
ENSGACG00000000849	clone I	3,19785	0,0007687	0,0124025
ENSGACG00000001127	clone I	1,80E+308	4,47E-006	0,00016756
ENSGACG00000001198	clone I	4,37351	0,0013312	0,0193595
ENSGACG00000001671	clone I	-2,99591	0,0004994	0,00872448
ENSGACG00000001749	clone I	2,91183	0,0001453	0,00314077
ENSGACG00000001763	clone I	3,13646	1,34E-006	6,00E-005
ENSGACG00000002902	clone I	3,30513	9,37E-007	4,43E-005
ENSGACG00000002933	clone I	3,55921	5,28E-008	3,72E-006
ENSGACG00000002955	clone I	3,71769	0	0
ENSGACG00000003003	clone I	3,44935	2,13E-009	2,28E-007
ENSGACG00000003420	clone I	-1,32249	0,0009942	0,0152893
ENSGACG00000003503	clone I	-2,25998	2,00E-005	0,00059715
ENSGACG00000003612,STK35 (1 of 2)	clone I	1,61227	5,53E-005	0,00140301
ENSGACG00000004079	clone I	3,52026	2,40E-006	9,88E-005
ENSGACG00000004200	clone I	3,87245	1,46E-008	1,22E-006
ENSGACG00000004247	clone I	1,80E+308	0,0004547	0,00807937
ENSGACG00000005904	clone I	1,82422	0,0004744	0,00836619
ENSGACG00000006044	clone I	3,1804	8,68E-006	0,00029408
ENSGACG00000006048	clone I	2,33507	0,0003743	0,00688626

gene	sample_2	log2(fold_change)	p_value	q_value
ENSGACG00000006109	clone I	3,44969	1,34E-006	6,01E-005
ENSGACG00000007447	clone I	-1,93989	2,89E-007	1,62E-005
ENSGACG00000007449	clone I	-2,20367	2,41E-005	0,00069822
ENSGACG00000007454	clone I	-1,46359	0,0028336	0,0354025
ENSGACG00000007661	clone I	3,90263	1,23E-007	7,75E-006
ENSGACG00000008353	clone I	1,60309	0,0012893	0,0188717
ENSGACG00000009409	clone I	2,56142	0,0007044	0,0115523
ENSGACG00000009417	clone I	1,5094	0,0014299	0,0204997
ENSGACG00000010050	clone I	1,44926	7,10E-006	0,00024826
ENSGACG00000010476	clone I	3,28382	6,72E-011	1,08E-008
ENSGACG00000010501	clone I	-1,13185	1,60E-006	6,99E-005
ENSGACG00000010623	clone I	7,62581	1,24E-009	1,42E-007
ENSGACG00000011767	clone I	2,98067	0,0039993	0,0464266
ENSGACG00000012654	clone I	1,80E+308	1,31E-006	5,90E-005
ENSGACG00000012657	clone I	6,35163	2,55E-009	2,67E-007
ENSGACG00000012962	clone I	5,7337	5,02E-005	0,00129382
ENSGACG00000013327	clone I	2,9605	0,0001526	0,00327103
ENSGACG00000014948	clone I	5,92349	1,70E-009	1,87E-007
ENSGACG00000015897	clone I	-0,466343	0	0
ENSGACG00000016379	clone I	1,00841	0,0015657	0,0220528
ENSGACG00000017093	clone I	0,574976	0,0014511	0,020743
ENSGACG00000018049	clone I	5,07397	0,0001475	0,00318105
ENSGACG00000018557,ENSGACG0000 0018560	clone I	0,799344	4,78E-008	3,41E-006
ENSGACG00000018802	clone I	1,93948	1,75E-005	0,00053396
ENSGACG00000018840	clone I	2,13567	9,12E-007	4,32E-005
ENSGACG00000018993	clone I	-1,45868	0,0005551	0,00950987
ENSGACG00000019023	clone I	0,453711	0,0004694	0,00829426
ENSGACG00000019252	clone I	1,31814	0,0025604	0,0326731
ENSGACG00000019744	clone I	1,21389	0,0004952	0,00866407
ENSGACG00000019952	clone I	1,52714	0,0029961	0,0370231
ENSGACG00000020145	clone I	2,47328	3,48E-006	0,00013543
ENSGACG00000020181	clone I	2,33056	2,60E-006	0,00010583
ENTPD1	clone I	0,405147	0,0007548	0,0122171
EPHA2 (1 of 2)	clone I	-0,411225	0,001256	0,0184807
F11R	clone I	-0,595993	0,0003122	0,00592568
FCGBP (1 of 2)	clone I	0,955827	0,0025933	0,0330062
FKBP5	clone I	4,09051	8,91E-012	1,78E-009
FLNC (2 of 2)	clone I	1,41296	2,37E-007	1,36E-005
FZD1	clone I	-1,33523	0,0041212	0,0475193
GADD45B (1 of 2)	clone I	1,28745	0,0004489	0,00799541
GATA2 (1 of 2)	clone I	-0,779088	5,02E-005	0,00129381
GCNT1	clone I	7,07117	5,00E-006	0,00018451
IDH1	clone I	-0,515671	0,0037348	0,0440147
KLF13	clone I	1,80E+308	0,0003868	0,00707433
KLF9	clone I	2,76989	9,27E-007	4,39E-005
MYBPC1	clone I	0,488438	2,61E-005	0,00074664
MYL7	clone I	7,97234	2,87E-010	3,91E-008
MYOM1 (1 of 2)	clone I	0,958314	0,0016399	0,0228865
NCOA7 (2 of 2)	clone I	-1,51921	0,0010537	0,0160297
NDUFS8 (2 of 2)	clone I	-0,314304	1,67E-005	0,00051148
NEB	clone I	0,579602	0,0002232	0,00448927
NFKBIA (1 of 2)	clone I	1,3429	0,000867	0,0136703

gene	sample_2	log2(fold_change)	p_value	q_value
NR1D2 (2 of 2)	clone I	2,57249	5,92E-009	5,57E-007
PAQR5	clone I	-0,621558	9,69E-005	0,00224123
PCTP	clone I	-0,490294	0,0001559	0,00332977
PDGFRA	clone I	1,0041	0,0006473	0,0107791
PIK3R1 (1 of 2)	clone I	1,22818	0,0001446	0,00312788
PNISR	clone I	0,665106	0,0008837	0,0138853
PPP1R15B	clone I	1,46665	0,0005836	0,00990473
RGS13 (2 of 2)	clone I	1,37077	0,0041918	0,0481519
SELE	clone I	1,76081	0,0008449	0,0133884
SLC25A43	clone I	0,915771	2,02E-005	0,00060263
SLC7A8	clone I	0,837094	0,0002611	0,00511129
SLC8A1 (2 of 2)	clone I	1,80E+308	0,0002751	0,00533715
SLCO2A1	clone I	1,43784	0,003383	0,0407239
SMOX	clone I	1,71728	2,47E-006	0,00010113
SOCS3 (1 of 2)	clone I	2,58154	5,22E-008	3,68E-006
SULT1E1	clone I	-0,374183	0,0004212	0,00758966
SULT6B1	clone I	-0,314315	2,67E-006	0,00010815
TG	clone I	2,06179	0,000914	0,0142743
THBS1 (2 of 2)	clone I	2,42189	1,00E-005	0,00033216
TIPRL	clone I	-0,370412	0,0009819	0,0151353
TNNC1	clone I	4,90297	3,81E-007	2,05E-005
TNNT2 (1 of 2)	clone I	5,24213	2,41E-008	1,89E-006
TSC22D3	clone I	2,18233	7,18E-006	0,00025055
TUFT1 (2 of 2)	clone I	0,905713	0,0004328	0,00776063
UBTD1 (2 of 2)	clone I	-0,9526	0,0002083	0,00423736
VWA1 (2 of 2)	clone I	-0,915985	1,10E-006	5,08E-005
ZFP36	clone I	1,56034	0,0007207	0,0117672
AADACL2	clone mix	-2,98837	4,28E-005	0,00113186
AARSD1	clone mix	-0,59341	0,002518	0,0322484
AASS	clone mix	1,3189	0,0023446	0,030466
ABCA1 (1 of 2)	clone mix	1,52269	0,0006071	0,0102301
ABCA1 (2 of 2)	clone mix	1,30216	0,0019408	0,0262009
ABI3BP	clone mix	2,08093	4,43E-007	2,32E-005
ABL2	clone mix	1,87075	1,78E-011	3,30E-009
ABR	clone mix	1,75035	2,50E-007	1,42E-005
ACAP1	clone mix	0,958463	5,40E-006	0,00019669
ACE	clone mix	2,25916	5,63E-009	5,34E-007
ACIN1	clone mix	1,25957	0,0013703	0,0198171
ACP1	clone mix	-1,40044	2,88E-008	2,21E-006
ACSL4	clone mix	1,25529	3,27E-007	1,79E-005
ACTA2	clone mix	2,0432	3,58E-005	0,00097342
ACTN2	clone mix	1,44252	0,0018249	0,0249441
ADAM19	clone mix	1,95255	0,0015112	0,0214318
ADAM8 (1 of 2)	clone mix	2,98115	3,05E-006	0,00012121
ADAMTS1	clone mix	1,32818	0,0042872	0,0489981
ADAMTS15 (2 of 2)	clone mix	2,07367	0,0021221	0,0281435
ADAMTS2	clone mix	1,6736	0,0005097	0,00887006
ADAMTSL4	clone mix	1,76124	0,0010944	0,0165317
AEBP1 (2 of 2)	clone mix	1,7704	2,36E-006	9,75E-005
AEBP2 (1 of 2),NDUFA5	clone mix	-1,25317	0,0007667	0,0123764
AFF4	clone mix	1,31134	0,001311	0,0191269
AK1	clone mix	-0,831149	0,001669	0,023212
AKAP11	clone mix	1,82963	1,42E-005	0,00044515

gene	sample_2	log2(fold_change)	p_value	q_value
AKAP13 (1 of 2)	clone mix	1,42365	0,0021055	0,0279672
AKAP13 (2 of 2)	clone mix	1,1726	0,0039878	0,046319
AKAP9	clone mix	1,23942	0,0017438	0,0240392
ALDH18A1 (1 of 2)	clone mix	0,66589	7,56E-006	0,00026166
ALDH1A2	clone mix	1,72314	1,82E-005	0,00055187
ALDH3B2	clone mix	1,45525	0,0003354	0,00628831
AMD1	clone mix	1,66411	0,0001273	0,00281343
AMPD3 (1 of 2)	clone mix	1,29514	1,34E-005	0,0004237
ANAPC16	clone mix	-1,53253	0,000208	0,00423315
ANGPTL2 (1 of 2)	clone mix	1,9765	0,0001468	0,00316686
ANGPTL2 (2 of 2)	clone mix	1,90234	0,001554	0,0219183
ANK3 (2 of 2)	clone mix	1,20681	0,0007019	0,0115186
ANKIB1	clone mix	1,84547	0,0001712	0,00360075
ANKRD11	clone mix	1,51751	0,0003192	0,00603549
ANO5 (2 of 2)	clone mix	1,52788	0,0005233	0,00906498
ANXA9	clone mix	-0,764217	5,63E-005	0,00142251
AOC2	clone mix	1,4928	0,00195	0,0262965
AP3D1	clone mix	1,21533	0,0039849	0,0462933
APPL2	clone mix	1,38412	0,0030678	0,0377067
ARHGAP21 (1 of 2)	clone mix	2,23518	3,95E-007	2,11E-005
ARHGAP24	clone mix	1,66713	0,0010807	0,0163628
ARHGAP29 (1 of 2)	clone mix	2,11859	5,56E-006	0,00020156
ARHGAP31	clone mix	2,10044	0,0012889	0,018867
ARHGAP40	clone mix	1,7626	0,0019038	0,0258016
ARHGAP6 (1 of 2)	clone mix	2,12721	0,0005658	0,00965918
ARHGEF11	clone mix	1,51459	0,0004812	0,00846367
ARHGEF17	clone mix	1,91161	0,0002196	0,00442999
ARHGEF26	clone mix	1,92709	0,0001727	0,00362646
ARID3A	clone mix	1,96505	3,86E-005	0,00103608
ARMC9	clone mix	1,64028	0,0004663	0,00825012
ARPC3	clone mix	-1,56115	0,0008984	0,0140731
ARPC4 (1 of 2)	clone mix	-1,48982	0,0008356	0,0132671
ARRDC2	clone mix	3,04941	2,11E-009	2,27E-007
ARVCF (1 of 2)	clone mix	1,84461	0,0002084	0,00424003
ASB2 (2 of 2)	clone mix	2,09231	0,0013435	0,0195048
ASB5	clone mix	2,09855	0,0001984	0,00407092
ASH1L	clone mix	1,1791	0,0030482	0,0375235
ASL	clone mix	-0,811455	5,28E-005	0,00134837
ASPN	clone mix	1,93933	0,0004179	0,00753915
ATG12	clone mix	-1,64264	0,0008327	0,0132286
ATP11C (2 of 2)	clone mix	1,25457	0,0016847	0,0233861
ATP13A3 (2 of 2)	clone mix	1,50644	0,0006143	0,0103301
ATP2A3	clone mix	1,24846	9,57E-007	4,51E-005
ATP2B4	clone mix	1,27099	0,0011649	0,0173922
ATP5J (1 of 2)	clone mix	-1,5082	0,0002848	0,00549194
ATP5O	clone mix	-1,52446	0,0042898	0,0490203
ATP8A1	clone mix	1,4227	0,0021857	0,0288037
B3GNT2	clone mix	2,32016	1,19E-005	0,00038341
BAG6 (1 of 2)	clone mix	1,0888	6,30E-006	0,00022415
BANF1	clone mix	-1,26732	0,0012015	0,0178286
BAZ2B	clone mix	1,67987	0,0003591	0,00665285
BCKDK	clone mix	0,590005	0,0030646	0,0376763
BCL9	clone mix	1,24393	0,0030697	0,0377251

gene	sample_2	log2(fold_change)	p_value	q_value
BCR (2 of 2)	clone mix	2,80207	1,27E-008	1,08E-006
BDH1	clone mix	1,22457	0,0025397	0,0324632
BICC1	clone mix	3,324	0,001689	0,023434
BIRC6	clone mix	0,978342	0,0005279	0,00912954
BLOC1S1	clone mix	-1,53113	0,0003052	0,00581429
BLVRB	clone mix	-0,772047	0,0009066	0,0141797
BMP1 (1 of 2)	clone mix	1,86276	3,08E-008	2,34E-006
BMPR2 (2 of 2)	clone mix	2,24372	0,0010162	0,0155629
BNIP1 (2 of 2)	clone mix	-1,32529	0,000901	0,014108
BOLA2	clone mix	-1,9282	0,0022006	0,0289595
BPNT1	clone mix	-0,600952	0,0006718	0,0111102
BRD1 (1 of 2)	clone mix	1,27229	3,61E-005	0,00097983
BRD2 (2 of 2)	clone mix	0,547968	0,0030335	0,0373808
BRD4	clone mix	1,1501	0,0031591	0,0385822
BTBD11 (1 of 2)	clone mix	1,32313	0,0031814	0,0387973
C14orf43 (2 of 2)	clone mix	2,07717	0,0001781	0,00372116
C14orf49	clone mix	1,27862	0,0006186	0,010388
C15orf57	clone mix	-0,891323	0,001932	0,0261065
C17orf61	clone mix	-1,5594	0,0003653	0,00674895
C19orf42	clone mix	-1,91338	0,0003903	0,00712739
C19orf53	clone mix	-1,38243	0,0037248	0,0439236
C1D	clone mix	-1,51477	0,003372	0,040617
C1orf116 (2 of 2)	clone mix	1,41683	0,0014907	0,0211973
C1orf31	clone mix	-1,38673	5,90E-005	0,00148057
C1orf51	clone mix	1,28825	0,0027556	0,0346259
C20orf194	clone mix	1,52852	0,0003874	0,00708348
C2orf40	clone mix	-1,51566	0,0041296	0,047595
C3 (6 of 8)	clone mix	1,25104	0,002269	0,029674
C3 (8 of 8)	clone mix	1,32199	0,0024086	0,0311274
C4A	clone mix	1,35585	0	0
C5orf43	clone mix	-1,19142	0,0021476	0,0284117
C6orf162	clone mix	-1,74666	0,0006626	0,0109863
C7 (2 of 2)	clone mix	1,59683	0,0001389	0,00302433
C7orf58	clone mix	1,37379	0,002064	0,027523
C7orf59	clone mix	-1,60346	3,44E-007	1,87E-005
C8orf59	clone mix	-1,85349	2,33E-006	9,64E-005
CABP5 (1 of 2)	clone mix	-5,73117	7,02E-007	3,46E-005
CAD	clone mix	1,05303	0,0025778	0,0328518
CALB2 (1 of 2)	clone mix	1,32122	0,0007421	0,0120503
CAMK1D (2 of 2)	clone mix	1,87079	0,0009895	0,0152318
CAMSAP2 (2 of 2)	clone mix	1,55046	0,0004149	0,00749462
CBX7 (2 of 2)	clone mix	1,49522	3,13E-005	0,0008689
CCBL1	clone mix	-0,671809	0,0031114	0,0381177
CCDC136 (1 of 2)	clone mix	3,12127	0,0017312	0,0239002
CCDC142	clone mix	1,15358	0,003731	0,0439816
CCDC72	clone mix	-1,58516	0,000122	0,00271532
CCDC80	clone mix	1,69627	0,000137	0,00298962
CCDC88C	clone mix	1,9504	0,0002248	0,00451625
CCNL1	clone mix	1,81294	7,22E-006	0,00025158
CCR9 (1 of 2)	clone mix	2,04877	5,43E-006	0,00019772
CCRN4L (1 of 2)	clone mix	2,80429	0,0002419	0,00479778
CD44	clone mix	1,62775	0,0001367	0,00298531
CDC14A (1 of 2)	clone mix	1,45073	0,0021572	0,0285113

gene	sample_2	log2(fold_change)	p_value	q_value
CDC42BPA	clone mix	1,32674	0,0015615	0,0220029
CDC42BPB	clone mix	1,18225	0,0007697	0,0124155
CDH11	clone mix	1,67931	0,0013827	0,0199588
CDH2 (1 of 2)	clone mix	1,69706	0,0019493	0,0262896
CDH5	clone mix	2,74703	4,16E-005	0,00110307
CEBPB	clone mix	2,95348	1,07E-010	1,63E-008
CELSR1	clone mix	1,75518	9,25E-005	0,00215477
CEND1	clone mix	-3,63043	0,0009381	0,0145841
CEP290	clone mix	2,02226	1,84E-005	0,00055671
CEP350	clone mix	1,37425	0,0003101	0,00589262
CETN3	clone mix	-1,4934	0,0015079	0,0213943
CGN (1 of 2)	clone mix	1,53293	0,0030707	0,0377352
CGNL1 (2 of 2)	clone mix	1,21401	0,0021746	0,0286897
CHCHD3 (2 of 2)	clone mix	1,03769	0,0015881	0,0223008
CHD3	clone mix	1,29535	0,0022629	0,0296077
CHD6	clone mix	1,3929	0,001017	0,0155732
CHD7	clone mix	1,20302	0,0024108	0,0311509
CHD8	clone mix	1,33526	0,0008148	0,0129988
CHGA	clone mix	1,16189	5,19E-005	0,00132987
CHL1 (1 of 2)	clone mix	1,91678	0,0027501	0,0345705
CHUK (1 of 2)	clone mix	0,859719	0,0002005	0,00410642
CIB1	clone mix	-1,14907	0,0039682	0,046144
CIC	clone mix	1,1916	0,0033414	0,0403279
CILP	clone mix	2,00354	0,0001957	0,00402452
CILP2	clone mix	3,13319	8,03E-007	3,88E-005
CISD3	clone mix	-1,07269	0,0002346	0,00467989
CKAP5	clone mix	1,10485	0,0037318	0,0439883
CKLF-CMTM1	clone mix	-1,35474	0,0042537	0,0487036
CLASP1 (1 of 2)	clone mix	2,03853	2,26E-005	0,00066044
CLASP2 (2 of 2)	clone mix	1,14394	0,0038008	0,0446195
CLDND1 (1 of 2)	clone mix	-1,14499	0,0026332	0,0334035
CLIC4	clone mix	2,538	3,24E-005	0,00089487
CLIP1 (1 of 2)	clone mix	1,06631	8,60E-009	7,72E-007
CLOCK	clone mix	1,31004	0,0025045	0,032108
CMIP	clone mix	1,25969	0,0022725	0,0297099
CNOT1	clone mix	1,03835	8,25E-007	3,97E-005
CNOT6	clone mix	1,24806	0,0038592	0,0451534
CNTN1 (1 of 2)	clone mix	2,52834	0,0002009	0,00411353
COL11A1 (2 of 2)	clone mix	2,93957	4,66E-009	4,52E-007
COL11A2	clone mix	2,2861	0,0001103	0,00249726
COL12A1 (1 of 2)	clone mix	1,85752	6,23E-006	0,0002222
COL12A1 (2 of 2)	clone mix	3,23831	2,18E-008	1,73E-006
COL15A1 (2 of 2)	clone mix	2,07771	0,0011376	0,0170612
COL16A1	clone mix	1,65595	4,13E-005	0,00109848
COL17A1 (1 of 2)	clone mix	1,14789	0,0039951	0,0463873
COL18A1 (2 of 2)	clone mix	1,39338	0,0014081	0,0202524
COL1A1 (2 of 2)	clone mix	1,37493	0	0
COL1A2	clone mix	1,9136	0,0001348	0,00295102
COL21A1	clone mix	1,53154	0,0027804	0,0348698
COL22A1	clone mix	2,56056	0,0001851	0,00384195
COL24A1	clone mix	1,27581	0,0022324	0,0292921
COL2A1 (1 of 2)	clone mix	1,77377	2,99E-005	0,00083738
COL4A1	clone mix	2,14359	3,84E-007	2,06E-005

gene	sample_2	log2(fold_change)	p_value	q_value
COL4A2	clone mix	1,84043	0,0004332	0,00776733
COL5A1	clone mix	1,9487	3,05E-006	0,00012111
COL5A2 (2 of 2)	clone mix	1,78346	0,0001601	0,00340433
COL5A3 (2 of 2)	clone mix	1,22147	0,0036237	0,0429831
COL6A1	clone mix	2,11634	6,00E-007	3,02E-005
COL6A2 (1 of 2)	clone mix	1,7478	2,04E-005	0,00060588
COL6A2 (2 of 2)	clone mix	1,62342	9,09E-005	0,00212345
COL6A3	clone mix	1,90043	1,39E-006	6,20E-005
COL6A6	clone mix	2,08236	1,32E-007	8,23E-006
COL7A1	clone mix	1,89201	8,70E-005	0,00204626
COL8A1 (1 of 2)	clone mix	1,76592	9,42E-005	0,00218682
COL8A2	clone mix	2,43965	4,58E-006	0,00017115
COLEC12 (2 of 2)	clone mix	1,94117	1,45E-005	0,00045485
COQ5	clone mix	-0,779522	0,000308	0,00585994
CORT	clone mix	-1,35618	0,0011724	0,0174825
COX7A2L	clone mix	-1,29134	0,001165	0,0173934
COX7C	clone mix	-2,01274	6,34E-007	3,17E-005
CREM	clone mix	1,57504	0,0009259	0,0144277
CRIPT	clone mix	-2,09269	6,43E-008	4,42E-006
CRLF1 (1 of 2)	clone mix	1,48172	0,0019984	0,0268244
CSNK1E (2 of 2)	clone mix	0,968664	3,22E-005	0,00089026
CSRNP1 (1 of 2)	clone mix	2,24237	5,96E-005	0,00149236
CSTA	clone mix	-1,88151	8,35E-006	0,00028449
CTBS	clone mix	-0,866002	9,03E-005	0,00211097
CTDSP1 (2 of 2)	clone mix	-0,853645	0,0003707	0,00683144
CXCL12 (2 of 2)	clone mix	1,0789	9,29E-006	0,00031148
CYP1B1	clone mix	2,72572	1,47E-008	1,23E-006
CYP26C1	clone mix	1,00656	0,0010326	0,0157686
CYP8B1	clone mix	1,47458	0,0022543	0,0295232
CYR61 (1 of 2)	clone mix	1,67213	7,69E-005	0,00184566
CYSLTR2	clone mix	1,51573	0,0025911	0,0329859
CYTH1 (1 of 2)	clone mix	1,20359	0,0029611	0,0366755
DAAM2	clone mix	1,59988	0,000434	0,00777921
DAB2	clone mix	2,01014	1,47E-008	1,23E-006
DAB2IP (1 of 2)	clone mix	1,32247	0,0012189	0,0180352
DAPK3	clone mix	1,28045	0,0043102	0,0492014
DAXX	clone mix	1,22873	0,0014052	0,0202195
DBI	clone mix	-1,55595	4,17E-011	7,06E-009
DCTN1 (2 of 2)	clone mix	0,695912	7,00E-007	3,45E-005
DCUN1D1	clone mix	-1,16085	0,0038463	0,0450365
DDIT4 (1 of 2)	clone mix	4,05636	1,98E-012	4,62E-010
DDX17 (1 of 3)	clone mix	1,34867	0,0020182	0,0270368
DENND2A (1 of 2)	clone mix	2,22538	0,0007434	0,0120666
DENND4A (2 of 2)	clone mix	4,69472	2,58E-011	4,59E-009
DHRS13 (1 of 3)	clone mix	-1,75812	5,00E-009	4,82E-007
DHTKD1	clone mix	1,09472	0,0019956	0,0267956
DIO3	clone mix	3,56329	1,02E-006	4,78E-005
DIP2B (1 of 2)	clone mix	1,64535	3,60E-005	0,0009774
DISP1	clone mix	1,49972	0,0014143	0,0203225
DLC1	clone mix	1,68455	0,0001073	0,00243964
DMD	clone mix	1,73201	2,65E-005	0,00075568
DMXL1	clone mix	1,33795	0,0006663	0,0110367
DMXL2	clone mix	1,30181	0,0019628	0,0264377

gene	sample_2	log2(fold_change)	p_value	q_value
DNAJC19	clone mix	-1,43261	0,0003223	0,00608485
DOCK10	clone mix	1,84711	4,62E-005	0,00120544
DOCK7	clone mix	1,56731	1,96E-009	2,12E-007
DOCK9 (1 of 2)	clone mix	1,44453	0,0002278	0,00456492
DOCK9 (2 of 2)	clone mix	1,45696	0,0006764	0,0111734
DOHH	clone mix	-1,04709	0,0015041	0,0213506
DPP7	clone mix	-0,800988	1,38E-010	2,04E-008
DPY30	clone mix	-1,78084	6,24E-005	0,00155013
DPYSL3	clone mix	2,11697	1,74E-005	0,00053074
DSC1	clone mix	1,4832	0,0014108	0,0202821
DST	clone mix	1,45994	6,00E-005	0,0015017
DUSP1	clone mix	1,92831	1,03E-005	0,00034032
DUSP5	clone mix	1,70009	9,64E-006	0,0003213
DUSP6	clone mix	2,71669	1,59E-007	9,66E-006
DUSP8	clone mix	2,04736	0,0020838	0,0277343
DYNLL1	clone mix	-2,20238	0	0
DYSF	clone mix	1,98601	0,000105	0,00239565
EBF3	clone mix	2,92109	2,07E-006	8,70E-005
ECM1	clone mix	1,54263	0,0029042	0,0361131
EDN2	clone mix	2,05346	0,0004538	0,00806777
EDNRA	clone mix	2,07892	6,49E-005	0,00160279
EFEMP2	clone mix	1,40916	0,001116	0,0167989
EGFR (1 of 2)	clone mix	1,38865	0,0003842	0,00703663
EGR1	clone mix	1,48617	0,0004036	0,00732797
EHD2 (1 of 2)	clone mix	2,06954	5,40E-006	0,00019675
EIF2AK3	clone mix	1,3932	0,0024091	0,0311335
EIF4G1 (2 of 2),FAM131A	clone mix	1,21872	0,0014755	0,021025
EIF4G3	clone mix	1,40106	0,0009831	0,0151505
ELK3	clone mix	1,25907	0,0034718	0,0415523
ELL (2 of 2)	clone mix	1,97803	0,0019199	0,0259727
ELL2	clone mix	0,68472	0,004177	0,0480197
ELL3 (1 of 2)	clone mix	1,4065	0,0003478	0,00647922
ELMOD2	clone mix	-1,06397	8,26E-010	9,94E-008
ELTD1	clone mix	1,35819	0,0014774	0,0210465
EMILIN2 (2 of 2)	clone mix	1,44294	0,0003236	0,00610372
ENSGACG00000000026	clone mix	2,28847	2,48E-005	0,00071627
ENSGACG00000000063	clone mix	1,85273	9,41E-005	0,00218509
ENSGACG00000000208	clone mix	3,57764	2,01E-005	0,00059826
ENSGACG00000000234,SULF2 (2 of 2)	clone mix	1,14983	0,0037429	0,0440886
ENSGACG00000000272	clone mix	1,35607	0,0010944	0,0165313
ENSGACG00000000300	clone mix	1,71123	0,000683	0,0112614
ENSGACG00000000336	clone mix	-0,723854	7,66E-005	0,00183993
ENSGACG00000000350	clone mix	-0,786931	0,0005159	0,00895946
ENSGACG00000000424	clone mix	-1,88833	0,0001249	0,00276941
ENSGACG00000000454	clone mix	-1,02347	8,17E-005	0,00194183
ENSGACG00000000849	clone mix	3,75332	5,26E-005	0,00134414
ENSGACG00000000989	clone mix	1,28943	0,000996	0,0153126
ENSGACG00000001072	clone mix	-1,25306	0,0015349	0,0217041
ENSGACG00000001172	clone mix	2,6896	0,0002327	0,00464711
ENSGACG00000001189	clone mix	-1,38062	0,0006639	0,0110042
ENSGACG00000001192	clone mix	1,21734	0,0033449	0,0403607
ENSGACG00000001319	clone mix	-1,46014	0,0003227	0,006091
ENSGACG00000001322	clone mix	-1,24313	0,0012484	0,0183904

gene	sample_2	log2(fold_change)	p_value	q_value
ENSGACG00000001373	clone mix	1,54372	0,0021236	0,028159
ENSGACG00000001460	clone mix	-1,68906	9,95E-006	0,0003302
ENSGACG00000001482	clone mix	-1,80E+308	0,0029358	0,0364263
ENSGACG00000001633	clone mix	-1,46904	0,0003363	0,00630341
ENSGACG00000001671	clone mix	-5,05472	8,61E-005	0,00202884
ENSGACG00000001749	clone mix	3,5425	1,90E-006	8,07E-005
ENSGACG00000001804	clone mix	-1,39224	0,0012648	0,0185834
ENSGACG00000001847	clone mix	-2,70142	1,25E-005	0,00039955
ENSGACG00000001919	clone mix	1,41213	0,0002523	0,00497016
ENSGACG00000002069	clone mix	-1,18715	9,14E-006	0,00030728
ENSGACG00000002123	clone mix	1,16484	0,0039318	0,0458199
ENSGACG00000002145	clone mix	2,3253	9,80E-008	6,36E-006
ENSGACG00000002153	clone mix	1,84736	0,0007793	0,0125423
ENSGACG00000002176	clone mix	1,2873	0,0030517	0,0375576
ENSGACG00000002243	clone mix	1,18819	1,24E-005	0,00039679
ENSGACG00000002354	clone mix	1,20796	2,74E-005	0,00077838
ENSGACG00000002748	clone mix	-1,18438	0,0020478	0,0273518
ENSGACG00000002918	clone mix	-4,25874	3,99E-006	0,00015215
ENSGACG00000002933	clone mix	1,80582	0,0039765	0,0462178
ENSGACG00000002952	clone mix	1,4924	0,0002654	0,00517984
ENSGACG00000003003	clone mix	1,83449	3,26E-007	1,79E-005
ENSGACG00000003019	clone mix	-1,5608	0,0004137	0,00747783
ENSGACG00000003132	clone mix	2,19703	5,17E-005	0,00132523
ENSGACG00000003234	clone mix	1,42018	0,0025513	0,0325793
ENSGACG00000003241	clone mix	-1,34058	0,0041588	0,0478573
ENSGACG00000003347	clone mix	0,945187	0,0038002	0,0446145
ENSGACG00000003404	clone mix	1,70974	4,46E-005	0,00117156
ENSGACG00000003405	clone mix	1,6694	0,0002859	0,00550988
ENSGACG00000003407	clone mix	1,90396	5,02E-006	0,0001849
ENSGACG00000003464	clone mix	1,09714	0,0027833	0,0348996
ENSGACG00000003503	clone mix	-2,70709	2,34E-007	1,35E-005
ENSGACG00000003835	clone mix	1,16495	0,0036875	0,0435802
ENSGACG00000003971	clone mix	1,986	4,19E-005	0,00111065
ENSGACG00000004060	clone mix	-1,1607	0,00189	0,0256546
ENSGACG00000004079	clone mix	2,18103	0,0007277	0,0118608
ENSGACG00000004139	clone mix	1,23773	0,0011242	0,016898
ENSGACG00000004200	clone mix	2,41456	8,48E-006	0,00028821
ENSGACG00000004211	clone mix	1,56138	0,0018495	0,0252152
ENSGACG00000004248	clone mix	1,15505	0,0040202	0,0466126
ENSGACG00000004599	clone mix	1,80E+308	0,0018689	0,0254236
ENSGACG00000004652	clone mix	-1,49589	0,0025749	0,0328235
ENSGACG00000004694	clone mix	-1,72877	0,0006867	0,0113122
ENSGACG00000004701	clone mix	-1,69121	0,0011055	0,0166689
ENSGACG00000004703	clone mix	-1,81915	0,0001009	0,00231751
ENSGACG00000004731	clone mix	1,01595	0,000272	0,00528624
ENSGACG00000004818	clone mix	-1,49542	0,0003691	0,00680708
ENSGACG00000005133	clone mix	-0,921689	0,0004189	0,00755459
ENSGACG00000005228	clone mix	1,29179	0,0030181	0,0372307
ENSGACG00000005363	clone mix	1,54865	0,0008259	0,0131404
ENSGACG00000005541	clone mix	1,36795	0,0014103	0,0202769
ENSGACG00000005569	clone mix	2,43577	9,19E-006	0,00030871
ENSGACG00000005736,SDC3	clone mix	1,39309	1,07E-005	0,00035122
ENSGACG00000005767	clone mix	1,34352	0,0007385	0,0120034

gene	sample_2	log2(fold_change)	p_value	q_value
ENSGACG00000005903	clone mix	-1,27527	0,0022855	0,029848
ENSGACG00000005904	clone mix	3,14706	1,93E-010	2,75E-008
ENSGACG00000006044	clone mix	2,5535	0,0001872	0,00387762
ENSGACG00000006048	clone mix	1,99105	0,0013807	0,0199361
ENSGACG00000006109	clone mix	2,03798	0,0011755	0,0175199
ENSGACG00000006530	clone mix	1,40026	0,0024209	0,031253
ENSGACG00000006908	clone mix	-2,9515	5,22E-011	8,61E-009
ENSGACG00000006931	clone mix	1,7093	0,0035178	0,041983
ENSGACG00000007329	clone mix	-1,5013	3,11E-015	1,26E-012
ENSGACG00000007447	clone mix	-1,40809	3,01E-005	0,00084281
ENSGACG00000007488	clone mix	3,37052	0,0032	0,0389743
ENSGACG00000007525	clone mix	2,22641	4,93E-006	0,00018202
ENSGACG00000007639	clone mix	1,2305	0,0005639	0,00963287
ENSGACG00000007673	clone mix	1,53829	0,0030153	0,0372052
ENSGACG00000007787	clone mix	1,17001	0,0030749	0,0377758
ENSGACG00000007796	clone mix	-1,25814	0,0013507	0,0195887
ENSGACG00000007854	clone mix	1,80E+308	0,0007251	0,0118264
ENSGACG00000007857	clone mix	-0,709295	0,0005278	0,00912784
ENSGACG00000007958	clone mix	0,591984	0,0003536	0,00656789
ENSGACG00000008205	clone mix	-1,28114	0,000845	0,0133902
ENSGACG00000008258	clone mix	2,17014	8,04E-005	0,00191669
ENSGACG00000008263	clone mix	1,22606	3,49E-005	0,00095409
ENSGACG00000008353	clone mix	2,79539	7,85E-009	7,13E-007
ENSGACG00000008466	clone mix	1,30148	0,0009631	0,0149
ENSGACG00000008485	clone mix	-1,07053	0,0004596	0,00815229
ENSGACG00000008510	clone mix	-1,20121	0,0017352	0,0239431
ENSGACG00000008661,ENSGACG00000008663	clone mix	1,19891	6,46E-005	0,00159707
ENSGACG00000008777	clone mix	1,6746	0,0012964	0,0189547
ENSGACG00000008819	clone mix	-1,46604	2,24E-006	9,32E-005
ENSGACG00000008820	clone mix	2,18134	0,0006684	0,0110647
ENSGACG00000008828	clone mix	-1,31017	0,0007893	0,0126709
ENSGACG00000009171	clone mix	-1,86502	1,74E-006	7,51E-005
ENSGACG00000009182	clone mix	0,821515	0,0004833	0,00849355
ENSGACG00000009200	clone mix	1,75203	7,98E-007	3,86E-005
ENSGACG00000009229	clone mix	-2,48882	2,22E-008	1,76E-006
ENSGACG00000009326	clone mix	-0,912265	0,0002976	0,00569642
ENSGACG00000009356	clone mix	1,86868	2,54E-005	0,00073013
ENSGACG00000009409	clone mix	-3,04254	5,98E-006	0,00021454
ENSGACG00000009417	clone mix	2,87517	8,55E-008	5,65E-006
ENSGACG00000009596	clone mix	1,33074	0,0004789	0,00842987
ENSGACG00000009715	clone mix	1,17048	0,0014491	0,0207207
ENSGACG00000009863	clone mix	2,12619	0,0002162	0,0043722
ENSGACG00000009946	clone mix	-1,63191	7,79E-005	0,0018659
ENSGACG00000010018	clone mix	1,95164	0,0002444	0,00483985
ENSGACG00000010050	clone mix	2,67786	7,24E-013	1,86E-010
ENSGACG00000010154	clone mix	-1,57825	0,0022428	0,0294027
ENSGACG00000010162	clone mix	1,522	0,0009343	0,0145353
ENSGACG00000010374	clone mix	-1,18904	0,0030734	0,0377616
ENSGACG00000010457	clone mix	-2,10177	4,66E-007	2,43E-005
ENSGACG00000010476	clone mix	4,33743	0	0
ENSGACG00000010501	clone mix	-1,34792	3,12E-009	3,19E-007
ENSGACG00000010548	clone mix	1,20325	0,0028774	0,0358387

gene	sample_2	log2(fold_change)	p_value	q_value
ENSGACG00000010688	clone mix	-0,791243	0,0036293	0,0430358
ENSGACG00000010749	clone mix	0,849583	0,0008352	0,0132613
ENSGACG00000010785	clone mix	-1,23175	0,000308	0,0058594
ENSGACG00000010905	clone mix	1,78136	0,0003582	0,00663963
ENSGACG00000010910	clone mix	3,45773	0,0002102	0,00427
ENSGACG00000011085	clone mix	1,40325	0,0029993	0,0370558
ENSGACG00000011111	clone mix	1,42744	0,0004054	0,0073543
ENSGACG00000011143	clone mix	1,7385	0,0006174	0,0103715
ENSGACG00000011165	clone mix	1,21107	0,0004797	0,00844171
ENSGACG00000011219	clone mix	-1,3095	0,0021986	0,0289373
ENSGACG00000011342	clone mix	0,913561	0,0040729	0,0470787
ENSGACG00000012174	clone mix	-2,2784	0,0005348	0,00922898
ENSGACG00000012247	clone mix	-1,34699	0,002937	0,0364383
ENSGACG00000012285	clone mix	2,00731	9,14E-005	0,00213412
ENSGACG00000012290	clone mix	2,5985	1,11E-007	7,09E-006
ENSGACG00000012340	clone mix	1,4346	0,0021623	0,0285647
ENSGACG00000012348	clone mix	-1,11961	0,0035734	0,0425099
ENSGACG00000012358	clone mix	2,45907	0,003922	0,0457317
ENSGACG00000012434	clone mix	1,37119	0,0008132	0,0129787
ENSGACG00000012548	clone mix	-1,82428	0,0005021	0,00876251
ENSGACG00000012556	clone mix	-1,52945	0,0003872	0,00708081
ENSGACG00000012592	clone mix	2,16546	1,67E-006	7,25E-005
ENSGACG00000012655	clone mix	1,02541	1,25E-005	0,00040031
ENSGACG00000012835	clone mix	1,7424	0,0004452	0,00794105
ENSGACG00000012912	clone mix	1,24444	0,0026153	0,0332262
ENSGACG00000012954	clone mix	-1,99583	0,0011209	0,0168576
ENSGACG00000013109	clone mix	0,670536	0,0006455	0,0107542
ENSGACG00000013161	clone mix	1,91657	6,83E-006	0,0002401
ENSGACG00000013327	clone mix	2,93684	0,0001402	0,00304868
ENSGACG00000013590	clone mix	-1,15408	0,002033	0,0271925
ENSGACG00000013762	clone mix	1,88156	7,65E-010	9,27E-008
ENSGACG00000013782	clone mix	2,03193	0,0008258	0,0131395
ENSGACG00000013891	clone mix	-2,57409	0,0026503	0,0335742
ENSGACG00000014109	clone mix	1,5978	3,33E-005	0,0009155
ENSGACG00000014131	clone mix	-1,39809	0,0014373	0,020585
ENSGACG00000014494	clone mix	1,47028	0,0005286	0,00913951
ENSGACG00000014579	clone mix	1,77056	0,0008492	0,0134424
ENSGACG00000014599	clone mix	1,63356	6,62E-005	0,00162915
ENSGACG00000014616	clone mix	0,496088	0,0022422	0,0293958
ENSGACG00000014629	clone mix	-0,781649	0,0028267	0,0353332
ENSGACG00000014744	clone mix	-0,42482	0,0042156	0,0483679
ENSGACG00000014774	clone mix	-1,46958	0,0005037	0,00878578
ENSGACG00000015058	clone mix	1,67001	0,004091	0,0472429
ENSGACG00000015110	clone mix	1,13082	0,0042244	0,0484471
ENSGACG00000015177	clone mix	1,21577	0,0025718	0,0327916
ENSGACG00000015193	clone mix	1,38119	0,002613	0,0332034
ENSGACG00000015196	clone mix	0,880938	0,0025656	0,0327283
ENSGACG00000015718	clone mix	-1,46391	0,0001828	0,00380123
ENSGACG00000015846	clone mix	1,87049	3,13E-005	0,00087065
ENSGACG00000015956	clone mix	2,2688	0,0002088	0,0042456
ENSGACG00000015960	clone mix	3,20456	0,0003268	0,00615466
ENSGACG00000016075	clone mix	1,41675	0,0032807	0,0397455
ENSGACG00000016174	clone mix	2,61135	0,0028941	0,0360107

gene	sample_2	log2(fold_change)	p_value	q_value
ENSGACG00000016379	clone mix	1,10143	0,0002404	0,00477396
ENSGACG00000016410	clone mix	1,26383	0,0022152	0,0291135
ENSGACG00000016422	clone mix	-1,9554	0,0039155	0,045671
ENSGACG00000016599	clone mix	-1,16004	0,0025838	0,0329144
ENSGACG00000016601	clone mix	2,05377	0,0001569	0,00334778
ENSGACG00000016901	clone mix	1,38676	0,0038727	0,0452799
ENSGACG00000016917	clone mix	2,13714	0,0007529	0,0121919
ENSGACG00000017045	clone mix	1,41113	0,0019758	0,0265813
ENSGACG00000017117	clone mix	2,23161	9,09E-005	0,00212356
ENSGACG00000017174	clone mix	1,39573	0,0021602	0,0285427
ENSGACG00000017278	clone mix	-1,089	0,0038541	0,0451073
ENSGACG00000017622	clone mix	1,44987	0,000337	0,00631358
ENSGACG00000017657	clone mix	-1,18118	0,0023365	0,0303797
ENSGACG00000017894	clone mix	1,76294	6,96E-005	0,00169847
ENSGACG00000017988	clone mix	-2,24129	6,83E-008	4,66E-006
ENSGACG00000017995	clone mix	-2,45774	5,36E-010	6,77E-008
ENSGACG00000018191	clone mix	1,52115	0,000537	0,00925842
ENSGACG00000018216	clone mix	1,20483	0,0023329	0,0303445
ENSGACG00000018380	clone mix	1,6284	0,0032907	0,0398408
ENSGACG00000018802	clone mix	3,00049	1,36E-009	1,54E-007
ENSGACG00000018832	clone mix	2,13146	0,0004639	0,00821494
ENSGACG00000018835	clone mix	1,48412	5,32E-007	2,72E-005
ENSGACG00000018840	clone mix	2,70347	1,47E-010	2,16E-008
ENSGACG00000018866	clone mix	1,6225	0,0010782	0,0163313
ENSGACG00000018954	clone mix	2,78159	0,0012747	0,0186976
ENSGACG00000018993	clone mix	-2,19321	4,37E-007	2,30E-005
ENSGACG00000019088	clone mix	1,62948	0,002848	0,0355455
ENSGACG00000019128	clone mix	1,49302	0,0012901	0,0188815
ENSGACG00000019173	clone mix	1,05771	0,0001847	0,00383513
ENSGACG00000019252	clone mix	1,31496	0,0013217	0,0192503
ENSGACG00000019285	clone mix	2,14907	0,0004728	0,00834292
ENSGACG00000019342	clone mix	2,36635	0,0033131	0,0400553
ENSGACG00000019361	clone mix	1,68073	0,0006436	0,0107284
ENSGACG00000019390	clone mix	-1,20156	0,0001435	0,00310904
ENSGACG00000019470	clone mix	2,24134	0,000185	0,00383962
ENSGACG00000019794	clone mix	-0,922832	0,0028706	0,0357706
ENSGACG00000019819	clone mix	-2,61279	1,77E-008	1,44E-006
ENSGACG00000019899	clone mix	1,38365	0,0033573	0,0404807
ENSGACG00000019921	clone mix	2,78947	2,01E-006	8,50E-005
ENSGACG00000019933	clone mix	1,35843	0,0007506	0,0121617
ENSGACG00000019951	clone mix	3,18536	8,78E-007	4,19E-005
ENSGACG00000019952	clone mix	2,87677	6,26E-010	7,77E-008
ENSGACG00000020003	clone mix	1,85921	0,0012234	0,0180896
ENSGACG00000020005	clone mix	2,60203	0,0032943	0,0398738
ENSGACG00000020034	clone mix	-3,26582	0,0029547	0,036613
ENSGACG00000020145	clone mix	2,90481	7,94E-009	7,21E-007
ENSGACG00000020180	clone mix	1,28424	0,0043138	0,0492315
ENSGACG00000020243	clone mix	-1,13963	0,0035015	0,0418289
ENSGACG00000020365	clone mix	-3,96316	4,82E-006	0,00017889
ENSGACG00000020469	clone mix	-1,48675	0,0005973	0,0100957
ENSGACG00000020633	clone mix	-3,96601	6,55E-010	8,09E-008
ENSGACG00000020852	clone mix	2,3146	5,85E-006	0,00021047
ENSGACG00000020858	clone mix	1,66655	0,0013909	0,020053

gene	sample_2	log2(fold_change)	p_value	q_value
ENTPD3	clone mix	0,817447	0,0040791	0,0471366
EP300 (1 of 2)	clone mix	1,47468	0,0002506	0,00494172
EP400NL	clone mix	1,1207	0,003227	0,0392352
EPHA3	clone mix	2,48924	0,0003471	0,00646924
ERBB2IP	clone mix	1,1431	0,0032956	0,0398865
ERGIC1	clone mix	1,03741	0,0008743	0,0137637
ERRFI1	clone mix	1,95878	0,0001082	0,00245595
ESYT1 (1 of 2)	clone mix	1,4769	0,0005427	0,00933842
EVC2	clone mix	1,07134	0,0027021	0,0340939
EXOC1	clone mix	0,793591	0,0008704	0,0137148
EXOSC1	clone mix	-1,64163	1,76E-005	0,00053487
EXOSC5	clone mix	-1,66835	0,0004797	0,00844117
EZH1	clone mix	1,15934	0,0031262	0,0382591
F3 (1 of 2)	clone mix	1,43614	0,0012001	0,0178116
F8	clone mix	1,62357	0,000141	0,0030629
FAM115A	clone mix	0,749156	0,0002881	0,00554526
FAM167B	clone mix	-1,2655	0,0001372	0,00299344
FAM193A	clone mix	1,18299	0,000172	0,00361372
FAM32A	clone mix	-1,4104	0,0002068	0,00421261
FAM65A	clone mix	2,29524	0,000421	0,00758596
FAM82A1	clone mix	1,23151	0,0040126	0,0465434
FAM96B	clone mix	-1,55313	0,0009965	0,0153182
FAR1	clone mix	1,36346	0,0007711	0,0124345
FAT1	clone mix	1,509	0,0002054	0,00418844
FBLN1 (1 of 2)	clone mix	1,24884	3,89E-007	2,08E-005
FBLN2 (1 of 2)	clone mix	1,86469	0,0003341	0,00626783
FBLN2 (2 of 2)	clone mix	2,47266	1,82E-006	7,81E-005
FBN1	clone mix	2,40121	3,97E-007	2,12E-005
FBN3	clone mix	2,90924	1,23E-008	1,06E-006
FCGBP (1 of 2)	clone mix	1,45989	4,66E-007	2,43E-005
FER1L6	clone mix	1,26646	0,0010117	0,0155067
FERMT2	clone mix	1,64941	0,0001787	0,00373046
FGD5 (2 of 2)	clone mix	2,7913	0,0020696	0,0275803
FGFR1 (2 of 2)	clone mix	1,30964	0,001157	0,0172951
FGFR2	clone mix	1,17367	0,0039425	0,0459178
FGFR4	clone mix	2,10564	0,0007507	0,0121631
FGL2	clone mix	2,01362	1,33E-005	0,00042305
FHL2 (1 of 2)	clone mix	-0,853669	0,0003674	0,0067802
FHL5	clone mix	-1,33072	1,60E-006	7,00E-005
FHOD1	clone mix	1,15929	1,76E-005	0,00053459
FIBIN (1 of 2)	clone mix	1,99351	0,0017506	0,0241158
FILIP1L	clone mix	2,16529	4,01E-007	2,13E-005
FKBP5	clone mix	5,18889	2,22E-015	9,22E-013
FLI1	clone mix	1,65068	0,0004886	0,008569
FLII	clone mix	1,14532	0,0026136	0,0332088
FLNA (2 of 2)	clone mix	1,33794	0,0005216	0,00904095
FLNC (2 of 2)	clone mix	2,1811	1,04E-009	1,22E-007
FLT1	clone mix	1,91872	0,0005644	0,00963953
FN1 (1 of 2)	clone mix	2,08289	8,96E-008	5,89E-006
FN1 (2 of 2)	clone mix	2,00699	5,06E-007	2,61E-005
FNBP4	clone mix	1,51856	0,000173	0,00363121
FOSL1	clone mix	3,79548	0,0039621	0,0460893
FOXK1	clone mix	1,31993	0,0011531	0,0172485

gene	sample_2	log2(fold_change)	p_value	q_value
FOXK2 (2 of 2)	clone mix	0,726217	0,0012626	0,018559
FREM1	clone mix	1,56928	0,0001193	0,00266554
FRK	clone mix	1,16932	0,0041834	0,0480759
FRMD4A	clone mix	2,14418	4,52E-005	0,00118374
FRMD4B (1 of 2)	clone mix	1,3493	0,0013543	0,0196324
FRY (1 of 2)	clone mix	1,5478	0,0001324	0,00290516
FRY (2 of 2)	clone mix	1,74599	5,05E-006	0,00018607
FRYL (1 of 2)	clone mix	1,25377	0,00119	0,0176919
FRZB	clone mix	1,06268	0,003559	0,0423744
FSTL1 (1 of 2)	clone mix	1,48993	0,0002524	0,00497146
FSTL3	clone mix	2,19555	3,34E-006	0,00013076
FUK	clone mix	1,34793	0,0013605	0,0197029
FUNDC1	clone mix	-0,618472	0,0005169	0,00897488
FUT4	clone mix	-1,2133	0,0002043	0,00417093
GADD45B (1 of 2)	clone mix	1,31273	9,59E-005	0,00222004
GADD45G (1 of 3)	clone mix	1,67327	0,0001723	0,00361841
GAK	clone mix	1,24254	0,0018373	0,0250823
GAL3ST1 (1 of 2)	clone mix	2,60358	0,0020498	0,0273743
GALM	clone mix	-1,04671	4,58E-008	3,29E-006
GALNTL1	clone mix	-1,22982	0,0014699	0,0209612
GAPVD1	clone mix	1,05938	0,0005107	0,00888559
GCNT1	clone mix	5,78438	0,0001946	0,00400541
GHR (1 of 2)	clone mix	1,20946	0,0039302	0,0458045
GLB1L	clone mix	1,885	0,0005731	0,00976072
GLG1 (1 of 2)	clone mix	1,18187	0,0034559	0,0414039
GLI2	clone mix	1,26719	0,0043446	0,0494997
GLUL (1 of 2)	clone mix	1,18276	0,0039508	0,0459911
GNAO1 (1 of 2)	clone mix	1,37946	0,0002282	0,00457157
GNGT1	clone mix	-1,80E+308	4,05E-007	2,15E-005
GOLGA2	clone mix	1,27538	0,0020549	0,0274264
GOLGA7 (2 of 2)	clone mix	-1,24047	0,0005407	0,0093098
GOSR1 (2 of 2)	clone mix	-1,69532	0,0001289	0,00284352
GPATCH8	clone mix	1,53484	9,68E-005	0,00223898
GPC4	clone mix	1,22116	0,0035679	0,0424563
GPR124	clone mix	1,40477	0,0036468	0,043197
GPR133	clone mix	2,08997	0,0002718	0,00528377
GRB10 (2 of 2)	clone mix	1,92341	0,0006084	0,0102474
GTF2H5	clone mix	-1,58058	0,0015103	0,0214209
H2AFV	clone mix	-1,68524	5,55E-005	0,00140579
HDAC4 (1 of 2)	clone mix	2,04922	3,46E-005	0,00094548
HELZ	clone mix	1,2447	0,0017369	0,0239623
HGF (2 of 2)	clone mix	2,18345	0,0033868	0,0407602
HGS	clone mix	1,11854	0,0040188	0,0465996
HIGD1A	clone mix	-1,21619	1,22E-007	7,68E-006
HIVEP1	clone mix	1,34371	0,0003884	0,0070986
HIVEP2 (1 of 2)	clone mix	1,44173	0,0001711	0,00359772
HLA-DMA (4 of 5)	clone mix	-1,62961	6,41E-005	0,0015862
HLF (1 of 2)	clone mix	1,56886	0,0013057	0,0190635
HM13	clone mix	1,00659	1,53E-005	0,00047405
HNMT (2 of 2)	clone mix	-1,28655	0,0005398	0,00929641
HNRNPUL1	clone mix	1,11921	0,0023539	0,0305587
HOOK3	clone mix	1,07486	0,0019126	0,0258923
HSD3B7	clone mix	1,27704	0,0017813	0,0244563

gene	sample_2	log2(fold_change)	p_value	q_value
HSPG2 (1 of 2)	clone mix	1,90905	8,21E-005	0,00195049
HSPG2 (2 of 2)	clone mix	2,42932	0,000215	0,0043526
HTT	clone mix	1,13888	0,0039399	0,0458928
HUWE1	clone mix	1,08798	2,23E-006	9,26E-005
IER3IP1	clone mix	-1,84029	0,0006459	0,0107599
IER5L (2 of 2)	clone mix	-1,7023	0,0001058	0,00241113
IGF1R (2 of 2)	clone mix	1,75874	0,0001682	0,00354904
IGFBP1 (1 of 2)	clone mix	2,84828	0,0003835	0,00702534
IL6ST	clone mix	1,19771	0,0018801	0,0255464
INPP4B	clone mix	1,04095	0,0002736	0,00531276
INPPL1	clone mix	1,55027	0,001002	0,0153876
INSR (2 of 2)	clone mix	1,22164	0,0023247	0,0302564
IRS2 (1 of 2)	clone mix	2,44104	1,90E-008	1,53E-006
IRS2 (2 of 2)	clone mix	1,26101	0,001887	0,0256232
ITCH (2 of 2)	clone mix	1,50676	0,0021509	0,0284449
ITGA1	clone mix	2,13788	3,24E-007	1,78E-005
ITGA2	clone mix	1,28825	0,0013395	0,0194558
ITGA4	clone mix	2,27446	0,0001005	0,00231031
ITGA5 (1 of 2)	clone mix	2,22833	0,0003431	0,0064079
ITGA8	clone mix	2,37947	0,0005793	0,00984406
ITGB2	clone mix	0,64577	6,10E-005	0,00152228
ITIH4 (1 of 2)	clone mix	-2,74219	0,0001092	0,00247491
ITIH4 (2 of 2)	clone mix	-3,22584	8,75E-005	0,00205648
ITIH5	clone mix	1,41706	0,0032643	0,0395911
ITPKC (1 of 2)	clone mix	1,77319	3,55E-005	0,00096693
ITPR1 (2 of 2)	clone mix	1,39985	0,0004621	0,00818921
ITPR2	clone mix	1,18149	0,0024181	0,0312248
ITPR3	clone mix	1,26078	0,0009958	0,0153095
ITSN2 (2 of 2)	clone mix	1,23929	0,0016317	0,0227914
JAG2	clone mix	1,52232	0,0008314	0,0132112
JAK1	clone mix	1,19508	0,0036571	0,0432964
JMJD1C	clone mix	1,46572	0,0008589	0,0135677
JUNB (1 of 2)	clone mix	2,62527	1,29E-008	1,10E-006
JUNB (2 of 2)	clone mix	2,1281	1,12E-005	0,00036411
KAT6B	clone mix	1,39374	7,50E-005	0,00180718
KDM2B (1 of 2)	clone mix	1,12231	0,0037736	0,0443727
KDM2B (2 of 2)	clone mix	1,24478	0,0021418	0,0283505
KDM6B	clone mix	2,39651	1,42E-007	8,77E-006
KDR	clone mix	1,47225	0,0024989	0,032052
KEAP1	clone mix	1,31854	0,0010766	0,016312
KIAA0182	clone mix	1,18573	0,0032195	0,0391611
KIAA0284 (2 of 2)	clone mix	0,945483	0,0014782	0,0210551
KIAA0907	clone mix	0,963339	2,94E-005	0,00082637
KIAA1033	clone mix	1,18341	0,003259	0,039541
KIAA1109	clone mix	1,45493	0,000256	0,00502931
KIAA1199	clone mix	1,64697	0,0008341	0,0132477
KIAA1217	clone mix	1,34335	0,0007845	0,0126104
KIAA1274	clone mix	1,27572	0,0027879	0,0349447
KIAA1797	clone mix	1,46796	0,0005628	0,00961892
KIF1B	clone mix	1,00748	0,0006031	0,0101757
KIF21A (1 of 2)	clone mix	1,58643	0,0009721	0,0150129
KIF3C (1 of 2)	clone mix	2,29334	3,49E-005	0,00095339
KLC1	clone mix	1,14795	0,0006371	0,0106428

gene	sample_2	log2(fold_change)	p_value	q_value
KLF13	clone mix	1,80E+308	1,15E-006	5,28E-005
KLF6 (1 of 2)	clone mix	1,72399	3,19E-005	0,00088284
KLF9	clone mix	3,87628	1,51E-012	3,63E-010
KLHDC10 (2 of 2)	clone mix	-2,96365	0,0029594	0,0366587
KLHL30	clone mix	1,63618	0,0014495	0,0207254
KLHL38 (2 of 2)	clone mix	2,18608	0,0009972	0,0153278
KRI1	clone mix	0,83717	0,0041333	0,0476279
KRT23 (5 of 7)	clone mix	-1,15449	2,22E-009	2,36E-007
LAMA2	clone mix	1,56706	0,0004522	0,00804558
LAMA3	clone mix	1,20688	0,002467	0,0317244
LAMA4	clone mix	1,69479	9,06E-005	0,00211783
LAMB2	clone mix	1,33861	0,0037058	0,0437497
LAMC2 (2 of 2)	clone mix	1,51831	3,88E-005	0,00104076
LAMC3	clone mix	1,68328	4,60E-005	0,00120217
LCP2	clone mix	1,02247	0,000185	0,00384046
LDLR (1 of 2)	clone mix	1,63578	0,0001714	0,00360418
LDLR (2 of 2)	clone mix	1,40693	0,0003628	0,00670906
LENG8	clone mix	1,75151	9,53E-006	0,00031823
LITAF	clone mix	-2,93932	0,0001449	0,00313416
LLPH	clone mix	-1,32634	0,0020929	0,0278333
LMOD1	clone mix	1,90133	0,0002115	0,00429239
LOX	clone mix	1,01333	0,001773	0,0243633
LOXL1	clone mix	1,41266	0,0028426	0,0354916
LOXL2 (1 of 2)	clone mix	2,05422	0,0002494	0,00492362
LOXL4	clone mix	1,7859	0,0029438	0,0365048
LPAR2 (2 of 2)	clone mix	-0,699581	0,0038246	0,0448359
LPHN1 (2 of 2)	clone mix	2,78901	1,28E-008	1,09E-006
LRP1 (1 of 2)	clone mix	1,54933	7,57E-005	0,00182137
LRP1 (2 of 2)	clone mix	2,09264	4,77E-008	3,40E-006
LRP4	clone mix	1,87782	2,25E-005	0,00065971
LRRC14B	clone mix	1,40134	0,004082	0,0471633
LRRC32	clone mix	1,97226	0,0004246	0,00763933
LRRC39	clone mix	-1,67212	0,0038726	0,0452792
LRRFIP1 (1 of 2)	clone mix	1,67544	2,03E-009	2,19E-007
LRRK2	clone mix	1,48702	0,0005256	0,00909851
LSM1	clone mix	-1,53817	0,0014148	0,0203286
LSM6	clone mix	-1,60661	0,0013211	0,019244
LTBP1	clone mix	1,58089	0,0004692	0,00829135
LTBP3	clone mix	1,77086	5,28E-005	0,0013494
LUM	clone mix	1,54568	0,0001427	0,00309388
LYST	clone mix	1,18814	0,0036561	0,0432867
LZIC	clone mix	-1,19959	3,96E-008	2,90E-006
MACF1	clone mix	1,31365	0,00137	0,0198136
MAD2L2	clone mix	-1,91643	1,42E-010	2,10E-008
MADD	clone mix	1,64519	0,0016384	0,0228686
MALT1	clone mix	1,20969	0,0008812	0,0138535
MAP3K6	clone mix	0,78318	0,0001139	0,00256364
MAP4K2	clone mix	1,38881	0,0002969	0,00568467
MAPK12 (2 of 2)	clone mix	0,819093	2,24E-006	9,30E-005
MAPK14 (1 of 2)	clone mix	1,23813	1,62E-005	0,00049806
MARK4 (2 of 2)	clone mix	1,32589	0,0039625	0,0460932
MAST2	clone mix	1,36967	0,0015534	0,0219114
MATR3	clone mix	1,84815	0,0001388	0,00302275

gene	sample_2	log2(fold_change)	p_value	q_value
MCAM (2 of 2)	clone mix	1,04019	7,53E-005	0,0018134
MCEE	clone mix	-1,67039	0,0002393	0,00475418
MDN1	clone mix	1,37261	0,0005874	0,00995799
MECOM	clone mix	1,67321	0,0023507	0,0305272
MED13 (1 of 2)	clone mix	1,29918	0,0023452	0,0304713
MEGF8	clone mix	1,2546	0,0016072	0,0225158
MET	clone mix	1,38607	0,001123	0,0168837
METTL10	clone mix	-1,28798	5,88E-006	0,00021129
METTL5	clone mix	-1,69459	0,0001791	0,00373836
MFGE8 (2 of 2)	clone mix	1,50353	0,0007317	0,011914
MGP	clone mix	1,7956	0,0031193	0,0381936
MGST1	clone mix	-1,49634	6,53E-005	0,00161157
MIB1	clone mix	1,41436	0,000736	0,0119716
MIB2	clone mix	1,40679	0,0015758	0,0221634
MID1 (2 of 2)	clone mix	1,57027	0,0021755	0,0286984
MINK1	clone mix	1,14903	0,0033775	0,0406713
MINOS1 (1 of 2)	clone mix	-1,67538	8,28E-005	0,00196317
MKL2 (2 of 2)	clone mix	2,65376	4,91E-008	3,49E-006
MKNK2	clone mix	1,85189	4,96E-006	0,00018319
MLL	clone mix	1,43732	0,0001306	0,00287415
MLL2	clone mix	1,29399	0,0006892	0,0113455
MLL3 (1 of 2)	clone mix	1,40997	0,0002661	0,00519204
MLL3 (2 of 2)	clone mix	1,36276	0,0012253	0,0181125
MMP14 (1 of 2)	clone mix	1,35097	0,0009403	0,0146108
MMP2	clone mix	1,74294	2,69E-005	0,00076687
MMP9	clone mix	1,60722	0	0
MORC4	clone mix	0,926759	6,56E-005	0,00161758
MRC2	clone mix	1,90768	0,0001228	0,00272932
MRPL14	clone mix	-1,33254	0,0019354	0,026144
MRPL18	clone mix	-1,38682	0,0017116	0,0236842
MRPL28	clone mix	-0,665718	0,0029699	0,0367605
MRPL33	clone mix	-1,43232	0,0001926	0,003971
MRPS10	clone mix	-1,59734	3,13E-012	6,98E-010
MRVI1	clone mix	3,14034	1,68E-006	7,27E-005
MTMR11	clone mix	1,68279	0,0039848	0,0462925
MTMR4	clone mix	1,18082	0,0025974	0,0330487
MXRA8 (2 of 2)	clone mix	1,49011	0,0003908	0,00713531
MYCBP2	clone mix	1,2928	0,0014512	0,020744
MYH10 (2 of 2)	clone mix	1,7458	0,0022821	0,0298136
MYH11 (1 of 2)	clone mix	2,24022	3,68E-006	0,00014203
MYLK	clone mix	1,77046	1,64E-005	0,000505
MYO1B	clone mix	1,47759	0,0005541	0,0094956
MYO1D	clone mix	1,17476	0,0041572	0,0478429
MYO5C	clone mix	1,5749	0,0004373	0,0078272
MYO9A (2 of 2)	clone mix	1,32125	6,13E-005	0,00152861
MYO9B (1 of 2)	clone mix	1,134	0,0033037	0,039963
MYOF (1 of 2)	clone mix	1,477	0,0003199	0,00604714
MYOF (2 of 2)	clone mix	1,17402	0,0029949	0,0370126
NAA10	clone mix	-1,27002	0,0012628	0,0185609
NACC2	clone mix	1,86546	0,0012114	0,0179476
NAV3	clone mix	2,0056	0,0006137	0,0103202
NCOA6	clone mix	1,22269	0,0040553	0,0469265
NDRG2	clone mix	1,38006	0,0014033	0,0201985

gene	sample_2	log2(fold_change)	p_value	q_value
NDUFA1	clone mix	-1,48889	0,0002415	0,00479196
NDUFA12	clone mix	-1,5868	4,28E-005	0,00113019
NDUFA13	clone mix	-1,58196	0,0001071	0,00243594
NDUFB1	clone mix	-1,57531	4,38E-005	0,00115282
NDUFB2	clone mix	-1,63432	0,0001443	0,00312288
NDUFB3	clone mix	-1,82146	8,96E-006	0,00030212
NDUFB8	clone mix	-1,5454	0,0001024	0,00234605
NDUFS6	clone mix	-1,24505	0,0023949	0,0309862
NEDD4L	clone mix	1,36545	0,001303	0,0190313
NF1	clone mix	1,20975	0,0021531	0,0284678
NFATC3	clone mix	1,15805	0,0041956	0,0481869
NFKBIA (1 of 2)	clone mix	2,16166	7,35E-010	8,96E-008
NHSL1	clone mix	1,30597	0,0024377	0,0314244
NID1 (1 of 2)	clone mix	1,36969	0,0009515	0,0147541
NKTR,ZBTB47	clone mix	1,16511	0,0006989	0,0114771
NLRC5	clone mix	1,23256	0,0040035	0,0464653
NR1D2 (2 of 2)	clone mix	3,31029	2,83E-009	2,93E-007
NRG2 (1 of 2)	clone mix	1,81825	0,0001758	0,00368067
NRK	clone mix	1,74381	0,0025825	0,0329008
NUAK1	clone mix	1,27433	0,0042871	0,0489973
NUCB2 (2 of 2)	clone mix	1,8959	0,001659	0,0231005
NXF3	clone mix	1,30415	0,0017087	0,023653
NYNRIN	clone mix	1,51887	0,0009451	0,0146712
OBSCN	clone mix	1,83204	0,0003255	0,00613406
OCRL	clone mix	1,62142	1,89E-006	8,04E-005
ODZ3 (1 of 2)	clone mix	1,53338	0,0003241	0,00611138
OGT	clone mix	1,28839	0,0016461	0,0229577
OLFML1	clone mix	1,63092	0,0009022	0,0141243
OLFML2A	clone mix	1,82337	1,37E-005	0,00043208
OLFML2B (2 of 2)	clone mix	2,10647	0,0002487	0,0049111
ORMDL3	clone mix	2,87915	0,0001076	0,00244483
OSBPL8	clone mix	1,34981	0,002417	0,0312137
OSMR (1 of 2)	clone mix	1,35592	0,001096	0,0165524
OTOF (1 of 2)	clone mix	2,66876	5,94E-005	0,00148805
PANK4	clone mix	1,19784	0,0029772	0,0368332
PARK2	clone mix	-0,828898	0,0033034	0,03996
PARP4	clone mix	1,19922	0,0040794	0,0471389
PCDH12	clone mix	2,55205	0,0006075	0,0102358
PCDH20	clone mix	2,46875	0,0001662	0,00351287
PCF11	clone mix	1,39614	0,0004896	0,00858334
PCK1	clone mix	3,39367	1,30E-005	0,00041336
PCNX	clone mix	1,03919	0,0035072	0,0418822
PCOLCE (2 of 2)	clone mix	0,972031	0,003598	0,0427445
PDE1B	clone mix	1,37799	0,0017127	0,0236959
PDGFRB	clone mix	1,48335	0,0036516	0,0432445
PDK2 (2 of 2)	clone mix	1,58189	0,0004716	0,00832604
PDS5B	clone mix	0,810839	0,0041886	0,048123
PFDN1	clone mix	-1,75764	1,98E-005	0,00059306
PFDN5	clone mix	-1,37492	1,43E-005	0,0004501
PGLYRP2 (1 of 2)	clone mix	1,83379	0,0002707	0,00526473
PHEX	clone mix	1,79068	0,0002922	0,00560992
PHKA1	clone mix	1,3131	0,0011424	0,0171184
PHLDB2 (1 of 2)	clone mix	1,09554	0,00051	0,00887444

gene	sample_2	log2(fold_change)	p_value	q_value
PHLDB2 (2 of 2)	clone mix	2,15268	1,01E-005	0,00033436
PI4KA (1 of 2)	clone mix	1,22285	0,0007949	0,0127443
PIGN	clone mix	1,00396	0,000689	0,0113429
PIK3C2A	clone mix	1,76895	1,92E-005	0,00057758
PIK3CB	clone mix	1,2076	0,0019858	0,0266883
PIK3CG	clone mix	1,34641	0,0027874	0,0349391
PIK3R1 (1 of 2)	clone mix	2,08068	3,20E-006	0,00012636
PIM3 (1 of 2)	clone mix	1,46414	0,0031027	0,0380374
PKD1	clone mix	2,36488	1,56E-007	9,50E-006
PKHD1L1	clone mix	0,912738	5,83E-005	0,00146519
PKN1 (1 of 2)	clone mix	1,13896	6,03E-005	0,00150745
PKN2	clone mix	0,713472	0,0040199	0,04661
PLCB2	clone mix	1,98429	2,56E-005	0,00073431
PLCB4	clone mix	1,81868	7,55E-006	0,00026142
PLCD4 (2 of 2)	clone mix	2,1633	1,40E-005	0,00043959
PLCE1	clone mix	1,421	0,0038989	0,0455173
PLCH2 (2 of 2)	clone mix	1,80E+308	0,0006945	0,0114191
PLD1 (1 of 2)	clone mix	1,28229	0,003515	0,0419579
PLEC (2 of 2)	clone mix	1,39999	0,0006586	0,010932
PLEKHA5 (1 of 2)	clone mix	1,44252	0,0024582	0,0316345
PLEKHA5 (2 of 2)	clone mix	1,93382	0,0026344	0,0334165
PLEKHA6	clone mix	1,11882	0,004205	0,0482705
PLEKHG4B	clone mix	1,55109	7,47E-005	0,00180225
PLOD2	clone mix	2,41154	1,71E-005	0,00052155
PNISR	clone mix	1,57074	4,44E-016	2,06E-013
PNPLA2	clone mix	2,79163	0,0002038	0,00416263
PODXL	clone mix	2,23457	0,0003851	0,00704968
POLR2A	clone mix	1,42182	0,0003365	0,00630568
POLR2I	clone mix	-1,83	6,20E-005	0,00154256
POLR3K	clone mix	-1,67895	0,0010649	0,0161697
POSTN (2 of 2)	clone mix	1,47413	0,0040138	0,0465538
PPDPF (1 of 2)	clone mix	-1,51358	9,15E-012	1,82E-009
PPM1J	clone mix	1,47926	2,06E-005	0,00061234
PPP1R15B	clone mix	2,0119	2,05E-006	8,64E-005
PPP2R3A	clone mix	1,4842	0,0009516	0,0147555
PPP2R5C	clone mix	1,11008	0,0001345	0,00294467
PPP4R1L	clone mix	1,02255	0,002142	0,0283528
PPT2	clone mix	2,3316	4,21E-007	2,23E-005
PPTC7 (1 of 2)	clone mix	1,54193	0,0006118	0,0102947
PRADC1	clone mix	-1,7438	0,0001433	0,00310418
PRDM16	clone mix	2,46786	0,0017668	0,0242928
PRDX3	clone mix	-0,556329	1,04E-009	1,22E-007
PRELP	clone mix	1,29964	0,0014764	0,0210352
PREX1	clone mix	1,65518	8,51E-005	0,0020101
PRKCA (2 of 2)	clone mix	1,26312	0,0003442	0,00642398
PRKDC	clone mix	1,05364	1,39E-005	0,00043887
PRR14L	clone mix	1,47179	0,0027958	0,0350235
PRRC2B	clone mix	1,12363	0,0038551	0,0451159
PSENEN	clone mix	-1,65368	4,31E-005	0,00113717
PSMA3	clone mix	-0,990015	0,0005136	0,00892639
PSMA8	clone mix	-1,23066	7,13E-005	0,00173444
PSME4 (1 of 2)	clone mix	1,29137	0,001305	0,0190559
PTGES3 (2 of 2)	clone mix	-1,1347	0,0035228	0,042031

gene	sample_2	log2(fold_change)	p_value	q_value
PTGIS (2 of 2)	clone mix	1,80526	2,23E-005	0,00065344
PTPMT1	clone mix	-1,05691	2,13E-013	6,14E-011
PTPN1	clone mix	1,62685	0,0006217	0,0104321
PTPN9	clone mix	2,81856	8,34E-005	0,00197533
PTPRB	clone mix	2,26292	1,84E-006	7,85E-005
PTPRD	clone mix	1,89604	5,25E-009	5,02E-007
PTPRF (2 of 2)	clone mix	1,31407	0,0035081	0,0418906
PTPRJ	clone mix	1,66511	7,46E-005	0,00180008
PTPRK	clone mix	1,26294	0,0034915	0,0417345
PTPRS (1 of 3)	clone mix	1,55095	0,0005758	0,00979633
PTTG1IP (1 of 2)	clone mix	-1,37292	0,0035685	0,0424611
PWP2	clone mix	0,967521	2,97E-005	0,00083166
PXDN	clone mix	1,6366	0,0001007	0,00231479
QRICH1 (2 of 2)	clone mix	1,0804	0,0025195	0,032263
RABGAP1L	clone mix	1,42795	0,0014061	0,0202292
RAD54L2 (1 of 2)	clone mix	1,31989	0,0022876	0,0298693
RALGAPB	clone mix	1,28552	0,0008716	0,0137304
RAPGEF1	clone mix	1,51866	0,0014003	0,0201643
RAPGEF6	clone mix	1,6209	0,0005116	0,00889854
RAPH1 (1 of 2)	clone mix	2,45057	0,0003405	0,00636735
RARG (2 of 2)	clone mix	1,54453	0,0009637	0,0149075
RASAL3 (2 of 2)	clone mix	1,23246	0,0043061	0,0491625
RASGEF1B (1 of 2)	clone mix	2,0876	0,0004269	0,00767428
RASGEF1B (2 of 2)	clone mix	3,50041	1,25E-007	7,85E-006
RASSF6	clone mix	-1,33047	0,0014837	0,0211169
RASSF7 (1 of 2)	clone mix	1,15176	0,0034465	0,0413172
RBM25 (1 of 2)	clone mix	1,56752	7,72E-005	0,00185206
RBM45	clone mix	0,806559	0,0009748	0,0150477
RBM5 (2 of 2)	clone mix	1,14031	0,0005176	0,00898436
RBMS1 (2 of 2)	clone mix	1,52473	2,79E-005	0,00078968
RECK	clone mix	1,58701	0,0025866	0,0329407
REEP5	clone mix	-1,38541	0,0024872	0,0319302
RERE	clone mix	1,17793	0,0025846	0,0329209
RGL1	clone mix	2,13087	1,15E-005	0,00037404
RGL2	clone mix	0,890003	0,0010272	0,0157002
RGS5	clone mix	0,590287	0,0025012	0,0320757
RHPN2	clone mix	1,34411	0,0014574	0,0208147
RICTOR	clone mix	1,24674	0,0017603	0,0242227
RIN3	clone mix	1,37589	0,000585	0,00992426
RNF19B	clone mix	1,5853	9,39E-006	0,00031426
RNPEPL1	clone mix	1,26631	0,0018535	0,025258
ROCK1	clone mix	1,1926	0,0013755	0,0198782
ROCK2 (1 of 2)	clone mix	1,5438	0,0004986	0,0087124
ROCK2 (2 of 2)	clone mix	1,26643	0,0015179	0,0215076
RPA3	clone mix	-1,81933	2,14E-005	0,00063159
RPL22L1	clone mix	-1,2272	0,0015563	0,0219441
RPLP2	clone mix	-1,47352	0,00115114	0,0172258
RPS29	clone mix	-1,91107	2,22E-016	1,07E-013
RPTOR	clone mix	1,47385	0,0007361	0,0119719
RYR1 (1 of 2)	clone mix	1,16688	0,003779	0,0444224
RYR1 (2 of 2)	clone mix	1,32321	0,0012067	0,017891
S100A1	clone mix	-4,206	6,62E-005	0,00162985
S100A10 (1 of 2)	clone mix	-1,83685	6,87E-006	0,00024112

gene	sample_2	log2(fold_change)	p_value	q_value
SAFB	clone mix	1,31669	0,0006592	0,0109403
SAMD10	clone mix	-1,48231	0,0025135	0,0322005
SAMSN1	clone mix	1,32175	0,0003426	0,00640068
SARNP	clone mix	-1,36723	0,0005113	0,00889393
SBNO2	clone mix	1,78291	4,87E-006	0,00018037
SCARA3	clone mix	1,78097	0,0023627	0,0306475
SCARF2	clone mix	2,72884	1,02E-005	0,00033579
SCGN (1 of 2)	clone mix	-1,96895	1,71E-005	0,00052319
SCTR	clone mix	-1,28593	0,0030624	0,0376535
SDC2	clone mix	1,14154	0,0043171	0,0492606
SDHAF2	clone mix	-0,778801	8,49E-005	0,00200615
SEC14L1 (1 of 2)	clone mix	1,32445	1,06E-005	0,00034817
SEC16A	clone mix	1,36654	0,0006502	0,0108178
SELE	clone mix	2,25665	3,53E-006	0,00013728
SELENBP1	clone mix	-2,66047	6,77E-007	3,35E-005
SEMA3D	clone mix	1,5052	0,0026232	0,0333052
SEMA4B (1 of 2)	clone mix	1,83003	0,001895	0,0257081
SEMA4C	clone mix	1,9183	0,0021004	0,0279119
SEPT9 (1 of 2)	clone mix	0,614001	0,0018448	0,0251641
SESN1	clone mix	1,35397	0,0016875	0,0234185
SF3B5	clone mix	-1,5325	9,41E-005	0,00218524
SFI1	clone mix	1,54495	0,0031433	0,038429
SFPQ	clone mix	0,990684	0,0005581	0,00955298
SFRP2	clone mix	1,83627	9,94E-005	0,00228861
SFSWAP	clone mix	1,57078	1,76E-006	7,58E-005
SH3BP1	clone mix	1,43575	4,31E-006	0,00016237
SH3BP2	clone mix	2,24389	0,0003691	0,00680614
SH3PXD2B	clone mix	1,67444	0,0004058	0,00736079
SHANK2	clone mix	2,20616	0,0009674	0,0149544
SHFM1	clone mix	-1,43562	0,0001754	0,00367245
SHROOM3	clone mix	1,86113	0,0001186	0,00265217
SIK1	clone mix	2,48444	1,61E-006	7,04E-005
SIK2	clone mix	1,39607	0,0003992	0,00726179
SKIL	clone mix	1,61697	0,0029608	0,0366725
SLC11A2 (1 of 2)	clone mix	1,45661	0,001681	0,0233435
SLC16A1 (1 of 2)	clone mix	1,76292	2,92E-005	0,00082045
SLC16A2	clone mix	2,45192	2,22E-005	0,0006524
SLC1A5	clone mix	1,79334	0,0001259	0,00278716
SLC20A1 (1 of 2)	clone mix	1,50606	0,0004984	0,00870914
SLC25A25 (2 of 2)	clone mix	1,86451	0,0005294	0,00915112
SLC27A2 (2 of 3)	clone mix	1,62602	0,0019832	0,0266592
SLC37A2 (1 of 2)	clone mix	0,710298	0,0015821	0,0222332
SLC38A10	clone mix	1,45508	0,002306	0,0300593
SLC38A2	clone mix	1,58625	0,0003151	0,0059706
SLC4A2 (3 of 3)	clone mix	2,01217	0,0017048	0,023608
SLC4A4 (1 of 2)	clone mix	0,759482	3,14E-007	1,73E-005
SLC9A5	clone mix	-3,91334	2,55E-012	5,80E-010
SLCO2A1	clone mix	2,67898	4,29E-009	4,21E-007
SLIRP	clone mix	-1,64959	0,0003749	0,00689572
SLIT1	clone mix	2,10058	1,95E-006	8,27E-005
SLIT2	clone mix	2,20422	0,000615	0,0103398
SLIT3	clone mix	1,6756	0,0001517	0,00325552
SMOX	clone mix	2,99311	1,95E-013	5,68E-011

gene	sample_2	log2(fold_change)	p_value	q_value
SMTN	clone mix	1,41508	0,0010022	0,0153897
SNRNP27	clone mix	-1,2544	0,0018229	0,024922
SNRNP70	clone mix	1,44364	4,65E-013	1,25E-010
SNRPD2	clone mix	-1,64929	2,98E-005	0,00083414
SNRPE	clone mix	-1,28508	0,0009913	0,0152543
SNX1 (2 of 2)	clone mix	1,02927	5,83E-005	0,00146557
SNX18 (1 of 2)	clone mix	1,61846	0,0019981	0,0268223
SNX33	clone mix	1,17631	0,0036154	0,0429039
SNX9	clone mix	0,705947	0,0016876	0,0234195
SOCS3 (1 of 2)	clone mix	3,72776	1,04E-014	3,85E-012
SOCS3 (2 of 2)	clone mix	2,97734	2,75E-006	0,00011111
SORBS3	clone mix	1,78808	0,0001495	0,00321661
SOS1	clone mix	1,17081	0,0001619	0,00343688
SPAG9 (1 of 2)	clone mix	1,38311	0,0008611	0,0135957
SPCS1	clone mix	-1,71541	1,15E-005	0,00037293
SPCS3	clone mix	-1,59879	5,79E-005	0,0014582
SPEN (2 of 2)	clone mix	1,43775	0,0002596	0,00508737
SPTBN1 (1 of 2)	clone mix	1,70488	4,62E-006	0,0001724
SPTBN1 (2 of 2)	clone mix	1,954	4,09E-007	2,17E-005
SRCAP	clone mix	1,49197	0,0009474	0,0147029
SREBF2	clone mix	1,47166	0,0010965	0,0165575
SRF (2 of 2)	clone mix	2,07322	0,0017872	0,0245192
SRGAP3 (2 of 2)	clone mix	1,36029	0,0005903	0,00999705
SRSF5	clone mix	1,61625	0,0001184	0,00264771
SRSF7	clone mix	0,975591	7,24E-005	0,00175606
STEAP4 (1 of 2)	clone mix	1,35154	0,0006004	0,0101377
STK17B	clone mix	1,34915	0,0019495	0,0262916
STMN1 (2 of 2)	clone mix	-1,44567	1,44E-011	2,75E-009
SULF1	clone mix	1,38388	0,0002092	0,00425412
SUMO4	clone mix	-1,58727	0,0001497	0,00322085
SUPT5H	clone mix	0,711749	5,96E-005	0,00149382
SUPT6H	clone mix	1,02009	7,62E-005	0,00183145
SWAP70 (1 of 2)	clone mix	1,55995	9,20E-007	4,36E-005
SYNE1 (2 of 2)	clone mix	1,48041	0,0002474	0,00488905
SYNE2 (3 of 3)	clone mix	1,2968	0,0014343	0,0205502
TANC1 (1 of 2)	clone mix	1,24175	4,23E-006	0,00016011
TANC2 (1 of 2)	clone mix	1,04652	0,0018308	0,025009
TAOK1 (1 of 2)	clone mix	1,45462	0,0007491	0,0121432
TARBP1	clone mix	1,58312	0,001339	0,019451
TARS	clone mix	0,910829	0,0040427	0,0468144
TATDN3	clone mix	-0,961499	2,31E-005	0,00067379
TBC1D1	clone mix	1,02151	0,0002348	0,00468332
TBC1D7	clone mix	-1,20832	0,002827	0,0353363
TBCB	clone mix	-1,59075	3,91E-006	0,00014949
TCERG1	clone mix	0,837936	0,001754	0,0241534
TCF3 (1 of 2)	clone mix	1,22193	0,0003945	0,00719105
TECPR2	clone mix	1,23381	0,0027174	0,0342437
TEF (1 of 2)	clone mix	2,6477	8,17E-008	5,44E-006
TENC1 (1 of 2)	clone mix	2,21059	9,11E-008	5,97E-006
TEP1	clone mix	1,36848	0,000428	0,00769127
TF	clone mix	-2,01686	0,0006484	0,0107935
TG	clone mix	4,10894	3,11E-015	1,26E-012
TGFB1	clone mix	1,54946	1,05E-005	0,00034558

gene	sample_2	log2(fold_change)	p_value	q_value
TGFB1I1	clone mix	2,25787	0,0005879	0,00996345
TGFBR3	clone mix	1,20837	0,001182	0,0175962
THBS1 (2 of 2)	clone mix	3,72154	4,96E-013	1,32E-010
THBS2 (1 of 2)	clone mix	2,41909	6,13E-006	0,00021913
THBS4 (1 of 2)	clone mix	1,80428	5,97E-006	0,00021416
THOC2	clone mix	1,16643	0,003106	0,0380681
THOC7	clone mix	-1,35791	0,0016033	0,0224724
THRA (1 of 2)	clone mix	1,73506	0,0042081	0,0482999
TIE1	clone mix	1,7574	0,0002071	0,00421822
TIMM8A	clone mix	-1,62349	7,08E-005	0,00172314
TIMM9	clone mix	-1,48041	0,0037115	0,0438023
TIMP2 (1 of 2)	clone mix	1,4363	0,0001471	0,003174
TIMP2 (2 of 2)	clone mix	1,28131	0,0016455	0,02295
TIMP3	clone mix	2,08806	2,57E-006	0,00010478
TINAGL1	clone mix	1,99684	1,59E-006	6,96E-005
TJP1 (2 of 2)	clone mix	1,54611	5,52E-005	0,0013997
TJP3	clone mix	1,16507	0,0026806	0,0338773
TK2	clone mix	-0,727228	0,0013378	0,019437
TMC8	clone mix	1,11575	9,12E-006	0,0003065
TMEM14E	clone mix	-1,51153	0,0007049	0,011559
TMEM18	clone mix	-1,58365	4,68E-005	0,00122017
TMEM2	clone mix	1,88846	0,0001453	0,00314141
TMEM54 (1 of 2)	clone mix	-1,12412	6,13E-013	1,60E-010
TMOD1	clone mix	1,56413	0,0030194	0,0372437
TNIK (2 of 2)	clone mix	1,09572	0,0036257	0,043003
TNKS (2 of 2)	clone mix	1,5979	0,0021728	0,0286705
TNNI2 (5 of 5)	clone mix	-2,3038	9,94E-005	0,00228963
TNPO1	clone mix	1,29952	0,0017628	0,0242486
TNRC18 (1 of 2)	clone mix	1,6305	0,0006087	0,0102516
TNRC18 (2 of 2)	clone mix	1,30764	0,0016956	0,0235072
TNRC6C (2 of 2)	clone mix	1,47264	0,0018324	0,0250261
TNS1 (1 of 2)	clone mix	1,75016	3,73E-005	0,00100768
TNS1 (2 of 2)	clone mix	1,93444	0,0003135	0,0059459
TOB1 (2 of 2)	clone mix	0,871034	0,0003049	0,00580974
TOP2B	clone mix	1,51499	0,0006864	0,0113076
TOR1B	clone mix	-0,648802	0,0014369	0,0205818
TPPP3	clone mix	1,61326	0,0040793	0,0471378
TRIM8 (1 of 2)	clone mix	1,27629	0,0034105	0,0409784
TRIO (2 of 2)	clone mix	1,55555	0,0003681	0,00679078
TRIP10 (1 of 2)	clone mix	1,45215	0,0028728	0,035794
TRPM4 (2 of 2)	clone mix	1,18494	0,003457	0,0414147
TRRAP	clone mix	1,24203	0,0026967	0,0340412
TSC22D3	clone mix	3,20421	7,42E-011	1,18E-008
TSHZ3 (2 of 2)	clone mix	1,88851	0,0016207	0,0226662
TTC14	clone mix	1,37838	0,0017181	0,0237531
TTC32	clone mix	-1,67312	0,0027037	0,0341089
TTC36	clone mix	-2,17972	1,43E-005	0,00044956
TTN	clone mix	1,85068	0,0001616	0,00343055
TXNDC17	clone mix	-1,25532	0,0020475	0,0273486
TXNL4A	clone mix	-1,40504	0,0003818	0,00699903
UBE3B	clone mix	1,2876	0,0037476	0,044131
UBL5	clone mix	-1,79158	1,83E-005	0,00055376
UBP1	clone mix	1,14038	0,0010214	0,0156282

gene	sample_2	log2(fold_change)	p_value	q_value
UBR4	clone mix	1,35428	0,0012627	0,0185597
UBTD1 (2 of 2)	clone mix	-1,0295	1,64E-007	9,90E-006
ULK2	clone mix	1,61131	0,0001342	0,0029383
UNC13B (2 of 2)	clone mix	1,78858	0,0012606	0,0185351
UPF1 (2 of 2)	clone mix	1,15737	0,0038849	0,0453915
UQCR10	clone mix	-1,37075	0,0019636	0,0264467
UQCRB	clone mix	-1,45922	0,0001982	0,00406727
UQCRH (1 of 2)	clone mix	-1,90668	5,90E-006	0,00021211
USO1	clone mix	0,692411	0,0023926	0,0309621
USP24	clone mix	1,34281	0,0007943	0,0127364
USP34	clone mix	1,22812	0,0016601	0,0231127
USP9X	clone mix	1,25591	0,00132	0,0192319
USPL1	clone mix	1,39397	0,0030682	0,03771
UTRN	clone mix	1,28776	0,0020937	0,0278423
UXT	clone mix	-1,34292	0,0029748	0,0368089
VAV3 (2 of 2)	clone mix	1,12506	0,0005817	0,00987833
VHL	clone mix	-1,24329	0,0016499	0,0229999
VIT	clone mix	1,28509	0,0010349	0,0157965
VPS13A	clone mix	1,30029	0,0006287	0,0105281
VPS13C	clone mix	1,07078	1,61E-013	4,77E-011
VPS13D	clone mix	1,3113	0,0010487	0,0159675
VWF	clone mix	2,02221	1,46E-006	6,46E-005
WAC (1 of 2)	clone mix	0,9681	0,0001862	0,00386105
WAPAL (2 of 2)	clone mix	0,650213	0,0018842	0,0255925
WASL	clone mix	0,738968	0,004353	0,0495703
WDFY3	clone mix	1,83562	3,94E-005	0,00105516
WDFY4	clone mix	1,02484	0,0001037	0,00237078
WDR90	clone mix	1,4556	0,0037671	0,0443133
WNK1 (1 of 2)	clone mix	1,17979	0,0030923	0,0379413
WNK1 (2 of 2)	clone mix	1,32838	0,0015632	0,022023
WSB2	clone mix	1,25118	0,0017601	0,0242205
XPO4 (1 of 2)	clone mix	1,1487	0,0037992	0,0446058
XRN2	clone mix	0,736139	0,004344	0,0494943
XYLT2	clone mix	2,03662	0,0029554	0,0366197
YEATS4	clone mix	-1,32467	0,0039827	0,0462731
YTHDC1	clone mix	1,28033	0,0035919	0,0426872
ZBTB20	clone mix	1,42414	0,002074	0,0276285
ZC3H11A	clone mix	1,49262	0,0001893	0,00391328
ZC3H12A (1 of 2)	clone mix	1,30748	0,0015109	0,0214279
ZC3H12A (2 of 2)	clone mix	1,1617	0,0038391	0,0449722
ZC3HAV1	clone mix	0,829933	8,28E-006	0,00028265
ZCCHC8	clone mix	0,760552	0,0010209	0,0156228
ZCRB1	clone mix	-1,25851	0,0043468	0,049518
ZEB2 (1 of 2)	clone mix	1,8126	0,0005175	0,00898338
ZFAND5 (1 of 2)	clone mix	1,40369	0,0020149	0,0270023
ZFC3H1	clone mix	1,65096	5,81E-007	2,94E-005
ZFHX3	clone mix	1,25615	0,0008133	0,0129802
ZFHX4	clone mix	1,9537	4,19E-005	0,00111064
ZFP36	clone mix	2,66095	4,12E-009	4,07E-007
ZHX2 (2 of 2)	clone mix	2,62291	0,0042073	0,0482935
ZNF292 (1 of 2)	clone mix	1,2329	0,0039968	0,046403
ZNF292 (2 of 2)	clone mix	1,52993	0,0006569	0,0109085
ZNF521	clone mix	1,87348	4,62E-005	0,0012066

gene	sample_2	log2(fold_change)	p_value	q_value
ZNF593	clone mix	-0,935372	0,0010378	0,0158333
ZNF646 (2 of 3)	clone mix	1,50275	0,0003858	0,0070605
ZNF711	clone mix	0,974845	0,0028841	0,0359072
ZNFX1	clone mix	1,64115	0,0002284	0,00457582
ZZEF1	clone mix	1,18647	0,0019496	0,0262921
ABL2	clone XII	1,71619	0,003217	0,0391373
ACP1	clone XII	-0,936496	0,0015726	0,0221283
ACSL4	clone XII	1,17819	2,20E-005	0,00064764
ADAM8 (1 of 2)	clone XII	2,81508	0,0005305	0,00916727
ADAMTS15 (2 of 2)	clone XII	2,4143	0,0041499	0,0477789
ADPRHL1	clone XII	4,69151	0,000127	0,0028064
ALPK3 (1 of 2)	clone XII	3,46598	0,0004928	0,00862902
ALPK3 (2 of 2)	clone XII	2,14886	0,0036776	0,0434877
ALPL	clone XII	1,18492	0,0035557	0,0423446
ANO9 (1 of 2)	clone XII	-0,748815	0,0037834	0,044463
AOC2	clone XII	2,51015	4,03E-006	0,00015373
ARRDC2	clone XII	2,44276	0,0016101	0,0225474
BAG3	clone XII	2,40186	0,0010202	0,0156133
BAG6 (1 of 2)	clone XII	0,849364	0,0014168	0,0203509
BAG6 (2 of 2)	clone XII	0,530867	0,0040542	0,0469169
BMP1 (1 of 2)	clone XII	1,65706	0,0039855	0,0462977
C4A	clone XII	1,15954	5,32E-009	5,08E-007
C6	clone XII	1,48911	0,0010866	0,0164358
CASQ2 (1 of 2)	clone XII	1,40759	0,003079	0,0378144
CBX7 (2 of 2)	clone XII	1,41355	0,0007368	0,0119811
CEBPB	clone XII	2,42574	0,0001205	0,00268807
CSNK1E (2 of 2)	clone XII	0,95828	0,0019388	0,0261808
DAB2	clone XII	1,47193	6,17E-005	0,00153559
DDIT4 (1 of 2)	clone XII	3,69054	2,10E-006	8,82E-005
DENND4A (2 of 2)	clone XII	3,45285	8,91E-005	0,00208854
DHRS13 (1 of 3)	clone XII	-1,49902	5,04E-006	0,00018578
DIO3	clone XII	3,01096	0,0006606	0,0109589
EDNRA	clone XII	2,11959	0,0033693	0,0405912
EHF	clone XII	-2,01067	0	0
EIF5B	clone XII	0,718096	0,0008796	0,0138336
ENSGACG00000000208	clone XII	3,44122	7,08E-005	0,00172361
ENSGACG00000000272	clone XII	2,02155	0,0007136	0,011674
ENSGACG00000000300	clone XII	2,21811	0,0014653	0,0209078
ENSGACG00000000849	clone XII	3,2855	0,0021198	0,0281181
ENSGACG00000001749	clone XII	2,97222	0,0003272	0,00616061
ENSGACG00000002902	clone XII	2,89507	0,0002357	0,00469788
ENSGACG00000002933	clone XII	3,33311	1,92E-006	8,14E-005
ENSGACG00000003003	clone XII	3,48081	0,0030598	0,0376296
ENSGACG00000003464	clone XII	1,44878	0,0037581	0,0442279
ENSGACG00000003612,STK35 (1 of 2)	clone XII	1,81609	1,92E-007	1,13E-005
ENSGACG00000004079	clone XII	4,49951	8,44E-006	0,00028709
ENSGACG00000004200	clone XII	2,31873	0,000464	0,00821685
ENSGACG00000005904	clone XII	2,9548	8,41E-006	0,00028631
ENSGACG00000006048	clone XII	2,6865	0,002418	0,0312234
ENSGACG00000006109	clone XII	5,29596	6,57E-006	0,00023243
ENSGACG00000006530	clone XII	1,98222	0,0010583	0,0160868
ENSGACG00000007447	clone XII	-1,68661	0,0004396	0,00786092
ENSGACG00000007661	clone XII	5,71207	3,10E-005	0,00086201

gene	sample_2	log2(fold_change)	p_value	q_value
ENSGACG00000008353	clone XII	2,38765	0,0008087	0,012922
ENSGACG00000008661,ENSGACG00000	clone XII	0,879168	0,0029556	0,0366216
ENSGACG00000008779	clone XII	-0,99187	8,00E-005	0,00190918
ENSGACG00000008872	clone XII	-1,22474	0,0039624	0,0460921
ENSGACG00000009229	clone XII	-2,08331	0,0003682	0,00679296
ENSGACG00000009520,ENSGACG00000	clone XII	1,0074	0,0030575	0,0376081
ENSGACG00000009715	clone XII	1,44465	0,0002091	0,00425162
ENSGACG00000009825	clone XII	2,23619	1,77E-007	1,06E-005
ENSGACG00000010050	clone XII	2,23323	6,46E-006	0,00022909
ENSGACG00000010476	clone XII	4,15084	1,61E-010	2,33E-008
ENSGACG00000010478	clone XII	1,98345	0,0041169	0,04748
ENSGACG00000010501	clone XII	-1,52744	4,78E-006	0,00017757
ENSGACG00000010623	clone XII	8,74215	7,37E-008	4,97E-006
ENSGACG00000011294	clone XII	1,5189	1,12E-005	0,00036514
ENSGACG00000011767	clone XII	3,52681	0,0035157	0,0419643
ENSGACG00000012657	clone XII	7,46295	1,85E-008	1,50E-006
ENSGACG00000012663	clone XII	2,72269	0,00033	0,00620401
ENSGACG00000013327	clone XII	3,31805	0,0002644	0,00516375
ENSGACG00000013782	clone XII	3,77565	1,16E-005	0,00037448
ENSGACG00000014109	clone XII	1,89089	0,004339	0,0494517
ENSGACG00000014948	clone XII	8,09567	3,06E-005	0,0008537
ENSGACG00000014960	clone XII	2,55214	0,0031035	0,0380444
ENSGACG00000018580	clone XII	2,30513	1,74E-005	0,00052994
ENSGACG00000018802	clone XII	2,16961	0,0002563	0,00503493
ENSGACG00000018840	clone XII	2,49532	2,57E-007	1,46E-005
ENSGACG00000019023	clone XII	0,647488	0,0014032	0,0201973
ENSGACG00000019819	clone XII	-1,78849	0,0031727	0,0387159
ENSGACG00000019951	clone XII	2,4068	0,0037367	0,0440323
ENSGACG00000019952	clone XII	2,48159	9,45E-005	0,00219424
ENSGACG00000020145	clone XII	3,16214	9,27E-007	4,39E-005
ENSGACG00000020852	clone XII	1,89304	0,001604	0,0224793
F8	clone XII	2,52914	0,0008433	0,0133667
FHL1 (1 of 2)	clone XII	1,29869	0,0016597	0,0231076
FHOD3 (1 of 2)	clone XII	2,44033	0,0013946	0,0200974
FKBP5	clone XII	4,47993	1,28E-008	1,09E-006
FMNL1 (2 of 2)	clone XII	0,608382	0,00331117	0,0400362
FOSL1	clone XII	4,41723	0,0018847	0,0255974
GADD45B (1 of 2)	clone XII	1,54716	0,0037936	0,0445552
GADD45G (1 of 3)	clone XII	2,01489	0,0005543	0,00949883
GLB1L	clone XII	2,05182	8,65E-005	0,00203729
GPX3	clone XII	2,88363	0,0039939	0,0463754
HGF (1 of 2)	clone XII	3,05781	0,0003716	0,0068446
HSP90AA1 (2 of 2)	clone XII	2,83595	0,0010858	0,0164249
IGFBP1 (1 of 2)	clone XII	2,76504	0,0042645	0,0488
IRS2 (1 of 2)	clone XII	2,06855	0,0019171	0,0259422
ITGA5 (1 of 2)	clone XII	2,69698	0,0026006	0,0330809
ITGB1 (1 of 2)	clone XII	0,629352	2,54E-005	0,00072976
JUNB (2 of 2)	clone XII	2,0575	0,0021262	0,0281882
KCNB1	clone XII	3,35689	3,52E-008	2,62E-006
KIAA0907	clone XII	1,04458	0,0002769	0,00536508
KLF9	clone XII	3,36244	1,65E-006	7,18E-005
KLHL30	clone XII	2,23929	0,0005901	0,009995
KLHL38 (2 of 2)	clone XII	3,06114	0,0001186	0,00265181

gene	sample_2	log2(fold_change)	p_value	q_value
LMOD2 (1 of 2)	clone XII	2,65843	0,0002852	0,00549748
LRRFIP1 (1 of 2)	clone XII	1,48271	1,28E-007	8,00E-006
MAD2L2	clone XII	-1,53477	0,0005821	0,0098846
MKL2 (2 of 2)	clone XII	2,06823	0,0028171	0,0352331
MMP9	clone XII	1,84036	0,0004848	0,00851444
MRPS10	clone XII	-0,949657	0,001061	0,0161199
MYL7	clone XII	8,00201	4,45E-007	2,33E-005
MYLK	clone XII	1,91033	0,0031178	0,03818
MYLK4 (1 of 2)	clone XII	3,66086	0,0002184	0,00441022
MYOM1 (2 of 2)	clone XII	0,845752	0,003683	0,0435377
NAPSA	clone XII	1,21821	4,34E-007	2,29E-005
NAV3	clone XII	2,72356	1,46E-005	0,00045693
NID2	clone XII	1,35594	0,0003728	0,00686296
NR1D2 (2 of 2)	clone XII	2,48143	0,0001907	0,00393907
OBSL1 (2 of 2)	clone XII	1,66439	0,0016022	0,0224604
PCDH20	clone XII	2,63281	0,0016473	0,022971
PDK2 (2 of 2)	clone XII	2,30963	0,000429	0,00770546
PDLIM2	clone XII	0,929548	0,0012074	0,0178988
PPP1R15B	clone XII	2,09803	0,0003971	0,00723149
PPT2	clone XII	1,88014	0,0041917	0,0481513
PTGIS (2 of 2)	clone XII	1,66641	0,0023446	0,0304657
PTRF (1 of 2)	clone XII	1,91687	0,0005214	0,00903934
RNF19B	clone XII	1,22362	0,0006173	0,0103695
RPS29	clone XII	-0,94273	0,0012327	0,0182012
SCN4A (2 of 2)	clone XII	3,59807	8,44E-006	0,00028706
SLC25A43	clone XII	1,12733	1,60E-005	0,00049419
SLC25A44 (2 of 2)	clone XII	-0,920373	0,0004977	0,00869976
SLC3A2 (2 of 2)	clone XII	1,82001	0,0023198	0,0302066
SLC41A3 (1 of 2)	clone XII	4,73896	0,000638	0,0106543
SLC4A2 (3 of 3)	clone XII	2,5205	0,0002663	0,00519505
SLCO2A1	clone XII	2,68145	4,63E-005	0,00120776
SMOX	clone XII	3,1819	4,31E-014	1,42E-011
SOCS3 (1 of 2)	clone XII	3,31067	4,85E-006	0,00017958
SOCS3 (2 of 2)	clone XII	2,51164	0,0021381	0,0283133
SORBS2	clone XII	4,1215	0,0002797	0,00541025
SVIL (1 of 2)	clone XII	1,17834	0,0027908	0,0349739
TEF (1 of 2)	clone XII	2,22288	0,0017015	0,0235716
TG	clone XII	2,53461	0,0017886	0,0245357
THBS1 (2 of 2)	clone XII	3,70595	2,17E-005	0,00063812
TIMELESS	clone XII	3,42301	0,0024441	0,0314901
TMEM54 (1 of 2)	clone XII	-0,735023	1,90E-006	8,07E-005
TNNC1	clone XII	6,68797	2,33E-007	1,34E-005
TNNT2 (1 of 2)	clone XII	6,18283	2,94E-007	1,64E-005
TRIM63	clone XII	2,08566	0,0013545	0,0196346
TSC22D3	clone XII	2,19202	0,0009183	0,0143307
UCP2	clone XII	2,02682	0,0019288	0,0260708
VWA1 (2 of 2)	clone XII	-0,778383	1,24E-012	3,03E-010
WAC (1 of 2)	clone XII	1,17662	9,66E-005	0,00223429
ZFP36	clone XII	2,24571	0,0016177	0,0226335

Supplementary table S.2.4 Putative immune system related genes in three-spined stickleback. Gene names were obtained either via the ensembl biomart filter, querying the *Homo sapiens* transcriptome for genes belonging to "immune system process" (GO:0002376), or via a published list containing immune genes identified in cod (*Gadus morhua*) and pipefish (*Syngnathus typhle*).

stickleback_gene_name	human_gene_name	source
ACIN1	ACIN1	ensembl biomart, HSA, GO:0002376
ACTR1B	ACTR1B	ensembl biomart, HSA, GO:0002376
ADA	ADA	ensembl biomart, HSA, GO:0002376
ADAM10	ADAM10	ensembl biomart, HSA, GO:0002376
ADAM17 (1 of 2)	ADAM17	ensembl biomart, HSA, GO:0002376
ADAM17 (2 of 2)	ADAM17	ensembl biomart, HSA, GO:0002376
ADAM8 (1 of 2)	ADAM8	ensembl biomart, HSA, GO:0002376
ADAM8 (2 of 2)	ADAM8	ensembl biomart, HSA, GO:0002376
ADAM9	ADAM9	ensembl biomart, HSA, GO:0002376
ADAMTS13	ADAMTS13	ensembl biomart, HSA, GO:0002376
ADAR	ADAR	ensembl biomart, HSA, GO:0002376
ADORA3 (1 of 2)	ADORA3	ensembl biomart, HSA, GO:0002376
ADORA3 (2 of 2)	ADORA3	ensembl biomart, HSA, GO:0002376
ADSS	ADSS	ensembl biomart, HSA, GO:0002376
ADSSL1	ADSSL1	ensembl biomart, HSA, GO:0002376
AICDA	AICDA	ensembl biomart, HSA, GO:0002376
AIMP1 (1 of 2)	AIMP1	ensembl biomart, HSA, GO:0002376
AIMP1 (2 of 2)	AIMP1	ensembl biomart, HSA, GO:0002376
AK7 (1 of 2)	AK7	ensembl biomart, HSA, GO:0002376
AK7 (2 of 2)	AK7	ensembl biomart, HSA, GO:0002376
AKIRIN2 (1 of 2)	AKIRIN2	ensembl biomart, HSA, GO:0002376
AKIRIN2 (2 of 2)	AKIRIN2	ensembl biomart, HSA, GO:0002376
AKT1	AKT1	ensembl biomart, HSA, GO:0002376
ALAS2	ALAS2	ensembl biomart, HSA, GO:0002376
ANGPT1	ANGPT1	ensembl biomart, HSA, GO:0002376
ANGPT2	ANGPT2	ensembl biomart, HSA, GO:0002376
ANK1 (1 of 2)	ANK1	ensembl biomart, HSA, GO:0002376
ANK1 (2 of 2)	ANK1	ensembl biomart, HSA, GO:0002376
ANXA1 (1 of 2)	ANXA1	ensembl biomart, HSA, GO:0002376
ANXA1 (2 of 2)	ANXA1	ensembl biomart, HSA, GO:0002376
ANXA3 (1 of 2)	ANXA3	ensembl biomart, HSA, GO:0002376
ANXA3 (2 of 2)	ANXA3	ensembl biomart, HSA, GO:0002376
AP1B1	AP1B1	ensembl biomart, HSA, GO:0002376
AP1G1	AP1G1	ensembl biomart, HSA, GO:0002376
AP1M1	AP1M1	ensembl biomart, HSA, GO:0002376
AP1M2	AP1M2	ensembl biomart, HSA, GO:0002376
AP1S1	AP1S1	ensembl biomart, HSA, GO:0002376
AP1S2 (1 of 2)	AP1S2	ensembl biomart, HSA, GO:0002376
AP1S2 (2 of 2)	AP1S2	ensembl biomart, HSA, GO:0002376
AP1S3 (1 of 2)	AP1S3	ensembl biomart, HSA, GO:0002376
AP2A1	AP2A1	ensembl biomart, HSA, GO:0002376
AP2A2	AP2A2	ensembl biomart, HSA, GO:0002376
AP2B1	AP2B1	ensembl biomart, HSA, GO:0002376
AP2M1	AP2M1	ensembl biomart, HSA, GO:0002376
AP2S1	AP2S1	ensembl biomart, HSA, GO:0002376
AP3B1 (1 of 2)	AP3B1	ensembl biomart, HSA, GO:0002376

stickleback_gene_name	human_gene_name	source
AP3B1 (2 of 2)	AP3B1	ensembl biomart, HSA, GO:0002376
AP3D1	AP3D1	ensembl biomart, HSA, GO:0002376
APC	APC	ensembl biomart, HSA, GO:0002376
APOB (1 of 5)	APOB	ensembl biomart, HSA, GO:0002376
APOB (2 of 5)	APOB	ensembl biomart, HSA, GO:0002376
APOB (3 of 5)	APOB	ensembl biomart, HSA, GO:0002376
APOB (4 of 5)	APOB	ensembl biomart, HSA, GO:0002376
APOB (5 of 5)	APOB	ensembl biomart, HSA, GO:0002376
APP (1 of 2)	APP	ensembl biomart, HSA, GO:0002376
APP (2 of 2)	APP	ensembl biomart, HSA, GO:0002376
AQP4	AQP4	ensembl biomart, HSA, GO:0002376
AQP9 (1 of 2)	AQP9	ensembl biomart, HSA, GO:0002376
AQP9 (2 of 2)	AQP9	ensembl biomart, HSA, GO:0002376
ARG2	ARG2	ensembl biomart, HSA, GO:0002376
ARHGEF5	ARHGEF5	ensembl biomart, HSA, GO:0002376
ASS1	ASS1	ensembl biomart, HSA, GO:0002376
ATF1	ATF1	ensembl biomart, HSA, GO:0002376
ATF2	ATF2	ensembl biomart, HSA, GO:0002376
ATG12	ATG12	ensembl biomart, HSA, GO:0002376
ATG5	ATG5	ensembl biomart, HSA, GO:0002376
ATG9A	ATG9A	ensembl biomart, HSA, GO:0002376
ATM (1 of 2)	ATM	ensembl biomart, HSA, GO:0002376
ATM (2 of 2)	ATM	ensembl biomart, HSA, GO:0002376
ATP1B1 (1 of 2)	ATP1B1	ensembl biomart, HSA, GO:0002376
ATP1B1 (2 of 2)	ATP1B1	ensembl biomart, HSA, GO:0002376
ATP1B2 (1 of 2)	ATP1B2	ensembl biomart, HSA, GO:0002376
ATP1B2 (2 of 2)	ATP1B2	ensembl biomart, HSA, GO:0002376
ATP1B3	ATP1B3	ensembl biomart, HSA, GO:0002376
ATP6V0A2 (1 of 2)	ATP6V0A2	ensembl biomart, HSA, GO:0002376
ATP6V0A2 (2 of 2)	ATP6V0A2	ensembl biomart, HSA, GO:0002376
ATP7A	ATP7A	ensembl biomart, HSA, GO:0002376
AXL	AXL	ensembl biomart, HSA, GO:0002376
B4GALT1	B4GALT1	ensembl biomart, HSA, GO:0002376
BANK1	BANK1	ensembl biomart, HSA, GO:0002376
BARX1	BARX1	ensembl biomart, HSA, GO:0002376
BAX	BAX	ensembl biomart, HSA, GO:0002376
BCAP31	BCAP31	ensembl biomart, HSA, GO:0002376
BCL10	BCL10	ensembl biomart, HSA, GO:0002376
BCL11A (1 of 2)	BCL11A	ensembl biomart, HSA, GO:0002376
BCL11A (2 of 2)	BCL11A	ensembl biomart, HSA, GO:0002376
BCL2	BCL2	ensembl biomart, HSA, GO:0002376
BCL2L1 (1 of 2)	BCL2L1	ensembl biomart, HSA, GO:0002376
BCL2L1 (2 of 2)	BCL2L1	ensembl biomart, HSA, GO:0002376
BCL6 (1 of 2)	BCL6	ensembl biomart, HSA, GO:0002376
BCL6 (2 of 2)	BCL6	ensembl biomart, HSA, GO:0002376
BDKRB2 (1 of 4)	BDKRB2	ensembl biomart, HSA, GO:0002376
BDKRB2 (2 of 4)	BDKRB2	ensembl biomart, HSA, GO:0002376
BDKRB2 (3 of 4)	BDKRB2	ensembl biomart, HSA, GO:0002376
BDKRB2 (4 of 4)	BDKRB2	ensembl biomart, HSA, GO:0002376
BECN1	BECN1	ensembl biomart, HSA, GO:0002376
BLM	BLM	ensembl biomart, HSA, GO:0002376
BLMH	BLMH	ensembl biomart, HSA, GO:0002376
BLNK	BLNK	ensembl biomart, HSA, GO:0002376

stickleback_gene_name	human_gene_name	source
BMI1	BMI1	ensembl biomart, HSA, GO:0002376
BMP4	BMP4	ensembl biomart, HSA, GO:0002376
BMP6	BMP6	ensembl biomart, HSA, GO:0002376
BMPR1A	BMPR1A	ensembl biomart, HSA, GO:0002376
BNIP3	BNIP3	ensembl biomart, HSA, GO:0002376
BNIP3L (1 of 2)	BNIP3L	ensembl biomart, HSA, GO:0002376
BNIP3L (2 of 2)	BNIP3L	ensembl biomart, HSA, GO:0002376
BPGM	BPGM	ensembl biomart, HSA, GO:0002376
BRCA2	BRCA2	ensembl biomart, HSA, GO:0002376
BTK	BTK	ensembl biomart, HSA, GO:0002376
C11orf82	C11orf82	ensembl biomart, HSA, GO:0002376
C1QBP	C1QBP	ensembl biomart, HSA, GO:0002376
C1QC	C1QC	ensembl biomart, HSA, GO:0002376
C3 (1 of 8)	C3	ensembl biomart, HSA, GO:0002376
C3 (2 of 8)	C3	ensembl biomart, HSA, GO:0002376
C3 (3 of 8)	C3	ensembl biomart, HSA, GO:0002376
C3 (4 of 8)	C3	ensembl biomart, HSA, GO:0002376
C3 (5 of 8)	C3	ensembl biomart, HSA, GO:0002376
C3 (6 of 8)	C3	ensembl biomart, HSA, GO:0002376
C3 (7 of 8)	C3	ensembl biomart, HSA, GO:0002376
C3 (8 of 8)	C3	ensembl biomart, HSA, GO:0002376
C5AR1	C5AR1	ensembl biomart, HSA, GO:0002376
C6	C6	ensembl biomart, HSA, GO:0002376
C7 (1 of 2)	C7	ensembl biomart, HSA, GO:0002376
C7 (2 of 2)	C7	ensembl biomart, HSA, GO:0002376
C8A	C8A	ensembl biomart, HSA, GO:0002376
C8B	C8B	ensembl biomart, HSA, GO:0002376
C8G	C8G	ensembl biomart, HSA, GO:0002376
C9	C9	ensembl biomart, HSA, GO:0002376
CACNB4 (1 of 2)	CACNB4	ensembl biomart, HSA, GO:0002376
CACNB4 (2 of 2)	CACNB4	ensembl biomart, HSA, GO:0002376
CALCA	CALCA	ensembl biomart, HSA, GO:0002376
CALCR	CALCR	ensembl biomart, HSA, GO:0002376
CAMK2A	CAMK2A	ensembl biomart, HSA, GO:0002376
CAMK4	CAMK4	ensembl biomart, HSA, GO:0002376
CANX	CANX	ensembl biomart, HSA, GO:0002376
CARD11	CARD11	ensembl biomart, HSA, GO:0002376
CARD9	CARD9	ensembl biomart, HSA, GO:0002376
CASP3 (1 of 4)	CASP3	ensembl biomart, HSA, GO:0002376
CASP3 (2 of 4)	CASP3	ensembl biomart, HSA, GO:0002376
CASP3 (3 of 4)	CASP3	ensembl biomart, HSA, GO:0002376
CASP3 (4 of 4)	CASP3	ensembl biomart, HSA, GO:0002376
CASP8	CASP8	ensembl biomart, HSA, GO:0002376
CAV1	CAV1	ensembl biomart, HSA, GO:0002376
CBFA2T3	CBFA2T3	ensembl biomart, HSA, GO:0002376
CBFB	CBFB	ensembl biomart, HSA, GO:0002376
CBLB	CBLB	ensembl biomart, HSA, GO:0002376
CCNB2 (1 of 2)	CCNB2	ensembl biomart, HSA, GO:0002376
CCNB2 (2 of 2)	CCNB2	ensembl biomart, HSA, GO:0002376
CCR6 (1 of 2)	CCR6	ensembl biomart, HSA, GO:0002376
CCR6 (2 of 2)	CCR6	ensembl biomart, HSA, GO:0002376
CCR9 (1 of 2)	CCR9	ensembl biomart, HSA, GO:0002376
CCR9 (2 of 2)	CCR9	ensembl biomart, HSA, GO:0002376

stickleback_gene_name	human_gene_name	source
CCRL1 (1 of 2)	CCRL1	ensembl biomart, HSA, GO:0002376
CCRL1 (2 of 2)	CCRL1	ensembl biomart, HSA, GO:0002376
CD164	CD164	ensembl biomart, HSA, GO:0002376
CD276	CD276	ensembl biomart, HSA, GO:0002376
CD74 (1 of 2)	CD74	ensembl biomart, HSA, GO:0002376
CD93	CD93	ensembl biomart, HSA, GO:0002376
CD97 (1 of 2)	CD97	ensembl biomart, HSA, GO:0002376
CD97 (2 of 2)	CD97	ensembl biomart, HSA, GO:0002376
CDK1	CDK1	ensembl biomart, HSA, GO:0002376
CDK13	CDK13	ensembl biomart, HSA, GO:0002376
CDK6	CDK6	ensembl biomart, HSA, GO:0002376
CENPE	CENPE	ensembl biomart, HSA, GO:0002376
CFB	CFB	ensembl biomart, HSA, GO:0002376
CFI	CFI	ensembl biomart, HSA, GO:0002376
CFP	CFP	ensembl biomart, HSA, GO:0002376
CHD7	CHD7	ensembl biomart, HSA, GO:0002376
CHIA	CHIA	ensembl biomart, HSA, GO:0002376
CHID1	CHID1	ensembl biomart, HSA, GO:0002376
CHRNA4	CHRNA4	ensembl biomart, HSA, GO:0002376
CHRNB2	CHRNB2	ensembl biomart, HSA, GO:0002376
CHST3 (1 of 2)	CHST3	ensembl biomart, HSA, GO:0002376
CHST3 (2 of 2)	CHST3	ensembl biomart, HSA, GO:0002376
CHUK (1 of 2)	CHUK	ensembl biomart, HSA, GO:0002376
CHUK (2 of 2)	CHUK	ensembl biomart, HSA, GO:0002376
CIAPIN1	CIAPIN1	ensembl biomart, HSA, GO:0002376
CLEC4M	CLEC4M	ensembl biomart, HSA, GO:0002376
CLNK	CLNK	ensembl biomart, HSA, GO:0002376
CLTA	CLTA	ensembl biomart, HSA, GO:0002376
CLU	CLU	ensembl biomart, HSA, GO:0002376
CMKLR1 (1 of 2)	CMKLR1	ensembl biomart, HSA, GO:0002376
CMKLR1 (2 of 2)	CMKLR1	ensembl biomart, HSA, GO:0002376
CNN2	CNN2	ensembl biomart, HSA, GO:0002376
COL1A1 (1 of 2)	COL1A1	ensembl biomart, HSA, GO:0002376
COL1A1 (2 of 2)	COL1A1	ensembl biomart, HSA, GO:0002376
COL1A2	COL1A2	ensembl biomart, HSA, GO:0002376
COL4A3BP (1 of 2)	COL4A3BP	ensembl biomart, HSA, GO:0002376
COL4A3BP (2 of 2)	COL4A3BP	ensembl biomart, HSA, GO:0002376
COLEC12 (1 of 2)	COLEC12	ensembl biomart, HSA, GO:0002376
COLEC12 (2 of 2)	COLEC12	ensembl biomart, HSA, GO:0002376
CORO1A	CORO1A	ensembl biomart, HSA, GO:0002376
CPLX2	CPLX2	ensembl biomart, HSA, GO:0002376
CRCP	CRCP	ensembl biomart, HSA, GO:0002376
CREB1 (1 of 2)	CREB1	ensembl biomart, HSA, GO:0002376
CREB1 (2 of 2)	CREB1	ensembl biomart, HSA, GO:0002376
CREBBP (1 of 2)	CREBBP	ensembl biomart, HSA, GO:0002376
CREBBP (2 of 2)	CREBBP	ensembl biomart, HSA, GO:0002376
CRHR1	CRHR1	ensembl biomart, HSA, GO:0002376
CRIP2 (1 of 2)	CRIP2	ensembl biomart, HSA, GO:0002376
CRIP2 (2 of 2)	CRIP2	ensembl biomart, HSA, GO:0002376
CRISP3	CRISP3	ensembl biomart, HSA, GO:0002376
CRKL	CRKL	ensembl biomart, HSA, GO:0002376
CSF1R (1 of 2)	CSF1R	ensembl biomart, HSA, GO:0002376
CSF1R (2 of 2)	CSF1R	ensembl biomart, HSA, GO:0002376

stickleback_gene_name	human_gene_name	source
CSK (1 of 2)	CSK	ensembl biomart, HSA, GO:0002376
CSK (2 of 2)	CSK	ensembl biomart, HSA, GO:0002376
CTNNBL1	CTNNBL1	ensembl biomart, HSA, GO:0002376
CTSB	CTSB	ensembl biomart, HSA, GO:0002376
CTSC	CTSC	ensembl biomart, HSA, GO:0002376
CTSD	CTSD	ensembl biomart, HSA, GO:0002376
CTSE	CTSE	ensembl biomart, HSA, GO:0002376
CTSF	CTSF	ensembl biomart, HSA, GO:0002376
CTSH	CTSH	ensembl biomart, HSA, GO:0002376
CTSK	CTSK	ensembl biomart, HSA, GO:0002376
CTSS (1 of 2)	CTSS	ensembl biomart, HSA, GO:0002376
CTSS (2 of 2)	CTSS	ensembl biomart, HSA, GO:0002376
CXADR	CXADR	ensembl biomart, HSA, GO:0002376
CXCL12 (1 of 2)	CXCL12	ensembl biomart, HSA, GO:0002376
CXCL12 (2 of 2)	CXCL12	ensembl biomart, HSA, GO:0002376
CXCR4 (1 of 2)	CXCR4	ensembl biomart, HSA, GO:0002376
CXCR4 (2 of 2)	CXCR4	ensembl biomart, HSA, GO:0002376
CYBA	CYBA	ensembl biomart, HSA, GO:0002376
CYBB	CYBB	ensembl biomart, HSA, GO:0002376
CYFIP2	CYFIP2	ensembl biomart, HSA, GO:0002376
CYP19A1 (1 of 2)	CYP19A1	ensembl biomart, HSA, GO:0002376
CYP19A1 (2 of 2)	CYP19A1	ensembl biomart, HSA, GO:0002376
CYP27B1	CYP27B1	ensembl biomart, HSA, GO:0002376
CYSLTR2	CYSLTR2	ensembl biomart, HSA, GO:0002376
DAB2	DAB2	ensembl biomart, HSA, GO:0002376
DCLRE1C	DCLRE1C	ensembl biomart, HSA, GO:0002376
DCTN1 (1 of 2)	DCTN1	ensembl biomart, HSA, GO:0002376
DCTN1 (2 of 2)	DCTN1	ensembl biomart, HSA, GO:0002376
DCTN6 (1 of 2)	DCTN6	ensembl biomart, HSA, GO:0002376
DCTN6 (2 of 2)	DCTN6	ensembl biomart, HSA, GO:0002376
DDOST	DDOST	ensembl biomart, HSA, GO:0002376
DICER1	DICER1	ensembl biomart, HSA, GO:0002376
DNAJA3 (1 of 2)	DNAJA3	ensembl biomart, HSA, GO:0002376
DNAJA3 (2 of 2)	DNAJA3	ensembl biomart, HSA, GO:0002376
DNASE2	DNASE2	ensembl biomart, HSA, GO:0002376
DNM2 (1 of 2)	DNM2	ensembl biomart, HSA, GO:0002376
DNM2 (2 of 2)	DNM2	ensembl biomart, HSA, GO:0002376
DOCK2	DOCK2	ensembl biomart, HSA, GO:0002376
DOK2	DOK2	ensembl biomart, HSA, GO:0002376
DUSP3	DUSP3	ensembl biomart, HSA, GO:0002376
DUSP4	DUSP4	ensembl biomart, HSA, GO:0002376
DUSP6	DUSP6	ensembl biomart, HSA, GO:0002376
DUSP7 (1 of 2)	DUSP7	ensembl biomart, HSA, GO:0002376
DYNC1H1	DYNC1H1	ensembl biomart, HSA, GO:0002376
DYNC1I1	DYNC1I1	ensembl biomart, HSA, GO:0002376
DYNC1I2 (1 of 2)	DYNC1I2	ensembl biomart, HSA, GO:0002376
DYNC1I2 (2 of 2)	DYNC1I2	ensembl biomart, HSA, GO:0002376
DYNC1LI2	DYNC1LI2	ensembl biomart, HSA, GO:0002376
DYNC2H1	DYNC2H1	ensembl biomart, HSA, GO:0002376
DYNC2LI1	DYNC2LI1	ensembl biomart, HSA, GO:0002376
DYNLL2	DYNLL2	ensembl biomart, HSA, GO:0002376
EBI3	EBI3	ensembl biomart, HSA, GO:0002376
EDA	EDA	ensembl biomart, HSA, GO:0002376

stickleback_gene_name	human_gene_name	source
EDN2	EDN2	ensembl biomart, HSA, GO:0002376
EDNRB (1 of 2)	EDNRB	ensembl biomart, HSA, GO:0002376
EDNRB (2 of 2)	EDNRB	ensembl biomart, HSA, GO:0002376
EFNA2	EFNA2	ensembl biomart, HSA, GO:0002376
EGR1	EGR1	ensembl biomart, HSA, GO:0002376
EIF2AK2 (1 of 2)	EIF2AK2	ensembl biomart, HSA, GO:0002376
EIF2AK2 (2 of 2)	EIF2AK2	ensembl biomart, HSA, GO:0002376
ELK1	ELK1	ensembl biomart, HSA, GO:0002376
ELMOD2	ELMOD2	ensembl biomart, HSA, GO:0002376
EMR2	EMR2	ensembl biomart, HSA, GO:0002376
ENDOU	ENDOU	ensembl biomart, HSA, GO:0002376
ENPP1	ENPP1	ensembl biomart, HSA, GO:0002376
ENPP2 (1 of 2)	ENPP2	ensembl biomart, HSA, GO:0002376
ENPP2 (2 of 2)	ENPP2	ensembl biomart, HSA, GO:0002376
EOMES (1 of 2)	EOMES	ensembl biomart, HSA, GO:0002376
EOMES (2 of 2)	EOMES	ensembl biomart, HSA, GO:0002376
EP300 (1 of 2)	EP300	ensembl biomart, HSA, GO:0002376
EP300 (2 of 2)	EP300	ensembl biomart, HSA, GO:0002376
EPAS1	EPAS1	ensembl biomart, HSA, GO:0002376
EPHA2 (1 of 2)	EPHA2	ensembl biomart, HSA, GO:0002376
EPHA2 (2 of 2)	EPHA2	ensembl biomart, HSA, GO:0002376
EPHB3 (1 of 2)	EPHB3	ensembl biomart, HSA, GO:0002376
EPHB3 (2 of 2)	EPHB3	ensembl biomart, HSA, GO:0002376
EPO	EPO	ensembl biomart, HSA, GO:0002376
ERAP1	ERAP1	ensembl biomart, HSA, GO:0002376
ERAP2	ERAP2	ensembl biomart, HSA, GO:0002376
ERCC1	ERCC1	ensembl biomart, HSA, GO:0002376
ERCC2	ERCC2	ensembl biomart, HSA, GO:0002376
ESAM	ESAM	ensembl biomart, HSA, GO:0002376
ETS1	ETS1	ensembl biomart, HSA, GO:0002376
EXO1	EXO1	ensembl biomart, HSA, GO:0002376
EXOC6	EXOC6	ensembl biomart, HSA, GO:0002376
EXOSC3	EXOSC3	ensembl biomart, HSA, GO:0002376
EXOSC4	EXOSC4	ensembl biomart, HSA, GO:0002376
EXOSC5	EXOSC5	ensembl biomart, HSA, GO:0002376
EXOSC6	EXOSC6	ensembl biomart, HSA, GO:0002376
EXOSC9	EXOSC9	ensembl biomart, HSA, GO:0002376
F11R	F11R	ensembl biomart, HSA, GO:0002376
FAM20C	FAM20C	ensembl biomart, HSA, GO:0002376
FAM65C	FAM65C	ensembl biomart, HSA, GO:0002376
FANCC	FANCC	ensembl biomart, HSA, GO:0002376
FECH	FECH	ensembl biomart, HSA, GO:0002376
FGF10 (1 of 2)	FGF10	ensembl biomart, HSA, GO:0002376
FGF10 (2 of 2)	FGF10	ensembl biomart, HSA, GO:0002376
FGF3	FGF3	ensembl biomart, HSA, GO:0002376
FGFR2	FGFR2	ensembl biomart, HSA, GO:0002376
FKBP1B	FKBP1B	ensembl biomart, HSA, GO:0002376
FLVCR1	FLVCR1	ensembl biomart, HSA, GO:0002376
FN1 (1 of 2)	FN1	ensembl biomart, HSA, GO:0002376
FN1 (2 of 2)	FN1	ensembl biomart, HSA, GO:0002376
FOS (1 of 2)	FOS	ensembl biomart, HSA, GO:0002376
FOS (2 of 2)	FOS	ensembl biomart, HSA, GO:0002376
FOXJ1	FOXJ1	ensembl biomart, HSA, GO:0002376

stickleback_gene_name	human_gene_name	source
FOXN1	FOXN1	ensembl biomart, HSA, GO:0002376
FOXP1	FOXP1	ensembl biomart, HSA, GO:0002376
FST	FST	ensembl biomart, HSA, GO:0002376
FYB	FYB	ensembl biomart, HSA, GO:0002376
FYN	FYN	ensembl biomart, HSA, GO:0002376
FZD5	FZD5	ensembl biomart, HSA, GO:0002376
FZD7	FZD7	ensembl biomart, HSA, GO:0002376
FZD8	FZD8	ensembl biomart, HSA, GO:0002376
FZD9	FZD9	ensembl biomart, HSA, GO:0002376
G6PD (1 of 2)	G6PD	ensembl biomart, HSA, GO:0002376
G6PD (2 of 2)	G6PD	ensembl biomart, HSA, GO:0002376
GAB2	GAB2	ensembl biomart, HSA, GO:0002376
GAB3	GAB3	ensembl biomart, HSA, GO:0002376
GALNT2	GALNT2	ensembl biomart, HSA, GO:0002376
GAS6	GAS6	ensembl biomart, HSA, GO:0002376
GATA2 (1 of 2)	GATA2	ensembl biomart, HSA, GO:0002376
GATA2 (2 of 2)	GATA2	ensembl biomart, HSA, GO:0002376
GCH1	GCH1	ensembl biomart, HSA, GO:0002376
GCNT3 (1 of 2)	GCNT3	ensembl biomart, HSA, GO:0002376
GCNT3 (2 of 2)	GCNT3	ensembl biomart, HSA, GO:0002376
GEM	GEM	ensembl biomart, HSA, GO:0002376
GLI3	GLI3	ensembl biomart, HSA, GO:0002376
GLRX5	GLRX5	ensembl biomart, HSA, GO:0002376
GNL1	GNL1	ensembl biomart, HSA, GO:0002376
GPAM	GPAM	ensembl biomart, HSA, GO:0002376
GPC3	GPC3	ensembl biomart, HSA, GO:0002376
GPR183	GPR183	ensembl biomart, HSA, GO:0002376
GPR65	GPR65	ensembl biomart, HSA, GO:0002376
GRAP2	GRAP2	ensembl biomart, HSA, GO:0002376
GRB14	GRB14	ensembl biomart, HSA, GO:0002376
GRB2	GRB2	ensembl biomart, HSA, GO:0002376
GRB7	GRB7	ensembl biomart, HSA, GO:0002376
GTPBP1	GTPBP1	ensembl biomart, HSA, GO:0002376
HAND2	HAND2	ensembl biomart, HSA, GO:0002376
HCK	HCK	ensembl biomart, HSA, GO:0002376
HCLS1	HCLS1	ensembl biomart, HSA, GO:0002376
HDAC4 (1 of 2)	HDAC4	ensembl biomart, HSA, GO:0002376
HDAC4 (2 of 2)	HDAC4	ensembl biomart, HSA, GO:0002376
HDAC5	HDAC5	ensembl biomart, HSA, GO:0002376
HDAC9	HDAC9	ensembl biomart, HSA, GO:0002376
HELLS	HELLS	ensembl biomart, HSA, GO:0002376
HHEX	HHEX	ensembl biomart, HSA, GO:0002376
HIF1A	HIF1A	ensembl biomart, HSA, GO:0002376
HIPK1 (1 of 2)	HIPK1	ensembl biomart, HSA, GO:0002376
HIPK1 (2 of 2)	HIPK1	ensembl biomart, HSA, GO:0002376
HIPK2	HIPK2	ensembl biomart, HSA, GO:0002376
HMGB1 (1 of 2)	HMGB1	ensembl biomart, HSA, GO:0002376
HMGB1 (2 of 2)	HMGB1	ensembl biomart, HSA, GO:0002376
HMGB2	HMGB2	ensembl biomart, HSA, GO:0002376
HOXA9	HOXA9	ensembl biomart, HSA, GO:0002376
HOXB4	HOXB4	ensembl biomart, HSA, GO:0002376
HPRT1	HPRT1	ensembl biomart, HSA, GO:0002376
HRAS	HRAS	ensembl biomart, HSA, GO:0002376

stickleback_gene_name	human_gene_name	source
HRH2 (1 of 2)	HRH2	ensembl biomart, HSA, GO:0002376
HRH2 (2 of 2)	HRH2	ensembl biomart, HSA, GO:0002376
HYAL2 (1 of 2)	HYAL2	ensembl biomart, HSA, GO:0002376
HYAL2 (2 of 2)	HYAL2	ensembl biomart, HSA, GO:0002376
ID2	ID2	ensembl biomart, HSA, GO:0002376
IFI35	IFI35	ensembl biomart, HSA, GO:0002376
IFIH1	IFIH1	ensembl biomart, HSA, GO:0002376
IGF1R (1 of 2)	IGF1R	ensembl biomart, HSA, GO:0002376
IGF1R (2 of 2)	IGF1R	ensembl biomart, HSA, GO:0002376
IK	IK	ensembl biomart, HSA, GO:0002376
IKBKAP	IKBKAP	ensembl biomart, HSA, GO:0002376
IKBKB	IKBKB	ensembl biomart, HSA, GO:0002376
IKBKE	IKBKE	ensembl biomart, HSA, GO:0002376
IKBKG	IKBKG	ensembl biomart, HSA, GO:0002376
IL10RB	IL10RB	ensembl biomart, HSA, GO:0002376
IL12B (3 of 3)	IL12B	ensembl biomart, HSA, GO:0002376
IL16	IL16	ensembl biomart, HSA, GO:0002376
IL1RAP	IL1RAP	ensembl biomart, HSA, GO:0002376
IL1RAPL1 (1 of 2)	IL1RAPL1	ensembl biomart, HSA, GO:0002376
IL1RAPL1 (2 of 2)	IL1RAPL1	ensembl biomart, HSA, GO:0002376
IL1RAPL2	IL1RAPL2	ensembl biomart, HSA, GO:0002376
IL1RL2	IL1RL2	ensembl biomart, HSA, GO:0002376
IL20RB	IL20RB	ensembl biomart, HSA, GO:0002376
IL2RG	IL2RG	ensembl biomart, HSA, GO:0002376
IL7R	IL7R	ensembl biomart, HSA, GO:0002376
ILF2	ILF2	ensembl biomart, HSA, GO:0002376
IMPDH1 (1 of 2)	IMPDH1	ensembl biomart, HSA, GO:0002376
INHA	INHA	ensembl biomart, HSA, GO:0002376
INHBA (1 of 2)	INHBA	ensembl biomart, HSA, GO:0002376
INHBA (2 of 2)	INHBA	ensembl biomart, HSA, GO:0002376
INPP5D	INPP5D	ensembl biomart, HSA, GO:0002376
INS	INS	ensembl biomart, HSA, GO:0002376
IP6K2 (1 of 2)	IP6K2	ensembl biomart, HSA, GO:0002376
IP6K2 (2 of 2)	IP6K2	ensembl biomart, HSA, GO:0002376
IRAK1	IRAK1	ensembl biomart, HSA, GO:0002376
IRAK3	IRAK3	ensembl biomart, HSA, GO:0002376
IRAK4	IRAK4	ensembl biomart, HSA, GO:0002376
IREB2	IREB2	ensembl biomart, HSA, GO:0002376
IRF2	IRF2	ensembl biomart, HSA, GO:0002376
IRF3	IRF3	ensembl biomart, HSA, GO:0002376
IRF4 (1 of 2)	IRF4	ensembl biomart, HSA, GO:0002376
IRF4 (2 of 2)	IRF4	ensembl biomart, HSA, GO:0002376
IRF5	IRF5	ensembl biomart, HSA, GO:0002376
IRF6	IRF6	ensembl biomart, HSA, GO:0002376
IRF7	IRF7	ensembl biomart, HSA, GO:0002376
IRF8	IRF8	ensembl biomart, HSA, GO:0002376
ITCH (1 of 2)	ITCH	ensembl biomart, HSA, GO:0002376
ITCH (2 of 2)	ITCH	ensembl biomart, HSA, GO:0002376
ITGA1	ITGA1	ensembl biomart, HSA, GO:0002376
ITGA5 (1 of 2)	ITGA5	ensembl biomart, HSA, GO:0002376
ITGA5 (2 of 2)	ITGA5	ensembl biomart, HSA, GO:0002376
ITGA6 (1 of 2)	ITGA6	ensembl biomart, HSA, GO:0002376
ITGA6 (2 of 2)	ITGA6	ensembl biomart, HSA, GO:0002376

stickleback_gene_name	human_gene_name	source
ITGA9	ITGA9	ensembl biomart, HSA, GO:0002376
ITGAV	ITGAV	ensembl biomart, HSA, GO:0002376
ITGB1 (1 of 2)	ITGB1	ensembl biomart, HSA, GO:0002376
ITGB1 (2 of 2)	ITGB1	ensembl biomart, HSA, GO:0002376
ITGB5	ITGB5	ensembl biomart, HSA, GO:0002376
ITK	ITK	ensembl biomart, HSA, GO:0002376
ITPKB	ITPKB	ensembl biomart, HSA, GO:0002376
JAG1 (1 of 2)	JAG1	ensembl biomart, HSA, GO:0002376
JAG1 (2 of 2)	JAG1	ensembl biomart, HSA, GO:0002376
JAG2	JAG2	ensembl biomart, HSA, GO:0002376
JAK1	JAK1	ensembl biomart, HSA, GO:0002376
JAK2 (1 of 2)	JAK2	ensembl biomart, HSA, GO:0002376
JAK2 (2 of 2)	JAK2	ensembl biomart, HSA, GO:0002376
JAM2 (1 of 2)	JAM2	ensembl biomart, HSA, GO:0002376
JAM2 (2 of 2)	JAM2	ensembl biomart, HSA, GO:0002376
JAM3 (1 of 2)	JAM3	ensembl biomart, HSA, GO:0002376
JAM3 (2 of 2)	JAM3	ensembl biomart, HSA, GO:0002376
JARID2	JARID2	ensembl biomart, HSA, GO:0002376
JMJD6	JMJD6	ensembl biomart, HSA, GO:0002376
JUN (1 of 2)	JUN	ensembl biomart, HSA, GO:0002376
JUN (2 of 2)	JUN	ensembl biomart, HSA, GO:0002376
JUNB (1 of 2)	JUNB	ensembl biomart, HSA, GO:0002376
JUNB (2 of 2)	JUNB	ensembl biomart, HSA, GO:0002376
KCNJ8	KCNJ8	ensembl biomart, HSA, GO:0002376
KIF11	KIF11	ensembl biomart, HSA, GO:0002376
KIF15	KIF15	ensembl biomart, HSA, GO:0002376
KIF18A	KIF18A	ensembl biomart, HSA, GO:0002376
KIF22	KIF22	ensembl biomart, HSA, GO:0002376
KIF23 (1 of 2)	KIF23	ensembl biomart, HSA, GO:0002376
KIF23 (2 of 2)	KIF23	ensembl biomart, HSA, GO:0002376
KIF26A (1 of 2)	KIF26A	ensembl biomart, HSA, GO:0002376
KIF26A (2 of 2)	KIF26A	ensembl biomart, HSA, GO:0002376
KIF2C	KIF2C	ensembl biomart, HSA, GO:0002376
KIF3A	KIF3A	ensembl biomart, HSA, GO:0002376
KIF3B	KIF3B	ensembl biomart, HSA, GO:0002376
KIF3C (1 of 2)	KIF3C	ensembl biomart, HSA, GO:0002376
KIF3C (2 of 2)	KIF3C	ensembl biomart, HSA, GO:0002376
KIF4A	KIF4A	ensembl biomart, HSA, GO:0002376
KIF5A (1 of 2)	KIF5A	ensembl biomart, HSA, GO:0002376
KIF5A (2 of 2)	KIF5A	ensembl biomart, HSA, GO:0002376
KIFAP3 (1 of 2)	KIFAP3	ensembl biomart, HSA, GO:0002376
KIFAP3 (2 of 2)	KIFAP3	ensembl biomart, HSA, GO:0002376
KIT	KIT	ensembl biomart, HSA, GO:0002376
KLC1	KLC1	ensembl biomart, HSA, GO:0002376
KLC2	KLC2	ensembl biomart, HSA, GO:0002376
KLF2 (1 of 2)	KLF2	ensembl biomart, HSA, GO:0002376
KLF2 (2 of 2)	KLF2	ensembl biomart, HSA, GO:0002376
KLF6 (1 of 2)	KLF6	ensembl biomart, HSA, GO:0002376
KLF6 (2 of 2)	KLF6	ensembl biomart, HSA, GO:0002376
KRAS	KRAS	ensembl biomart, HSA, GO:0002376
KYNU	KYNU	ensembl biomart, HSA, GO:0002376
L1CAM	L1CAM	ensembl biomart, HSA, GO:0002376
LCK	LCK	ensembl biomart, HSA, GO:0002376

stickleback_gene_name	human_gene_name	source
LEF1	LEF1	ensembl biomart, HSA, GO:0002376
LGALS1 (1 of 3)	LGALS1	ensembl biomart, HSA, GO:0002376
LGALS1 (2 of 3)	LGALS1	ensembl biomart, HSA, GO:0002376
LGALS1 (3 of 3)	LGALS1	ensembl biomart, HSA, GO:0002376
LGALS3	LGALS3	ensembl biomart, HSA, GO:0002376
LGALS8 (1 of 2)	LGALS8	ensembl biomart, HSA, GO:0002376
LGALS8 (2 of 2)	LGALS8	ensembl biomart, HSA, GO:0002376
LGMN	LGMN	ensembl biomart, HSA, GO:0002376
LIG4	LIG4	ensembl biomart, HSA, GO:0002376
LMO4	LMO4	ensembl biomart, HSA, GO:0002376
LNPEP	LNPEP	ensembl biomart, HSA, GO:0002376
LRRC17	LRRC17	ensembl biomart, HSA, GO:0002376
LRRC8A (1 of 2)	LRRC8A	ensembl biomart, HSA, GO:0002376
LRRC8A (2 of 2)	LRRC8A	ensembl biomart, HSA, GO:0002376
LYL1	LYL1	ensembl biomart, HSA, GO:0002376
LYN	LYN	ensembl biomart, HSA, GO:0002376
LYST	LYST	ensembl biomart, HSA, GO:0002376
MAEA	MAEA	ensembl biomart, HSA, GO:0002376
MAG	MAG	ensembl biomart, HSA, GO:0002376
MALT1	MALT1	ensembl biomart, HSA, GO:0002376
MAP2K1	MAP2K1	ensembl biomart, HSA, GO:0002376
MAP2K2 (1 of 2)	MAP2K2	ensembl biomart, HSA, GO:0002376
MAP2K2 (2 of 2)	MAP2K2	ensembl biomart, HSA, GO:0002376
MAP2K4	MAP2K4	ensembl biomart, HSA, GO:0002376
MAP2K6	MAP2K6	ensembl biomart, HSA, GO:0002376
MAP2K7	MAP2K7	ensembl biomart, HSA, GO:0002376
MAP3K7	MAP3K7	ensembl biomart, HSA, GO:0002376
MAP3K8	MAP3K8	ensembl biomart, HSA, GO:0002376
MAP4K2	MAP4K2	ensembl biomart, HSA, GO:0002376
MAPK1	MAPK1	ensembl biomart, HSA, GO:0002376
MAPK10	MAPK10	ensembl biomart, HSA, GO:0002376
MAPK11	MAPK11	ensembl biomart, HSA, GO:0002376
MAPK14 (1 of 2)	MAPK14	ensembl biomart, HSA, GO:0002376
MAPK14 (2 of 2)	MAPK14	ensembl biomart, HSA, GO:0002376
MAPK7	MAPK7	ensembl biomart, HSA, GO:0002376
MAPK8 (1 of 2)	MAPK8	ensembl biomart, HSA, GO:0002376
MAPK8 (2 of 2)	MAPK8	ensembl biomart, HSA, GO:0002376
MAPK9	MAPK9	ensembl biomart, HSA, GO:0002376
MAPKAP1	MAPKAP1	ensembl biomart, HSA, GO:0002376
MAPKAPK2	MAPKAPK2	ensembl biomart, HSA, GO:0002376
MARCO	MARCO	ensembl biomart, HSA, GO:0002376
MASP1 (1 of 2)	MASP1	ensembl biomart, HSA, GO:0002376
MASP1 (2 of 2)	MASP1	ensembl biomart, HSA, GO:0002376
MAVS	MAVS	ensembl biomart, HSA, GO:0002376
MBP	MBP	ensembl biomart, HSA, GO:0002376
MECOM	MECOM	ensembl biomart, HSA, GO:0002376
MED1	MED1	ensembl biomart, HSA, GO:0002376
MEF2A	MEF2A	ensembl biomart, HSA, GO:0002376
MEF2C (1 of 2)	MEF2C	ensembl biomart, HSA, GO:0002376
MEF2C (2 of 2)	MEF2C	ensembl biomart, HSA, GO:0002376
MELK	MELK	ensembl biomart, HSA, GO:0002376
MEN1	MEN1	ensembl biomart, HSA, GO:0002376
MERTK	MERTK	ensembl biomart, HSA, GO:0002376

stickleback_gene_name	human_gene_name	source
MFAP2	MFAP2	ensembl biomart, HSA, GO:0002376
MINK1	MINK1	ensembl biomart, HSA, GO:0002376
MITF (1 of 2)	MITF	ensembl biomart, HSA, GO:0002376
MITF (2 of 2)	MITF	ensembl biomart, HSA, GO:0002376
MIXL1	MIXL1	ensembl biomart, HSA, GO:0002376
MKNK2	MKNK2	ensembl biomart, HSA, GO:0002376
MLF1	MLF1	ensembl biomart, HSA, GO:0002376
MLH1	MLH1	ensembl biomart, HSA, GO:0002376
MLL	MLL	ensembl biomart, HSA, GO:0002376
MLL5	MLL5	ensembl biomart, HSA, GO:0002376
MPZL2 (1 of 2)	MPZL2	ensembl biomart, HSA, GO:0002376
MPZL2 (2 of 2)	MPZL2	ensembl biomart, HSA, GO:0002376
MSH2	MSH2	ensembl biomart, HSA, GO:0002376
MSN (1 of 2)	MSN	ensembl biomart, HSA, GO:0002376
MSN (2 of 2)	MSN	ensembl biomart, HSA, GO:0002376
MST1R (1 of 2)	MST1R	ensembl biomart, HSA, GO:0002376
MST1R (2 of 2)	MST1R	ensembl biomart, HSA, GO:0002376
MYB	MYB	ensembl biomart, HSA, GO:0002376
MYD88	MYD88	ensembl biomart, HSA, GO:0002376
MYH9 (1 of 2)	MYH9	ensembl biomart, HSA, GO:0002376
MYH9 (2 of 2)	MYH9	ensembl biomart, HSA, GO:0002376
MYLPF (1 of 2)	MYLPF	ensembl biomart, HSA, GO:0002376
MYLPF (2 of 2)	MYLPF	ensembl biomart, HSA, GO:0002376
MYO1E	MYO1E	ensembl biomart, HSA, GO:0002376
MYO1F	MYO1F	ensembl biomart, HSA, GO:0002376
MYO9B (1 of 2)	MYO9B	ensembl biomart, HSA, GO:0002376
MYO9B (2 of 2)	MYO9B	ensembl biomart, HSA, GO:0002376
NBEAL2	NBEAL2	ensembl biomart, HSA, GO:0002376
NBN	NBN	ensembl biomart, HSA, GO:0002376
NCAM1 (1 of 2)	NCAM1	ensembl biomart, HSA, GO:0002376
NCAM1 (2 of 2)	NCAM1	ensembl biomart, HSA, GO:0002376
NCF1	NCF1	ensembl biomart, HSA, GO:0002376
NCF2	NCF2	ensembl biomart, HSA, GO:0002376
NCK1	NCK1	ensembl biomart, HSA, GO:0002376
NCK2	NCK2	ensembl biomart, HSA, GO:0002376
NCKAP1L	NCKAP1L	ensembl biomart, HSA, GO:0002376
NCOA6	NCOA6	ensembl biomart, HSA, GO:0002376
NCSTN	NCSTN	ensembl biomart, HSA, GO:0002376
NDRG1 (1 of 2)	NDRG1	ensembl biomart, HSA, GO:0002376
NDRG1 (2 of 2)	NDRG1	ensembl biomart, HSA, GO:0002376
NEDD4	NEDD4	ensembl biomart, HSA, GO:0002376
NFATC2	NFATC2	ensembl biomart, HSA, GO:0002376
NFKB1	NFKB1	ensembl biomart, HSA, GO:0002376
NFKB2	NFKB2	ensembl biomart, HSA, GO:0002376
NFKBIA (1 of 2)	NFKBIA	ensembl biomart, HSA, GO:0002376
NFKBIA (2 of 2)	NFKBIA	ensembl biomart, HSA, GO:0002376
NHEJ1	NHEJ1	ensembl biomart, HSA, GO:0002376
NKAP	NKAP	ensembl biomart, HSA, GO:0002376
NKX2-3	NKX2-3	ensembl biomart, HSA, GO:0002376
NKX2-5	NKX2-5	ensembl biomart, HSA, GO:0002376
NKX3-2	NKX3-2	ensembl biomart, HSA, GO:0002376
NLRC5	NLRC5	ensembl biomart, HSA, GO:0002376
NLRX1	NLRX1	ensembl biomart, HSA, GO:0002376

stickleback_gene_name	human_gene_name	source
NOD1	NOD1	ensembl biomart, HSA, GO:0002376
NOD2	NOD2	ensembl biomart, HSA, GO:0002376
NOTCH1 (1 of 2)	NOTCH1	ensembl biomart, HSA, GO:0002376
NOTCH1 (2 of 2)	NOTCH1	ensembl biomart, HSA, GO:0002376
NPEPPS	NPEPPS	ensembl biomart, HSA, GO:0002376
NTRK1	NTRK1	ensembl biomart, HSA, GO:0002376
NUB1	NUB1	ensembl biomart, HSA, GO:0002376
NUP85	NUP85	ensembl biomart, HSA, GO:0002376
ONECUT1	ONECUT1	ensembl biomart, HSA, GO:0002376
OPRD1 (1 of 2)	OPRD1	ensembl biomart, HSA, GO:0002376
OPRD1 (2 of 2)	OPRD1	ensembl biomart, HSA, GO:0002376
OPRK1 (1 of 2)	OPRK1	ensembl biomart, HSA, GO:0002376
OPRK1 (2 of 2)	OPRK1	ensembl biomart, HSA, GO:0002376
OSBPL1A (1 of 2)	OSBPL1A	ensembl biomart, HSA, GO:0002376
OSBPL1A (2 of 2)	OSBPL1A	ensembl biomart, HSA, GO:0002376
OSTM1	OSTM1	ensembl biomart, HSA, GO:0002376
OTUD5	OTUD5	ensembl biomart, HSA, GO:0002376
PAFAH1B1 (1 of 2)	PAFAH1B1	ensembl biomart, HSA, GO:0002376
PAFAH1B1 (2 of 2)	PAFAH1B1	ensembl biomart, HSA, GO:0002376
PAG1	PAG1	ensembl biomart, HSA, GO:0002376
PAK1 (1 of 2)	PAK1	ensembl biomart, HSA, GO:0002376
PAK1 (2 of 2)	PAK1	ensembl biomart, HSA, GO:0002376
PAK2 (1 of 2)	PAK2	ensembl biomart, HSA, GO:0002376
PAK2 (2 of 2)	PAK2	ensembl biomart, HSA, GO:0002376
PANX1 (1 of 2)	PANX1	ensembl biomart, HSA, GO:0002376
PANX1 (2 of 2)	PANX1	ensembl biomart, HSA, GO:0002376
PAX1	PAX1	ensembl biomart, HSA, GO:0002376
PAX5	PAX5	ensembl biomart, HSA, GO:0002376
PBX1 (1 of 2)	PBX1	ensembl biomart, HSA, GO:0002376
PBX1 (2 of 2)	PBX1	ensembl biomart, HSA, GO:0002376
PCID2 (1 of 2)	PCID2	ensembl biomart, HSA, GO:0002376
PCID2 (2 of 2)	PCID2	ensembl biomart, HSA, GO:0002376
PDE1B	PDE1B	ensembl biomart, HSA, GO:0002376
PDE2A	PDE2A	ensembl biomart, HSA, GO:0002376
PDE4B (2 of 2)	PDE4B	ensembl biomart, HSA, GO:0002376
PDE4D	PDE4D	ensembl biomart, HSA, GO:0002376
PDGFB (1 of 2)	PDGFB	ensembl biomart, HSA, GO:0002376
PDGFB (2 of 2)	PDGFB	ensembl biomart, HSA, GO:0002376
PDIA3	PDIA3	ensembl biomart, HSA, GO:0002376
PDPK1	PDPK1	ensembl biomart, HSA, GO:0002376
PFDN1	PFDN1	ensembl biomart, HSA, GO:0002376
PGLYRP2 (1 of 2)	PGLYRP2	ensembl biomart, HSA, GO:0002376
PGLYRP2 (2 of 2)	PGLYRP2	ensembl biomart, HSA, GO:0002376
PGM3	PGM3	ensembl biomart, HSA, GO:0002376
PI4K2A	PI4K2A	ensembl biomart, HSA, GO:0002376
PIAS1 (1 of 2)	PIAS1	ensembl biomart, HSA, GO:0002376
PIAS1 (2 of 2)	PIAS1	ensembl biomart, HSA, GO:0002376
PIK3C3	PIK3C3	ensembl biomart, HSA, GO:0002376
PIK3CB	PIK3CB	ensembl biomart, HSA, GO:0002376
PIK3CG	PIK3CG	ensembl biomart, HSA, GO:0002376
PIK3R1 (1 of 2)	PIK3R1	ensembl biomart, HSA, GO:0002376
PIK3R1 (2 of 2)	PIK3R1	ensembl biomart, HSA, GO:0002376
PIK3R2 (1 of 2)	PIK3R2	ensembl biomart, HSA, GO:0002376

stickleback_gene_name	human_gene_name	source
PIK3R2 (2 of 2)	PIK3R2	ensembl biomart, HSA, GO:0002376
PIK3R3	PIK3R3	ensembl biomart, HSA, GO:0002376
PIK3R4	PIK3R4	ensembl biomart, HSA, GO:0002376
PIN1	PIN1	ensembl biomart, HSA, GO:0002376
PIP4K2A	PIP4K2A	ensembl biomart, HSA, GO:0002376
PIP5K1C (1 of 2)	PIP5K1C	ensembl biomart, HSA, GO:0002376
PIP5K1C (2 of 2)	PIP5K1C	ensembl biomart, HSA, GO:0002376
PITX2	PITX2	ensembl biomart, HSA, GO:0002376
PKHD1L1	PKHD1L1	ensembl biomart, HSA, GO:0002376
PKNOX1	PKNOX1	ensembl biomart, HSA, GO:0002376
PLEK	PLEK	ensembl biomart, HSA, GO:0002376
PLEKHA1 (1 of 2)	PLEKHA1	ensembl biomart, HSA, GO:0002376
PLEKHA1 (2 of 2)	PLEKHA1	ensembl biomart, HSA, GO:0002376
PLG	PLG	ensembl biomart, HSA, GO:0002376
PMS2	PMS2	ensembl biomart, HSA, GO:0002376
PODXL	PODXL	ensembl biomart, HSA, GO:0002376
PODXL2	PODXL2	ensembl biomart, HSA, GO:0002376
POU1F1	POU1F1	ensembl biomart, HSA, GO:0002376
POU2F2 (1 of 2)	POU2F2	ensembl biomart, HSA, GO:0002376
POU2F2 (2 of 2)	POU2F2	ensembl biomart, HSA, GO:0002376
PPARG	PPARG	ensembl biomart, HSA, GO:0002376
PRDX1	PRDX1	ensembl biomart, HSA, GO:0002376
PRDX3	PRDX3	ensembl biomart, HSA, GO:0002376
PRELID1	PRELID1	ensembl biomart, HSA, GO:0002376
PREX1	PREX1	ensembl biomart, HSA, GO:0002376
PRF1 (1 of 5)	PRF1	ensembl biomart, HSA, GO:0002376
PRF1 (2 of 5)	PRF1	ensembl biomart, HSA, GO:0002376
PRF1 (3 of 5)	PRF1	ensembl biomart, HSA, GO:0002376
PRF1 (4 of 5)	PRF1	ensembl biomart, HSA, GO:0002376
PRF1 (5 of 5)	PRF1	ensembl biomart, HSA, GO:0002376
PRG4	PRG4	ensembl biomart, HSA, GO:0002376
PRKCA (1 of 2)	PRKCA	ensembl biomart, HSA, GO:0002376
PRKCA (2 of 2)	PRKCA	ensembl biomart, HSA, GO:0002376
PRKCB (1 of 2)	PRKCB	ensembl biomart, HSA, GO:0002376
PRKCB (2 of 2)	PRKCB	ensembl biomart, HSA, GO:0002376
PRKCD (1 of 2)	PRKCD	ensembl biomart, HSA, GO:0002376
PRKCD (2 of 2)	PRKCD	ensembl biomart, HSA, GO:0002376
PRKCE (1 of 2)	PRKCE	ensembl biomart, HSA, GO:0002376
PRKCE (2 of 2)	PRKCE	ensembl biomart, HSA, GO:0002376
PRKCQ	PRKCQ	ensembl biomart, HSA, GO:0002376
PRKCSH	PRKCSH	ensembl biomart, HSA, GO:0002376
PRKD2	PRKD2	ensembl biomart, HSA, GO:0002376
PRKDC	PRKDC	ensembl biomart, HSA, GO:0002376
PRKRA	PRKRA	ensembl biomart, HSA, GO:0002376
PRKX	PRKX	ensembl biomart, HSA, GO:0002376
PRLR (1 of 2)	PRLR	ensembl biomart, HSA, GO:0002376
PRLR (2 of 2)	PRLR	ensembl biomart, HSA, GO:0002376
PSEN1	PSEN1	ensembl biomart, HSA, GO:0002376
PSMA4 (1 of 2)	PSMA4	ensembl biomart, HSA, GO:0002376
PSMA4 (2 of 2)	PSMA4	ensembl biomart, HSA, GO:0002376
PSMA6 (1 of 2)	PSMA6	ensembl biomart, HSA, GO:0002376
PSMA6 (2 of 2)	PSMA6	ensembl biomart, HSA, GO:0002376
PSMB8 (1 of 10)	PSMB8	ensembl biomart, HSA, GO:0002376

stickleback_gene_name	human_gene_name	source
PSMB8 (10 of 10)	PSMB8	ensembl biomart, HSA, GO:0002376
PSMB8 (2 of 10)	PSMB8	ensembl biomart, HSA, GO:0002376
PSMB8 (3 of 10)	PSMB8	ensembl biomart, HSA, GO:0002376
PSMB8 (4 of 10)	PSMB8	ensembl biomart, HSA, GO:0002376
PSMB8 (5 of 10)	PSMB8	ensembl biomart, HSA, GO:0002376
PSMB8 (6 of 10)	PSMB8	ensembl biomart, HSA, GO:0002376
PSMB8 (7 of 10)	PSMB8	ensembl biomart, HSA, GO:0002376
PSMB8 (8 of 10)	PSMB8	ensembl biomart, HSA, GO:0002376
PSMB8 (9 of 10)	PSMB8	ensembl biomart, HSA, GO:0002376
PSMB9 (1 of 5)	PSMB9	ensembl biomart, HSA, GO:0002376
PSMB9 (2 of 5)	PSMB9	ensembl biomart, HSA, GO:0002376
PSMB9 (3 of 5)	PSMB9	ensembl biomart, HSA, GO:0002376
PSMB9 (4 of 5)	PSMB9	ensembl biomart, HSA, GO:0002376
PSMB9 (5 of 5)	PSMB9	ensembl biomart, HSA, GO:0002376
PSMD11 (1 of 2)	PSMD11	ensembl biomart, HSA, GO:0002376
PSMD11 (2 of 2)	PSMD11	ensembl biomart, HSA, GO:0002376
PSMD4 (2 of 2)	PSMD4	ensembl biomart, HSA, GO:0002376
PSME4 (1 of 2)	PSME4	ensembl biomart, HSA, GO:0002376
PSME4 (2 of 2)	PSME4	ensembl biomart, HSA, GO:0002376
PSTPIP1 (1 of 2)	PSTPIP1	ensembl biomart, HSA, GO:0002376
PSTPIP1 (2 of 2)	PSTPIP1	ensembl biomart, HSA, GO:0002376
PTAFR	PTAFR	ensembl biomart, HSA, GO:0002376
PTBP3	PTBP3	ensembl biomart, HSA, GO:0002376
PTEN (1 of 2)	PTEN	ensembl biomart, HSA, GO:0002376
PTEN (2 of 2)	PTEN	ensembl biomart, HSA, GO:0002376
PTGDR2 (1 of 3)	PTGDR2	ensembl biomart, HSA, GO:0002376
PTGDR2 (2 of 3)	PTGDR2	ensembl biomart, HSA, GO:0002376
PTGDR2 (3 of 3)	PTGDR2	ensembl biomart, HSA, GO:0002376
PTGER4 (1 of 2)	PTGER4	ensembl biomart, HSA, GO:0002376
PTGER4 (2 of 2)	PTGER4	ensembl biomart, HSA, GO:0002376
PTK2B (1 of 2)	PTK2B	ensembl biomart, HSA, GO:0002376
PTK2B (2 of 2)	PTK2B	ensembl biomart, HSA, GO:0002376
PTPN1	PTPN1	ensembl biomart, HSA, GO:0002376
PTPN11	PTPN11	ensembl biomart, HSA, GO:0002376
PTPN2 (1 of 2)	PTPN2	ensembl biomart, HSA, GO:0002376
PTPN2 (2 of 2)	PTPN2	ensembl biomart, HSA, GO:0002376
PTPN22	PTPN22	ensembl biomart, HSA, GO:0002376
PTPN6	PTPN6	ensembl biomart, HSA, GO:0002376
PTPRC	PTPRC	ensembl biomart, HSA, GO:0002376
PTPRO	PTPRO	ensembl biomart, HSA, GO:0002376
PTX3	PTX3	ensembl biomart, HSA, GO:0002376
PVRL1 (1 of 2)	PVRL1	ensembl biomart, HSA, GO:0002376
PVRL1 (2 of 2)	PVRL1	ensembl biomart, HSA, GO:0002376
RAB27A	RAB27A	ensembl biomart, HSA, GO:0002376
RAB7A (1 of 2)	RAB7A	ensembl biomart, HSA, GO:0002376
RAB7A (2 of 2)	RAB7A	ensembl biomart, HSA, GO:0002376
RAC1 (1 of 2)	RAC1	ensembl biomart, HSA, GO:0002376
RAC1 (2 of 2)	RAC1	ensembl biomart, HSA, GO:0002376
RACGAP1	RACGAP1	ensembl biomart, HSA, GO:0002376
RAG1	RAG1	ensembl biomart, HSA, GO:0002376
RAG2	RAG2	ensembl biomart, HSA, GO:0002376
RASGRP4	RASGRP4	ensembl biomart, HSA, GO:0002376
RB1	RB1	ensembl biomart, HSA, GO:0002376

stickleback_gene_name	human_gene_name	source
RBCK1	RBCK1	ensembl biomart, HSA, GO:0002376
RBM15 (1 of 2)	RBM15	ensembl biomart, HSA, GO:0002376
RBM15 (2 of 2)	RBM15	ensembl biomart, HSA, GO:0002376
RELA	RELA	ensembl biomart, HSA, GO:0002376
RELB	RELB	ensembl biomart, HSA, GO:0002376
RET	RET	ensembl biomart, HSA, GO:0002376
RFX1 (1 of 2)	RFX1	ensembl biomart, HSA, GO:0002376
RFX1 (2 of 2)	RFX1	ensembl biomart, HSA, GO:0002376
RGCC	RGCC	ensembl biomart, HSA, GO:0002376
RGS1	RGS1	ensembl biomart, HSA, GO:0002376
RHOH	RHOH	ensembl biomart, HSA, GO:0002376
RICTOR	RICTOR	ensembl biomart, HSA, GO:0002376
RILP	RILP	ensembl biomart, HSA, GO:0002376
RIPK2	RIPK2	ensembl biomart, HSA, GO:0002376
RIPK3	RIPK3	ensembl biomart, HSA, GO:0002376
RNF168	RNF168	ensembl biomart, HSA, GO:0002376
RNF8	RNF8	ensembl biomart, HSA, GO:0002376
ROCK1	ROCK1	ensembl biomart, HSA, GO:0002376
RORC	RORC	ensembl biomart, HSA, GO:0002376
RPA1 (1 of 2)	RPA1	ensembl biomart, HSA, GO:0002376
RPA1 (2 of 2)	RPA1	ensembl biomart, HSA, GO:0002376
RPL22 (1 of 2)	RPL22	ensembl biomart, HSA, GO:0002376
RPL22 (2 of 2)	RPL22	ensembl biomart, HSA, GO:0002376
RPS14	RPS14	ensembl biomart, HSA, GO:0002376
RPS19	RPS19	ensembl biomart, HSA, GO:0002376
RPS27A	RPS27A	ensembl biomart, HSA, GO:0002376
RPS6KA1	RPS6KA1	ensembl biomart, HSA, GO:0002376
RPS6KA2	RPS6KA2	ensembl biomart, HSA, GO:0002376
RPS6KA3	RPS6KA3	ensembl biomart, HSA, GO:0002376
RPS6KA5	RPS6KA5	ensembl biomart, HSA, GO:0002376
RSAD2	RSAD2	ensembl biomart, HSA, GO:0002376
RTKN2	RTKN2	ensembl biomart, HSA, GO:0002376
RUNX1	RUNX1	ensembl biomart, HSA, GO:0002376
RUNX2	RUNX2	ensembl biomart, HSA, GO:0002376
S100B	S100B	ensembl biomart, HSA, GO:0002376
S1PR4	S1PR4	ensembl biomart, HSA, GO:0002376
SATB1	SATB1	ensembl biomart, HSA, GO:0002376
SBDS	SBDS	ensembl biomart, HSA, GO:0002376
SCG2 (1 of 2)	SCG2	ensembl biomart, HSA, GO:0002376
SCG2 (2 of 2)	SCG2	ensembl biomart, HSA, GO:0002376
SEC61A1 (1 of 2)	SEC61A1	ensembl biomart, HSA, GO:0002376
SEC61A1 (2 of 2)	SEC61A1	ensembl biomart, HSA, GO:0002376
SEC61B	SEC61B	ensembl biomart, HSA, GO:0002376
SEMA7A (1 of 2)	SEMA7A	ensembl biomart, HSA, GO:0002376
SEMA7A (2 of 2)	SEMA7A	ensembl biomart, HSA, GO:0002376
SERPING1	SERPING1	ensembl biomart, HSA, GO:0002376
SFRP1	SFRP1	ensembl biomart, HSA, GO:0002376
SFRP2	SFRP2	ensembl biomart, HSA, GO:0002376
SFXN1	SFXN1	ensembl biomart, HSA, GO:0002376
SGPL1	SGPL1	ensembl biomart, HSA, GO:0002376
SH2B2	SH2B2	ensembl biomart, HSA, GO:0002376
SH2B3	SH2B3	ensembl biomart, HSA, GO:0002376
SH2D1A	SH2D1A	ensembl biomart, HSA, GO:0002376

stickleback_gene_name	human_gene_name	source
SH2D1B	SH2D1B	ensembl biomart, HSA, GO:0002376
SH3GL2 (1 of 2)	SH3GL2	ensembl biomart, HSA, GO:0002376
SH3GL2 (2 of 2)	SH3GL2	ensembl biomart, HSA, GO:0002376
SHH	SHH	ensembl biomart, HSA, GO:0002376
SIGIRR	SIGIRR	ensembl biomart, HSA, GO:0002376
SIKE1	SIKE1	ensembl biomart, HSA, GO:0002376
SIX1	SIX1	ensembl biomart, HSA, GO:0002376
SIX4	SIX4	ensembl biomart, HSA, GO:0002376
SKAP1	SKAP1	ensembl biomart, HSA, GO:0002376
SKAP2	SKAP2	ensembl biomart, HSA, GO:0002376
SKIL	SKIL	ensembl biomart, HSA, GO:0002376
SLC11A2 (1 of 2)	SLC11A2	ensembl biomart, HSA, GO:0002376
SLC11A2 (2 of 2)	SLC11A2	ensembl biomart, HSA, GO:0002376
SLC16A1 (1 of 2)	SLC16A1	ensembl biomart, HSA, GO:0002376
SLC16A1 (2 of 2)	SLC16A1	ensembl biomart, HSA, GO:0002376
SLC16A3 (1 of 2)	SLC16A3	ensembl biomart, HSA, GO:0002376
SLC16A3 (2 of 2)	SLC16A3	ensembl biomart, HSA, GO:0002376
SLC25A38 (1 of 2)	SLC25A38	ensembl biomart, HSA, GO:0002376
SLC25A38 (2 of 2)	SLC25A38	ensembl biomart, HSA, GO:0002376
SLC3A2 (1 of 2)	SLC3A2	ensembl biomart, HSA, GO:0002376
SLC3A2 (2 of 2)	SLC3A2	ensembl biomart, HSA, GO:0002376
SLC7A10 (1 of 2)	SLC7A10	ensembl biomart, HSA, GO:0002376
SLC7A10 (2 of 2)	SLC7A10	ensembl biomart, HSA, GO:0002376
SLC7A9 (1 of 2)	SLC7A9	ensembl biomart, HSA, GO:0002376
SLC7A9 (2 of 2)	SLC7A9	ensembl biomart, HSA, GO:0002376
SMAD3	SMAD3	ensembl biomart, HSA, GO:0002376
SMAD6	SMAD6	ensembl biomart, HSA, GO:0002376
SMARCA4	SMARCA4	ensembl biomart, HSA, GO:0002376
SNRK	SNRK	ensembl biomart, HSA, GO:0002376
SOCS1 (1 of 2)	SOCS1	ensembl biomart, HSA, GO:0002376
SOCS1 (2 of 2)	SOCS1	ensembl biomart, HSA, GO:0002376
SOCS3 (1 of 2)	SOCS3	ensembl biomart, HSA, GO:0002376
SOCS3 (2 of 2)	SOCS3	ensembl biomart, HSA, GO:0002376
SOD1	SOD1	ensembl biomart, HSA, GO:0002376
SOD2	SOD2	ensembl biomart, HSA, GO:0002376
SOX4 (1 of 2)	SOX4	ensembl biomart, HSA, GO:0002376
SOX4 (2 of 2)	SOX4	ensembl biomart, HSA, GO:0002376
SP1	SP1	ensembl biomart, HSA, GO:0002376
SP2	SP2	ensembl biomart, HSA, GO:0002376
SP3 (1 of 2)	SP3	ensembl biomart, HSA, GO:0002376
SP3 (2 of 2)	SP3	ensembl biomart, HSA, GO:0002376
SP7	SP7	ensembl biomart, HSA, GO:0002376
SPI1 (1 of 2)	SPI1	ensembl biomart, HSA, GO:0002376
SPI1 (2 of 2)	SPI1	ensembl biomart, HSA, GO:0002376
SPON2	SPON2	ensembl biomart, HSA, GO:0002376
SPTB	SPTB	ensembl biomart, HSA, GO:0002376
SPTBN2	SPTBN2	ensembl biomart, HSA, GO:0002376
SRC (1 of 2)	SRC	ensembl biomart, HSA, GO:0002376
SRC (2 of 2)	SRC	ensembl biomart, HSA, GO:0002376
SRF (1 of 2)	SRF	ensembl biomart, HSA, GO:0002376
SRF (2 of 2)	SRF	ensembl biomart, HSA, GO:0002376
SRPK1 (1 of 2)	SRPK1	ensembl biomart, HSA, GO:0002376
SRPK1 (2 of 2)	SRPK1	ensembl biomart, HSA, GO:0002376

stickleback_gene_name	human_gene_name	source
SRPK2	SRPK2	ensembl biomart, HSA, GO:0002376
ST6GAL1	ST6GAL1	ensembl biomart, HSA, GO:0002376
STAR (1 of 2)	STAR	ensembl biomart, HSA, GO:0002376
STAR (2 of 2)	STAR	ensembl biomart, HSA, GO:0002376
STAT1	STAT1	ensembl biomart, HSA, GO:0002376
STK3	STK3	ensembl biomart, HSA, GO:0002376
STK4	STK4	ensembl biomart, HSA, GO:0002376
STXBP2	STXBP2	ensembl biomart, HSA, GO:0002376
STXBP3	STXBP3	ensembl biomart, HSA, GO:0002376
SUMO1	SUMO1	ensembl biomart, HSA, GO:0002376
SUSD2	SUSD2	ensembl biomart, HSA, GO:0002376
SWAP70 (1 of 2)	SWAP70	ensembl biomart, HSA, GO:0002376
SWAP70 (2 of 2)	SWAP70	ensembl biomart, HSA, GO:0002376
SYK	SYK	ensembl biomart, HSA, GO:0002376
TAB2	TAB2	ensembl biomart, HSA, GO:0002376
TAB3	TAB3	ensembl biomart, HSA, GO:0002376
TACC3	TACC3	ensembl biomart, HSA, GO:0002376
TAL1	TAL1	ensembl biomart, HSA, GO:0002376
TANK	TANK	ensembl biomart, HSA, GO:0002376
TAP1	TAP1	ensembl biomart, HSA, GO:0002376
TAPBP (1 of 7)	TAPBP	ensembl biomart, HSA, GO:0002376
TAPBP (2 of 7)	TAPBP	ensembl biomart, HSA, GO:0002376
TAPBP (3 of 7)	TAPBP	ensembl biomart, HSA, GO:0002376
TAPBP (4 of 7)	TAPBP	ensembl biomart, HSA, GO:0002376
TAPBP (5 of 7)	TAPBP	ensembl biomart, HSA, GO:0002376
TAPBPL	TAPBPL	ensembl biomart, HSA, GO:0002376
TAX1BP1 (1 of 2)	TAX1BP1	ensembl biomart, HSA, GO:0002376
TAX1BP1 (2 of 2)	TAX1BP1	ensembl biomart, HSA, GO:0002376
TAZ	TAZ	ensembl biomart, HSA, GO:0002376
TBK1	TBK1	ensembl biomart, HSA, GO:0002376
TBKBP1 (1 of 2)	TBKBP1	ensembl biomart, HSA, GO:0002376
TBKBP1 (2 of 2)	TBKBP1	ensembl biomart, HSA, GO:0002376
TBX1	TBX1	ensembl biomart, HSA, GO:0002376
TCF12	TCF12	ensembl biomart, HSA, GO:0002376
TCF21	TCF21	ensembl biomart, HSA, GO:0002376
TCF3 (1 of 2)	TCF3	ensembl biomart, HSA, GO:0002376
TCF3 (2 of 2)	TCF3	ensembl biomart, HSA, GO:0002376
TEC	TEC	ensembl biomart, HSA, GO:0002376
TESC (1 of 2)	TESC	ensembl biomart, HSA, GO:0002376
TESC (2 of 2)	TESC	ensembl biomart, HSA, GO:0002376
TET2	TET2	ensembl biomart, HSA, GO:0002376
TFEB	TFEB	ensembl biomart, HSA, GO:0002376
TFRC (1 of 2)	TFRC	ensembl biomart, HSA, GO:0002376
TFRC (2 of 2)	TFRC	ensembl biomart, HSA, GO:0002376
TGFB1	TGFB1	ensembl biomart, HSA, GO:0002376
TGFB2	TGFB2	ensembl biomart, HSA, GO:0002376
TGFBR1	TGFBR1	ensembl biomart, HSA, GO:0002376
TGFBR2 (1 of 2)	TGFBR2	ensembl biomart, HSA, GO:0002376
TGFBR2 (2 of 2)	TGFBR2	ensembl biomart, HSA, GO:0002376
TGFBR3	TGFBR3	ensembl biomart, HSA, GO:0002376
THBD	THBD	ensembl biomart, HSA, GO:0002376
THBS1 (1 of 2)	THBS1	ensembl biomart, HSA, GO:0002376
THBS1 (2 of 2)	THBS1	ensembl biomart, HSA, GO:0002376

stickleback_gene_name	human_gene_name	source
THOC5	THOC5	ensembl biomart, HSA, GO:0002376
THRA (1 of 2)	THRA	ensembl biomart, HSA, GO:0002376
THRA (2 of 2)	THRA	ensembl biomart, HSA, GO:0002376
TINAGL1	TINAGL1	ensembl biomart, HSA, GO:0002376
TLR2	TLR2	ensembl biomart, HSA, GO:0002376
TLR5 (1 of 3)	TLR5	ensembl biomart, HSA, GO:0002376
TLR5 (2 of 3)	TLR5	ensembl biomart, HSA, GO:0002376
TLR5 (3 of 3)	TLR5	ensembl biomart, HSA, GO:0002376
TLR7	TLR7	ensembl biomart, HSA, GO:0002376
TLR9	TLR9	ensembl biomart, HSA, GO:0002376
TLX1	TLX1	ensembl biomart, HSA, GO:0002376
TMEM173	TMEM173	ensembl biomart, HSA, GO:0002376
TMX1	TMX1	ensembl biomart, HSA, GO:0002376
TNFAIP1	TNFAIP1	ensembl biomart, HSA, GO:0002376
TNFAIP3	TNFAIP3	ensembl biomart, HSA, GO:0002376
TNFAIP8L2	TNFAIP8L2	ensembl biomart, HSA, GO:0002376
TNFRSF14	TNFRSF14	ensembl biomart, HSA, GO:0002376
TNFRSF1B	TNFRSF1B	ensembl biomart, HSA, GO:0002376
TNIP1	TNIP1	ensembl biomart, HSA, GO:0002376
TNIP2	TNIP2	ensembl biomart, HSA, GO:0002376
TNRC6C (1 of 2)	TNRC6C	ensembl biomart, HSA, GO:0002376
TNRC6C (2 of 2)	TNRC6C	ensembl biomart, HSA, GO:0002376
TP53	TP53	ensembl biomart, HSA, GO:0002376
TPD52	TPD52	ensembl biomart, HSA, GO:0002376
TPO	TPO	ensembl biomart, HSA, GO:0002376
TPP2	TPP2	ensembl biomart, HSA, GO:0002376
TRAF2 (1 of 2)	TRAF2	ensembl biomart, HSA, GO:0002376
TRAF2 (2 of 2)	TRAF2	ensembl biomart, HSA, GO:0002376
TRAF3IP2	TRAF3IP2	ensembl biomart, HSA, GO:0002376
TRAF6	TRAF6	ensembl biomart, HSA, GO:0002376
TRIM25 (1 of 2)	TRIM25	ensembl biomart, HSA, GO:0002376
TRIM25 (2 of 2)	TRIM25	ensembl biomart, HSA, GO:0002376
TRIM32	TRIM32	ensembl biomart, HSA, GO:0002376
TRPM4 (1 of 2)	TRPM4	ensembl biomart, HSA, GO:0002376
TRPM4 (2 of 2)	TRPM4	ensembl biomart, HSA, GO:0002376
TSHR (1 of 2)	TSHR	ensembl biomart, HSA, GO:0002376
TSHR (2 of 2)	TSHR	ensembl biomart, HSA, GO:0002376
TTC7A	TTC7A	ensembl biomart, HSA, GO:0002376
TUBB	TUBB	ensembl biomart, HSA, GO:0002376
TUSC2 (1 of 2)	TUSC2	ensembl biomart, HSA, GO:0002376
TUSC2 (2 of 2)	TUSC2	ensembl biomart, HSA, GO:0002376
TXK	TXK	ensembl biomart, HSA, GO:0002376
TXNIP	TXNIP	ensembl biomart, HSA, GO:0002376
TXNRD2	TXNRD2	ensembl biomart, HSA, GO:0002376
TYK2	TYK2	ensembl biomart, HSA, GO:0002376
TYR (1 of 2)	TYR	ensembl biomart, HSA, GO:0002376
TYR (2 of 2)	TYR	ensembl biomart, HSA, GO:0002376
TYRO3	TYRO3	ensembl biomart, HSA, GO:0002376
UBA52	UBA52	ensembl biomart, HSA, GO:0002376
UBA7	UBA7	ensembl biomart, HSA, GO:0002376
UBE2A	UBE2A	ensembl biomart, HSA, GO:0002376
UNG	UNG	ensembl biomart, HSA, GO:0002376
USP18	USP18	ensembl biomart, HSA, GO:0002376

stickleback_gene_name	human_gene_name	source
VAMP7	VAMP7	ensembl biomart, HSA, GO:0002376
VASP	VASP	ensembl biomart, HSA, GO:0002376
VAV1	VAV1	ensembl biomart, HSA, GO:0002376
VAV3 (1 of 2)	VAV3	ensembl biomart, HSA, GO:0002376
VAV3 (2 of 2)	VAV3	ensembl biomart, HSA, GO:0002376
VCAM1	VCAM1	ensembl biomart, HSA, GO:0002376
VEGFA (1 of 2)	VEGFA	ensembl biomart, HSA, GO:0002376
VEGFA (2 of 2)	VEGFA	ensembl biomart, HSA, GO:0002376
VIPR1 (1 of 2)	VIPR1	ensembl biomart, HSA, GO:0002376
VIPR1 (2 of 2)	VIPR1	ensembl biomart, HSA, GO:0002376
VPS33A	VPS33A	ensembl biomart, HSA, GO:0002376
VTN (1 of 2)	VTN	ensembl biomart, HSA, GO:0002376
VTN (2 of 2)	VTN	ensembl biomart, HSA, GO:0002376
WAS	WAS	ensembl biomart, HSA, GO:0002376
WNT1	WNT1	ensembl biomart, HSA, GO:0002376
WNT10B	WNT10B	ensembl biomart, HSA, GO:0002376
WNT2B (1 of 2)	WNT2B	ensembl biomart, HSA, GO:0002376
WNT2B (2 of 2)	WNT2B	ensembl biomart, HSA, GO:0002376
WNT3	WNT3	ensembl biomart, HSA, GO:0002376
WNT4	WNT4	ensembl biomart, HSA, GO:0002376
WNT5A	WNT5A	ensembl biomart, HSA, GO:0002376
XBP1	XBP1	ensembl biomart, HSA, GO:0002376
XRCC5	XRCC5	ensembl biomart, HSA, GO:0002376
XRCC6	XRCC6	ensembl biomart, HSA, GO:0002376
YES1 (1 of 2)	YES1	ensembl biomart, HSA, GO:0002376
YES1 (2 of 2)	YES1	ensembl biomart, HSA, GO:0002376
YTHDF2	YTHDF2	ensembl biomart, HSA, GO:0002376
ZBTB16	ZBTB16	ensembl biomart, HSA, GO:0002376
ZC3H8	ZC3H8	ensembl biomart, HSA, GO:0002376
ZC3HAV1	ZC3HAV1	ensembl biomart, HSA, GO:0002376
ZEB1 (1 of 2)	ZEB1	ensembl biomart, HSA, GO:0002376
ZEB1 (2 of 2)	ZEB1	ensembl biomart, HSA, GO:0002376
ZFAT	ZFAT	ensembl biomart, HSA, GO:0002376
ZFP36L1	ZFP36L1	ensembl biomart, HSA, GO:0002376
ZFPM1	ZFPM1	ensembl biomart, HSA, GO:0002376
C1QTNF4 (1 of 2)	C1QTNF4	Star et al. 2011; Haase et al. 2013
C1QTNF4 (2 of 2)	C1QTNF4	Star et al. 2011; Haase et al. 2013
C1QTNF5	C1QTNF5	Star et al. 2011; Haase et al. 2013
C4A	C4	Star et al. 2011; Haase et al. 2013
CCR7	CCR7	Star et al. 2011; Haase et al. 2013
CD226	CD226	Star et al. 2011; Haase et al. 2013
CD3E	CD3E	Star et al. 2011; Haase et al. 2013
CD74 (2 of 2)	CD74	Star et al. 2011; Haase et al. 2013
CD79A	CD79A	Star et al. 2011; Haase et al. 2013
CD79B	CD79B	Star et al. 2011; Haase et al. 2013
CXCR3	CXCR3	Star et al. 2011; Haase et al. 2013
ENSGACG00000000336	MHC II beta	Star et al. 2011; Haase et al. 2013
ENSGACG00000000478	TNF	Star et al. 2011; Haase et al. 2013
ENSGACG00000000569	IgM	Star et al. 2011; Haase et al. 2013
ENSGACG00000001729	IL8	Star et al. 2011; Haase et al. 2013
ENSGACG00000001745	TLR18	Star et al. 2011; Haase et al. 2013

stickleback_gene_name	human_gene_name	source
ENSGACG00000001805	TRGC	Star et al. 2011; Haase et al. 2013
ENSGACG00000001919	MHC I	Star et al. 2011; Haase et al. 2013
ENSGACG00000003030	C1QTNF3	Star et al. 2011; Haase et al. 2013
ENSGACG00000005289	TRBC	Star et al. 2011; Haase et al. 2013
ENSGACG00000005449	TLR22	Star et al. 2011; Haase et al. 2013
ENSGACG00000008369	AIRE	Star et al. 2011; Haase et al. 2013
ENSGACG00000008375	AIRE	Star et al. 2011; Haase et al. 2013
ENSGACG00000008397	TLR13	Star et al. 2011; Haase et al. 2013
ENSGACG00000008945	CD8A	Star et al. 2011; Haase et al. 2013
ENSGACG00000008960	CD8B	Star et al. 2011; Haase et al. 2013
ENSGACG00000009282	Fas	Star et al. 2011; Haase et al. 2013
ENSGACG00000009364	TLR21	Star et al. 2011; Haase et al. 2013
ENSGACG00000009832	CD4	Star et al. 2011; Haase et al. 2013
ENSGACG00000012763	IgM	Star et al. 2011; Haase et al. 2013
ENSGACG00000012766	IgM	Star et al. 2011; Haase et al. 2013
ENSGACG00000012767	IgD	Star et al. 2011; Haase et al. 2013
ENSGACG00000012769	IgM	Star et al. 2011; Haase et al. 2013
ENSGACG00000012781	IgD	Star et al. 2011; Haase et al. 2013
ENSGACG00000012783	IgM	Star et al. 2011; Haase et al. 2013
ENSGACG00000012792	IgM	Star et al. 2011; Haase et al. 2013
ENSGACG00000012797	IgD	Star et al. 2011; Haase et al. 2013
ENSGACG00000012799	IgM	Star et al. 2011; Haase et al. 2013
ENSGACG00000012804	IgM	Star et al. 2011; Haase et al. 2013
ENSGACG00000012809	IgM	Star et al. 2011; Haase et al. 2013
ENSGACG00000013031	GZMB	Star et al. 2011; Haase et al. 2013
ENSGACG00000013372	TNF	Star et al. 2011; Haase et al. 2013
ENSGACG00000014811	C5	Star et al. 2011; Haase et al. 2013
ENSGACG00000014852	C1QTNF3	Star et al. 2011; Haase et al. 2013
ENSGACG00000015763	TRGC	Star et al. 2011; Haase et al. 2013
ENSGACG00000016298	IL4RA	Star et al. 2011; Haase et al. 2013
ENSGACG00000017257	FasL	Star et al. 2011; Haase et al. 2013
ENSGACG00000017271	IL15	Star et al. 2011; Haase et al. 2013
ENSGACG00000019078	IL8	Star et al. 2011; Haase et al. 2013
ENSGACG00000019282	B2M	Star et al. 2011; Haase et al. 2013
ENSGACG00000019287	B2M	Star et al. 2011; Haase et al. 2013
FOXP3	FOXP3	Star et al. 2011; Haase et al. 2013
HLA-DMA (5 of 5)	MHC II alpha	Star et al. 2011; Haase et al. 2013
IGBP1	IGBP1	Star et al. 2011; Haase et al. 2013
IL12B (1 of 3)	IL12B	Star et al. 2011; Haase et al. 2013
IL12B (2 of 3)	IL12B	Star et al. 2011; Haase et al. 2013
IL12RB2	IL12RB2	Star et al. 2011; Haase et al. 2013
IL17D (1 of 2)	IL17D	Star et al. 2011; Haase et al. 2013
IL17D (2 of 2)	IL17D	Star et al. 2011; Haase et al. 2013
IL17RA (1 of 2)	IL17RA	Star et al. 2011; Haase et al. 2013
IL17RA (2 of 2)	IL17RA	Star et al. 2011; Haase et al. 2013
IL17RD	IL17RD	Star et al. 2011; Haase et al. 2013
IL1B	IL1B	Star et al. 2011; Haase et al. 2013
IL2RB	IL2RB	Star et al. 2011; Haase et al. 2013
IL6ST	IL6ST	Star et al. 2011; Haase et al. 2013
PSMB1	PSMB1	Star et al. 2011; Haase et al. 2013
PSMB10	PSMB10	Star et al. 2011; Haase et al. 2013
PSMB2	PSMB2	Star et al. 2011; Haase et al. 2013
PSMB3	PSMB3	Star et al. 2011; Haase et al. 2013

stickleback_gene_name	human_gene_name	source
PSMB4	PSMB4	Star et al. 2011; Haase et al. 2013
PSMB5	PSMB5	Star et al. 2011; Haase et al. 2013
PSMB6	PSMB6	Star et al. 2011; Haase et al. 2013
PSMB7	PSMB7	Star et al. 2011; Haase et al. 2013
PSME1	PSME1	Star et al. 2011; Haase et al. 2013
PSME2	PSME2	Star et al. 2011; Haase et al. 2013
PSME3	PSME3	Star et al. 2011; Haase et al. 2013
RFX7 (1 of 2)	RFX7	Star et al. 2011; Haase et al. 2013
RFX7 (2 of 2)	RFX7	Star et al. 2011; Haase et al. 2013
RFXANK	RFXANK	Star et al. 2011; Haase et al. 2013
RFXAP	RFXAP	Star et al. 2011; Haase et al. 2013
TAPBP (6 of 7)	TAPBP	Star et al. 2011; Haase et al. 2013
TAPBP (7 of 7)	TAPBP	Star et al. 2011; Haase et al. 2013
TLR6	TLR1	Star et al. 2011; Haase et al. 2013
TLR8	TLR8	Star et al. 2011; Haase et al. 2013
UNC93B1	UNC93B	Star et al. 2011; Haase et al. 2013

Supplementary table S.2.5 Enriched GO terms. Shown are GO-terms (GO-ID, GO-term) of the group "Biological Process" found to be overrepresented in a given test-set tested against the whole set of identified *G. aculeatus* genes. Given are number of genes per GO-term in test- (#Test) and reference-set (#Ref) with p-values and FDR corrections.

test-set	GO-ID	GO-term	FDR	p-value	#Test	#Ref
total up-regulated in head kidney	GO:0032502	developmental process	2,46E-02	6,04E-04	101	4465
total up-regulated in head kidney	GO:0007275	multicellular organismal development	2,69E-02	7,96E-04	96	4216
total up-regulated in head kidney	GO:0032501	multicellular organismal process	2,69E-02	8,05E-04	96	4225
total up-regulated in head kidney	GO:0048869	cellular developmental process	3,98E-02	1,54E-03	61	2455
total up-regulated in head kidney	GO:0030154	cell differentiation	3,98E-02	1,54E-03	61	2455
total up-regulated in head kidney	GO:0009653	anatomical structure morphogenesis	3,98E-02	1,62E-03	58	2315
total up-regulated in head kidney	GO:0048856	anatomical structure development	3,98E-02	1,63E-03	58	2317
total down-regulated in head kidney	GO:0008152	metabolic process	4,53E-10	3,69E-12	182	7196
total down-regulated in head kidney	GO:0009056	catabolic process	4,36E-08	4,74E-10	70	1875
total down-regulated in head kidney	GO:0006629	lipid metabolic process	5,97E-05	1,14E-06	37	893
total down-regulated in head kidney	GO:0009605	response to external stimulus	7,57E-05	1,65E-06	46	1264
total down-regulated in head kidney	GO:0005975	carbohydrate metabolic process	3,82E-03	1,24E-04	25	627
total down-regulated in head kidney	GO:0019748	secondary metabolic process	9,22E-03	3,38E-04	8	94
total down-regulated in head kidney	GO:0006950	response to stress	9,22E-03	3,51E-04	58	2144
total up-regulated in gill	GO:0032502	developmental process	1,13E-18	6,12E-21	340	4226
total up-regulated in gill	GO:0032501	multicellular organismal process	4,70E-18	3,83E-20	324	3997
total up-regulated in gill	GO:0007275	multicellular organismal development	5,03E-18	5,46E-20	323	3989
total up-regulated in gill	GO:0050789	regulation of biological process	4,76E-13	1,16E-14	455	6800
total up-regulated in gill	GO:0065007	biological regulation	1,20E-12	3,26E-14	459	6916
total up-regulated in gill	GO:0009653	anatomical structure morphogenesis	2,36E-10	9,12E-12	184	2189
total up-regulated in gill	GO:0048856	anatomical structure development	2,36E-10	9,82E-12	184	2191
total up-regulated in gill	GO:0007010	cytoskeleton organization	2,36E-10	1,03E-11	79	652
total up-regulated in gill	GO:0050896	response to stimulus	3,56E-10	1,64E-11	352	5120
total up-regulated in gill	GO:0048869	cellular developmental process	4,10E-10	2,12E-11	191	2325
total up-regulated in gill	GO:0030154	cell differentiation	4,10E-10	2,12E-11	191	2325
total up-regulated in gill	GO:0016043	cellular component organization	4,87E-09	3,05E-10	265	3664

test-set	GO-ID	GO-term	FDR	p-value	#Test	#Ref
total up-regulated in gill	GO:0071840	cellular component organization or biogenesis	4,87E-09	3,05E-10	265	3664
total up-regulated in gill	GO:0007165	signal transduction	3,72E-08	2,59E-09	257	3604
total up-regulated in gill	GO:0009790	embryo development	3,72E-08	2,66E-09	107	1142
total up-regulated in gill	GO:0051716	cellular response to stimulus	3,72E-08	2,66E-09	257	3605
total up-regulated in gill	GO:0050794	regulation of cellular process	3,72E-08	2,73E-09	257	3606
total up-regulated in gill	GO:0009605	response to external stimulus	2,21E-07	1,80E-08	108	1202
total up-regulated in gill	GO:0023052	signaling	4,52E-06	4,79E-07	267	4006
total up-regulated in gill	GO:0009719	response to endogenous stimulus	1,78E-05	1,94E-06	67	704
total up-regulated in gill	GO:0006464	cellular protein modification process	1,95E-05	2,22E-06	144	1923
total up-regulated in gill	GO:0043412	macromolecule modification	1,95E-05	2,22E-06	144	1923
total up-regulated in gill	GO:0006996	organelle organization	3,56E-05	4,16E-06	133	1763
total up-regulated in gill	GO:0071841	cellular component organization or biogenesis at cellular level	3,89E-05	4,76E-06	133	1768
total up-regulated in gill	GO:0071842	cellular component organization at cellular level	3,89E-05	4,76E-06	133	1768
total up-regulated in gill	GO:0009987	cellular process	1,26E-04	1,58E-05	504	8771
total up-regulated in gill	GO:0008283	cell proliferation	5,11E-04	7,08E-05	88	1127
total up-regulated in gill	GO:0008219	cell death	6,20E-04	8,76E-05	101	1347
total up-regulated in gill	GO:0016265	death	6,58E-04	9,47E-05	101	1350
total up-regulated in gill	GO:0044267	cellular protein metabolic process	7,81E-03	1,23E-03	150	2319
total up-regulated in gill	GO:0006950	response to stress	1,75E-02	2,99E-03	133	2069
total up-regulated in gill	GO:0019538	protein metabolic process	2,61E-02	4,68E-03	185	3045
total down-regulated in gill	GO:0006091	generation of precursor metabolites and energy	9,69E-03	6,83E-05	16	386

Supplementary table S.2.6 Differentially expressed immune-related genes in head kidney tissue of *G. aculeatus*. Shown are differentially expressed genes and their corresponding treatment, including FPKM values for control (control_val) and treatment (treatment_val). The log2-fold change shows if there is up- or down-regulation of a given gene due to the parasite treatment. Only significant differences shown.

gene	treatment	control_val	treatment_val	log2(fold_change)
APOB (5 of 5)	clone I	397,857	2,52703	-7,29866
PGLYRP2 (2 of 2)	clone I	302,534	2,23121	-7,08313
APOB (1 of 5)	clone I	142,41	1,13425	-6,97217
C8G	clone I	564,245	4,5427	-6,95663
C3 (1 of 8)	clone I	253,781	2,14946	-6,88346
C8B	clone I	189,341	1,62499	-6,86441
C3 (4 of 8)	clone I	862,33	8,5632	-6,65395
VTN (2 of 2)	clone I	52,3546	0,527891	-6,63193
C3 (5 of 8)	clone I	131,06	1,43388	-6,51416
C3 (3 of 8)	clone I	159,784	1,87542	-6,41276
PLG	clone I	216,823	2,54515	-6,41262
CFP	clone I	95,5085	1,17732	-6,34205
C8A	clone I	107,029	1,39908	-6,25739
SUSD2	clone I	9,21498	0,148896	-5,9516
C9	clone I	141,829	2,39006	-5,89096
ENSGACG00000003030	clone I	50,9171	0,928614	-5,77693
G6PD (2 of 2)	clone I	13,1035	0,242406	-5,75639
ENSGACG00000014811	clone I	107,827	2,36189	-5,51263
C3 (2 of 8)	clone I	100,881	2,30492	-5,45179
ENSGACG00000014852	clone I	56,6342	2,57792	-4,45739
PVRL1 (2 of 2)	clone I	11,0099	0,514717	-4,41888
CFB	clone I	76,4034	3,73169	-4,35573
SERPING1	clone I	265,943	13,3341	-4,31792
C6	clone I	98,9399	6,35633	-3,96029
ENPP2 (2 of 2)	clone I	39,8483	2,61654	-3,92879
KYNU	clone I	9,8258	0,762041	-3,68863
C7 (1 of 2)	clone I	20,5733	1,85433	-3,47181
ADSSL1	clone I	22,0206	2,48666	-3,14657
C3 (8 of 8)	clone I	24,4008	2,94383	-3,05116
MYLPF (2 of 2)	clone I	141,621	20,0123	-2,82307
C3 (7 of 8)	clone I	25,5542	3,86762	-2,72404
ADAMTS13	clone I	6,34378	1,61993	-1,96941
HYAL2 (1 of 2)	clone I	14,5824	32,8338	1,17095
IRF4 (2 of 2)	clone I	24,12	64,276	1,41405
JUNB (1 of 2)	clone I	14,9186	76,5929	2,3601
ENSGACG00000016298	clone I	21,2148	136,593	2,68674
PRF1 (2 of 5)	clone I	2,84543	19,7145	2,79254
THBS1 (2 of 2)	clone I	5,34663	41,8024	2,96688
SOCS3 (2 of 2)	clone I	6,09284	69,9715	3,52158
JUNB (2 of 2)	clone I	4,48677	68,0492	3,92283
SOCS3 (1 of 2)	clone I	8,54547	277,545	5,02142
VTN (1 of 2)	clone mix	290,729	0,291691	-9,96102
C8B	clone mix	189,341	0,246136	-9,58731
PGLYRP2 (2 of 2)	clone mix	302,534	0,491203	-9,26656
PLG	clone mix	216,823	0,38897	-9,12264

gene	treatment	control_val	treatment_val	log2(fold_change)
APOB (5 of 5)	clone mix	397,857	0,736573	-9,07721
C8G	clone mix	564,245	1,19664	-8,88119
ENSGACG00000014811	clone mix	107,827	0,302411	-8,47799
APOB (1 of 5)	clone mix	142,41	0,401887	-8,46904
C8A	clone mix	107,029	0,371097	-8,172
C3 (4 of 8)	clone mix	862,33	3,43326	-7,97252
C3 (3 of 8)	clone mix	159,784	0,846626	-7,56018
CFP	clone mix	95,5085	0,510596	-7,5473
C3 (5 of 8)	clone mix	131,06	0,811535	-7,33536
C3 (1 of 8)	clone mix	253,781	1,58069	-7,32688
C9	clone mix	141,829	1,58198	-6,48627
SUSD2	clone mix	9,21498	0,107208	-6,4255
C3 (2 of 8)	clone mix	100,881	1,47385	-6,09692
ENSGACG00000003030	clone mix	50,9171	1,36813	-5,21788
CFB	clone mix	76,4034	2,06039	-5,21265
G6PD (2 of 2)	clone mix	13,1035	0,459733	-4,83302
ENSGACG00000014852	clone mix	56,6342	2,01001	-4,8164
VTN (2 of 2)	clone mix	52,3546	2,73782	-4,25722
SERPING1	clone mix	265,943	17,0305	-3,96492
C6	clone mix	98,9399	6,54284	-3,91856
ENPP2 (2 of 2)	clone mix	39,8483	3,13234	-3,66921
C3 (8 of 8)	clone mix	24,4008	3,10237	-2,97549
IRF4 (2 of 2)	clone mix	24,12	83,3801	1,78947
ITGA5 (1 of 2)	clone mix	3,89684	19,3759	2,31389
THBS1 (2 of 2)	clone mix	5,34663	28,5636	2,41748
ENSGACG00000016298	clone mix	21,2148	124,818	2,55669
SOCS3 (2 of 2)	clone mix	6,09284	47,1337	2,95157
SIX1	clone mix	2,98137	31,7399	3,41225
JUNB (2 of 2)	clone mix	4,48677	47,7688	3,41232
PIP5K1C (2 of 2)	clone mix	0,832627	10,2316	3,61921
ATP1B3	clone mix	3,11375	55,4923	4,15556
CRIP2 (2 of 2)	clone mix	2,78183	50,6523	4,18652
ADSSL1	clone mix	22,0206	439,238	4,31808
MEF2C (2 of 2)	clone mix	1,28259	30,988	4,59457
SOCS3 (1 of 2)	clone mix	8,54547	230,874	4,7558
MLF1	clone mix	0,781018	21,7563	4,79993
MYLPF (1 of 2)	clone mix	1,35951	2943,02	11,08
PVRL1 (2 of 2)	clone XII	11,0099	0,538633	-4,35336
MYLPF (2 of 2)	clone XII	141,621	16,6078	-3,0921
COL1A1 (2 of 2)	clone XII	57,8938	25,687	-1,17237
ZC3HAV1	clone XII	35,2857	21,6113	-0,707299
ADAMTS13	clone XII	6,34378	11,0225	0,797039
IRF4 (2 of 2)	clone XII	24,12	115,193	2,25575
RGCC	clone XII	28,2047	157,304	2,47955
ENSGACG00000016298	clone XII	21,2148	135,673	2,67699
CYP27B1	clone XII	7,50464	51,4143	2,77632
THBS1 (2 of 2)	clone XII	5,34663	37,0327	2,7921
JUNB (1 of 2)	clone XII	14,9186	106,155	2,83099
CCR9 (1 of 2)	clone XII	2,60228	31,9553	3,61821
CRIP2 (2 of 2)	clone XII	2,78183	39,5776	3,83058
PIP5K1C (2 of 2)	clone XII	0,832627	12,8216	3,94477
JUNB (2 of 2)	clone XII	4,48677	102,8	4,51802
SOCS3 (2 of 2)	clone XII	6,09284	140,181	4,52403

gene	treatment	control_val	treatment_val	log2(fold_change)
ENSGACG00000014852	clone XII	56,6342	2208,16	5,28503
ENSGACG00000003030	clone XII	50,9171	2822,85	5,79286
SOCS3 (1 of 2)	clone XII	8,54547	632,269	6,20923

Supplementary table S.2.7 Differentially expressed immune-related genes in gill tissue of *G. aculeatus*. Shown are differentially expressed genes and their corresponding treatment, including FPKM values for control (control_val) and treatment (treatment_val). The log2-fold change shows if there is up- or down-regulation of a given gene due to the parasite treatment. Only significant differences shown.

gene	treatment	control_val	treatment_val	log2(fold_change)
GATA2 (1 of 2)	clone I	110,657	64,4838	-0,779088
CASP3 (4 of 4)	clone I	450,008	269,981	-0,73709
F11R	clone I	282,828	187,116	-0,595993
EPHA2 (1 of 2)	clone I	24,5537	18,464	-0,411225
COL1A1 (2 of 2)	clone I	120,383	195,736	0,701278
C4A	clone I	26,6354	44,8943	0,753185
PIK3R1 (1 of 2)	clone I	32,8272	76,9047	1,22818
NFKBIA (1 of 2)	clone I	101,293	256,941	1,3429
CCR9 (1 of 2)	clone I	15,7446	43,8927	1,47913
THBS1 (2 of 2)	clone I	2,65074	14,2046	2,42189
SOCS3 (1 of 2)	clone I	25,2321	151,034	2,58154
PFDN1	clone mix	113,611	33,5984	-1,75764
EXOSC5	clone mix	89,0188	28,0065	-1,66835
ATG12	clone mix	50,5042	16,175	-1,64264
ELMOD2	clone mix	99,0101	47,3581	-1,06397
ENSGACG00000000336	clone mix	646,991	391,739	-0,723854
PRDX3	clone mix	128,492	87,3783	-0,556329
DCTN1 (2 of 2)	clone mix	21,9148	35,4999	0,695912
ZC3HAV1	clone mix	57,9356	102,987	0,829933
CHUK (1 of 2)	clone mix	15,6785	28,4516	0,859719
PKHD1L1	clone mix	3,33013	6,26935	0,912738
PRKDC	clone mix	5,5653	11,5522	1,05364
CXCL12 (2 of 2)	clone mix	180,438	381,163	1,0789
VAV3 (2 of 2)	clone mix	7,66529	16,7189	1,12506
MYO9B (1 of 2)	clone mix	11,7707	25,8328	1,134
KLC1	clone mix	10,2467	22,7065	1,14795
MINK1	clone mix	12,5942	27,9295	1,14903
FGFR2	clone mix	38,7514	87,4171	1,17367
TRPM4 (2 of 2)	clone mix	16,1638	36,749	1,18494
LYST	clone mix	2,52577	5,75517	1,18814
ROCK1	clone mix	19,4466	44,4478	1,1926
JAK1	clone mix	42,4953	97,2966	1,19508
IL6ST	clone mix	19,5226	44,7802	1,19771
CHD7	clone mix	6,55623	15,0938	1,20302
PIK3CB	clone mix	18,7046	43,1989	1,2076
TGFBR3	clone mix	15,8447	36,6134	1,20837
MALT1	clone mix	5,48002	12,6746	1,20969
AP3D1	clone mix	10,9076	25,3267	1,21533
TCF3 (1 of 2)	clone mix	12,5922	29,3723	1,22193
NCOA6	clone mix	6,04059	14,0976	1,22269
NLRC5	clone mix	7,72544	18,1536	1,23256
MAPK14 (1 of 2)	clone mix	36,8271	86,8727	1,23813
RICTOR	clone mix	7,93354	18,8267	1,24674
C3 (6 of 8)	clone mix	2,23888	5,32882	1,25104

gene	treatment	control_val	treatment_val	log2(fold_change)
ACIN1	clonemix	21,5025	51,4822	1,25957
PRKCA (2 of 2)	clonemix	7,20845	17,3013	1,26312
PSME4 (1 of 2)	clonemix	11,7679	28,8033	1,29137
C3 (8 of 8)	clonemix	1,66511	4,16296	1,32199
PIK3CG	clonemix	7,73283	19,6629	1,34641
C4A	clonemix	26,6354	68,1728	1,35585
COL1A1 (2 of 2)	clonemix	120,383	312,219	1,37493
PDE1B	clonemix	11,871	30,8535	1,37799
MAP4K2	clonemix	10,3164	27,0149	1,38881
ENSGACG00000001919	clonemix	118,854	316,304	1,41213
MLL	clonemix	3,41602	9,25116	1,43732
SLC11A2 (1 of 2)	clonemix	8,2926	22,76	1,45661
TNRC6C (2 of 2)	clonemix	2,86844	7,96076	1,47264
EP300 (1 of 2)	clonemix	3,93953	10,9489	1,47468
EGR1	clonemix	17,677	49,5211	1,48617
ITCH (2 of 2)	clonemix	4,34254	12,3402	1,50676
CYSLTR2	clonemix	8,98739	25,6988	1,51573
JAG2	clonemix	3,96985	11,4035	1,52232
TGFB1	clonemix	19,2995	56,4909	1,54946
SWAP70 (1 of 2)	clonemix	25,7638	75,9629	1,55995
C7 (2 of 2)	clonemix	11,3621	34,368	1,59683
SKIL	clonemix	5,59669	17,1667	1,61697
PTPN1	clonemix	12,4365	38,4085	1,62685
PREX1	clonemix	7,1903	22,6468	1,65518
MECOM	clonemix	2,79049	8,89955	1,67321
KLF6 (1 of 2)	clonemix	38,6488	127,676	1,72399
THRA (1 of 2)	clonemix	6,17339	20,5508	1,73506
IGF1R (2 of 2)	clonemix	3,76793	12,7508	1,75874
SLC16A1 (1 of 2)	clonemix	10,4441	35,4457	1,76292
PGLYRP2 (1 of 2)	clonemix	12,1395	43,2742	1,83379
SFRP2	clonemix	14,8646	53,0794	1,83627
MKNK2	clonemix	61,4839	221,94	1,85189
COL1A2	clonemix	67,0945	252,776	1,9136
COLEC12 (2 of 2)	clonemix	6,56252	25,2012	1,94117
TINAGL1	clonemix	18,6589	74,4725	1,99684
FN1 (2 of 2)	clonemix	5,47172	21,9932	2,00699
DAB2	clonemix	5,07582	20,4465	2,01014
CCR9 (1 of 2)	clonemix	15,7446	65,1434	2,04877
HDAC4 (1 of 2)	clonemix	3,84143	15,899	2,04922
EDN2	clonemix	9,09681	37,761	2,05346
SRF (2 of 2)	clonemix	2,85015	11,9942	2,07322
PIK3R1 (1 of 2)	clonemix	32,8272	138,861	2,08068
FN1 (1 of 2)	clonemix	11,812	50,042	2,08289
JUNB (2 of 2)	clonemix	15,1382	66,1757	2,1281
ITGA1	clonemix	8,11723	35,7251	2,13788
NFKBIA (1 of 2)	clonemix	101,293	453,214	2,16166
ITGA5 (1 of 2)	clonemix	1,8522	8,67928	2,22833
PODXL	clonemix	6,93071	32,6175	2,23457
KIF3C (1 of 2)	clonemix	2,13274	10,4545	2,29334
JUNB (1 of 2)	clonemix	22,0675	136,157	2,62527
DUSP6	clonemix	8,66461	56,9579	2,71669
SOCS3 (2 of 2)	clonemix	8,34668	65,733	2,97734
ADAM8 (1 of 2)	clonemix	1,99632	15,7632	2,98115

gene	treatment	control_val	treatment_val	log2(fold_change)
THBS1 (2 of 2)	clone mix	2,65074	34,9675	3,72154
SOCS3 (1 of 2)	clone mix	25,2321	334,289	3,72776
ITGB1 (1 of 2)	clone XII	35,9397	55,5941	0,629352
C4A	clone XII	26,6354	59,4999	1,15954
DAB2	clone XII	5,07582	14,08	1,47193
C6	clone XII	3,91636	10,9939	1,48911
SLC3A2 (2 of 2)	clone XII	57,6051	203,394	1,82001
JUNB (2 of 2)	clone XII	15,1382	63,0149	2,0575
SOCS3 (2 of 2)	clone XII	8,34668	47,5986	2,51164
ITGA5 (1 of 2)	clone XII	1,8522	12,0105	2,69698
ADAM8 (1 of 2)	clone XII	1,99632	14,0493	2,81508
SOCS3 (1 of 2)	clone XII	25,2321	250,36	3,31067
THBS1 (2 of 2)	clone XII	2,65074	34,5915	3,70595

Appendix Chapter 3

Supplementary table S.3.1 Number of reads per sample, including treatment, fish family, organ type, flowcell lane number, total reads and mapped reads. Seven samples from gills were of reduced quality and had to be removed from further analysis. This led to 2 samples of M-C and XII-M and 3 samples of M-M, I-M and XII-XII in gills as well as 4 samples for all remaining treatments, resulting in 57 individual libraries.

sample	fish family	treatment	organ	lane no	total reads	aligned reads	% aligned
30	10-2x1	M-C	gills	L003	23200292	10673872	46,01
31	10-13x12	M-C	gills	L007	13843090	7269757	52,52
32	10-13x12	M-M	gills	L002	15338700	5590881	36,45
33	10-11x16	M-M	gills	L008	9388988	4603250	49,03
34	10-10x15	M-M	gills	L008	13518952	6765327	50,04
35	10-2x1	I-C	gills	L002	11469604	6214717	54,18
36	10-13x12	I-C	gills	L001	15699134	9302945	59,26
37	10-10x15	I-C	gills	L005	9427674	4985903	52,89
38	10-11x16	I-C	gills	L005	9696188	5067788	52,27
39	10-13x12	I-M	gills	L001	14100266	7211746	51,15
40	10-2x1	I-M	gills	L001	16578380	9333477	56,30
41	10-11x16	I-M	gills	L007	5347532	2592101	48,47
42	10-2x1	I-I	gills	L001	4063104	2291667	56,40
43	10-13x12	I-I	gills	L003	14077882	6987047	49,63
44	10-11x16	I-I	gills	L004	6580812	3040312	46,20
45	10-10x15	I-I	gills	L006	4209734	2198714	52,23
46	10-13x12	XII-C	gills	L001	22333120	12833446	57,46
47	10-2x1	XII-C	gills	L002	10633172	5381299	50,61
48	10-11x16	XII-C	gills	L005	5259256	2753246	52,35
49	10-10x15	XII-C	gills	L003	17222058	10103310	58,66
50	10-2x1	XII-M	gills	L004	11213700	5480842	48,88
51	10-10x15	XII-M	gills	L005	6136364	3248372	52,94
52	10-13x12	XII-XII	gills	L003	15972590	8927896	55,90
53	10-11x16	XII-XII	gills	L006	13032102	7691739	59,02
54	10-10x15	XII-XII	gills	L008	10406320	4868582	46,78
55	10-2x1	M-C	head kidney	L004	19397972	10114604	52,14
56	10-13x12	M-C	head kidney	L002	18125592	10561800	58,27
57	10-11x16	M-C	head kidney	L006	21368720	13513779	63,24
58	10-10x15	M-C	head kidney	L007	27882162	14601208	52,37
59	10-13x12	M-M	head kidney	L005	17938740	9686640	54,00
60	10-2x1	M-M	head kidney	L002	14743006	8639596	58,60
61	10-11x16	M-M	head kidney	L001	26166842	15671690	59,89
62	10-10x15	M-M	head kidney	L008	22917476	11210711	48,92
63	10-2x1	I-C	head kidney	L002	15901786	9654649	60,71
64	10-13x12	I-C	head kidney	L001	21585752	12516032	57,98
65	10-10x15	I-C	head kidney	L007	13507136	7198480	53,29
66	10-11x16	I-C	head kidney	L007	19187590	9882590	51,51
67	10-13x12	I-M	head kidney	L001	29708146	17022959	57,30
68	10-2x1	I-M	head kidney	L005	9385772	5185492	55,25
69	10-11x16	I-M	head kidney	L007	14238190	7842227	55,08
70	10-10x15	I-M	head kidney	L008	17588174	9551118	54,30
71	10-2x1	I-I	head kidney	L001	20113408	13216210	65,71
72	10-13x12	I-I	head kidney	L006	23300234	14747637	63,29
73	10-11x16	I-I	head kidney	L003	17524576	10753016	61,36
74	10-10x15	I-I	head kidney	L006	15238958	9376244	61,53

sample	fish family	treatment	organ	lane no	total reads	aligned reads	% aligned
75	10-13x12	XII-C	head kidney	L003	20949002	11779921	56,23
76	10-2x1	XII-C	head kidney	L004	14624880	8093626	55,34
77	10-11x16	XII-C	head kidney	L004	16929110	9576694	56,57
78	10-10x15	XII-C	head kidney	L004	23834444	12169141	51,06
79	10-2x1	XII-M	head kidney	L003	27035170	16038620	59,33
80	10-13x12	XII-M	head kidney	L003	25921982	14714739	56,77
81	10-10x15	XII-M	head kidney	L006	35427104	21128950	59,64
82	10-11x16	XII-M	head kidney	L006	18137748	11393160	62,81
83	10-2x1	XII-XII	head kidney	L002	20256484	11087272	54,73
84	10-13x12	XII-XII	head kidney	L002	23309590	12869852	55,21
85	10-11x16	XII-XII	head kidney	L005	38346330	20984672	54,72
86	10-10x15	XII-XII	head kidney	L007	13026678	7185444	55,16

Supplementary table S.3.2 Cufflinks output, list of differentially expressed genes in head kidney tissue of three-spined sticklebacks. Differentially expressed is defined by comparison to pre-exposed controls (I-C, XII-C or M-C). The term "gene" is the name for a specific gene as taken from the *G. aculeatus* reference genome, "sample_1" is the preexposure control group, "sample_2" the infection treatment group, log2(fold change) displays the transformed fold change in "sample_2" compared to "sample_1", p value and q value are given for each test (only significant differences shown).

gene	sample_1	sample_2	log2(fold_change)	p_value	q_value
A1CF	I-C	I-I	3,2036	0,0022239	0,029203
ACTN2	I-C	I-I	-9,76437	5,15E-008	3,64E-006
ADPRHL1	I-C	I-I	-7,39486	2,42E-007	1,38E-005
ALPK3 (1 of 2)	I-C	I-I	-6,94988	0,0005625	0,00961366
APOB (2 of 5)	I-C	I-I	3,40812	5,57E-006	0,00020195
APOE (2 of 2)	I-C	I-I	3,48032	0,0043787	0,0497963
ASB10	I-C	I-I	-7,03418	0,0017174	0,0237451
BMP10 (2 of 2)	I-C	I-I	-1,80E+308	0,0022095	0,029054
CAP2	I-C	I-I	-4,88706	8,8544E-04	0,0139076
CHRM2 (1 of 2)	I-C	I-I	-4,05351	0,0032527	0,039484
CKMT2 (1 of 2)	I-C	I-I	-5,44235	1,88E-005	0,00056622
COMTD1 (2 of 2)	I-C	I-I	1,80E+308	0,0007038	0,0115437
CSRP3	I-C	I-I	-8,35771	1,91E-006	8,14E-005
CUZD1	I-C	I-I	4,13725	0,0004637	0,00821235
DES	I-C	I-I	-5,54369	0,0015245	0,0215832
ELMOD2	I-C	I-I	0,950604	5,59E-011	9,15E-009
ENSGACG00000000115	I-C	I-I	-3,54206	7,02E-005	0,0017111
ENSGACG00000000272	I-C	I-I	-5,34753	0,00011243	0,00253701
ENSGACG00000000300	I-C	I-I	-5,57803	0,0003628	0,00671037
ENSGACG00000001073	I-C	I-I	-5,8439	0,0002577	0,00505692
ENSGACG00000001559	I-C	I-I	1,54286	0,0019455	0,0262497
ENSGACG00000002089	I-C	I-I	-4,90571	0,0005155	0,00895473
ENSGACG00000003351	I-C	I-I	-4,36197	0,0012195	0,0180416
ENSGACG00000003435	I-C	I-I	3,40672	0,0010413	0,0158758
ENSGACG00000003787	I-C	I-I	1,6804	0,0001988	0,00407695
ENSGACG00000004463	I-C	I-I	3,67183	0,0002604	0,00510036
ENSGACG00000005994	I-C	I-I	-5,28514	7,13E-005	0,00173349
ENSGACG00000006109	I-C	I-I	-5,20298	0,001911	0,0258757
ENSGACG00000006644	I-C	I-I	2,84275	0,0009159	0,0142995
ENSGACG00000006829	I-C	I-I	3,91479	4,24E-005	0,00112144
ENSGACG00000006908	I-C	I-I	2,11471	0,0010229	0,0156465
ENSGACG00000007505	I-C	I-I	3,42935	0,0014793	0,0210679
ENSGACG00000007661	I-C	I-I	-8,52956	2,85E-005	0,00080373
ENSGACG00000009801	I-C	I-I	-0,929019	1,81E-005	0,00054907
ENSGACG00000009821	I-C	I-I	-6,51937	5,78E-006	0,00020822
ENSGACG00000009825	I-C	I-I	1,77626	3,99E-008	2,92E-006
ENSGACG00000010126	I-C	I-I	-9,32576	3,77E-010	4,97E-008
ENSGACG00000010623	I-C	I-I	-9,96683	4,33E-006	0,00016313
ENSGACG00000011294	I-C	I-I	-2,81859	0,0005336	0,00921181
ENSGACG00000012657	I-C	I-I	-8,84593	2,37E-006	9,76E-005
ENSGACG00000012663	I-C	I-I	-6,21131	1,2123E-04	0,00270081
ENSGACG00000013782	I-C	I-I	-6,71836	2,64E-005	0,0007535
ENSGACG00000014948	I-C	I-I	-12,0484	0,0001029	0,00235484

gene	sample_1	sample_2	log2(fold_change)	p_value	q_value
ENSGACG00000014960	I-C	I-I	-9,34773	7,05E-009	6,49E-007
ENSGACG00000015168	I-C	I-I	-4,32944	0,001492	0,0212132
ENSGACG00000015464	I-C	I-I	1,07663	0,000847	0,0134155
ENSGACG00000016813	I-C	I-I	-4,01863	4,49E-010	5,80E-008
ENSGACG00000017681	I-C	I-I	2,1781	0	0
ENSGACG00000017758	I-C	I-I	4,33209	0,001764	0,0242613
ENSGACG00000019454	I-C	I-I	3,37742	0,0020256	0,0271166
ENSGACG00000019517	I-C	I-I	4,63325	0,000233	0,0046527
ENSGACG00000019604	I-C	I-I	1,75918	0,0018373	0,0250825
ENSGACG00000019744	I-C	I-I	-8,2213	9,57E-010	1,13E-007
ENSGACG00000019784	I-C	I-I	-5,37535	0,0006856	0,011297
ENSGACG00000020653	I-C	I-I	3,75858	7,79E-005	0,00186652
ENSGACG00000020852	I-C	I-I	-0,866915	0,0005954	0,0100692
F9 (2 of 2)	I-C	I-I	2,11605	0,0010282	0,0157123
FABP1	I-C	I-I	4,24325	0,0001413	0,00306845
FBXO40 (1 of 3)	I-C	I-I	-6,03503	8,25E-005	0,00195831
FGF8 (2 of 2)	I-C	I-I	-7,17864	4,78E-005	0,00124014
FHL2 (1 of 2)	I-C	I-I	-6,36153	6,58E-005	0,00162077
FHOD3 (1 of 2)	I-C	I-I	-4,38783	0,0017679	0,0243055
FLNC (2 of 2)	I-C	I-I	-6,84303	3,02E-005	0,00084467
FOXA3	I-C	I-I	3,44121	0,0021748	0,0286915
G6PC (1 of 2)	I-C	I-I	3,81217	0,0036596	0,0433184
GAPDH (1 of 2)	I-C	I-I	-5,46821	0,000939	0,0145956
HAO1	I-C	I-I	2,82325	3,47E-009	3,50E-007
HSP90AA1 (2 of 2)	I-C	I-I	-5,81598	0,0004204	0,00757666
HSPB7	I-C	I-I	-5,74368	0,0002557	0,00502486
IGFBP1 (1 of 2)	I-C	I-I	4,68339	0,0006887	0,0113397
IGFBP2 (2 of 2)	I-C	I-I	3,62982	0,0029777	0,0368385
KBTBD12	I-C	I-I	-4,59262	0,00311129	0,0381166
KCNH2 (2 of 2)	I-C	I-I	-8,86128	2,00E-006	8,46E-005
KCNJ14	I-C	I-I	-4,38144	0,0020864	0,0277639
KCNJ5	I-C	I-I	-5,17193	0,00014311	0,00310119
KLHL31	I-C	I-I	-5,70514	0,0009157	0,0142964
LDB3	I-C	I-I	-5,27519	0,0015756	0,0221617
LMOD2 (1 of 2)	I-C	I-I	-5,89506	2,60E-005	0,00074495
LRG1	I-C	I-I	3,22671	0,0014649	0,0209036
LRRC10	I-C	I-I	-3,65971	0,0022374	0,029345
MASP1 (2 of 2)	I-C	I-I	4,11019	0,0014483	0,0207118
MSRB2	I-C	I-I	2,89639	0,00113461	0,0170253
MYL7	I-C	I-I	-9,23	1,10E-006	5,08E-005
MYLK4 (1 of 2)	I-C	I-I	-8,58864	4,04E-005	0,00107837
MYLK4 (2 of 2)	I-C	I-I	-5,90449	0,0003307	0,00621669
MYO18A (2 of 2)	I-C	I-I	-6,25441	0,0001551	0,00331456
MYOZ2 (1 of 2)	I-C	I-I	-6,99721	5,16E-007	2,65E-005
NDUFA4 (2 of 2)	I-C	I-I	-4,516	0,0041298	0,0475971
NEBL	I-C	I-I	-4,57686	0,0013342	0,0193943
NEURL2	I-C	I-I	-5,66264	9,64E-005	0,00223017
NEXN	I-C	I-I	-6,13821	7,83E-005	0,00187541
NRAP	I-C	I-I	-5,11863	0,0003417	0,0063863
PCK1	I-C	I-I	5,30571	1,04E-006	4,82E-005
PDLIM1	I-C	I-I	-5,57631	0,0001959	0,00402836
PIK3IP1	I-C	I-I	-0,439696	0,0036948	0,0436465
PLA2G12B (1 of 2)	I-C	I-I	4,38859	0,0017699	0,0243288

gene	sample_1	sample_2	log2(fold_change)	p_value	q_value
PRG4	I-C	I-I	3,88188	0,0012575	0,0184982
RASAL1	I-C	I-I	4,96106	0,0030906	0,0379258
RGR	I-C	I-I	-4,50471	0,0024052	0,031093
RGS5	I-C	I-I	-1,04667	2,42E-006	9,93E-005
RRAD	I-C	I-I	-4,13646	0,00291	0,0361699
SCN4A (2 of 2)	I-C	I-I	-6,31184	0,0005568	0,0095339
SCN4B (1 of 2)	I-C	I-I	-5,88474	2,72E-005	0,00077369
SLC13A3	I-C	I-I	3,3038	0,0023183	0,030191
SLC22A16	I-C	I-I	2,95895	0,0030439	0,0374805
SLC25A43	I-C	I-I	-2,21571	0,0027089	0,0341623
SLC41A3 (1 of 2)	I-C	I-I	-6,68688	8,26E-006	0,00028215
SMPX	I-C	I-I	-5,4675	3,1745E-04	0,00600772
SORBS2	I-C	I-I	-5,54165	0,0002906	0,00558465
SPP2	I-C	I-I	2,95744	0,0025063	0,0321261
STX2 (2 of 2)	I-C	I-I	1,14427	0,0008787	0,0138221
SYNPO2L (2 of 2)	I-C	I-I	-8,49299	2,23E-008	1,77E-006
TBX5	I-C	I-I	-7,20804	0,0001651	0,0034942
TEKT4	I-C	I-I	-8,79113	8,45E-008	5,60E-006
TMEM182	I-C	I-I	-3,86601	0,00011533	0,00259158
TMOD1	I-C	I-I	-3,64097	1,6207E-04	0,00343936
TNNC1	I-C	I-I	-10,7505	3,22E-007	1,77E-005
TNNT2 (1 of 2)	I-C	I-I	-9,44077	1,54E-006	6,75E-005
TRIM55 (1 of 2)	I-C	I-I	-6,03454	0,0003517	0,00653795
TTN	I-C	I-I	-5,6439	0,0015707	0,0221066
TXLNB (1 of 2)	I-C	I-I	-4,79872	4,3172E-04	0,00774481
TXLNB (2 of 2)	I-C	I-I	-5,19878	0,0008945	0,0140236
UNC119 (2 of 2)	I-C	I-I	-6,20599	0,0005308	0,00917109
USP13	I-C	I-I	-5,1325	0,0003673	0,00677983
USP28	I-C	I-I	-5,15739	0,0007556	0,0122272
VTN (2 of 2)	I-C	I-I	1,79699	1,62E-006	7,07E-005
ACTN2	I-C	I-M	-9,64766	7,94E-008	5,30E-006
ADPRHL1	I-C	I-M	-1,80E+308	0,0007273	0,011855
ALPK3 (1 of 2)	I-C	I-M	-6,2787	8,50E-005	0,00200787
APOBEC2 (2 of 2)	I-C	I-M	-5,94001	0,0013633	0,0197365
ASB10	I-C	I-M	-7,29938	0,0016941	0,0234895
BMP10 (2 of 2)	I-C	I-M	-8,31862	1,30E-006	5,86E-005
CAP2	I-C	I-M	-5,19012	0,0007241	0,0118134
CAV3	I-C	I-M	-4,84283	0,0040926	0,0472586
CD2	I-C	I-M	1,26396	0,002573	0,0328042
CKMT2 (1 of 2)	I-C	I-M	-6,08517	0,00011364	0,00255961
COX6B1 (1 of 2)	I-C	I-M	-4,49974	0,0015801	0,0222111
CSRP3	I-C	I-M	-1,80E+308	0,0021666	0,0286077
DES	I-C	I-M	-7,90155	3,33E-005	0,00091747
ENSGACG00000000115	I-C	I-M	-3,9053	7,61E-005	0,00182976
ENSGACG00000000272	I-C	I-M	-6,18776	1,41E-005	0,0004443
ENSGACG00000000300	I-C	I-M	-6,07926	0,004199	0,0482167
ENSGACG00000001073	I-C	I-M	-6,08942	0,0001258	0,00278648
ENSGACG00000002089	I-C	I-M	-5,65334	0,0007307	0,0119005
ENSGACG00000002830	I-C	I-M	-5,82383	0,0016229	0,0226912
ENSGACG00000003351	I-C	I-M	-5,05096	0,0002222	0,00447343
ENSGACG00000004239	I-C	I-M	1,22532	3,50E-007	1,90E-005
ENSGACG00000005760	I-C	I-M	1,47151	0,0023884	0,0309173
ENSGACG00000005994	I-C	I-M	-5,06538	0,0002038	0,00416163

gene	sample_1	sample_2	log2(fold_change)	p_value	q_value
ENSGACG00000006109	I-C	I-M	-4,96385	0,0030368	0,0374111
ENSGACG00000007661	I-C	I-M	-9,58726	7,41E-006	0,00025721
ENSGACG00000009821	I-C	I-M	-5,37486	0,0001338	0,00293145
ENSGACG00000009825	I-C	I-M	1,31201	0,0004598	0,00815422
ENSGACG00000010126	I-C	I-M	-9,11835	4,30E-011	7,25E-009
ENSGACG00000010375	I-C	I-M	0,503829	0,000607	0,0102285
ENSGACG00000010623	I-C	I-M	-8,98926	1,01E-005	0,00033418
ENSGACG00000012654	I-C	I-M	-7,58903	2,36E-005	0,00068562
ENSGACG00000012657	I-C	I-M	-9,69557	6,11E-007	3,07E-005
ENSGACG00000012663	I-C	I-M	-6,2842	0,000182	0,00378736
ENSGACG00000013782	I-C	I-M	-8,31958	1,19E-006	5,43E-005
ENSGACG00000014948	I-C	I-M	-10,83	0,0004092	0,00741153
ENSGACG00000014960	I-C	I-M	-9,94095	2,92E-009	3,01E-007
ENSGACG00000016813	I-C	I-M	-3,55478	0,000106	0,00241466
ENSGACG00000018706	I-C	I-M	-5,64052	0,0024523	0,031576
ENSGACG00000019744	I-C	I-M	-8,70632	1,79E-007	1,07E-005
ENSGACG00000019784	I-C	I-M	-5,91224	0,000489	0,00857414
FBRSL1	I-C	I-M	0,587013	0,0013918	0,0200639
FBXO40 (1 of 3)	I-C	I-M	-4,43413	0,0002857	0,00550594
FGF8 (2 of 2)	I-C	I-M	-1,80E+308	0,0038188	0,0447832
FHL2 (1 of 2)	I-C	I-M	-6,47491	0,0002713	0,00527475
FOSL1	I-C	I-M	6,24922	5,71E-005	0,00144035
GAPDH (1 of 2)	I-C	I-M	-6,36137	0,00016	0,0034015
GPM6B (2 of 2)	I-C	I-M	1,86623	0	0
GZMM (2 of 5)	I-C	I-M	-1,24609	1,02E-005	0,0003377
HSP90AA1 (2 of 2)	I-C	I-M	-5,16525	0,0006415	0,0107001
HSPB7	I-C	I-M	-6,06835	0,0001861	0,00385942
IL22RA1	I-C	I-M	6,65357	1,77E-007	1,06E-005
JPH2	I-C	I-M	-4,2612	0,0007527	0,0121896
KCNH2 (2 of 2)	I-C	I-M	-7,2939	0,0005836	0,00990548
KLHL31	I-C	I-M	-6,41344	0,0004331	0,00776472
LDB3	I-C	I-M	-5,29263	0,0007259	0,0118366
LRRC10	I-C	I-M	-5,83602	0,0021321	0,0282501
MMP9	I-C	I-M	2,93848	0,0022669	0,0296505
MYL7	I-C	I-M	-9,58177	7,13E-007	3,50E-005
MYLK4 (2 of 2)	I-C	I-M	-4,29637	0,0018583	0,0253093
MYO18A (2 of 2)	I-C	I-M	-5,63737	4,73E-005	0,00123105
MYOZ2 (1 of 2)	I-C	I-M	-1,80E+308	0,0031884	0,0388637
NAV3	I-C	I-M	-2,88097	0,0003515	0,00653484
NEURL2	I-C	I-M	-5,32465	0,0002759	0,00534957
NEXN	I-C	I-M	-6,95422	2,62E-006	0,00010654
NUDC	I-C	I-M	0,60157	0,001437	0,0205825
OBSL1 (2 of 2)	I-C	I-M	-3,59071	0,0023857	0,0308886
PDLIM1	I-C	I-M	-5,01518	0,0003547	0,00658534
PFKM (2 of 2)	I-C	I-M	-4,32162	0,001694	0,0234893
PGAM2	I-C	I-M	-4,71721	0,0012638	0,0185711
PYGM (2 of 2)	I-C	I-M	-4,82057	0,000834	0,0132458
RALY	I-C	I-M	3,27138	0,004244	0,0486187
SARDH	I-C	I-M	0,845349	0,0007201	0,0117598
SCN4A (2 of 2)	I-C	I-M	-5,61785	1,46E-005	0,00045688
SCN4B (1 of 2)	I-C	I-M	-4,6932	5,33E-005	0,00136033
SLC41A3 (1 of 2)	I-C	I-M	-6,29454	5,99E-005	0,00149977
SLC7A6	I-C	I-M	-4,73045	0,0031039	0,0380482

gene	sample_1	sample_2	log2(fold_change)	p_value	q_value
SLC8A1 (2 of 2)	I-C	I-M	-8,19525	1,27E-008	1,08E-006
SMPX	I-C	I-M	-4,7602	0,0029474	0,0365408
SNTB1	I-C	I-M	1,19752	0,0004171	0,00752695
SYNPO2L (2 of 2)	I-C	I-M	-7,84385	8,72E-009	7,82E-007
TBX5	I-C	I-M	-1,80E+308	0,0025359	0,0324265
TEKT4	I-C	I-M	-7,27979	7,71E-008	5,17E-006
TMEM182	I-C	I-M	-4,41403	4,94E-005	0,00127469
TMOD1	I-C	I-M	-4,67481	0,0003427	0,00640146
TNNC1	I-C	I-M	-10,7611	4,16E-007	2,21E-005
TNNT2 (1 of 2)	I-C	I-M	-9,03996	8,01E-007	3,87E-005
TPM2	I-C	I-M	-2,01832	0,0006089	0,0102537
TRIM55 (1 of 2)	I-C	I-M	-5,54131	0,0029788	0,0368492
TTN	I-C	I-M	-6,78561	0,000245	0,00485106
TXLNB (1 of 2)	I-C	I-M	-6,14956	1,22E-005	0,00039175
TXLNB (2 of 2)	I-C	I-M	-6,31793	0,0001073	0,00243889
UGP2 (1 of 2)	I-C	I-M	0,632532	0,0003415	0,00638288
UNC119 (2 of 2)	I-C	I-M	-4,83963	0,0005432	0,0093443
USP13	I-C	I-M	-5,6379	0,0003843	0,00703771
USP28	I-C	I-M	-6,42494	0,000275	0,00533523
A1CF	M-C	M-M	6,24562	2,80E-005	0,00079265
ABCB11	M-C	M-M	3,99804	0,0014103	0,020277
ABCB4	M-C	M-M	5,64531	0,0003517	0,00653902
ABCC11	M-C	M-M	4,03032	0,0036797	0,0435067
ACMSD	M-C	M-M	4,54276	0,001329	0,019336
ADAMTS13	M-C	M-M	3,28212	0,0022013	0,0289666
ADSSL1	M-C	M-M	-3,21472	4,6361E-04	0,00821118
AGR2	M-C	M-M	4,78149	0,0007701	0,0124214
AGT	M-C	M-M	6,91082	2,99E-007	1,66E-005
AGXT (1 of 2)	M-C	M-M	6,43777	3,41E-006	0,00013333
AGXT (2 of 2)	M-C	M-M	5,77562	7,21E-005	0,0017491
AGXT2 (1 of 2)	M-C	M-M	4,22101	0,0031646	0,0386356
AHSG	M-C	M-M	6,88328	1,58E-009	1,76E-007
ALDH8A1	M-C	M-M	4,06988	0,00211352	0,028054
ALLC	M-C	M-M	5,12333	3,99E-005	0,00106523
AMDHD1	M-C	M-M	3,98926	0,0014018	0,0201816
AMN	M-C	M-M	4,88142	0,0031865	0,0388457
ANGPTL3 (1 of 2)	M-C	M-M	4,71893	0,0016751	0,0232799
APOA1	M-C	M-M	6,32992	7,89E-005	0,00188727
APOB (1 of 5)	M-C	M-M	5,26128	6,60E-005	0,0016248
APOB (5 of 5)	M-C	M-M	6,19346	3,33E-010	4,45E-008
APOH (2 of 2)	M-C	M-M	4,39094	0,0019767	0,0265904
ARG1	M-C	M-M	3,29273	0,0012339	0,0182174
ARL14 (2 of 2)	M-C	M-M	6,06266	0,0001719	0,00361185
ASGR1	M-C	M-M	4,78904	0,0003742	0,00688546
ATP2A1 (1 of 2)	M-C	M-M	-4,51672	2,26E-006	9,37E-005
ATP2A1 (2 of 2)	M-C	M-M	-5,49328	1,22E-007	7,69E-006
BCO2 (3 of 3)	M-C	M-M	4,66599	2,05E-005	0,00060817
C3 (1 of 8)	M-C	M-M	5,26274	1,83E-005	0,00055388
C3 (2 of 8)	M-C	M-M	5,98528	1,48E-005	0,0004609
C3 (3 of 8)	M-C	M-M	5,53618	4,52E-005	0,00118481
C3 (4 of 8)	M-C	M-M	5,73688	0,0002215	0,00446176
C3 (5 of 8)	M-C	M-M	5,20093	1,0283E-04	0,0023544
C6orf58	M-C	M-M	4,60758	0,0003858	0,00705953

gene	sample_1	sample_2	log2(fold_change)	p_value	q_value
C8A	M-C	M-M	5,9133	9,50E-006	0,0003173
C8B	M-C	M-M	5,78051	3,13E-005	0,00087079
C8G	M-C	M-M	5,77978	4,83E-005	0,00125181
C9	M-C	M-M	4,90788	0,0001662	0,00351147
CASQ1 (1 of 2)	M-C	M-M	-6,37873	1,44E-007	8,87E-006
CETP	M-C	M-M	5,98376	4,12E-006	0,00015642
CFB	M-C	M-M	3,0643	0,00321159	0,0390877
CFP	M-C	M-M	4,19919	0,0009356	0,0145522
CHIA	M-C	M-M	6,02963	0,0004688	0,00828558
CHRNA3	M-C	M-M	-0,57589	0,0010359	0,015809
CIDEB	M-C	M-M	5,1474	0,0001788	0,00373299
CKM (1 of 2)	M-C	M-M	-5,12307	3,52E-007	1,91E-005
CLIC5 (1 of 2)	M-C	M-M	5,71021	0,0004508	0,00802405
CNDP1	M-C	M-M	5,01556	1,87E-005	0,00056515
CNGB1 (1 of 2)	M-C	M-M	2,45307	0,0021937	0,0288866
CYP24A1	M-C	M-M	6,23321	1,49E-014	5,35E-012
CYP2C9	M-C	M-M	5,44079	0,0003941	0,00718528
CYP2J2 (1 of 6)	M-C	M-M	4,44073	1,13E-005	0,00036846
CYP2J2 (2 of 6)	M-C	M-M	6,14929	4,17E-006	0,00015805
CYP2J2 (3 of 6)	M-C	M-M	5,24812	4,23E-008	3,07E-006
CYP2R1	M-C	M-M	4,82016	0,000318	0,00601638
CYP2W1 (1 of 5)	M-C	M-M	6,79932	1,47E-006	6,48E-005
CYP7A1	M-C	M-M	3,33197	0	0
CYP8B1	M-C	M-M	4,7681	0,0001261	0,00279186
DIABLO (1 of 2)	M-C	M-M	6,83145	7,30E-006	0,00025404
DNAJC22	M-C	M-M	1,80E+308	0,0015695	0,0220934
DPYS	M-C	M-M	5,5907	0,0002286	0,00457873
ENPP2 (2 of 2)	M-C	M-M	3,37469	0,0034235	0,0411006
ENSGACG00000000007	M-C	M-M	4,67798	0,0004701	0,00830421
ENSGACG00000001260	M-C	M-M	5,46537	5,69E-005	0,00143703
ENSGACG00000001432	M-C	M-M	4,97537	0,00014611	0,00315546
ENSGACG00000001522	M-C	M-M	-4,2287	0,0002878	0,00554095
ENSGACG00000001559	M-C	M-M	4,22704	0,0001733	0,00363691
ENSGACG00000001733	M-C	M-M	5,1101	9,11E-006	0,00030625
ENSGACG00000001742	M-C	M-M	2,6669	0,0007754	0,0124921
ENSGACG00000002738	M-C	M-M	-4,01513	0,000636	0,0106266
ENSGACG00000003003	M-C	M-M	-3,70792	0,0005422	0,00933051
ENSGACG00000003030	M-C	M-M	9,62865	5,41E-012	1,14E-009
ENSGACG00000003435	M-C	M-M	6,45185	0,0007708	0,0124303
ENSGACG00000003461	M-C	M-M	6,14974	1,53E-005	0,00047633
ENSGACG00000003467	M-C	M-M	5,61175	0,0004184	0,00754595
ENSGACG00000003473	M-C	M-M	5,46971	7,44E-005	0,00179517
ENSGACG00000003787	M-C	M-M	2,94554	0	0
ENSGACG00000004413	M-C	M-M	5,86328	2,27E-005	0,00066346
ENSGACG00000004463	M-C	M-M	4,60709	0,0015058	0,0213705
ENSGACG00000004949	M-C	M-M	3,96517	2,8213E-04	0,00544833
ENSGACG00000005023	M-C	M-M	-5,47101	6,59E-006	0,00023302
ENSGACG00000005067	M-C	M-M	4,02377	0,00211347	0,0280536
ENSGACG00000005883	M-C	M-M	4,61765	1,25E-006	5,66E-005
ENSGACG00000006029	M-C	M-M	6,04219	0,0005613	0,00959752
ENSGACG00000006545	M-C	M-M	5,27466	0,0001228	0,00273037
ENSGACG00000006644	M-C	M-M	5,36298	0,0010872	0,0164436
ENSGACG00000006829	M-C	M-M	7,07357	4,20E-009	4,13E-007

gene	sample_1	sample_2	log2(fold_change)	p_value	q_value
ENSGACG00000006833	M-C	M-M	5,84302	3,44E-006	0,00013439
ENSGACG00000007507	M-C	M-M	3,35701	0,0039474	0,0459603
ENSGACG00000007642	M-C	M-M	5,98434	0,0004817	0,00847061
ENSGACG00000007954	M-C	M-M	7,3361	3,85E-006	0,00014749
ENSGACG00000009173	M-C	M-M	5,9581	1,97E-005	0,00058806
ENSGACG00000009188	M-C	M-M	-2,47104	0,0014231	0,0204226
ENSGACG00000009487	M-C	M-M	-3,78187	0,0009491	0,014723
ENSGACG00000009583	M-C	M-M	5,62105	2,6187E-04	0,0051243
ENSGACG00000009592	M-C	M-M	5,95863	1,60E-006	7,01E-005
ENSGACG00000009633	M-C	M-M	2,75675	0,0013846	0,0199791
ENSGACG00000009825	M-C	M-M	1,34487	7,99E-010	9,65E-008
ENSGACG00000009880	M-C	M-M	5,57323	9,95E-005	0,00229026
ENSGACG00000009952	M-C	M-M	5,12916	0,0006316	0,0105678
ENSGACG00000010000	M-C	M-M	-5,94143	3,04E-008	2,30E-006
ENSGACG00000010018	M-C	M-M	-6,62659	1,50E-008	1,25E-006
ENSGACG00000010145	M-C	M-M	4,93497	0,0001854	0,0038471
ENSGACG00000010162	M-C	M-M	-4,31931	2,27E-005	0,00066396
ENSGACG00000010184	M-C	M-M	-3,4648	0,0006446	0,0107417
ENSGACG00000010196	M-C	M-M	4,65302	0,0004149	0,00749462
ENSGACG00000010933	M-C	M-M	5,31005	1,0224E-04	0,00234339
ENSGACG00000011392	M-C	M-M	5,70172	2,81E-005	0,00079489
ENSGACG00000011617	M-C	M-M	6,16466	4,83E-005	0,00125223
ENSGACG00000011846	M-C	M-M	5,60779	0,0002875	0,00553541
ENSGACG00000011851	M-C	M-M	5,86459	4,33E-005	0,00114232
ENSGACG00000011882	M-C	M-M	5,20515	0,0015766	0,0221725
ENSGACG00000012174	M-C	M-M	-3,58147	8,20E-005	0,00194795
ENSGACG00000012414	M-C	M-M	5,15713	0,0001317	0,00289356
ENSGACG00000012954	M-C	M-M	-3,77862	1,10E-005	0,00035836
ENSGACG00000014109	M-C	M-M	5,47222	8,61E-005	0,00202883
ENSGACG00000014348	M-C	M-M	5,09804	2,35E-005	0,00068479
ENSGACG00000014699	M-C	M-M	6,19778	3,44E-005	0,00094125
ENSGACG00000014752	M-C	M-M	-4,82586	2,76E-005	0,0007829
ENSGACG00000014811	M-C	M-M	6,65685	9,60E-007	4,51E-005
ENSGACG00000014852	M-C	M-M	10,8211	1,85E-010	2,65E-008
ENSGACG00000014936	M-C	M-M	-3,7129	0,0002613	0,00511462
ENSGACG00000015265	M-C	M-M	-4,17962	1,2652E-04	0,00279855
ENSGACG00000015411	M-C	M-M	6,40136	2,20E-006	9,16E-005
ENSGACG00000015464	M-C	M-M	5,98062	8,11E-010	9,77E-008
ENSGACG00000015472	M-C	M-M	5,99218	5,44E-006	0,00019804
ENSGACG00000015778	M-C	M-M	-3,82298	0,0025228	0,0322959
ENSGACG00000015857	M-C	M-M	7,00018	1,11E-005	0,00036094
ENSGACG00000015947	M-C	M-M	4,44314	0,000254	0,00499673
ENSGACG00000016045	M-C	M-M	-5,53644	2,51E-005	0,00072251
ENSGACG00000016093	M-C	M-M	4,51974	3,9652E-04	0,00722161
ENSGACG00000016104	M-C	M-M	5,44205	8,86E-005	0,00207823
ENSGACG00000016669	M-C	M-M	2,73153	0,0007121	0,0116543
ENSGACG00000016696	M-C	M-M	6,8339	1,00E-007	6,50E-006
ENSGACG00000017681	M-C	M-M	5,74959	1,81E-006	7,78E-005
ENSGACG00000017683	M-C	M-M	-5,53279	4,63E-006	0,00017276
ENSGACG00000018499	M-C	M-M	-4,38961	0,00119316	0,0177292
ENSGACG00000019066	M-C	M-M	5,7524	3,55E-006	0,00013774
ENSGACG00000019454	M-C	M-M	6,03869	0,0003832	0,00702085
ENSGACG00000020047	M-C	M-M	6,66654	1,75E-009	1,92E-007

gene	sample_1	sample_2	log2(fold_change)	p_value	q_value
ENSGACG00000020249	M-C	M-M	5,01505	0,0035233	0,0420346
ENSGACG00000020653	M-C	M-M	6,50554	3,30E-009	3,35E-007
ENSGACG00000020873	M-C	M-M	5,14516	0,0025018	0,0320825
ENSGACG00000020917	M-C	M-M	5,79828	6,89E-005	0,00168523
F10	M-C	M-M	5,58018	2,50E-005	0,00072125
F2	M-C	M-M	5,60026	6,95E-005	0,00169704
F5	M-C	M-M	5,50362	7,89E-005	0,00188668
F9 (2 of 2)	M-C	M-M	6,00649	2,10E-007	1,23E-005
FABP1	M-C	M-M	7,74625	8,43E-007	4,04E-005
FAH	M-C	M-M	4,42413	1,39E-005	0,00043933
FBLN1 (1 of 2)	M-C	M-M	-0,917771	0,0024044	0,0310855
FBRSL1	M-C	M-M	-0,557799	0,0019804	0,0266297
FCGBP (1 of 2)	M-C	M-M	5,07081	8,59E-006	0,00029154
FETUB (1 of 3)	M-C	M-M	4,14972	0,001091	0,0164912
FETUB (2 of 3)	M-C	M-M	4,07071	0,0013078	0,0190893
FETUB (3 of 3)	M-C	M-M	6,55603	7,16E-006	0,0002499
FGA	M-C	M-M	6,77778	1,59E-006	6,96E-005
FGB	M-C	M-M	6,62879	5,40E-006	0,00019685
FGG	M-C	M-M	5,96574	1,81E-005	0,00054815
G6PC (1 of 2)	M-C	M-M	5,85552	3,30E-005	0,00090933
GLS2 (2 of 2)	M-C	M-M	6,36035	0,0004599	0,00815645
GPD1 (1 of 2)	M-C	M-M	-1,4928	0,0019326	0,0261131
GZMM (2 of 5)	M-C	M-M	1,3619	0,0004615	0,00818037
GZMM (3 of 5)	M-C	M-M	1,28727	1,08E-008	9,40E-007
HAAO	M-C	M-M	5,41247	7,88E-005	0,00188452
HABP2 (1 of 2)	M-C	M-M	5,13962	0,00031114	0,00590876
HABP2 (2 of 2)	M-C	M-M	5,91924	2,51E-005	0,0007232
HAL	M-C	M-M	3,72502	0,0026886	0,0339588
HAO1	M-C	M-M	4,60131	0,0010306	0,0157434
HNF4A	M-C	M-M	4,83063	0,0001548	0,00330979
HPD	M-C	M-M	6,04037	1,61E-005	0,00049636
HPX	M-C	M-M	5,67667	3,81E-005	0,00102634
IGFALS	M-C	M-M	4,50715	0,0007642	0,012343
IGFBP1 (2 of 2)	M-C	M-M	5,80698	4,78E-005	0,00124184
IGFBP2 (2 of 2)	M-C	M-M	4,81498	8,18E-005	0,00194368
IGSF5 (2 of 2)	M-C	M-M	6,19839	0,00011658	0,00261475
ILDR1 (1 of 2)	M-C	M-M	4,14478	0,0002195	0,00442888
ITIH2	M-C	M-M	5,80062	9,90E-008	6,42E-006
ITIH4 (2 of 2)	M-C	M-M	3,9729	0,0012956	0,0189457
JPH1 (1 of 2)	M-C	M-M	-3,78824	0,0018578	0,025304
KBTBD10 (1 of 2)	M-C	M-M	-4,59477	0,0019222	0,025998
KL	M-C	M-M	4,49569	0,0010204	0,0156159
KNG1	M-C	M-M	5,48807	7,25E-005	0,00175758
KRT23 (5 of 7)	M-C	M-M	3,58565	2,98E-007	1,65E-005
KRT23 (7 of 7)	M-C	M-M	2,7991	0,001293	0,0189156
LECT2	M-C	M-M	5,31565	0,0001454	0,00314255
LRG1	M-C	M-M	5,19845	0,0003334	0,00625793
LYZ	M-C	M-M	5,93342	1,53E-006	6,73E-005
METTL21C (2 of 2)	M-C	M-M	-4,10782	6,72E-005	0,00165062
MIOX	M-C	M-M	4,97903	0,000179	0,00373511
MLXIPL	M-C	M-M	4,46709	0,0002513	0,00495426
MOGAT2	M-C	M-M	3,56468	0,0024555	0,031607
MSS51	M-C	M-M	-4,30853	0,0005946	0,0100571

gene	sample_1	sample_2	log2(fold_change)	p_value	q_value
MST1P9	M-C	M-M	7,05333	5,39E-007	2,76E-005
MYL1	M-C	M-M	-5,70375	1,34E-007	8,33E-006
MYLPF (2 of 2)	M-C	M-M	-4,07478	4,07E-005	0,00108503
MYOZ1 (1 of 2)	M-C	M-M	-4,50465	0,0004539	0,00806938
MYOZ3	M-C	M-M	-4,40583	0,002466	0,0317135
NME4	M-C	M-M	5,34205	0,0004373	0,00782696
NR1H4	M-C	M-M	5,52203	0,0003486	0,00649137
PDP2	M-C	M-M	-0,366836	7,79E-005	0,00186591
PFKM (1 of 2)	M-C	M-M	-4,90846	0,0001236	0,0027454
PGLYRP2 (2 of 2)	M-C	M-M	5,53778	8,16E-007	3,93E-005
PPP2R3A	M-C	M-M	0,927903	0,00115311	0,0172488
PRHOXNB	M-C	M-M	5,94863	4,84E-005	0,00125439
PROC	M-C	M-M	6,43658	3,10E-008	2,35E-006
PRODH2	M-C	M-M	4,6795	0,0019388	0,0261804
PROZ (2 of 2)	M-C	M-M	5,90506	5,47E-009	5,20E-007
PVRL1 (2 of 2)	M-C	M-M	6,35052	0,000345	0,00643759
S100P	M-C	M-M	3,50431	0,0033453	0,0403631
SARDH	M-C	M-M	0,582095	0,0001591	0,00338658
SERPINC1	M-C	M-M	5,98177	2,53E-005	0,0007286
SERPIND1	M-C	M-M	6,07295	9,09E-007	4,31E-005
SERPINF2	M-C	M-M	6,2221	5,35E-005	0,00136383
SERPING1	M-C	M-M	3,52804	0,0031747	0,0387338
SHBG	M-C	M-M	5,96357	2,55E-005	0,00073195
SLC13A5 (2 of 2)	M-C	M-M	5,92329	0,000108	0,00245162
SLC27A2 (1 of 3)	M-C	M-M	5,6876	0,0001529	0,00327576
SLC2A2	M-C	M-M	5,6952	2,52E-005	0,00072683
SLC7A2	M-C	M-M	3,84217	0,0023661	0,0306822
SOAT2	M-C	M-M	5,21256	0,0004722	0,00833495
SPP2	M-C	M-M	4,28619	0,00113018	0,0169712
SUSD2	M-C	M-M	5,13608	0,0025921	0,0329943
TAT	M-C	M-M	5,21289	1,41E-009	1,59E-007
TDO2	M-C	M-M	6,59428	8,43E-006	0,00028677
TEKT4	M-C	M-M	4,75554	0,0028254	0,0353207
TF	M-C	M-M	5,75935	4,35E-005	0,00114636
TFPI2	M-C	M-M	0,598114	0,0007498	0,0121518
TFR2	M-C	M-M	3,74899	0,0026551	0,0336226
TLR3	M-C	M-M	3,37072	0,0009229	0,0143896
TM4SF4	M-C	M-M	4,29681	0,0001445	0,00312712
TNNC2 (1 of 2)	M-C	M-M	-4,79011	1,32E-005	0,00042025
TNNC2 (2 of 2)	M-C	M-M	-5,38302	0,0010514	0,016002
TNNI2 (1 of 5)	M-C	M-M	-4,77831	5,71E-005	0,00144014
TNNI2 (3 of 5)	M-C	M-M	-5,21657	5,21E-006	0,00019084
TNNT2 (2 of 2)	M-C	M-M	-4,27072	0,0018992	0,0257503
TNNT3 (2 of 2)	M-C	M-M	-4,452	0,0005714	0,00973583
TPM2	M-C	M-M	-1,87407	1,57E-007	9,56E-006
TPM3	M-C	M-M	-4,70612	7,81E-005	0,00187
TYMP	M-C	M-M	3,97764	5,2713E-04	0,00911956
UCP1	M-C	M-M	6,83445	5,89E-008	4,09E-006
A1CF	XII-C	XII-M	-2,87689	0,0003476	0,00647631
ACMSD	XII-C	XII-M	-3,1883	0,0004881	0,00856181
ACSF2 (2 of 2)	XII-C	XII-M	-2,11376	5,7549E-04	0,00979296
ADPRH	XII-C	XII-M	-3,5771	0,0005685	0,00969665
ADSSL1	XII-C	XII-M	-5,36915	2,90E-006	0,00011608

gene	sample_1	sample_2	log2(fold_change)	p_value	q_value
AKR1D1 (2 of 2)	XII-C	XII-M	-3,36545	0,0004056	0,0073574
ALDH1L1	XII-C	XII-M	-3,25056	0,0039664	0,0461282
ALDH8A1	XII-C	XII-M	-3,93858	0,0003254	0,0061321
ALDH9A1 (1 of 2)	XII-C	XII-M	-1,81403	0,0002268	0,00454894
ALLC	XII-C	XII-M	-3,79422	7,80E-006	0,00026869
AMDHD1	XII-C	XII-M	-2,9679	0,0036603	0,0433248
AMPD1	XII-C	XII-M	-6,714	3,12E-007	1,72E-005
ANXA6	XII-C	XII-M	-3,4597	0,00119203	0,0177152
APOA1	XII-C	XII-M	-3,65138	2,13E-014	7,46E-012
APOB (2 of 5)	XII-C	XII-M	-2,62482	3,26E-005	0,00089905
APOBEC2 (2 of 2)	XII-C	XII-M	-3,65362	0,00211815	0,0281008
APOD (2 of 6),GGH	XII-C	XII-M	-3,1916	0,0002714	0,00527652
APOE (2 of 2)	XII-C	XII-M	-3,31803	9,15E-005	0,00213584
APOH (2 of 2)	XII-C	XII-M	-3,56939	0,0004924	0,00862323
ARG1	XII-C	XII-M	-3,38239	0,000648	0,0107872
ARHGEF38 (1 of 2)	XII-C	XII-M	-3,24751	0,0025694	0,0327669
ASPA	XII-C	XII-M	-1,15453	4,12E-011	6,98E-009
ASPDH	XII-C	XII-M	-3,87172	0,0029515	0,0365806
ATP1B3	XII-C	XII-M	-3,38417	0,0039333	0,0458332
ATP2A1 (2 of 2)	XII-C	XII-M	-7,35967	1,35E-005	0,00042802
BCO2 (3 of 3)	XII-C	XII-M	-1,66564	0,0021682	0,0286251
C7 (1 of 2)	XII-C	XII-M	-3,16896	7,1826E-04	0,0117355
C8A	XII-C	XII-M	-3,45414	0,0037053	0,0437449
C8G	XII-C	XII-M	-3,34482	0,0017357	0,0239487
CAP2	XII-C	XII-M	-3,02215	0,0018987	0,0257471
CASQ1 (1 of 2)	XII-C	XII-M	-5,46807	5,57E-006	0,000202
CASQ1 (2 of 2)	XII-C	XII-M	-4,38539	0,001719	0,0237624
CAV3	XII-C	XII-M	-4,48323	0,0003448	0,00643374
CETP	XII-C	XII-M	-4,39802	2,86E-006	0,00011461
CFB	XII-C	XII-M	-2,90205	0,0036628	0,0433486
CFP	XII-C	XII-M	-3,41843	0,0023365	0,0303797
CKM (1 of 2)	XII-C	XII-M	-6,36357	1,28E-005	0,00040712
CKM (2 of 2)	XII-C	XII-M	-6,60937	1,11E-006	5,13E-005
CKMT2 (1 of 2)	XII-C	XII-M	-6,95729	0	0
CLIC5 (1 of 2)	XII-C	XII-M	-4,18101	0,0002567	0,00504054
CNDP1	XII-C	XII-M	-1,10377	0,0040346	0,0467396
CPB2	XII-C	XII-M	-3,33232	0,0002213	0,00445846
CREG2	XII-C	XII-M	-0,845928	5,21E-005	0,00133331
CTDSPL (1 of 2)	XII-C	XII-M	-0,967501	0,0030522	0,037561
CYP24A1	XII-C	XII-M	-3,87659	1,15E-007	7,28E-006
CYP2J2 (1 of 6)	XII-C	XII-M	-2,78071	0	0
CYP2J2 (3 of 6)	XII-C	XII-M	-2,67426	0,00119314	0,017729
DES	XII-C	XII-M	-6,28617	3,01E-007	1,67E-005
DGAT2	XII-C	XII-M	-2,86578	0,0017923	0,024577
DHRS7C (1 of 2)	XII-C	XII-M	-5,35042	0,0013992	0,0201522
DHRS7C (2 of 2)	XII-C	XII-M	-3,87493	1,4791E-04	0,00318789
DHRS9	XII-C	XII-M	-1,61946	5,05E-005	0,00129979
DIABLO (1 of 2)	XII-C	XII-M	-2,82574	8,66E-006	0,00029358
DPYS	XII-C	XII-M	-2,30337	0,0001498	0,00322237
ENO3	XII-C	XII-M	-2,36195	0,0016655	0,0231726
ENSGACG00000000114	XII-C	XII-M	-3,21377	4,73E-005	0,00122976
ENSGACG00000000115	XII-C	XII-M	-2,70189	1,6121E-04	0,003424
ENSGACG00000000151	XII-C	XII-M	-0,800817	0,0042786	0,0489215

gene	sample_1	sample_2	log2(fold_change)	p_value	q_value
ENSGACG00000000272	XII-C	XII-M	-6,01347	6,60E-006	0,00023336
ENSGACG00000000300	XII-C	XII-M	-6,09147	3,06E-005	0,000853
ENSGACG00000001522	XII-C	XII-M	-4,73009	2,02E-006	8,53E-005
ENSGACG00000001733	XII-C	XII-M	-3,16082	2,59E-010	3,56E-008
ENSGACG00000001742	XII-C	XII-M	-1,89094	1,18E-010	1,78E-008
ENSGACG00000001978	XII-C	XII-M	-2,83034	0,0004302	0,00772234
ENSGACG00000002089	XII-C	XII-M	-4,61267	0,0001339	0,0029334
ENSGACG00000002525	XII-C	XII-M	-2,91193	0,0010545	0,0160397
ENSGACG00000002902	XII-C	XII-M	-7,4906	5,07E-011	8,40E-009
ENSGACG00000003003	XII-C	XII-M	-9,33196	2,53E-009	2,66E-007
ENSGACG00000003030	XII-C	XII-M	-4,28505	1,12E-005	0,00036349
ENSGACG00000003435	XII-C	XII-M	-3,60097	0,0025202	0,0322693
ENSGACG00000004200	XII-C	XII-M	-8,40032	2,17E-008	1,73E-006
ENSGACG00000004413	XII-C	XII-M	-3,08145	0,00113201	0,0169936
ENSGACG00000004971	XII-C	XII-M	-4,90615	0,0001202	0,00268286
ENSGACG00000005023	XII-C	XII-M	-7,00563	7,30E-008	4,93E-006
ENSGACG00000005264	XII-C	XII-M	-4,05955	0,0002502	0,00493606
ENSGACG00000005547	XII-C	XII-M	-2,63618	0,0026928	0,0340023
ENSGACG00000005712	XII-C	XII-M	-3,43393	0,0010564	0,0160627
ENSGACG00000005883	XII-C	XII-M	-2,96456	0,0008809	0,0138494
ENSGACG00000006275	XII-C	XII-M	2,09221	1,46E-005	0,00045765
ENSGACG00000006596	XII-C	XII-M	0,578624	0,0005764	0,00980449
ENSGACG00000006644	XII-C	XII-M	-2,16565	0,004016	0,0465743
ENSGACG00000006829	XII-C	XII-M	-2,17378	0,0017751	0,0243868
ENSGACG00000007038	XII-C	XII-M	-3,23105	0,0025639	0,0327103
ENSGACG00000007337	XII-C	XII-M	-2,81681	0,00291175	0,0361865
ENSGACG00000007642	XII-C	XII-M	-3,22114	0,0021794	0,0287382
ENSGACG00000007954	XII-C	XII-M	-4,1734	8,51E-007	4,08E-005
ENSGACG00000009173	XII-C	XII-M	-3,12941	0,0018042	0,024709
ENSGACG00000009409	XII-C	XII-M	-6,84666	1,84E-008	1,49E-006
ENSGACG00000009487	XII-C	XII-M	-4,58873	1,4353E-04	0,00310904
ENSGACG00000009825	XII-C	XII-M	-0,879274	1,12E-006	5,16E-005
ENSGACG00000009880	XII-C	XII-M	-4,56852	0,000261	0,00511025
ENSGACG00000009883	XII-C	XII-M	-4,7449	0,0001069	0,00243186
ENSGACG00000009952	XII-C	XII-M	-3,78567	0,0001303	0,00286735
ENSGACG00000010000	XII-C	XII-M	-8,69877	2,30E-005	0,00067263
ENSGACG00000010018	XII-C	XII-M	-9,7993	1,33E-007	8,28E-006
ENSGACG00000010145	XII-C	XII-M	-2,87259	0,0021371	0,0283024
ENSGACG00000010184	XII-C	XII-M	-3,65125	0,0005803	0,0098589
ENSGACG00000010476	XII-C	XII-M	-3,479	0,0002634	0,00514872
ENSGACG00000010817	XII-C	XII-M	-1,84174	0,0042411	0,048594
ENSGACG00000011392	XII-C	XII-M	-4,08726	2,16E-005	0,0006367
ENSGACG00000012174	XII-C	XII-M	-6,60891	6,13E-007	3,08E-005
ENSGACG00000012381	XII-C	XII-M	-2,83143	2,68E-006	0,0001084
ENSGACG00000012390	XII-C	XII-M	-2,35146	0,0001824	0,0037941
ENSGACG00000012473	XII-C	XII-M	-4,25735	0,0006335	0,0105935
ENSGACG00000012954	XII-C	XII-M	-6,1241	6,60E-006	0,00023325
ENSGACG00000012962	XII-C	XII-M	-7,56529	0,00011897	0,00265936
ENSGACG00000013583	XII-C	XII-M	-4,12164	8,17E-005	0,00194218
ENSGACG00000013650	XII-C	XII-M	-0,743087	0,0033321	0,0402362
ENSGACG00000013769	XII-C	XII-M	-2,87741	0,0025775	0,0328483
ENSGACG00000014699	XII-C	XII-M	-3,37912	0,0015875	0,0222944
ENSGACG00000014752	XII-C	XII-M	-6,52499	1,84E-007	1,10E-005

gene	sample_1	sample_2	log2(fold_change)	p_value	q_value
ENSGACG00000014852	XII-C	XII-M	-3,53238	1,26E-005	0,00040256
ENSGACG00000014922	XII-C	XII-M	-4,5155	1,75E-005	0,00053356
ENSGACG00000014936	XII-C	XII-M	3,17084	0,0009946	0,0152948
ENSGACG00000015168	XII-C	XII-M	-4,75285	3,36E-005	0,0009231
ENSGACG00000015265	XII-C	XII-M	-7,05323	0,0007311	0,0119061
ENSGACG00000015411	XII-C	XII-M	-1,77773	0,00193511	0,0261409
ENSGACG00000015778	XII-C	XII-M	-6,31283	5,36E-007	2,74E-005
ENSGACG00000016045	XII-C	XII-M	-7,71005	8,69E-008	5,73E-006
ENSGACG00000016093	XII-C	XII-M	-4,07242	0,0010529	0,0160193
ENSGACG00000016104	XII-C	XII-M	-3,41047	0,0034602	0,0414456
ENSGACG00000016168	XII-C	XII-M	-6,78966	0,00115664	0,0172911
ENSGACG00000016696	XII-C	XII-M	-4,56031	0,0004561	0,00810209
ENSGACG00000017681	XII-C	XII-M	-2,38263	8,88E-016	3,93E-013
ENSGACG00000017683	XII-C	XII-M	-6,52447	3,39E-007	1,85E-005
ENSGACG00000018499	XII-C	XII-M	-6,39319	0,0001064	0,00242083
ENSGACG00000018908	XII-C	XII-M	-4,89097	0,0024535	0,0315875
ENSGACG00000019023	XII-C	XII-M	-7,00841	1,22E-014	4,46E-012
ENSGACG00000019066	XII-C	XII-M	-3,23974	0,0028869	0,0359365
ENSGACG00000019517	XII-C	XII-M	-3,66643	0,0006066	0,0102237
ENSGACG00000019604	XII-C	XII-M	-2,299	3,4363E-04	0,00641571
ENSGACG00000019784	XII-C	XII-M	-6,13487	5,40E-006	0,00019667
ENSGACG00000020047	XII-C	XII-M	-4,01956	5,40E-005	0,00137375
ENSGACG00000020187	XII-C	XII-M	-3,28241	7,76E-005	0,00185966
ENSGACG00000020566	XII-C	XII-M	-3,50073	0,0015819	0,0222317
EPS8L3 (1 of 2)	XII-C	XII-M	-4,0189	0,0009995	0,0153563
EVC2	XII-C	XII-M	-0,98378	0,0004226	0,00761004
FABP1	XII-C	XII-M	-3,90124	6,80E-006	0,00023923
FABP2 (2 of 2)	XII-C	XII-M	-5,2038	4,99E-005	0,00128726
FAH	XII-C	XII-M	-2,89783	8,09E-005	0,00192601
FETUB (1 of 3)	XII-C	XII-M	-3,14504	0,0040449	0,0468342
FLNC (2 of 2)	XII-C	XII-M	-3,75227	0,0004518	0,00803918
FOXA3	XII-C	XII-M	-3,66987	0,0009538	0,0147822
FRZB	XII-C	XII-M	-1,66235	0,0038263	0,0448519
G6PC (1 of 2)	XII-C	XII-M	-4,09482	0,0003772	0,00692938
G6PC (2 of 2)	XII-C	XII-M	-3,27963	0,0019743	0,0265647
GAPDH (1 of 2)	XII-C	XII-M	-5,29299	0	0
GAS6	XII-C	XII-M	-0,639669	0,001506	0,021372
GPD1 (1 of 2)	XII-C	XII-M	-2,70678	2,92E-005	0,00082077
HAAO	XII-C	XII-M	-3,62198	9,45E-005	0,0021927
HABP2 (1 of 2)	XII-C	XII-M	-4,18856	0,0002267	0,00454624
HAO1	XII-C	XII-M	-2,67585	0,0003933	0,00717215
HGD	XII-C	XII-M	-3,25357	0,000484	0,00850298
HHATL (2 of 2)	XII-C	XII-M	-6,04086	2,51E-006	0,00010246
HNMT (2 of 2)	XII-C	XII-M	-3,72634	2,3508E-04	0,00468741
HPX	XII-C	XII-M	-3,8271	0,00174511	0,0240543
HRC	XII-C	XII-M	-7,50299	0,0007529	0,0121917
HSPB1	XII-C	XII-M	-1,90803	0,0031962	0,0389384
ILDR1 (1 of 2)	XII-C	XII-M	-2,51245	0,0010014	0,0153796
IRF6	XII-C	XII-M	-3,96646	0,0019251	0,0260303
ITGA6 (1 of 2)	XII-C	XII-M	0,736352	0,0019063	0,0258261
JPH1 (1 of 2)	XII-C	XII-M	-4,24635	0,0005317	0,00918377
KBTBD10 (1 of 2)	XII-C	XII-M	-5,33849	1,6873E-04	0,00355703
KBTBD12	XII-C	XII-M	-4,43153	0,0007407	0,0120317

gene	sample_1	sample_2	log2(fold_change)	p_value	q_value
KL	XII-C	XII-M	-3,488	3,17E-005	0,00087919
KLHL31	XII-C	XII-M	-6,88991	2,77E-007	1,56E-005
KMO	XII-C	XII-M	-3,10414	0,0025837	0,0329131
LECT2	XII-C	XII-M	-2,92558	0,0007247	0,0118212
LRG1	XII-C	XII-M	-3,52995	7,92E-005	0,00189251
LYZ	XII-C	XII-M	-3,85804	6,14E-007	3,08E-005
MAT1A (2 of 2)	XII-C	XII-M	-4,7146	8,43E-009	7,59E-007
MFRP	XII-C	XII-M	-3,58496	0,0010824	0,0163828
MMP25	XII-C	XII-M	0,476968	1,60E-010	2,32E-008
MOGAT2	XII-C	XII-M	-3,70157	0,00112391	0,0168945
MSRB2	XII-C	XII-M	-3,85737	0,0026453	0,0335243
MST1P9	XII-C	XII-M	-2,78873	0,0038728	0,0452808
MYBPC1	XII-C	XII-M	-5,16371	0,0002356	0,00469522
MYL1	XII-C	XII-M	-5,93064	1,64E-007	9,89E-006
MYLPF (1 of 2)	XII-C	XII-M	-8,88641	1,89E-006	8,05E-005
MYLPF (2 of 2)	XII-C	XII-M	-3,75924	1,84E-006	7,87E-005
MYOM1 (2 of 2)	XII-C	XII-M	-6,12449	3,95E-005	0,0010576
MYOZ1 (1 of 2)	XII-C	XII-M	-7,87043	9,97E-005	0,00229572
NEXN	XII-C	XII-M	-4,07985	0,0031254	0,038251
NIPSNAP1	XII-C	XII-M	-3,21626	0,0001044	0,00238373
NR1H4	XII-C	XII-M	-2,852	0,0006153	0,0103433
OVGP1 (3 of 5)	XII-C	XII-M	-3,85687	6,68E-005	0,0016413
PABPC4	XII-C	XII-M	-5,84423	5,81E-007	2,94E-005
PCK1	XII-C	XII-M	-4,42309	0,0008987	0,0140776
PCSK6	XII-C	XII-M	-3,46911	0,0013662	0,019769
PDK2 (2 of 2)	XII-C	XII-M	-2,30364	0,0035904	0,0426724
PDLIM1	XII-C	XII-M	-5,38613	1,64E-005	0,00050355
PFKM (1 of 2)	XII-C	XII-M	-7,5262	2,3153E-04	0,00462795
PFKM (2 of 2)	XII-C	XII-M	-4,64196	6,77E-005	0,00166094
PGAM2	XII-C	XII-M	-5,72095	9,51E-007	4,48E-005
PGLYRP2 (1 of 2)	XII-C	XII-M	-3,49429	0,0031968	0,0389444
PGLYRP2 (2 of 2)	XII-C	XII-M	-3,40134	6,22E-012	1,30E-009
PIGB	XII-C	XII-M	0,493949	1,43E-008	1,20E-006
PLP1 (2 of 2)	XII-C	XII-M	-2,166	0,0025678	0,0327492
PPDPF (2 of 2)	XII-C	XII-M	-3,09571	9,10E-005	0,00212569
PPP1R27 (1 of 2)	XII-C	XII-M	-5,06258	0,0029084	0,0361533
PRHOXNB	XII-C	XII-M	-3,2034	0,0009474	0,0147021
PROC	XII-C	XII-M	-4,43566	8,45E-006	0,00028757
PROZ (2 of 2)	XII-C	XII-M	-3,23525	0,0001369	0,0029875
PYGM (2 of 2)	XII-C	XII-M	-5,49794	1,04E-006	4,82E-005
RPL3L	XII-C	XII-M	-6,03545	7,87E-007	3,81E-005
RXRG	XII-C	XII-M	-0,879282	0,0008476	0,0134217
SERPINF2	XII-C	XII-M	-3,39122	6,60E-005	0,00162611
SLC22A14	XII-C	XII-M	-3,07062	0,0041962	0,0481914
SLC25A34	XII-C	XII-M	-3,67291	3,3969E-04	0,00635442
SLC25A43	XII-C	XII-M	-3,45582	2,21E-007	1,28E-005
SRL (1 of 2)	XII-C	XII-M	-3,68227	0,0002717	0,00528142
SUSD2	XII-C	XII-M	-2,74687	0,0007321	0,0119191
TM4SF4	XII-C	XII-M	-3,09077	0,004015	0,0465646
TMEM182	XII-C	XII-M	-5,19931	0,0004543	0,00807509
TMOD4	XII-C	XII-M	-0,746368	3,18E-005	0,00088118
TNNC2 (1 of 2)	XII-C	XII-M	-5,67162	3,24E-007	1,78E-005
TNNI2 (1 of 5)	XII-C	XII-M	-4,61371	2,26E-005	0,00066158

gene	sample_1	sample_2	log2(fold_change)	p_value	q_value
TNNI2 (3 of 5)	XII-C	XII-M	-4,60935	1,63E-005	0,00050239
TNNI2 (4 of 5)	XII-C	XII-M	-4,8571	0,0009413	0,0146232
TNNI2 (5 of 5)	XII-C	XII-M	-6,23533	3,60E-008	2,67E-006
TNNT2 (2 of 2)	XII-C	XII-M	-3,68396	0,0040998	0,0473256
TNNT3 (2 of 2)	XII-C	XII-M	-3,83573	0,0012204	0,0180527
TPM3	XII-C	XII-M	-6,30816	1,07E-006	4,97E-005
TTC36	XII-C	XII-M	-3,06072	0,001208	0,017906
TTN	XII-C	XII-M	-6,60355	1,35E-006	6,05E-005
TXLNB (1 of 2)	XII-C	XII-M	-5,53162	3,17E-006	0,00012505
TXLNB (2 of 2)	XII-C	XII-M	-5,58446	6,17E-006	0,00022018
UCP2	XII-C	XII-M	-4,03948	7,20E-005	0,00174716
UNC45B	XII-C	XII-M	-4,2868	0,0010164	0,0155647
UPP2	XII-C	XII-M	-3,06534	0,0005105	0,00888149
USP13	XII-C	XII-M	-5,38417	0,0001803	0,00375815
USP28	XII-C	XII-M	-6,85629	4,50E-006	0,00016855
ZNFX1	XII-C	XII-M	1,29777	0,0002668	0,00520323
A1CF	XII-C	XII-XII	-7,51722	7,20E-011	1,15E-008
ABCB11	XII-C	XII-XII	-6,08197	1,13E-006	5,17E-005
ABCB4	XII-C	XII-XII	-5,42162	1,58E-006	6,91E-005
ABCC11	XII-C	XII-XII	-4,85898	3,95E-006	0,00015087
ABCD1	XII-C	XII-XII	-2,72092	0,0010014	0,0153802
ABHD15	XII-C	XII-XII	-3,43352	0,0017066	0,0236295
ABT1,ENSGACG00000000296	XII-C	XII-XII	1,12021	3,61E-005	0,00098022
ACMSD	XII-C	XII-XII	-6,46402	2,06E-006	8,66E-005
ACSF2 (2 of 2)	XII-C	XII-XII	-3,91682	3,36E-006	0,00013148
ADPRH	XII-C	XII-XII	-2,04532	0,0026334	0,0334063
AGT	XII-C	XII-XII	-6,6314	1,98E-007	1,16E-005
AGXT (1 of 2)	XII-C	XII-XII	-8,52796	1,36E-008	1,15E-006
AGXT (2 of 2)	XII-C	XII-XII	-9,28692	2,34E-006	9,65E-005
AGXT2 (1 of 2)	XII-C	XII-XII	-4,65837	1,44E-005	0,0004503
AGXT2L1	XII-C	XII-XII	-4,38033	4,23E-005	0,00111874
AHSG	XII-C	XII-XII	-8,31774	8,23E-009	7,43E-007
AKR1D1 (1 of 2)	XII-C	XII-XII	-4,06505	0,0035064	0,0418746
AKR1D1 (2 of 2)	XII-C	XII-XII	-7,24717	1,67E-007	1,00E-005
ALDH1L1	XII-C	XII-XII	-4,95421	2,00E-005	0,00059809
ALDH8A1	XII-C	XII-XII	-5,97735	1,02E-007	6,61E-006
ALDH9A1 (1 of 2)	XII-C	XII-XII	-1,5425	0,0022923	0,0299175
ALDOB	XII-C	XII-XII	-4,51104	0,0028026	0,0350892
ALLC	XII-C	XII-XII	-5,17299	1,27E-006	5,72E-005
ALYREF (2 of 2)	XII-C	XII-XII	0,943266	0,0001482	0,00319298
AMDHD1	XII-C	XII-XII	-3,6914	0,0002859	0,00550945
AMPD1	XII-C	XII-XII	-4,62513	1,75E-007	1,05E-005
AP2S1	XII-C	XII-XII	0,812851	0,0034419	0,0412744
APOA1	XII-C	XII-XII	-8,57937	0	0
APOB (1 of 5)	XII-C	XII-XII	-6,89567	4,63E-006	0,00017283
APOB (5 of 5)	XII-C	XII-XII	-7,53838	2,22E-016	1,07E-013
APOD (2 of 6),GGH	XII-C	XII-XII	-4,552	3,14E-005	0,00087222
APOE (2 of 2)	XII-C	XII-XII	-7,34671	2,59E-008	2,01E-006
APOF	XII-C	XII-XII	-4,09164	0,0030861	0,0378826
APOH (1 of 2)	XII-C	XII-XII	-4,12864	0,0012929	0,0189141
APOH (2 of 2)	XII-C	XII-XII	-7,02804	2,41E-007	1,38E-005
ARG1	XII-C	XII-XII	-4,8008	0,0004827	0,00848497
ARHGEF38 (1 of 2)	XII-C	XII-XII	-5,16472	4,76E-005	0,00123607

gene	sample_1	sample_2	log2(fold_change)	p_value	q_value
ASGR1	XII-C	XII-XII	-6,57355	2,04E-006	8,59E-005
BCO2 (3 of 3)	XII-C	XII-XII	-6,03272	0,0004642	0,00821956
C3 (1 of 8)	XII-C	XII-XII	-6,88341	2,17E-009	2,33E-007
C3 (2 of 8)	XII-C	XII-XII	-6,58022	6,09E-007	3,06E-005
C3 (3 of 8)	XII-C	XII-XII	-7,08703	1,75E-006	7,53E-005
C3 (4 of 8)	XII-C	XII-XII	-7,54974	0,0010764	0,0163095
C3 (5 of 8)	XII-C	XII-XII	-6,80613	3,04E-006	0,0001209
C4A	XII-C	XII-XII	-1,30456	3,71E-006	0,00014306
C7orf10	XII-C	XII-XII	0,533861	0,0024214	0,0312575
C8A	XII-C	XII-XII	-7,64739	4,30E-007	2,27E-005
C8G	XII-C	XII-XII	-8,67221	1,71E-010	2,46E-008
C9	XII-C	XII-XII	-7,06315	3,28E-007	1,80E-005
CA6 (1 of 2)	XII-C	XII-XII	3,18591	2,01E-005	0,00059918
CA6 (2 of 2)	XII-C	XII-XII	2,97804	0,0013638	0,0197407
CASQ1 (2 of 2)	XII-C	XII-XII	-4,4447	0,0005719	0,00974304
CDCA7L	XII-C	XII-XII	0,597531	0,0030247	0,0372948
CDK1	XII-C	XII-XII	1,68752	0,00221141	0,0290741
CDO1	XII-C	XII-XII	-3,20155	0,000467	0,00826046
CELA1 (1 of 2)	XII-C	XII-XII	-4,96738	0,0005856	0,00993326
CETP	XII-C	XII-XII	-8,08857	4,10E-011	6,95E-009
CFB	XII-C	XII-XII	-4,61178	1,52E-005	0,00047235
CFP	XII-C	XII-XII	-5,52123	6,14E-006	0,00021927
CIDEB	XII-C	XII-XII	-5,7993	1,22E-006	5,56E-005
CLDN2	XII-C	XII-XII	-3,93385	0,0027759	0,0348271
CLIC5 (1 of 2)	XII-C	XII-XII	-5,08877	0,000769	0,0124069
CNDP1	XII-C	XII-XII	-6,36507	1,11E-007	7,08E-006
CPT1B	XII-C	XII-XII	-2,6732	0,003792	0,0445406
CREB3L3	XII-C	XII-XII	-4,56019	0,0004262	0,00766375
CREG2	XII-C	XII-XII	-0,897494	2,84E-013	7,99E-011
CYP24A1	XII-C	XII-XII	-6,37246	1,12E-010	1,70E-008
CYP2C9	XII-C	XII-XII	-6,28678	0,0005455	0,00937755
CYP2J2 (1 of 6)	XII-C	XII-XII	-5,84391	1,08E-008	9,44E-007
CYP2J2 (2 of 6)	XII-C	XII-XII	-6,76922	5,40E-007	2,76E-005
CYP2J2 (3 of 6)	XII-C	XII-XII	-7,1205	7,55E-009	6,90E-007
CYP2J2 (6 of 6)	XII-C	XII-XII	-2,36835	0,0018905	0,0256592
CYP2W1 (1 of 5)	XII-C	XII-XII	-6,7401	2,60E-010	3,57E-008
CYP2W1 (4 of 5)	XII-C	XII-XII	-3,72082	0,0026303	0,0333768
CYP8B1	XII-C	XII-XII	-4,52562	8,18E-005	0,00194319
DDX52	XII-C	XII-XII	0,757169	0,0003369	0,00631291
DGAT2	XII-C	XII-XII	-4,92008	3,91E-006	0,00014964
DHRS9	XII-C	XII-XII	-1,64067	1,82E-005	0,00055195
DIABLO (1 of 2)	XII-C	XII-XII	-8,60729	9,85E-013	2,46E-010
DMGDH	XII-C	XII-XII	-4,83162	8,56E-005	0,00201899
DPYS	XII-C	XII-XII	-6,23866	7,78E-007	3,78E-005
EGFR (2 of 2)	XII-C	XII-XII	-3,02412	0,0008259	0,0131409
ENPP2 (2 of 2)	XII-C	XII-XII	-3,70527	0,000465	0,00823156
ENSGACG00000000007	XII-C	XII-XII	-7,191	8,54E-008	5,65E-006
ENSGACG00000000231	XII-C	XII-XII	-4,4589	0,0002266	0,00454534
ENSGACG00000000300	XII-C	XII-XII	-2,87947	0,0034504	0,0413537
ENSGACG00000000343	XII-C	XII-XII	3,72336	0,0014767	0,0210383
ENSGACG00000001260	XII-C	XII-XII	-7,25094	1,95E-008	1,57E-006
ENSGACG00000001261	XII-C	XII-XII	-4,32806	0,0001017	0,00233307
ENSGACG00000001432	XII-C	XII-XII	-7,36476	1,91E-007	1,13E-005

gene	sample_1	sample_2	log2(fold_change)	p_value	q_value
ENSGACG00000001522	XII-C	XII-XII	-3,43377	0,0002402	0,00476969
ENSGACG00000001733	XII-C	XII-XII	-5,98875	1,28E-013	3,86E-011
ENSGACG00000001742	XII-C	XII-XII	-2,10345	9,82E-010	1,16E-007
ENSGACG00000001978	XII-C	XII-XII	-2,36981	0,0015264	0,0216056
ENSGACG00000002258	XII-C	XII-XII	1,72588	5,91E-005	0,00148256
ENSGACG00000002525	XII-C	XII-XII	-3,10225	0,0002756	0,00534469
ENSGACG00000002902	XII-C	XII-XII	-4,75149	7,27E-007	3,56E-005
ENSGACG00000003003	XII-C	XII-XII	-4,89348	5,10E-005	0,00131122
ENSGACG00000003030	XII-C	XII-XII	-7,97925	3,73E-006	0,00014361
ENSGACG00000003435	XII-C	XII-XII	-6,86558	0,0028188	0,0352497
ENSGACG00000003461	XII-C	XII-XII	-8,48332	9,58E-008	6,24E-006
ENSGACG00000003467	XII-C	XII-XII	-8,74649	0,00061188	0,0102952
ENSGACG00000003473	XII-C	XII-XII	-8,56034	3,80E-008	2,80E-006
ENSGACG00000003808	XII-C	XII-XII	-2,98768	0,0042829	0,0489589
ENSGACG00000004324	XII-C	XII-XII	1,26285	0,0006256	0,0104852
ENSGACG00000004413	XII-C	XII-XII	-7,71113	1,37E-009	1,56E-007
ENSGACG00000004816	XII-C	XII-XII	-3,72473	0,0020276	0,0271378
ENSGACG00000004822	XII-C	XII-XII	-3,74578	0,0021765	0,0287084
ENSGACG00000004971	XII-C	XII-XII	-3,27661	0,0038137	0,0447359
ENSGACG00000005067	XII-C	XII-XII	-3,29208	0,0008034	0,0128537
ENSGACG00000005264	XII-C	XII-XII	-5,51687	0,0009832	0,0151515
ENSGACG00000005421	XII-C	XII-XII	-2,11599	0,0006903	0,0113616
ENSGACG00000005482	XII-C	XII-XII	-3,12259	0,0001096	0,00248234
ENSGACG00000005547	XII-C	XII-XII	-3,14895	0,0002701	0,00525637
ENSGACG00000005712	XII-C	XII-XII	-2,64471	0,0024751	0,031805
ENSGACG00000005883	XII-C	XII-XII	-5,17259	3,21E-008	2,42E-006
ENSGACG00000005916	XII-C	XII-XII	-4,21456	0,00119459	0,0177469
ENSGACG00000006351	XII-C	XII-XII	-3,68324	0,0028738	0,0358035
ENSGACG00000006545	XII-C	XII-XII	-7,91367	3,99E-006	0,00015216
ENSGACG00000006644	XII-C	XII-XII	-6,99104	0,000184	0,00382292
ENSGACG00000006790	XII-C	XII-XII	-2,65138	0,0035709	0,0424861
ENSGACG00000006829	XII-C	XII-XII	-1,80E+308	0,000647	0,0107749
ENSGACG00000006833	XII-C	XII-XII	-6,0804	0,00113973	0,0170871
ENSGACG00000007038	XII-C	XII-XII	-7,04772	2,33E-005	0,0006798
ENSGACG00000007040	XII-C	XII-XII	-5,77756	4,92E-005	0,00127169
ENSGACG00000007337	XII-C	XII-XII	-3,00513	0,00111003	0,0167248
ENSGACG00000007447	XII-C	XII-XII	1,09673	0,0010148	0,015546
ENSGACG00000007505	XII-C	XII-XII	-4,4772	0,0003981	0,00724532
ENSGACG00000007507	XII-C	XII-XII	-3,55635	0,0038678	0,0452352
ENSGACG00000007640	XII-C	XII-XII	-6,08411	7,82E-006	0,00026935
ENSGACG00000007954	XII-C	XII-XII	-10,1081	4,43E-005	0,00116422
ENSGACG00000008370	XII-C	XII-XII	-4,06104	0,0003052	0,00581541
ENSGACG00000009173	XII-C	XII-XII	-7,89168	4,25E-009	4,18E-007
ENSGACG00000009409	XII-C	XII-XII	-4,09979	2,09E-005	0,00061973
ENSGACG00000009487	XII-C	XII-XII	-3,5846	0,001409	0,0202627
ENSGACG00000009583	XII-C	XII-XII	-5,63332	6,21E-006	0,00022136
ENSGACG00000009880	XII-C	XII-XII	-9,32224	1,01E-009	1,19E-007
ENSGACG00000009883	XII-C	XII-XII	-9,27892	1,74E-006	7,49E-005
ENSGACG00000009946	XII-C	XII-XII	-2,71579	0,0035297	0,0420991
ENSGACG00000009952	XII-C	XII-XII	-7,31101	0,0043207	0,0492917
ENSGACG00000010050	XII-C	XII-XII	1,50022	1,0724E-04	0,00243777
ENSGACG00000010145	XII-C	XII-XII	-5,96844	1,75E-007	1,05E-005
ENSGACG00000010196	XII-C	XII-XII	-6,77733	5,63E-009	5,34E-007

gene	sample_1	sample_2	log2(fold_change)	p_value	q_value
ENSGACG00000010933	XII-C	XII-XII	-8,13177	8,90E-011	1,38E-008
ENSGACG00000011392	XII-C	XII-XII	-9,0509	8,92E-009	7,97E-007
ENSGACG00000011617	XII-C	XII-XII	-8,02247	2,36E-005	0,00068516
ENSGACG00000011633	XII-C	XII-XII	-2,85175	0,0022073	0,0290311
ENSGACG00000011784,POLR3	XII-C	XII-XII	-2,5935	0,0025282	0,0323498
ENSGACG00000011846	XII-C	XII-XII	-7,07136	1,15E-006	5,28E-005
ENSGACG00000012381	XII-C	XII-XII	-7,01659	3,80E-014	1,27E-011
ENSGACG00000012390	XII-C	XII-XII	-3,07	0	0
ENSGACG00000012414	XII-C	XII-XII	-8,10942	3,58E-009	3,60E-007
ENSGACG00000012473	XII-C	XII-XII	-3,72154	0,00117663	0,0175327
ENSGACG00000013354	XII-C	XII-XII	-2,33371	0,003722	0,0438987
ENSGACG00000013449	XII-C	XII-XII	-3,50995	0,0009424	0,0146377
ENSGACG00000013769	XII-C	XII-XII	-1,80E+308	0,0018301	0,0250022
ENSGACG00000013793	XII-C	XII-XII	-5,0342	0,000355	0,00658907
ENSGACG00000014348	XII-C	XII-XII	-6,14615	6,34E-007	3,17E-005
ENSGACG00000014675	XII-C	XII-XII	-2,36636	0,0021484	0,0284203
ENSGACG00000014699	XII-C	XII-XII	-6,0074	8,01E-007	3,87E-005
ENSGACG00000014811	XII-C	XII-XII	-7,76487	3,46E-008	2,58E-006
ENSGACG00000014852	XII-C	XII-XII	-7,7671	1,16E-007	7,37E-006
ENSGACG00000015110	XII-C	XII-XII	2,98331	4,80E-005	0,00124524
ENSGACG00000015411	XII-C	XII-XII	-8,3239	1,88E-008	1,52E-006
ENSGACG00000015472	XII-C	XII-XII	-7,38266	1,27E-007	7,97E-006
ENSGACG00000015857	XII-C	XII-XII	-8,96505	2,70E-008	2,08E-006
ENSGACG00000015947	XII-C	XII-XII	-7,06088	1,21E-008	1,04E-006
ENSGACG00000016093	XII-C	XII-XII	-6,64913	2,70E-006	0,00010933
ENSGACG00000016104	XII-C	XII-XII	-9,61668	5,03E-012	1,07E-009
ENSGACG00000016696	XII-C	XII-XII	-7,19733	1,81E-006	7,76E-005
ENSGACG00000017299	XII-C	XII-XII	-4,08743	0,0024548	0,0316005
ENSGACG00000017681	XII-C	XII-XII	-7,58563	3,87E-010	5,09E-008
ENSGACG00000018177	XII-C	XII-XII	-1,80E+308	0,0002979	0,00570002
ENSGACG00000019066	XII-C	XII-XII	-7,10928	1,16E-008	9,99E-007
ENSGACG00000019517	XII-C	XII-XII	-5,24987	0,000109	0,00247067
ENSGACG00000019573	XII-C	XII-XII	3,40115	9,74E-005	0,00225013
ENSGACG00000019574	XII-C	XII-XII	3,81195	0,0006014	0,0101522
ENSGACG00000019604	XII-C	XII-XII	-7,15937	8,50E-005	0,00200882
ENSGACG00000020047	XII-C	XII-XII	-8,53774	1,77E-011	3,29E-009
ENSGACG00000020090	XII-C	XII-XII	-3,72569	0,0013093	0,0191061
ENSGACG00000020187	XII-C	XII-XII	-7,17322	7,92E-009	7,19E-007
ENSGACG00000020249	XII-C	XII-XII	-5,46179	0,0014566	0,0208052
ENSGACG00000020566	XII-C	XII-XII	-5,86274	1,53E-006	6,72E-005
ENSGACG00000020653	XII-C	XII-XII	-8,09134	3,51E-005	0,00095862
ENSGACG00000020917	XII-C	XII-XII	-6,49915	4,68E-007	2,44E-005
ENTPD4	XII-C	XII-XII	0,504471	0,0027217	0,0342867
EPS8L1 (1 of 2)	XII-C	XII-XII	-3,7175	0,0019135	0,0259035
F10	XII-C	XII-XII	-7,06153	1,78E-007	1,06E-005
F2	XII-C	XII-XII	-6,56292	0,0002169	0,00438502
F3 (1 of 2)	XII-C	XII-XII	1,01909	0,0018092	0,0247661
F5	XII-C	XII-XII	-6,8013	2,77E-007	1,55E-005
F9 (1 of 2)	XII-C	XII-XII	-5,28131	7,01E-005	0,00170843
F9 (2 of 2)	XII-C	XII-XII	-6,12098	7,55E-005	0,0018186
FABP1	XII-C	XII-XII	-8,75221	1,57E-007	9,57E-006
FAH	XII-C	XII-XII	-5,10059	1,10E-007	7,03E-006
FETUB (1 of 3)	XII-C	XII-XII	-5,3291	9,95E-006	0,00033001

gene	sample_1	sample_2	log2(fold_change)	p_value	q_value
FETUB (2 of 3)	XII-C	XII-XII	-5,73088	0,0001934	0,00398442
FETUB (3 of 3)	XII-C	XII-XII	-8,38638	2,58E-007	1,46E-005
FGA	XII-C	XII-XII	-8,68709	7,85E-010	9,49E-008
FGB	XII-C	XII-XII	-8,03609	8,57E-007	4,10E-005
FGG	XII-C	XII-XII	-8,17159	1,63E-007	9,86E-006
FOSL1	XII-C	XII-XII	3,03083	7,0278E-04	0,0115304
FOXA3	XII-C	XII-XII	-1,80E+308	0,0027277	0,0343451
FRZB	XII-C	XII-XII	-2,20519	0,0002259	0,00453376
G0S2	XII-C	XII-XII	-3,83279	0,0035308	0,0421091
G6PC (1 of 2)	XII-C	XII-XII	-5,71699	2,24E-005	0,00065546
G6PC (2 of 2)	XII-C	XII-XII	-4,68469	0,0001273	0,00281333
GALNTL1	XII-C	XII-XII	-2,31879	0,0033668	0,0405682
GAPDH (1 of 2)	XII-C	XII-XII	-2,26748	7,07E-006	0,00024734
GAPDH (2 of 2)	XII-C	XII-XII	-7,28283	2,13E-006	8,91E-005
GCGR (1 of 2)	XII-C	XII-XII	-3,67698	0,0010869	0,0164391
GLUL (1 of 2)	XII-C	XII-XII	1,77433	0,0001455	0,00314527
GPD1 (1 of 2)	XII-C	XII-XII	-2,04913	0,0006686	0,0110677
GPX4 (2 of 4)	XII-C	XII-XII	-3,47483	0,000604	0,0101879
GSTZ1	XII-C	XII-XII	-3,73852	0,00047	0,00830396
HAAO	XII-C	XII-XII	-7,74734	3,79E-010	5,00E-008
HABP2 (1 of 2)	XII-C	XII-XII	-9,00813	5,89E-005	0,00147832
HABP2 (2 of 2)	XII-C	XII-XII	-8,16428	1,46E-005	0,00045678
HAL	XII-C	XII-XII	-6,61141	3,82E-006	0,00014649
HAO1	XII-C	XII-XII	-8,32644	0,00010118	0,00232351
HGD	XII-C	XII-XII	-6,00458	6,65E-009	6,17E-007
HM13	XII-C	XII-XII	0,537757	5,20E-005	0,00133246
HNF1A	XII-C	XII-XII	-5,16401	0,0001798	0,00374914
HNF4A	XII-C	XII-XII	-5,49691	0,0003609	0,006681
HNMT (2 of 2)	XII-C	XII-XII	-4,47289	1,26E-005	0,00040345
HPD	XII-C	XII-XII	-7,82797	2,90E-008	2,22E-006
HPN	XII-C	XII-XII	-3,91839	0,0021232	0,0281559
HPX	XII-C	XII-XII	-8,00512	7,52E-008	5,06E-006
IGFALS	XII-C	XII-XII	-5,70818	8,72E-006	0,00029509
IGFBP2 (2 of 2)	XII-C	XII-XII	-6,03781	2,36E-005	0,00068488
IGSF5 (2 of 2)	XII-C	XII-XII	-5,58862	7,45E-005	0,00179775
IL22RA1	XII-C	XII-XII	4,31099	0,0001592	0,00338933
ILDR1 (1 of 2)	XII-C	XII-XII	-1,80E+308	0,0003163	0,00598984
IRF6	XII-C	XII-XII	-2,95084	0,0024466	0,0315164
IRG1	XII-C	XII-XII	2,76104	0,0042936	0,0490534
ITIH2	XII-C	XII-XII	-8,00117	2,68E-009	2,79E-007
ITIH4 (2 of 2)	XII-C	XII-XII	-5,24343	0,00021118	0,00428705
IYD	XII-C	XII-XII	-3,55342	0,0004852	0,00851954
KIF23 (2 of 2)	XII-C	XII-XII	1,27243	0,0003008	0,00574566
KL	XII-C	XII-XII	-7,62037	3,35E-009	3,40E-007
KMO	XII-C	XII-XII	-4,72131	7,44E-006	0,00025809
KNG1	XII-C	XII-XII	-8,61511	2,47E-009	2,60E-007
KYNU	XII-C	XII-XII	-4,39218	0,000274	0,00531895
LCAT,PLA2G15	XII-C	XII-XII	-1,66457	0,0029535	0,036601
LECT2	XII-C	XII-XII	-7,91313	7,08E-010	8,66E-008
LMNA (2 of 2)	XII-C	XII-XII	-4,27443	0,0016144	0,0225961
LRG1	XII-C	XII-XII	-8,5673	2,98E-007	1,66E-005
LRRFIP1 (1 of 2)	XII-C	XII-XII	1,09215	6,29E-007	3,15E-005
LYZ	XII-C	XII-XII	-8,5563	4,44E-016	2,06E-013

gene	sample_1	sample_2	log2(fold_change)	p_value	q_value
LZTR1	XII-C	XII-XII	0,237536	0,0010107	0,0154952
MASP1 (2 of 2)	XII-C	XII-XII	-5,11288	0,0032125	0,039095
MAT1A (2 of 2)	XII-C	XII-XII	-8,85453	5,53E-014	1,79E-011
MFRP	XII-C	XII-XII	-3,37713	0,0023103	0,0301058
MINPP1 (1 of 2)	XII-C	XII-XII	-4,24108	0,0003291	0,00618973
MIOX	XII-C	XII-XII	-7,31873	1,52E-007	9,27E-006
MLXIPL	XII-C	XII-XII	-4,69301	0,0004363	0,00781249
MPZL3	XII-C	XII-XII	-4,52466	0,0043382	0,0494444
MSRB2	XII-C	XII-XII	-1,80E+308	0,000849	0,0134406
MST1P9	XII-C	XII-XII	-6,89453	4,26E-009	4,19E-007
MTTP	XII-C	XII-XII	-3,76032	0,0001632	0,00345999
MXD4	XII-C	XII-XII	1,12127	0,0002279	0,00456725
MYBPC1	XII-C	XII-XII	-3,96875	0,0002656	0,00518394
MYL1	XII-C	XII-XII	-2,82616	0,0039828	0,0462739
MYLPF (2 of 2)	XII-C	XII-XII	-3,70764	1,89E-006	8,05E-005
MYOM1 (2 of 2)	XII-C	XII-XII	-2,62032	1,01E-005	0,00033356
NAALADL1	XII-C	XII-XII	-3,43984	0,0005435	0,00934889
NFE2	XII-C	XII-XII	2,04937	0,0043365	0,0494301
NIPSNAP1	XII-C	XII-XII	-6,25706	1,54E-005	0,00047749
NME4	XII-C	XII-XII	-6,9648	6,51E-007	3,24E-005
NPC1L1	XII-C	XII-XII	-4,61176	0,0005219	0,0090457
NR1H4	XII-C	XII-XII	-1,80E+308	0,0026053	0,0331266
NR5A2	XII-C	XII-XII	-4,62559	0,0041602	0,0478695
OVGP1 (3 of 5)	XII-C	XII-XII	-8,08742	3,03E-009	3,12E-007
PACSIN3	XII-C	XII-XII	-3,74296	0,0017306	0,0238935
PCSK6	XII-C	XII-XII	-5,69553	1,00E-005	0,00033269
PFKM (2 of 2)	XII-C	XII-XII	-3,30888	3,46E-008	2,58E-006
PGAM2	XII-C	XII-XII	-2,88107	0,0014061	0,0202302
PGLYRP2 (2 of 2)	XII-C	XII-XII	-7,95708	7,99E-014	2,51E-011
PIPOX	XII-C	XII-XII	-4,25245	0,0005806	0,00986331
PLA2G12B (1 of 2)	XII-C	XII-XII	-5,48194	0,0036104	0,0428589
PLG	XII-C	XII-XII	-8,21339	5,50E-009	5,23E-007
PLP1 (2 of 2)	XII-C	XII-XII	-2,41914	0,0022698	0,0296819
PRHOXNB	XII-C	XII-XII	-1,80E+308	0,002062	0,0275018
PROC	XII-C	XII-XII	-7,78684	9,08E-007	4,31E-005
PROM1 (1 of 2)	XII-C	XII-XII	-4,54218	0,00087	0,0137093
PROZ (2 of 2)	XII-C	XII-XII	-7,82426	1,68E-006	7,27E-005
PRPF40A	XII-C	XII-XII	0,769123	0,001589	0,02231
PYGM (2 of 2)	XII-C	XII-XII	-3,40174	0,0002153	0,00435671
QPCT	XII-C	XII-XII	-3,03856	0,0034602	0,0414456
QPRT	XII-C	XII-XII	-4,13468	0,0026738	0,0338111
RPA1 (1 of 2)	XII-C	XII-XII	1,31239	0,00116631	0,017409
SAP30L	XII-C	XII-XII	0,879816	0,0022394	0,0293659
SDC2	XII-C	XII-XII	-2,66123	0,0013388	0,0194486
SERPINC1	XII-C	XII-XII	-8,20089	7,26E-008	4,91E-006
SERPIND1	XII-C	XII-XII	-7,7105	1,37E-008	1,16E-006
SERPINF2	XII-C	XII-XII	-8,10694	4,25E-013	1,15E-010
SERPING1	XII-C	XII-XII	-4,04635	0,0004561	0,00810117
SHBG	XII-C	XII-XII	-7,38051	2,57E-008	1,99E-006
SLC13A3	XII-C	XII-XII	-4,76312	0,0002362	0,00470487
SLC13A5 (2 of 2)	XII-C	XII-XII	-5,91348	2,51E-006	0,0001024
SLC1A5	XII-C	XII-XII	2,28973	1,8527E-04	0,00384474
SLC22A13	XII-C	XII-XII	-1,80E+308	0,0004896	0,0085833

gene	sample_1	sample_2	log2(fold_change)	p_value	q_value
SLC22A14	XII-C	XII-XII	-4,85527	4,26E-005	0,00112749
SLC22A16	XII-C	XII-XII	-6,69477	9,10E-005	0,00212407
SLC25A34	XII-C	XII-XII	-2,46962	0,00329433	0,0398738
SLC26A5	XII-C	XII-XII	0,615251	0,00325789	0,0395304
SLC27A2 (1 of 3)	XII-C	XII-XII	-7,17104	3,04E-005	0,000848856
SLC27A6	XII-C	XII-XII	-2,9555	0,00189705	0,0257288
SLC2A2	XII-C	XII-XII	-1,80E+308	0,00339695	0,0408539
SLC39A8	XII-C	XII-XII	-3,92423	0,00136215	0,0197224
SLC7A2	XII-C	XII-XII	-3,88851	0,00176167	0,0242373
SNX12	XII-C	XII-XII	0,649493	0,001358	0,0196733
SOAT2	XII-C	XII-XII	-4,45959	0,00048914	0,00857645
SRM	XII-C	XII-XII	1,17942	0,00038921	0,00711141
SRSF9	XII-C	XII-XII	0,670511	4,28E-005	0,00113022
ST3GAL1 (1 of 8)	XII-C	XII-XII	-4,82043	0,00187842	0,0255287
STXBP2	XII-C	XII-XII	0,692237	0,00307866	0,0378117
SUSD2	XII-C	XII-XII	-6,4171	1,30E-005	0,000413161
TDO2	XII-C	XII-XII	-8,37441	3,64E-009	3,65E-007
TF	XII-C	XII-XII	-8,21765	0,00018047	0,00376166
TFR2	XII-C	XII-XII	-4,25283	0,00023493	0,00468486
THNSL2	XII-C	XII-XII	-0,831918	2,38E-005	0,000689916
TIMM50	XII-C	XII-XII	0,709383	5,80E-005	0,00145943
TLR3	XII-C	XII-XII	-3,97338	0,00021677	0,00438191
TM4SF4	XII-C	XII-XII	-6,70081	8,59E-005	0,00202479
TM4SF5	XII-C	XII-XII	-3,39837	0,00192896	0,0260721
TMEM182	XII-C	XII-XII	-2,21797	0,00299143	0,0369786
TMEM79 (1 of 2)	XII-C	XII-XII	-4,53034	0,00367515	0,0434645
TNNC2 (1 of 2)	XII-C	XII-XII	-2,93937	0,00262468	0,0333213
TNNI2 (1 of 5)	XII-C	XII-XII	-3,82846	0,00025989	0,00509279
TNNI2 (3 of 5)	XII-C	XII-XII	-4,54901	5,30E-006	0,000193659
TNNI2 (5 of 5)	XII-C	XII-XII	-5,66183	1,51E-006	6,63E-005
TNNT3 (2 of 2)	XII-C	XII-XII	-3,60576	0,00056963	0,00971136
TSPAN9 (2 of 2)	XII-C	XII-XII	-1,0148	0,00142326	0,0204243
TTC36	XII-C	XII-XII	-5,06853	3,83E-006	0,00014688
TTC38	XII-C	XII-XII	-0,820873	0,00409224	0,047255
TYMP	XII-C	XII-XII	-4,34513	2,48E-005	0,00071659
UCP1	XII-C	XII-XII	-7,30858	2,00E-007	1,18E-005
UPP2	XII-C	XII-XII	-6,6475	1,62E-008	1,34E-006
WDR5	XII-C	XII-XII	0,527287	0,00252738	0,0323415
XRCC3	XII-C	XII-XII	0,918695	2,13E-008	1,69E-006

Supplementary table S.3.3 Cufflinks output, list of differentially expressed genes in gill tissue of three-spined sticklebacks. Differentially expressed is defined by comparison to pre-exposed controls (I-C, XII-C or M-C). The term "gene" is the name for a specific gene as taken from the *G. aculeatus* reference genome, "sample_1" is the preexposure control group, "sample_2" the infection treatment group, log2(fold change) displays the transformed fold change in "sample_2" compared to "sample_1", p value and q value are given for each test (only significant differences shown).

gene	sample_1	sample_2	log2(fold_change)	p_value	q_value
ACP1	I-C	I-I	1,06638	0,00188273	0,0255759
ACSL4	I-C	I-I	0,49783	0,00338968	0,0407872
AK1	I-C	I-I	1,63774	4,38E-006	0,000164731
ALDH18A1 (1 of 2)	I-C	I-I	0,886864	3,57E-007	1,93E-005
ALDH9A1 (2 of 2)	I-C	I-I	0,726761	2,95E-005	0,000827829
ALYREF (2 of 2)	I-C	I-I	1,13775	6,40E-010	7,93E-008
ASB5	I-C	I-I	2,90346	0,00060106	0,0101474
ATP6AP1 (1 of 2)	I-C	I-I	1,2358	4,89E-005	0,00126448
ATP6V0D2	I-C	I-I	3,87103	0,00275609	0,034631
B3GNTL1	I-C	I-I	1,28126	4,29E-007	2,26E-005
C15orf57	I-C	I-I	1,03196	0,00340856	0,0409596
C7orf59	I-C	I-I	1,88722	0,00438419	0,0498426
CASP3 (4 of 4)	I-C	I-I	0,645245	0,000826204	0,0131441
CCBL1	I-C	I-I	1,05635	5,49E-009	5,22E-007
CD2	I-C	I-I	1,03392	0,000980042	0,0151135
CHAC1 (2 of 2)	I-C	I-I	0,969798	3,99E-007	2,12E-005
CHCHD3 (2 of 2)	I-C	I-I	1,08492	0,00272945	0,0343629
CISH	I-C	I-I	2,47561	6,10E-005	0,00152153
COL6A3	I-C	I-I	-1,92174	0,0028733	0,0357981
COQ5	I-C	I-I	0,98473	5,11E-010	6,49E-008
COX7C	I-C	I-I	2,19668	0,00302125	0,0372623
CPO (2 of 2)	I-C	I-I	2,80016	0,00429951	0,0491038
CPSF2	I-C	I-I	0,929871	0,00099175	0,0152592
CRISP3	I-C	I-I	2,97095	0,00327134	0,0396586
CRYBA2	I-C	I-I	3,13098	0,00269028	0,0339761
CSTF2	I-C	I-I	1,04323	1,61E-005	0,000495787
CTH	I-C	I-I	1,07274	0,00393627	0,0458599
DBI	I-C	I-I	1,78594	1,43E-005	0,000448044
DDIT4 (1 of 2)	I-C	I-I	2,95025	0,000714356	0,0116846
DDX52	I-C	I-I	1,0189	0,000424042	0,00763117
DHRS13 (1 of 3)	I-C	I-I	1,28681	0,00149223	0,0212159
EID3	I-C	I-I	0,675838	0,000607343	0,010233
EIF2B2	I-C	I-I	0,88029	0,00117131	0,0174703
ELMOD2	I-C	I-I	1,30915	0,000500722	0,00874306
ENSGACG00000000114	I-C	I-I	1,56736	1,70E-006	7,35E-005
ENSGACG00000000115	I-C	I-I	1,55557	0,000142435	0,00308912
ENSGACG00000000757	I-C	I-I	3,18189	0,00336644	0,0405647
ENSGACG00000000834	I-C	I-I	1,00379	0,000117098	0,00262449
ENSGACG00000001124	I-C	I-I	1,59435	0,000694043	0,0114126
ENSGACG00000001198	I-C	I-I	3,21099	0,000752633	0,0121886
ENSGACG00000001322	I-C	I-I	2,20745	0,00334191	0,0403328
ENSGACG00000001635	I-C	I-I	1,42546	0,00319916	0,0389661
ENSGACG00000001648	I-C	I-I	3,58982	0,00171703	0,023742

gene	sample_1	sample_2	log2(fold_change)	p_value	q_value
ENSGACG00000001729	I-C	I-I	2,4157	0,00417295	0,0479837
ENSGACG00000001763	I-C	I-I	2,0235	0,000267686	0,00521725
ENSGACG00000002769	I-C	I-I	1,03171	0,00185684	0,0252939
ENSGACG00000003226	I-C	I-I	0,874845	0,000209286	0,0042549
ENSGACG00000003971	I-C	I-I	3,37565	2,29E-005	0,000669683
ENSGACG00000005133	I-C	I-I	1,31844	0,00032417	0,00611326
ENSGACG00000005365	I-C	I-I	2,17623	0,000502121	0,00876338
ENSGACG00000005981	I-C	I-I	1,18629	2,02E-005	0,000601023
ENSGACG00000006029	I-C	I-I	2,37547	0,00364034	0,0431371
ENSGACG00000006710	I-C	I-I	1,99109	0,0027825	0,0348908
ENSGACG00000006806	I-C	I-I	2,77749	0,00318877	0,0388671
ENSGACG00000008485	I-C	I-I	0,982145	0,00287469	0,0358127
ENSGACG00000009076	I-C	I-I	2,76015	0,00135729	0,0196653
ENSGACG00000009358	I-C	I-I	2,99512	0,000733518	0,0119382
ENSGACG00000009801	I-C	I-I	0,896846	0,00230943	0,0300963
ENSGACG00000010497	I-C	I-I	1,73235	1,58E-007	9,62E-006
ENSGACG00000010623	I-C	I-I	2,27464	0,00324131	0,0393744
ENSGACG00000011672	I-C	I-I	3,88202	3,98E-006	0,000151799
ENSGACG00000012562	I-C	I-I	3,20219	0,00296942	0,0367558
ENSGACG00000012566	I-C	I-I	3,45481	0,000480476	0,00845246
ENSGACG00000012607	I-C	I-I	1,01719	9,94E-005	0,00228999
ENSGACG00000012639	I-C	I-I	2,18533	0,0039085	0,045607
ENSGACG00000013327	I-C	I-I	2,95465	0,00156358	0,022027
ENSGACG00000013361	I-C	I-I	3,53802	0,0016694	0,0232164
ENSGACG00000013652	I-C	I-I	1,76264	0,00152393	0,0215761
ENSGACG00000013891	I-C	I-I	3,84069	0,000388135	0,00709501
ENSGACG00000014148	I-C	I-I	3,34201	0,00201381	0,0269901
ENSGACG00000014312	I-C	I-I	2,62637	0,000265642	0,00518421
ENSGACG00000014407	I-C	I-I	1,03785	0,00341764	0,0410464
ENSGACG00000015818	I-C	I-I	3,43061	7,07E-005	0,00172233
ENSGACG00000016608	I-C	I-I	2,80008	0,00257915	0,0328654
ENSGACG00000016724	I-C	I-I	0,696547	3,05E-007	1,69E-005
ENSGACG00000017825	I-C	I-I	0,913188	0,00390363	0,0455611
ENSGACG00000018049	I-C	I-I	3,40445	2,58E-005	0,000739363
ENSGACG00000018764	I-C	I-I	3,89666	4,20E-006	0,000158898
ENSGACG00000018802	I-C	I-I	2,9241	0,000937802	0,0145807
ENSGACG00000018840	I-C	I-I	2,59236	0,000112284	0,00253432
ENSGACG00000018977	I-C	I-I	2,59047	0,00269386	0,034013
ENSGACG00000019770	I-C	I-I	1,37867	0,00257472	0,0328216
ENSGACG00000020145	I-C	I-I	2,57998	0,0005864	0,00994376
ENSGACG00000020181	I-C	I-I	2,29866	0,0021429	0,0283617
ENSGACG00000020365	I-C	I-I	2,83295	1,39E-005	0,000437539
ENSGACG00000020633	I-C	I-I	3,03704	0,000382222	0,0070059
ENSGACG00000020931, ENSGACG00000020932, ENSGACG00000020933, ENSGACG00000020934	I-C	I-I	2,38429	0,000799165	0,0127988
ENTPD2	I-C	I-I	1,19221	0,00141111	0,0202856
FADD	I-C	I-I	1,17767	1,00E-011	1,98E-009
FAM102B (2 of 2)	I-C	I-I	1,25105	7,50E-006	0,000259858
FBP2	I-C	I-I	1,3125	0,000161148	0,00342288
FGFR1OP2	I-C	I-I	0,970075	0,00295421	0,0366082
FKBP5	I-C	I-I	2,97127	0,000340462	0,00636661
FLOT2 (1 of 2)	I-C	I-I	0,450472	0,0036068	0,042824

gene	sample_1	sample_2	log2(fold_change)	p_value	q_value
FMNL1 (2 of 2)	I-C	I-I	0,68415	9,71E-009	8,58E-007
FTSJ1	I-C	I-I	1,15193	0,000398657	0,00725401
FUT4	I-C	I-I	1,34105	0,00213094	0,0282378
GADD45B (1 of 2)	I-C	I-I	2,27733	0,000239548	0,00475894
GAPDH (1 of 2)	I-C	I-I	1,37251	0,00374502	0,0441091
GLRX2	I-C	I-I	1,49421	8,27E-005	0,00196099
GPANK1	I-C	I-I	0,973576	6,21E-005	0,00154427
GPN1	I-C	I-I	1,22154	1,11E-006	5,10E-005
GRAP2	I-C	I-I	1,37326	0,0014083	0,0202553
GTF2F1	I-C	I-I	0,94963	0,00261937	0,0332673
GZMA	I-C	I-I	2,42166	0,00204452	0,0273172
HSD11B1L	I-C	I-I	1,13767	0,000115713	0,00259858
HVCN1	I-C	I-I	2,65315	0,000387873	0,007091
ILDR1 (1 of 2)	I-C	I-I	1,05748	0,00112328	0,0168865
ILDR1 (2 of 2)	I-C	I-I	0,553309	0,000586235	0,00994133
KCNB1	I-C	I-I	-2,58894	0,00365761	0,043301
KLF9	I-C	I-I	2,80781	0,000703385	0,011539
L2HGDH	I-C	I-I	0,866441	0,00235475	0,0305672
LACC1	I-C	I-I	1,0269	0,0035357	0,0421552
LGALS4	I-C	I-I	5,64768	0,000302023	0,0057651
LGALS8 (2 of 2)	I-C	I-I	1,24388	0,00403732	0,0467663
LMOD3	I-C	I-I	2,21197	0,000998973	0,0153501
LRP1 (2 of 2)	I-C	I-I	-1,78102	0,00297638	0,0368252
LSM6	I-C	I-I	2,31994	0,000776713	0,0125091
LZIC	I-C	I-I	0,783218	1,33E-009	1,51E-007
MAP1LC3A	I-C	I-I	0,879106	2,60E-007	1,48E-005
MFAP1	I-C	I-I	0,895563	0,000978245	0,0150917
MLYCD	I-C	I-I	1,3359	0,00324271	0,0393889
MRPL12	I-C	I-I	0,886142	0,000182471	0,00379602
MRPL28	I-C	I-I	0,953263	0,000806661	0,0128961
MRPL39	I-C	I-I	1,32642	0,000107106	0,00243518
MRPS10	I-C	I-I	1,14308	5,17E-006	0,000189807
MRPS31	I-C	I-I	1,02423	1,07E-007	6,86E-006
MYCL1 (1 of 2)	I-C	I-I	3,0125	0,00205085	0,027386
NARFL	I-C	I-I	0,829697	0,0022408	0,0293808
NEK4	I-C	I-I	0,676057	0,00366856	0,0434021
PARS2	I-C	I-I	0,544981	0,00132514	0,0192914
PDIA5	I-C	I-I	1,38609	0	0
PFKFB1	I-C	I-I	1,08331	0,00209807	0,0278881
PGLYRP2 (1 of 2)	I-C	I-I	1,94663	0,00205357	0,0274135
PHKG1	I-C	I-I	1,65527	0,000992454	0,0152683
PPDPF (1 of 2)	I-C	I-I	1,63668	0,00364742	0,0432035
PPM1H (2 of 2)	I-C	I-I	1,02397	0,000106684	0,00242709
PPP2R5E	I-C	I-I	0,51421	3,32E-005	0,00091505
PRMT7	I-C	I-I	1,34676	0,0016437	0,0229308
RAC2	I-C	I-I	1,2381	0,00433946	0,049455
RAG1	I-C	I-I	3,50958	8,07E-005	0,00192261
RAG2	I-C	I-I	4,01033	0,000107311	0,00243911
RARS	I-C	I-I	1,00136	5,75E-005	0,00144848
RASSF5	I-C	I-I	0,797388	0,000227582	0,0045616
RBBP5	I-C	I-I	0,969692	1,36E-011	2,60E-009
RBM19	I-C	I-I	0,716089	0,00102302	0,0156489
RHOT1 (1 of 2)	I-C	I-I	0,43465	0,00324319	0,0393923

gene	sample_1	sample_2	log2(fold_change)	p_value	q_value
RPS24	I-C	I-I	1,35074	0,000117143	0,00262536
RPS6KA4	I-C	I-I	0,71365	0,00213822	0,0283146
RPUSD4	I-C	I-I	0,91908	4,43E-005	0,00116332
SCN1B (2 of 2)	I-C	I-I	3,882	4,14E-005	0,00109967
SERBP1 (1 of 2)	I-C	I-I	0,766833	0,0023779	0,0308064
SLC3A2 (2 of 2)	I-C	I-I	2,12421	0,0022725	0,0297099
SLC7A8	I-C	I-I	1,20664	1,85E-011	3,42E-009
SMC5	I-C	I-I	0,990069	1,11E-015	4,85E-013
SMOX	I-C	I-I	1,63219	7,63E-009	6,96E-007
SMPD4	I-C	I-I	1,59214	1,93E-005	0,00057896
SMPDL3A	I-C	I-I	0,460075	5,76E-006	0,000207861
SNUPN	I-C	I-I	0,914031	1,34E-008	1,13E-006
SOCS3 (1 of 2)	I-C	I-I	2,27549	0,00148691	0,0211533
SPCS2	I-C	I-I	1,18677	3,29E-005	0,000906846
SPG21	I-C	I-I	1,00015	4,38E-005	0,00115339
SRM	I-C	I-I	1,50633	0,00230483	0,0300473
STMN1 (2 of 2)	I-C	I-I	1,59407	0,00354076	0,0422032
STOML2 (1 of 2)	I-C	I-I	1,01677	0,000889959	0,0139658
STOML2 (2 of 2)	I-C	I-I	0,962673	0,00143353	0,0205415
SULT6B1	I-C	I-I	1,1455	0,00220091	0,0289623
SURF1	I-C	I-I	1,3086	0,00204043	0,0272724
SVIL (2 of 2)	I-C	I-I	1,8684	0,00324804	0,0394372
TF	I-C	I-I	2,53567	0,00143598	0,0205701
TG	I-C	I-I	-3,21798	0,00285178	0,0355834
TMEM182	I-C	I-I	1,34652	0,000263586	0,005151
TMOD4	I-C	I-I	1,28638	5,27E-005	0,00134623
TNNC1	I-C	I-I	2,77367	0,00438272	0,0498299
TOM1 (2 of 2)	I-C	I-I	0,715083	0,00207351	0,0276229
TOMM40 (1 of 2)	I-C	I-I	0,858374	1,02E-007	6,58E-006
TRAF3	I-C	I-I	0,863206	0,000207282	0,00422076
TSC22D3	I-C	I-I	2,4211	0,00233233	0,0303389
TTC9C	I-C	I-I	0,925316	0,00133853	0,0194454
TXNDC17	I-C	I-I	1,74545	0,00192318	0,0260089
U3	I-C	I-I	3,53431	0,00216907	0,0286344
U3	I-C	I-I	3,53431	0,00216907	0,0286344
UNC45A	I-C	I-I	0,579195	0,000903231	0,0141367
UROS	I-C	I-I	1,02671	0,00336672	0,0405675
USP48	I-C	I-I	0,689672	6,21E-006	0,000221617
VIPR1 (2 of 2)	I-C	I-I	2,81637	0,00109823	0,0165802
VTCN1	I-C	I-I	2,25646	0,00302807	0,0373262
WDR24	I-C	I-I	0,50504	0,000480249	0,00844928
WDR5	I-C	I-I	0,771969	0,000636995	0,0106405
ZNF259	I-C	I-I	1,38251	2,12E-007	1,24E-005
MON2	I-C	I-M	1,06885	0,00148111	0,0210887
ABL2	I-C	I-M	1,89206	5,23E-005	0,00133767
ACTR6	I-C	I-M	1,52946	0,00291511	0,0362214
ADSS	I-C	I-M	1,52778	0,00108634	0,0164322
ALDH18A1 (1 of 2)	I-C	I-M	1,08821	0,000428026	0,00769105
ALPL	I-C	I-M	1,62133	0,00141912	0,0203767
ALYREF (2 of 2)	I-C	I-M	1,22517	1,85E-005	0,000559078
ANGPTL1 (2 of 2)	I-C	I-M	3,29055	0,000993256	0,0152782
ASPN	I-C	I-M	2,18377	0,000530808	0,00917169
ATF6	I-C	I-M	0,872526	2,16E-006	9,02E-005

gene	sample_1	sample_2	log2(fold_change)	p_value	q_value
BIN2	I-C	I-M	1,05867	3,56E-007	1,93E-005
C4A	I-C	I-M	1,84794	3,77E-005	0,00101746
C6	I-C	I-M	2,16836	1,36E-005	0,000429667
C7 (1 of 2)	I-C	I-M	3,05243	0,00130068	0,0190043
CACNA1S (1 of 2)	I-C	I-M	1,49291	7,71E-006	0,000266149
CAD	I-C	I-M	1,45629	0,00346048	0,0414473
CAMK1D (2 of 2)	I-C	I-M	2,29053	0,00328369	0,039774
CASP3 (4 of 4)	I-C	I-M	2,13822	7,08E-006	0,000247391
CASP8	I-C	I-M	1,11152	6,77E-005	0,00166045
CBX7 (2 of 2)	I-C	I-M	1,75388	3,77E-005	0,00101746
CCR9 (1 of 2)	I-C	I-M	2,29269	2,30E-005	0,000671488
CD248 (2 of 2)	I-C	I-M	3,04138	0,00251313	0,0321969
CD44	I-C	I-M	2,62774	1,35E-008	1,14E-006
CDC42	I-C	I-M	0,611439	0,00168893	0,0234333
CEBPB	I-C	I-M	2,54166	0,000953958	0,0147839
CERS2 (2 of 2)	I-C	I-M	0,955292	7,99E-007	3,86E-005
CISH	I-C	I-M	2,27586	2,69E-005	0,000767433
CKMT1A	I-C	I-M	1,48923	0,00019705	0,00404708
CMPK2	I-C	I-M	1,97821	0,00310836	0,0380897
CNOT1	I-C	I-M	0,996233	0,000350483	0,00652017
COX15	I-C	I-M	0,899073	5,02E-011	8,32E-009
CPA1	I-C	I-M	2,18017	0,00282842	0,0353506
CPSF2	I-C	I-M	1,04553	1,73E-007	1,04E-005
CPZ (2 of 2)	I-C	I-M	1,54866	0,00413938	0,0476845
CREBL2	I-C	I-M	1,16863	0,00365412	0,043268
CSTF2	I-C	I-M	1,36713	1,34E-005	0,000424193
CTDSPL (2 of 2)	I-C	I-M	0,627914	0,0041673	0,0479327
CYP1B1	I-C	I-M	2,43897	0,00136674	0,0197759
DAB2	I-C	I-M	1,83943	4,30E-005	0,00113591
DCLK2 (1 of 2)	I-C	I-M	3,16682	0,00169243	0,0234719
DCPS	I-C	I-M	1,35279	3,01E-006	0,000119695
DDIT4 (1 of 2)	I-C	I-M	3,98875	7,15E-005	0,0017384
DENND4A (2 of 2)	I-C	I-M	3,88648	9,24E-005	0,002153
DHX58	I-C	I-M	2,25817	0,00206034	0,0274845
DIO3	I-C	I-M	2,90881	0,00328669	0,0398025
DIS3	I-C	I-M	0,82111	0,0014665	0,0209225
DOCK1	I-C	I-M	0,963102	1,31E-011	2,52E-009
DUOX1	I-C	I-M	2,51376	0,00048636	0,00853666
DUS3L	I-C	I-M	0,586906	0,000633645	0,0105948
EIF2D	I-C	I-M	1,21843	6,30E-006	0,000224228
EIF4H	I-C	I-M	0,95837	0,000327267	0,00616107
EIF5B	I-C	I-M	1,3542	3,09E-007	1,71E-005
ELL2	I-C	I-M	0,915836	2,19E-008	1,74E-006
ENSGACG00000000082, SUSD3	I-C	I-M	1,01735	1,30E-005	0,000412817
ENSGACG00000000208	I-C	I-M	3,00768	2,17E-005	0,000638112
ENSGACG00000000614	I-C	I-M	2,76621	0	0
ENSGACG00000001531	I-C	I-M	2,98674	2,24E-005	0,000655901
ENSGACG00000001749	I-C	I-M	2,77919	0,000130531	0,00287229
ENSGACG00000002265	I-C	I-M	1,37301	1,87E-006	7,98E-005
ENSGACG00000002541	I-C	I-M	4,6613	0,000545188	0,00937295
ENSGACG00000003446	I-C	I-M	2,59278	0,000198101	0,00406506
ENSGACG00000003503	I-C	I-M	2,92817	7,95E-005	0,00189741

gene	sample_1	sample_2	log2(fold_change)	p_value	q_value
ENSGACG00000004324	I-C	I-M	1,26338	0,000547165	0,00940077
ENSGACG00000004759	I-C	I-M	1,27472	0,00214189	0,0283519
ENSGACG00000005049	I-C	I-M	3,50272	7,62E-007	3,71E-005
ENSGACG00000005904	I-C	I-M	3,16034	0,00025651	0,00503772
ENSGACG00000005965	I-C	I-M	0,85924	0,000892028	0,0139927
ENSGACG00000005981	I-C	I-M	1,05193	0,00350671	0,0418781
ENSGACG00000006109	I-C	I-M	3,65915	9,57E-005	0,00221709
ENSGACG00000006357	I-C	I-M	3,1351	0,000665758	0,0110298
ENSGACG00000006596	I-C	I-M	1,53666	0,00115816	0,01731
ENSGACG00000006681	I-C	I-M	1,19149	0,00142858	0,020485
ENSGACG00000006710	I-C	I-M	3,09743	3,13E-005	0,000868852
ENSGACG00000006711	I-C	I-M	3,03448	0,00178908	0,02454
ENSGACG00000007150	I-C	I-M	0,92807	0,00236222	0,0306424
ENSGACG00000007176	I-C	I-M	1,80283	0,00340144	0,0408941
ENSGACG00000007442	I-C	I-M	0,998806	0,00179979	0,0246604
ENSGACG00000007525	I-C	I-M	2,00529	0,00390317	0,0455571
ENSGACG00000007661	I-C	I-M	3,63522	0,00012041	0,00268589
ENSGACG00000007958	I-C	I-M	1,20692	2,65E-005	0,000756153
ENSGACG00000008153	I-C	I-M	1,83097	0,00030165	0,00575908
ENSGACG00000009076	I-C	I-M	4,70901	1,33E-008	1,13E-006
ENSGACG00000009188	I-C	I-M	4,04831	7,14E-008	4,84E-006
ENSGACG00000009200	I-C	I-M	4,753	1,30E-013	3,92E-011
ENSGACG00000009358	I-C	I-M	2,90268	0,000855537	0,0135238
ENSGACG00000009414	I-C	I-M	3,36886	0,00215052	0,0284419
ENSGACG00000009546	I-C	I-M	3,46036	0,000467568	0,00826813
ENSGACG00000009763	I-C	I-M	3,81412	0,000223497	0,00449411
ENSGACG00000009770	I-C	I-M	3,88164	2,26E-007	1,31E-005
ENSGACG00000009801	I-C	I-M	0,80729	0,00351478	0,0419562
ENSGACG00000009825	I-C	I-M	1,92495	4,50E-005	0,00117901
ENSGACG00000010476	I-C	I-M	2,60605	0,00198565	0,0266868
ENSGACG00000010623	I-C	I-M	4,63542	6,70E-006	0,00023619
ENSGACG00000010664	I-C	I-M	1,14168	0,00309508	0,0379672
ENSGACG00000010749	I-C	I-M	1,36807	0,00406738	0,0470304
ENSGACG00000011040	I-C	I-M	1,83449	0,00222028	0,0291659
ENSGACG00000011120	I-C	I-M	0,694891	0,000109177	0,00247482
ENSGACG00000011407	I-C	I-M	0,715788	0,00051256	0,00891181
ENSGACG00000011542	I-C	I-M	1,02289	0,000112786	0,00254372
ENSGACG00000012607	I-C	I-M	1,20567	0,000112292	0,00253446
ENSGACG00000012655	I-C	I-M	1,44394	0,00114954	0,017206
ENSGACG00000012657	I-C	I-M	3,53076	0,000162153	0,00344087
ENSGACG00000012663	I-C	I-M	2,36157	0,003076	0,037786
ENSGACG00000012695	I-C	I-M	2,47566	0,00231449	0,0301489
ENSGACG00000012769	I-C	I-M	2,04814	2,82E-008	2,17E-006
ENSGACG00000012792	I-C	I-M	4,30345	0,000861727	0,0136037
ENSGACG00000012829	I-C	I-M	1,0905	4,04E-011	6,86E-009
ENSGACG00000013029	I-C	I-M	3,06833	0,00142452	0,0204374
ENSGACG00000013109	I-C	I-M	1,12987	0,00036995	0,00681951
ENSGACG00000013214	I-C	I-M	3,36096	0,000640668	0,0106892
ENSGACG00000013327	I-C	I-M	2,89018	0,00305625	0,0375972
ENSGACG00000013631	I-C	I-M	1,71895	0,000119549	0,00266978
ENSGACG00000014312	I-C	I-M	2,26132	0,00329104	0,0398434
ENSGACG00000014540	I-C	I-M	3,91986	0	0
ENSGACG00000014574	I-C	I-M	0,679278	0,000644243	0,0107375

gene	sample_1	sample_2	log2(fold_change)	p_value	q_value
ENSGACG00000014936	I-C	I-M	3,50652	5,16E-005	0,00132397
ENSGACG00000014948	I-C	I-M	6,28768	4,42E-009	4,32E-007
ENSGACG00000015960	I-C	I-M	3,46228	5,24E-006	0,000191765
ENSGACG00000015986	I-C	I-M	0,870942	0,00342369	0,0411013
ENSGACG00000016298	I-C	I-M	1,81407	0,00241281	0,0311713
ENSGACG00000016724	I-C	I-M	1,06166	0	0
ENSGACG00000016848	I-C	I-M	1,67218	0,00026554	0,00518246
ENSGACG00000017050	I-C	I-M	2,53586	0,00350063	0,0418207
ENSGACG00000017123	I-C	I-M	2,61392	0,00295858	0,0366512
ENSGACG00000017259	I-C	I-M	2,00066	0,00172743	0,0238584
ENSGACG00000017758	I-C	I-M	6,46246	1,53E-005	0,000476551
ENSGACG00000018764	I-C	I-M	3,26023	0,000154213	0,00329976
ENSGACG00000018802	I-C	I-M	3,10299	0,000384739	0,00704477
ENSGACG00000018835	I-C	I-M	1,46006	0,000488635	0,008569
ENSGACG00000018840	I-C	I-M	3,66367	9,71E-009	8,58E-007
ENSGACG00000018850	I-C	I-M	3,57985	0,00287508	0,035816
ENSGACG00000019285	I-C	I-M	2,67125	0,00118819	0,0176694
ENSGACG00000019470	I-C	I-M	3,19185	7,44E-005	0,00179677
ENSGACG00000019938	I-C	I-M	0,728692	0,000260917	0,00510905
ENSGACG00000019951	I-C	I-M	2,6078	0,00427866	0,0489218
ENSGACG00000019952	I-C	I-M	2,81172	0,000948147	0,014712
ENSGACG00000020145	I-C	I-M	2,27389	0,000783491	0,0125973
ENSGACG00000020181	I-C	I-M	3,15752	3,00E-005	0,000840122
ENSGACG00000020219	I-C	I-M	0,886338	0,000277586	0,00537635
ENSGACG00000020490	I-C	I-M	3,10006	0,00401087	0,046528
ENSGACG00000020491	I-C	I-M	2,94495	0,000973301	0,0150278
ENSGACG00000020790	I-C	I-M	1,0346	0,00106624	0,0161864
ENTPD4	I-C	I-M	1,23502	9,08E-005	0,00212151
EPSTI1	I-C	I-M	2,70934	0,000323242	0,00609884
ERGIC1	I-C	I-M	1,71616	4,45E-006	0,000166868
ETV6	I-C	I-M	0,950886	1,36E-007	8,43E-006
EWSR1	I-C	I-M	1,03754	0,000728191	0,0118674
F2RL3	I-C	I-M	2,86443	0,00255694	0,0326383
FADD	I-C	I-M	1,22118	0,00291527	0,0362229
FAM102B (2 of 2)	I-C	I-M	1,4647	0,000439794	0,00786403
FAM180A (1 of 2)	I-C	I-M	3,41038	0,000748979	0,012141
FBLN1 (1 of 2)	I-C	I-M	1,30147	0,00305994	0,0376309
FCGBP (1 of 2)	I-C	I-M	1,09567	0,00116094	0,0173446
FGFR1OP2	I-C	I-M	1,31959	0,00149917	0,0212945
FKBP5	I-C	I-M	4,86639	4,19E-005	0,00111109
FTSJ1	I-C	I-M	1,20516	6,51E-005	0,00160698
GADD45B (1 of 2)	I-C	I-M	2,65248	4,39E-007	2,31E-005
GALM	I-C	I-M	0,738199	0,00257233	0,0327969
GJA5 (1 of 2)	I-C	I-M	5,22662	0,00409095	0,0472429
GPR137	I-C	I-M	0,966046	0,00357746	0,0425481
GTF2F1	I-C	I-M	1,26571	2,56E-006	0,000104313
GZMM (4 of 5)	I-C	I-M	1,67667	6,31E-011	1,02E-008
HHATL (1 of 2)	I-C	I-M	3,32727	0,00228957	0,0298889
HS6ST1	I-C	I-M	0,608438	0,00046495	0,00823045
HVCN1	I-C	I-M	2,35532	0,000822359	0,0130962
HYAL2 (1 of 2)	I-C	I-M	1,52474	0,00150965	0,0214143
ILDR1 (2 of 2)	I-C	I-M	0,85305	0,000931022	0,0144929
ISG15	I-C	I-M	2,66096	0,000304127	0,00579806

gene	sample_1	sample_2	log2(fold_change)	p_value	q_value
ITGA11 (1 of 2)	I-C	I-M	2,74568	0,00249837	0,0320474
ITGB1 (1 of 2)	I-C	I-M	0,946666	4,47E-008	3,22E-006
KIFAP3 (2 of 2)	I-C	I-M	1,03014	0,0038685	0,0452418
KLC1	I-C	I-M	1,00953	0,000365214	0,00674725
KLF13	I-C	I-M	4,1442	9,71E-005	0,00224445
KLF9	I-C	I-M	3,72975	3,14E-005	0,000872921
KRI1	I-C	I-M	1,29271	5,13E-008	3,63E-006
KRT80	I-C	I-M	3,41722	1,95E-006	8,27E-005
LCP2	I-C	I-M	1,36991	0,000530739	0,00917084
LRRFIP1 (1 of 2)	I-C	I-M	1,19566	0,000295029	0,00565485
LRRFIP2	I-C	I-M	0,99874	0,00169823	0,0235373
MAP1LC3A	I-C	I-M	0,621759	1,49E-005	0,000465732
MAPRE2	I-C	I-M	1,01253	0,000206462	0,00420673
MCAM (2 of 2)	I-C	I-M	1,16257	0,00328312	0,0397681
MCM3	I-C	I-M	2,24767	0,00169026	0,0234478
MFAP1	I-C	I-M	1,33406	3,66E-005	0,000992268
MGAT4B	I-C	I-M	1,13257	0,000819311	0,0130577
MMP25	I-C	I-M	1,50576	0,000230605	0,00461249
MORC4	I-C	I-M	1,05565	0,000259505	0,00508642
MOV10 (2 of 2)	I-C	I-M	1,99391	0,00381933	0,0447884
MPHOSPH10	I-C	I-M	1,57077	0,000247008	0,00488312
MRPL12	I-C	I-M	1,17684	0,00069362	0,0114065
MRPL15	I-C	I-M	1,02273	0,00152302	0,0215661
MRPL39	I-C	I-M	0,974951	0,00108191	0,0163768
MRPS31	I-C	I-M	1,27377	8,87E-005	0,00208105
MTDH (2 of 2)	I-C	I-M	1,31645	0,00308782	0,0378998
MTRR	I-C	I-M	0,638102	0,00389216	0,0454552
MYL7	I-C	I-M	4,22341	3,48E-005	0,000951378
MYLK4 (1 of 2)	I-C	I-M	3,7669	0,000549077	0,00942798
MYOM1 (1 of 2)	I-C	I-M	1,95576	1,18E-005	0,000380382
MYOM1 (2 of 2)	I-C	I-M	1,27327	3,32E-009	3,37E-007
NARFL	I-C	I-M	0,733371	2,43E-005	0,000703521
NCF1	I-C	I-M	1,89572	0,00276216	0,0346887
NCKIPSD	I-C	I-M	1,3988	0,000865544	0,013652
NFKBIA (1 of 2)	I-C	I-M	2,18021	0,00253209	0,0323896
NOM1	I-C	I-M	0,792943	0,00144785	0,0207067
NR1D2 (2 of 2)	I-C	I-M	3,09906	0,000259578	0,00508752
NUCB2 (2 of 2)	I-C	I-M	2,71066	0,00117244	0,0174835
NUPL1	I-C	I-M	1,128	0,000129899	0,0028607
NVL	I-C	I-M	1,23471	3,21E-005	0,000888554
OPHN1	I-C	I-M	0,635895	0,000202813	0,00414521
OPTN	I-C	I-M	0,759271	8,36E-012	1,68E-009
OSBPL3 (1 of 2)	I-C	I-M	1,04762	0,00096956	0,0149808
PARS2	I-C	I-M	0,529033	1,88E-011	3,47E-009
PCDH20	I-C	I-M	2,62026	0,00418458	0,0480874
PDP2	I-C	I-M	1,14294	0,00420974	0,0483147
PDS5B	I-C	I-M	0,754104	4,60E-005	0,00120119
PIK3R1 (1 of 2)	I-C	I-M	1,74812	0,00411594	0,0474713
PIK3R5 (2 of 2)	I-C	I-M	1,10862	0,00428277	0,0489579
PLCG2	I-C	I-M	0,829402	0,000313967	0,00595382
PLP1 (2 of 2)	I-C	I-M	2,1978	0,00389698	0,0454986
POLD1	I-C	I-M	0,700675	1,12E-006	5,16E-005
POLR2B	I-C	I-M	0,996298	0,0024775	0,0318306

gene	sample_1	sample_2	log2(fold_change)	p_value	q_value
PPM1H (2 of 2)	I-C	I-M	1,48719	0,00356839	0,0424609
PPP1R14B	I-C	I-M	2,63327	0,00292787	0,0363458
PPP1R15B	I-C	I-M	1,99898	0,00424356	0,0486158
PPP2R5E	I-C	I-M	0,860695	3,61E-006	0,000139669
PRDX6 (2 of 2)	I-C	I-M	1,02055	3,99E-013	1,09E-010
PRPF40A	I-C	I-M	1,36377	0,000471303	0,00832185
PRPSAP1 (2 of 2)	I-C	I-M	0,593619	0,00428633	0,0489911
PTPRS (2 of 3)	I-C	I-M	0,898658	4,87E-008	3,47E-006
PTRF (1 of 2)	I-C	I-M	1,63566	0,000968339	0,0149666
PWP2	I-C	I-M	1,3502	5,38E-005	0,00137133
RANBP1	I-C	I-M	0,987749	0,00033277	0,00624786
RARS	I-C	I-M	1,19501	3,17E-011	5,53E-009
RASSF5	I-C	I-M	1,05653	0,000924479	0,0144102
RBM19	I-C	I-M	0,919554	3,72E-006	0,000143539
RBM42	I-C	I-M	1,06579	0,000391725	0,00714915
RG9MTD2	I-C	I-M	0,630802	0,00066012	0,0109528
RGL3 (1 of 2)	I-C	I-M	1,69844	0,00039726	0,00723326
RIOK2	I-C	I-M	1,36975	0,000447195	0,00797139
RNF19B	I-C	I-M	2,07154	2,18E-006	9,08E-005
RNFT1	I-C	I-M	0,70227	0,000501664	0,00875665
RPS6KA4	I-C	I-M	1,04107	2,65E-005	0,000757513
RRP1B	I-C	I-M	1,37957	0,000171989	0,00361367
RSAD2	I-C	I-M	2,49104	0,000578266	0,00983014
SELE	I-C	I-M	1,17534	0,000476153	0,00839148
SEMA4D	I-C	I-M	1,37756	0,0011326	0,0170007
SERPINE1	I-C	I-M	2,65261	0,00178948	0,0245447
SHANK2	I-C	I-M	2,18331	0,00107597	0,016305
SLC1A5	I-C	I-M	1,9729	9,09E-005	0,00212313
SLC25A33	I-C	I-M	1,18603	0,00207304	0,0276177
SLC39A10	I-C	I-M	0,957977	7,59E-005	0,00182642
SLC41A3 (1 of 2)	I-C	I-M	4,37094	0,000655333	0,0108877
SLC7A8	I-C	I-M	1,61711	6,66E-016	3,01E-013
SLC8A1 (2 of 2)	I-C	I-M	5,58777	6,03E-006	0,000215867
SMARCE1 (2 of 2)	I-C	I-M	1,08602	0,00137672	0,0198921
SMC5	I-C	I-M	1,31481	3,28E-012	7,28E-010
SMOX	I-C	I-M	2,53788	7,49E-005	0,00180538
SNX12	I-C	I-M	0,920203	0,00436271	0,0496568
SNX13	I-C	I-M	0,75892	0,00146333	0,0208847
SNX9	I-C	I-M	0,965161	7,85E-005	0,00187972
SOCS3 (1 of 2)	I-C	I-M	3,74379	1,17E-005	0,000378595
SORBS2	I-C	I-M	3,48741	0,000146088	0,00315511
SPPL2A	I-C	I-M	0,974997	0,000144286	0,00312263
SRPX	I-C	I-M	1,35546	0,00344038	0,0412596
STIM1	I-C	I-M	0,921522	6,97E-006	0,000244235
STRBP	I-C	I-M	0,934622	0,00228921	0,0298858
STX4	I-C	I-M	0,940211	0,00142799	0,0204784
SULF1	I-C	I-M	1,13507	0,00408549	0,0471958
SULT6B1	I-C	I-M	0,655797	0,00211935	0,0281132
SUPT5H	I-C	I-M	1,02087	2,19E-005	0,000645199
TEF (1 of 2)	I-C	I-M	2,8033	0,00119597	0,017763
THBS3	I-C	I-M	2,54505	0,00425576	0,0487205
TMED1 (1 of 2)	I-C	I-M	1,25847	0,00347665	0,041597
TMEM106C	I-C	I-M	1,62367	0,000185233	0,00384414

gene	sample_1	sample_2	log2(fold_change)	p_value	q_value
TMEM199	I-C	I-M	0,864675	3,09E-006	0,000122634
TNFRSF11B	I-C	I-M	1,16415	0,00343001	0,0411626
TNNC1	I-C	I-M	4,47998	2,44E-005	0,000705583
TNNT2 (1 of 2)	I-C	I-M	4,26987	1,51E-005	0,000470594
TPPP3	I-C	I-M	2,33528	0,00300923	0,0371484
TPRG1	I-C	I-M	1,0428	0,000967586	0,0149569
TPST1	I-C	I-M	0,97765	0,000691708	0,0113802
TRAK1 (2 of 2)	I-C	I-M	3,97189	0,00119518	0,0177538
TSC22D3	I-C	I-M	3,58433	2,49E-005	0,000718902
USP18	I-C	I-M	2,66969	0,000116195	0,00260743
USP48	I-C	I-M	0,814339	0,000161789	0,00343435
WAPAL (2 of 2)	I-C	I-M	0,960089	3,14E-006	0,000124147
WAS	I-C	I-M	0,997456	0,00325192	0,0394757
WDR18	I-C	I-M	0,878972	1,09E-006	5,04E-005
XRN2	I-C	I-M	1,15834	0,00175428	0,0241567
ACSL1 (2 of 2)	M-C	M-M	1,65265	0,000406212	0,00736623
ADAL	M-C	M-M	1,49976	0,0015622	0,022011
C3 (4 of 8)	M-C	M-M	2,72071	0,00337134	0,0406105
C7 (1 of 2)	M-C	M-M	3,34781	0,00324309	0,0393916
CCNA2	M-C	M-M	1,8344	0,00263274	0,0333991
CKMT1A	M-C	M-M	-1,43781	1,51E-006	6,64E-005
CPXM1	M-C	M-M	1,00298	0,00184884	0,0252067
DDHD1 (2 of 2)	M-C	M-M	3,62399	0,00204759	0,0273497
DENND4A (2 of 2)	M-C	M-M	3,83644	0,000503117	0,00877755
DHCR24	M-C	M-M	0,874502	0,000729086	0,0118796
DIO3	M-C	M-M	3,12496	0,0020047	0,0268918
EIF2A	M-C	M-M	0,568932	0,000895932	0,0140422
ELOVL1 (1 of 2)	M-C	M-M	0,786506	1,99E-005	0,000593461
ELTD1	M-C	M-M	1,52572	9,66E-005	0,00223425
ENSGACG00000000208	M-C	M-M	2,7523	0,00107398	0,0162817
ENSGACG00000000343	M-C	M-M	4,25363	0,00106093	0,0161194
ENSGACG00000000614	M-C	M-M	0,907927	0,00251866	0,0322545
ENSGACG00000000621	M-C	M-M	8,50865	0	0
ENSGACG00000000869	M-C	M-M	3,73545	1,77E-006	7,63E-005
ENSGACG00000001010	M-C	M-M	5,92861	0,00295368	0,0366026
ENSGACG00000001198	M-C	M-M	3,75758	0,000309282	0,00587914
ENSGACG00000001671	M-C	M-M	-8,20722	7,06E-005	0,00171863
ENSGACG00000001749	M-C	M-M	2,35486	7,60E-006	0,00026292
ENSGACG00000001763	M-C	M-M	2,86805	1,16E-010	1,75E-008
ENSGACG00000006908	M-C	M-M	3,3289	3,25E-011	5,66E-009
ENSGACG00000007987	M-C	M-M	0,994184	0,000320104	0,00605036
ENSGACG00000009358	M-C	M-M	3,97651	0,00059571	0,0100735
ENSGACG00000009417	M-C	M-M	2,9753	0,00385354	0,0451032
ENSGACG00000009825	M-C	M-M	2,34259	6,51E-006	0,000230516
ENSGACG00000010476	M-C	M-M	4,08073	6,77E-005	0,00166036
ENSGACG00000012566	M-C	M-M	3,59543	0,00342276	0,0410931
ENSGACG00000013327	M-C	M-M	2,93033	0,000549438	0,00943285
ENSGACG00000013762	M-C	M-M	2,15453	1,02E-005	0,000338165
ENSGACG00000018001	M-C	M-M	1,42208	0,00384598	0,0450342
ENSGACG00000018840	M-C	M-M	2,48087	0,000764526	0,0123473
ENSGACG00000019470	M-C	M-M	3,16318	0,00128272	0,0187942
ENSGACG00000020145	M-C	M-M	2,41396	0,00176216	0,0242422
ENSGACG00000020181	M-C	M-M	2,56403	0,00410982	0,0474147

gene	sample_1	sample_2	log2(fold_change)	p_value	q_value
ENSGACG00000020490	M-C	M-M	3,3051	0,000595099	0,0100648
ENSGACG00000020660	M-C	M-M	3,44192	0,00275552	0,0346252
ERGIC1	M-C	M-M	1,6229	0,00250116	0,0320753
FKBP5	M-C	M-M	4,07403	0,000155896	0,00332943
GALM	M-C	M-M	0,974542	3,88E-005	0,00104086
GPX4 (1 of 4)	M-C	M-M	1,73764	0,000171898	0,00361207
GRM8 (2 of 2)	M-C	M-M	2,56568	0,00282738	0,0353399
HVCN1	M-C	M-M	2,33557	0,00171338	0,0237027
KLF9	M-C	M-M	3,34425	0,000208518	0,00424141
MAD2L2	M-C	M-M	0,487597	0,00393528	0,0458513
MMP25	M-C	M-M	1,36323	0,00020528	0,00418704
PIK3R5 (2 of 2)	M-C	M-M	0,77712	0,00101375	0,0155324
RNF19B	M-C	M-M	1,54668	0,00145359	0,0207728
SELE	M-C	M-M	1,36423	0,000175677	0,00367787
SLC1A5	M-C	M-M	1,57872	0,003847	0,0450437
SLC25A4	M-C	M-M	-0,840952	0,000290043	0,00557635
SMOX	M-C	M-M	2,79924	0,00244695	0,03152
TDO2	M-C	M-M	3,8335	0,00406195	0,0469863
TEF (2 of 2)	M-C	M-M	1,05854	9,74E-006	0,000324307
THBS1 (2 of 2)	M-C	M-M	3,72156	0,000805716	0,0128832
ACP1	XII-C	XII-M	-1,02258	0,00298756	0,0369387
ACTA2	XII-C	XII-M	2,54557	4,44E-005	0,00116734
ACTN2	XII-C	XII-M	1,72356	0,00434163	0,049474
ADAL	XII-C	XII-M	-1,31015	0,000155602	0,00332405
AK1	XII-C	XII-M	-1,70418	0,00107505	0,0162938
AP2S1	XII-C	XII-M	-1,23273	0,00155945	0,0219806
BLVRB	XII-C	XII-M	-1,73601	0,00110515	0,0166649
BMP10 (2 of 2)	XII-C	XII-M	3,14122	0,00377331	0,0443699
C4A	XII-C	XII-M	-1,4211	4,88E-006	0,000180477
CACNA1S (1 of 2)	XII-C	XII-M	-0,980371	0,00310541	0,0380622
CBX7 (2 of 2)	XII-C	XII-M	-1,3165	0,000910071	0,0142242
CKB (2 of 2)	XII-C	XII-M	2,88304	0,00438945	0,0498891
CLDN15 (2 of 2)	XII-C	XII-M	-1,80E+308	0,000574403	0,00977743
COL24A1	XII-C	XII-M	-1,72575	0,0011195	0,0168405
CPT1A	XII-C	XII-M	-0,803261	0,000106372	0,00242109
CREG2	XII-C	XII-M	-0,93678	0,000911894	0,0142478
CXCL12 (2 of 2)	XII-C	XII-M	-1,72844	2,07E-006	8,69E-005
CYB5B	XII-C	XII-M	-1,49855	0,00109538	0,0165438
DTWD2	XII-C	XII-M	-1,27167	0,00439115	0,049903
DYNLT3 (1 of 2)	XII-C	XII-M	-1,69182	0,00116681	0,017415
ENSGACG00000000115	XII-C	XII-M	1,21472	0,00220717	0,0290297
ENSGACG00000000621	XII-C	XII-M	-1,80E+308	0,000377712	0,00693715
ENSGACG00000000834	XII-C	XII-M	-1,07662	0,00263071	0,03338
ENSGACG00000000887	XII-C	XII-M	-3,0523	5,47E-006	0,000198962
ENSGACG00000001016	XII-C	XII-M	-1,80E+308	1,39E-005	0,000438312
ENSGACG00000001322	XII-C	XII-M	-2,80974	0,000307883	0,00585737
ENSGACG00000001973	XII-C	XII-M	-1,17824	1,11E-006	5,12E-005
ENSGACG00000002145	XII-C	XII-M	-2,29666	0,00126318	0,0185645
ENSGACG00000002223	XII-C	XII-M	1,80E+308	1,93E-005	0,000577912
ENSGACG00000002281	XII-C	XII-M	-1,80E+308	0,00423925	0,0485783
ENSGACG00000002955	XII-C	XII-M	-0,996822	8,05E-005	0,00191847
ENSGACG00000003503	XII-C	XII-M	3,19732	8,47E-007	4,06E-005
ENSGACG00000004079	XII-C	XII-M	2,56893	0,000347154	0,00647032

gene	sample_1	sample_2	log2(fold_change)	p_value	q_value
ENSGACG00000005421	XII-C	XII-M	-1,32211	0,00428882	0,0490116
ENSGACG00000007661	XII-C	XII-M	3,1826	0,000188706	0,00390359
ENSGACG00000007857	XII-C	XII-M	-1,09781	1,46E-006	6,47E-005
ENSGACG00000007950	XII-C	XII-M	-4,81711	0,00327485	0,0396934
ENSGACG00000008587	XII-C	XII-M	-2,11846	0,0030949	0,0379651
ENSGACG00000008869	XII-C	XII-M	-3,10093	0,000351288	0,00653212
ENSGACG00000009014	XII-C	XII-M	-2,32146	0,00128166	0,0187809
ENSGACG00000009076	XII-C	XII-M	-2,75242	0,00273241	0,0343938
ENSGACG00000009188	XII-C	XII-M	-3,01286	0,00162336	0,0226964
ENSGACG00000009200	XII-C	XII-M	-3,48024	7,51E-005	0,00181091
ENSGACG00000009821	XII-C	XII-M	2,54524	0,00326088	0,0395593
ENSGACG00000012554	XII-C	XII-M	-1,98145	0,0025289	0,0323569
ENSGACG00000012797	XII-C	XII-M	-2,45115	0,00201953	0,0270521
ENSGACG00000012799	XII-C	XII-M	-2,44042	0,000948531	0,0147168
ENSGACG00000012962	XII-C	XII-M	4,34904	3,91E-005	0,00104714
ENSGACG00000013695	XII-C	XII-M	-2,58075	0,00221029	0,0290625
ENSGACG00000013782	XII-C	XII-M	2,99059	7,02E-006	0,000245818
ENSGACG00000013891	XII-C	XII-M	-4,08485	0,000271714	0,00528182
ENSGACG00000013918	XII-C	XII-M	-2,24376	0,00257104	0,0327841
ENSGACG00000014131	XII-C	XII-M	-2,93419	0,000641185	0,0106958
ENSGACG00000014250	XII-C	XII-M	-4,28056	0,00108046	0,0163593
ENSGACG00000014402	XII-C	XII-M	-2,29219	0,00217272	0,02867
ENSGACG00000014540	XII-C	XII-M	4,44896	0	0
ENSGACG00000014547	XII-C	XII-M	-3,2554	1,24E-005	0,000397603
ENSGACG00000014629	XII-C	XII-M	-1,58755	1,18E-005	0,000381569
ENSGACG00000015524	XII-C	XII-M	-1,24754	0,00205081	0,0273857
ENSGACG00000015818	XII-C	XII-M	3,91081	0,00394012	0,0458949
ENSGACG00000015897	XII-C	XII-M	-0,607423	0,0005398	0,0092968
ENSGACG00000016379	XII-C	XII-M	-1,00928	0,000467089	0,00826108
ENSGACG00000017105	XII-C	XII-M	-1,304	0,00106447	0,0161653
ENSGACG00000017373	XII-C	XII-M	-2,06368	0,00361475	0,0428979
ENSGACG00000018049	XII-C	XII-M	4,52522	0,000754657	0,0122155
ENSGACG00000018138	XII-C	XII-M	-2,78729	0,000222793	0,00448288
ENSGACG00000019173	XII-C	XII-M	-1,12944	0,000535122	0,00923297
ENSGACG00000019933	XII-C	XII-M	-2,337	5,94E-005	0,00148914
ENSGACG00000020034	XII-C	XII-M	-4,27551	8,51E-005	0,00201008
ENSGACG00000020365	XII-C	XII-M	-2,68098	0,00169319	0,0234798
FHL5	XII-C	XII-M	-1,99379	7,33E-013	1,88E-010
GALNT8 (2 of 2)	XII-C	XII-M	-3,94196	2,05E-005	0,000608777
GATA4	XII-C	XII-M	1,80E+308	0,000863143	0,0136213
GRIN1 (1 of 2)	XII-C	XII-M	3,67203	0,00138389	0,0199711
HSD17B10	XII-C	XII-M	-0,56101	0,00266943	0,0337672
IGKC (1 of 24)	XII-C	XII-M	-2,46711	0,000378934	0,00695572
IQGAP2	XII-C	XII-M	-0,99391	0,0013501	0,0195816
IREB2	XII-C	XII-M	-1,3334	2,15E-005	0,000633304
ISG15	XII-C	XII-M	-2,6577	0,000859133	0,0135704
KCNH2 (2 of 2)	XII-C	XII-M	2,74522	0,00333451	0,0402604
KRT80	XII-C	XII-M	3,28477	2,25E-007	1,30E-005
LZIC	XII-C	XII-M	-1,16155	4,97E-005	0,00128157
MAD2L2	XII-C	XII-M	-1,33933	4,01E-010	5,24E-008
MEP1A (2 of 2)	XII-C	XII-M	-2,36676	0,000484938	0,00851623
MLYCD	XII-C	XII-M	-1,25466	0,0033207	0,0401275
MPEG1	XII-C	XII-M	-1,67578	0,00432543	0,0493345

gene	sample_1	sample_2	log2(fold_change)	p_value	q_value
MPG	XII-C	XII-M	-2,66881	0,000360158	0,00666957
MRPL28	XII-C	XII-M	-1,21976	5,22E-007	2,68E-005
MRPS10	XII-C	XII-M	-0,902243	0,000562783	0,00961805
MYBPC2 (1 of 2)	XII-C	XII-M	-1,33345	0,00252917	0,0323596
MYLK4 (1 of 2)	XII-C	XII-M	3,13032	0,00222181	0,0291808
MYOM1 (2 of 2)	XII-C	XII-M	-0,641081	7,23E-005	0,00175367
MYOZ1 (1 of 2)	XII-C	XII-M	-2,11366	0,00415329	0,0478094
NCKIPSD	XII-C	XII-M	-1,6209	0,000592411	0,0100274
NEB	XII-C	XII-M	-1,60573	1,18E-005	0,000379978
PFKM (1 of 2)	XII-C	XII-M	-1,36188	0,000294732	0,0056498
RANBP1	XII-C	XII-M	-0,8463	0,000239732	0,00476212
REPS1	XII-C	XII-M	-1,46348	0,00272318	0,0343016
RSRC2	XII-C	XII-M	-0,756344	0,000327078	0,00615803
RYR1 (2 of 2)	XII-C	XII-M	-1,87082	0,00101808	0,0155864
SLC41A3 (1 of 2)	XII-C	XII-M	4,3497	0,000620083	0,0104097
SLC4A4 (1 of 2)	XII-C	XII-M	-0,618281	0,00115703	0,0172956
SLC8A1 (2 of 2)	XII-C	XII-M	3,40203	2,18E-011	3,96E-009
SORBS2	XII-C	XII-M	3,40704	6,26E-005	0,00155514
SPPL2A	XII-C	XII-M	-0,546297	0,00359356	0,0427036
STOML2 (2 of 2)	XII-C	XII-M	-0,705211	3,10E-005	0,000861952
TF	XII-C	XII-M	-2,34864	0,00393212	0,0458231
TMEM54 (1 of 2)	XII-C	XII-M	-0,681608	0,00439144	0,0499056
TMOD4	XII-C	XII-M	-1,59469	1,26E-011	2,44E-009
TRDN	XII-C	XII-M	-1,41674	0,000148808	0,00320355
TTC38	XII-C	XII-M	-1,21994	0,00170875	0,0236531
TYMP	XII-C	XII-M	-3,50109	3,43E-005	0,000940746
TYRP1 (1 of 2)	XII-C	XII-M	-1,89179	0,0033432	0,0403453
UROS	XII-C	XII-M	-1,14915	7,33E-005	0,00177322
WDR19	XII-C	XII-M	-2,43017	0,000298937	0,00571645
ACP1	XII-C	XII-XII	-1,53551	5,88E-006	0,000211444
ADAL	XII-C	XII-XII	-1,01735	0,000309222	0,00587822
ADCK3 (1 of 2)	XII-C	XII-XII	-0,635055	6,80E-007	3,36E-005
ADI1	XII-C	XII-XII	-1,86492	0,0037275	0,0439481
ADPRH	XII-C	XII-XII	-2,09513	5,20E-006	0,000190681
ADPRHL1	XII-C	XII-XII	-5,20503	5,71E-005	0,00144081
AK1	XII-C	XII-XII	-1,747	0,000799162	0,0127988
ALDH16A1	XII-C	XII-XII	-1,46557	1,36E-006	6,08E-005
ATG12	XII-C	XII-XII	-2,29584	0,00230763	0,0300774
ATP6V0D1	XII-C	XII-XII	-0,729465	0,00240924	0,0311353
BACE2	XII-C	XII-XII	-1,79742	0,00250627	0,0321256
BLOC1S3	XII-C	XII-XII	-1,8091	0,000453999	0,00807103
BLVRB	XII-C	XII-XII	-2,09286	5,86E-005	0,00147198
C10orf57	XII-C	XII-XII	-2,12205	0,00362975	0,0430398
C15orf57	XII-C	XII-XII	-1,27658	0,00114076	0,0170991
C17orf61	XII-C	XII-XII	-2,17153	0,00266183	0,0336905
C18orf32	XII-C	XII-XII	-2,60773	0,000767088	0,0123816
C19orf42	XII-C	XII-XII	-2,44489	0,00137583	0,0198818
C1orf31	XII-C	XII-XII	-2,17846	0,0015004	0,0213087
C2orf40	XII-C	XII-XII	-1,89709	0,00144253	0,0206461
C6orf162	XII-C	XII-XII	-2,2193	0,00257725	0,0328463
CBR4	XII-C	XII-XII	-2,18368	0,00327701	0,0397137
CCDC115	XII-C	XII-XII	-2,32883	0,00312532	0,038251
CDKN2B	XII-C	XII-XII	-1,77829	0,00414495	0,0477346

gene	sample_1	sample_2	log2(fold_change)	p_value	q_value
CHAC1 (2 of 2)	XII-C	XII-XII	-1,09943	0,000272905	0,00530108
CISD3	XII-C	XII-XII	-1,77448	3,44E-005	0,000941118
CKMT1A	XII-C	XII-XII	0,730322	7,24E-005	0,00175609
CKMT2 (1 of 2)	XII-C	XII-XII	-1,37151	0,000342504	0,00639858
CLDN15 (2 of 2)	XII-C	XII-XII	-1,80E+308	0,000574403	0,00977743
COX7A2L	XII-C	XII-XII	-2,18444	0,00377384	0,0443743
CREG2	XII-C	XII-XII	-1,37572	1,28E-008	1,09E-006
CRTAM	XII-C	XII-XII	-1,60521	1,44E-005	0,00045053
CSRP3	XII-C	XII-XII	-3,05447	0,00427279	0,0488722
CTU1	XII-C	XII-XII	-1,505	0,00394352	0,045926
CYB5B	XII-C	XII-XII	-1,47152	0,00103136	0,0157527
DBI	XII-C	XII-XII	-1,94279	0,00215932	0,0285333
DDRGK1	XII-C	XII-XII	-0,875264	0,00117426	0,017505
DHRS13 (1 of 3)	XII-C	XII-XII	-1,9928	2,43E-005	0,000703925
DTWD2	XII-C	XII-XII	-1,31896	0,000937553	0,0145776
DYNLT3 (1 of 2)	XII-C	XII-XII	-1,82759	0,000444962	0,00793853
EAPP	XII-C	XII-XII	-1,29824	0,000252703	0,00497633
EIF4H	XII-C	XII-XII	-0,724285	0,000744629	0,0120837
ENSGACG00000000040	XII-C	XII-XII	-1,37349	0,00160349	0,0224743
ENSGACG00000000082,!	XII-C	XII-XII	-0,810912	1,73E-005	0,000527485
ENSGACG00000000336	XII-C	XII-XII	-1,29954	0,00167892	0,0233221
ENSGACG00000000424	XII-C	XII-XII	-2,21174	0,002017	0,0270242
ENSGACG00000000621	XII-C	XII-XII	-6,67698	3,01E-008	2,29E-006
ENSGACG00000000869	XII-C	XII-XII	4,40716	1,07E-005	0,000350016
ENSGACG00000000964	XII-C	XII-XII	-1,17258	0,00121498	0,0179888
ENSGACG00000001016	XII-C	XII-XII	-1,80E+308	1,39E-005	0,000438312
ENSGACG00000001033	XII-C	XII-XII	-2,31236	0,00224017	0,029374
ENSGACG00000001322	XII-C	XII-XII	-2,94311	0,000189814	0,00392239
ENSGACG00000001344	XII-C	XII-XII	-2,6432	0,00305019	0,0375428
ENSGACG00000001633	XII-C	XII-XII	-1,95688	0,00210379	0,027949
ENSGACG00000001857	XII-C	XII-XII	-1,74202	2,93E-005	0,000822186
ENSGACG00000001884	XII-C	XII-XII	-0,838885	0,000465426	0,00823714
ENSGACG00000002281	XII-C	XII-XII	-1,80E+308	0,00423925	0,0485783
ENSGACG00000002450	XII-C	XII-XII	-1,39357	0,00371811	0,0438624
ENSGACG00000003132	XII-C	XII-XII	-1,80E+308	0,00240456	0,0310867
ENSGACG00000003456	XII-C	XII-XII	-2,70673	0,000190045	0,00392649
ENSGACG00000003467	XII-C	XII-XII	-2,61765	0,00134743	0,0195514
ENSGACG00000005018	XII-C	XII-XII	-2,1148	0,00191701	0,0259417
ENSGACG00000005421	XII-C	XII-XII	-1,24496	0,00356919	0,0424683
ENSGACG00000005683	XII-C	XII-XII	2,57136	0,00258183	0,0328937
ENSGACG00000005975	XII-C	XII-XII	-1,13613	6,12E-005	0,0015272
ENSGACG00000006019	XII-C	XII-XII	-2,16696	5,58E-005	0,001413
ENSGACG00000006204	XII-C	XII-XII	-2,53576	0,00176632	0,0242881
ENSGACG00000007447	XII-C	XII-XII	-1,58803	2,53E-007	1,44E-005
ENSGACG00000007546	XII-C	XII-XII	-1,84247	4,75E-005	0,00123467
ENSGACG00000007661	XII-C	XII-XII	-2,85701	0,00089657	0,0140504
ENSGACG00000007761	XII-C	XII-XII	-1,56566	0,00398779	0,046319
ENSGACG00000007857	XII-C	XII-XII	-1,54702	5,08E-011	8,41E-009
ENSGACG00000007950	XII-C	XII-XII	-4,47084	4,58E-005	0,00119843
ENSGACG00000008764	XII-C	XII-XII	-1,38475	0,00251422	0,0322091
ENSGACG00000009211	XII-C	XII-XII	-2,27841	0,00298346	0,0368967
ENSGACG00000009229	XII-C	XII-XII	-4,16666	2,18E-006	9,10E-005
ENSGACG00000009409	XII-C	XII-XII	-4,67818	1,62E-006	7,07E-005

gene	sample_1	sample_2	log2(fold_change)	p_value	q_value
ENSGACG00000009417	XII-C	XII-XII	1,87456	0,00191831	0,0259552
ENSGACG00000010400	XII-C	XII-XII	-3,60869	3,56E-005	0,000969458
ENSGACG00000010501	XII-C	XII-XII	-1,39245	8,24E-008	5,47E-006
ENSGACG00000010623	XII-C	XII-XII	-8,9327	1,76E-008	1,44E-006
ENSGACG00000010643	XII-C	XII-XII	-1,29378	0,00331233	0,0400478
ENSGACG00000010888	XII-C	XII-XII	-3,68651	0,000967311	0,0149535
ENSGACG00000010896	XII-C	XII-XII	-3,13415	0,00365516	0,0432779
ENSGACG00000010933	XII-C	XII-XII	-3,32155	0,0011112	0,0167396
ENSGACG00000011120	XII-C	XII-XII	-0,989832	0,00027078	0,00526687
ENSGACG00000011294	XII-C	XII-XII	-2,05827	8,86E-006	0,000299254
ENSGACG00000011542	XII-C	XII-XII	-0,67284	0,00227398	0,0297265
ENSGACG00000011617	XII-C	XII-XII	-3,31753	0,000436991	0,00782254
ENSGACG00000012375	XII-C	XII-XII	-2,1792	0,00358087	0,0425809
ENSGACG00000012607	XII-C	XII-XII	-0,681049	0,000511673	0,00889879
ENSGACG00000012639	XII-C	XII-XII	-2,16845	0,00309066	0,0379265
ENSGACG00000012654	XII-C	XII-XII	-8,05799	1,77E-005	0,000538289
ENSGACG00000012657	XII-C	XII-XII	-9,80076	2,33E-009	2,47E-007
ENSGACG00000012781	XII-C	XII-XII	-2,5856	0,000890445	0,013972
ENSGACG00000012783	XII-C	XII-XII	-2,18468	0,00300959	0,0371516
ENSGACG00000012797	XII-C	XII-XII	-2,76255	0,000514936	0,00894615
ENSGACG00000012799	XII-C	XII-XII	-2,69946	0,000236614	0,00471186
ENSGACG00000013652	XII-C	XII-XII	-1,70586	1,57E-005	0,000486918
ENSGACG00000013871	XII-C	XII-XII	-2,68559	0,000423505	0,00762325
ENSGACG00000013891	XII-C	XII-XII	-4,95161	1,63E-005	0,000502762
ENSGACG00000013918	XII-C	XII-XII	-3,0927	0,000223724	0,00449783
ENSGACG00000014099	XII-C	XII-XII	-6,32001	0,000288798	0,00555664
ENSGACG00000014250	XII-C	XII-XII	-4,68041	0,000282455	0,00545371
ENSGACG00000014315	XII-C	XII-XII	-2,82704	0,000207975	0,00423238
ENSGACG00000014547	XII-C	XII-XII	-2,32138	0,000379408	0,00696301
ENSGACG00000014601	XII-C	XII-XII	-2,48256	0,000633424	0,0105919
ENSGACG00000014629	XII-C	XII-XII	-2,02122	3,41E-008	2,55E-006
ENSGACG00000014655	XII-C	XII-XII	-2,2616	0,00350841	0,0418934
ENSGACG00000014948	XII-C	XII-XII	-4,60299	2,04E-005	0,000607357
ENSGACG00000015628	XII-C	XII-XII	-2,36594	0,00118956	0,0176859
ENSGACG00000015818	XII-C	XII-XII	4,83375	0,000285252	0,00549901
ENSGACG00000015897	XII-C	XII-XII	-1,27281	0	0
ENSGACG00000016409	XII-C	XII-XII	-2,85154	0,00185073	0,0252276
ENSGACG00000016422	XII-C	XII-XII	-2,57647	2,32E-006	9,61E-005
ENSGACG00000016618	XII-C	XII-XII	-0,886272	0,0014457	0,020682
ENSGACG00000017022	XII-C	XII-XII	-2,17934	0,00261713	0,0332454
ENSGACG00000017119	XII-C	XII-XII	-1,86369	0,00341765	0,0410464
ENSGACG00000017373	XII-C	XII-XII	-2,7038	0,000155989	0,00333097
ENSGACG00000018049	XII-C	XII-XII	5,48649	4,95E-005	0,00127765
ENSGACG00000019078	XII-C	XII-XII	-2,21467	0,00137303	0,019849
ENSGACG00000019173	XII-C	XII-XII	-0,661639	0,0040881	0,0472168
ENSGACG00000019390	XII-C	XII-XII	-1,71775	0,000863382	0,0136244
ENSGACG00000019581	XII-C	XII-XII	-2,63441	0,000307383	0,00584919
ENSGACG00000019627	XII-C	XII-XII	-2,1919	0,00366178	0,0433396
ENSGACG00000019770	XII-C	XII-XII	-1,5099	0,00254847	0,0325522
ENSGACG00000020034	XII-C	XII-XII	-4,5031	1,76E-005	0,000534335
ENSGACG00000020365	XII-C	XII-XII	-2,54221	0,0019117	0,0258831
ENSGACG00000020403	XII-C	XII-XII	-1,33093	0,00135174	0,0196013
FAM132B	XII-C	XII-XII	-1,88161	0,00297368	0,0367983

gene	sample_1	sample_2	log2(fold_change)	p_value	q_value
FAM151B	XII-C	XII-XII	-1,47488	0,00111701	0,016811
FAM167B	XII-C	XII-XII	-1,93204	0,00019205	0,00396176
FAM55C (4 of 8)	XII-C	XII-XII	2,44667	0,00192745	0,0260559
FAM96B	XII-C	XII-XII	-2,12226	0,00272705	0,0343389
FCGBP (1 of 2)	XII-C	XII-XII	1,11778	0,000469877	0,00830164
FHL5	XII-C	XII-XII	-2,42105	0	0
FKBP5	XII-C	XII-XII	2,90362	4,53E-005	0,00118577
GALM	XII-C	XII-XII	-1,96901	0,000440142	0,00786896
GAPDH (1 of 2)	XII-C	XII-XII	-0,916309	2,47E-005	0,000713586
GCDH (1 of 2)	XII-C	XII-XII	-0,884634	0	0
GCNT1	XII-C	XII-XII	2,44138	0,000140063	0,00304611
GEM	XII-C	XII-XII	-3,08182	0,00440146	0,0499958
GLTPD1	XII-C	XII-XII	-1,88935	0,00438718	0,0498698
GNPTG	XII-C	XII-XII	-1,42836	0,00197235	0,0265441
GOSR1 (2 of 2)	XII-C	XII-XII	-2,24254	0,00253675	0,0324348
GP1BB	XII-C	XII-XII	-2,08305	0,0028203	0,0352668
GPANK1	XII-C	XII-XII	-1,26792	0,000683235	0,0112656
GZMA	XII-C	XII-XII	-2,52529	0,000194744	0,00400804
HBM	XII-C	XII-XII	-2,20318	0,00174002	0,023997
HERC4	XII-C	XII-XII	-0,832232	0,00107758	0,0163239
HIST1H1T	XII-C	XII-XII	-2,07656	0,00224885	0,0294662
HLA-DMA (4 of 5)	XII-C	XII-XII	-2,5597	0,00255126	0,0325793
HNMT (2 of 2)	XII-C	XII-XII	-2,47248	0,00230014	0,0299998
HSD17B10	XII-C	XII-XII	-1,38806	0	0
IER3IP1	XII-C	XII-XII	-2,48344	0,000745628	0,0120971
IER5L (2 of 2)	XII-C	XII-XII	-2,1169	0,00305635	0,037598
IFT20	XII-C	XII-XII	-2,51506	0,00133305	0,0193808
IFT80	XII-C	XII-XII	-0,827042	0,00315778	0,0385695
IGKC (1 of 24)	XII-C	XII-XII	-3,8186	4,24E-006	0,000160175
IGKC (12 of 24)	XII-C	XII-XII	-4,80445	0,00435787	0,0496125
IGKC (15 of 24)	XII-C	XII-XII	-4,12615	0,000307482	0,00585091
IGKC (17 of 24)	XII-C	XII-XII	-4,57546	0,00117278	0,0174877
IGKC (4 of 24)	XII-C	XII-XII	-3,77034	0,000942892	0,0146437
ILDR1 (1 of 2)	XII-C	XII-XII	-1,00837	0,00417389	0,0479907
IRF4 (2 of 2)	XII-C	XII-XII	-2,57593	0,000129152	0,00284723
LDHD	XII-C	XII-XII	-1,7586	0,00428869	0,0490105
LGALS8 (2 of 2)	XII-C	XII-XII	-1,80283	0,000754317	0,0122111
LPAR2 (2 of 2)	XII-C	XII-XII	-1,52445	0,00126689	0,0186078
LRRC10	XII-C	XII-XII	-3,59324	0,00366052	0,0433273
LRRC39	XII-C	XII-XII	-2,60888	9,56E-005	0,00221427
LSM6	XII-C	XII-XII	-2,0142	0,00438535	0,0498523
LZIC	XII-C	XII-XII	-1,40845	4,72E-008	3,38E-006
MAD2L2	XII-C	XII-XII	-1,91893	0	0
METTL10	XII-C	XII-XII	-1,70618	0,000800979	0,0128221
METTL5	XII-C	XII-XII	-2,00067	0,0026621	0,0336933
MFSD2A (1 of 2)	XII-C	XII-XII	-1,05012	0,00348505	0,0416744
MINOS1 (1 of 2)	XII-C	XII-XII	-2,33586	0,00222955	0,0292627
MLYCD	XII-C	XII-XII	-1,16221	0,00242119	0,0312563
MPLKIP	XII-C	XII-XII	-1,77642	0,00202493	0,0271103
MRPL12	XII-C	XII-XII	-0,748151	0,00391883	0,0457017
MRPL15	XII-C	XII-XII	-0,879514	0,000428675	0,00770038
MRPL19	XII-C	XII-XII	-1,00699	0,00014249	0,00309018
MRPL28	XII-C	XII-XII	-1,38321	1,19E-010	1,80E-008

gene	sample_1	sample_2	log2(fold_change)	p_value	q_value
MRPS10	XII-C	XII-XII	-1,94523	1,21E-012	2,95E-010
MRPS24	XII-C	XII-XII	-1,87955	0,00382143	0,0448068
MRPS28	XII-C	XII-XII	-2,28462	0,000870863	0,0137199
MRPS31	XII-C	XII-XII	-0,990626	1,40E-007	8,63E-006
MYBPC3	XII-C	XII-XII	-2,21774	0,00130682	0,0190777
MYL7	XII-C	XII-XII	-9,6997	1,23E-008	1,06E-006
MYOM1 (2 of 2)	XII-C	XII-XII	-0,733483	1,46E-013	4,35E-011
NAPSA	XII-C	XII-XII	-0,724385	0,00265038	0,0335756
NCKIPSD	XII-C	XII-XII	-1,32399	0,0026075	0,03315
NDUFB1	XII-C	XII-XII	-2,28121	0,00404949	0,0468738
NDUFB2	XII-C	XII-XII	-2,21198	0,00427402	0,0488833
NEURL2	XII-C	XII-XII	-2,77606	0,00322076	0,0391733
NT5C	XII-C	XII-XII	-1,27345	0,00277182	0,034785
NXT2	XII-C	XII-XII	-2,6926	0,000939975	0,0146075
PFKM (1 of 2)	XII-C	XII-XII	-1,11129	0,0038835	0,0453793
PIGB	XII-C	XII-XII	-1,27992	0,000173849	0,0036462
PIK3IP1	XII-C	XII-XII	-0,836943	5,47E-006	0,000198887
PLD4	XII-C	XII-XII	-2,22806	0,0030462	0,0375022
PPDPF (1 of 2)	XII-C	XII-XII	-1,82248	9,41E-005	0,00218564
PRADC1	XII-C	XII-XII	-1,4514	0,00128686	0,0188422
PRKAG3 (2 of 2)	XII-C	XII-XII	-2,28641	0,00391174	0,045638
PTCD3	XII-C	XII-XII	-0,64423	0,00284796	0,0355449
PTS	XII-C	XII-XII	-2,94802	0,00288764	0,0359441
PVRL1 (2 of 2)	XII-C	XII-XII	1,80E+308	0,00028023	0,0054186
RDH8 (1 of 2)	XII-C	XII-XII	-1,13695	0,00387236	0,0452771
RGMB	XII-C	XII-XII	-1,82986	0,00202683	0,0271293
RHBDL2	XII-C	XII-XII	-0,923793	0,000481145	0,00846259
RMND5B	XII-C	XII-XII	-0,833435	0,00194115	0,026204
RPA3	XII-C	XII-XII	-2,10338	0,00378758	0,0445029
RPS24	XII-C	XII-XII	-1,7706	3,14E-007	1,73E-005
RPS29	XII-C	XII-XII	-2,35633	0,00111128	0,0167406
RRAD	XII-C	XII-XII	-3,26701	0,0026881	0,0339537
SCTR	XII-C	XII-XII	-2,02566	0,00390582	0,0455821
SEPHS2	XII-C	XII-XII	-1,58403	0,000285042	0,00549584
SERBP1 (1 of 2)	XII-C	XII-XII	-0,743406	0,00407758	0,0471231
SH3BP5	XII-C	XII-XII	-1,41421	0,00372185	0,0438973
SLC25A37	XII-C	XII-XII	-1,52099	7,85E-005	0,00187823
SLC25A43	XII-C	XII-XII	-0,892083	1,35E-006	6,05E-005
SLC35C1	XII-C	XII-XII	-1,03646	0,00372148	0,0438941
SLC46A3	XII-C	XII-XII	-1,88678	0,00218798	0,0288272
SLC4A4 (1 of 2)	XII-C	XII-XII	-0,560978	1,95E-005	0,000583546
SLCO2B1	XII-C	XII-XII	-0,466404	4,39E-011	7,39E-009
SNX14	XII-C	XII-XII	-0,911407	0,00213708	0,0283024
SOCS1 (2 of 2)	XII-C	XII-XII	-2,1492	0,0024328	0,0313745
SPCS2	XII-C	XII-XII	-1,22291	3,56E-005	0,000969074
SPG21	XII-C	XII-XII	-0,773409	0,000842736	0,013359
SPPL2A	XII-C	XII-XII	-0,991912	4,27E-010	5,54E-008
STOML2 (2 of 2)	XII-C	XII-XII	-1,10531	0	0
TAL1	XII-C	XII-XII	-2,27421	0,00391056	0,0456269
TBCA	XII-C	XII-XII	-1,31508	0,00159684	0,0223987
TDO2	XII-C	XII-XII	-2,48774	0,00214148	0,0283477
TF	XII-C	XII-XII	-2,55465	0,000694077	0,011413
TFPI2	XII-C	XII-XII	-1,84437	0,000360012	0,00666721

gene	sample_1	sample_2	log2(fold_change)	p_value	q_value
THBS1 (2 of 2)	XII-C	XII-XII	2,47397	0,000908149	0,0142002
TIFA	XII-C	XII-XII	-1,91228	0,00239611	0,0309984
TK2	XII-C	XII-XII	-1,24255	0,0023515	0,0305359
TMEM14E	XII-C	XII-XII	-1,96681	0,00410269	0,0473507
TMEM182	XII-C	XII-XII	-1,31999	0,000423897	0,00762913
TMEM183A	XII-C	XII-XII	-1,05048	0,000211902	0,00429934
TMEM54 (1 of 2)	XII-C	XII-XII	-1,36264	4,40E-009	4,31E-007
TMOD4	XII-C	XII-XII	-1,63869	7,62E-014	2,40E-011
TNNC1	XII-C	XII-XII	-5,82709	6,05E-007	3,04E-005
TNNI2 (5 of 5)	XII-C	XII-XII	-3,38388	0,000743147	0,0120635
TNNT2 (1 of 2)	XII-C	XII-XII	-6,92757	4,04E-008	2,95E-006
TOM1 (2 of 2)	XII-C	XII-XII	-0,907007	0,00286219	0,0356855
TRDN	XII-C	XII-XII	-1,33111	7,11E-005	0,0017288
TTC32	XII-C	XII-XII	-2,2248	0,00130766	0,019088
TTC36	XII-C	XII-XII	-2,33456	0,00136678	0,0197763
TTC38	XII-C	XII-XII	-1,21289	0,000893866	0,0140165
TTC9C	XII-C	XII-XII	-1,39674	7,59E-008	5,10E-006
TXNDC17	XII-C	XII-XII	-2,26596	7,29E-005	0,00176523
UROS	XII-C	XII-XII	-1,4419	7,44E-007	3,63E-005
WDR18	XII-C	XII-XII	-0,844971	0,000729012	0,0118787
WDR5	XII-C	XII-XII	-0,731655	0,0010035	0,0154058
XCR1 (1 of 2)	XII-C	XII-XII	-2,49098	0,00299241	0,0369881

Supplementary table S.3.4 GO terms from the biological process ontology that were significantly over- or underrepresented in different treatment groups ("Tested") when compared to a reference group ("Reference"). Groups consisted of genes that were either unique to a specific treatment groups (e.g. I only) or all genes differentially expressed within a given treatment group (e.g. all XII-XII). For a general representation of GO terms, treatments were also tested against the transcriptome.

tested	reference	organ	GO-ID	term	representation	FDR
I only	M only	head kidney	GO: 0071840	cellular component organization or biogenesis	under	0,009
I only	M only	head kidney	GO: 0016043	cellular component organization	under	0,009
I only	M only	head kidney	GO: 0007010	cytoskeleton organization	under	0,009
I only	M only	head kidney	GO: 0006996	organelle organization	under	0,009
I only	M only	head kidney	GO: 0071841	cellular component organization or biogenesis at cellular level	under	0,009
I only	M only	head kidney	GO: 0071842	cellular component organization at cellular level	under	0,009
I only	M only	head kidney	GO: 0048869	cellular developmental process	under	0,009
I only	M only	head kidney	GO: 0009653	anatomical structure morphogenesis	under	0,009
I only	M only	head kidney	GO: 0030154	cell differentiation	under	0,009
I only	M only	head kidney	GO: 0048856	anatomical structure development	under	0,049
XII only	XII-XII only	gills	GO: 0032502	developmental process	under	0,022
XII only	XII-XII only	gills	GO: 0009987	cellular process	under	0,034
XII only	XII-XII only	gills	GO: 0007275	multicellular organismal development	under	0,049
XII only	XII-XII only	gills	GO: 0032501	multicellular organismal process	under	0,049
I-M only	M-M only	head kidney	GO: 0048856	anatomical structure development	over	4,80E
I-M only	M-M only	head kidney	GO: 0009653	anatomical structure morphogenesis	over	4,80E
I-M only	M-M only	head kidney	GO: 0030154	cell differentiation	over	0,006
I-M only	M-M only	head kidney	GO: 0048869	cellular developmental process	over	0,006
I-M only	M-M only	head kidney	GO: 0007010	cytoskeleton organization	over	0,010
I-M only	M-M only	head kidney	GO: 0009987	cellular process	over	0,010
I-M only	M-M only	head kidney	GO: 0016043	cellular component organization	over	0,010
I-M only	M-M only	head kidney	GO: 0071840	cellular component organization or biogenesis	over	0,010
I-M only	M-M only	head kidney	GO: 0034641	cellular nitrogen compound metabolic process	over	0,010
I-M only	M-M only	head kidney	GO: 0006139	nucleobase-containing compound metabolic process	over	0,010

tested	reference	organ	GO-ID	term	representation	FDR
I-M only	M-M only	head kidney	GO: 0006807	nitrogen compound metabolic process	over	0,010
I-M only	M-M only	head kidney	GO: 0044237	cellular metabolic process	over	0,017
I-M only	M-M only	head kidney	GO: 0009790	embryo development	over	0,021
I-M only	M-M only	head kidney	GO: 0006996	organelle organization	over	0,026
I-M only	M-M only	head kidney	GO: 0071841	cellular component organization or biogenesis at cellular level	over	0,026
I-M only	M-M only	head kidney	GO: 0071842	cellular component organization at cellular level	over	0,026
I-M only	M-M only	head kidney	GO: 0032501	multicellular organismal process	over	0,037
I-M only	M-M only	head kidney	GO: 0032502	developmental process	over	0,037
I-M only	M-M only	head kidney	GO: 0007275	multicellular organismal development	over	0,037
I only	I-I only	head kidney	GO: 0009653	anatomical structure morphogenesis	under	3,40E
I only	I-I only	head kidney	GO: 0007010	cytoskeleton organization	under	6,79E
I only	I-I only	head kidney	GO: 0048856	anatomical structure development	under	6,79E
I only	I-I only	head kidney	GO: 0048869	cellular developmental process	under	6,79E
I only	I-I only	head kidney	GO: 0030154	cell differentiation	under	6,79E
I only	I-I only	head kidney	GO: 0006996	organelle organization	under	9,64E
I only	I-I only	head kidney	GO: 0071841	cellular component organization or biogenesis at cellular level	under	9,64E
I only	I-I only	head kidney	GO: 0071842	cellular component organization at cellular level	under	9,64E
I only	I-I only	head kidney	GO: 0071840	cellular component organization or biogenesis	under	0,002
I only	I-I only	head kidney	GO: 0016043	cellular component organization	under	0,002
I only	I-I only	head kidney	GO: 0050789	regulation of biological process	under	0,013
I only	I-I only	head kidney	GO: 0009987	cellular process	under	0,016
I only	I-I only	head kidney	GO: 0007275	multicellular organismal development	under	0,016
I only	I-I only	head kidney	GO: 0032501	multicellular organismal process	under	0,016
I only	I-I only	head kidney	GO: 0032502	developmental process	under	0,016
I only	I-I only	head kidney	GO: 0065007	biological regulation	under	0,016
I only	I-I only	head kidney	GO: 0009056	catabolic process	under	0,021
I only	I-I only	head kidney	GO: 0009790	embryo development	under	0,021
I only	I-I only	head kidney	GO: 0034641	cellular nitrogen compound metabolic process	under	0,021

tested	reference	organ	GO-ID	term	representation	FDR
I only	I-I only	head kidney	GO: 0006139	nucleobase-containing compound metabolic process	under	0,021
I only	I-I only	head kidney	GO: 0006807	nitrogen compound metabolic process	under	0,021
I only	I-I only	head kidney	GO: 0044237	cellular metabolic process	under	0,026
I only	I-I only	head kidney	GO: 0051179	localization	under	0,050
I only	I-I only	head kidney	GO: 0051234	establishment of localization	under	0,050
I only	I-I only	head kidney	GO: 0006810	transport	under	0,050
I-I only	XII-XII only	head kidney	GO: 0009653	anatomical structure morphogenesis	over	0,006
I-I only	XII-XII only	head kidney	GO: 0006996	organelle organization	over	0,010
I-I only	XII-XII only	head kidney	GO: 0007010	cytoskeleton organization	over	0,010
I-I only	XII-XII only	head kidney	GO: 0071841	cellular component organization or biogenesis at cellular level	over	0,010
I-I only	XII-XII only	head kidney	GO: 0071842	cellular component organization at cellular level	over	0,010
I-I only	XII-XII only	head kidney	GO: 0050789	regulation of biological process	over	0,011
I-I only	XII-XII only	head kidney	GO: 0048856	anatomical structure development	over	0,022
I-I only	XII-XII only	head kidney	GO: 0065007	biological regulation	over	0,028
I-I only	XII-XII only	head kidney	GO: 0016043	cellular component organization	over	0,038
I-I only	XII-XII only	head kidney	GO: 0071840	cellular component organization or biogenesis	over	0,038
I-I only	XII-XII only	head kidney	GO: 0051234	establishment of localization	over	0,048
I-I only	XII-XII only	head kidney	GO: 0051179	localization	over	0,048
I-I only	XII-XII only	head kidney	GO: 0006810	transport	over	0,048
I-I only	M-M only	head kidney	GO: 0009653	anatomical structure morphogenesis	over	0,006
I-I only	M-M only	head kidney	GO: 0006996	organelle organization	over	0,010
I-I only	M-M only	head kidney	GO: 0007010	cytoskeleton organization	over	0,010
I-I only	M-M only	head kidney	GO: 0071841	cellular component organization or biogenesis at cellular level	over	0,010
I-I only	M-M only	head kidney	GO: 0071842	cellular component organization at cellular level	over	0,010
I-I only	M-M only	head kidney	GO: 0050789	regulation of biological process	over	0,011
I-I only	M-M only	head kidney	GO: 0048856	anatomical structure development	over	0,022
I-I only	M-M only	head kidney	GO: 0065007	biological regulation	over	0,028
I-I only	M-M only	head kidney	GO: 0016043	cellular component organization	over	0,038

tested	reference	organ	GO-ID	term	representation	FDR
I-I only	M-M only	head kidney	GO: 0071840	cellular component organization or biogenesis	over	0,038
I-I only	M-M only	head kidney	GO: 0051234	establishment of localization	over	0,048
I-I only	M-M only	head kidney	GO: 0051179	localization	over	0,048
I-I only	M-M only	head kidney	GO: 0006810	transport	over	0,048
I-I and I-M	XII-XII and XII-M	head kidney	GO: 0009653	anatomical structure morphogenesis	over	0,006
I-I and I-M	XII-XII and XII-M	head kidney	GO: 0048869	cellular developmental process	over	0,006
I-I and I-M	XII-XII and XII-M	head kidney	GO: 0030154	cell differentiation	over	0,006
I-I and I-M	XII-XII and XII-M	head kidney	GO: 0006996	organelle organization	over	0,006
I-I and I-M	XII-XII and XII-M	head kidney	GO: 0071841	cellular component organization or biogenesis at cellular level	over	0,006
I-I and I-M	XII-XII and XII-M	head kidney	GO: 0071842	cellular component organization at cellular level	over	0,006
I-I and I-M	XII-XII and XII-M	head kidney	GO: 0007010	cytoskeleton organization	over	0,006
I-I and I-M	XII-XII and XII-M	head kidney	GO: 0071840	cellular component organization or biogenesis	over	0,006
I-I and I-M	XII-XII and XII-M	head kidney	GO: 0016043	cellular component organization	over	0,006
I-I and I-M	XII-XII and XII-M	head kidney	GO: 0050789	regulation of biological process	over	0,023
I-I and I-M	XII-XII and XII-M	head kidney	GO: 0065007	biological regulation	over	0,031
I-I and I-M	XII-XII and XII-M	head kidney	GO: 0048856	anatomical structure development	over	0,038
I-I and I-M	XII-XII and XII-M	head kidney	GO: 0044237	cellular metabolic process	over	0,038
I-I and I-M	XII-XII and XII-M	head kidney	GO: 0051179	localization	over	0,038
I-I and I-M	XII-XII and XII-M	head kidney	GO: 0051234	establishment of localization	over	0,038
I-I and I-M	XII-XII and XII-M	head kidney	GO: 0006810	transport	over	0,038
I-I and I-M	XII-XII and XII-M	head kidney	GO: 0009987	cellular process	over	0,042
I-M only	XII-M only	head kidney	GO: 0050789	regulation of biological process	over	0,037
all I-I	transcriptome	head kidney	GO: 0007010	cytoskeleton organization	over	8,23E
all XII-XII	transcriptome	head kidney	GO: 0050789	regulation of biological process	under	0,001
all XII-XII	transcriptome	head kidney	GO: 0065007	biological regulation	under	0,001
all XII-XII	transcriptome	head kidney	GO: 0050794	regulation of cellular process	under	0,028
all XII-XII	transcriptome	head kidney	GO: 0051716	cellular response to stimulus	under	0,028
all XII-XII	transcriptome	head kidney	GO: 0007165	signal transduction	under	0,028

tested	reference	organ	GO-ID	term	representation	FDR
all XII-XII	transcriptome	head kidney	GO: 0009987	cellular process	under	0,035
all consecutive	transcriptome	head kidney	GO: 0050789	regulation of biological process	under	0,006
all consecutive	transcriptome	head kidney	GO: 0008283	cell proliferation	under	0,007
all consecutive	transcriptome	head kidney	GO: 0065007	biological regulation	under	0,007
all consecutive	transcriptome	head kidney	GO: 0050794	regulation of cellular process	under	0,023
all consecutive	transcriptome	head kidney	GO: 0051716	cellular response to stimulus	under	0,023
all consecutive	transcriptome	head kidney	GO: 0007165	signal transduction	under	0,023
all consecutive	transcriptome	head kidney	GO: 0044260	cellular macromolecule metabolic process	under	0,024
all consecutive	transcriptome	head kidney	GO: 0007010	cytoskeleton organization	over	0,035
all consecutive	transcriptome	head kidney	GO: 0023052	signaling	under	0,041

Supplementary table S.3.5 Differentially expressed immune-related genes in head kidney tissue of *G. aculeatus*. Shown are differentially expressed genes and their corresponding pre-exposure control (sample_1) and final treatment (sample_2). The log2-fold change shows if there is up- or down-regulation of a given gene due to the parasite treatment compared to the respective pre-exposure control. Only significant differences shown.

gene	sample_1	sample_2	log2_foldchange
ELMOD2	I-C	I-I	0,950604
VTN (2 of 2)	I-C	I-I	1,79699
APOB (2 of 5)	I-C	I-I	3,40812
PRG4	I-C	I-I	3,88188
MASP1 (2 of 2)	I-C	I-I	4,11019
MYLPF (2 of 2)	M-C	M-M	-4,07478
ADSSL1	M-C	M-M	-3,21472
CFB	M-C	M-M	3,0643
ADAMTS13	M-C	M-M	3,28212
ENPP2 (2 of 2)	M-C	M-M	3,37469
SERPING1	M-C	M-M	3,52804
CFP	M-C	M-M	4,19919
C9	M-C	M-M	4,90788
SUSD2	M-C	M-M	5,13608
C3 (5 of 8)	M-C	M-M	5,20093
APOB (1 of 5)	M-C	M-M	5,26128
C3 (1 of 8)	M-C	M-M	5,26274
C3 (3 of 8)	M-C	M-M	5,53618
PGLYRP2 (2 of 2)	M-C	M-M	5,53778
C3 (4 of 8)	M-C	M-M	5,73688
C8G	M-C	M-M	5,77978
C8B	M-C	M-M	5,78051
C8A	M-C	M-M	5,9133
C3 (2 of 8)	M-C	M-M	5,98528
CHIA	M-C	M-M	6,02963
APOB (5 of 5)	M-C	M-M	6,19346
PVRL1 (2 of 2)	M-C	M-M	6,35052
ENSGACG00000014811	M-C	M-M	6,65685
ENSGACG00000003030	M-C	M-M	9,62865
ENSGACG00000014852	M-C	M-M	10,8211
MYLPF (1 of 2)	XII-C	XII-M	-8,88641
ADSSL1	XII-C	XII-M	-5,36915
ENSGACG00000003030	XII-C	XII-M	-4,28505
IRF6	XII-C	XII-M	-3,96646
MYLPF (2 of 2)	XII-C	XII-M	-3,75924
ENSGACG00000014852	XII-C	XII-M	-3,53238
PGLYRP2 (1 of 2)	XII-C	XII-M	-3,49429
C8A	XII-C	XII-M	-3,45414
CFP	XII-C	XII-M	-3,41843
PGLYRP2 (2 of 2)	XII-C	XII-M	-3,40134
ATP1B3	XII-C	XII-M	-3,38417
C8G	XII-C	XII-M	-3,34482
C7 (1 of 2)	XII-C	XII-M	-3,16896
CFB	XII-C	XII-M	-2,90205
SUSD2	XII-C	XII-M	-2,74687

gene	sample_1	sample_2	log2_foldchange
APOB (2 of 5)	XII-C	XII-M	-2,62482
GAS6	XII-C	XII-M	-0,639669
ITGA6 (1 of 2)	XII-C	XII-M	0,736352
C8G	XII-C	XII-XII	-8,67221
PLG	XII-C	XII-XII	-8,21339
ENSGACG00000003030	XII-C	XII-XII	-7,97925
PGLYRP2 (2 of 2)	XII-C	XII-XII	-7,95708
ENSGACG00000014852	XII-C	XII-XII	-7,7671
ENSGACG00000014811	XII-C	XII-XII	-7,76487
C8A	XII-C	XII-XII	-7,64739
C3 (4 of 8)	XII-C	XII-XII	-7,54974
APOB (5 of 5)	XII-C	XII-XII	-7,53838
C3 (3 of 8)	XII-C	XII-XII	-7,08703
C9	XII-C	XII-XII	-7,06315
APOB (1 of 5)	XII-C	XII-XII	-6,89567
C3 (1 of 8)	XII-C	XII-XII	-6,88341
C3 (5 of 8)	XII-C	XII-XII	-6,80613
C3 (2 of 8)	XII-C	XII-XII	-6,58022
SUSD2	XII-C	XII-XII	-6,4171
CFP	XII-C	XII-XII	-5,52123
MASP1 (2 of 2)	XII-C	XII-XII	-5,11288
CFB	XII-C	XII-XII	-4,61178
KYNU	XII-C	XII-XII	-4,39218
SERPING1	XII-C	XII-XII	-4,04635
MYLPF (2 of 2)	XII-C	XII-XII	-3,70764
ENPP2 (2 of 2)	XII-C	XII-XII	-3,70527
IRF6	XII-C	XII-XII	-2,95084
C4A	XII-C	XII-XII	-1,30456
STXBP2	XII-C	XII-XII	0,692237
AP2S1	XII-C	XII-XII	0,812851
KIF23 (2 of 2)	XII-C	XII-XII	1,27243
RPA1 (1 of 2)	XII-C	XII-XII	1,31239
CDK1	XII-C	XII-XII	1,68752

Supplementary table S.3.6 Differentially expressed immune-related genes in gill tissue of *G. aculeatus*. Shown are differentially expressed genes and their corresponding pre-exposure control (sample_1) and final treatment (sample_2). The log2-fold change shows if there is up- or down-regulation of a given gene due to the parasite treatment compared to the respective pre-exposure control. Only significant differences shown.

gene	sample_1	sample_2	log2_foldchange
CASP3 (4 of 4)	I-C	I-I	0,645245
LGALS8 (2 of 2)	I-C	I-I	1,24388
ELMOD2	I-C	I-I	1,30915
GRAP2	I-C	I-I	1,37326
PGLYRP2 (1 of 2)	I-C	I-I	1,94663
SLC3A2 (2 of 2)	I-C	I-I	2,12421
SOCS3 (1 of 2)	I-C	I-I	2,27549
ENSGACG00000001729	I-C	I-I	2,4157
VIPR1 (2 of 2)	I-C	I-I	2,81637
CRISP3	I-C	I-I	2,97095
RAG1	I-C	I-I	3,50958
RAG2	I-C	I-I	4,01033
ITGB1 (1 of 2)	I-C	I-M	0,946666
WAS	I-C	I-M	0,997456
KLC1	I-C	I-M	1,00953
KIFAP3 (2 of 2)	I-C	I-M	1,03014
CASP8	I-C	I-M	1,11152
HYAL2 (1 of 2)	I-C	I-M	1,52474
ADSS	I-C	I-M	1,52778
PIK3R1 (1 of 2)	I-C	I-M	1,74812
ENSGACG00000016298	I-C	I-M	1,81407
DAB2	I-C	I-M	1,83943
C4A	I-C	I-M	1,84794
NCF1	I-C	I-M	1,89572
ENSGACG00000012769	I-C	I-M	2,04814
CASP3 (4 of 4)	I-C	I-M	2,13822
C6	I-C	I-M	2,16836
NFKBIA (1 of 2)	I-C	I-M	2,18021
CCR9 (1 of 2)	I-C	I-M	2,29269
RSAD2	I-C	I-M	2,49104
USP18	I-C	I-M	2,66969
C7 (1 of 2)	I-C	I-M	3,05243
SOCS3 (1 of 2)	I-C	I-M	3,74379
ENSGACG00000012792	I-C	I-M	4,30345
C3 (4 of 8)	M-C	M-M	2,72071
C7 (1 of 2)	M-C	M-M	3,34781
THBS1 (2 of 2)	M-C	M-M	3,72156
ENSGACG00000012797	XII-C	XII-M	-2,45115
ENSGACG00000012799	XII-C	XII-M	-2,44042
CXCL12 (2 of 2)	XII-C	XII-M	-1,72844
C4A	XII-C	XII-M	-1,4211
IREB2	XII-C	XII-M	-1,3334
AP2S1	XII-C	XII-M	-1,23273
GEM	XII-C	XII-XII	-3,08182
ENSGACG00000012797	XII-C	XII-XII	-2,76255

gene	sample_1	sample_2	log2_foldchange
ENSGACG00000012799	XII-C	XII-XII	-2,69946
ENSGACG00000012781	XII-C	XII-XII	-2,5856
IRF4 (2 of 2)	XII-C	XII-XII	-2,57593
ATG12	XII-C	XII-XII	-2,29584
TAL1	XII-C	XII-XII	-2,27421
ENSGACG00000019078	XII-C	XII-XII	-2,21467
ENSGACG00000012783	XII-C	XII-XII	-2,18468
SOCS1 (2 of 2)	XII-C	XII-XII	-2,1492
LGALS8 (2 of 2)	XII-C	XII-XII	-1,80283
ENSGACG00000000336	XII-C	XII-XII	-1,29954
THBS1 (2 of 2)	XII-C	XII-XII	2,47397
PVRL1 (2 of 2)	XII-C	XII-XII	1,80E+308